CELL-PENETRATING PEPTIDES

Processes and Applications

Ülo Langel

CRC PRESS
PHARMACOLOGY & TOXICOLOGY SERIES

CELL-PENETRATING PEPTIDES

Processes and Applications

Pharmacology and Toxicology: Basic and Clinical Aspects

Mannfred A. Hollinger, Series Editor
University of California, Davis

Published Titles

Biomedical Applications of Computer Modeling, 2001, Arthur Christopoulos
Molecular Bases of Anesthesia, 2001, Eric Moody and Phil Skolnick
Manual of Immunological Methods, 1999, Pauline Brousseau, Yves Payette, Helen Tryphonas, Barry Blakley, Herman Boermans, Denis Flipo, Michel Fournier
CNS Injuries: Cellular Responses and Pharmacological Strategies, 1999, Martin Berry and Ann Logan
*Infectious Diseases in Immunocompromised Hosts,*1998, Vassil St. Georgiev
Pharmacology of Antimuscarinic Agents, 1998, Laszlo Gyermek
Basis of Toxicity Testing, *Second Edition,* 1997, Donald J. Ecobichon
Anabolic Treatments for Osteoporosis, 1997, James F. Whitfield and Paul Morley
Antibody Therapeutics, 1997, William J. Harris and John R. Adair
Muscarinic Receptor Subtypes in Smooth Muscle, 1997, Richard M. Eglen
Antisense Oligodeonucleotides as Novel Pharmacological Therapeutic Agents, 1997, Benjamin Weiss
Airway Wall Remodelling in Asthma, 1996, A.G. Stewart
Drug Delivery Systems, 1996, Vasant V. Ranade and Mannfred A. Hollinger
Brain Mechanisms and Psychotropic Drugs, 1996, Andrius Baskys and Gary Remington
Receptor Dynamics in Neural Development, 1996, Christopher A. Shaw
Ryanodine Receptors, 1996, Vincenzo Sorrentino
Therapeutic Modulation of Cytokines, 1996, M.W. Bodmer and Brian Henderson
Pharmacology in Exercise and Sport, 1996, Satu M. Somani
Placental Pharmacology, 1996, B. V. Rama Sastry
Pharmacological Effects of Ethanol on the Nervous System, 1996, Richard A. Deitrich
Immunopharmaceuticals, 1996, Edward S. Kimball
Chemoattractant Ligands and Their Receptors, 1996, Richard Horuk
Pharmacological Regulation of Gene Expression in the CNS, 1996, Kalpana Merchant
Experimental Models of Mucosal Inflammation, 1995, Timothy S. Gaginella
Human Growth Hormone Pharmacology: Basic and Clinical Aspects, 1995, Kathleen T. Shiverick and Arlan Rosenbloom
Placental Toxicology, 1995, B. V. Rama Sastry
Stealth Liposomes, 1995, Danilo Lasic and Frank Martin
TAXOL®: Science and Applications, 1995, Matthew Suffness
Endothelin Receptors: From the Gene to the Human, 1995, Robert R. Ruffolo, Jr.
Alternative Methodologies for the Safety Evaluation of Chemicals in the Cosmetic Industry,1995, Nicola Loprieno
Phospholipase A_2 in Clinical Inflammation: Molecular Approaches to Pathophysiology, 1995, Keith B. Glaser and Peter Vadas
Serotonin and Gastrointestinal Function, 1995, Timothy S. Gaginella and James J. Galligan
Chemical and Structural Approaches to Rational Drug Design, 1994, David B. Weiner and William V. Williams
Biological Approaches to Rational Drug Design, 1994, David B. Weiner and William V. Williams

Pharmacology and Toxicology: Basic and Clinical Aspects

Published Titles (*Continued*)

Direct and Allosteric Control of Glutamate Receptors, 1994, M. Palfreyman, I. Reynolds, and P. Skolnick
Genomic and Non-Genomic Effects of Aldosterone, 1994, Martin Wehling
Peroxisome Proliferators: Unique Inducers of Drug-Metabolizing Enzymes, 1994, David E. Moody
Angiotensin II Receptors, Volume I: Molecular Biology, Biochemistry, Pharmacology, and Clinical Perspectives, 1994, Robert R. Ruffolo, Jr.
Angiotensin II Receptors, Volume II: Medicinal Chemistry, 1994, Robert R. Ruffolo, Jr.
Beneficial and Toxic Effects of Aspirin, 1993, Susan E. Feinman
Preclinical and Clinical Modulation of Anticancer Drugs, 1993, Kenneth D. Tew, Peter Houghton, and Janet Houghton
In Vitro *Methods of Toxicology*, 1992, Ronald R. Watson
Human Drug Metabolism from Molecular Biology to Man, 1992, Elizabeth Jeffreys
Platelet Activating Factor Receptor: Signal Mechanisms and Molecular Biology, 1992, Shivendra D. Shukla
Biopharmaceutics of Ocular Drug Delivery, 1992, Peter Edman
Pharmacology of the Skin, 1991, Hasan Mukhtar
Inflammatory Cells and Mediators in Bronchial Asthma, 1990, Devendra K. Agrawal and Robert G. Townley
Cell Death: The Role of PARP, 2000, Csaba Szabó
Immune Interferon: Properties and Clincial Applications, 2000, Roumen Tsanev and Ivan Ivanov

CELL-PENETRATING PEPTIDES

Processes and Applications

Ülo Langel

CRC PRESS

Boca Raton London New York Washington, D.C.

Library of Congress Cataloging-in-Publication Data

Langel, Ulo.
Cell-penetrating peptides : processes and applications / by Ulo Langel.
p. cm. -- (Pharmacology and toxicology)
Includes bibliographical references and index.
ISBN 0-8493-1141-1 (alk. paper)
1. Peptides--Physiological transport. 2. Drug carriers (Pharmacy) I. Title. II. Pharmacology & toxicology (Boca Raton, Fla.)

QP552.P4 L364 2002
572'.65--dc21

2002017437

Visit the CRC Press Web site at www.crcpress.com

International Standard Book Number 0-8493-1141-1
Library of Congress Card Number 2002017437
Printed in the United States of America 1 2 3 4 5 6 7 8 9 0
Printed on acid-free paper

Preface

In the past 7 to 8 years, a new research field has emerged based on the finding that several short peptides, called cell-penetrating peptides or CPPs, are able to translocate across plasma membranes in a nonreceptor-mediated fashion.

The field started with discoveries in 1988 that the HIV-coded Tat regulatory protein could be taken up by cells when added to culture media,[1,2] and in 1991 that the homeodomain of Antennapedia (a *Drosophila* homeoprotein) was internalized by cells in a receptor-independent manner.[3] In an attempt to better understand the mechanism of internalization, the Antennapedia homeodomain was studied by site-directed mutagenesis; in 1994 it was found that the third helix (amino acids 43 to 58) of the homeodomain of Antennapedia is necessary and sufficient for translocation. This resulted in development of pAntp(43–58) (later called penetratin) and its variants by Professor Alain Prochiantz' group.[4] Shorter Tat-derived sequences with cell-penetrating properties were introduced in parallel.[5]

The discovery that short peptides are able to penetrate into living cells is especially exciting because, today, the CPPs have been shown to provide a new method for cellular delivery of a wide array of molecular cargos.

Biological cell membranes define the cell as a compartment with respect to ions and small and large molecules, including peptides, proteins, and oligonucleotides. Gradients of ions and metabolites are built up across the plasma membranes; special transport proteins, such as carriers, pumps, and gated ion channels, regulate import and export of substances across the plasma membrane together with endocytotic processes. Most of these conventional intracellular delivery processes are ATP-dependent and can be saturated. They suffer from strong limitations in terms of the chemical variability of transported molecules and delivery capacity because the number of the carriers is fixed in the cell and can vary only within narrow limits.

The relative inefficiency and cytotoxicity of modern synthetic DNA delivery systems has been one of the driving forces behind the development of novel cellular delivery vectors. The need to import plasmids and antisense oligonucleotides into cells in sufficient amounts led to the use of nonphysiological and possibly traumatic approaches such as electroporation and lipofection. In addition to being relatively harmful and nonspecific, the latter approaches do not allow targeting to individual cell types. Therefore, development of novel, highly efficient delivery systems applicable to basic and clinical research is highly desirable.

CPPs hold promise of becoming complementary among endogenous transporters, viral transfection, lipofection, and electroporation. CPPs are gentler; the variation of their sequence and inclusion of intracellular addresses may assist their selectivity in terms of delivery.

This handbook is the first effort to collect information available about CPPs. It is divided into three sections: classes of CPPs (Section I), possible mechanisms of action of CPPs (Section II), and applications of CPPs (Section III). The contributors

to the handbook are prominent researchers in the field of CPPs who, together, have been involved in all aspects of CPP development, from discovery of CPPs to their biomedical applications. I acknowledge every contributor for his or her excellent work.

Classes of cell-penetrating peptides

Several families of CPPs are known today, mostly derived from naturally occurring proteins by making use of different *ad hoc* principles in choice of sequences. The original sequences of such CPP families are represented below. These particular sequences fall within some criteria for CPP definition, i.e., they consist of less than 30 amino acids, their cellular internalization is seemingly receptor- or protein-independent and occurs at 4°C, and they have been applied for cellular delivery of cargoes.

Examples of CPPs introduced by different research groups

1. Penetratin[4]	RQIKIWFQNRRMKWKK
2. Tat fragment (48–60)[5]	GRKKRRQRRRPPQC
3. Signal sequence-based peptides[6]	GALFLGWLGAAGSTMGAWSQPKKKRKV
4. pVEC[8]	LLIILRRRIRKQAHAHSK
5. Transportan[9]	GWTLNSAGYLLKINLKALAALAKKIL
6. Amphiphilic model peptide[10]	KLALKLALKALKAALKLA
7. Arg_9[11]	RRRRRRRRR

Sequences 1 to 4 are derived from naturally occurring proteins; sequences 5 to 7 represent artificial synthetic or chimeric peptides. Many analogs discussed in the following chapters exist for several of these parent peptides.

CPPs were first derived from naturally occurring proteins like Antennapedia of *Drosophila*, Tat of HIV-1, and VP22 of HSV (protein transduction domains, PTD), followed soon by designed chimeric peptides like MTS–NLS and transportan, model peptides, and other PTDs.[7,12,13] Numerous analogs of the above-mentioned CPPs have been designed and synthesized, giving rise to families of respective peptides. Both classes of CPPs, whether protein-derived and designed or combined, have been vastly expanded by new peptides and derivatives. The motifs responsible for penetration are generalized, at least for some CPPs, and this information has fueled design and successful application of poly-arginine-mimicking peptoids.[14] Examples of these CPPs are described in detail in Chapters 1 through 7.

Although these chapters cover most described CPPs today, some constantly emerging CPPs or, more exactly, novel vector developments are not included in this handbook. These include the lipophilization approach,[15-17] design of 7TM receptor antagonists,[18] and, possibly, some very recent developments that have not been tested carefully yet.

Mechanisms of cell penetration

Among the many short peptides applied in drug delivery, the choice of CPPs presented in this book is somehow arbitrary since the term *receptor* or *protein-independent* uptake is complicated to define. For simplification, internalization "at 4°C" has been included in the definition. Clearly, further studies on CPP uptake mechanisms are necessary before a consensus definition of CPPs can be proposed. In Chapters 8 through 14 possible mechanisms of cellular uptake of CPPs are discussed.

We have to admit that today, despite numerous studies carried out in the field, the mechanism of uptake of CPPs is still not clarified. In addition, it is likely that mechanisms may differ between distinct CPPs.

However, we feel that the CPPs shown earlier differ from other classes of peptides used in drug delivery, in particular peptides recognized by cell-surface receptors, because they are captured by cells in absence of a chiral receptor, or even when endocytosis has been blocked. This difference has a very high impact in cargo delivery, since CPPs and their cargoes do not accumulate in endosomes and lysosomes and thus have better access in the same time to other compartments less sensitive to degradation. The uptake mechanisms of CPPs also differ from those of a wide variety of toxins and antimicrobial peptides, as they do not form pores within the membranes. Therefore, this handbook describes the latter class of membrane-active peptides only briefly. Chapter 14 has signal sequences as its subject due to possible mechanistic similarities between the uptake of these peptides and that of CPPs.

Attempts have been made to extract structural information that would predict the uptake process of the transport peptides. Positive charges in side chains of Lys/Arg, amphiphilicity of the peptide, presence of Trp or Phe residues in certain positions, and length of the polypeptide chain have been proposed as crucial factors determining cellular uptake. However, general rules for cellular uptake of peptides are only beginning to emerge. Therefore, rational design of novel transport peptides, sequence comparison, SAR studies, molecular modeling, biophysical characterization, and multivariate analysis will be necessary for successful application of CPPS in research and therapy. These topics are discussed throughout the handbook, particularly in Section II.

Applications of CPPs

Traditionally, polypeptides and oligonucleotides are considered of limited therapeutical value because of their low biomembrane permeability and their relatively rapid degradation. This is an obstacle to their use in biomedical research and as pharmaceutical substances. Indeed, the possibility to manipulate intracellular biological targets would increase if large-sized hydrophilic compounds could be addressed intracellularly, without severe limitation on amounts inherent to the necessity to cross lipid bilayers. Thus, the discovery that CPPs translocate across the plasma membrane of live cells and permit intracellular transport of cargoes, such as conjugated peptides, proteins, oligonucleotides, λ phages, and nanoparticles has opened new possibilities in biomedical research and therapy. In Section III, several such applications are covered, including methods for CPP conjugation and microbial applications.

In conclusion, a constantly growing number of cell-penetrating peptides are available today and have been applied for cellular delivery of a variety of bioactive cargoes with seemingly no strict size limit. This handbook summarizes that which has already been achieved. Although the mechanisms of cellular uptake of CPPs are not yet clarified, attempts have been and are being made to help solve this question, thus opening the way to rational design of peptidic and nonpeptidic carriers. Clinical applications will then be within reach.

Ülo Langel

REFERENCES

1. Green, M. and Loewenstein, P.M., Autonomous functional domains of chemically synthesized human immunodeficiency virus tat trans-activator protein, *Cell,* 55*,* 1179, 1988.
2. Frankel, A.D. and Pabo, C.O., Cellular uptake of the tat protein from human immunodeficiency virus, *Cell,* 55*,* 1189, 1988.
3. Joliot, A. et al., Antennapedia homeobox peptide regulates neural morphogenesis, *Proc. Natl. Acad. Sci. U.S.A.,* 88*,* 1864, 1991.
4. Derossi, D. et al., The third helix of the Antennapedia homeodomain translocates through biological membranes, *J. Biol. Chem.,* 269*,* 10444, 1994.
5. Vivès, E., Brodin, P., and Lebleu, B., A truncated HIV-1 Tat protein basic domain rapidly translocates through the plasma membrane and accumulates in the cell nucleus, *J. Biol. Chem.,* 272*,* 16010, 1997.
6. Chaloin, L. et al., Design of carrier peptide–oligonucleotide conjugates with rapid membrane translocation and nuclear localization properties, *Biochem. Biophys. Res. Commun.,* 243*,* 601, 1998.
7. Chang, M. et al., Dissecting G protein-coupled receptor signaling pathways with membrane-permeable blocking peptides, *J. Biol. Chem.,* 275*,* 7021, 2000.
8. Elmquist, A. et al., VE-Cadherin-derived cell-penetrating peptide, pVEC, with carrier functions, *Exp. Cell Res.,* 269*,* 237, 2001.
9. Pooga, M. et al., Cell penetration by transportan, *FASEB J.,* 12*,* 67, 1998.
10. Oehlke, J. et al., Evidence for extensive and nonspecific translocation of oligopeptides across plasma membranes of mammalian cells, *Biochim. Biophys. Acta,* 1330*,* 50, 1997.
11. Mitchell, D.J. et al., Polyarginine enters cells more efficiently than other polycationic homopolymers, *J. Pept. Res.,* 56*,* 318, 2000.
12. Mi, Z. et al., Characterization of a class of cationic peptides able to facilitate efficient protein transduction *in vitro* and *in vivo*, *Mol. Ther.,* 2*,* 339, 2000.
13. Han, K. et al., Efficient intracellular delivery of GFP by homeodomains of Drosophila Fushi-tarazu and Engrailed proteins, *Mol. Cells,* 10*,* 728, 2000.
14. Wender, P.A. et al., The design, synthesis, and evaluation of molecules that enable or enhance cellular uptake: peptoid molecular transporters, *Proc. Natl. Acad. Sci. USA,* 97*,* 13003, 2000.
15. Gudmundsson, O.S. et al., Coumarinic acid-based cyclic prodrugs of opioid peptides that exhibit metabolic stability to peptidases and excellent cellular permeability, *Pharmac. Res.,* 16*,* 7, 1999.
16. Eichholtz, T. et al., A myristoylated pseudosubstrate peptide, a novel protein kinase C inhibitor, *J. Biol. Chem.,* 268*,* 1982, 1993.
17. Vegners, R., Cunningham, C.C., and Janmey, P.A., Cell-permeant peptide derivatives based on the phosphoinositide binding site of gelsolin, in *Peptides 1998,* Bajusz, S. and Hudesz, F., Eds., Akademiai Kiado, Budapest, 82, 1999.
18. Tarasova, N.L., Rice, W.G., and Michejda, C.J., Inhibition of G-protein-coupled receptor function by disruption of transmembrane domain interactions, *J. Biol. Chem.,* 274, 34911, 1999.

Editor

Ülo Langel is a professor at the department of neurochemistry and neurotoxicology, Stockholm University, Sweden. Dr. Langel graduated from Tartu University, Tartu, Estonia, as a bioorganic chemist in 1974; he has received his Ph.D. twice: in 1980 from Tartu University (bioorganic chemistry), and in 1993 from Tartu University and Stockholm University (biochemistry and neurochemistry). His professional experience includes a career at Tartu University (from junior research fellow to associate professor and visiting professor, from 1974 to the present); The Scripps Research Institute, La Jolla, California (associate professor, 2000 to 2001); and Stockholm University (from research fellow to associate professor and professor, from 1987 to the present).

Professor Langel has been selected as a fellow member of the International Neuropeptide Society (1995), and is also a member of the International Society for Neurochemistry, European Peptide Society, Swedish Biochemical Society, and Estonian Biochemical Society. He has been awarded a White Star Order, 4th class, by Estonian Republic. Dr. Langel has been an invited lecturer at numerous international conferences and is co-author of more than 140 scientific articles and 5 patents.

Contributors

Mats Andersson
Microbiology and Tumour Biology Center (MTC)
Karolinska Institutet
Stockholm, Sweden

Frédéric Basyn
Center for Numerical Molecular Biophysics
Faculté Universitaire des Sciences Agronomiques
Gembloux, Belgium

Michelle Becker–Hapak
Howard Hughes Medical Institute
Department of Cellular and Molecular Medicine
University of California–San Diego
School of Medicine
La Jolla, California

Michael Bienert
Institute of Molecular Pharmacology
Berlin, Germany

Olivier Bouffioux
Center for Numerical Molecular Biophysics
Faculté Universitaire des Sciences Agronomiques
Gembloux, Belgium

Robert Brasseur
Center for Numerical Molecular Biophysics
Faculté Agronomique
Gembloux, Belgium

Laurent Chaloin
Centre de Recherches de Biochimie Macromoléculaire
Biophysics Department
Montpellier, France

Gilles Divita
Centre de Recherches de Biochimie Macromoléculaire
Biophysics Department
Montpellier, France
The Scripps Research Institute
Department of Molecular Biology
La Jolla, California

Steven F. Dowdy
Howard Hughes Medical Institute
Department of Cellular and Molecular Medicine
University of California–San Diego
School of Medicine
La Jolla, California

Edmond Dupont
Ecole Normale Supérieure
Paris, France

Anna Elmquist
Department of Neurochemistry and Neurotoxicology
Arrhenius Laboratories
Stockholm University
Stockholm, Sweden

L.E. Göran Eriksson
Department of Biochemistry and Biophysics
Stockholm University
Stockholm, Sweden

Liam Good
Center for Genomics and Bioinformatics (CGB)
Karolinska Institutet
Stockholm, Sweden

Astrid Gräslund
Department of Biochemistry and Biophysics
Stockholm University
Stockholm, Sweden

K.R. Gunaratna
Center for Genomics and Bioinformatics (CGB)
Karolinska Institutet
Stockholm, Sweden

Frédéric Heitz
Centre de Recherches de Biochimie Macromoléculaire
Biophysics Department
Montpellier, France

Mattias Hällbrink
Department of Neurochemistry and Neurotoxicology
Arrhenius Laboratories
Stockholm University
Stockholm, Sweden

Alain Joliot
Ecole Normale Supérieure
Paris, France

Erik Kreider
CellGate Inc.
Sunnyvale, California

Ülo Langel
Department of Neurochemistry and Neurotoxicology
Arrhenius Laboratories
Stockholm University
Stockholm, Sweden

Bernard Lebleu
Institut de Génétique Moléculaire
Université de Montpellier
Montpellier, France

Yao-Zhong Lin
Department of Microbiology and Immunology
Vanderbilt University School of Medicine
Nashville, Tennessee

Maria Lindgren
Department of Neurochemistry and Neurotoxicology
Arrhenius Laboratories
Stockholm University
Stockholm, Sweden

May C. Morris
Centre de Recherches de Biochimie Macromoléculaire
Biophysics Department
Montpellier, France
The Scripps Research Institute
Department of Molecular Biology
La Jolla, California

Kenta Nakai
Human Genome Center
The Institute of Medical Science
The University of Tokyo
Tokyo, Japan

Johannes Oehlke
Institute of Molecular Pharmacology
Berlin, Germany

Kanaka Pattabiraman
Department of Chemistry
Stanford University
Stanford, California

Erin T. Pelkey
Department of Chemistry
Stanford University
Stanford, California

Margus Pooga
Estonian Biocentre
Tartu, Estonia

Alain Prochiantz
Ecole Normale Supérieure
Paris, France

René Rezsohazy
Unit of Developmental Genetics
Université Catholique de Louvain
Bruxelles, Belgium

Jonathan B. Rothbard
CellGate Inc.
Sunnyvale, California

Kristen Sadler
Department of Microbiology and Immunology
Vanderbilt University School of Medicine
Nashville, Tennessee

Ursel Soomets
Department of Biochemistry
University of Tartu
Tartu, Estonia

James P. Tam
Department of Microbiology and Immunology
Vanderbilt University
Nashville, Tennessee

Ching-Hsuan Tung
Center for Molecular Imaging Research
Massachusetts General Hospital
Harvard Medical School
Charlestown, Massachusetts

Andres Valkna
Laboratory of Molecular Genetics
National Institute of Chemical Physics and Biophysics
Tallinn, Estonia

Christopher L. VanDeusen
Department of Chemistry
Stanford University
Stanford, California

Nicole Van Mau
Centre de Recherches de Biochimie Macromoléculaire
Biophysics Department
Montpellier, France

Eric Vivès
Institut de Génétique Moléculaire
Université de Montpellier
Montpellier, France

Jehangir S. Wadia
Howard Hughes Medical Institute
Department of Cellular and Molecular Medicine
University of California–San Diego
School of Medicine
La Jolla, California

Ralph Weissleder
Center for Molecular Imaging Research
Massachusetts General Hospital
Harvard Medical School
Charlestown, Massachusetts

Paul A. Wender
Department of Chemistry
Stanford University
Stanford, California

Burkhard Wiesner
Institute of Molecular Pharmacology
Berlin, Germany

Lee Wright
CellGate Inc.
Sunnyvale, California

Bryan L. Wylie
CellGate Inc.
Sunnyvale, California

Matjaž Zorko
Institute of Biochemistry
Ljubljana, Slovenia

Contents

Section I

Classes of Cell-Penetrating Peptides

1 The Tat-Derived Cell-Penetrating Peptide

Eric Vivès and Bernard Lebleu

CONTENTS

1.1 INTRODUCTION

Rapid progress in functional genomics analysis, biotechnology, and bio-organic chemistry in recent years has led to potential new drug classes. They include peptides, monoclonal antibodies (or antibody fragments), antisense oligonucleotides, ribozymes, catalytic DNA fragments, decoy DNA, interfering double-stranded RNA (RNAi), aptamers, and, of course, recombinant proteins and plasmid DNA (Lebleu[1] and references therein). Delivering these relatively large molecular weight and usually hydrophilic "informational" molecules at their most appropriate site, e.g., in the right intracellular compartment of the targeted tissue, is a formidable challenge that is still far from being met satisfactorily. Expression from recombinant viral vectors has been developed for the *in situ* production of recombinant proteins, ribozymes, or antisense RNAs. This strategy cannot be easily applied to all cases mentioned previously and has its own limitations in terms of efficiency, safety, or tissue targeting. Numerous nonviral delivery vectors have been engineered in order to bypass biological barriers; most of them are still at an early stage of development and generally suffer from poor efficiency compared to viral vectors.

Our own efforts along these lines have originated from a long-term interest in synthetic oligo- and polynucleotides, namely, double-stranded RNAs as interferon

0-8493-1141-1/02/$0.00+$1.50

(IFN) inducers, 2-5A activators of RNaseL, and antisense oligonucleotides. In this context, an early experiment indicates how appropriate delivery could benefit the field of nucleic acids therapeutics. Synthetic double-stranded RNA (ds RNA) as poly(I).poly(C) have been used as IFN inducers in several cell cultures or even in animal models. Approximately 10^5 molecules of poly(I).poly(C) are requested to induce IFN production[2] when incubated in a cell culture model, while a few molecules suffice to promote IFN induction when poly(I).poly(C) is directly microinjected into HeLa cell nuclei.[3] Somatic cell microinjection cannot be applied to a large number of cells and is therefore limited in its application; hence the search for alternative routes to bypass cellular membranes.

Various polycationic polymers have proven useful to promote the internalization of drugs or even macromolecules. One of the most extensively studied in this respect has been poly(L-lysine) following initial studies by Shen and Ryser. They established that chemical conjugation of methotrexate or proteins to poly(L-lysine) allowed significantly improved internalization in various cell types.[4,5]

We adapted this strategy to the intracellular delivery of 2-5A oligonucleotides (ODNs)[6] and antisense ODNs.[7] A large improvement in cytoplasmic delivery and biological activity was recorded in these experiments. Uptake took place through adsorptive endocytosis; release of the conjugated oligonucleotide probably took place in an endocytic compartment through degradation of most (if not all) of the polybasic amino acid carrier by cellular esterases. Poly(L-lysine)-based delivery vectors have also been engineered for the delivery of plasmid DNA, but transfection yields were low compared to those of viral vectors.[8]

Moreover, internalization through an endocytic compartment leads to entrapment and, to a large part, degradation of the transported biomolecules in lysosomes. Combination with endosome-disrupting agents or amphipathic fusogenic peptides improved transfection efficiency at the expense of additional complexity of these synthetic delivery vehicles (reviewed in Curiel[9]). Despite numerous studies, the future of this strategy for the systemic delivery of genes or other drugs is hampered by serious drawbacks such as complexity, toxicity for certain cell lines, and immunogenicity including complement activation.

A new strategy has emerged in recent years starting from the serendipitous and surprising observation that some cellular proteins could be taken up by intact cells when incubated in the culture medium. Interestingly, two of the most studied cell-penetrating proteins are trans-activating factors: the *Drosophila* Antennapedia protein (whose properties will be reviewed extensively here) and the human immunodeficiency virus (HIV)-coded Tat regulatory protein.

1.2 TAT CELLULAR UPTAKE: FROM INITIAL DATA ON THE FULL-LENGTH TAT PROTEIN TO THE DEFINITION OF A 9-MER CELL-PENETRATING PEPTIDE

The HIV-coded Tat regulatory protein has been extensively studied by virologists since the deletion of its gene has shown that it was essential for virus replication.[10] It is an 86-amino-acids-long nuclear protein which binds to the viral TAR region,

increases the processivity of RNA polymerase, and transactivates the viral promoter (see Reference 11 for a review). In the course of studies aimed at setting up a convenient transactivation assay, two groups independently discovered that a purified full-length Tat protein could be taken up by cells and was able to promote the transcription of a reporter gene driven by the HIV LTR promoter.[12,13] Tat-mediated transactivation in these assays was largely stimulated by lysosomotropic amines as chloroquine or monensin in keeping with an endocytic pathway of internalization.

In a series of papers, Fawell et al. later established that cross-linking of recombinant proteins as β-galactosidase or horseradish peroxydase to a Tat peptide (extending from amino acids 37 to 72) encompassing the Tat basic domain allowed their uptake in various cell lines.[14] Likewise, a shorter Tat sequence (amino acids 37 to 62) allowed the efficient internalization of a Fab antibody fragment.[15] Intriguingly, uptake of the full-length Tat protein or of a Tat protein conjugate was increased upon Tat biotinylation.[16] These initial studies already pointed to the potential utilization of Tat-derived peptides as vehicles for the cellular delivery of chemically conjugated biomolecules.

At about the same time, Derossi et al. described the transmembrane passage of the homeodomain of the *Drosophila* Antennapedia protein and its receptor-independent uptake mechanism.[17] In the initial publication, internalization within nerve cells and translocation to the nucleus were ascribed to the amphipathic character of a 16-amino-acids-long region in the homeodomain third helix.[18]

Based on these publications and as a first step towards engineering potentially new delivery vectors, we decided to search for the shortest Tat-derived peptide still able to cross cellular membranes efficiently. The following considerations guided these studies:

1. A peptide-based delivery vector should be as short as possible in order to reduce its cost.
2. Transactivation properties and toxicity (neurotoxicity, in particular) associated with long Tat-derived peptides should be avoided.[19,20]

Although structure–activity studies had not been performed, the 37–72 region of Tat encompasses two potentially important structural regions:

1. An N-terminal portion, extending from amino acids 39 to 49, which could adopt an amphipathic α-helix type configuration, as proposed on the basis of circular dichroïsm studies.[21]
2. A stretch of basic amino acids extending from positions 49 to 59 which is highly conserved among HIV-1 isolates. Moreover, the GRKKR sequence (amino acids 48 to 52) was supposed to act as a nuclear localization signal.[22]

A peptide extending from amino acids residues 38 to 60 was thus synthesized as reference material since it overlapped these two potentially important domains. Internalization in HeLa cells, as well as in a variety of other cell lines, was established by fluorescence microscopy.[23] Cellular internalization and intracellular distribution

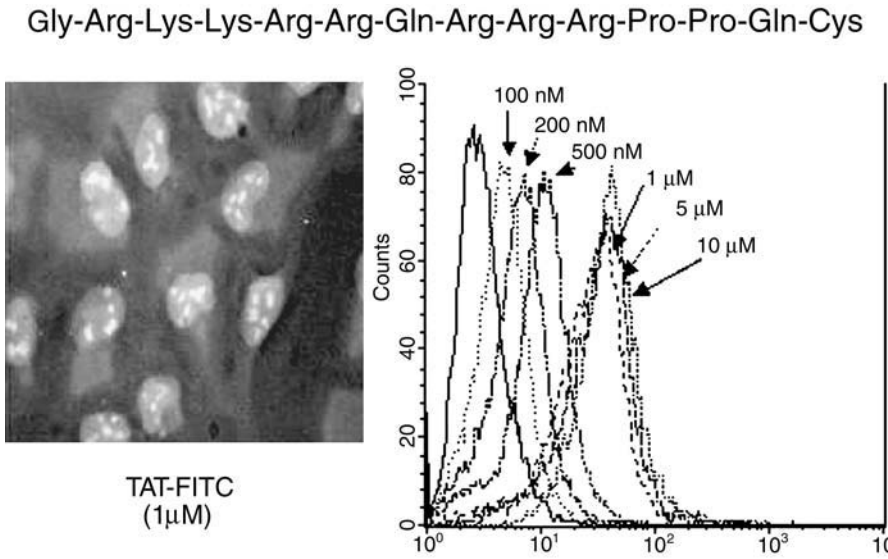

FIGURE 1.1 Cellular internalization of the Tat peptide. The primary sequence of the Tat peptide is indicated in the three-letter code. Left panel: fluorescence microscopy study of the internalization of the fluoresceinated Tat peptide: U2OS cells were incubated for 30 min at 37°C with 1 μ*M* of fluorescein-labeled Tat peptide. Peptide shows a nuclear localization with a nucleolar concentration as previously shown in HeLa cells.[23] Right panel: FACS analysis of the uptake of a rhodamine-labeled Tat peptide in HeLa cells. Extracellular concentrations of peptide were as indicated on the scheme. Peptide internalization could be easily detected from 100 n*M* concentration. Signal appeared to saturate above 1 μ*M* concentration.

have been monitored by various protocols in order to avoid potential artefacts. In most cases, the Tat-derived peptides were conjugated through an additional C-terminal cysteinyl residue to fluorescein and fluorescence distribution was analyzed on formaldehyde fixed cells or in living cells, according to published protocols.[23] Alternatively, the intracellular distribution of Tat has been analyzed by indirect immunofluorescence with a monoclonal antibody specific to the Tat basic domain.

Since uptake of the Antennapedia third helix had been ascribed to an amphipathic helix, we then compared the cellular internalization of a series of Tat-derived peptides carrying deletions. The importance of the basic region was confirmed by the lack of uptake of a peptide including the full α-helix domain but carrying deletions in the C-terminal cluster of basic amino acids (peptides 38–54). The 48–60 peptide encompassing the basic amino acids stretch and lacking the potential α-helix was the most efficiently internalized (Figure 1.1).

Interestingly, amino acids substitutions in the Antennapedia homeodomain also ruled out the importance of the α-amphipathic helix configuration for cellular internalization.[17] The next issues to establish were whether this sequence could be shortened without loss of internalization efficiency and whether its strong basic character was essential. A series of progressive deletions and amino acids replacements (Ala scan) were performed, as summarized in Figure 1.2.

Primary sequence of the Tat peptides	Relative uptake efficacy	Ref.
FITKALGISYGRKKRRQRRRPPQC	+	22
LGISYGRKKRRQRRRPPQC	++	22
FITKALGISYGRKKRRQC	–	22
GRKKRRQRRRPPQC	++++	22
GRKKRRQRRRC	++++	33
GRKKRRQRARPPQC	++	33
GRKKRRQARAPPQC	+	33
GRKKRRQRRPPQC	++	33
GRKKRRQRPPQC	+/–	33
GRKKRRQPPQC	–	33
RKKRRQRRR	+++++	51
RRRQRRKKR	++++++	47
RRRQRRKKR	++++++	47

FIGURE 1.2 Primary structure of the synthesized Tat peptides and structure activity study of the uptake. Relative cellular internalization was evaluated by the mean intensity of the fluorescent signal observed by microscopy[23,33] or by FACS[47] and compared to the intensity of the peptide shown in Figure 1.1. The sequence with the shortest sequence and the higher signal corresponds to RKKRRQRRR. Peptides with amino acids under *d*-conformation are written in italic.

These studies thus established that the high content in basic amino acids was essential and that little could be modified without rapidly losing cellular uptake efficiency; these points will be discussed in more detail in Section 1.4. Altogether these data provided the first demonstration that a 9-mer basic amino acids-rich Tat sequence (Arg-Lys-Lys-Arg-Arg-Gln-Arg-Arg-Arg) was strictly requested but was sufficient to be efficiently taken up by cells and to accumulate in the nuclei. Interestingly, this Tat-derived cell-penetrating peptide contains information for membrane translocation as well as a nuclear localization signal domain allowing nuclear transfer, thus providing a first example, to our knowledge, of dual functions within a single short peptide.

1.3 APPLICATIONS FOR THE DELIVERY OF BIOMOLECULES

As mentioned earlier, a major challenge in biotechnology is the design of vectors that will permit (or improve) the cellular internalization of hydrophilic biomolecules. We initially focused on small biopolymers as antisense oligonucleotides and non-permeant peptides. Synthetic oligonucleotides (ODN) allow various and potent strategies to control gene expression through specific interactions with DNA (by triple helix formation through Hoogsteen base-pairing), to RNA (antisense ODN and ribozymes), or even to proteins (decoy RNA or DNA and aptamers). Despite several clinical trials underway, cellular uptake and escape from the endocytic compartments are important bottlenecks in the development of these technologies. Our strategy within this field has consisted in conjugating an ODN derivative

carrying a pyridine sulfenyl-activated thiol function at its 5′end with the free sulfhydryl group of a cystein residue added to the C-terminal end of the Tat-transporting peptide, as outlined in Figure 1.3.[24] This strategy allowed the coupling of activated ODN to the carrier peptide with a good yield, provided high salt concentration and acetonitrile were added during the coupling reaction to prevent precipitation.

It is generally assumed that the intracellular environment is reductive, thus favoring the dissociation of the cargo ODN from the transporting peptide after cellular internalization.[25] As shown in Figure 1.4, the chemical conjugation of a 19-mer rhodamine-labeled ODN to the Tat peptide allows cellular internalization and nuclear delivery of the transported ODN. Whether dissociation of the ODN cargo from the transporting Tat peptide actually took place after cell uptake was impossible to assess in these experiments. Indeed, short ODN have a strong nuclear tropism, once introduced in the cell cytoplasm,[26] and will therefore co-localize in nuclei with Tat peptides.

Along the same lines, a 20-mer phosphorothioate ODN analogue complementary to the ribosome-binding site of the P-glycoprotein mRNA was conjugated to the Tat cell-penetrating peptide (CPP) through a disulfide bridge as well.[27] Interestingly, the biological activity of this ODN was more efficient in the presence of serum, unlike most nucleic acid delivery agents.[28] A specific inhibition of P-glycoprotein expression was attained at submicromolar concentration, while much higher levels were required in the absence of a delivery vehicle in the same experimental model.[29] This is, to our knowledge, the only system in which the usefulness of Tat-conjugation has been documented for the administration of antisense ODN. Coupling antisense ODN and PNA to the Antennapedia CPP has also been documented on several models, as will be reviewed in a separate chapter in this book. Impressively, PNAs conjugated to the Antennapedia CPP penetrate the blood–brain barrier after *in vivo* administration to rats.[30]

Altogether, CPPs appear to be valuable tools for the administration of antisense ODN and PNA even in an *in vivo* setting. This is particularly important since very few synthetic nucleic acid delivery vehicles have yet proven to be useful *in vivo*. Although no experimental evidence has been produced to our knowledge, conjugation to CPP could be useful as well for the delivery of decoy oligonucleotides, ribozymes, aptamers, or RNAi (responsible for double-stranded RNA-mediated interference).

As mentioned earlier, we initially aimed at conjugating transported ODN and the Tat peptide through a disulfide bridge, a strategy also used by the group of

---

FIGURE 1.3 (opposite) Peptide (or oligonucleotide [ODN]) Tat-CPP-conjugate synthesis scheme. Peptide (left) or ODN (right) were synthesized with an additional sulfhydryl group to allow an easy coupling step to the Tat CPP. Cystein can be incorporated at one (or the other) end of the transported peptide while the SH group can be linked to the 5′ (or 3′) terminus of an ODN during the synthesis. This thiol group can then be easily activated using 2,2′-dithiopyridine.[24] After isolation of the activated compounds, the coupling through disulfide bridge formation with the Tat peptide can be performed. This strategy allows the quantitative formation of the heterodimer (peptide-TatCPP or ODN-TatCPP) only. For fluorescent microscopy or FACS analysis purposes, chimeras can be specifically labeled through an amino group by using a succinimidyl dye.

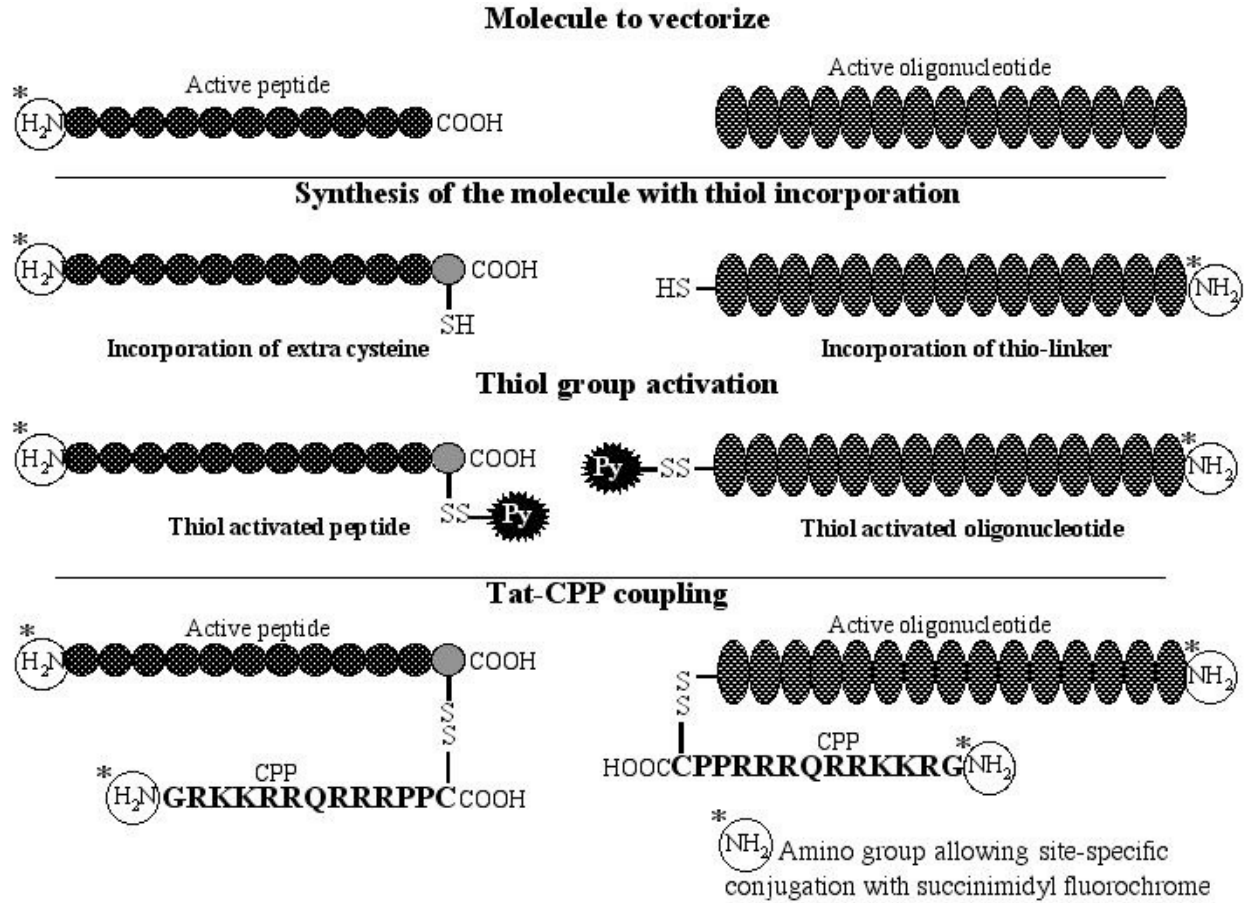
Molecule to vectorize
Active peptide
COOH
Active oligonucleotide
Synthesis of the molecule with thiol incorporation
COOH
SH
Incorporation of extra cysteine
HS
Incorporation of thio-linker
Thiol group activation
COOH
SS
Py
Thiol activated peptide
Py
SS
Thiol activated oligonucleotide
Tat-CPP coupling
Active peptide
COOH
CPP
GRKKRRQRRRPPC
Active oligonucleotide
CPP
HOOCCPPRRRQRRKKRG
Amino group allowing site-specific conjugation with succinimidyl fluorochrome

FIGURE 1.3

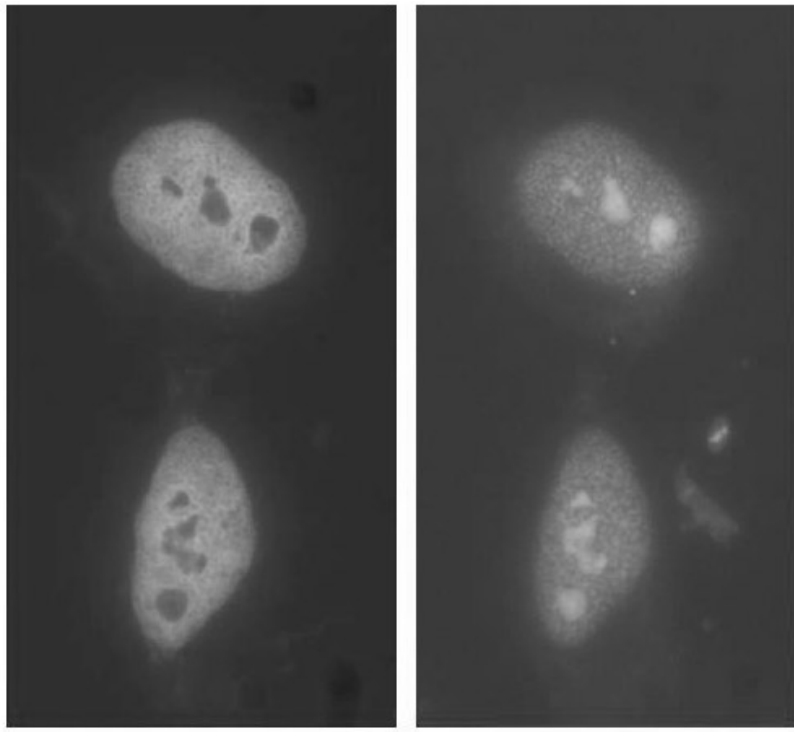

FIGURE 1.4 Internalization of a Rhodamine-labeled ODN-Tat CPP in HeLa cells. Tat-SS-5′-ODN-3′-Rhodamine conjugate was incubated with HeLa cells for 30 min at 37°C. Cells were fixed and the intracellular fluorescence distribution was observed by fluorescence microscopy. (a) Hoescht staining showing the cell nuclei; (b) immunofluorescence detection of the chimera, indicating nuclear accumulation.

R.L. Juliano.[28,29] We reasoned that this would be the ideal situation to allow intracellular release of a minimally modified antisense ODN and thus avoid the risk of changing hybridization properties.

An alternative strategy would consist in stable conjugation (through a thioether or an amide bond, for example) of the antisense ODN to the carrier Tat peptide. Cationic peptide conjugation should indeed accelerate hybridization by increasing the effective ODN concentration at the target sequence.[31] Whether this will occur at the expense of diminished sequence-specific recognition should be verified.

A second class of medium-size biomolecules of interest to us consisted of nonpermeant peptides. Recall that biological processes (for instance, intracellular signaling cascades) often involve complex networks of protein–protein interactions. Rapid technological developments in functional genomics have allowed the identification of peptide domains involved in protein–ligand recognition in increasing number, thus paving the way for design of peptidic competitors. A severe limitation to the use of peptides in intact cells and, as a consequence, to their development as

potential drugs is their inability to cross biological membranes (see Reference 32 for a review).

As for antisense ODN, our initial strategy has consisted in the chemical conjugation of the Tat-transporting peptide with the peptide of interest through a disulfide bridge (Figure 1.3). As a model system, we used a 15-mer peptide (TA9) corresponding to the N-terminal region of the HIV-1 Tat protein (amino acids 2 to 15) whose intracellular distribution could be monitored by indirect immunofluorescence with a specific monoclonal antibody. This peptide was synthesized with an additional C-terminal cysteine residue to allow condensation to the Tat carrier peptide (Tat 48–60) through a disulfide bridge. The conjugation of TA9 to the Tat carrier peptide allowed its cellular uptake and nuclear accumulation. No internalization was observed with the free TA9 peptide or with a DTT-reduced conjugate.[33] As for antisense ODN, we could not ascertain in these experiments whether or how rapidly effective reduction of the disulfide bridge took place after cellular uptake.

An alternative strategy consisted in the chemical synthesis of a chimeric peptide in which the transported peptide and the carrier Tat peptide were fused through a regular amide (peptidic) bond, thus leading to a stable conjugate. We chose as a model system a 17–mer p53-derived peptide known to inhibit the Mdm2–p53 interaction and, consequently, to stabilize p53 and activate p53-dependent biological responses (reviewed in Lane[34]). The cellular uptake and the intracellular distribution of the Tat-transported p53 peptide were monitored by indirect immunofluorescence with specific antibodies, as shown in Figure 1.5.

Particularly interesting along these lines is the development of peptidic agonists or antagonists of intracellular signaling cascades and their vectorization through Tat or Antennapedia CPP conjugation, as reviewed by Dunican and Doherty.[32] Another interesting application is the conjugation to Tat of antigenic peptides, a strategy that allows their delivery in antigen-presenting cells and the generation of CTL-epitopes even in TAP-deficient cells.[35]

In these experiments, conjugation through a reducible disulfide bridge or synthesis of a tandem peptide carrying contiguous cargo and transporting peptides have both been used. To our knowledge, no direct comparison of the biological response of the two approaches has been made in the same model in terms of efficiency and selectivity. Moreover, actual dissociation of the cargo peptide from its delivery vehicle has not been followed.

Somewhat unexpectedly, Schwarze and colleagues[36] established that β-galactosidase (as well as a number of other full-length proteins) could be delivered into cells when carrying a fused Tat basic domain (amino acids 47 to 57) at its N-terminal end *ex vivo* and *in vivo* after intraperitoneal injection into mice. This seminal observation has raised the possibility of delivering proteins into cells as an alternative to plasmid delivery, as reviewed by Ford et al.[37] Protein transduction and gene delivery have limitations and advantages and we will need more data before appreciating their respective futures and fields of application. Protein delivery will be reviewed in this book by Dowdy et al., and so will not be discussed more extensively here.

Gene therapy could also benefit from these recent advances in the design of cell-penetrating peptides. Recall that nonviral gene delivery vectors are still in their

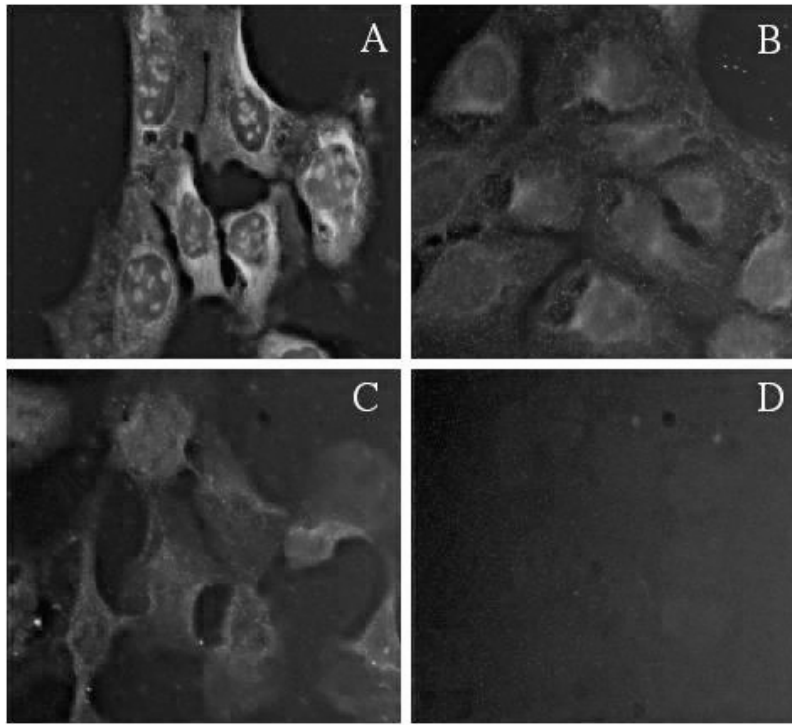

FIGURE 1.5 (Color Figure 1.5 follows p. 14.) Tat-CPP mediated intracellular delivery of a p53 peptide. Panel A: 10 μ*M* of the tandem peptide was incubated on U2OS cells for 30 min at 37°C. p53 cellular entry was assessed by indirect immunofluorescence using an anti-p53 antibody (DO-1). Nucleolar and cytoplasmic detection of the conjugate can be visualized. Panel B: U2OS cells were incubated with 50 μ*M* of p53. Only the background level could be detected. This background corresponded to the endogeneous p53 as assessed by treating cells with the anti-p53 antibody alone (Panel C). Panel D: control corresponding to the incubation of cells with the fluorescein-labeled secondary antibody.

infancy and are poorly efficient compared to retrovirus- or adenovirus-based viral vectors. Trapping in the endocytic compartments and poor translocation from the cytoplasm to the nuclei are generally recognized as limiting steps of synthetic DNA delivery systems. In keeping with these limitations, endosome-disrupting agents (for instance, inactivated adenovirus particles) greatly increase the efficiency of nonviral plasmid DNA delivery,[38] as stated in the introduction. Both limitations could, in theory, be alleviated by cell-penetrating peptides such as Tat or Antennapedia. In a recent publication, Eguchi and colleagues[39] fused the protein transduction domain of Tat (amino acids 43–60) to the N-terminal end of bacteriophage lambda D-head protein displayed in multiple copies (420 copies) at the surface of the phage particle. These engineered phage particles allowed the transfection in mammalian cells of a reporter luciferase gene with an efficiency superior to the widely used cationic lipids.

Tat-mediated intracellular delivery of bacteriophages has moved us to the field of particulate material. Along the same lines, a series of publications by Weissleder et al.[40,41] have described the derivatization of biocompatible magnetic nanoparticles (with a mean diameter of several nanometers) by Tat peptides and their uptake in hematopoietic and neural progenitor cells for *in vivo* imaging purposes.

Finally, Tat peptides have been attached to the surface of liposomes (with a mean diameter of 200 nm) via a polyethylene glycol spacer at an average of 500 Tat-peptide per particle.[42] Cytoplasmic uptake of these relatively large particles has been documented, provided that multipoint attachment between the Tat-coated liposomes and the cell surface was allowed. Whether liposomes-encapsulated material will be released in the cytoplasm has not been established yet.

1.4 MECHANISM OF CELLULAR UPTAKE AND NUCLEAR TRANSLOCATION

1.4.1 Mechanism of Uptake of the Full-Length Tat Protein

In their seminal paper, Mann and Frankel[43] established that the Tat protein (although a slightly truncated form extending from amino acids 1 to 72 was used) was internalized in HeLa cells by absorptive endocytosis. All experimental controversies argue for lack of specific receptors but binding involved electrostatic interactions with cell surface components that could be inhibited by polyanions as heparin. Alternative mechanisms to endocytosis might, however, be involved for cellular uptake since low temperature incubation (4°C) inhibited Tat-mediated transactivation in HeLa cells but not in H9 lymphoid cells. Conversely, the punctuated cytoplasmic staining observed when a rhodamine-labeled Tat protein was incubated with HeLa cells over short periods of times was also characteristic of an endocytic uptake mechanism.

Heparin binds to ubiquitary cell surface heparan sulfate proteoglycans; therefore, it was tempting to postulate that they might act as receptors for the Tat protein. Both genetic and biochemical evidence for such a mechanism have recently been provided by Tyagi et al.,[44] at least for the full-length Tat-GFP fusion construct used in these experiments. Interestingly, heparan sulfate-binding proteins share common characteristics with the Tat basic domain, and mutations or modifications of arginine residues in this domain inhibit Tat uptake. Although heparan sulfate proteoglyeans are expressed in most tissues, alternative Tat ligands might be involved in cellular uptake. In neurons, for example, LRP (or low-density lipoprotein receptor-related protein) bind the Tat protein through its core domain (amino acids 38 to 48). Tat is thereafter internalized by endocytosis and transported to the neuronal nuclei.[45] The Tat protein also binds to several integrin receptors through the RGD sequence located at their C-terminal end.[46]

1.4.2 The Tat CPP Does Not Enter Cells via a Known Mechanism

As stated above, heparan sulfate proteoglycan receptors are required for uptake of the full-length Tat protein.[44] However, we obtained convincing data showing that

the short HIV-1 Tat peptide did not enter cells via this receptor type (Silhol et al., in press). Briefly, we made use of various CHO mutant cell lines totally or partially deficient in the expression of heparan sulfate proteoglycans[44] and clearly established that rhodamin- or fluorescein-labeled Tat CPP was normally taken up in these mutant cell lines. The internalization of the Tat peptide in these cell lines was monitored in parallel by fluorescence microscopy and by FACS scan analysis. In addition, the digestion of HS receptors by heparinase III prior to incubation with the Tat entities abolished the internalization of the GFP-fused Tat protein, but did not alter the uptake of the Tat CPP (Silhol et al., in press).

Tat CPP cellular entry does not seem to involve the endocytosis pathway since the incubation of cells with Tat fluorochrome-labeled peptides never induced the characteristic punctuated cellular labeling of endocytic vesicles.[23] This is not definitive proof, however, since passage through the endocytic compartment could be very transient as observed with cationic lipids delivery. On the other hand, it was recently reported that sodium azide, which inhibits the cellular oxidative phosphorylation process, prevented Tat peptide analogues uptake,[47] in keeping with an energy-dependant pathway.

In contradiction to these latter data, low temperature (4°C) incubation of cells with short Tat peptides containing the full cluster of basic amino acids did not abolish internalization.[23] Internalization of the Tat CPP uptake at low temperature also took place when the short Tat peptide was chemically bound to liposomes[42] or was complexed to a chelating moiety.[48] Although internalization of the Tat CPP takes place at low temperature, a quantitative evaluation performed by FACS analysis indicated a decrease of the level of Tat CPP internalization during incubation at low temperature (Silhol et al., in press). Likewise, a 60% reduction of the internalization rate of the Antennapedia CPP has been recently demonstrated by FACS analysis.[49] Here again, fluorescence microscopy analysis of the Antennapedia CPP distribution had not revealed a diminished uptake at low temperature.[17]

Whether slightly reduced CPP uptake at low temperature is really significant must be further analyzed. Along these lines, another CPP peptide called Transportan, designed from the fusion of a peptide derived from the neuropeptide galanin and the mastoparan, was also shown to translocate efficiently through the plasma membrane at 4 and 0°C.[50] Despite these apparently contradictory results between sodium azide treatment and low temperature incubation, data indicate that endocytosis is not the major pathway allowing the cellular uptake of the Tat peptide.

1.4.3 Molecular Aspects of Tat CPP Uptake

Internalization of these CPPs in various cell lines did not involve the presence of a specific cellular receptor or transporter, as demonstrated for the Antennapedia peptide[17] and discussed in another section in this book. The same conclusion could also be made for the Tat CPP since several analogues derived from the Tat peptide retained their ability to be internalized in cells. The more convincing results, which excluded a receptor interaction, have been provided by the use of a Tat CPP assembled with *d*-amino acid derivatives (*inverso*) and from a Tat CPP synthesized from the C-terminal end to the N-terminal end (usually called *retro* sequence).[47,51] The

uptake of the Tat peptide derivative containing *retro* and *inverso* sequences was also evaluated.

All these analogues were even more efficiently internalized than the native Tat peptide sequence.[47] The higher uptake of the *inverso* peptides was explained by their higher stability against protease digestion in serum-containing media[47] and, therefore, by the higher concentration of intact peptide to be internalized by cells. However, the higher uptake of the *retro* peptide (corresponding to the sequence $Tat_{57}RRRQRRKKR_{49})$[47] cannot be explained by an increased metabolic stability.

The analysis of the primary sequence of Antennapedia, Transportan, and Tat CPP reveals a high content of basic amino acids. For the Tat peptide, the importance of the basic residues has been rapidly pointed out by our group since we performed the deletion or substitution of arginine residues.[33] The lack of a single basic residue led to strong reduction of the intracellular fluorescent signal.[33] These results were confirmed recently by FACS scan analysis with systematic substitution by an alanine residue of each amino acid of the $Tat_{49–57}$ peptide.[47] In this latter work, substitution of a single lysine residue also reduced dramatically (up to 90%) the cellular uptake of the Tat peptide, thus confirming the importance of the cationic charges.

The primary sequence of the Tat peptide does not seem to be a key feature for cell uptake since several analogues, such as a scrambled sequence, were tested without noticeable variation of the cellular uptake intensity (Vivès et al., unpublished results). Therefore, Tat peptide cellular internalization occurred, provided the total number of basic amino acids was left unchanged, thus confirming the key role of the cationic charge. These structure–activity data ruled out the involvement of a receptor or transporter-mediated mechanism in the cellular internalization of the Tat peptide.

The importance of the basic residues in the membrane translocation process of these CPPs led several groups to test the cellular uptake of other polycationic molecules. One of the more interesting studies in this field analyzed the internalization of various cationic homopolymers such as poly-Arginine, poly-Histidine, poly-Lysine, and poly-Ornithine.[52] The cellular uptake of the poly-Arginine polymer appeared to be far more effective than the uptake of the other polybasic sequences.[52] Such data not only pointed out the requirement of several polycationic charges along the peptide sequence, but also indicated a preference for the guanidinium group of the arginine side-chain.

Along this line, several arginine-rich peptides, such as flock house virus (FHV) or HIV Rev protein-derived peptides, are also taken up by cells.[51] The length of the poly-arginine tract also seems critical since the 9-arginine-long homopolymer is the most efficiently internalized.[47,51] Interestingly, longer homopolymers have a reduced translocating activity,[51] thus indicating a critical length of the Tat-derived CPP for optimal cellular uptake. Another considered factor has been the effect of side-chain length of arginine residues on cell uptake[52] by using arginine analogues with various numbers of methylene groups incorporated along their lateral side-chain. Results showed that uptake was proportional to the length of the side-chain.

In conclusion, the critical aspects for improving the cellular Tat-derived CPP uptake appeared to be the presence of a high number of guanidinium groups along a short linear sequence, and an appropriate exposure of these residues to still unknown cellular components implicated in the membrane translocation process.

1.4.4 Cellular Aspects of Tat CPP Uptake

The internalization of Tat-derived CPP is not cell specific because all cell lines tested so far in our laboratory efficiently entrapped the native Tat-translocating peptide. Additional data in the literature confirmed the broad panel of cells allowing Tat peptide uptake. These include cell types such as monocyte or macrophage progenitors that are poorly transfected by traditional methods.[53] Importantly, Tat peptide-conjugated molecules were also shown to pass through the blood–brain barrier, which is a highly selective biological membrane;[36] Tat-derived peptides, such as a short homopolymer of arginine, efficiently cross the skin stratum corneum.[54]

Tat uptake by these different cell types most probably involves a common cellular component or a common process of entry that still remains to be highlighted. However, some indications from the literature raise interesting features about Tat (and CPP-related peptides) cellular uptake. The absence of perinuclear punctuation after incubation of cells with fluorescence-labeled Tat peptides (References 23, for native Tat CPP, and 47 for Tat-derived peptide) and the important uptake at low temperature excluded the endocytosis pathway, as previously discussed. Pinocytosis and potocytosis, a caveolae-mediated uptake (see References 55 and 56 for recent reviews), could be involved in the translocation of the Tat peptide and its derivatives, since potocytosis is poorly sensitive to temperature.[57] In line with this possibility, a reduction of the uptake of a Tat peptide-displaying phage was observed in the presence of inhibitors of caveolae formation such as nystatin or fillipin.[39] However, other inhibitors of caveolae formation such as okadaic acid did not inhibit the uptake of a fluorescein-labeled Tat CPP.[23] The huge difference in the nature and size of these Tat-conjugated entities (a bacteriophage vs. a small peptide) could explain these apparent contradictory results; the possible involvement of caveolae in CPP uptake remains to be convincingly established.

It was shown that this Tat CPP peptide was able to vectorize various cargo molecules (from small peptide to phage or ferromagnetic particles) inside cells.[14,15,27,28,33,36,39,58-62] Whether a single pathway is involved in all cases has yet to be evaluated. Whether binding to other cell surface determinants (for instance, to polar lipid heads) is required has also to be further investigated. Along this line, the requirement of an appropriate exposure of the Tat peptide at the surface of liposomes to allow their cellular uptake has been highlighted.[42] This feature strongly suggests that a direct interaction with unknown cellular entities is requested to trigger the internalization process.

1.5 CONCLUSION AND PERSPECTIVES

As discussed in Section 1.4 and other chapters in this book, short natural or synthetic basic peptides unexpectedly allowed a mechanism not involving cell surface receptors and not mediated by endocytosis to cross biological barriers. Whether the formation of inverted micelles, as proposed for the Antennapedia peptide,[63] or caveolae might be involved as suggested by Eguchi et al.[39] is the object of ongoing experiments.

TABLE 1.1
Various Examples of Tat-CPP Vectorization

Cargo molecule	Tat sequence link type	Cell type	Ref.
Anti-tetanus F(ab′)2 fragments	$Tat_{37–72}$ disulfide bridge	NG108-15 neurohybridoma cells Rev-2-T6 lymphoma cells	61
Oligonucleotide (20 mer)	$Tat_{49–60}$ disulfide bridge	3T3 fibroblast cells	28
Phosphopeptide (10 mer)	$Tat_{48–57}$ co-incubation	T84 colonic epithelial cells	65
IB protein derived peptide (20 mer)	$Tat_{48–59}$ tandem	βTC-3 insulin secreting cells	59
Ferromagnetic particles	$Tat_{48–58}$ disulfide bridge	C17.2 mouse neural progenitor cells Human $CD4^+$ lymphocyte Mouse splenocytes	41
Liposomes	$Tat_{47–57}$ Amide bond	H9C2 rat embryonic cardiac myocytes BT20 human breast tumor LLC mouse lung carcinoma	42
Technetium-99	$Tat_{48–57}$ Metal chelator	Human Jurkat cells	48
Phage	$Tat_{43–60}$ Fusion construct	COS-1 fibroblast cells 3T3 fibroblast cells 293 human embryonal kidney cells	39

As summarized in Section 1.3, Tat-mediated delivery of a wide collection of cargo molecules from medium-size material (oligonucleotides or peptides) to large particles (phages or liposomes) has already been achieved (as summarized in Table 1.1). Most of these applications have been described recently and more studies will be required before their full potential and their limitations will be delineated.

As usual in an emerging field, unsuccessful experiments have seldom been reported. Our poor understanding of the mechanism of internalization of Tat peptide conjugates and their intracellular fate renders interpretation of successes and failures difficult. As an example, Tat-antisense ODN conjugates failed to exert a significant inhibition of P-glycoprotein expression when the targeted cells were incubated in the absence of serum, although they were efficient in serum-supplemented culture medium.[28] As another example, Falnes et al.[64] did not succeed in detecting a cytotoxic effect of diphteria toxin A-chain after fusion to the Tat or to the VP22 CPP, despite cell surface binding.

The ability to promote cellular uptake of various biomolecules in cell cultures by a strategy that bypasses the hostile environment of endocytic vesicles can be considered a highly significant achievement. Interestingly, Tat-mediated delivery has been successfully applied to cell types difficult to transfect by usual methodologies, e.g., monocyte or macrophage progenitors.[53] Important indications have been provided for the delivery (or release) of transported cargo to the nuclei (as a consequence

of the natural tropism of this nuclear localization signal-containing peptide), the cytoplasm[54] or even the endoplasmic reticulum and the trans-Golgi network.[35] Whether additional motifs will allow selective accumulation within one cellular compartment has not been demonstrated, to our knowledge.

Importantly as well, a few publications have established the possibility of achieving Tat-mediated delivery *in vivo* after intraperitoneal administration.[36] Comprehensive studies of biodistribution have not been published, but evidence for delivery of the cargo to various tissues and for crossing the blood–brain barrier has been provided (Schwarze et al.,[36] for instance).

Although no sign of toxicity has been reported yet in *ex vivo* and *in vivo* experiments, obviously more must be done to assess the safety of Tat-based delivery vectors. Potential toxicity for the central nervous system and immunogenicity of Tat conjugates must be tested before considering potential clinical applications.

A potential drawback of the strategy in some applications might be the apparent lack of selectivity of Tat-mediated drug delivery. Whether some of these Tat-based delivery vehicles might be equipped with cell-targeting motifs allowing their preferential accumulation in a given tissue or cell type has still to be achieved. Likewise, combination with polymeric or particulate material might permit a controlled-release of Tat-conjugated drugs, but, to our knowledge, this strategy has not been investigated.

ACKNOWLEDGMENTS

Work in the authors' laboratory is supported by the Centre National de la Recherche Scientifique (CNRS) and by grants from l' Agence de la Recherche sur le Cancer (ARC) and the Ligue Nationale Française Contre le Cancer (LNFCC).

REFERENCES

1. Lebleu, B., Delivering information-rich drugs prospects and challenges, *Trends Biotechnol.,* 14, 109–110, 1996.
2. Gordon, J. and Minks, M.A., The interferon renaissance: molecular aspects of induction and action, *Microbiol. Rev.,* 45, 244–266, 1981.
3. Silhol, M., Huez, G., and Lebleu, B., An antiviral state induced in HeLa cells by microinjected poly(rI).poly(rC), *J. Gen. Virol.,* 67, 1867–1873, 1986.
4. Shen, W.C. and Ryser, H.J., Conjugation of poly-L-lysine to albumin and horseradish peroxidase: a novel method of enhancing the cellular uptake of proteins, *Proc. Natl. Acad. Sci. USA,* 75, 1872–1876, 1978.
5. Shen, W.C. and Ryser, H.J., Poly (L-lysine) and poly (D-lysine) conjugates of methotrexate: different inhibitory effect on drug resistant cells, *Mol. Pharmacol.,* 16, 614–622, 1979.
6. Bayard, B., Bisbal, C., and Lebleu, B., Activation of ribonuclease L by (2′-5′)(A)4-poly(L-lysine) conjugates in intact cells, *Biochemistry,* 25, 3730–3736, 1986.
7. Lemaitre, M., Bayard, B., and Lebleu, B., Specific antiviral activity of a poly(L-lysine)-conjugated oligodeoxyribonucleotide sequence complementary to vesicular stomatitis virus N protein mRNA initiation site, *Proc. Natl. Acad. Sci. USA,* 84, 648–652, 1987.

8. Wagner, E. et al., Transferrin-polycation conjugates as carriers for DNA uptake into cells, *Proc. Natl. Acad. Sci. USA,* 87, 3410–3414, 1990.
9. Curiel, D.T., High-efficiency gene transfer mediated by adenovirus-polylysine-DNA complexes, *Ann. NY Acad. Sci.,* 716, 36–56, 1994.
10. Dayton, A.I. et al., The trans-activator gene of the human T cell lymphotropic virus type III is required for replication, *Cell,* 44, 941–947, 1986.
11. Jeang, K.T., Xiao, H., and Rich, E.A., Multifaceted activities of the HIV-1 transactivator of transcription, Tat, *J. Biol. Chem.,* 274, 28837–28840, 1999.
12. Frankel, A.D. and Pabo, C.O., Cellular uptake of the Tat protein from human immunodeficiency virus, *Cell,* 55, 1189–1193, 1988.
13. Green, M. and Loewenstein, P.M., Autonomous functional domains of chemically synthesized human immunodeficiency virus Tat trans-activator protein, *Cell,* 55, 1179–1188, 1988.
14. Fawell, S. et al., Tat-mediated delivery of heterologous proteins into cells, *Proc. Natl. Acad. Sci. USA,* 91, 664–668, 1994.
15. Anderson, D.C. et al., Tumor cell retention of antibody Fab fragments is enhanced by an attached HIV Tat protein-derived peptide, *Biochem. Biophys. Res. Commun.,* 194, 876–884, 1993.
16. Chen, L.L. et al., Increased cellular uptake of the human immunodeficiency virus-1 Tat protein after modification with biotin, *Anal. Biochem.,* 227, 168–175, 1995.
17. Derossi, D. et al., Cell internalization of the third helix of the Antennapedia homeodomain is receptor-independent, *J. Biol. Chem.,* 271, 18188–18193, 1996.
18. Derossi, D. et al., The third helix of the Antennapedia homeodomain translocates through biological membranes, *J. Biol. Chem.,* 269, 10444–10450, 1994.
19. Sabatier, J.-M. et al., Evidence for neurotoxic activity of tat from human immunodeficiency virus type 1, *J. Virol.,* 65, 961–967, 1991.
20. Perez, A. et al., Evaluation of HIV-1 Tat induced neurotoxicity in rat cortical cell culture, *J. Neurovirol.,* 7, 1–10, 2001.
21. Loret, E.P. et al., Activating region of HIV-1 Tat protein: vacuum UV circular dichroism and energy minimization, *Biochemistry,* 30, 6013–6023, 1991.
22. Ruben, S. et al., Structural and functional characterization of human immunodeficiency virus tat protein, *J. Virol.,* 63, 1–8, 1989.
23. Vivès, E., Brodin, P., and Lebleu, B., A truncated HIV-1 Tat protein basic domain rapidly translocates through the plasma membrane and accumulates in the cell nucleus, *J. Biol. Chem.,* 272, 16010–16017, 1997.
24. Vivès, E. and Lebleu, B., Selective coupling of a highly basic peptide to an oligonucleotide, *Tetrahedron Lett.,* 38, 1183–1186, 1997.
25. Feener, E.P., Shen, W.C., and Ryser, H.J., Cleavage of disulfide bonds in endocytosed macromolecules. A processing not associated with lysosomes or endosomes, *J. Biol. Chem.,* 265, 18780–18785, 1990.
26. Leonetti, J.P. et al., Intracellular distribution of microinjected antisense oligonucleotides, *Proc. Natl. Acad. Sci. USA,* 88, 2702–2706, 1991.
27. Hughes, J. et al., *In vitro* transport and delivery of antisense oligonucleotides, *Methods Enzymol.,* 313, 342–358, 2000.
28. Astriab–Fisher, A. et al., Antisense inhibition of P-glycoprotein expression using peptide-oligonucleotide conjugates, *Biochem. Pharmacol.,* 60, 83–90, 2000.
29. Alahari, S.K. et al., Inhibition of expression of the multidrug resistance-associated P-glycoprotein by phosphorothioate and 5′ cholesterol-conjugated phosphorothioate antisense oligonucleotides, *Mol. Pharmacol.,* 50, 808–819, 1996.

30. Pooga, M. et al., Cell penetrating PNA constructs regulate galanin receptor levels and modify pain transmission *in vivo*, *Nat. Biotechnol.,* 16, 857–861, 1998.
31. Wei, Z. et al., Hybridization properties of oligodeoxynucleotide pairs bridged by polyarginine peptides, *Nucleic Acids Res.,* 24, 655–661, 1996.
32. Dunican, D.J. and Doherty, P., Designing cell-permeant phosphopeptides to modulate intracellular signaling pathways, *Biopolymers,* 60, 45–60, 2001.
33. Vivès, E. et al., Structure activity relationship study of the plasma membrane translocating potential of a short peptide from HIV-1 Tat protein, *Lett. Peptide Sci.,* 4, 429–436, 1997.
34. Lane, D., Awakening angels, *Nature,* 394, 616–617, 1998.
35. Lu, J. et al., TAP-independent presentation of CTL epitopes by Trojan antigens, *J. Immunol.,* 166, 7063–7071, 2001.
36. Schwarze, S.R. et al., *In vivo* protein transduction: delivery of a biologically active protein into the mouse, *Science,* 285, 1569–1572, 1999.
37. Ford, K.G. et al., Protein transduction: an alternative to genetic intervention? *Gene Ther.,* 8, 1–4, 2001.
38. Curiel, D.T. et al., Adenovirus enhancement of transferrin-polylysine-mediated gene delivery, *Proc. Natl. Acad. Sci. USA,* 88, 8850–8854, 1991.
39. Eguchi, A. et al., Protein transduction domain of HIV-1 Tat protein promotes efficient delivery of DNA into mammalian cells, *J. Biol. Chem.,* 276, 26204–26210, 2001.
40. Weissleder, R. et al., *In vivo* magnetic resonance imaging of transgene expression, *Nat. Med.,* 6, 351–355, 2000.
41. Lewin, M. et al., Tat peptide-derivatized magnetic nanoparticles allow *in vivo* tracking and recovery of progenitor cells, *Nat. Biotechnol.,* 18, 410–414, 2000.
42. Torchilin, V.P. et al., TAT peptide on the surface of liposomes affords their efficient intracellular delivery even at low temperature and in the presence of metabolic inhibitors, *Proc. Natl. Acad. Sci. USA,* 98, 8786–8791, 2001.
43. Mann, D.A. and Frankel, A.D., Endocytosis and targeting of exogenous HIV-1 Tat protein, *Embo. J.,* 10, 1733–1739, 1991.
44. Tyagi, M. et al., Internalization of HIV-1 tat requires cell surface heparan sulfate proteoglycans, *J. Biol. Chem.,* 276, 3254–3261, 2001.
45. Liu, Y. et al., Uptake of HIV-1 Tat protein mediated by low-density lipoprotein receptor-related protein disrupts the neuronal metabolic balance of the receptor ligands, *Nat. Med.,* 6, 1380–1387, 2000.
46. Barillari, G.R. et al., The Tat protein of human immunodeficiency virus type 1, a growth factor for AIDS Kaposi sarcoma and cytokine-activated vascular cells, induces adhesion of the same cell types by using integrin receptors recognizing the RGD amino acid sequence, *Proc. Natl. Acad. Sci U.S.A.,* 90, 7941–7945, 1993.
47. Wender, P.A. et al., The design, synthesis, and evaluation of molecules that enable or enhance cellular uptake: peptoid molecular transporters, *Proc. Natl. Acad. Sci. USA,* 97, 13003–13008, 2000.
48. Polyakov, V. et al., Novel Tat-peptide chelates for direct transduction of technetium-99m and rhenium into human cells for imaging and radiotherapy, *Bioconjug. Chem.,* 11, 762–771, 2000.
49. Drin, G. et al., Physico-chemical requirements for cellular uptake of pAntp peptide. Role of lipid-binding affinity, *Eur. J. Biochem.,* 268, 1304–1314, 2001.
50. Pooga, M. et al., Cell penetration by transportan, *FASEB J.,* 12, 67–77, 1998.
51. Futaki, S. et al., Arginine-rich peptides. An abundant source of membrane-permeable peptides having potential as carriers for intracellular protein delivery, *J. Biol. Chem.,* 276, 5836–5840, 2001.

52. Mitchell, D.J. et al., Polyarginine enters cells more efficiently than other polycationic homopolymers, *J. Pept. Res.,* 56, 318–325, 2000.
53. Abu-Amer, Y. et al., TAT fusion proteins containing tyrosine 42-deleted IkappaBalpha arrest osteoclastogenesis, *J. Biol. Chem.,* 276, 30499–30503, 2001.
54. Rothbard, J.B. et al., Conjugation of arginine oligomers to cyclosporin A facilitates topical delivery and inhibition of inflammation, *Nat. Med.,* 6, 1253–1257, 2000.
55. Kurzchalia, T.V. and Parton, R.G., Membrane microdomains and caveolae, *Curr. Opin. Cell. Biol.,* 11, 424–431, 1999.
56. Gumbleton, M., Abulrob, A.G., and Campbell, L., Caveolae: an alternative membrane transport compartment, *Pharm. Res.,* 17, 1035–1048, 2000.
57. Anderson, R.G. et al., Potocytosis: sequestration and transport of small molecules by caveolae, *Science,* 255, 410–411, 1992.
58. Dostmann, W.R. et al., Highly specific, membrane-permeant peptide blockers of cGMP-dependent protein kinase Ialpha inhibit NO-induced cerebral dilation, *Proc. Natl. Acad. Sci. USA,* 97, 14772–14777, 2000.
59. Bonny, C. et al., Cell-permeable peptide inhibitors of JNK: novel blockers of beta-cell death, *Diabetes,* 50, 77–82, 2001.
60. Li, H. et al., Cholesterol binding at the cholesterol recognition/interaction amino acid consensus (CRAC) of the peripheral-type benzodiazepine receptor and inhibition of steroidogenesis by an HIV TAT-CRAC peptide, *Proc. Natl. Acad. Sci. USA,* 98, 1267–1272, 2001.
61. Stein, S. et al., A disulfide conjugate between anti-tetanus antibodies and HIV (37-72) Tat neutralizes tetanus toxin inside chromaffin cells, *FEBS Lett.,* 458, 383–386, 1999.
62. Caron, N.J. et al., Intracellular delivery of a Tat-eGFP fusion protein into muscle cells, *Mol. Ther.,* 3, 310–318, 2001.
63. Prochiantz, A., Getting hydrophilic compounds into cells: lessons from homeopeptides, *Curr. Opin. Neurobiol.,* 6, 629–634, 1996.
64. Falnes, P.O., Wesche, J., and Olsnes, S., Ability of the Tat basic domain and VP22 to mediate cell binding, but not membrane translocation of the diphtheria toxin A-fragment, *Biochemistry,* 40, 4349–4358, 2001.
65. Taylor, C.T. et al., Phosphorylation-dependent targeting of cAMP response element binding protein to the ubiquitin/proteasome pathway in hypoxia, *Proc. Natl. Acad. Sci. USA,* 97, 12091–12096, 2000.

2 Penetratins

Edmond Dupont, Alain Joliot, and Alain Prochiantz

CONTENTS

0-8493-1141-1/02/$0.00+$1.50

2.1 INTRODUCTION

Homeoproteins are transcription factors involved in several biologic processes, primarily during development. They were first discovered in *Drosophila* and later in all metazoans and plants. They bind DNA through a 60-amino-acid-long sequence, the homeodomain. This homeodomain is highly conserved across homeoproteins and species and composed of three α-helices, the third of which is more particularly dedicated to recognition of the DNA target site.[1] In addition to their role in pattern formation during development, homeoproteins can act later to refine or maintain neuronal connections in invertebrates and vertebrates. Indeed, mutations in homeogenes lead to modifications in axon pathfinding,[2-4] and synapse formation.[5-7] This suggests that homeoproteins probably help to define the important plasticity characterizing the vertebrate nervous system.

2.2 HOMEOPROTEIN-DERIVED PEPTIDIC VECTORS

2.2.1 The Antennapedia Homeodomain

To analyze the role of homeoproteins in neuronal morphogenesis, we developed a protocol aimed at antagonizing transcriptional activity of endogenous homeoproteins.

TABLE 2.1
Behavior of AntpHD Mutants

Hoemodomain	Sequence[a]	Internalization	DNA binding	Biological effect
	35 60			
AntpHD	-AHALCLT*ERQIKIWFQNRRMKWKKEN*	+++	+++	+++
AntpHD 50A	-A**Y**ALCLT*ERQIKIWFA**N**RRMKWKKEN*	+++	+	–
AntpHD 40P2	-AHALC**PP***ERQIKIWFQNRRMKWKKEN*	++	–	–
AntpHD 48S	-AHALCLT*ERQIK------**S**NRRMKWKKEN*	–	–	–

[a] Only residues 35 to 60 are shown.

Note: The third helix is in italics; mutations and deletions are shown in bold.

This was achieved through the mechanical internalization of FITC-labeled homeodomains into live postmitotic neurons.[8-10] The addition of exogenous *Drosophila* Antennapedia homeodomain induced strong neurite outgrowth that was attributed to competition between the homeodomain and endogenous homeoproteins for their binding sites.[10] During these experiments the translocation of the Antennapedia homeodomain (AntpHD) across biological membranes, followed by its nuclear addressing, was discovered. This observation was later extended to several homeodomains and full-length homeoproteins, leading to the concept of messenger proteins.[11]

In an attempt to analyze the neurite-promoting function of the homeodomain and its mechanism of action, three different point mutations were introduced (Table 2.1).[12-14] AntpHD 50A has a glutamine/alanine substitution in position 50 of the homeodomain (position 9 in the third helix), a position important for the specificity of protein and DNA interactions. In AntpHD 48S, a single serine residue replaces three amino acids (tryptophan 48, phenylalanine 49, and glutamine 50). Trp 48 and Phe 49 are conserved in all homeodomains and important for the homeodomain structure. AntpHD 40P2 has a substitution of two amino acids located in the turn between helices 2 and 3 (leucine 40 and threonine 41) by two prolines. The DNA-binding capacity of the three mutants is either decreased (AntpHD 50A) or completely abolished (AntpHD 48S and AntpHD 40P2) and translocation into live cells is lost only in the AntpHD 48S mutant.[13] Biological activity (neurite outgrowth stimulation) is lost in all cases.[12-14]

2.2.2 The Penetratin-1 Peptide

The results with AntpHD 48S suggested the presence of a cell translocation sequence in the third helix. The 16 amino acids of the helix (amino acids 43 to 58, Table 2.2) were synthesized and internalization into live cells was followed and observed thanks to a N-terminal biotin.[15] Shorter versions of the same peptide, with N-ter or C-ter deletions, are not internalized, suggesting that this peptide, hereafter penetratin, is necessary and sufficient for internalization. By deleting more amino acids starting from the N terminus, Fischer et al. have more recently described a shorter (seven amino acids) penetratin-derived peptide with internalization properties (see Section 2.3.1.4).[16]

TABLE 2.2
Internalization of Penetratin and Its Derivatives

Peptide	Sequence	Internalization	Subcellular distribution
43–58	RQIKIWFQNRRMKWKK	+++	N > C
58–43	KKWKMRRNQFWIKIQR	+++	N > C
D43–58	RQIKIWFQNRRMKWKK	+++	N > C
Pro50	RQIKIWF**P**NRRMKWKK	+++	N > C
3P	RQ**P**KIWF**P**NRRM**P**WKK	+++	C > N
Met–Arg	RQIKIWFQN**M**R**R**KWKK	+++	N > C
7Arg	RQI**R**IWFQNRRM**R**W**RR**	+++	N > C
W/R	R**RWRR**W**WRRWWRR**W**RR**	+++	N > C
45–58	IKIWFQNRRMKWKK	++	N > C
52–58	RRMKWKK	++	N > C
48–58	WFQNRRMKWKK	+	N > C
47–58	IWFQNRRMKWKK	+	N > C
46–58	KIWFQNRRMKWKK	+	N > C
43–57	RQIKIWFQNRRMKWK	–	–
43–54	RQIKIWFQNRRM	–	–
2Phe	RQIKI**F**FQNRRMK**F**KK	–	–
41–55	TERQIKIWFQNRRMK	–	–
46–60	KIWFQNRRMK	–	–

Similarly, to AntpHD, penetratin is internalized by an energy-independent mechanism at both 4 and 37°C, has access to the cytoplasm and nucleus, from which it can be retrieved without apparent degradation.[15] Translocation has been observed in all cell types and in 100% of the cells. It is not concentration-dependent between 10 p*M* and 100 μ*M* and, below 10 μ*M*, toxicity is rare and cell-type dependent. The presence of three arginine and three lysine residues confers to the peptide an isoelectric point above 12. Finally, although penetratin can be represented under the form of an amphipathic helix, circular dichroism experiments have shown that it is poorly structured in water and adopts an α-helical structure only in a hydrophobic environment.[15]

2.3 HOW DO PENETRATIN PEPTIDES CROSS CELLULAR MEMBRANES?

Penetratin internalization mechanisms were investigated through a chemical approach. Two groups of data have emerged, gathered from structure and function studies in biological systems and from biophysical and biochemical approaches in purely artificial systems.

2.3.1 Influence of Structural Parameters on Peptide Translocation

Several derivatives from the original penetratin-1 sequence have been chemically synthesized (Table 2.2). They were generated to address the following points. Is

there a chiral recognition mechanism between penetratins and a membrane receptor? Do helicity and amphiphilicity influence translocation? What is the minimal sequence required for internalization? What is the relative importance of each residue of penetratin-1 in the internalization process?

2.3.1.1 Chirality

Two peptides were synthesized, a 43–58 peptide composed of D-amino acids (D-penetratin-1) and an *inverso* form of the 43–58 peptide: the 58–43 peptide. These peptides are internalized as efficiently as penetratin-1 at 4 and 37°C, demonstrating that a chiral membrane receptor is not required for cellular translocation.[15,17] Additionally, accumulation of D-penetratin-1 was increased because of the resistance of D-peptides to proteolysis. Fluid phase endocytosis does not require a membrane receptor, cannot be saturated, and is not inhibited at 4°C, three characteristics resembling those of penetratin. However, peptide localization by electronic microscopy showed no endocytotic figures and demonstrated an accumulation in the cytoplasm and nucleus, thus precluding fluid phase endocytosis.[17]

2.3.1.2 Helicity

Peptide helicity was broken by introducing one (Pro50) or three (3Pro) prolines within the sequence (Table 2.2).[17] In Pro50, glutamine in position 50 is replaced by a proline; in 3Pro, glutamine 50, isoleucine 45, and lysine 55 are replaced by prolines. Neither modification hampered peptide internalization at 4 or 37°C, suggesting that a helical structure is not required. However, the subcellular localization of 3Pro differed from that of penetratin-1 as it was not conveyed to the cell nucleus. This suggested that nuclear addressing and accumulation is sequence-dependent and does not simply reflect the small size of the peptides.

Recently, Fischer et al. have analyzed the importance of the penetratin secondary structure by constraining its conformation.[16] Cyclic peptides were obtained through the addition of N- and C-terminal cysteines followed by air oxidation at an elevated pH. The linear form of the mutant peptide is internalized, but the cyclic one is not, suggesting that the secondary structure is important for translocation.

2.3.1.3 Amphiphilicity

To address the role of amphiphilicity a penetratin-1 mutant with two phenylalanines in place of tryptophans 48 and 56 (Table 2.2) was tested.[15] This double mutant was not internalized, demonstrating that amphiphilicity is not sufficient to mediate internalization. This experiment also suggested that one or both tryptophans are crucial. More recent data,[16,18] and the internalization of the homeodomain of Engrailed which lacks tryptophan 56,[19] demonstrates that tryptophan 48 is a key residue. It is noteworthy that this residue has been conserved in all homeodomains.

2.3.1.4 Sequence Length

Two shorter peptides encompassing amino acids 41 to 55 or 46 to 60 (Table 2.2) do not translocate into live cells.[15,17] This suggested that the N- and C-terminal residues

are crucial for translocation into neuronal cells. Fischer et al. studied the effect of successive truncations of the 43–58 peptide.[16] C-terminal truncations had a dramatic negative effect on cellular translocation (43–57 and 43–54 mutants, Table 2.2); the deletion of only the last Lys residue strongly impaired peptide penetration. In contrast, N-terminal truncations were less detrimental, allowing the definition of a heptamere (Arg-Arg-Met-Lys-Trp-Lys-Lys, Table 2.2) internalized with 60% efficiency, compared to full-length penetratin-1. The latter result, at odds with earlier reports,[15,17] could be explained by the different types of cells used (immortalized HaCat fibroblasts and lung cancer A549 cell lines instead of neurons). Another unexplored possibility is the different spacers (amino-pentanoic acid or β-alanine) used to separate the peptide from the biotin moiety.

2.3.1.5 Relative Importance of Each Individual Residue

In two separate studies, each amino acid of the penetratin-1 sequence was substituted by alanine-scanning.[16,18] These two studies differ by cell types (human HaCat and A549 vs. human transformed leukemia cells K562) and by mode of detection (biotin and NBD fluorochrome (7-nitrobenz-2-oxa-1, 3-diazol-4-yl)). The two reports confirm the key role of several basic residues: Lys 58, Lys 57, Lys 55, Arg 53, Arg 52, and Lys 46. The role of hydrophobic residues is less clear, with a distinct controversy on the function of Trp48 and Trp56.[15,16,18]

Taken together, the results from all groups suggest the involvement of basic residues and of at least one tryptophan in the translocation process. This proposition has been confirmed by biophysical experiments demonstrating a role of charged groups in lipid binding and of one tryptophan in lipid destabilization and peptide translocation.

2.3.2 Peptide–Lipid Interactions

Translocation of the penetratin peptides does not require chiral receptors and does not involve classical endocytosis. Fluid phase pinocytosis can be excluded on the basis of ultrastructural studies that failed to reveal any association of penetratins with vesicular structures; internalization through inverted micelles was proposed. This model is based on the induction of inverted micelles by tryptophan residues,[20] and on the capacity of penetratins to form multimer in the presence of SDS and to lower the critical micellar concentration in the presence of lipids.[15,21]

To evaluate the implication of inverted micelles in peptide translocation, *in vitro* peptide and lipid interactions were analyzed by several laboratories. These experiments were based on fluorescence spectroscopy, circular dichroism (CD), and nuclear magnetic resonance (NMR) of proton (^{1}H-NMR) and phosphorus (^{31}P-NMR). The first series of experiments with ^{31}P-NMR demonstrated that the addition of penetratin peptides to lipids from embryonic rat brains induces formation of inverted micelles.[15,21] In contrast, the double Phe non-internalized variant failed to induce inverted micelle formation (unpublished results). Furthermore, ^{1}H-NMR spectroscopy demonstrated that the conformational flexibility of the peptide backbones allows their adaptation to the concave surface of an SDS micelle and the convex surface of an inverted micelle.[21]

In a second set of experiments, the interaction of peptides with phospholipids of various compositions and with SDS was characterized and the induced peptide structure was determined. In the presence of SDS, penetratin adopts an α-helical structure.[15,21-23] In SDS micelles (^{1}H-NMR with paramagnetic probes) penetratin-1 forms a straight helix.[22] The C terminus of the helix is deep in the SDS micelle and its N terminus is near the surface of the micelle, with two residues (Arg 43 and Gln 44) sticking outside.

Structural studies were also achieved with synthetic lipids. CD spectroscopy showed that, although penetratin-1 adopts a random coil structure in an aqueous environment, it becomes structured in the presence of negatively charged phospholipids. At a low peptide to lipid ratio (1:325), the peptide adopts α-helical conformation.[18] At a high peptide to lipid ratio (1:10), the peptide forms antiparallel β-sheet.[23] Indeed, Persson et al. have observed that above a 1:12.5 peptide to negatively charged-lipid ratio, penetratin peptides induce vesicle aggregation, with concomitant conformational transition from α-helix to antiparallel β-sheet.[24] Moreover, following the vesicle aggregation process, they have monitored a spontaneous vesicle disaggregation that may reflect penetratin translocation in phospholipid vesicles.

Another study on phospholipid monolayers with modulation infra-red reflection absorption spectroscopy (PM-IRRAS) suggests that penetratin-1 is adsorbed parallel to the surface of negatively charged phospholipid layers and adopts a β-sheet structure.[25]

Since bilayer model membranes are more biomimetic than monolayers, Fragneto et al. have analyzed the behavior of penetratin peptides in the bilayer model.[26,27] By neutron and x-ray reflectivity, they were able to measure accurately bilayer structural changes induced by penetratin peptides. They showed that penetratin added to a bilayer of negatively charged phospholipids provokes more than a doubling of its roughness and suggested that the peptide is mainly located in the lipid headgroups, not in the acyl chains.

2.3.3 Proposed Model of Penetratin Internalization

In summary, a model can be proposed that takes into account all structure and function and biophysical and biochemical studies on penetratin-1 and its derivatives.[17,28,29] These studies preclude classical endocytosis, fluid-phase potocytosis, and pore formation. This last point recently has been addressed[30] and new results agree with earlier data demonstrating that the addition of penetratin-1 to lipid monolayers or cells does not induce pore formation (as evaluated by the passage of ions). Our working hypothesis is that penetratin peptides interact directly with negatively charged lipids or sugar components, presumably through an electrostatic interaction and that this interaction is followed by destabilization of the lipid bilayer and formation of inverted micelles in which the peptides are trapped (Figure 2.1). Eventually a fraction of the micelles will open on the cytoplasmic side, thus allowing intracellular delivery. In this model, penetratin is always kept in a hydrophilic environment, included in the cavity of the micelle, and delivered from the extracellular medium to the cytoplasm of the cell. This translocation mechanism led us to speculate that hydrophilic molecules linked to penetratin peptides would also be internalized.

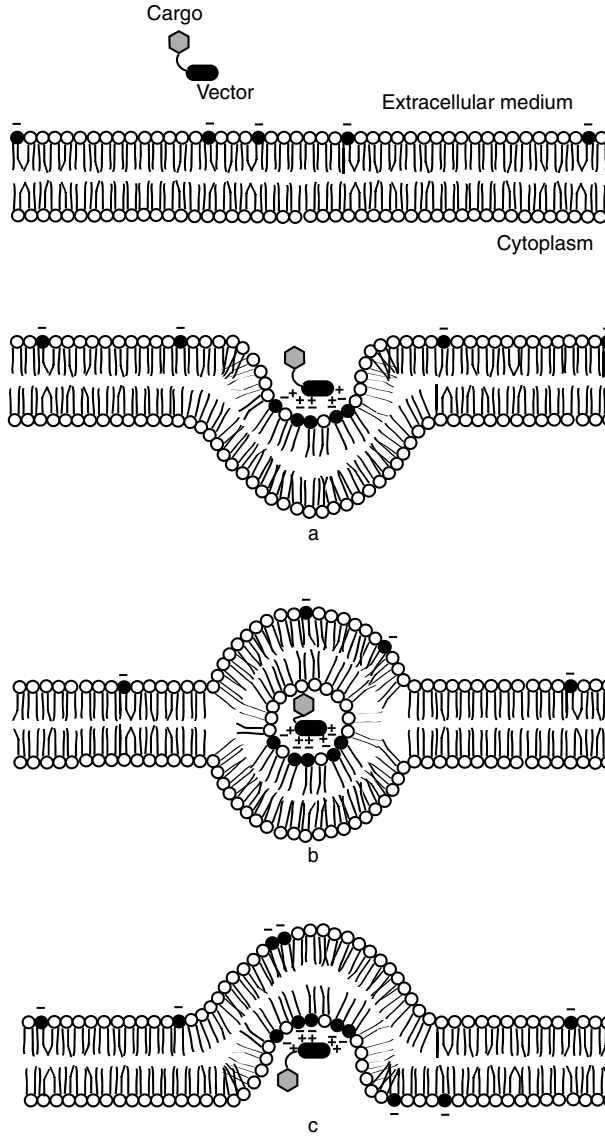

FIGURE 2.1 Model for intracellular translocation of penetratin peptides. (a) According to biophysical studies of peptide and lipid interactions, the peptide binds to the membrane through electrostatic interactions; (b) tryptophane residues destabilize the membrane and provoke the formation of inverted micelles; (c) upon restoration of the planar bilayer, the peptide is delivered to the cell cytoplasm.

2.4 DELIVERY OF HYDROPHILIC CARGOES INTO LIVE CELLS WITH PENETRATIN VECTORS

Since first reports demonstrating the efficient cell delivery of hydrophilic molecules linked to penetratin or AntpHD,[31-33] several applications have been developed thanks to the Antennapedia homeodomain, its third helix, and several variants (for reviews see References 28, 29, 34, and 35). Penetratin and penetratin-derived peptides have been used successfully to deliver chemical molecules, proteins, oligopeptides, oligonucleotides, and peptide-nucleic acids into live cells, *in vitro* and *in vivo*. The next paragraphs describe the mode of linkage and highlight some typical applications. A more comprehensive list of cargoes delivered by this vector system is presented in Table 2.3.

2.4.1 Principles of Cargo–Vector Linkage

One of the first applications has been to link and internalize oligonucleotides bearing a free thiol group to the cysteine naturally present in the β-turn between the second and the third helix of AntpHD.[36] AntpHD was also used to deliver recombinant polypeptides of different lengths (Table 2.3). In that case, the cargo sequences were fused to the C terminus of AntpHD and the fusion proteins expressed in *Escherichia coli* were purified thanks to the heparin-binding properties of the homeodomain. However, most of the experiments were achieved with the penetratin-1 peptide. The three main types of coupling protocols used are illustrated in Figure 2.2.

In a first protocol, penetratin is synthesized with an additional N-terminal-activated cysteine, protected by a nitro-pyridinium group that prevents peptide homodimerization and facilitates disulfide bond formation with the reactive thiol present on the cargo. This method is advantageous in that the cargo is released free in the cytoplasm as a result of disulfide bond breakage in the reductive cytoplasmic milieu.

In a second method, the cargo and vector are chemically synthesized in continuity. In that case, no coupling reaction is necessary. These first two methods also allow the internalization of modified peptides like phospho-peptides or peptide nucleic acid (PNA). Another possible modification is biotinylation; this modification is useful to follow the peptide in the cells and to purify any molecule interacting with internalized cargoes.

The third method consists in the preparation of fusion polypeptides by *in vitro* recombination. The fusion is expressed in *E. coli* and purified easily due to the heparin-binding properties of the third helix. Alternatively, the fusion protein can incorporate a poly-histidine or GST sequence for purification on ion columns or gluthathion, respectively. Indeed a tag (HA, myc, etc.) and a protease site allowing removal of the GST moiety can be added to the construction. Because of low cost, this is a method of choice when long cargoes are needed.

2.4.2 Vectorization with AntpHD

2.4.2.1 AntpHD-Mediated Internalization of Oligonucleotides

The first applications were developed with the entire homeodomain. AntpHD has been used to internalize antisense oligonucleotides against the β-amyloid precursor

TABLE 2.3
Cargoes Internalized *In Vitro* and *In Vivo* with AntpHD-Derived Peptidic Vectors

Type of cargo	Length	Vector	Cargo effect	Ref.
Entire protein				
$p16^{INK4A}$	156 aa	Penetratin	Induces replicative senescence	71
Oligopeptide				
PKC	14 aa	AntpHD	Inhibits PKC activity in neurons	31
PKC-ε	9 aa	Penetratin	Inhibits PKC-ε activity in rabbit cardiomyocytes	58
cGPK	8 aa	Penetratin	Inhibits cGMP kinase in cerebral arteries	59
SSeKS	16 aa	Penetratin	Inhibits SSeKS binding to cyclinD1	51
ICE	6 aa	Penetratin	Blocks ICE proteases	43
EGF-R	9 aa	Penetratin	Inhibits EGF and PDGF stimulated mitosis	39
FGF-R1	9 aa	Penetratin	Inhibits FGF-R signaling in neurons	60
$p75^{NTR}$	35 aa	Penetratin	Suppresses neuronal death promoted by the chopper domain of $p75^{NTR}$	82
Pcw3	41 aa	AntpHD	T-cell activation	40, 41
OVA-K	8 aa	Penetratin	T-cell activation and protection against ovalbumin expressing tumor cell line	74
Rab 13	41 aa	AntpHD	Inhibits prolactin exocytosis	33
Grb10	16 aa	Penetratin	Blocks PDGF and insulin-stimulated mitogenesis	38
PSM	16 aa	Penetratin	Blocks PDGF and insulin-stimulated mitogenesi	39
Cav1	19 aa	Penetratin	Inhibits NO synthesis and inflammation	75
Met-R	19 aa	Penetratin	Inhibits Met kinase activity	63
CD44	13 aa	Penetratin	Inhibits CD44 activation	61
$p16^{INK4A}$	20 aa	Penetratin	Inhibits cyclin D1-CDK4 activity	45, 46
$p16^{INK4A}$	20 aa	Penetratin	Inhibits cyclin D1-CDK4 mediated cell-spreading on vitronectin	48
$p16^{INK4A}$	20 aa	Penetratin	Inhibits transformation of pancreatic tumor cells	47
$p21^{Waf1/Cip1}$	20 aa	Penetratin	Inhibits PCNA activity and promotes growth arrest of $p53^{-/-}$ cells	80
$p21^{Waf1/Cip1}$	26 aa	Penetratin	Inhibits cyclin D1/CDK4 and cyclin E/CDK2 activity and kills human lymphoma cells	83
elF4e	12 aa	Penetratin	Blocks elF4e-induced transformation	52
p53/E1B	17 aa	Penetratin	Inhibits E1B binding to p53	53
p53	95 aa	Penetratin	Inhibits p53-mediated apoptosis	54
cMyc	14 aa	Penetratin	Inhibits cancerization of human breast cancer cells	56, 57
E2F-1	8 aa	Penetratin	Inhibits cyclin A/E-CDK2 activity	49
Oligonucleotide				
SOD1	21 mer	Penetratin	Inhibits SOD1 in PC12 cells	42
β-APP	25 mer	AntpHD	Inhibits β-APP in neurons	32
$p21^{Waf1/Cip1}$	21 mer	AntpHD	Inhibits $p21^{Waf1/Cip1}$ in human gliomas	37
HAND	18 mer	Penetratin	Inhibits the bHLH factor HAND in neural crest cells	81

TABLE 2.3 (continued)
Cargoes Internalized *In Vitro* and *In Vivo* with AntpHD-Derived Peptidic Vectors

Type of cargo	Length	Vector	Cargo effect	Ref.
PNA				
GalR1	21 mer	Penetratin	Down regulates Galanin receptor R1 *in vivo*	67
Telomerase	13 mer	Penetratin	Inhibits telomerase in melanoma cells	65, 66
Chemical drug				
Doxorubicin		Penetratin	Doxorubicin crosses BBB	78

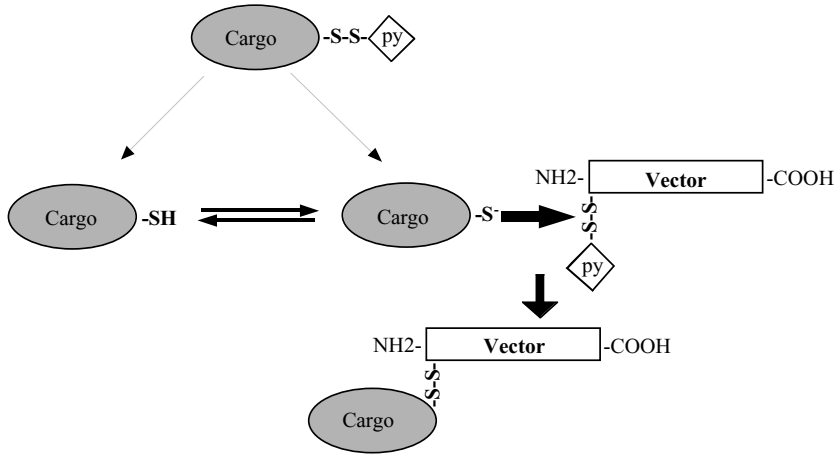

FIGURE 2.2 Two modes of coupling cargoes to Penetratin peptides: (1) linkage requiring disulfide bond formation. Cargo and vector are synthesized with a cysteine in which the thiol group is protected with a pyridinium group (py). The pyridinium on the cargo is removed either by dithiothreitol (DTT), in the case of oligonucleotides, or by tris-(2-carboxyethyl) phosphine hydrochloride (TCEP). (2) Chemical synthesis in tandem. The cargo (a peptide in this case) is synthesized in tandem with the vector. (3) Alternatively, fusion peptides (vector and cargo) can be expressed in *E. Coli* and purified.

protein (APP) into neurons developing *in vitro*.[32] Internalized antisense oligonucleotides caused a transient inhibition of β-APP synthesis and of neurite elongation at concentrations in the n*M* range. A more recent example is the overcoming of radio resistance in human gliomas by AntpHD-coupled $p21^{WAF1/CIP1}$ antisense oligonucleotides.[37] Malignant gliomas are tumors highly resistant against γ-irradiation that overexpress the cyclin-CDK inhibitor protein p21. This overexpression enhances survival and suppresses apoptosis after γ-irradiation. The pretreatment of cells with antisense oligonucleotides, coupled to AntpHD, enhanced γ-irradiation-induced apoptosis and cytotoxicity in radioresistant glioma cells.

However, the success of strategies based on the internalization of oligonucleotides is highly dependent on the stability of the oligonucleotides and the half-life of the target protein. Therefore, we believe that, when possible, internalizing a peptide with direct target antagonizing activity represents a better approach.

2.4.2.2 AntpHD-Mediated Internalization of Polypeptides

2.4.2.2.1 In Vitro

In a study aimed at understanding the role of small GTP-binding proteins in prolactin exocytosis, several fusion peptides were constructed linking AntpHD to 30 to 40 amino acids derived from the C-terminal domains of rab1, rab2, and rab3.[33] After internalization by anterior rat pituitary cells, only rab3 C terminus blocked prolactin exocytosis. AntpHD-coupled peptides have also been used to inactivate tyrosine-kinase membrane receptors like PDGF-receptor, IGF-I receptor, and insulin receptor. To that end, Grb10 binding to the activated cytoplasmic domain of the receptors has been inhibited by internalizing phosphopeptides that bind Grb10 SH2 and SH3 adaptor domains.[38] A similar protocol was used to study the function of another cellular partner of PDGF, IGF-I, and insulin receptors: PSM (proline-rich, PH SH2 domain-containing signaling mediator).[39] Similarly, to Grb10, PSM possesses SH2 and SH3 adaptor domains and an AntpHD-coupled peptide mimetic of the proline-rich putative SH3 domain-binding region interfered with PDGF, IGF-I, and insulin, but not with EGF-induced DNA synthesis. As in the case of Grb10, PSM is a positive effector for mitogenic signals triggered by PDGF, IGF-I, or insulin and SH2 and SH3 domains determine the specificity of PSM action in each mitogenic pathway.

2.4.2.2.2 In Vivo

The first *in vivo* application of AntpHD-mediated vectorization was the induction of T-cell responses by a peptide derived from the HLA-cw3 cytotoxic-T-cell epitope. AntpHD-based fusion peptides, expressing the 170–179 amino acids from HLA-Cw3 or 147–156 amino acids from influenza nucleoprotein with flanking proteasome recognition sites, were addressed into the cell cytoplasm to allow their presentation in the MHC-I context.[40] Peptide presentation led to the priming of cytotoxic T cells *in vitro* and *in vivo* (after intraperitoneal injection). *In vivo* efficiency in antigen presentation required that the peptide be associated with negative charges under the form of SDS or polysialic acid. Although this was not investigated, it is believed that negative charges protect the peptide from degradation and favor its diffusion within the organism.

In a more recent report, Chikh et al. have shown that the addition of liposomes stabilizes AntpHD-Cw3 and protects it against degradation.[41] Association with liposomes is spontaneous regardless of lipid composition; about 50% of the tethered peptide can also be exchanged from these liposomes. Moreover, this association with liposomes confers a partial resistance against protease degradation and does not alter the capacity of the recombinant peptide to be internalized in macrophages and dendritic cells and to prime T-cell response *in vivo* through the MHC-I pathway.

2.4.3 Vectorization with Penetratin Peptide, *In Vitro* Studies

2.4.3.1 Oligonucleotide and Oligopeptide Delivery

In this section we shall only consider the *in vitro* delivery of oligopeptides and oligonucleotides. A specific section is devoted to full-length proteins and to *in vivo* approaches. Two main domains of application (cell death and cell cycle and signal transduction) will be developed.

2.4.3.1.1 Cell Death and Cell Cycle Regulation

Several pathways lead to apoptosis in PC12 cells (nitric oxide (NO), withdrawal of trophic factors). Incubation of PC12 cells with an antisense oligonucleotide against superoxyde dismutase 1 (SOD-1) mRNA efficiently decreases SOD-1 activity (50 to 60%) and promotes apoptotic cell death specifically induced by accumulation of NO.[42] A 100-fold increase in antisense efficiency on both effects was observed after linkage to penetratin-1 by a disulfide bridge.[36] When linked to penetratin, oligonucleotide internalization became insensitive to the presence of serum during incubation.

In the same experimental model, incubation of PC12 cells with a penetratin-linked oligopeptide which mimics the catalytic site of interleukin 1β-converting enzyme (ICE)-like proteases protected cells from apoptosis.[43] Equivalent effects were obtained with the permeant competitive ICE inhibitor ZVAD-FMK, but at much higher concentrations (200-fold). Two different penetratin-linked cargoes (SOD antisense, ICE oligopeptide) have been used simultaneously without interference.

Penetratin peptides have been used to interfere with the cell cycle, in particular to antagonize the interaction between cyclins and cyclin-dependent kinases (CDK). Cell cycle inhibitors, also tumor suppressors, are grouped in two families: the $p21^{Cip1/Waf1}$ family (including p21, p27, and p57) and the p16 family (including $p15^{INK4b}$, $p16^{INK4b}$, $p18^{INK4c}$, and $p19^{INK4d}$).[44] P16 CDK2/INK4A is deleted or mutated in a large number of human cancers and its overexpression blocks transition through the G1/S phase of the cell cycle. P16 binding blocks CDK 4,CDK 6 activity and pRb phosphorylation. Peptides derived from the p16 binding domain to CDK4, CDK6 and internalized after penetratin linkage mimicked the p16 inhibitory action on CDK4 and CDK6 and prevented pRb phosphorylation and cell cycle progression.[45,46]

Inhibition of pRb phosphorylation in pancreatic cancer cells devoid of endogenous p16 activity was also obtained by Fujimoto et al.[47] Indeed, they restored a p16 function using the same peptide as Fahraeus et al.[45,46] Consequently, the growth of cancer cells was inhibited through arrest in G_1. Another study with p16-derived

peptides also demonstrated that p16 inhibits $\alpha_v\beta_3$ integrin-mediated cell spreading on vitronectin.[48]

Penetratin vectors have also been directed against downstream targets of pRb. Members of E2F transcription factors family are positive effectors of the cell cycle and downstream targets of pRb. Unphosphorylated pRb is able to sequester E2F, converting it from a transcriptional activator to a trancriptional repressor. Consequently, disruption of the pRb/E2F complex can lead to oncogenesis. Among proteins regulating E2F, cyclin A/CDK2 complexes neutralize E2F DNA-binding. Chen et al. have designed peptides corresponding to the cyclin A/CDK2-binding site on E2F.[49] Coupled to penetratin, these peptides were able to kill transformed cells in which E2F was already deregulated by pRb inactivation. It is noteworthy that the same team has recently identified about 12 peptides able to antagonize *in vitro* E2F-1 and cyclin A activity.[50] The potential anticancer effect of cell-permeant versions of the peptides (coupled to penetratin) is presently tested on tumor cells.

The tumor suppressor SSeCKS (sarc-suppressed C kinase substrate) also blocks the G1/S transition through an interaction with cyclin D1. Internalization with penetratin of the SSeCKS sequence responsible for this interaction demonstrated that SSeCKS anchors cyclin D1 in the cytoplasm, thus giving a molecular basis to G1/S arrest induced by SSeCKS.[51]

Another study with penetratin-coupled antagonizing peptides was conducted to evaluate the role of the translation initiation factor eIF4E in cellular transformation.[52] Over-expression of eIF4E is oncogenic and found in a number of human cancers; eIF4E activity can be blocked by eIF4E binding proteins (4E-BPs). Peptides after eIF4E-binding motifs found in 4E-Bps and introduced into cells designed bound eIF4E and induced massive apoptosis, thus revealing an involvement of this protein in the control of cell death not related to its known role in mRNA translation.

The tumor suppressor protein p53 is frequently targeted by oncoproteins in transformed cells. This is typically the case for adenovirus early region 1B protein (E1B), which binds and inactivates p53 through its sequestration in the cytoplasm. Penetratin-coupled peptides corresponding to the p53-binding site of E1B disrupted p53-E1B interaction allowing p53 nuclear addressing and restoring cell cycle arrest.[53]

Chemotherapy or radiation therapy activates p53-mediated processes in sensitive tissues. Thus p53 may be an appropriate target to reduce damages made to normal tissues during cancer therapies. Using a selection of genetic suppressor elements (GSE) from a library of randomly fragmented p53 cDNA, Mittelman and Gudkov have isolated p53-derived antagonizing peptides.[54] One of them, GSE56, was fused to penetratin and the fusion protein was shown to attenuate p53-mediated transactivation and reduce anticancer treatment side effects.[55]

Transcription factor c-Myc is a positive effector of cell proliferation; the misregulation of its activity can lead to cell transformation. To counteract its activity, Giorello et al. have developed penetratin-coupled inhibitory peptides.[56] These peptides were efficiently internalized in Myc-transformed human breast cancer cells and suppressed their transformation characteristics. Efficiency was improved by synthesizing their *retro-inverso* forms; these new peptides were more potent (5 to 10 times) and more stable (30 to 35 times) than their natural counterparts.[57]

2.4.3.1.2 Regulation of Signal Transduction

Intracellular protein kinase C (PKC) activity was down-regulated in neurons by the penetratin-coupled PKC pseudo-substrate, provoking growth cone collapse.[31] This confirmed PKC involvement in the transduction of extracellular signals regulating axon elongation. Penetratin-coupled inhibitory peptides targeting protein kinase C epsilon (PKC-ε) have highlighted its role in the protection of ischemic rabbit cardiomyocyte against osmotic shock.[58]

Another intracellular kinase, the cGMP-dependent protein kinase I (cGPK) was impaired by peptide blockers fused to penetratin. This inhibition into cerebral arteries cultured *in vitro* revealed a central role of the kinase in promoting NO-induced vasodilatation.[59]

The intracytoplasmic interactions between fibroblast growth factor receptor 1 (FGFR1) and SH2 (sarc-homology 2) domain of phospholipase C have been antagonized with a penetratin-coupled phosphopeptide corresponding to the phosphorylated site of the cytoplasmic domain of FGFR1.[60] This inhibited phospholipid hydrolysis stimulated by basic FGF and, in consequence, neurite outgrowth stimulated by basic FGF.

Peck and Isacke have analyzed the signaling pathway induced by an extracellular matrix glycosaminoglycan, the hyaluronan, which leads to cell migration.[61] Protein CD44, the hyaluronan transmembrane receptor, plays an essential role in many physiological events, including tumor progression, lymphocyte homing, and tissue morphogenesis. Hyaluronan binding to CD44 induces its phosphorylation on a serine crucial for hyaluronan-dependent cell migration. Penetratin-linked peptides mimicking endogenous phosphorylation sites blocked CD44-induced cell migration without reducing its expression or ability to bind hyaluronan. Penetratin-coupled peptides have also been used to analyze the signaling pathways of other glycosaminoglycans and their role in neuronal polarity.[62]

Still in the cell migration area, the binding of HGF (hepatocyte growth factor) to its receptor (c-Met) leads to invasive growth, an essential developmental event also implicated in tumor metastasis. The first event in this cascade is receptor autophosphorylation. Peptides interfering with HGF-induced c-Met autophosphorylation coupled to penetratin, once internalized in normal and transformed epithelial cells, blocked c-Met kinase and invasive growth.[63]

2.4.3.2 Delivery of Peptide Nucleic Acids (PNAs)

PNAs are oligonucleotides in which the sugar-phosphate backbone has been replaced by a neutral peptidic backbone;[64] they bind complementary RNA and DNA in a parallel or antiparallel orientation. Compared to deoxy-oligonucleotides, they present the advantage of forming extremely stable PNA–DNA or PNA–RNA duplexes. Moreover, PNAs are highly resistant to proteases and nucleases and inhibit gene expression at transcriptional and translational levels. Unfortunately, PNAs are poorly internalized by live cells. Three reports have demonstrated that eucaryotic cells efficiently take up penetratin-coupled PNAs *in vitro*[65,66] and *in vivo*.[34,67]

In vitro delivery of PNA using penetratin-1 was demonstrated in human prostate tumor cells[66] and human melanoma cell lines;[65] the aim was to investigate the effect

of two inhibitory PNAs on the catalytic activity of human telomerase. Telomerase function in normal cells is to maintain chromosome integrity, but several reports raise the question of telomerase implication in cell immortality and cancer. From a therapeutic point of view, it is of interest to block telomerase activity in transformed cells. To add telomeric repeats to the end of chromosomes, telomerase copies a small RNA sequence complementary to DNA. The strategy used here was to internalize two PNAs, an 11mer and a 13mer designed to cover the 5′-proximal region of the RNA and thus to inhibit human telomerase activity. The 13mer PNA coupled to penetratin through a disulfide-bound down-regulated telomerase activity in intact live cells, but the doubling time of the treated cells was only slightly decreased and telomeres were not shortened.[65]

A more successful use of PNAs linked to penetratin-1 was the antagonizing of the biological activity of galanin, a peptide neuromediator involved in pain transduction (see the section devoted to *in vivo* use of penetratin-derived peptides).

2.4.3.3 Delivery of Entire Proteins

AntpHD and penetratin are able to deliver large molecular weight protein into live cells. Among them are homeoproteins like Engrailed, HoxA-5, HoxB-4, HoxC-8, Pax 6, HoxC-4, Emx2, and Otx2[68-70] (unpublished results).

A good example of the successful delivery of entire proteins fused to penetratin-1 is the study of the replicative senescence phenomenon. Genetically programmed senescence is induced when cells approach their limit of population doubling. Interestingly, $p16^{INK4b}$ RNA and protein levels rise as cells enter senescence, but there was no evidence that p16 accumulation drives senescence. Using penetratin-1 to internalize $p16^{INK4b}$ into human diploid fibroblasts, Kato et al. have shown that $p16^{INK4b}$, but not a functionally compromised variant, provokes G1 arrest.[71] This arrest is certainly due to inhibition of pRb phosphorylation and the arrested cells display a senescent phenotype, strongly suggesting that $p16^{INK4b}$ is implicated in replicative senescence.

2.4.3.4 Chemical Drug Delivery

Doxorubicin, an anthracyclin, is a commonly used anticancer drug. Anthracyclins are among the most active antitumor compounds. Not only do they, as intercalating agents, induce DNA damage but they also bind cell surface acidic phospholipids, like cardiolipids, and induce necrosis and apoptosis via the sphingomyelin–ceramide pathway. However, anthracyclin treatments often lead to multidrug-resistant tumors through an enhanced expression of a multidrug-resistance gene (mdr). This gene encodes a 170-kD protein called the P-glycoprotein (Pgp) that actively transports several cytotoxic agents out of the cells.[72]

To overcome this problem, Mazel et al. have covalently linked doxorubicin to the penetratin N terminus and tested this conjugate in human erythroleukemia K562 cells.[73] Doxo-penetratin was about 20-fold more effective than doxorubicin alone to kill K562 doxorubicin-resistant cells. This suggests that the mode of internalization of penetratin, very likely through inverted micelles, allows the conjugate to escape Pgp activity.

2.4.4 *In Vivo* Internalization with Penetratin-Derived Vectors

2.4.4.1 Immune System

Similarly, to Schutze-Redelmeier et al. with AntpHD,[40] Pietersz et al. have demonstrated that penetratin efficiently targets antigenic peptides to the MHC-I complex.[74] Penetratin-coupled 9mer peptides corresponding to CTL epitopes have been successfully and rapidly imported into the cytosol of peritoneal exudate cells (PEC). Moreover, an 8mer peptide derived from ovalbumin (SIINFKEL) and coupled to penetratin induced a T-cell response after injection in mice and protected them against the development of tumor cell line E.G7-OVA expressing ovalbumin.

2.4.4.2 Delivery of Peptides in Blood Vessels

To appreciate further the role of caveolin-1 (the primary coat protein of caveolae) in signal transduction, Bucci et al. synthesized a hybrid peptide containing penetratin and the caveolin-1 scaffolding domain (19 aa).[75] Mice blood vessels and endothelial cells efficiently took up the peptide *ex vivo* and *in vivo*. Consequently, acetylcholine-induced vasodilatation and nitric oxyde production in isolated mouse aortic rings were selectively inhibited. Moreover, systemic administration of the peptide in mice suppressed acute inflammation and vascular leak as efficiently as a glucocorticoid or endothelial nitric oxyde synthase (eNOS) inhibitors.

2.4.4.3 Direct Perfusion Inside the Central Nervous System

Bolton et al. have evaluated the brain response induced by fluorescent penetratin after intrathecal injection into the striatum or the lateral ventricles of the rat brain.[76] Injection of 10 μg of penetratin in the striatum provoked neurotoxic cell death and an inflammatory response. Injections of 1 μg or less resulted in low toxicity with some spreading of the peptides, followed by its uptake, primarily by neurons. Penetratin injected in the lateral ventricle was internalized by ependymal cells bordering the ventricle but did not enter the parenchyme, or only very poorly. When injected at the periphery, penetratin-1 did not disrupt the blood-brain barrier (BBB) and Bolton et al. did not detect the peptide in rat brain 24 h after a 2-mg/kg intravenous injection.

Penetratin has been used *in vivo* to deliver PNAs into the central nervous system (CNS).[34,67] Galanin is a widely distributed neuropeptide involved in several biological effects. Galanin receptor type 1 (Gal R1) is highly conserved between species and abundant in the hypothalamus, hippocampus, and spinal cord.[77] PNAs designed to down-regulate the expression of the Gal R1 gene were covalently coupled to the N terminus of penetratin-1 by a disulfide bond. These PNAs down-regulated Gal R1 receptor expression by human Bowles melanoma cells and *in vivo* after intrathecal delivery at the level of the dorsal spinal cord. Down-regulation in the spinal cord decreased galanin binding and inhibited the C-fiber stimulation-induced facilitation of the rat flexor reflex, a response monitoring Gal R1 activity.

2.4.4.4 The Blood–Brain Barrier

Following the intravenous injection of a doxorubicin-penetratin peptide, Rousselle et al. have observed its passage into rat brain parenchyma.[78] These data are at odds

with the absence of BBB crossing reported by Bolton et al.[76] However, the conditions within the two experiments are very different. In particular, Rousselle et al. used radioactive doxorubicine coupled to a penetratin peptide composed of D-amino acids (2.5 mg/kg) and quantified brain accumulation 30 min after injection. In contrast, Bolton et al. used a fluorescent compound (2.0 mg/kg) linked to normal penetratin and quantified its presence in the brain 24 h after injection. The two approaches thus differ in terms of protocols and also of sensitivity, not to mention the modification of the vector (D vs. L amino acids).

Drug delivery to the brain is often restricted by the BBB that regulates the exchange of substances between brain and blood. The protein Pgp, which participates in the multidrug-resistance phenomenon (see above), has been detected at the luminal site of the endothelial cells of the BBB.[79] As a consequence, the brain availability of several drugs and, in particular, of anticancer drugs is extremely low, a likely explanation for the failure of brain tumor chemotherapy. The crossing of doxorubicin was analyzed by the *in situ* brain perfusion technique or by intravenous injection.[78] The amount of penetratin-coupled doxorubicin transported into the brain was 20-fold higher than that of free doxorubicin, without BBB disruption. These results demonstrate that penetratin peptides might be used as very efficient and safe means to deliver drugs across the BBB.

2.5 EXPERIMENTAL PROCEDURES

2.5.1 AntpHD and Penetratin

2.5.1.1 AntpHD and Penetratin Labeling

In order to be visualized, the AntpHD and penetratin peptides must be coupled to a fluorochrome (FITC, NBD TRITC, or CY3), to a biotin residue, or radioactively labeled. AntpHD can be labeled during synthesis in *E.Coli* with [^{35}S] methionine, or postsynthesis with FITC (Sigma), CY3 monofunctional dye (Amersham), or sulfo-NHS-biotin (Pierce). Penetratin can be coupled to fluorochromes, biotine,[15] or radioactive molecule[78] during synthesis, or postsynthesis as for AntpHD.

2.5.1.1.1 FITC Labeling Postsynthesis

Solutions

1. 1 *M* sodium bicarbonate buffer, pH 9.3: dissolve 0.84 g NaHCO3 in 9 ml deionized water. Adjust to pH 9.3 with NaOH and complete to 10 ml with deionized water. This solution should be stored at 4°C and used within one week.
2. Phosphate buffer saline, pH 7.2 (Life Technologies).
3. 1 *M* glycine: dissolve 7.5 g in 80 ml distilled water. Adjust to 100 ml with distilled water.
4. FITC dye (Molecular Probes).

Steps

1. Dilute 1 mg peptide in 200 µl of 50 m*M* sodium bicarbonate buffer, pH 9.3 (final concentration).

2. Add 10 to 50 molar ratio of reactive FITC dye to the peptide solution.
3. Incubate for 2 h at 4°C with gentle agitation.
4. Add 100 m*M* glycine (final concentration) and incubate for 2 h at 4°C (glycine deactivates free FITC). Purify the peptide by dialysis (spectrapor membranes, cut off 1000 d, Spectrum) against PBS at 4°C overnight with at least four changes. Purify the labeled AntpHD by gel filtration (microspin columns bio gel p6, Biorad) or by dialysis (spectrapor membranes, cut off 3000 d, Spectrum) against PBS at 4°C overnight with at least four changes.

2.5.1.1.2 Biotinylation Postsynthesis

Solutions

1. 100 m*M* sodium bicarbonate buffer, pH 8.5: dissolve 1.7 g NaHCO3 in 180 ml distilled water. Adjust to pH 8.5 with NaOH and complete to 200 ml with distilled water.
2. 1 *M* glycine: dissolve 7.5 g in 80 ml distilled water. Adjust to 100 ml with distilled water.
3. Sulfo-NHS-biotin (MW 443.42).

Steps

1. Dilute 1 mg peptide in 1 ml 50 m*M* sodium bicarbonate buffer, pH 8.5 (final concentration).
2. Dissolve a 5-*M* ratio of Sulfo-NHS-biotin (biotin/peptide) directly in the tube (alternatively, Sulfo-NHS-biotin can be predissolved in bicarbonate buffer just before use).
3. Incubate for 2 h at 4°C.
4. Add 100 m*M* glycine (final concentration) and incubate for 2 h at 4°C (glycine deactivates free Sulfo-NHS-biotin).

2.5.1.2 Internalization of AntpHD or Penetratin Peptides

Solutions

1. Culture medium.
2. Ethanol/acetic acid (9:1): mix 90 ml ethanol with 10 ml acetic acid. Store at –20°C. Do not store more than 1 week.
3. PBS 10% NCS (or FCS): dilute 10 ml of 10 × PBS (Life Technologies) in 80 ml distilled water. Add 10 ml NCS.
4. PBS 500 m*M* NaCl: dilute 10 ml of 10 × PBS (Life Technologies) and 10 ml 5 *M* NaCl in 100 ml distilled water.

Only for internalization of coupled peptide:

5. 1 *M* $MgCl_2$: dissolve 20.3 g $MgCl_2$. $6H_2O$ in 80 ml distilled water. Adjust to 100 ml with distilled water.
6. 10× deoxyribonuclease I (300 µg/ml): dissolve 1 mg DNase I in 3.2 ml PBS. Add 67 µl of 1 *M* $MgCl_2$. Filter, sterilize, and store at –20°C in aliquots.

Steps

1. Grow cells on glass coverslips; 10^4 to 5×10^4 cells/well in a 24-well plate at the time of coupled oligonucleotide addition is usually appropriate.
2. Dilute the coupled oligonucleotide product in fresh culture medium (500 µl/well) at a final concentration of 100 n*M* and add it to the cells after removal of the culture medium. For coupled peptides, dilute the product at a final concentration of 10 µ*M* and 30 µgl/ml. DNase I can be added to the culture medium during peptide incubation in order to reduce nonspecific binding of the vector to DNA released from dead cells.
3. Incubate for 2 h in normal culture conditions.
4. Wash the cells twice with fresh culture medium.
5. Wash the cells briefly with PBS 500 m*M* NaCl (to reduce nonspecific binding on the cell surface).

2.5.1.3 Detection of Internalized AntpHD or Penetratin

2.5.1.3.1 Detection of Peptides in Live Cells

This kind of observation is possible only with fluorochrome-labeled peptides; in that case, live cells are directly observed under a fluorescence microscope and can alternatively be sorted isolated with a FACS-Scan.

2.5.1.3.2 Detection of Biotin-Labeled Peptides

1. Fix cells in a solution of ethanol/acetic acid (9:1) for 5 min at –20°C.
2. Wash the cells three times for 5 min with PBS.
3. Incubate the cells in PBS 10% NCS for 30 min at room temperature.
4. Wash the cells three times for 5 min with PBS.
5. Incubate the cells with FITC-streptavidin in PBS 10% NCS for 30 min at room temperature.
6. Wash the cells three times for 2 min with PBS.
7. Wash the cells with distilled water.
8. Air-dry the coverslips and mount them in antifading medium (DAKO) before examination with a fluorescence microscope.

2.5.1.3.3 Detection of Radioactive Peptides Detection

Count directly with a scintillation counter.

2.5.2 AntpHD and Penetratin-Coupled Cargoes

2.5.2.1 Cargo–Vector Linkage

2.5.2.1.1 Oligonucleotides and PNAs

The principle of the coupling reaction is the formation of a disulfide bond between the vector and the cargo molecules (Figure 2.2). At one extremity the vector contains a disulfide pyridinium function that is highly reactive when incubated with free SH groups but which cannot react with itself, thus preventing the formation of homodimers. Penetratin-l is supplied in this form (activated penetratin-1), otherwise the function can be added at the N-terminal end of the peptide during synthesis (e.g.,

see Reference 31). Coupling requires the presence of an SH group at either end of the oligonucleotide. Modified oligonucleotides are available commercially with a thiol or disulfide pyridinium group.

Solutions

1. 5 × SDS sample buffer: to make 20 ml, add 0.97 g Tris, 2 g SDS, 10 ml glycerol (87%), and 0.5% bromophenol blue. Dissolve in distilled water and adjust to pH 6.8.
2. 5 × reducing SDS sample buffer: 20 ml 5 × SDS sample buffer containing 1.5 g DTT.

Steps

1. Resuspend separately the oligonucleotide and the vector in distilled water (1 to 10 mg/ml).
2. Quickly add an equimolar amount of vector to the oligonucleotide (after resuspension oligonucleotides can form homodimers; even if this reaction is relatively slow it is preferable to add the vector rapidly). Occasionally, a small precipitate may appear. If so, the sample can be incubated at 65°C for 15 min and, if the precipitate persists, 1 *M* NaCl or 20% DMSO (final concentration) can be added.
3. Incubate for 2 h at 37°C.
4. Keep a 5-µg aliquot for testing the yield of the reaction and store the remaining aliquots at –80°C.
5. Dilute 5 µg of the coupled product in 1 × SDS sample buffer (final concentration). Run the sample on 20% SDS-PAGE with no reducing agent. The same amount of coupled product diluted in 1 × reducing SDS sample buffer or vector alone can be run as control.
6. Stain the gel with Coomassie blue. The yield of the reaction is routinely above 50%.

2.5.2.1.2 Peptide

Basically, the coupling procedure is identical to the coupling with an oligonucleotide except that TCEP is preferred to DTT as the reducing agent. The cargo peptide must be ordered or synthesized with a disulfide pyridinium group or a cysteine at one end, except if a cysteine is already in the peptide sequence. If this is the case, the vector will react with the internal cysteine.[43] This does not affect the capacity of internalization.

Solutions

1. TCEP (MW 286.65): resuspend TCEP in distilled water at the appropriate concentration.

Steps

1. Resuspend separately the vector and the peptide in distilled and degazed water (1 to 10 mg/ml). If the peptide is not hydrosoluble, it can be resuspended in an appropriate mixture of water and DMSO or water and dimethylformamide without interference with the coupling reaction.

2. Treat the peptide with an equimolar amount of TCEP and incubate for 5 min at room temperature (TCEP should not be in excess).
3. Mix the solution with an equimolar amount of vector.
4. Incubate for 1 h at 37°C.
5. Keep 2 µg for gel analysis and store the coupled product at –80°C in aliquots. If desired, the coupled product can be purified by HPLC.
6. Dilute 2 µg of the coupled product in 1 × SDS sample buffer (final concentration). Run the sample on 20% SDS-PAGE without reducing agent. The same amount of the coupled product diluted in 1 × reducing SDS sample buffer or vector and peptide alone can be run as control.
7. Stain the gel with Coomassie blue. The yield of the reaction is routinely above 50%.

2.5.2.1.3 Direct Linkage

The cargo can be chemically synthesized in tandem with the vector;[60] this method is possible when the cargo is a peptide or a chemical molecule (fluorochromes, biotin). However, once internalized, an s–s coupled peptide is likely to be separated from the vector because of the reducing intracellular medium. This is not the case for a chimerical molecule.

2.5.2.1.4 Fusion Proteins in Bacteria

Fusion peptides comprising the AntpHD or penetratin peptides can be expressed in *E. coli* and purified. AntpHD fusion protein can be purified on heparin columns.

2.5.2.1.5 Decoupling Reaction

Incubation of cells with the decoupled product is a useful control for both fluorescent and nonfluorescent oligonucleotides. Alternatively, oligonucleotide or vector alone can be used.

Solution

1. 1 *M* cysteine (MW 121.2): dissolve 1.2 g cysteine in 10 ml distilled water.

Steps

1. Incubate the coupled product for 15 min at 37°C with 1 m*M* DTT (final concentration). If the cargo or vector alone is used as control it can be incubated with a tenfold molar ratio of cysteine in order to prevent terminal SH group reaction with free SH present at the cell surface.

2.5.2.2 Internalization and Detection of Vector–Cargo Fusion Molecules

Procedures are basically the same as those described for vector alone except that the cargo can be labeled for detection in place of the vector. As oligonucleotides and peptides, PNAs fused to AntpHD and penetratin can be visualized after internalization in cells when coupled to a fluorochrome[66] or to a biotin residue. One advantage of the vector is that internalization efficacy is almost insensitive to all common culture media (RPMI, DMEM-FI2) and unmodified by the presence of

FCS (10%) or horse serum (10%). Internalization can be done on cells grown on plastic or glass (coated or not with polylysine, laminin, collagen).

The only crucial point is that the coupled product must be diluted in the culture medium before its addition on cells. Because of the rapidity of the internalization process, direct addition of the concentrated product on cells can lead to a heterogeneous distribution among cells.

2.5.2.2.1 Oligonucleotide Internalization

The following protocol is appropriate for antisense oligonucleotide experiments, but optimal concentration and incubation time must be determined in each case. Internalization and intracellular distribution of the cargo can be visualized by using a labeled oligonucleotide. Doubly modified oligonucleotides containing an SH modification at the 3′ end and a fluorescein or a biotin at the opposite end are commercially available.

Steps

1. Grow the cells in appropriate medium. The number of cells is an important parameter; 10^5 cells/well in a 24-well plate at the time of coupled oligonucleotide addition is usually appropriate.
2. Dilute the coupled oligonucleotide in 500 µL fresh culture medium (1 µ*M* to 1 n*M* final) and add it to the cells after removal of the culture medium (if present, DMSO concentration should not exceed 0.1%).
3. Incubate the cells in normal culture conditions until needed. The effect of the oligonucleotide can be evaluated a few hours after its addition (see Section 2.4). Because of the limited stability of intracellular oligonucleotides, biological effects should be evaluated within 2 days.
4. If culture times longer than 1 day are required after treatment, repeat the treatment every 24 h. Proceed as in step 2.

2.5.2.2.2 Peptide Internalization

The ability to internalize small peptides is a promising feature of homeodomain-derived vectors. Internalized peptides can exert direct effects on biological functions, which can be monitored as early as a few minutes after their addition;[31] the effects can last up to 8 days.[43] In contrast with oligonucleotides, peptide internalization can be greatly affected by its amino acid sequence. Even if the vector has been used successfully with different kinds of peptides, it is preferable to test internalization in each case. In order to be visualized, cargo peptide can be labeled as described for penetratin (Section 2.5.1.1).

Solutions

1. 1 *M* $MgCl_2$: dissolve 20.3 g $MgCl_2 \cdot 6H_2O$ in 80 ml distilled water. Adjust to 100 ml with distilled water.
2. 10× deoxyribonuclease I (300 µg/ml): dissolve 1 mg DNase I in 3.2 ml PBS. Add 67 µl of 1 *M* $MgCl_2$. Filtrate, sterilize, and store at –20°C in aliquots.

Step

1. Peptide–vector internalization is identical to oligonucleotide–vector internalization, except that 30 µg/ml DNase I can be added to the culture medium during peptide incubation in order to reduce nonspecific binding of the vector to DNA released from dead cells.

2.5.3 Comments

AntpHD and penetratin transduction properties can be exploited in all cases when delivery of exogenous hydrophilic compounds in cells or tissues is required. The diversity of molecules delivered with these vectors (peptides, proteins, oligonucleotides, PNAs, and chemical substances) allows several experimental approaches. To date, a wide range of biological phenomena have been studied, perturbed, or corrected due to these peptidic vectors (Table 2.3). They are particularly well suited for dissecting mechanistic aspects of regulations mediated by complex protein–protein interactions, like signal transduction pathways or cell cycle regulation (see Section 2.4.3.1). Penetratin vectors are also promising in therapeutics: they have been employed to correct hyperproliferative disorders often leading to cancerization (see Sections 2.4.3.1 and 2.4.4.3); they are also good vectors to bypass *in vivo* tight barriers and detoxification systems such as, respectively, the BBB and the MDR system (see Sections 2.4.3.4 and 2.4.4.3). The consequence is an important potentiation of the cargo molecule in terms of accessibility to the targeted tissue and of biological effect.

The cell type in which peptides will be delivered is not a critical parameter, since penetratin-cargo hybrids are efficiently delivered in many cell types: PC12, rat, and mice primary neurons, 3T3, COS-7, MDCK, K562, SAOS, U2OS, MCF-7, Hela, ES, myotubes.

In general, whatever cargo is chosen, the solubility of cargo–vector hybrid is important. Lack of solubility is often due to neutralization of charges between the two molecules and can be improved by avoiding the use of PBS, increasing the ionic strength, or adding a small percentage of DMSO.

2.5.3.1 Oligopeptides

Concerning oligopeptides, the efficacy of delivery will depend on structure or conformation of the fusion hybrid. There is no absolute rule, and oligopeptides up to 156 aa have been successfully delivered in cells so far (see Table 2.3). The concentration of the coupled product to be used is variable: in general 2 to 20 µ*M* in most applications; time of treatment is also variable, depending on the biological effect observed. Shortest times (10 min to 2 h) are preferred when responses are believed to be rapid, such as for molecules involved in signal transduction, longer times for prolonged biological effects such as differentiation, proliferation, apoptosis (2 to 48 h). The only data demonstrating *in vivo* delivery of oligopeptides (mice blood vessels[75]) report systemic intraperitoneal injections of 0.3 mg/kg of the fusion peptide (35 aa) and a monitored short-term biological effect (on inflammation) 45 min after injection, and a long-term biological effect 24 h after injection (on vascular leakage).

2.5.3.2 Oligonucleotides

As in every antisense strategy, there is no general rule for obtention of a biological effect. For example, the abundance of the target mRNA, the stability of the cognate protein, and the percentage of inhibition necessary to obtain an effect are usual limiting factors. However, several parameters must be considered. The design of the oligonucleotide must minimize the possibility of secondary structure formation and of cross-hybridization with other RNAs. The site of translation start is often chosen as a target but, when possible, it is preferable to test several oligonucleotides that hybridize with different portions of the target mRNA. Fifteen to twenty-five base oligonucleotides are usually adequate. Longer oligonucleotides are not always more efficient and can reduce the efficacy of internalization. Phosphorothioate analogues of oligonucleotides with a longer half-life can be used, but precipitation with the vector often occurs during the coupling reaction. The concentration of coupled oligonucleotide hybrids is variable; as a general rule, the coupled oligonucleotide is 100- to 1000-fold more active than the uncoupled oligonucleotide. Generally, maximal effects are obtained with 10 to 100 n*M* and targeted proteins are down-regulated after 1 to 3 h of treatment.

2.5.3.3 Peptide Nucleic Acids

According to the technical data available for the PNA–penetratin hybrids, no toxicity was observed for concentrations up to 150 μ*M* with 21 mer PNAs. Concentrations used range *ex vivo* from 35 to 350 n*M*; the only *in vivo* study reports the use of 150 μ*M* of PNA–penetratin conjugate delivered by intrathecal injections to target the galanin receptor in rat CNS. Biological effects were obtained *ex vivo* from 30 min to 5 h following treatment, and *in vivo* after 48 h of treatment.[67]

2.5.3.4 Drugs

Two publications reported targeting penetratin-coupled anticancer drug doxorubicin *ex vivo* in transformed K562 human cells and *in vivo* through BBB of rats. Maximal biological effect (killing of transformed cells) was obtained *ex vivo* after 48 h of treatment (4 μ*M* of hybrid peptide vs. 120 μ*M* of free doxorubicin).[73] Doxorubicin transfer through BBB was 20-fold more efficient when coupled to penetratin than uncoupled. Delivery into the brain was observed rapidly after the intravenous injection of 2.5 mg peptide/kg body weight, within 30 min after the injection.[56,57,78,80-83]

REFERENCES

1. Gehring, W.J. et al., Homeodomain-DNA recognition, *Cell*, 78, 211, 1994.
2. Doe, C.Q. and Scott, M.P., Segmentation and homeotic gene function in the developing nervous system of Drosophila, *Trends Neurosci.*, 11, 101, 1988.
3. Doe, C.Q. et al., Control of neuronal fate by the *Drosophila* segmentation gene even-skipped, *Nature*, 333, 376, 1988.
4. Le Mouellic, H. et al., Homeosis in the mouse induced by a null mutation in the Hox-3.1 gene, *Cell*, 69, 251, 1992.

5. Miller, D.M. et al., C. elegans unc-4 gene encodes a homeodomain protein that determines the pattern of synaptic input to specific motor neurons, *Nature*, 355, 841, 1992.
6. Tiret, L. et al., Increased apoptosis of motoneurons and altered somatotopic maps in the brachial spinal cord of Hoxc-8-deficient mice, *Development*, 125, 279, 1998.
7. White, J.G. et al., Mutations in the Caenorhabditis elegans unc-4 gene alter the synaptic input to ventral cord motor neurons, *Nature*, 355, 838, 1992.
8. Ayala, J. et al., The product of rab2, a small GTP binding protein, increases neuronal adhesion, and neurite growth *in vitro*, *Neuron*, 4, 797, 1990.
9. Borasio, G.D. et al., Ras p21 protein promotes survival and fiber outgrowth of cultured embryonic neurons, *Neuron*, 2, 1087, 1989.
10. Joliot, A. et al., Antennapedia homeobox peptide regulates neural morphogenesis, *Proc. Natl. Acad. Sci. USA,* 88, 1864, 1991.
11. Prochiantz, A., Messenger proteins, *J. Soc. Biol.*, 194, 119, 2000.
12. Bloch–Gallego, E. et al., Antennapedia homeobox peptide enhances growth and branching of embryonic chicken motoneurons *in vitro*, *J. Cell. Biol.*, 120, 485, 1993.
13. Le Roux, I. et al., Neurotrophic activity of the Antennapedia homeodomain depends on its specific DNA-binding properties, *Proc. Natl. Acad. Sci. USA,* 90, 9120, 1993.
14. Le Roux, I. et al., Promoter-specific regulation of gene expression by an exogenously added homedomain that promotes neurite growth, *FEBS Lett.*, 368, 311, 1995.
15. Derossi, D. et al., The third helix of the Antennapedia homeodomain translocates through biological membranes, *J. Biol. Chem.*, 269, 10444, 1994.
16. Fischer, P.M. et al., Structure-activity relationship of truncated and substituted analogues of the intracellular delivery vector Penetratin, *J. Pept. Res.*, 55, 163, 2000.
17. Derossi, D. et al., Cell internalization of the third helix of the Antennapedia homeodomain is receptor-independent, *J. Biol. Chem.*, 271, 18188, 1996.
18. Drin, G. et al., Physico-chemical requirements for cellular uptake of pAntp peptide. Role of lipid-binding affinity, *Eur. J. Biochem.*, 268, 1304, 2001.
19. Mainguy, G. et al., An induction gene trap for identifying a homeoprotein-regulated locus, *Nat. Biotechnol.*, 18, 746, 2000.
20. de Kruijff, B. et al., Molecular aspects of the bilayer stabilization induced by poly(L-lysines) of varying size in cardiolipin liposomes, *Biochim. Biophys. Acta*, 820, 295, 1985.
21. Berlose, J.P. et al., Conformational and associative behaviours of the third helix of antennapedia homeodomain in membrane-mimetic environments, *Eur. J. Biochem.*, 242, 372, 1996.
22. Lindberg, M. and Graslund, A., The position of the cell penetrating peptide penetratin in SDS micelles determined by NMR, *FEBS Lett.*, 497, 39, 2001.
23. Magzoub, M. et al., Interaction and structure induction of cell-penetrating peptides in the presence of phospholipid vesicles, *Biochim. Biophys. Acta*, 1512, 77, 2001.
24. Persson, D. et al., Penetratin-induced aggregation and subsequent dissociation of negatively charged phospholipid vesicles, *FEBS Lett.*, 25245, 1, 2001.
25. Bellet–Amalric, E. et al., Interaction of the third helix of Antennapedia homeodomain and a phospholipid monolayer, studied by ellipsometry and PM-IRRAS at the air-water interface, *Biochim. Biophys. Acta*, 1467, 131, 2000.
26. Fragneto, G. et al., Neutron and x-ray reflectivity studies at solid–liquid interfaces: the interactions of a peptide with model membranes, *Physica B*, 276, 2000.
27. Fragneto, G. et al., Interaction of the third helix of Antennapedia homeodomain with a deposited phospholipid bilayer: a neutron reflectivity structural study, *Langmuir*, 16, 4581, 2000.

28. Derossi, D. et al., Trojan peptides: the penetratin system for intracellular delivery, *Trends Cell Biol.*, 8, 84, 1998.
29. Prochiantz, A., Messenger proteins: homeoproteins, TAT and others, *Curr. Opin. Cell Biol.*, 12, 400, 2000.
30. Thoren, P.E. et al., The antennapedia peptide penetratin translocates across lipid bilayers — the first direct observation, *FEBS Lett.*, 482, 265, 2000.
31. Theodore, L. et al., Intraneuronal delivery of protein kinase C pseudosubstrate leads to growth cone collapse, *J. Neurosci.*, 15, 7158, 1995.
32. Allinquant, B. et al., Downregulation of amyloid precursor protein inhibits neurite outgrowth *in vitro*, *J. Cell. Biol.*, 128, 919, 1995.
33. Perez, F. et al., Rab3A and rab3b carboxy-terminal peptides are both potent and specific inhibitors of prolactin release by rat cultured anterior pituitary cells, *Mol. Endocrinol.*, 8, 1278, 1994.
34. Prochiantz, A., Peptide nucleic acid smugglers, *Nat. Biotechnol.*, 16, 819, 1998.
35. Lindgren, M. et al., Cell-penetrating peptides, *Trends Pharmacol. Sci.*, 21, 99, 2000.
36. Troy, C.M. et al., Downregulation of Cu/Zn superoxide dismutase leads to cell death via the nitric oxide-peroxynitrite pathway, *J. Neurosci.*, 16, 253, 1996.
37. Kokunai, T. et al., Overcoming of radioresistance in human gliomas by p21WAF1/CIP1 antisense oligonucleotide, *J. Neurooncol.*, 51, 111, 2001.
38. Wang, J. et al., Grb10, a positive, stimulatory signaling adapter in platelet-derived growth factor BB-, insulin-like growth factor I-, and insulin-mediated mitogenesis, *Mol. Cell Biol.*, 19, 6217, 1999.
39. Riedel, H. et al., PSM, a mediator of PDGF-BB-, IGF-I-, and insulin-stimulated mitogenesis, *Oncogene*, 19, 39, 2000.
40. Schutze-Redelmeier, M.P. et al., Introduction of exogenous antigens into the MHC class I processing and presentation pathway by *Drosophila* Antennapedia homeodomain primes cytotoxic T cells *in vivo*, *J. Immunol.*, 157, 650, 1996.
41. Chikh, G. et al., Characterization of hybrid CTL epitope delivery systems consisting of the Antennapedia homeodomain peptide vector formulated in liposomes, *J. Immunol. Methods*, 254, 119, 2001.
42. Troy, C.M. and Shelanski, M.L., Down-regulation of copper/zinc superoxide dismutase causes apoptotic death in PC12 neuronal cells, *Proc. Natl. Acad. Sci. USA,* 91, 6384, 1994.
43. Troy, C.M. et al., The contrasting roles of ICE family proteases and interleukin-1beta in apoptosis induced by trophic factor withdrawal and by copper/zinc superoxide dismutase down-regulation, *Proc. Natl. Acad. Sci. USA,* 93, 5635, 1996.
44. Sherr, C.J. and Roberts, J.M., CDK inhibitors: positive and negative regulators of G1-phase progression, *Genes Dev.*, 13, 1501, 1999.
45. Fahraeus, R. et al., Inhibition of pRb phosphorylation and cell-cycle progression by a 20- residue peptide derived from p16CDKN2/INK4A, *Curr. Biol.*, 6, 84, 1996.
46. Fahraeus, R. et al., Characterization of the cyclin-dependent kinase inhibitory domain of the INK4 family as a model for a synthetic tumour suppressor molecule, *Oncogene*, 16, 587, 1998.
47. Fujimoto, K. et al., Inhibition of pRb phosphorylation and cell cycle progression by an antennapedia-p16(INK4A) fusion peptide in pancreatic cancer cells, *Cancer Lett.*, 159, 151, 2000.
48. Fahraeus, R. and Lane, D.P., The p16(INK4a) tumour suppressor protein inhibits alphavbeta3 integrin-mediated cell spreading on vitronectin by blocking PKC-dependent localization of alphavbeta3 to focal contacts, *Embo. J.*, 18, 2106, 1999.

49. Chen, Y.N. et al., Selective killing of transformed cells by cyclin/cyclin-dependent kinase 2 antagonists, *Proc. Natl. Acad. Sci. USA,* 96, 4325, 1999.
50. Sharma, S.K. et al., Identification of E2F-1/Cyclin A antagonists, *Bioorg. Med. Chem. Lett.*, 11, 2449, 2001.
51. Lin, X. et al., SSeCKS, a major protein kinase C substrate with tumor suppressor activity, regulates G(1) — >S progression by controlling the expression and cellular compartmentalization of cyclin D, *Mol. Cell Biol.*, 20, 7259, 2000.
52. Herbert, T.P. et al., Rapid induction of apoptosis mediated by peptides that bind initiation factor eIF4E, *Curr. Biol.*, 10, 793, 2000.
53. Hutton, F.G. et al., Consequences of disruption of the interaction between p53 and the larger adenovirus early region 1B protein in adenovirus E1 transformed human cells, *Oncogene*, 19, 452, 2000.
54. Mittelman, J.M. and Gudkov, A.V., Generation of p53 suppressor peptide from the fragment of p53 protein, *Somat. Cell Mol. Genet.*, 25, 115, 1999.
55. Komarov, P.G. et al., A chemical inhibitor of p53 that protects mice from the side effects of cancer therapy, *Science*, 285, 1733, 1999.
56. Giorello, L., et al., Inhibition of cancer cell growth and c-Myc transcriptional activity by a c-Myc helix 1-type peptide fused to an internalization sequence, *Cancer Res.*, 58, 3654, 1998.
57. Pescarolo, M.P. et al., A *retro-inverso* peptide homologous to helix 1 of c-Myc is a potent and specific inhibitor of proliferation in different cellular systems, *FASEB J.*, 15, 31, 2001.
58. Liu, G.S. et al., Protein kinase C-epsilon is responsible for the protection of preconditioning in rabbit cardiomyocytes, *J. Mol. Cell Cardiol.*, 31, 1937, 1999.
59. Dostmann, W.R. et al., Highly specific, membrane-permeant peptide blockers of cGMP-dependent protein kinase Ialpha inhibit NO-induced cerebral dilation, *Proc. Natl. Acad. Sci. USA,* 97, 14772, 2000.
60. Hall, H. et al., Inhibition of FGF-stimulated phosphatidylinositol hydrolysis and neurite outgrowth by a cell-membrane permeable phosphopeptide, *Curr. Biol.*, 6, 580, 1996.
61. Peck, D. and Isacke, C.M., Hyaluronan-dependent cell migration can be blocked by a CD44 cytoplasmic domain peptide containing a phosphoserine at position 325, *J. Cell Sci.*, 111, 1595, 1998.
62. Calvet, S. et al., Identification of a signaling pathway activated specifically in the somatodendritic compartment by a heparan sulfate that regulates dendrite growth, *J. Neurosci.*, 18, 9751, 1998.
63. Bardelli, A. et al., A peptide representing the carboxyl-terminal tail of the met receptor inhibits kinase activity and invasive growth, *J. Biol. Chem.*, 274, 29274, 1999.
64. Nielsen, P.E., Peptide nucleic acids as therapeutic agents, *Curr. Opin. Struct. Biol.*, 9, 353, 1999.
65. Villa, R. et al., Inhibition of telomerase activity by a cell-penetrating peptide nucleic acid construct in human melanoma cells, *FEBS Lett.*, 473, 241, 2000.
66. Simmons, C.G. et al., Synthesis and membrane permeability of PNA-peptide conjugate, *Bioorg. Med. Chem. Lett.*, 7, 3001, 1997.
67. Pooga, M. et al., Cell penetrating PNA constructs regulate galanin receptor levels and modify pain transmission *in vivo*, *Nat. Biotechnol.*, 16, 857, 1998.
68. Maizel, A. et al., A short region of its homeodomain is necessary for engrailed nuclear export and secretion, *Development*, 126, 3183, 1999.
69. Joliot, A. et al., Identification of a signal sequence necessary for the unconventional secretion of engrailed homeoprotein, *Curr. Biol.*, 8, 856, 1998.

70. Chatelin, L. et al., Transcription factor hoxa-5 is taken up by cells in culture and conveyed to their nuclei, *Mech. Dev.*, 55, 111, 1996.
71. Kato, D. et al., Features of replicative senescence induced by direct addition of antennapedia-p16INK4A fusion protein to human diploid fibroblasts, *FEBS Lett.*, 427, 203, 1998.
72. Broxterman, H.J. et al., Multidrug resistance proteins and other drug transport-related resistance to natural product agents, *Curr. Opin. Oncol.*, 7, 532, 1995.
73. Mazel, M. et al., Doxorubicin-peptide conjugates overcome multidrug resistance, *Anticancer Drugs*, 12, 107, 2001.
74. Pietersz, G.A. et al., A 16-mer peptide (RQIKIWFQNRRMKWKK) from Antennapedia preferentially targets the class I pathway, *Vaccine*, 19, 1397, 2001.
75. Bucci, M. et al., *In vivo* delivery of the caveolin-1 scaffolding domain inhibits nitric oxide synthesis and reduces inflammation, *Nat. Med.*, 6, 1362, 2000.
76. Bolton, S.J. et al., Cellular uptake and spread of the cell-permeable peptide penetratin in adult rat brain, *Eur. J. Neurosci.*, 12, 2847, 2000.
77. Burgevin, M.C. et al., Cloning, pharmacological characterization, and anatomical distribution of a rat cDNA encoding for a galanin receptor, *J. Mol. Neurosci.*, 6, 33, 1995.
78. Rousselle, C. et al., New advances in the transport of doxorubicin through the blood-brain barrier by a peptide vector-mediated strategy, *Mol. Pharmacol.*, 57, 679, 2000.
79. Cordon–Cardo, C. et al., Multidrug-resistance gene (P-glycoprotein) is expressed by endothelial cells at blood-brain barrier sites, *Proc. Natl. Acad. Sci. USA,* 86, 695, 1989.
80. Cayrol, C. et al., p21 binding to PCNA causes G1 and G2 cell cycle arrest in p53-deficient cells, *Oncogene*, 16, 311, 1998.
81. Howard, M. et al., Expression of HAND gene products may be sufficient for the differentiation of avian neural crest-derived cells into catecholaminergic neurons in culture, *Dev. Biol.*, 215, 62, 1999.
82. Coulson, E.J. et al., Chopper, a new death domain of the p75 neurotrophin receptor that mediates rapid neuronal cell death, *J. Biol. Chem.*, 275, 30537, 2000.
83. Mutoh, M. et al., A p21(Waf1/Cip1)carboxyl-terminal peptide exhibited cyclin-dependent kinase-inhibitory activity and cytotoxicity when introduced into human cells, *Cancer Res.*, 59, 3480, 1999.

3 Transportans

Margus Pooga, Mattias Hällbrink, and Ülo Langel

CONTENTS

3.1 INTRODUCTION

The first discovered cell-penetrating peptides (CPPs) were derived from naturally occurring proteins like the Antennapedia homeodomain of Drosophila,[1] Tat of HIV-1,[2] and VP22 of HSV,[3] followed soon by designed chimeric peptides like MTS-NLS,[4] transportan,[5] and model peptides.[6] Numerous analogues of these CPPs have now been designed and synthesized, giving rise to families of respective peptides. Both classes of CPPs, protein-derived and designed or combined, have been vastly expanded by new peptides and derivatives. In this chapter we summarize the discovery, properties, and application of the cell-penetrating peptide transportan and its analogues.

3.2 THE DISCOVERY OF TRANSPORTAN

The predecessor of transportan, galparan, comprises a fragment of the neuropeptide galanin (1–13) and the wasp venom peptide mastoparan.[7] (Table 3.1) It was designed under a program aimed at creating galanin receptor ligands by using a chimeric

0-8493-1141-1/02/$0.00+$1.50

TABLE 3.1
Sequences and Uptake Parameters of Mastoparan (MP), Transportan (TP), and Transportan Analogues (TP2 to TP16)

	Sequence	Length[a] (a.a.)	Cellular uptake[b] 0°C	Cellular uptake[b] 37°C	Speed of uptake, $\tau_{0.5}$ (min)
Galparan	GWTLNSAGYLLGPINLKALAALAKKIL	27	nd	nd	nd
TP	GWTLNSAGYLLGK[c]INLKALAALAKKIL	27	+++	+++	3.4
TP2	GWTLNSAGYLLGK[c]INLKAKAALAKKLL	27	++	++	
TP3	$C_6H_5CH_2CO$(D-Y(Me))FQNRPRYK[c]-(Ahx) -INLKALAALAKKIL		++	++	nd
TP4	GWTLNSAGYLLGK[c]FLPLILRKIVTAL	26	—	—	—
TP5	GWTLNPAGYLLGK[c]INLKALAALAKKIL	27	+	+	nd
TP6	GWTLNPPGYLLGK[c]INLKALAALAKKIL	27	+	+	nd
TP7	...LNSAGYLLGK[c]INLKALAALAKKIL	24	+++	+++	4.3
TP8	.....LLGK[c]INLKALAALAKKIL	18	—	+/–	—
TP9	GWTLNSAGYLLGK[c]..LKALAALAKKIL	25	+++	+++	6.5
TP10	.....AGYLLGK[c]INLKALAALAKKIL	21	+++	+++	8.6
TP11	GWTLNS.....K[c]INLKALAALAKKIL	21	+	+	nd
TP12	...LNSAGYLLGK[c]..LKALAALAKKIL	22	++	++	10.7
TP13	...LNSAGYLLGK[c]....ALAALAKKIL	20	—	+/–	—
TP14	.....AGYLLGK[c]..LKALAALAKKIL	19	++	++	nd
TP15	...LNSAGYLLGK[c]..LKALAALAK…	19	—	+/–	—
TP16	GWTLNSAGYLLGK[c]INLKAPAALAKKIL	27	—	+/–	—
MP	[d]INLKALAALAKKIL	14	+	+	nd

[a] Number of amino acid residues.
[b] Detection of biotin by indirect immunofluorescence: +++ denotes comparable, ++ or + decreased, and +/– weak uptake in relation to that of transportan.
[c] Biotinylated at ε-amino group of Lys.
[d] Biotinylated at the N terminus.

strategy. The combination of these two peptides was motivated by the following observations:

1. Galanin (1–13) had been shown to be the smallest fragment of this neuropeptide that exhibited a reasonably high affinity toward the galanin receptor type 1.[8]
2. Many chimeric galanin receptor ligands were shown to possess very high affinity to galanin receptors. They consisted of galanin (1–13) in N terminus and a fragment of other neuropeptide or just a stretch of hydrophobic amino acids in C terminus.[9]
3. The C-terminal part of the chimeras was suspected to interact primarily with cellular membranes rather than with the receptor protein. Therefore, mastoparan, known to interact with lipid membranes, was used to C-terminally extend galanin (1–13) in order to increase the affinity toward membranes.[7]

Indeed, galparan is a high affinity ligand for the galanin receptor present in the Bowes melanoma cell line.[7] Unexpectedly, *in vivo* studies on acetylcholine release in rat brain showed that galparan dose dependently increased acetylcholine release in a PTX-dependent manner,[10] as could be expected from a mastoparan-based peptide, but was opposite to the effects of galanin. In a further study, galparan, contrary to mastoparan, was shown to stimulate the Na^+/K^+-ATPase in rat hippocampal membranes where galanin had no effect.[7] Thus, it is obvious that galparan is a peptide with different properties from those of the parent peptides.

Moreover, galparan was shown to be a strong stimulator of the release of insulin from rat β-cells.[11] Again, contrary to the effects of the parent peptides, the effect is reversible and not dependent on PTX- or CTX-sensitive G proteins, PKA, PKC, or intracellular Ca^{2+} levels.

In principle, the effects of galparan could be caused by extra- or intracellular action of the peptide. In order to follow the mode of binding and cellular localization of galparan, a labeled peptide was required. It was expected that the free N terminus of galparan would be necessary for binding to galanin receptors in Bowes cells as well as for accomplishing its effects in other assays. Consequently, it was necessary to introduce a reporter group into the peptide chain.

Because a substitution of Pro^{13} to a Lys in the galanin peptide did not influence the affinity of the peptide for the galanin receptor,[12] a similar substitution of the Pro to Lys was introduced in galparan.[5] The Lys residue possesses an amino group on its side chain that is a convenient attachment point for a suitable reporter group. Biotin was used as a reporter group because it was considered a less disturbing modification compared to the widely used fluorophores, which possibly interact with plasma membranes. Indirect detection of biotin is more time consuming than direct visualization of a chromophore, but enables greater flexibility of methods.[5]

Strikingly, whereas cells incubated with similarly substituted galanin showed almost no intracellular staining in indirect immunofluorescence experiments, those incubated with the biotinylated galparan analogue were heavily labeled both in the cytoplasm and nucleus. In the hope that the new peptide could be used as a carrier vector, the peptide was named transportan.[5]

3.3 CELL PENETRATION OF TRANSPORTAN

Transportan is a 27-amino-acid-long peptide (Table 3.1) with properties of a typical cell-penetrating peptide. It enters cells rapidly at both physiological and low temperature, predominantly without using endocytosis or active transport.[5]

Incubation of cells with biotinyl-transportan-containing culture medium for 1 min at 37°C is sufficient for insertion of the peptide into plasma membrane, where it is easily detected by indirect immunofluorescence. In the following 5 to 10 min, transportan distributes to the nuclear envelope and other intracellular membranous structures. Subsequently, it concentrates in the nuclear envelope and inside the nuclei (Figure 3.1A). Lowering the incubation temperature decelerates but does not abolish translocation of transportan into cells (Figure 3.1D). The distribution of biotinyl-transportan in cells incubated at 37°C or 0 to 4°C is very similar, showing a preference of the peptide for membrane structures.

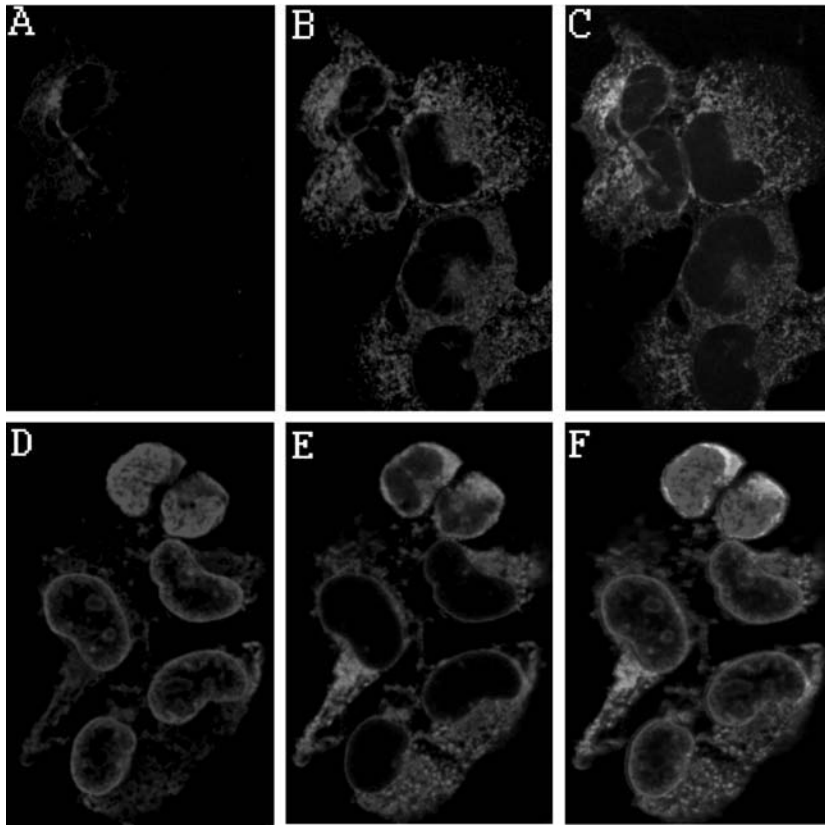

FIGURE 3.1 (Color Figure 3.1 follows p. 14.) Confocal microphotographs showing internalization of biotinyl-transportan. Bowes cells were incubated with 10 μ*M* biotinyl-transportan at 0˚C (A to C) or at 37˚C (D to F) for 60 min. Transportan was visualized by streptavidin-Texas Red (A, D) and membranes were stained with concanavalin A-FITC (B, E); the combined image is shown on C, F. (Reprinted from Pooga, M. et al., *FASEB J.,* 12, 67, 1998. With permission.)

However, there is one principal difference in respective cellular localization: after 1 h incubation at 0°C, the peptide does not accumulate in the nuclei. The reason for this is not clear yet, but could be explained by a slower redistribution of the peptide in the cell interior or a lower degree of intranuclear accumulation giving a concentration under the detection limit for this method. In addition, degradation of transportan in the cells at 37°C, but not at 0°C, can lead to formation of fragments capable of nuclear translocation. However, the analysis of internalized transportan by electrophoresis indicated the presence of intact transportan, but not the shorter fragments, which makes nuclear translocation after partial degradation of transportan less probable.

The nature of the cytosolic structures in which transportan concentrates was assessed using the fluorescently labeled lectin concanavalin A (Con A). Con A binds to glycoproteins with high mannose content and also stains, along with the plasma membrane and nuclear envelope, different intracellular membranous structures, and

especially the endoplasmic reticulum (Figure 3.1B, E). The combined image of peptide and Con A-TRITC localization in Bowes melanoma cells shows a preferential targeting of biotinyl-transportan to membranous structures, both at 0°C and 37°C (Figure 3.1C, F). Furthermore, we suggest the nucleoli to be the intranuclear structures where transportan concentrates, since the staining of the nucleoli with acridine orange coincided with localization of the peptide.[5]

The mechanism of cell entry of transportan remains unknown. Translocation of transportan into cells is probably not mediated by specific receptors in the plasma membrane, since the internalization of biotinyl-transportan cannot be blocked by preincubation of cells with tenfold excess of its "parent" compounds: galanin, mastoparan, or galparan. Other indirect evidence points to nonreceptor-mediated cell entry of transportan: we have not yet found a cell line that does not internalize the peptide. Moreover, for transportan, protein-mediated uptake can be excluded because extensive cross-linking of proteins on the cell surface does not abolish internalization of the peptide.[5]

In order to study the role of endocytosis in the internalization of transportan, hyperosmolar solution conditions and lowered temperature were used to suppress endocytosis. Clathrin-dependent endocytosis is inhibited by more than 90% in hyperosmolar solution through blockage of clathrin-coated pit formation.[13] In 0.45 *M* sucrose solution, Bowes cells shrink and change morphology slightly, but internalization of biotinyl-transportan is not markedly affected. Lowering temperature below 18°C abolishes endocytosis, but cellular translocation of transportan is not abolished even at 4 or 0°C. Thus, the cell entry of transportan is not an active cellular process and not directly fueled by ATP energy.

Transportan penetrates into cells rapidly; in a suspension of human melanoma Bowes cells, the half maximal intracellular concentration is reached in 3 to 5 min at 37°C as estimated from uptake experiments with radioactively labeled ([^{125}I]-Tyr^{9},N$^{\varepsilon 13}$-biotinyl)-transportan. The translocation into cells attached on plastic is slower, but still in the same time scale. Moreover, transportan not only enters cells, but also concentrates there. At first, using radioactively labeled transportan, we estimated that the intracellular transportan concentration at saturation exceeds the extracellular by at least twofold. More careful estimation of the cell volume revealed that the extent of intracellular accumulation of transportan is at least 20-fold.[14]

However, great care has to be taken when interpreting uptake data as cellular penetration only, since plasma membrane adsorption and uptake by endocytotic mechanisms also contributed in our uptake experiment using either radioactively or fluorophore-labeled transportan.

3.4 PROPERTIES OF TRANSPORTAN

The N-terminal part of transportan corresponds to the fragment of the neuropeptide galanin that is the main determinant of binding to type 1 galanin receptors (GalR1). Hence, binding of biotinyl-transportan to galanin receptors in Bowes cell membranes was expected. Biotinyl-transportan showed high affinity toward galanin receptors (K_D = 17 n*M*), exceeding that of the galanin fragment (1–13) several-fold, and of

fragment (1–12) — the galanin-derived sequence in transportan — more than 100-fold. However, biotinyl-transportan bound to galanin receptors less avidly than its predecessor, galparan ($K_D = 6.4$). The drop in affinity is probably due to replacement of galanin's Pro[13] in galparan to N^{ε}-biotinyl-Lys in transportan. As has been pointed out, even though transportan can bind to galanin receptors and thereby induce receptor-mediated endocytosis, this process is not determining the cell entry of this peptide.[5]

Mastoparan, the other component of transportan, is probably responsible for most of its unexpected properties. A family of 14-amino-acid-long peptides, mastoparans are one of the best studied amphiphilic peptides.[15] In aqueous solution, mastoparan is unfolded, but forms an amphiphilic α-helix[16] in the presence of lipids. Furthermore, mastoparan has been shown to penetrate into cell membranes and into cells.

The representatives of the mastoparan family of peptides show various biological activities such as degranulation of mast cells, activation of phospholipase A_2 and C, and release of histamine from mast cells, catecholamines from chromaffin cells, serotonin from platelets, and insulin from Rin m5F cells (for a review see Soomets et al.[15]).

Functional responses to the peptide have been proposed to result, at least partly, from activation of G-proteins[17] and the direct interaction of mastoparan with GTP-binding proteins has been demonstrated.[18] The activation is exerted through stimulation of GDP/GTP exchange analogously to G-protein-coupled receptors, indicating that mastoparans mimic receptors in ligand-bound conformation.[17] Therefore, we have studied the influence of transportan and all its analogues on GTPase activity. Contrary to mastoparan that activates GTPases, transportan, as well as its predecessor galparan, inhibits basal activity of GTPases[19] in Bowes cell membranes. However, to reveal the inhibitory activity, a rather high concentration of transportan is necessary (EC_{50} 21 μ*M*). The inhibitory effect is suggested to be caused by a direct interaction of transportan with the enzymes or possibly by changes of membrane properties or structure.[5] It is not clear what relevance this has in cells at the concentration of transportan used to deliver cargo into the cell.

3.5 STRUCTURE–ACTIVITY RELATIONSHIP OF TRANSPORTAN

To evaluate the significance of either part of the transportan sequence in cellular penetration and interactions with the signal transduction machinery, we changed the galanin or mastoparan moieties to different bioactive peptides.[14,20] The C-terminal half, mastoparan, is known to bind G-proteins, mimicking receptors in active conformation. In order to decrease this specific side effect, we designed TP 2, in which the mastoparan part was changed to the inactive analogue, mastoparan 17.[14]

In order to elucidate the role of the N-terminal hormone part, the galanin part was changed to a vasopressin V_{1a} selective antagonist and coupled to the mastoparan part through a 6-aminohexanoic linker producing TP 3, even though the predecessor of transportan 3, M391, was shown to bind to the V_{1a} vasopressin receptor with high affinity[21] and also exhibited nonreceptor-mediated biological activity. Finally, since it was thought that the amphiphilic helix is an important structural motif for membrane interaction, crabrolin, an amphiphilic peptide of hornet venom, was substituted for mastoparan in the sequence of TP 4.[22]

In the penetration studies performed with transportan and its analogues, transportan and TP 2 (galanin (1–12)-Lys-mastoparan 17) showed comparable uptake. TP 3 was found to be localized mainly to the plasma membrane rather than inside the cells, probably due to structural differences between galanin and vasopressin antagonist moieties. The TP 4 did not insert into the plasma membrane or enter the cells in a detectable amount; hence the mastoparan part with its amphipathic properties seems to contribute vastly to the ability of these peptides to traverse the cellular membranes.[14]

Penetratin and Tat-peptide are shorter than transportan, but still possess ability to penetrate into cells. In order to find the shortest transportan analogue with no or low biological activity that has similar cell-penetrating properties as the original peptide, we synthesized different deletion analogues of transportan (Table 3.1).[23]

Deletion of three or six residues from the N terminus of transportan (TP 7, TP 10) or the first two residues of the mastoparan part (TP 9) did not change the cellular penetration ability of the peptides. All three peptides could be detected in the cytoplasm and nucleus of Bowes cells. This lends further support for a nonendocytotic uptake mechanism for the transportans, since Trp^2 and Asn^5, which have been shown to be necessary for high affinity binding of this N-terminal fragment to the galanin receptor,[8] are not present in TP 10 molecule.

However, truncation of nine amino acid residues from the N terminus (TP 8) diminished the cellular penetration and deletion of amino acids 7 to 12 (TP 11) drastically decreased the uptake, possibly hinting at significance of the tyrosine in position 9.

It has been shown that mastoparan, the C-terminal part of transportan, penetrates into cell membranes and can be internalized to some small degree.[15] Therefore, it could be expected that the mastoparan part of transportan would be important in the uptake of this peptide. TP 9, where two amino acids in the N terminus of the mastoparan part are deleted, showed similar uptake as transportan in Bowes cells. Building on this, we deleted three (TP 12) or six (TP 14) amino acids from the N terminus of TP 9, respectively. The uptake of both peptides was significant, but somewhat lower than for transportan 9. Transportans 13 and 15, where a Lys residue has been deleted from the mastoparan part, did not show any detectable cellular uptake, pointing to the importance of positive charges for cell penetration.[23]

3.6 TRANSPORTAN AS DELIVERY VECTOR

3.6.1 Delivery of Peptides

In order to measure the delivery kinetics of transportan, constructs based on energy transfer quenching of the 2-amino-benzoic acid fluorophore were used.[24] The fluorophore is compatible with *t*-Boc chemistry, is resistant to photo-bleaching, and has a well-characterized amino acid-like quencher. The fluorophore model peptide cargo and the quencher CPP were connected by a disulfide bond that should be rapidly reduced in the cellular interior. After cleavage of the construct, the fluorescence intensity increased at least tenfold. This allowed us to follow the uptake of the peptide–cargo construct in real time without time-consuming cell isolation steps.

The total uptake displayed a roughly linear dependence of the amount of total construct in the experiment, showing that the transport mechanism was not saturated and that the upper limit of construct import (if such limits exist) was not reached within the concentration range used. At saturation, the cargo concentration inside the cells was about 400-fold higher than that which remained extracellularly, showing that transportan is indeed very efficient in delivering small peptides to the cytoplasm. In this assay, rate of transportan uptake was shown to be close to the rate obtained with the peptide itself. Moreover, transportan uptake was shown not to be disturbed by the presence of 10% fetal bovine serum in the incubation medium.

3.6.2 Delivery of PNA

Synthetic molecules that can specifically inhibit translation or transcription hold great promise as potential antisense and antigene drugs. The novel DNA mimics polyamide/peptide nucleic acid (PNA);[25] locked (LNA)[26] and morpholino nucleic acids[27] have probably the highest potential as antisense reagents, since they reveal high stability in biological fluids as well as *in vivo* conditions in general. Moreover, they show low toxicity and strong, specific pairing with complementary single-stranded RNA/DNA.

Among these DNA analogues, PNA with a noncharged achiral polyamide backbone to which the nucleobases are attached is one of the best studied.[28] Unfortunately, the uptake of unmodified PNA by most cell types in culture as well as *in vivo* is poor, especially at low or medium concentrations.[29] Consequently, in order to reach intracellular PNA concentration necessary for biological action, high or extremely high extracellular (20 to 100 μ*M*) concentrations are usually applied.[30]

To circumvent this problem, we used transportan to facilitate the cellular uptake of PNA. A disulfide bond was formed between an extra cysteine on $^{\varepsilon\text{-NH}}\text{Lys}^{13}$ of transportan and the biotinyl-Cys of PNA oligomer. Usually 4 to 8 h incubation with 10 to 20 μ*M* biotinyl-PNA is needed to yield intracellular concentration detectable by indirect immunofluorescence. In contrast, transportan-PNA constructs (TP-PNA) enter cells at remarkable speed; 5 to 10 min incubation of Bowes melanoma cells with 2 to 3 μ*M* TP-PNA is sufficient for internalization of detectable amounts of biotinyl-PNA. Prolonging incubation to 2 to 4 h leads to accumulation of PNA in the cells and concentrations as low as 0.1 μ*M* extracellular TP-PNA lead to a cellular concentration detectable by fluorescence.[29]

The cellular internalization of unmodified PNA at high concentrations results predominantly in granular staining, suggesting that the cells take up "naked" PNA by constitutive (or induced) endocytosis. After 4 to 8 h incubation, the delivered PNA is trapped in vesicular structures like endosomes or lysosomes and stays inactive. Later the staining spreads in the cell and is localized more diffusely, implying that part of the PNA has been liberated from lysosomes.

The cellular distribution of transportan-delivered PNA resembles that of transportan only at very initial steps of internalization (up to 5 min). Later their localizations do not overlap, confirming that, in the cell interior, the cargo is liberated from the carrier peptide after disulfide bond reduction and can follow its own signals for intracellular routing.

A 21-mer antisense PNA complementary to type 1 galanin receptor mRNA, delivered into Bowes melanoma cells either by transportan or penetratin, led to decrease of the level of the protein by more than 90% after 36 h at 3 μ*M* concentration of the construct. Moreover, *de novo* synthesis of GalR1 protein was blocked or reduced below the level of detection upon treatment of Bowes cells with the cell-penetrating PNA constructs. Antisense PNA cell-penetrating constructs are applicable in cells growing in culture and also *in vivo*. Administration of PNA constructs targeting the analogous region of the rat GalR1 mRNA into the lumbar spinal cord in rat leads to a profound down-regulation of galanin-binding sites. The loss of galanin-binding sites is accompanied by a reduction of the inhibition of galanin on the facilitation of the flexor reflex, suggesting that galanin receptors of type 1 mediate this physiological effect of galanin.[29]

3.6.3 Delivery of Proteins

In addition to small- or medium-sized hydrophilic biomolecules like peptides and oligonucleotides, proteins can also be transduced into a cell's interior by cell-penetrating peptides (for review, see Swartze et al.[31]).

We have studied whether transportan is able to convey proteins, ranging in molecular weight from 30 to 150 kDa, into cells by coupling transportan to the proteins with different coupling strategies. The connection of transportan to peptides or PNA oligomers via a disulfide bond enabled the transduction of the molecules into cells with subsequent liberation in the cytosol.[29] Hence, the disulfide bond was used to couple transportan with the green fluorescent protein (GFP) (Figure 3.2A).[32] Incubation of COS-7 cells for 10 min with 0.5 μ*M* construct suffices for GFP to insert into the membrane and translocate into cytosol. In 1 h most of the GFP fluorescence located to cytoplasmic membranes and, to a smaller extent, to the plasma membrane as judged by the presence of reticular structures detected by fluorescence microscopy and confocal laser scanning microscopy.

Treatment of GFP-S-S-TP adduct with dithiothreitol (DTT) before applying to the cells completely abolished GFP internalization, thus suggesting that the coupling of GFP to transportan is indeed necessary for translocation into the cells. However, when DTT was added to the medium after incubation with constructs, no decrease in fluorescence intensity was detected in either the cytosol or plasma membrane. This shows that transportan does not simply function as a membrane anchor for the protein.

The fluorescence of GFP is detectable at all stages of its cell translocation: in the solution surrounding the cells, in the plasma membrane, and inside the cells. The staining was seen both diffusely and in granular or vesicular structures. Since native GFP has a very tight barrel-shaped structure which must be preserved to be able to fluoresce, we suggest that GFP is not unfolded upon the passage across the membrane or in the cell interior. We may conclude that, even if unfolding of proteins facilitates its transduction into the cells, as was suggested previously,[33] it is not obligatory.

The 30-kDa green fluorescent protein is a rather small protein, but its efficient transportan-assisted translocation into cells inspired us to continue with bigger

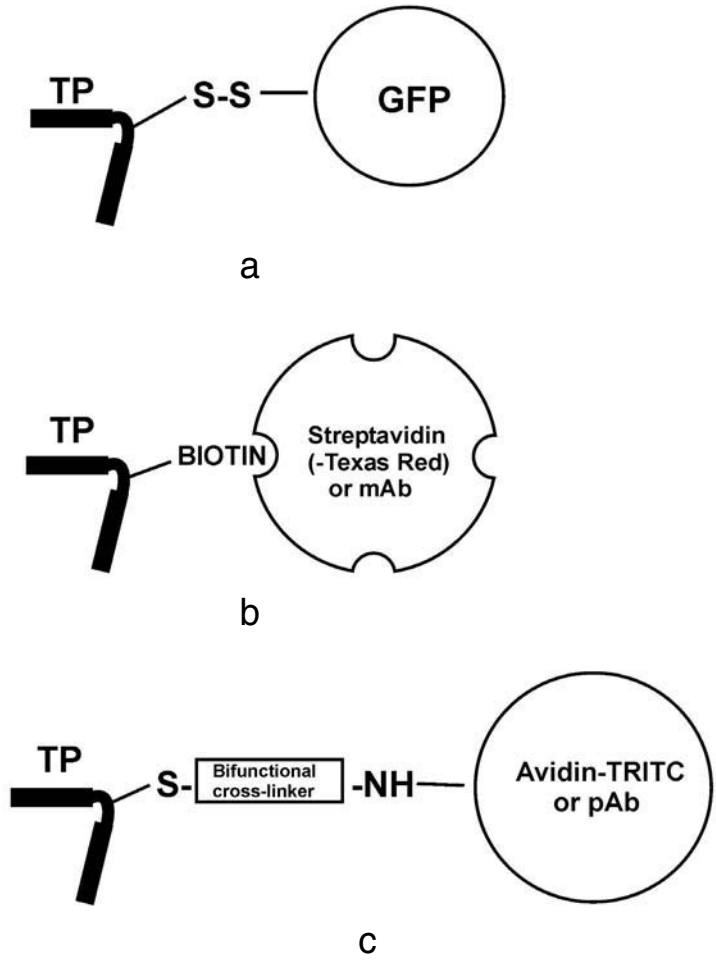

FIGURE 3.2 Coupling of transportan (TP) to different cargoes: (a) thiol group of Cys or biotin coupled to the side chain of Lys^{13} of TP; (b) primary amino group of the cargo protein or, specifically, a biotin-binding site of streptavidin and biotin antibody; (c) bifunctional cross-linker covalently coupling Cys in TP with primary amino groups of the cargo protein.

proteins. Thus, the delivery capacity of transportan was estimated using avidin of about 70 kDa and antibodies of 150 kDa molecular weight.

A bifunctional cross-linker SMCC [succinimidyl-4-(maleimidomethyl)-cyclohexane-1-carboxylate][34] was used to connect transportan and a cargo protein (Figure 3.2c), in order to obtain more stable conjugates than the disulfide-bridged adducts and to avoid the necessity of introducing extra cysteine into the protein to be delivered.

Commonly, the protein of interest is expressed in bacteria as a fusion with the cell-penetrating sequence and the construct is purified by applying different chromatographic methods. However, if the pure protein is available in sufficient amounts or its expression as a fusion protein with CPP sequence is cumbersome (e.g., antibodies), then chemical cross-linking of protein to a delivery peptide is a good alternative. Moreover, more than one CPP molecule could be coupled per molecule of the protein of interest by the chemical cross-link, which could facilitate the cell entry of bigger proteins. However, there are some drawbacks as well. The delivered protein cannot be dissociated from the transporter in the cells and the modification of functional domains of proteins by the cross-linker could lead to decrease or even loss of activity or function.

We chose TRITC-labeled avidin as the first medium-sized protein. The construct was prepared from avidin–TRITC and Cys-($^{N,\varepsilon}$Lys^{13})transportan by first coupling the cross-linker to the amino groups of avidin and then linking transportan via the sulfhydryl groups. The cellular uptake of the resulting TP–avidin–TRITC construct was rapid; in 5 min the red fluorescent signal was detectable in the plasma membrane of COS-7 or Bowes melanoma cells. After 30 min, staining was detectable all over the cytosol. It was mainly localized granularly, but some diffuse staining was present as well.

Modification of antibodies with transportan following the same cross-linking protocol enabled them to translocate into cultured cells. The time scale of internalization and the cellular distribution of transportan-conjugated antibodies were analogous to those of avidin–transportan constructs. We derivatized polyclonal antibodies recognizing human mitochondrial NifS protein with transportan. The ability of the antibodies to recognize the antigen was not lost upon conjugation with the delivery peptide, since detection of NifS protein by transportan-modified antibodies was not compromised in Western analysis. However, whether the cell-transduced antibodies are competent to find and bind their intracellular target and thereby to modulate its activity is not clear so far. We may conclude that transportan can carry relatively big proteins with molecular mass at least up to 150 kDa across the plasma membrane into the cell interior.

The possibility of utilizing a noncovalent complex of the transport peptide and a cargo molecule for delivery has not been studied so far. To fill this gap, we took advantage of the capability of avidin and streptavidin to form an extremely stable complex with biotin or biotin-labeled molecules. Streptavidin alone or in combination with the unlabeled cell-penetrating peptide cannot traverse the plasma membrane (Figure 3.3B). However, coapplication of biotinylated transportan along with streptavidin Texas Red conjugate into the culture medium led to intense staining of the plasma membrane of the cells in 5 to 15 min, confirming that, in solution, biotinylated transportan associated with labeled streptavidin (Figure 3.2b) and targeted the formed complexes into the plasma membrane. At 15 min, but more markedly at 30 min and later, transportan–streptavidin complexes had relocated from plasma membrane into cortical cytoplasm and were detectable in the perinuclear area of a cell (Figure 3.3A).

Internalized streptavidin–Texas Red (or its complexes with biotinyl–transportan) gave rise to weak diffuse staining of the cytosol with strong punctuate accumulation,

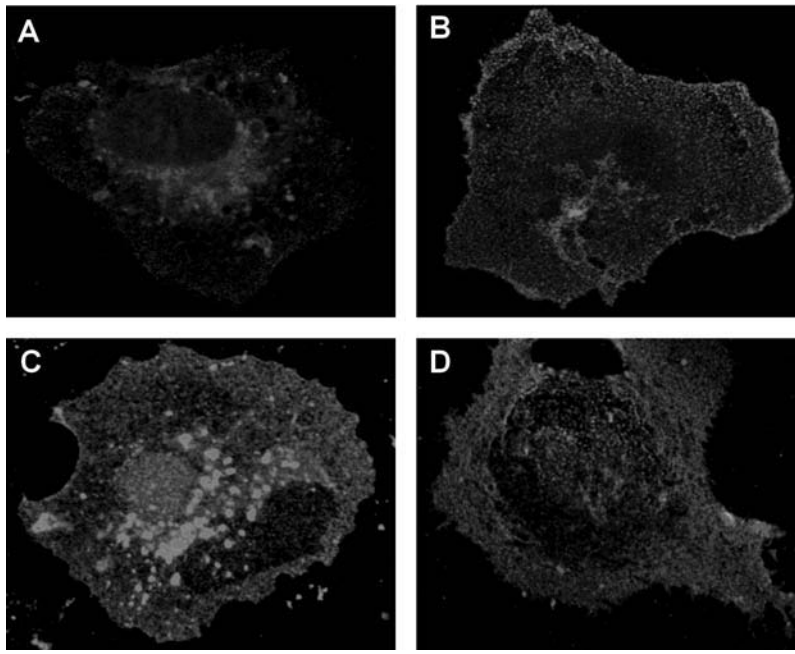

FIGURE 3.3 (Color Figure 3.3 follows p. 14.) (A) Delivery of streptavidin-Texas Red conjugate (SA-TxR) by biotinyl-transportan (bTP) into COS-7 cells. The cells were incubated for 2 h at 37°C with 2 μ*M* biotinyl-transportan and streptavidin-Texas Red (red) (1:100 dilution) in IMDM. (B) Nonbiotinylated transportan was applied into the culture medium along with SA-TxR. The plasma membrane was visualized with concanavalin A-FITC (green) (2 μg/ml). (C) Delivery of anti-biotin monoclonal antibody into Bowes cells by biotinyl-transportan. Cells were incubated with 2 μ*M* bTP and 1 μg/ml anti-biotin antibody (clone 33 "Boehringer–Mannheim") in culture medium for 2 h at 37ºC and stained after fixation with anti-mouse-FITC ("Sigma" 1:100). (D) Uptake of bTP-SA-TxR at 0°C (2 h incubation).

indicating that part of the delivered proteins was probably confined to vesicular substructures or concentrated in specific regions or organelles. The cellular distribution of streptavidin–Texas Red that had been translocated into the cells as a noncovalent complex with biotinyl–transportan was, in general, very similar to that observed for covalent transportan–avidin–TRITC constructs. We may conclude that covalent coupling of the transport peptide to a cargo protein is actually not obligatory, and their strong complexing is also sufficient for efficient transduction of a protein into cells.

Streptavidin has exceptionally high affinity towards biotin and forms very stable complexes with biotinyl–transportan. However, how strongly the delivery peptide must associate with a protein in order to guarantee transfer of a protein from outside to inside the cells is not known. Antibiotin monoclonal antibodies bind biotin with affinity several orders of magnitude lower than streptavidin does. Therefore, we investigated whether the interaction between the biotin moiety of transportan and

antibiotin antibodies is strong enough to enable insertion of formed complexes into plasma membrane of cells and following translocation into the cytosol. Indeed, antibiotin monoclonal antibodies are detectable in COS-7 cells after 1 to 2 h of incubation with complexes of biotinyl–transportan with antibiotin monoclonal antibodies at 37°C (Figure 3.3C).

The respective antibody localizes in the perinuclear and cortical areas of COS-7 cells as well as in the plasma membrane, confirming that transportan has succeeded to convey noncovalently bound antibodies into a cell's interior. Seemingly, the interaction between the transporter peptide and a cargo molecule (protein in this assay) must not necessarily be extra strong for delivery to occur; complexes of medium stability can be utilized, too.

The localization of the transduced proteins inside the cells is of primary importance to understanding whether they retain intactness and activity and if they are localized or trapped into organelles or accessibly in cytoplasm. Peptide-assisted cell transduction of the larger proteins has usually led to a granular-reticular pattern of intracellular distribution. The observed pattern suggests that delivered protein resides mainly in vesicular structures and that endocytosis could be responsible for most of the peptide-mediated protein translocation.

Consequently, we incubated COS-7 cells on ice in order to abolish endocytosis in tissue culture medium containing complexes of biotinyl–transportan with streptavidin–Texas Red conjugate. Incubation of cells with the respective complexes for 2 h on ice yielded a marked staining of the plasma membrane (Figure 3.3D) suggesting that, even at very low temperatures, transportan can target protein cargoes to the plasma membrane of cells and probably is able to penetrate into the membrane. Surprisingly, we observed some weak staining of cytosol in the vicinity of plasma membrane and also in the perinuclear area. Consequently, lowering the temperature cannot completely abolish internalization of transportan–protein complexes, implying that endocytosis is not the only mechanism involved in peptide-mediated cellular translocation of proteins.

Electron microscopy was used in order to get a more detailed view on the cellular structures where proteins reside after transportan-assisted delivery. Analogously to the fluorescence microscopy experiment, we applied biotinyl–transportan along with streptavidin labeled with colloidal gold into the culture medium. Despite the bulkiness of the label on the protein (the diameter of the gold particle is 10 nm), streptavidin–gold conjugate is translocated into cells by biotinyl–transportan. Inside the cells, delivered streptavidin resides mainly in a granulo-vesicular manner in structures, some of which are surrounded by membrane, but also diffusely in cytoplasm.

Localization of streptavidin–gold conjugates outside membrane-surrounded vesicles and diffusely in the cytoplasm after only 15 min of incubation suggests that the transportan-aided uptake of proteins cannot be explained solely by endocytosis. In principle, a possibility exists that the cell-delivered protein has escaped from clathrin coated vesicles or early endosomes and been able to localize into cytoplasm. However, since streptavidin–gold conjugates are diffusely localized in the cytoplasm already at the initial stages of internalization, this explanation is less plausible.

The general localization pattern of cell-delivered streptavidin obtained by fluorescence and electron microscopy is very similar. However, the results of electron microscopy studies suggest that, in parallel with endocytosis, another poorly understood process governs transportan-aided cellular translocation of proteins. Electron microscopy studies reveal also that conglomerates containing several labeled streptavidin and biotinyl–transportan molecules can cross the plasma membrane and enter the cells, showing the applicability of peptide-mediated transport for big supramolecular complexes.

3.7 METHODOLOGICAL CONSIDERATIONS

3.7.1 Cargo–CPP Conjugation Strategies

Several types of conjugation strategies have previously been used including pH-sensitive linkers, the reduction-sensitive disulfide bond, and direct backbone fusion. As CPPs have a cellular distribution and possible biochemical actions of their own, a labile bond between them and a cargo molecule would be advantageous. However, for larger cargo sizes in which the uptake rates are lower, the extracellular stability of the disulfide bond could be too low and a stable bond could be more favorable. Consequently, we have chosen to use disulfide bonds for smaller molecules and stable cross-linkers for larger cargo.

3.7.2 Disulfide Heterodimers

For synthesis of unsymmetrical disulfides between transport peptides and Cys-containing cargo, the 3-nitro-2-pyridinesulphenyl (Npys) derivative of Cys was coupled to the ε-amino group of Lys^{13} in transportan, or N terminally in the other CPPs. The S-Npys-protected peptides have been shown to react rapidly with thiols to form disulfides.[35] Because the ring nitrogen acts as an internal base in the reaction, it can be performed in low pH, which suppresses homodimer formation.

The constructs were synthesized using different solvent systems. However, a deoxygenated mixture of 3:2:1 DMSO/NMP/0.1 *M* sodium acetate, pH 4.5, gave the highest yield for peptides and PNA. The mixture was stirred gently overnight under nitrogen gas. In the case of peptide or PNA–CPP constructs, purification was performed on the reverse phase HPLC column and the final yield of the construct was around 30 to 50%.

3.7.3 Conjugation of Transportan to Proteins

For synthesis of the GFP–transportan construct, covalent protein dimers were reduced by incubating purified recombinant GFP with DTT. Residual DTT and salts were removed by gel filtration on Sephadex G-15 column. For the transportan–GFP conjugation, several solvent systems were tested and the best was found to be deoxygenated 40 m*M* Hepes buffer, pH 7.2, which contained 0.1 *M* KCl and 30% (v/v) ethanol.

For cross-linking of transportan to avidin–TRITC or antibodies, the proteins were modified with a fourfold molar excess of a bifunctional cross-linker succinimidyl-4-(N-maleimidomethyl)-cyclohexane-1-carboxylate (SMCC) in 0.1 *M* phosphate buffer, pH 8.5, for 5 min, as described by Peeters et al.[34] Nonreacted cross-linker was removed by gel filtration on Sephadex G-15 in 0.1 *M* phosphate buffer, pH 6.7, and the SMCC-modified protein was subsequently reacted overnight with transportan–cysteine using twofold molar excess of peptide.

Studies of the internalization of peptides into cells require a method of visualization, such as including a label to their sequences. Many commercially available labels, e.g., fluorescein, rhodamine, biotin, and digoxigenin, can be applied to label free amino groups in the sequence of peptides. Alternatively, radioactively labeled peptides can be used to characterize the internalization process quantitatively.

We have used biotinylated peptides because biotinylation can easily be performed using solid phase peptide synthesis. The internalization of the biotinylated peptides can be followed using indirect immunofluorescence. This method for visualization of the biotinyl label includes treatment of cells with biotinyl–peptides, permeabilization of cells, and subsequent treatment with an avidin or streptavidin–fluorochrome conjugate. Streptavidin is less basic and is not glycosylated, therefore showing fewer nonspecific reactions such as interactions with lectins or acidic groups on proteins or membranes, as compared to avidin.

In our studies, cells were treated with biotinylated peptides and, after permeabilization, were stained with streptavidin–FITC or avidin–TRITC and visualized under a fluorescence microscope. Two alternative fixation methods were used. First, cells were fixed and permeabilized simultaneously with methanol. As both fixing and permabilization occur in parallel, some of the peptides associated with the plasma membrane could be redistributed into the cell. The other method used was to fix cells first with paraformaldehyde and subsequently permeabilize with Hepes buffer/Triton X-100 mixture. This treatment should exclude the possibility of washing noninternalized peptides into the cell. However, in our experiments similar results were obtained with both methods.

3.8 STRUCTURAL ORGANIZATION OF TRANSPORTAN

Circular dichroism studies reveal that, in water, transportan behaves as a random coil and does not fold into any stable structure.[36] In the presence of SDS micelles, transportan adopts a secondary structure consisting of 60% helicity. The helix is localized in mastoparan part and galanin-derived N-terminal part is less structured. However, both parts are almost buried in the SDS micelles, leaving only the central connecting part of transportan clearly exposed to the solution, as shown by NMR studies. Considering these data, the interaction of transportan with membranes can be hypothesized. The mastoparan helix is inserted deeply into lipid bilayer with its axis perpendicular to the membrane interface; the connecting segment, containing the Lys residue where the labels and cargoes are coupled, protrudes from the membrane. The N terminus is residing partly in the membrane interface and is buried partly in the membrane.[36]

The molecular modeling of interaction of transportan and its analogues yields structures that correspond well to NMR data on the peptide in SDS micelles. The C-terminal part of the transportan analogues is predicted to be buried in the membrane; the only exception is TP15, whose N terminus becomes buried in the membrane. Both Lys residues of C terminus of the longest peptides (TP, TP7, and TP9) may reach the opposite side of the membrane, while the aromatic residues of the N terminal and the biotinyl group remain anchored in the first phospholipid polar head area.

According to calculation of the molecular hydrophobic potentials (MHP),[37] the N-terminal part is hydrophilic due to the presence of threonine, serine, or aromatic residues. Strikingly, TP15 has an inverted orientation, although this is the sole peptide that has a charged hydrophilic lysine residue instead of Lys-Ile-Leu in the C terminus. Thus, the most important features that determine the orientation of cell penetrating peptides in the membrane are peptide length and location of aromatic and lysine residues in the terminal regions of the sequence.

The transportan analogues have stable positions when inserted into the membrane, but their orientations in relation to the membrane surface differ. Therefore, we tried to group the results according to angle and depth of penetration into the membrane, a classification tightly correlated to peptide size. Two predicted parameters may be correlated with the ability of the peptides to traverse phospholipid membranes. First, an oblique orientation relative to the membrane plane seems to be important, since peptides predicted to have a more parallel orientation in relation to the membrane (angle less than 40 to 45°) internalize efficiently. In contrast, short peptides (22 amino acids or less) with more perpendicular orientation internalize poorly (e.g., TP 11), if at all (TP 13 and TP 15). Second, transportan and its derivatives of 24–25 amino acids, i.e., long analogues, penetrate into cells more efficiently. The increased length of the peptide seems to facilitate penetration into the hydrophobic core. Shorter peptides (less than 21 residues) may not reach the second leaflet and are therefore too short to span the lipid bilayer.

Although transportan is in random-coil formation when water solution, it seems to be organized as an ensemble of different multimers, ranging from predominant dimers to molecular assemblies with high molecular weight. Multimerization can be induced by the interaction of peptide with detergent micelles or membrane lipids, as suggested by Derossi et al.[1] However, when we used biotinyl–transportan to transduce the tagged streptavidin into cells, we often observed formation of large, labeled rod-like structures in both electron and fluorescence microscopy, probably generated due to multimerization of transportan in solution.[38] Huge assemblies form preferentially when streptavidin is incubated with biotinyl–transportan in a small volume, for a long time, or at high concentration, lending more support to the probable multimerization of transportan in solution. Both penetratin and transportan tend to form multimers and assemblies in solution; whether this is coincident or somehow related to their ability to penetrate into cells is not clear yet.

We have demonstrated that transportan, a chimera consisting of galanin (1–13) coupled to mastoparan (1–14) is a cell-penetrating peptide. Furthermore, the uptake of transportan is probably not receptor or energy dependent. Transportan can be shortened by at least six amino acids and modified with respect to its amphiphilicity,

and still retain efficient uptake. Moreover, transportan can deliver proteins in a native, folded state of up to at least 150 kDa to the cytoplasm of living cells.

ACKNOWLEDGMENTS

This work was supported by grants from the EC Biotechnology Project BIO4-98-0227, Swedish Research Councils TFR and NFR, and Estonian Science Foundation (ESF4007).

REFERENCES

1. Derossi, D. et al., The third helix of the Antennapedia homeodomain translocates through biological membranes, *J. Biol. Chem.,* 269, 10444, 1994.
2. Vivés, E., Brodin, P., and Lebleu, B., A truncated HIV-1 Tat protein basic domain rapidly translocates through the plasma membrane and accumulates in the cell nucleus, *J. Biol. Chem.,* 272, 16010, 1997.
3. Elliott, G. and O'Hare, P., Intercellular trafficking and protein delivery by a herpesvirus structural protein, *Cell,* 88, 223, 1997.
4. Chaloin, L. et al., Conformations of primary amphipathic carrier peptides in membrane mimicking environments, *Biochemistry,* 36, 11179, 1997.
5. Pooga, M. et al., Cell penetration by transportan, *FASEB J.,* 12, 67, 1998.
6. Oehlke, J. et al., Cellular uptake of an alpha-helical amphipathic model peptide with the potential to deliver polar compounds into the cell interior nonendocytically, *Biochim. Biophys. Acta.,* 1414, 127, 1998.
7. Langel, Ü. et al., A galanin-mastoparan chimeric peptide activates the Na^+,K^+-ATPase and reverses its inhibition by ouabain, *Regul. Pept.,* 62, 47, 1996.
8. Land, T. et al., Linear and cyclic N-terminal galanin fragments and analogs as ligands at the hypothalamic galanin receptor, *Int. J. Pept. Protein. Res.,* 38, 267, 1991.
9. Langel, Ü., Land, T., and Bartfai, T., Design of chimeric peptide ligands to galanin receptors and substance P receptors, *Int. J. Pept. Protein. Res.,* 39, 516, 1992.
10. Consolo, S. et al., Galparan induces *in vivo* acetylcholine release in the frontal cortex, *Brain Res.,* 756, 174, 1997.
11. Östenson, C-G. et al., Galparan: a powerful insulin-releasing chimeric peptide acting at a novel site, *Endocrinology,* 138, 3308, 1997.
12. Pooga, M. et al., Novel galanin receptor ligands, *J. Pept. Res.,* 51, 65, 1998.
13. Heuser, J.E. and Anderson, R.G., Hypertonic media inhibit receptor-mediated endocytosis by blocking clathrin-coated pit formation, *J. Cell. Biol.,* 108, 389, 1989.
14. Lindgren, M. et al., Translocation properties of novel cell penetrating transportan and penetratin analogues, *Bioconjug. Chem.,* 11, 619, 2000.
15. Soomets, U. et al., From galanin and mastoparan to galparan and transportan, *Curr. Top. Pept. Protein. Res.,* 2, 83, 1997.
16. Higashijima, T. et al., Conformational change of mastoparan from wasp venom on binding with phospholipid membrane, *FEBS Lett.,* 152, 227, 1983.
17. Higashijima, T. et al., Mastoparan, a peptide toxin from wasp venom, mimics receptors by activating GTP-binding regulatory proteins (G proteins), *J. Biol. Chem.,* 263, 6491, 1988.
18. Mousli, M. et al., G protein activation: a receptor-independent mode of action for cationic amphiphilic neuropeptides and venom peptides, *Trends Pharmacol. Sci.,* 11, 358, 1990.

19. Zorko, M. et al., Differential regulation of GTPase activity by mastoparan and galparan, *Arch. Biochem. Biophys.,* 349, 321, 1998.
20. Pooga, M. et al., Galanin-based peptides, galparan and transportan, with receptor-dependent and independent activities, *Ann. N.Y. Acad. Sci.,* 863, 450, 1998.
21. Hällbrink, M. et al., Effects of vasopressin-mastoparan chimeric peptides on insulin release and G-protein activity, *Regul. Pept.,* 82, 45, 1999.
22. Krishnakumari, V. and Nagaraj, R., Antimicrobial and hemolytic activities of crabrolin, a 13-residue peptide from the venom of the European hornet, *Vespa crabro,* and its analogs, *J. Pept. Res.,* 50, 88, 1997.
23. Soomets, U. et al., Deletion analogues of transportan, *Biochim. Biophys. Acta,* 1467, 165, 2000.
24. Meldal, M. and Breddam, K., Anthranilamide and nitrotyrosine as a donor-acceptor pair in internally quenched fluorescent substrates for endopeptidases: multicolumn peptide synthesis of enzyme substrates for subtilisin Carlsberg and pepsin, *Anal. Biochem.,* 195, 141, 1991.
25. Nielsen, P.E. et al., Sequence-selective recognition of DNA by strand displacement with a thymine-substituted polyamide, *Science,* 254, 1497–1500, 1991.
26. Kumar, R. et al., The first analogues of LNA (locked nucleic acids): phosphorothioate-LNA and 2′-thio-LNA, *Bioorg. Med. Chem. Lett.,* 8, 2219, 1998.
27. Summerton, J., Morpholino antisense oligomers: the case for an RNase H-independent structural type, *Biochim. Biophys. Acta,* 1489, 141, 1999.
28. Ray, A. and Nordén, B., Peptide nucleic acid (PNA): its medical and biotechnical applications and promise for the future, *FASEB J.,* 14, 1041, 2000.
29. Pooga, M. et al., Cell penetrating PNA constructs regulate galanin receptor levels and modify pain transmission *in vivo*, *Nat. Biotechnol.,* 16, 857, 1998.
30. Sei, S. et al., Identification of a key target sequence to block human immunodeficiency virus type 1 replication within the gag-pol transframe domain, *J. Virol.,* 74, 4621, 2000.
31. Schwarze, S.R., Hruska, K.A., and Dowdy, S.F., Protein transduction: unrestricted delivery into all cells? *Trends Cell. Biol.,* 10, 290, 2000.
32. Tsien, R.Y., The green fluorescent protein, *Annu. Rev. Biochem.,* 67, 509, 1988.
33. Schwarze, S.R. et al., *In vivo* protein transduction: delivery of a biologically active protein into the mouse, *Science,* 285, 1569, 1999.
34. Peeters, J.M. et al., Comparison of four bifunctional reagents for coupling peptides to proteins and the effect of the three moieties on the immunogenicity of the conjugates, *J. Immunol. Methods,* 120, 133, 1989.
35. Bernatowicz, M.S., Matsueda, R., and Matsueda, G.R., Preparation of Boc-[S-(3-nitro-2-pyridinesulfenyl)]-cysteine and its use for unsymmetrical disulfide bond formation, *Int. J. Pept. Protein. Res.,* 28, 107, 1986.
36. Lindberg, M. et al., Secondary structure and position of the cell-penetrating peptide transportan in SDS micelles as determined by NMR, *Biochemistry,* 40, 3141, 2001.
37. Brasseur, R., Differentiation of lipid-associating helices by use of three-dimensional molecular hydrophobicity potential calculations, *J. Biol. Chem.,* 266, 16120, 1991.
38. Pooga, M. et al., Cellular translocation of proteins by transportan, *FASEB J.,* 15, 1400, 2001.

4 Model Amphipathic Peptides

Johannes Oehlke, Burkhard Wiesner, and Michael Bienert

CONTENTS

0-8493-1141-1/02/$0.00+$1.50

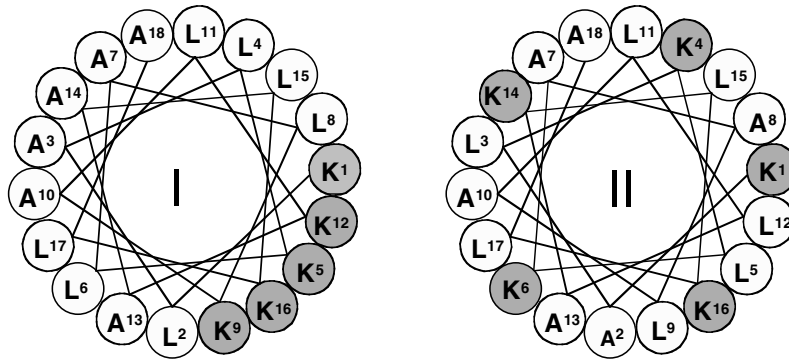

FIGURE 4.1 Helical wheel projections of the amphipathic and nonamphipathic peptide pairs I and II.

ABSTRACT

The term MAPs (model amphipathic peptides) designates a group of peptides derived from the α-helical amphipathic model peptide KLALKLALKALKAALKLA-NH_2, which is taken up by mammalian cells in a nonendocytic way. The mechanism of the cellular uptake of MAPs proved to be highly complex and involves energy-dependent as well as -independent processes to a comparable extent. Stepwise structural alterations with respect to chain length, charge, and helix parameters failed to provide information about essential structural requirements for the cellular uptake of MAP. Instead, evidence was found for a structure-independent cellular uptake of all investigated peptides, an enrichment within the cell of amphipathic members of the series, and a rapid washout of the nonamphipathic ones. Extensive translocation into the cell interior was also found for disulfide-bridged peptide and phosphorothioate oligonucleotide conjugates with MAPs. However, no improvement with respect to the cellular uptake of naked oligonucleotides was observed for the peptide–phosphorothioate oligonucleotide conjugates.

4.1 INTRODUCING HISTORY

The term MAPs (model amphipathic peptides[1]) designates a group of peptides derived from the α-helical amphipathic model peptide KLALKLALKAL-KAALKLA-NH_2 (I, Figure 4.1), originally designed by Steiner et al.[2] and initially used in our group for biophysical studies on interactions of bioactive helical amphipathic peptides with lipidic interfaces.[3-7] Throughout the course of these studies mammalian cells were exposed to the fluorescein-labeled helical amphipathic and nonamphipathic pair I and II (KALKLKLALALLAKLKLA-NH_2, Figure 4.1) and to the all-D-amino acid analog and double-D-amino acid analogs of I in order to obtain information about the influence of amphipathicity on adsorption to the cell surface.

Confocal laser scanning microscopy (CLSM)-monitoring of these experiments revealed unexpectedly extensive intracellular fluorescence after exposure to I and

its D-amino acid analog, but not after incubation with its nonamphipathic counterpart II and a double D-amino acid with impaired amphipathicity;[8] this suggested an amphipathicity-dependent cellular uptake. Internalization of the synthetic peptide I and its D-analog was observed even at 0°C and after energy depletion[8] analogous to that reported for the natural Antennapedia sequence[9] indicating a nonendocytic mode of uptake. Further studies confirmed these surprising initial observations and provided evidence for the involvement of various nonendocytic mechanisms in this process.[10]

4.2 MECHANISTIC ASPECTS OF THE CELLULAR UPTAKE OF MAPs

4.2.1 Quantitation of Internalized MAPs

MAPs exhibit strong membrane lytic properties at concentrations above 4 μ*M*;[10] thus cellular uptake experiments must be confined to concentrations below this value in order to avoid bias of the results by pore formation. The resulting peptide levels in the cell lysates nevertheless proved sufficient for HPLC analysis by fluorescence detection. The surface-bound portion of cell-associated MAPs found in the cell lysates, however, exceeded that actually internalized by about tenfold.[10] Therefore precise discrimination of both peptide fractions was required as a precondition for quantitative deductions. Such discrimination was achieved by treatment of the peptide-exposed, washed cells with diazotized 2-nitroaniline.[10] This reagent, previously shown to modify surface-bound primary amino compounds while leaving those within the cell intact,[11] has the crucial advantage of being highly reactive even at 0°C, so that bias of the results by counteracting efflux processes, strongly attenuated or suppressed at this temperature, is minimized. By contrast, acid washing of the peptide-loaded cells (5 min at 0°C with HAc/NaCl, 0.2 *M*/0.05 *M*), a procedure commonly used to strip surface-bound peptides, failed to remove I from the cell surface (loss <5%).[10]

4.2.2 Cellular Uptake of I at 37 and 0°C in Comparison with That of Its All-D Analog and That of the Antennapedia Sequence XV

The HPLC-determined quantity of intact I internalized after 30 min (Figure 4.2) corresponded to an approximately fivefold enrichment within the cell,[10] which, considering that the endosomal compartment comprises only about 10% of cell volume,[12] contradicted an endocytic mode of uptake. The high uptake of I observed at 0°C strongly supports this conclusion (Figure 4.2).

With the all-D-amino acid analog of I and the Antennapedia peptide XV,[9] uptake at 37 and 0°C similar to that of the parent peptide was observed (Figure 4.2), ruling out sterically specific interactions on the internalization of MAPs and suggesting an analogy to the cellular uptake of protein-derived cell-penetrating peptides.[1,13,14] The differences between the internalized quantities of I and its all-D-analog can be explained by the resistance of the latter towards metabolic breakdown.[10]

No internalization could be detected by this protocol for II, the nonamphipathic analog of I.[10] These findings led to the initial conclusion that amphipathicity is

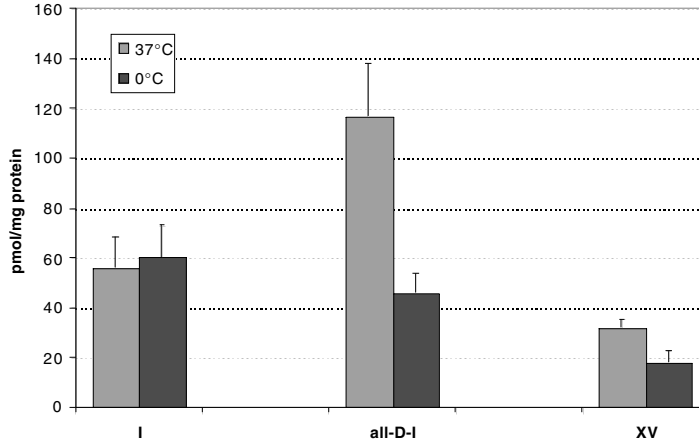

FIGURE 4.2 Intact fractions of cell-associated peptide after exposing LKB Ez 7 cells for 30 min at 37 and at 0°C to 1.8 μ*M* I, the all-D enantiomer of I, and the Antennapedia peptide XV[9] and subsequent treatment with diazotized 2-nitroaniline. Before exposure to the peptide at 0°C the cells were incubated in DPBSG for 60 min at 0°C. Each bar represents the mean of three samples ± SD.

essential for this type of peptide to enter mammalian cells; this was modified later, in that amphipathicity mediates only retrieval within the cell, combined with reduced efflux (see below). Likewise, the inability to detect cellular uptake of II also argues against a significant contribution from endocytosis to the internalization of I. If adsorptive endocytosis were to be the predominant mechanism for the uptake, then peptide II should also be internalized to a clearly measurable degree, since this derivative, which possesses the same number of positive charges as I, has been found to be adsorbed extensively to the cell surface (to about 30% to that of cell-associated I).[8]

4.2.3 Effects of Factors Known to Affect Endocytosis or Transport Protein Function on the Cellular Uptake of I

Figure 4.3 shows the effects of energy depletion, lowered temperature, pH, and ionic composition of the incubation buffer, and of additives known to affect endocytosis or to inhibit mdrp or MRP and the large anion transporter, respectively, upon internalization of I into aortic endothelial cells. With the exception of calcium depletion and vincristine treatment, the total quantity of internalized I was affected significantly in all cases. Potassium depletion (known to inhibit clathrin-dependent endocytosis[15,16]) elevation of lysosomal pH by 100 μ*M* chloroquine,[17] disturbance of endosomal transport by 5 μ*M* Brefeldin A,[18] addition of DNP-S-glutathione (100 μ*M*) (an inhibitor of MRP and the large anion transporter MOAT[19,20]), and depletion of magnesium had no effect upon internalization of I.[10]

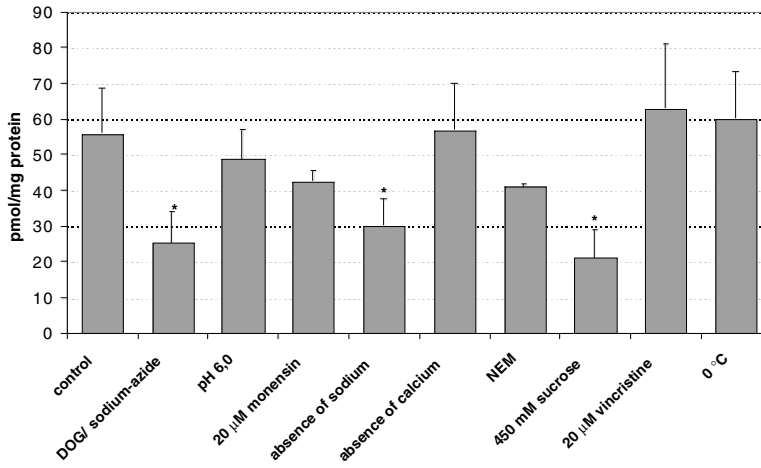

FIGURE 4.3 Intact fractions of cell-associated peptide after exposing LKB Ez 7 cells for 30 min at 37°C to 1.8 μ*M* I dissolved in DPBSG (control and NEM, respectively), in DPBSG adjusted with HCl to pH 6.0, in sodium-free buffer (DPBSG with NaCl and phosphates replaced by 137 m*M* choline chloride and 10 m*M* HEPES, respectively), in DPBSG without calcium (absence of calcium), in DPBS containing 25 m*M* 2-deoxyglucose/10 m*M* sodium azide (DOG/sodium azide) or 20 μ*M* monensin or 20 μ*M* vincristine, respectively, and in DPBSG at 0°C, followed by treatment with diazotized 2-nitroaniline. Before exposure to the peptide, the cells used for the NEM, DOG/sodium azide and 0°C experiments were incubated at 37°C for 5 min in DPBSG containing 1 m*M* N-ethylmaleimide and subsequently rinsed three times with DPBSG (NEM), or incubated for 60 min at 37°C in DPBS containing 25 m*M* 2-deoxyglucose/10 m*M* sodium azide (DOG/sodium azide), or in DPBSG for 60 min at 0°C, respectively. Each bar represents the mean of three samples ± SD. The differences between the respective controls and the asterisk-labeled bars are statistically significant at $p \leq 0.05$ (Student's *t* test).

The observed energy-dependent component of the uptake of I would normally, according to established knowledge, imply an endocytic mechanism. The results of the experiments conducted with I, however, provide arguments for and against this. As outlined earlier, the high quantity of internalized I and complete lack of cellular uptake of its nonamphipathic analog II are contraindicative of an endocytic mechanism. Further arguments against the significant involvement of endocytosis are the absence of any effect of potassium depletion and the significant inhibitive effect of sodium depletion. On the other hand, the strong effects of energy depletion, lowered temperature, alteration of internal and external pH, presence of hyperosmolar sucrose, and pretreatment with NEM are commonly considered characteristic of clathrin-dependent[15,21,22] or cavaeolae-mediated endocytosis,[23,24] respectively.

It should be noted, however, that these effects might also be explained by translocation events mediated by carrier proteins or proceeding across protein channels, which have often been found to exhibit pH and energy dependence.[25-27] In the

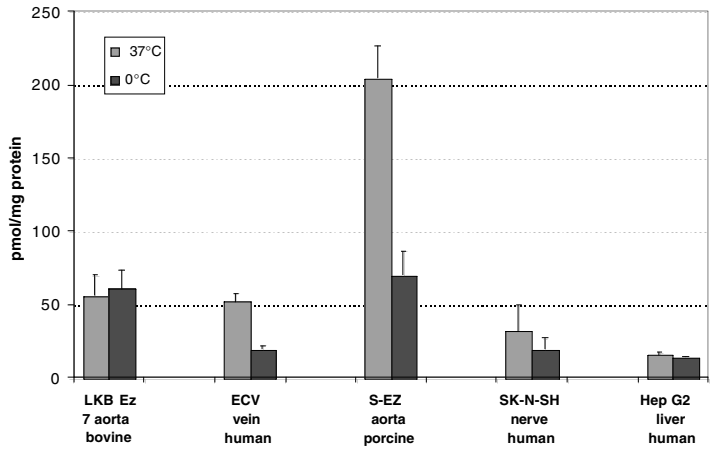

FIGURE 4.4 Intact fractions of cell-associated peptide after exposing various cell types from different species and organs for 30 min at 37 and at 0°C to 1.8 μ*M* I, the all-D enantiomer of I, and the Antennapedia peptide XV[9] and subsequent treatment with diazotized 2-nitroaniline. Before exposure to the peptide at 0°C the cells were incubated in DPBSG for 60 min at 0°C. Each bar represents the mean of three samples ± SD.

same way, the effect of hyperosmolar sucrose might be interpreted as the effect of membrane shrinking due to hyperosmolar stress.[28]

Taken together and based on data currently available, an unequivocal decision for either of the mechanisms discussed appears impossible. In context, however, these data imply that multiple, probably nonendocytic mechanisms are involved in the uptake into mammalian cells of MAPs.

4.2.4 Uptake of MAPs into Various Cell Types from Different Species and Organs

After exposure to I of endothelial cells from other species, as well as other cell types, an extensive uptake of I at 37 and 0°C with significant variability was observed in all cases (Figure 4.4). These findings indicated that nonendocytic mechanisms responsible for the cellular uptake of MAPs were generally operative.

4.3 INVESTIGATION OF STRUCTURAL REQUIREMENTS FOR CELLULAR UPTAKE OF MAPs

4.3.1 Influence of Hydrophobicity, Hydrophobic Moment, and Size of the Hydrophilic Face on Cellular Uptake of Helical Peptides

The cellular uptake of a series derived from I by exchange of Leu-11 against the internal fluorescent probe Trp and by stepwise alterations of hydrophobicity, hydrophobic moment, and hydrophilic face (with retention of positive charge and helix-forming propensity) was assessed by the earlier described HPLC protocol (Table 4.1;

TABLE 4.1
Internalization of Peptide into Aortic Endothelial Cells and Fluorescein Leakage

Peptide composition	pmol internalized peptide/mg protein	Fluorescein leakage related to that of KLA1-exposed cells	H	μ	Φ (°)	α-helix (%) 50% TFE
KLALKLALKAW-KAALKLA-NH_2	161 ± 21	1.0 ± 0.09	–0.025	0.329	80	73
KLALKAALKAW-KAAAKLA-NH_2	15 ± 6	0.75 ± 0.14	–0.056	0.329	80	68
KLALKAAAKAW-KAAAKAA-NH_2	<10	0.79 ± 0.12	–0.087	0.329	80	59
KITLKLAIKAW-KLALKAA-NH_2	47 ± 7	0.98 ± 0.16	–0.027	0.284	80	69
KIAAKSIAKIW-KSILKIA-NH_2	68 ± 2	1.46 ± 0.36	–0.026	0.406	80	64
KALAKALAKLW-KALAKAA-NH_2	149 ± 20	1.21 ± 0.11	–0.056	0.391	80	67
KLALKLALKWA-KLALKAA-NH_2	15 ± 4	0.75 ± 0.14	–0.025	0.320	80	61
KLLAKAAKKWL-LLALKAA-NH_2	29 ± 14	0.72 ± 0.10	–0.025	0.300	100	60
KLLAKAALKWL-LKALKAA-NH_2	44 ± 10	1.39 ± 0.42	–0.025	0.295	120	55
KALKKLLAKWL-AAAKALL-NH_2	218 ± 31	1.42 ± 0.17	–0.025	0.299	140	62
KLAAALLKKWK-KLAAALL-NH_2	226 ± 19	0.94 ± 0.12	–0.025	0.297	160	60
KALAALLKKWA-KLLAALK-NH_2	341 ± 58	0.89 ± 0.09	–0.025	0.291	180	62

Note: After preloading with fluorescein diacetate and exposure for 30 min at 37°C to 4.5 μ*M* solutions in DPBSG of I-related peptides showing stepwise alterations of the helix parameters hydrophobicity (H), hydrophobic moment (μ), and hydrophilic face (Φ).

Reference 29). In order to facilitate monitoring of toxic effects of the respective peptides by leakage of fluorescein from the cell interior after preloading with diacetylfluorescein, a generally slightly toxic peptide concentration of 5 μ*M* was chosen for these experiments. Under these conditions the parent peptide I induced 30% fluorescein leakage.[10] That the results obtained at the slightly toxic 5 μ*M* peptide concentration were not biased significantly by partial damage to the plasma membrane was ascertained by additional experiments performed at the nontoxic 2 μ*M* peptide concentration that led to analogous results.[29]

Clear cellular uptake and pore-forming activity were found in almost all cases (Table 4.1). No unambigous correlation, however, either between physicochemical parameters and uptake behavior pore-forming activity or between uptake behavior and pore-forming activity was apparent from the data. Generally these findings argue against a decisive role of any of the altered helix parameters on cellular uptake.

4.3.2 Influence of Molecular Size, Charge, and Primary Structure

Table 4.2 summarizes results of cell experiments performed with a series derived from I by alterations in chain length, charge- and helix-forming propensity, and an N-terminal carboxy fluorescein tag. Comparison with the results obtained with the tryptophan-labeled series is justified by the similar uptake and toxicity found for related pairs of tryptophan- and fluorescein-labeled analogs.[29]

Reduction of chain length by two amino acid residues had no significant influence upon the amount of internalized peptide (III, Table 4.2). Shortening the molecule by four amino acid residues, either N or C terminally, however, resulted in a substantial loss of uptake and membrane toxicity (IV, V, Table 4.2), suggesting that a minimum chain length corresponding to four complete helix turns was essential.

Replacement of two of the five lysines of the molecule by glutamine residues reduced the uptake markedly, accompanied by a clear reduction in membrane toxicity (VII, Table 4.2). Surprisingly, further elimination of basic lysine side chains resulted in significantly enhanced internalization (VIII, IX, Table 4.2), even when the noticeable contributions of surface-bound peptide to the quantity of IX measured in the cell lysate are taken into consideration. In the case of IX (and also of X) the lack of side chain amino groups prevented the differentiation of surface-bound from internalized peptide fractions by means of diazotized 2-nitroaniline. That IX has been actually internalized at least comparably to I is suggested by the threefold increase in the level of fluorescent metabolites in the cell lysate of IX-treated cells compared to that found after exposure to I.[29] CLSM (see below) revealed a similar image for both I- and IX-treated cells, again indicating comparable uptake. Reduction of the helix-forming propensity by Ala–Gly replacement strongly impaired the degree of internalization (VI, Table 4.2). Taken together, these results imply that helical amphipathicity is the most decisive structural requirement of MAPs for achieving high intracellular concentrations.

Additional uptake experiments performed with two pairs of helical amphipathic and nonamphipathic peptides, unrelated to I and with a lower net charge (XI to XIV, Table 4.2), confirmed the crucial role of amphipathicity and likewise the conclusion that net positive charge is not decisive in this context.[29] Clear cellular uptake of a

TABLE 4.2
Internalization of Peptide into Aortic Endothelial Cells and Fluorescein Leakage

Peptide	Peptide composition	pmol internalized peptide/mg protein	Fluorescein leakage related to that of I-exposed cells[a]	H	μ	Φ (°)	α-helix TFE	α-helix SDS
I	KLALKLALKALK-AALKLA-NH_2	228 ± 54	1.0 ± 0.38	–0.0161	0.3339	80	60	68
III	KLALKLALKAL-KAALK-NH_2	218 ± 23	3.13 ± 0.47	–0.0161	0.3339	80	52	61
IV	KLALKALKAAL-KLA-NH_2	<30	0.30 ± 0.18	–0.0317	0.3358	60	45	51
V	KLALKLALKAL-KAA-NH_2	<30	0.43 ± 0.25	–0.0317	0.330	80	50	59
VI	KLGLKLGLKGLK-GGLKLG-NH_2	<30	0.33 ± 0.19	–0.0461	0.313	80	13	8
VII	KLALKLALKALQ-AALQLA-NH_2	42 ± 12.4	0.59 ± 0.23	0.0294	0.2912	80	53	66
VIII	KLALQLALQALQ-AALQLA-NH_2	461 ± 44	1.03 ± 0.10	0.075	0.2505	80	78	78
IX	QLALQLALQALQ-AALQLA-NH_2	5670 ± 3971[b]	0.95 ± 0.62	0.0978	0.234	80	72	72
X	ELALELALEALE-AALELA-NH_2	135 ± 14.6[b]	0.34 ± 0.28	0.117	0.216	80	84	21
XI	LKTLATALTKLA-KTLTTL-NH_2	539 ± 80	0.88 ± 0.35	–0.025	0.3414	160	95	79
XII	LLKTTALLKTTA-LLKTTA-NH_2	n.d.[c]	0.57 ± 0.17	–0.025	0	360	74	39
XIII	LKTLTETLKELT-KTLTEL-NH_2	141 ± 54	0.79 ± 0.32	–0.170	0.387	220	78	56
XIV	LLKTTELLKTTE-LLKTTE-NH_2	n.d.[c]	0.42 ± 0.15	–0.170	0	360	52	17
XV	RQIKIWFQNRR-MKWKK-NH_2	216 ± 58	0.29 ± 0.10	–0.4822	0.1652	280	29	23

Note: After preloading with fluorescein diacetate and exposure for 30 min at 37°C to 4.5 μ*M* solutions in DPBSG of N-terminally fluorescein-labeled I-related peptides with alterations in chain length, charge and helix parameters, to I-nonrelated amphipathic/nonamphipathic peptide pairs (XI/XII, XIII/XIV), possessing reduced net charge with respect to I, and to the natural cell permeable Antennapedia peptide XV.[9,13]

[a] Fluorescein content of I exposed cells/fluorescein content of peptide exposed cells.

[b] No discrimination between internalized and surface-bound peptide possible with diazotized. 2- nitroaniline because of the lack of modifiable side chain amino groups.

[c] Nondetectable.

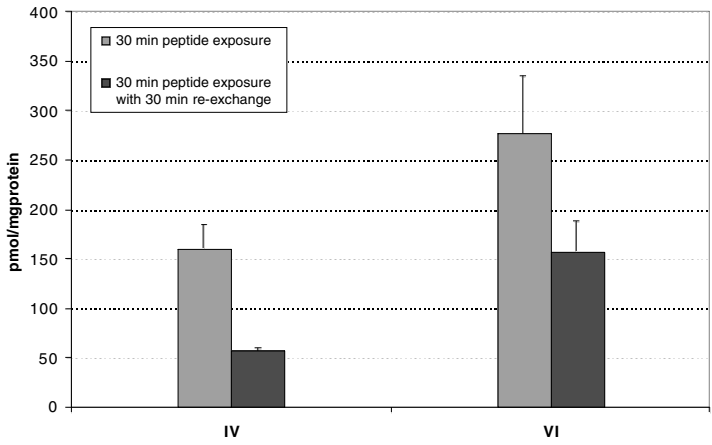

FIGURE 4.5 Intact fractions of cell-associated peptide after exposing LKB Ez 7 cells for 30 min at 37°C to 50 μ*M* IV and VI with and without exposure to fresh DPBSG for 30 min at 37°C prior to washing and treatment with diazotized 2-nitroaniline. Each bar represents the mean of three samples ± SD.

comparable order as found with I was observed for the amphipathic peptides XI and XIII. For the nonamphipathic counterparts, XII and XIV, containing charged residues uniformly distributed around the helix, no internalization was detectable. The notion that the net positive charge is of lower importance for entry into the cell interior was further supported by the similar degree of internalization found for the Antennapedia peptide XV,[9] which possesses two positive side chains more than I (Table 4.2).

Common quantitation protocols, as the HPLC approach applied here, presuppose removal of the vast excess of analyte in the incubation solution by a multiple wash process. The wash steps are normally performed in the cold in order to suppress bias of the results by energy-dependent efflux processes. Since, however, MAPs are able to cross the plasma membrane in the cold, the possibility could not be ruled out that the uptake results obtained might be biased by a rapid wash-out. Initial evidence that the inability to detect cellular uptake of the nonamphipathic peptides by the described HPLC protocol indeed reflected that only poor internalization combined with a rapid wash-out was provided by uptake experiments performed at 50 μ*M* concentration using peptides IV and VI. Under such conditions clear internalization of these unstructured peptides, which were nontoxic even at this high concentration,[29] was detected by the HPLC protocol (Figure 4.5). Likewise, Figure 4.5 illustrates an extensive escape of these peptides from preloaded cells, whereas for the amphipathic parent, peptide I, no significant efflux was measurable under the same conditions.[10] This suggested that the low intracellular levels (relative to those of the external medium) achieved with peptides IV and VI are at least partially due to wash-out.

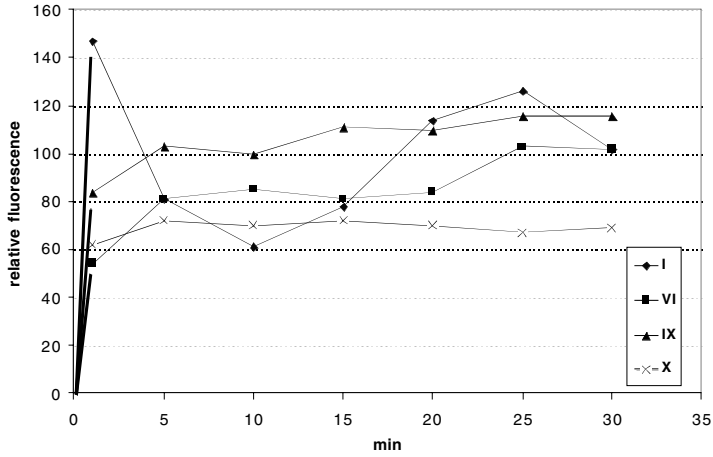

FIGURE 4.6 Time course of the fluorescence intensity within the cytosol after exposure of LKB Ez7 cells at 37°C to 1 μ*M* I, VI, IX, or X, respectively, normalized to the fluorescence intensity of the external peptide solution at time point 0.

4.3.3 Monitoring of Cellular Uptake of MAPs by an On-Line CLSM Protocol That Avoids Bias of Results by Wash-Out

The notion that nonamphipathic peptides of the MAP series are also able to penetrate mammalian plasma membranes could be confirmed by using an on-line CLSM protocol for monitoring cellular uptake. This protocol enabled measurement of the intracellular fluorescence in the presence of external fluorescent substrate,[30,31] thus avoiding bias of the results by wash-out. The correction of the measured intracellular fluorescence by out-of-focus contributions of the extracellular fluorescence was achieved in this protocol by means of the function of the axial response of the microscope, which was itself determined using the cell-impermeant dye carboxyfluorescein.[31] These on-line CLSM studies revealed an extensive and very rapid translocation of both amphipathic and non-amphipathic I-related peptides across mammalian plasma membranes proceeding to a comparable extent within a few minutes (Figure 4.6; see Reference 32).

In most cases, the fluorescence appeared evenly distributed throughout the cytosol and nucleus, accompanied by a perinuclear punctuate pattern, suggesting that nonendocytic as well as endocytic modes of uptake are involved. The predominance of nonendocytic processes was indicated by the fact that exposure of the cells at 0°C to the peptides also led to extensive intracellular fluorescence, with the signals not significantly different from those at 37°C.[32]

A different fluorescence pattern, however, now exhibiting analogy to the results obtained by the HPLC protocol (Figure 4.7), was observed after multiple cold washing of the peptide-exposed cells.[32] In washed cells preloaded with peptides of

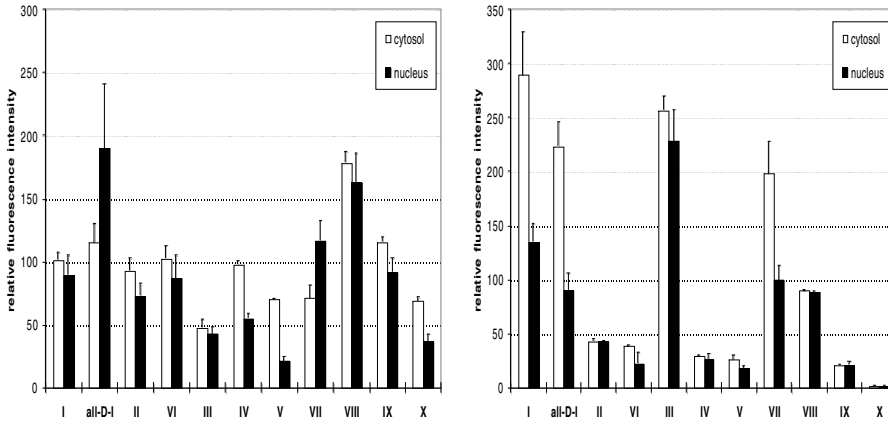

FIGURE 4.7 Fluorescence intensity of internalized peptides in the cytosol and nucleus after exposure of LKB Ez7 cells for 30 min at 37°C to 1 μ*M* I and I-derived peptides (A) and subsequent washing with cold PBS (B), normalized to the fluorescence intensity of the external peptide solution. Each bar represents the mean from three cells ± S.E.M.

lower positive charge, chain length, or amphipathicity than the parent compound I, substantially reduced fluorescence intensities were found, whereas high fluorescence intensities were observed in cells treated with those peptides proven to be extensively internalized by HPLC measurements (Figure 4.7b). These findings further confirm the conclusion that wash processes can substantially bias results of peptide uptake experiments.

Quantitative deductions from the fluorescence intensities measured by CLSM were only possible in combination with parallel HPLC determinations, since the high relative intensities of the cytosolic fluorescence in Figure 4.7b are biased by alterations of the peptide's environment and aggregation status.[32]

HPLC analysis of the wash fluids revealed that the peak corresponding to the intact peptide represented more than 90% of the detected fluorescence in all cases, indicating that metabolites or fluorescent contaminants were unlikely to have contributed significantly to the wash-out fraction. CLSM monitoring of cells exposed to the I-unrelated helical amphipathic and nonamphipathic pairs XI to XIV (Table 4.2) as well as to the natural vector peptides derived from the Antennapedia homeodomain (XV; see Reference 9) and from the Kaposi-fibroblast growth factor (Fluos-AAVALLPAVLLALLAP-NH_2 (XVI); Reference 33) led to similar results to those obtained with the MAP series (Figure 4.8). The on-line CLSM protocol revealed extensive internalization in all cases, even for nonamphipathic peptides XIII and XV (undetectable within the cell by the HPLC protocol) and significant losses of cytosolic and nuclear fluorescence after washing, particularly in the cases of the nonamphipathic peptides (Figure 4.8).

Exposure to other cell types of I-derived peptides resulted in a consistently high intracellular fluorescence in all cases, which was distinctive for each cell type

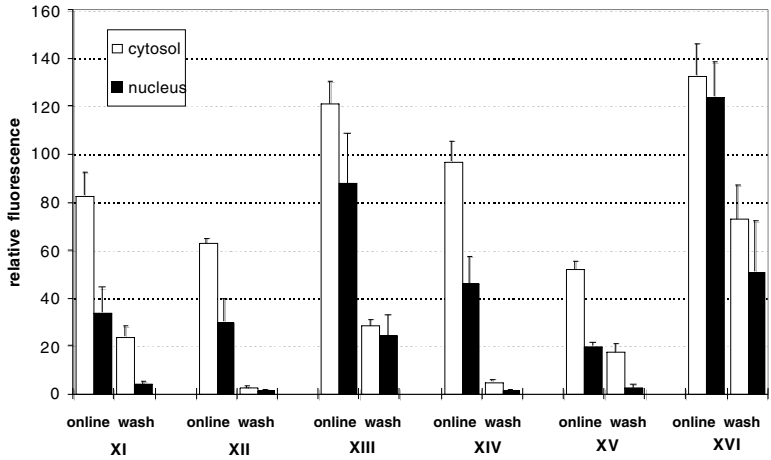

FIGURE 4.8 Fluorescence intensity of internalized peptides in the cytosol and nucleus after exposure of LKB Ez7 cells for 30 min at 37°C to 1 μ*M* helical model peptides not related to I and to the natural vector peptides XV[9] and XVI,[33] with and without subsequent washing with cold PBS, normalized to the fluorescence intensity of the external peptide solution. Each bar represents the mean from three cells ± S.E.M.

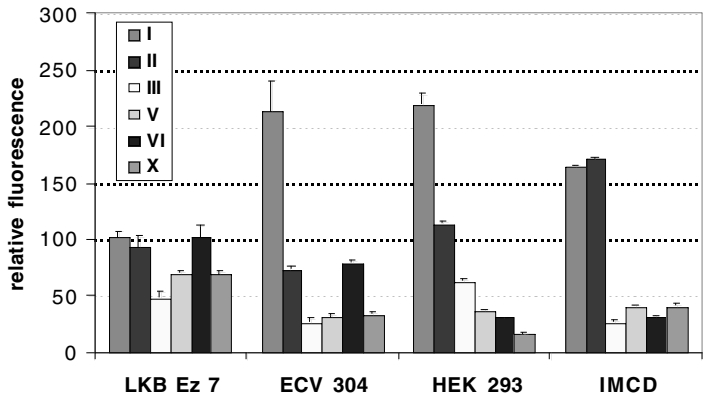

FIGURE 4.9 Intensity of the cytosolic fluorescence after exposure of different cell types for 30 min at 37°C to 1 μ*M* I and I-derived peptides, normalized to the fluorescence intensity of the external peptide solution. Each bar represents the mean from three cells ± S.E.M.

(Figure 4.9; Reference 32). Virtually identical effects to those described earlier for LKB Ez 7 on the intracellular fluorescence at reduced temperature and after cold washing were also observed for the other cell types investigated. These observations

indicate a promising basis for the development of vector peptides with increased cell specificy.

Taken together, the CLSM results suggest that amphipathicity is without importance for the translocation of peptides across mammalian plasma membranes, but that it mediates enrichment within the cell interior and increases resistance against wash-out. With a view to practical applications, therefore, substantial obstacles connected with the use of amphipathic peptides, such as membrane toxicity, high aggregation propensity, and related solubility problems, appear avoidable.

4.4 ABILITY OF MAPs TO SHUTTLE POLAR BIOACTIVE COMPOUNDS INTO CYTOSOL AND NUCLEUS OF MAMMALIAN CELLS

First attempts to assess the suitability of MAPs for introducing polar compounds of biological interest into the cell interior of mammalian cells were performed using disufide bridged conjugates of I with the negatively charged SH2 domain-binding peptide pYEEWE and with the positively charged SV40 nuclear localization sequence PKKKRKV. CLSM revealed internalization into the cytosol similarly to I for both conjugates and enrichment within the nucleus for the conjugate bearing the SV40 sequence.[10]

Further experiments using the tripeptide SLV, the consensus sequence for the FAP-1 binding domain of the intracellular C terminus of the apoptosis-inducing receptor Fas,[34] and the polymerase II-inhibiting cyclic mushroom peptide amanitin[35,36] were performed to examine the ability of such conjugates to elicit biological effects within the cell after being tagged to I.

Human Fas (APO-1/CD95) is an apoptosis-inducing member of the tumor necrosis factor receptor superfamily.[34,37] In the inactive state, a negative regulatory domain of Fas is captured by Fas-associated-phosphatase-1 (FAP-1),[38] which blocks binding of adaptors (e.g., FADD) and subsequent caspase activation.[34,39] Yanagisawa et al. recently showed that cytoplasmic microinjection of the simple N-terminally protected tripeptide Ac-SLV, the consensus sequence for the FAP-1 binding domain of Fas, inhibited the Fas-FAP-1-binding and dramatically enhanced Fas-mediated apoptosis.[40] Figure 4.10 shows that externally administered I, bearing the tripeptide SLV C terminally, is able specifically to activate caspase 8, the initial reaction of the apoptosis cascade.[41,42] The specificity is indicated by the inactivity of the components alone and of the N terminally with the SLV-sequence-tagged I (Figure 4.10; Reference 43). Replacement of I by the natural Antennapedia sequence[9] resulted in similar biological activity (Figure 4.10), indicating comparable shuttling ability for MAPs and natural vector peptide.

Disulfide bridging of I or the Antennapedia peptide[9] to the mushroom toxin amanitin similarly augmented the toxicity of this cyclic peptide (Figure 4.11; Reference 44), revealing the extensive and comparable shuttling ability of both cell-penetrating peptides. For amanitin alone a tenfold higher concentration was required for eliciting a toxicity comparable to that of its conjugates.[44]

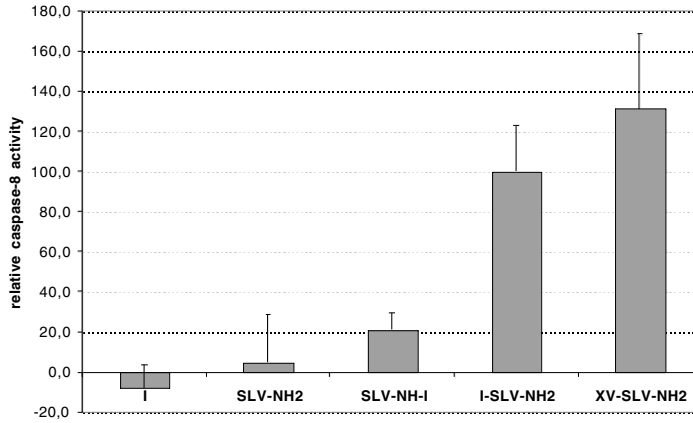

FIGURE 4.10 Relative caspase-8 activity induced in ECV-304 cells after incubation with 0.5 μ*M* I, I tagged N or C terminally with SLV, XV tagged C terminally with SLV or with SLV-NH_2 for 120 min at 37°C. Each bar represents the mean of three experiments ± S.E.M.

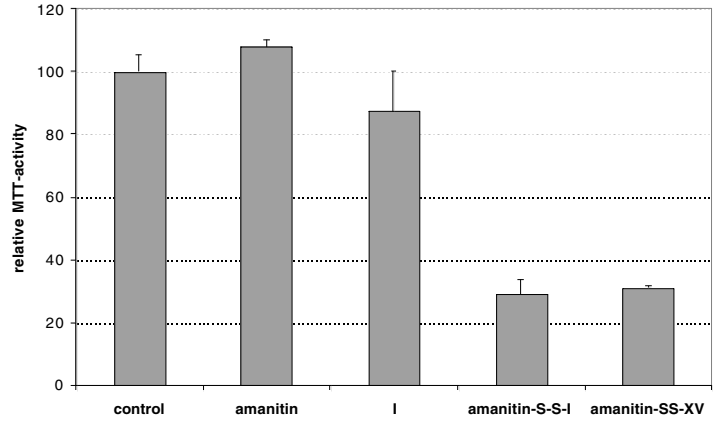

FIGURE 4.11 Relative viability of LKB Ez 7 cells determined by the MTT-method[55] after incubation with 1 μ*M* α-amanitin, I and disulfide-bridged constructs of amanitin and I or XV for 48 h at 37°C. The peptides were administered twice, at 0 and 24 h. Each bar represents the mean of three experiments ± S.E.M.

Extensive and comparable translocation into the cell interior was also found for the oligonucleotide conjugates with MAPs and the Antennapedia peptide when phosphorothioate oligonucleotides were used as the cargo molecule.[45] Surprisingly, no improvement with respect to the cellular uptake of naked oligonucleotides was observed (Figure 4.12); however, the opposite, an inhibiting effect of the peptide moiety on the membrane permeation of the oligonucleotide dependent on cell type

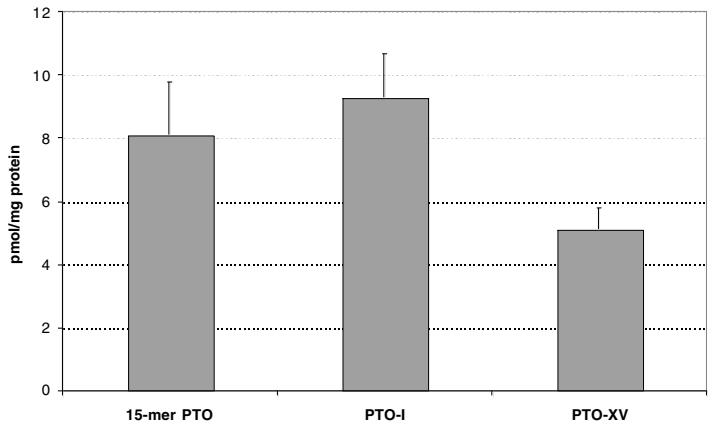

FIGURE 4.12 Quantities of internalized oligonucleotide after exposure of CHO cells to 0.5 μ*M* 15-mer PTO alone and conjugated to peptides I and XV for 30 min at 37°C determined by gel-capillary electrophoresis with laser-induced fluorescence detection. Each bar represents the mean from three cells ± SEM.

and oligonucleotide length, appeared to operate.[45] Aspects other than membrane translocation ability — probably interactions with nucleic acid binding proteins — might thus have more importance for the biological activity of oligonucleotides and oligonucleotide–peptide conjugates.

In context, the outlined results obtained with peptides and oligonucleotides as cargo molecules provide strong evidence for cell-penetrating ability of conjugates between MAPs and hydrophilic bioactive compounds and for a shuttling activity of MAPs comparable to that of natural protein-derived cell-penetrating peptides.

4.5 OTHER MODEL AMPHIPATHIC PEPTIDES APPLIED IN UPTAKE STUDIES

Although this chapter summarizes mainly the uptake studies of our own group using I-derived peptides, efforts of other groups in designing amphipathic peptides in order to improve the cellular uptake of biomolecules will be briefly reviewed next.

A quite simple decapeptide, (KFF)3K was shown by Vaara and Porro[46] to act synergistically with antibiotics against gram-negative bacteria, propably due to its cell wall-permeating properties. This peptide, which possesses no significant intrinsic antibacterial activity, was conjugated to 12- and 15-mer anti-*lacZ* PNAs via a flexible ethylene glycol linker. The PNA–peptide conjugates were 15- to 20-fold more active in inhibiting *lacZ* expression in *E. coli* than the corresponding PNAs without attached peptides.[47] Obviously, proline-containing, nonhelical peptides such as ILPWKWP-WWPWRRGC are also able to carry PNA oligomers into bacteria, and the corresponding peptide–PNA conjugates evoke the inhibition of bacterial growth. (For conjugates of other peptides with ODNs see the review of Tung and Stein.[48])

A cationic amphipathic peptide, very similar to the I-derived series, WEAKLAKALAKALAKHLAKALAKALKACEA (KALA), was designed by Wyman et al.[49] The KALA repeat was chosen to bind DNA, while the glutamic acid residues were inserted to improve water solubility at physiological pH. Although cellular uptake of the peptide was not demonstrated, KALA was shown to promote the uptake of ODNs after formation of noncovalent KALA-ODN complexes. KALA modifies especially the intracellular distribution and increases the nuclear accumulation of ODNs by redistribution from punctate cytoplasmic regions into the nucleus.[49]

Niidome et al.[50] studied binding of α-helical, cationic peptides to plasmid DNA and their gene transfer ability. Peptides such as Ac-LARLLARLLARLLARLLARLLARLLARL-$NHCH_3$ form aggregates with plasmid DNA, which are internalized by an endocytotic pathway. Obviously, the endosomal or lysosomal membrane-pertubing activity of the peptide moiety allows rapid transfer of the peptide–DNA complex from the endosomal compartment into the cytosol. Glutamic acid residues-containing peptides such as GLFEAIAEFIEGGWEGLIEGCA (E5CA) or LAELLAELLAEL undergo a conformational change when the pH shifts from neutral to 5 or 6, inducing a transient permeabilization of the plasma membrane or membranes of the endosomal compartment.[51-53] On the basis of these findings, the acidification of the extracellular medium in the presence of the E5CA peptide was suggested in order to improve cellular uptake of antisense ODNs into the cytosol and nucleus.[51]

4.6 EXPERIMENTAL

4.6.1 Cell Culture

Cells were seeded at an initial density 5×10^4 cells/cm^2 in 24-well culture plates and cultured at 37°C in a humidified 5% CO_2 containing air environment for 4 days without replacing the medium. For CLSM, 10^4 cells on 22×22 mm coverslips were cultured analogously.

4.6.2 Uptake Experiments

After removal of the medium, the cell layers were rinsed two times at 37°C with Dulbecco's phosphate buffered saline (DPBS; Biochrom KG, Berlin) supplemented with 1 g/l D-glucose (DPBSG) and subsequently exposed, unless indicated otherwise, at 37°C for 30 min to 500 µl of the peptide solutions in DPBSG. Thereafter, the incubation solutions were removed, the cells were washed two times with ice-cold PBS, incubated with 500 µl of ice-cold PBS and treated with diazotized 2-nitroaniline as described previously[11] in order to modify any surface-bound peptide.

In brief, 50 µl 0.6 *M* $NaNO_2$ was added to 400 µl ethanol/water 1/1 v/v containing 2-nitroaniline (0.06 *M*) and HCl (0.125 *M*). After standing for 5 min at ambient temperature, 10 µl of this reagent was added to the ice-cold PBS covering the cell layer and allowed to react for 10 min at 0°C. After aspiration of the diazo reagent, the cells were washed two times with ice-cold PBS and finally lysed with 0.2 ml 0.1% Triton X-100 containing 10 mmol/l trifluoroacetic acid for 2 h at 0°C. The

resulting lysate was used for HPLC analysis and for protein determination according to Bradford.[54]

To measure the pore forming propensity of the peptides, the cells were pre-exposed to a 12-μ*M* solution of fluorescein diacetate in DPBSG (containing 0.5% DMSO) for 15 min at 37°C. After aspiration of the fluorescein diacetate solution, the cells were rinsed four times with DPBSG 37°C and then exposed to the peptides. Since a noticeable export of fluorescein generated within the cells was also observed for the control cells (half-life time at 37°C, 9 min) an exact time regime was required for the wash steps to optimize reliability.

4.6.3 HPLC Analysis

HPLC was performed using a Bischoff-HPLC-gradient system (Leonberg, Germany) with a Polyencap A 300, 5 μm column (250 × 4 mm I.D.), with precolumns containing the same adsorbent and a Fluorescence HPLC-Monitor RF-551 (Shimadzu).

Up to 200 μl of the cell lysates were passed through a precolumn containing 60 mg of Polyencap (A 300, 5 μm), which was subsequently connected to the HPLC system. The elution was carried out with 0.01 *M* TFA (A) and acetonitrile/water 9/1 (B) at a flow rate of 1.0 ml/min with gradients from 30 to 45% B (0 to 10 min) and 45 to 80% B (15 to 20 min) for peptides, and 30 to 60% B (0 to 15 min) and 60 to 80% B (15 to 20 min) for peptide conjugates. Quantitation was performed by fluorescence measurement at 520 nm after excitation at 445 nm by means of calibration lines obtained with the parent peptides under identical conditions. For unknown metabolites, a twofold molar fluorescence intensity than that found during HPLC for I was used for quantitation, based on the generally two- to threefold higher molar fluorescence intensities observed for HPLC peaks of characterized derivatives of I, which had lower structure-forming propensity.

4.6.4 Confocal Laser Scanning Microscopy (CLSM)

4.6.4.1 Fluorescence Imaging at 37°C, On-Line

The coverslips carrying coherent cell formations as well as single cells were overlayed with 1 ml PBS and the initial microscopy was performed without peptide solution (control image). Thereafter, the buffer was aspirated and the cells were exposed to 1 ml of a 1-μ*M* solution of the peptide in DPBS for 30 min; fluorescence images were monitored at 5-min intervals.

Fluorescence imaging after incubation for 30 min at 37°C and subsequent washing: cells were exposed for 30 min at 37°C to 1 μ*M* peptide in DPBS and subsequently washed four times with ice-cold PBS. The intracellular fluorescence signal was measured by CLSM.

Fluorescence imaging after incubation for 30 min at 4°C without subsequent washing: cells were precooled for 30 min at 0 to 4°C in DPBS and then exposed to 1 ml of 1 μ*M* peptide in DPBSG for 30 min at 0 to 4°C. Fluorescence images were monitored at 5-min intervals.

At the end of each protocol the integrity of the plasma membrane was verified by addition of trypan blue and measurement of the trypan blue fluorescence (λexc = 543 nm, λem > 590 nm).

To monitor the fluorescence images and measure the fluorescence intensities an LSM 410 invert confocal laser scanning microscope (Carl Zeiss, Jena GmbH, Jena, Germany) was used. Excitation was performed at 488 nm (Fluos) or 543 nm (Trypan Blue) using an argon-krypton or helium-neon laser and a dichroitic mirror FT 510 or NT 543/80/20 for respective wavelength selection. Emission was measured at wavelengths >515 or >570 nm with cut-off filters LP 515 and LP 570, respectively, in front of the detector. The fluorescence intensities inside and outside the cell were recorded in predetermined regions of interest (ROIs, 16 × 16 pixel; 30 scans with a scan time of 2 sec with double averaging) as described by Lorenz et al.[30] The background fluorescence intensity was determined before addition of the peptide solution for 300 sec. For measurement of the intracellular fluorescence, three ROIs were selected in the cytosol and one in the nucleus of three cells in such a manner that the diffuse fluorescence could be recorded without interference with vesicular fluorescence.

The intracellular fluorescence signal was corrected for contributions from the extracellular fluorescence arising from nonideal confocal properties of the CLSM by estimating the distribution function of sensitivity in the Z direction of the microscope, according to Wiesner et al.[31]

4.6.4.2 Measurement of Axial Response of the Confocal System

Dye solution of 400 µl (carboxyfluorescein or fluorescein-labeled peptide; 1.25 µ*M*) was transferred to the cover slip. The fluorescence of the dye and the reflection signal of the excitation source were detected in a two-channel measurement. The scan plane (XY-plane) was moved in 1-µm steps in the Z direction up to 200 µm, beginning at the middle of the cover slip. Adjacent to the optical boundary (cover slip-dye) the step width was decreased to 0.2 µm. At each step a two-channel image (512 × 512 pixel) with a scan time of 2 sec and a double averaging was captured. The intensities of the fluorescence and reflection signals were obtained directly from the single-channel image after each scan. The values of the intensities were stored according to the Z position. The registration of the reflection signal was used for determining the Z position of the optical boundary.

4.6.4.3 Calculation of Contributions from Out-of-Focus Planes to Intracellular Fluorescence Intensity

After preincubating the cells for 10 min with 1.25 µ*M* solutions of the dye or the flurescently labeled peptide respectively, and subsequent transfer of 400 µl of the cell suspension to the cover slip, optical measurements were performed using the experimental setup that follows.

The XY-plane was positioned in the middle of a cell in the Z-axis using the reflection and the transmission modes of the microscope. Regions of interest (ROIs, 16 × 16 pixel) were fixed between the center of the cell and the extracellular medium.

The fluorescence intensity in each ROI was recorded as the mean of 30 scans with a scan time of 2 sec with double averaging. The reflection mode was used to determine the cell geometry and each different ΔZ_n in the Z direction from the center of ROI to the extracellular medium. Thereby the distances ΔZ_n were obtained with the knowledge of the dimension of cell, the Z position at the cell, and the positions of ROIs at the focal plane by simple mathematical calculation. The values of the fluorescence intensities of the ROIs and the distances of the ΔZ_n values were stored for later computation.

REFERENCES

1. Lindgren, M. et al., Cell-penetrating peptides, *Trends Pharmacol. Sci.,* 21, 99, 2000.
2. Steiner, V. et al., Retention behaviour of a template-assembled synthetic protein and its amphiphilic building blocks on reversed-phase columns, *J. Chromatogr.,* 586, 43, 1991.
3. Rothemund, S. et al., Peptide destabilization by two adjacent D-amino acids in single-stranded amphipathic alpha-helices, *Pept. Res.,* 9, 79, 1996.
4. Rothemund, S. et al., Recognition of alpha-helical peptide structures using high-performance liquid chromatographic retention data for D-amino acid analogues: influence of peptide amphipathicity and of stationary phase hydrophobicity, *J. Chromatogr.,* 689, 219, 1995.
5. Krause, E. et al., Location of an amphipathic alpha-helix in peptides using reversed-phase HPLC retention behavior of D-amino acid analogs, *Anal. Chem.,* 67, 252, 1995.
6. Dathe, M. et al., Hydrophobicity, hydrophobic moment and angle subtended by charged residues modulate antibacterial and haemolytic activity of amphipathic helical peptides, *FEBS Lett.,* 403, 208, 1997.
7. Cross, L.J. et al., Influence of alpha-helicity, amphipathicity and D-amino acid incorporation on the peptide-induced mast cell activation, *Eur. J. Pharmacol.,* 291, 291, 1995.
8. Oehlke, J. et al., Nonendocytic, amphipathicity dependent cellular uptake of helical model peptides, *Protein Pept. Lett.,* 3, 393, 1996.
9. Derossi, D. et al., The third helix of the Antennapedia homeodomain translocates through biological membranes, *J. Biol. Chem.,* 269, 10444, 1994.
10. Oehlke, J. et al., Cellular uptake of an alpha-helical amphipathic model peptide with the potential to deliver polar compounds into the cell interior non-endocytically, *Biochim. Biophys. Acta,* 1414, 127, 1998.
11. Oehlke, J., Savoly, B., and Blasig, I.E., Utilization of endothelial cell monolayers of low tightness for estimation of transcellular transport characteristics of hydrophilic compounds, *Eur. J. Pharm. Sci.,* 2, 365, 1994.
12. Guillot, F.L., Audus, K.L., and Raub, T.J., Fluid-phase endocytosis by primary cultures of bovine brain microvessel endothelial cell monolayers, *Microvasc. Res.,* 39, 1, 1990.
13. Prochiantz, A., Getting hydrophilic compounds into cells: lessons from homeopeptides, *Curr. Opin. Neurobiol.,* 6, 629, 1996.
14. Hawiger, J., Cellular import of functional peptides to block intracellular signaling, *Curr. Opin. Immunol.,* 9, 189, 1997.
15. Mellman, I., Endocytosis and molecular sorting, *Annu. Rev. Cell Dev. Biol.,* 12, 575, 1996.

16. Hansen, S.H., Sandvig, K., and van-Deurs, B., Clathrin and HA2 adaptors: effects of potassium depletion, hypertonic medium, and cytosol acidification, *J. Cell Biol.,* 121, 61, 1993.
17. Ohkuma, S. and Poole, B., Fluorescence probe measurement of the intralysosomal pH in living cells and the perturbation of pH by various agents, *Proc. Natl. Acad. Sci. U.S.A.,* 75, 3327, 1978.
18. Lippincott–Schwartz, J. et al., Rapid redistribution of Golgi proteins into the ER in cells treated with brefeldin A: evidence for membrane cycling from Golgi to ER, *Cell,* 56, 801, 1989.
19. Cole, S.P. et al., Overexpression of a transporter gene in a multidrug-resistant human lung cancer cell line, *Science,* 258, 1650, 1992.
20. Ballatori, N. et al., Carrier-mediated uptake of lucifer yellow in skate and rat hepatocytes: a fluid-phase marker revisited, *Am. J. Physiol.,* 277, G896-G904, 1999.
21. Steinman, R.M. et al., Endocytosis and the recycling of plasma membrane, *J. Cell Biol.,* 96, 1, 1983.
22. Schmid, S.L. and Carter, L.L., ATP is required for receptor-mediated endocytosis in intact cells, *J. Cell Biol.,* 111, 2307, 1990.
23. Schnitzer, J.E., Allard, J., and Oh, P., NEM inhibits transcytosis, endocytosis, and capillary permeability: implication of caveolae fusion in endothelia, *Am. J. Physiol.,* 268, H48–H55, 1995.
24. Anderson, R.G. et al., Potocytosis: sequestration and transport of small molecules by caveolae, *Science,* 255, 410, 1992.
25. Marger, M.D. and Saier, M.H., A major superfamily of transmembrane facilitators that catalyse uniport, symport and antiport, *Trends Biochem. Sci.,* 18, 13, 1993.
26. Nikaido, H., Prevention of drug access to bacterial targets: permeability barriers and active efflux, *Science,* 264, 382, 1994.
27. Schatz, G. and Dobberstein, B., Common principles of protein translocation across membranes, *Science,* 271, 1519, 1996.
28. Paul, S. et al., Structure and *in vitro* substrate specificity of the murine multidrug resistance-associated protein, *Biochemistry,* 35, 13647, 1996.
29. Scheller, A. et al., Structural requirements for cellular uptake of alpha-helical amphipathic peptides, *J. Pept. Sci.,* 5, 185, 1999.
30. Lorenz, D. et al., Mechanism of peptide-induced mast cell degranulation — translocation and patch-clamp studies, *J. Gen. Physiol.,* 112, 577, 1998.
31. Wiesner, B. et al., Measurement of intracellular fluorescence in the presence of a strong extracellular fluorescence using confocal laser scanning microscopy, *Anal. Biochem.,* submitted.
32. Scheller, A. et al., Evidence for an amphipathicity independent cellular uptake of amphipathic cell-penetrating peptides, *Eur. J. Biochem.,* 267, 6043, 2000.
33. Lin, Y.Z. et al., Inhibition of nuclear translocation of transcription factor NF- kappa B by a synthetic peptide containing a cell membrane-permeable motif and nuclear localization sequence, *J. Biol. Chem.,* 270, 14255, 1995.
34. Ashkenazi, A. and Dixit, V.M., Death receptors: signaling and modulation, *Science,* 281, 1305, 1998.
35. Wieland, T., Poisonous principles of mushrooms of the genus Amanita. Four-carbon amines acting on the central nervous system and cell-destroying cyclic peptides are produced, *Science,* 159, 946, 1968.
36. Faulstich, H. and Wieland, T., New aspects of amanitin and phalloidin poisoning, *Adv. Exp. Med. Biol.,* 391, 309, 1996.

37. Itoh, N. et al., The polypeptide encoded by the cDNA for human cell surface antigen Fas can mediate apoptosis, *Cell,* 66, 233, 1991.
38. Sato, T. et al., FAP-1: a protein tyrosine phosphatase that associates with Fas, *Science,* 268, 411, 1995.
39. Kumar, S. and Colussi, P.A., Prodomains-adaptors-oligomerization: the pursuit of caspase activation in apoptosis, *Trends Biochem. Sci.,* 24, 1, 1999.
40. Yanagisawa, J. et al., The molecular interaction of Fas and FAP-1 — a tripeptide blocker of human Fas interaction with FAP-1 promotes Fas-induced apoptosis, *J. Biol. Chem.,* 272, 8539, 1997.
41. Muzio, M. et al., FLICE, a novel FADD-homologous ICE/CED-3-like protease, is recruited to the CD95 (Fas/APO-1) death-inducing signaling complex, *Cell,* 85, 817, 1996.
42. Boldin, M.P. et al., Involvement of MACH, a novel MORT1/FADD-interacting protease, in Fas/APO-1- and TNF receptor-induced cell death, *Cell,* 85, 803, 1996.
43. Scheller, A., Melzig, M., and Oehlke, J., Induction of caspase-8 in human cells by the extracellular administration of peptides containing a C-terminal SLV sequence, *Lett. Pept. Sci.,* in press.
44. Oehlke, J., Bienert, M., and Faulstich, H., *Lett. Pept. Sci.,* in preparation.
45. Oehlke, J. et al., Cellular uptake of antisense oligonucleotides after complexing or conjugation with cell-penetrating model peptides, *Bioconjugate Chem.,* in preparation.
46. Vaara, M. and Porro, M., Group of peptides that act synergistically with hydrophobic antibiotics against gram-negative enteric bacteria, *Antimicrob. Agents Chemother.,* 40, 1801, 1996.
47. Good, L. et al., Bactericidal antisense effects of peptide-PNA conjugates, *Nat. Biotechnol.,* 19, 360, 2001.
48. Tung, C.H. and Stein, S., Preparation and applications of peptide-oligonucleotide conjugates, *Bioconjugate Chem.,* 11, 605, 2000.
49. Wyman, T.B. et al., Design, synthesis, and characterization of a cationic peptide that binds to nucleic acids and permeabilizes bilayers, *Biochemistry,* 36, 3008, 1997.
50. Niidome, T. et al., Binding of cationic alpha-helical peptides to plasmid DNA and their gene transfer abilities into cells, *J Biol. Chem.,* 272, 15307, 1997.
51. Pichon, C. et al., Cytosolic and nuclear delivery of oligonucleotides mediated by an amphiphilic anionic peptide, *Antisense. Nucleic. Acid. Drug Dev.,* 7, 335, 1997.
52. Ohmori, N. et al., The enhancing effect of anionic alpha-helical peptide on cationic peptide-mediating transfection systems, *Biochem. Biophys. Res. Commun.,* 235, 726, 1997.
53. Takahashi, S., Conformation of membrane fusion-active 20-residue peptides with or without lipid bilayers. Implication of alpha-helix formation for membrane fusion, *Biochemistry,* 29, 6257, 1990.
54. Bradford, M.M., A rapid and sensitive method for the quantitation of microgram quantities of protein utilizing the principle of protein-dye binding, *Anal. Biochem.,* 72, 248, 1976.
55. Mosmann, T., Rapid colorimetric assay for cellular growth and survival: application to proliferation and cytotoxicity assays, *J. Immunol. Methods,* 65, 55, 1983.

5 Signal Sequence-Based Cell-Penetrating Peptides and Their Applications for Gene Delivery

May C. Morris, Laurent Chaloin, Frédéric Heitz, and Gilles Divita

CONTENTS

0-8493-1141-1/02/$0.00+$1.50

5.1 INTRODUCTION

Over the past 10 years, substantial progress has been made in the development of cell-penetrating peptide-based drug delivery systems. This was directly correlated with the dramatic acceleration in the production of new therapeutic molecules because the cell delivery systems described until then were restricted by very specific issues. As such, the goal became to design short synthetic peptides which would incorporate cellular addresses and intramolecular routing signals and to formulate synthetic peptide cargo complexes which could overcome both extracellular and intracellular limitations.[1-5] Cell-penetrating peptides present several advantages in that they are modulable, lack immunogenicity, easy to produce, and can incorporate a number of specific attributes required for efficient cargo delivery. They have been shown efficiently to introduce drugs, antisense DNA, PNA, oligonucleotides, and small proteins into cells *in vivo* and *in vitro*.[4-9]

In the design of cell-penetrating peptides, the two main barriers to overcome are the cell membrane and the nuclear membrane. Signal sequence-based cell-penetrating peptides described in the literature can be subdivided into two types: natural peptides and chimeric peptides. The main cell routing elements are termed import signals and nuclear localization sequences (NLSs) and are presumed to function in most eukaryotic cells. Efficient uptake into cells in the absence of specific receptors or transporters and escape from the endosomal or lysosomal compartments are additional obstacles to be surmounted and therefore key parameters to be considered in the rational design and engineering of cell-penetrating peptides.

Although the nucleus represents a major barrier, it also constitutes one of the major targets for drug and gene therapy. Indeed, cell-penetrating peptides containing NLS have been extensively used for drug and cargo delivery, with the NLS either directly incorporated in the formulation or cross-linked to the cell-penetrating peptide or even to its cargo.[6-10] This chapter will highlight characteristics of NLS-based peptides designed to address the nucleus and will discuss why understanding the mechanism of nuclear import and of structural features of cell-penetrating peptides is essential for improvement of *in vivo* drug therapy.

5.2 SIGNAL SEQUENCE: THE NUCLEAR LOCALIZATION SEQUENCE

5.2.1 Introduction: The Nuclear Localization Sequence

Although the nucleus constitutes one of the major cellular compartments to be targeted, nuclear delivery of drugs and DNA is limited by the selectivity of the nuclear envelope. Indeed, in the case of gene therapy, for example, expression of transcripts can only take place following delivery into the nucleus. However, transport of therapeutic DNA from the cytoplasm into the nucleus constitutes one of the major limiting steps in nondividing cells. Fortunately, over the last few years, the structure and molecular mechanisms of nuclear transport have been characterized in detail, thereby enabling more appropriate design of cell-penetrating peptides

aimed at targeting the nucleus.[11,12] The nuclear transport process is facilitated by nuclear import signal sequences, the best documented group of which comprises the NLSs. NLSs are characteristic short sequences that can be further subdivided into monopartite or bipartite signals when they consist, respectively, of one or two clusters of four or more basic amino acids (lysine or arginine).[12-14]

Understanding the nuclear transport mechanism of macromolecules, together with characterization of a large number of potential NLSs and their regulation, has enabled the development of new tools that can be directly applied to the improvement of drug delivery systems. In eukaryotic cells, most of the natural NLSs are bipartite, consisting of two short cationic domains separated by a spacer of 10 to 12 residues. The best characterized bipartite NLS is that of nucleoplasmin[15] with the minimal sequence KRPAATKKAGQAKKKL. Among monopartite NLS, the best characterized is a short sequence, ^{126}PKKKRKV^{132}, derived from SV40 (simian virus 40) large T antigen.[16] Lys^{128} is essential for NLS activity, as mutation of this residue to an Asn or a Thr completely abolishes nuclear targeting.[17] In contrast, mutation of the other basic residues is less dramatic for nuclear translocation.[11,18]

This NLS has been extensively used for coupling cargoes (protein, peptide, DNA, or ODN) and has been shown to improve crossing of the nuclear membrane.[9,10] In addition to its cationic domains, NLS contain a few characteristic components, including an α-helix destabilizing proline or glycine residue upstream or downstream of the cluster of basic residues and a cluster of acidic residues upstream or downstream of or within the spacer. Serine residues located in or around the cationic cluster are usually essential for transport and have been implicated as phosphorylation sites.[9,20] Finally, hydrophobic aromatic residues (Trp or Tyr) are excluded from the NLS or from the spacer of the bipartite NLS.

5.2.2 Mechanism of Nuclear Transport

The most widely utilized pathway for nuclear import is mediated by NLSs (Table 5.1 and Figure 5.1). Although there appears to be a lack of primary sequence homology between the different NLS sequences described, they all bind the same family of cytoplasmic receptors termed importins or karyopherins. The importin β pathway is one of the best described, with import substrates binding importin β either directly or through the adaptor protein importin α.[13,18-22]

Transport of macromolecules between the cytoplasm and the nucleus generally occurs through the nuclear pore complex (NPC). The NPC is a large multimeric complex of about 125 MDa containing 50 to 100 different proteins, termed nucleoporins,[18,22] that forms an inner pore smaller than 9 nm in diameter. In theory molecules smaller than 9 nm in diameter or around 60 kDa can diffuse passively through the central channel of the NPC. However, small molecule delivery is also controlled by cellular events and other signals such as cytoplasmic retention signals and phosphorylation, which may block nuclear entry and render it more selective. In contrast, entry into the nucleus of larger molecules including proteins or DNA requires an active signal-mediated transport process facilitated by NLS signals. This nuclear transfer through the NPC involves a network of proteins and is dependent

TABLE 5.1
NLS-Containing Cell-Penetrating Peptides

Proteins	Minimal NLS	Ref.
SV 40 Large T	PKKKRKV	16
P101	CGPGSDDEAAADAQHAAPPKKKRKVGY	16, 17
Nucleoplasmin	KRPAATKKAGQAKKKKL	15
HIV-1 Tat	GRKKRRQRRRPPQ	42
Yeast mat a2	NKIPIKD	5
HIV-1 rev	RRNRRRRW	42
Polyomavirus Vp1	APKRKSGVSK	38
NF-kB	VQRKRQKLMP	10, 68
M9	NQSSNFGPMKGGNFGGRSSGPYGGGGQYFAKPRNQGGY	29–31
Vpr	DTWTGVEALIRILQQLLFIHFRIGCRHSRIGIIQQRRTRNGA	37, 38, 41
FP-NLS (MPG)	GALFLGFLGAAGSTMGAWSQPKKKRKV	50, 51
SP-NLS	MGLGLHLLVLAAALQGAWSQPKKKRK	47, 48
SN50	AAVALLPAVLLALLAPVQRKRQKLMP	10, 68

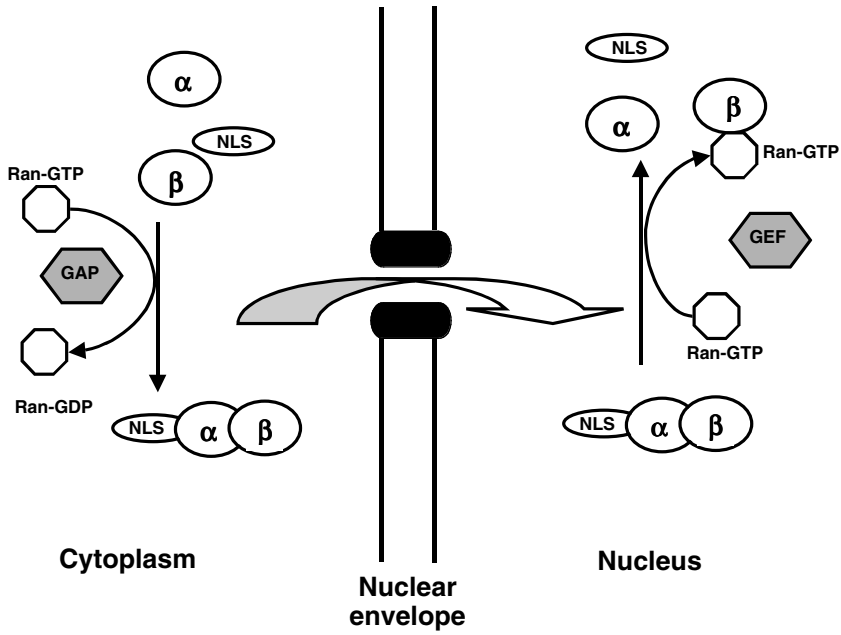

FIGURE 5.1 Mechanism of NLS-dependent nuclear import pathway. The formation of the trimeric complex among an NLS containing cargo, importin α, and importin β takes place in the cytoplasm. This is followed by docking of the trimeric complex to the NPC, then translocation through the central channel, and finally Ran-GTP-mediated dissociation of the complex and release of the cargo into the nucleus.

on ATP. As for small molecules, cytoplasmic retention sequences and regulatory phosphorylation can modulate transport of larger molecules through the NPC.[14,22-24]

Transport across the NPC basically involves four major steps, initiated by binding of an NLS to importin α in the cytoplasm, which strengthens the interaction of the latter with importin β. Importin β is responsible for the translocation of the importin and cargo complex through the pore. This is followed by docking of the cargo and importin complex to the cytoplasmic periphery of the NPC, then transport through the pore, which involves hydrophobic clusters of aromatic residues (Phe) from specific nucleoporins.[24,25] Once in the nucleus, the complex finally dissociates in an energy-dependent mechanism, followed by recycling of the transport factors to the cytoplasm, thus releasing them for the next import cycle. Transfer through the pore is facilitated by a series of factors including the small GTPase protein Ran (ras-related nuclear protein), the nuclear transport factor-2 (NTF-2), and the chromatin-bound guanine exchange factor RCC1. The small GTPase Ran confers directionality to the nuclear import system: Ran-GTPase allows association of the cargo and importin complex in its GDP-form in the cytoplasmic compartment, whereas its GTP-form dissociates the complex in the nucleus.

Once in the nucleus, importin β binds to Ran-GTP, which induces dissociation of the import complex, and importin α is then recycled to the cytoplasm. The binding of the cargo and importin complex to the cytoplasmic face of the NPC is ATP-independent, whereas its nuclear accumulation is dependent on ATP. The GDP and GTP-forms of Ran are maintained, respectively, by the Ran GTPase activity protein 1 (GAP) in the cytoplasm and the nucleotide exchange factor Ran-GEF in the nucleoplasm. A recent study has revealed that the interaction of importin β and importin α confers very high affinity to the complex for mono or bipartite NLS. After translocation of the heterotrimeric complex to the nuclear compartment, Ran-GTP induces dissociation of the importin β and importin α complex, which favors release of the cargo in the nucleus and converts importin α into an auto-inhibited conformation, thereby preventing it from binding to nuclear proteins.[26-28]

Another major pathway of nuclear delivery has been described for the M9 NLS sequence that mediates bidirectional transport of ribonucleoprotein hrRNP A1. M9 is a short signal sequence of 38 residues rich in glycine and aromatic residues, encoding an NLS as well as an NES sequence. Nuclear transport is mediated by interaction with the transport receptor protein transportin 1 (TRN1), a member of the importin family of nucleocytoplasmic transport factors.[29] Several M9-like sequences containing NLS–NES import and export sequences that overlap have been identified.[29,30] A similar sequence, characterized by an NLS–NES, has been described for Tap proteins involved in export of nuclear mRNA. Although their sequence is not similar to that of M9, they seem to be involved in the same import mechanism as transportin proteins. As for the β importin pathway, dissociation between transportin 1/M9 NLS is induced by Ran-GTP.[29-31]

5.2.3 NLS Involved in the Delivery of Active Cargo

Synthetic NLS-containing peptides have been extensively used to improve the nuclear delivery of cargoes (drugs, DNA). They have been attached to cargoes or

combined with other transfection methods to facilitate delivery into the nucleus (see Table 5.1).

Most of these studies were performed with the sequence derived from SV40 large T antigen NLS PKKKRKV. This sequence was associated with either membrane-penetrating peptides or cationic peptides, but also directly linked to cargoes.[5,8,9] Several studies were performed with an optimized NLS sequence derived from SV40 large T antigen NLS (peptide P101) CGPGDDEAAADAQHAAPPKKKRKVGY, which contains the NLS signature PKKKRKV together with the flanking serine phosphorylation site S^{112}DDE recognized by the protein kinase CK2.[32] This phosphorylation was shown to improve binding of the NLS sequence to a receptor such as importin α and consequently to enhance the rate of nuclear import. In peptide P101, a combination of this NLS with polylysine enabled the demonstration of a direct correlation among the presence of the NLS, recognition by the nuclear import machinery, and the enhancement of transfection efficiency.[17,33,34]

The NLS sequence M9 is a cellular NLS from heterogeneous nuclear ribonucleoprotein hnRNP A1, a major nuclear pre-mRNA-binding protein. The sequence of M9 constitutes a nonclassical NLS, NQSSNFGPMKGGNFGGRSSGPYGGGGQYFAKPRNQGGY, which is recognized by the importin β like shuttle protein transportin I.[35] Nuclear import based on the use of M9 sequence is extremely efficient and has been resorted to in order to improve nuclear delivery of drugs and DNA.[30,31,36]

Viruses achieve nuclear entry mostly during mitosis. However, several viruses succeed in entering the nucleus through interaction of viral components with cellular importin molecules. Although this mechanism is not well described, a few nonclassical NLSs have been proposed to be involved and have further been used for nuclear delivery.[37] Adenoviruses require dissociation of their viral components prior to entry into the nucleus. In contrast, in the case of lentiviruses, the preintegration complex enters the nucleus intact.[38] The protein Vpr is involved in the nuclear import of the HIV preintegration complex and contains a nonclassical NLS at its C terminus, DTWTGVEALIRILQQLLFIHFRIGCRHSRIGIIQQRRTRNGA, that allows nuclear import to be mediated independently of the importin or transportin pathways. Vpr has been proposed to interact directly with the NPC in an energy-independent fashion. The NLS derived from the HIV viral protein Vpr has been used successfully in transfection experiments.[37] The C-terminal domain of Vpr (Vpr^{52-96}) has been shown to interact with and condense DNA and to mediate DNA transfection through the endosomal pathway, but in a pH-independent manner.[39-41]

A large number of NLSs or putative NLSs have been described, such as the putative NLS found in the amino terminus of yeast α-mating factor, Q-KIPIK-N, which is capable of enhancing delivery of beta galactosidase into the nucleus. More recently, the HIV-1 Tat peptide or HIV Rev has also been proposed to represent an NLS domain recognized directly by importin β rather than by importin α.[42] Tat peptide can play a double targeting role, by first delivering its cargo into the cytosol, then to the nucleus. A peptide sequence issued from the 20 first residues of the adenovirus fiber protein was used to improve transfection of human cells. This peptide AKRARLSTSFNPVYPYEDES contains a hydrophobic domain FNPVYPY, specific for receptor-mediated endocytosis and the NLS motif KRARLSTSF, which together favor delivery of proteins into the nucleus.[38,43]

5.3 NLS-CONTAINING CELL-PENETRATING PEPTIDES

5.3.1 Signal Sequence-Based Peptides: Import and Targeting Signals

Bifunctional peptide sequences containing NLS have been designed to overcome both cytoplasmic and nuclear entry barriers. The poor permeability of the plasma membrane of eukaryotic cells to drugs or DNA represents the first limiting barrier to the development of therapeutic molecules. A series of peptides able to cross the plasma membrane have been described and will be developed in detail in other chapters of this book. Here we will essentially focus on chimeric cell-penetrating peptides in which a nuclear targeting sequence has been coupled to an import peptide sequence.[5,7,9]

In general, cell-penetrating peptide-based import signals must be capable of directing the movement of a cargo across the cell membrane into the cytoplasm of most of the cells, either by transient membrane permeabilization or through the endocytotic pathway by receptor-mediated endocytosis. In order to facilitate the rapid internalization of NLS-containing peptides, import signal sequences selective to specific cells and receptors have been used.[9,10] However, the delivery of chemotherapeutic drugs imported through this mechanism appears to be limited to certain cell lines. To address this issue, several short import signal sequence peptides have been coupled to NLSs and can be divided into three major classes: hydrophobic, amphiphatic, or cationic peptides.[4]

5.3.2 Import Signal Sequences

The first class of import signal sequences corresponds to the hydrophobic region of various signal sequences termed membrane-permeable sequences (MPSs).[10,44] MPSs are about 20 amino acids long and adopt a characteristic helical conformation under membrane mimetic environment, irrespective of their distinct primary sequences. They are capable of crossing the cell membrane and importing covalently attached functional domains from other intracellular proteins. A series of peptides have been described so far, including the Src homology 2 (SH2) domain of Grb2,[45] human integrins β1, β3,[46] and the sequence signal of Kaposi fibroblast growth factor (K-FGF) AAVAALLPAVLLALLAP.[8,10] The mechanism of internalization of these peptides does not require receptor proteins and is independent of the classical endocytotic pathway.[10] The alpha-helical structure of these peptides seems to be required for penetration but is not sufficient by itself for cellular delivery. Studies have demonstrated that the versatility of the structure of the hydrophobic domain is important for cell penetration.

A series of peptide fusion sequences and signal sequences have also been used, including the hydrophobic signal sequence from the Caiiman crocodylus immunoglobulin light chain signal sequence and fusion sequence from HIV gp41 fusion peptide.[47-52] Peptides such as IgV (light) chain of caiman crocodylus associated with an NLS and helical h-FGF were shown to adopt a beta strand fold.[47] Such sequences have been fused to the NLS of SV40 large T antigen to target the nucleus of cells and to deliver antisense oligonucleotides, peptides, plasmid DNA, and drugs.[48-51]

Amphipathic sequences contain a periodicity of hydrophobic and polar residues, such as the fusion peptide of influenza hemaglutinin (HA-2),[53-55] and related synthetic analogs called GALA, KALA,[56,57] JTS1,[58] and Hel 11.7.[59] Import signal peptides have been demonstrated to interact with cellular membranes and lipid bilayers, resulting in fusion events with the membrane. The conformation of these peptides is sensitive to the pH: acidic pH induces a conformational change from random coil to a helical transition that induces leakage of vesicular contents. They have been used in association with an NLS in order to improve release from the endosomes of different formulations.[53]

Another class of cell-penetrating peptides corresponds to the protein transduction domains and includes the third helix of Antennapedia,[53] Tat HIV protein,[2] VP22 protein,[61,62] and transportan.[63] These peptides have been proposed to enter the cell through a mechanism independent of the endosomal pathway and will be described in detail in other chapters of this book.

5.3.3 Applications for NLS in Cell-Penetrating Peptides

NLS peptides covalently linked to a variety of proteins have already been demonstrated to increase the potential for nuclear localization and to confer nuclear localization to nonnuclear proteins. Moreover, NLSs have been associated with different hydrophobic cell-penetrating peptides in order to favor membrane crossing of nuclear targeting cargoes. Finally, NLSs have been associated with cationic peptides or motifs to facilitate DNA binding and compaction for gene delivery.[8-10]

Several bifunctional peptides containing NLS have been described (Table 5.1). Braden et al. have proposed a bifunctional peptide (PNA–NLS) combining a peptide nucleic acid (PNA) with the core nuclear localization sequence of SV40 for gene delivery. PNAs are synthetic molecules which bind DNA with high affinity and specificity.[64,65] They have been used to label specific locations of DNA with high interactive specificity and stability.[66] PNA–NLS associated with polyethyleimide dramatically increase the nuclear uptake of oligonucleotides and facilitate plasmid transfection in an NLS-dependent fashion. PNA–NLS-conjugated molecules constitute a promising tool for therapeutic gene therapy and have recently been used successfully for *in vivo* nuclear delivery of ODN.[67] However, one of the limitations of this approach resides in the choice of the PNA target site to promote efficient transfection.

The NLS of NFkB p50 subunit was coupled with the cell membrane-permeable motif carrier derived from the hydrophobic region of the signal peptide of Kaposi fibroblast growth factor (K-FGF). This cell penetrating peptide was shown to block intracellular recognition of the NLS and to inhibit nuclear translocation of NF-κB transcription factor. The authors demonstrated that the biological effects were due to the NLS, as transport was energy dependent and completely abolished upon mutation or deletion of the NLS.[68]

Several studies have shown that cross-linking an NLS to polycationic peptides (pLys) can enhance transfection by specifically conferring recognition by nuclear import receptors. Peptide P101 associated with polylysine improves recognition by

the nuclear import machinery and enhances transfection efficiency.[33,34] An interesting system was described using a recombinant fusion peptide containing a Gal4 DNA-binding domain associated to a fragment of the invasin protein of Yersinia pseudotuberculosis.[69] The Gal4 moiety of the system confers DNA-binding and nuclear targeting characteristics through a mechanism independent of the importin β pathway. However, Gal4 DNA-binding and nuclear targeting properties are mutually exclusive, leading to inefficient transport of DNA into the nucleus. In order to use the inherent property of Gal4 to bind DNA and preserve nuclear targeting characteristics, the Gal4 peptide was coupled with SV40 NLS polylysine. Association of Gal4 with an NLS has been used to improve its transfection efficiency.[69,70]

Bacterial NLSs containing proteins were also used for nuclear import of DNA into mammalian cells. *Agrobacterium* virulence proteins VirD2 and VirE2 have been demonstrated to be efficient in promoting DNA delivery into Hela cells. Nuclear import is dependent on α importin and Ran GTP protein.[71]

Peptide vehicles that integrate multiple targeting and routing signals are often limited due to synthetic constraints and domain presentation issues associated with linear assemblies of efficient NLS-conjugated proteins. For example, the simple cross-linking between an NLS and an MPS does not work in numerous cases, and insertion of a linker sequence is essential to preserve the properties of these domains.[72] In order to control these parameters, branched peptides or L-oligomers have been developed containing cytoplasmic translocating sequence signals and nuclear localization signals. L-oligomers corresponding to peptides that integrate multiple targeting and routing signals have been developed involving polylysine and NLS. These branched peptides have been used as nonviral transfection agents for the delivery of proteins and genes.[4,73] Branched peptides are rapidly internalized by endocytosis and can target and accumulate in different subcellular compartments.[4,74]

The signal sequence of the Ig(v) light chain of caiman crocodilus or the fusion peptide of HIV-1 gp41 has been associated to the hydrophilic nuclear localization sequence of SV40 large T antigen[5] to develop a single chain peptide-vector (FP-NLS: GALFLGFLGAAGSTMGAWSQPKKKRKV referred to hereafter as MPG or SP-NLS: MGLGLHLLVLAAALQGAWSQPKKKRK) which efficiently delivers short oligonucleotides and drugs into a wide variety of cell lines independently of the endosomal pathway.[48-51] The FP-NLS peptide family interacts strongly with nucleic acids through its NLS domain and forms peptide–peptide interactions through the gp41 hydrophobic domain, thus generating a peptide cage around the plasmid. After crossing the cell membrane, the presence of the NLS domain promotes rapid delivery of the plasmid into the nucleus.

Structural and mechanistic investigations have revealed that the flexibility between the two domains of MPG is crucial for gene delivery and can be improved by adding a linker sequence between the fusion and the NLS motifs.[5,75] MPG was shown to deliver small hydrophobic peptides using a similar nonendosomal pathway. Activity of this peptide is associated to a very versatile structure, and greatest activity is associated with β-strand structure, whereas α-helical folding is associated with toxicity. MPG activity is independent of the endosomal pathway and its NLS enables it to deliver and express transgenes in the nucleus of nondividing cells (Figure 5.4).

A similar strategy has been used to develop a short amphipathic peptide carrier for protein delivery. This peptide carrier (chariot) contains three domains: a hydrophobic tryptophan-rich motif, an NLS domain derived from the SV40 large T antigen, and a spacer domain which improves flexibility and integrity of the hydrophobic and the hydrophilic domains. Chariot is able to efficiently deliver a variety of peptides and proteins into several cell lines in a fully biologically active form, without the need for prior chemical covalent coupling or denaturation steps.[52]

5.4 UTILIZATION OF THE NLS PATHWAY FOR NUCLEAR IMPORT OF GENE DELIVERY VECTORS

5.4.1 Challenges in Gene Delivery

In the past 5 years the potential hazards of viral vectors as well as their immunogenicity have led research in the field of gene therapy to focus at least in part on the design of new tools and methods for gene delivery. In this respect, the major challenge resides in the design of nonviral vectors that can compensate for the poor permeability of the cell membrane to nucleic acids and improve intracellular trafficking and nuclear delivery of genes into target cells with minimal toxicity.[5,9,76-78] Nonviral systems present several advantages over viral systems, in that they are simple to use, easily produced, do not induce specific immune responses, and are less cytotoxic. Cell-penetrating peptides constitute an interesting subclass among nonviral gene delivery systems. The challenge in peptide-based gene delivery systems is to define the ideal formulation that satisfies most of the major requirements: (1) reversible binding to cargo or DNA, (2) cellular or tissue specificity essential for *in vivo* gene delivery, (3) membrane fusogenic or disruptive activities, and (4) ability to promote nuclear translocation of plasmids (Figure 5.2).

One of the major issues in gene therapy is the dependency of delivery systems on the mitotic activity of cells, illustrated by lack of efficient delivery into nondividing cells. This is primarily due to the inability of most nonviral gene delivery systems to translocate plasmids into the nucleus of nondividing cells. Several modifications of plasmid DNA have been proposed to improve their interaction with the nuclear import machinery, including additional cloning of specific DNA sequences recognized by transcription factors, the attachment of glycosylated moieties, or of synthetic peptides containing a nuclear localization signal.[79,80] Alternatively, NLSs have been incorporated into nonviral gene delivery systems and either noncovalently or covalently linked to the cargo or the DNA. Except for a few examples, incorporation of an NLS significantly increases the efficiency of transfection. However, in contrast to their effect on proteins, NLSs do not appear to improve nuclear targeting of DNA; significantly in most cases, NLS simply improves formation of DNA and peptide complexes through electrostatic interactions.[8,9]

5.4.2 Noncovalent Incorporation of Nuclear Localization Sequences

Noncovalent attachment of the NLS can be achieved by taking advantage of the cationic residues within the NLS or by fusion or covalent binding of the NLS to a

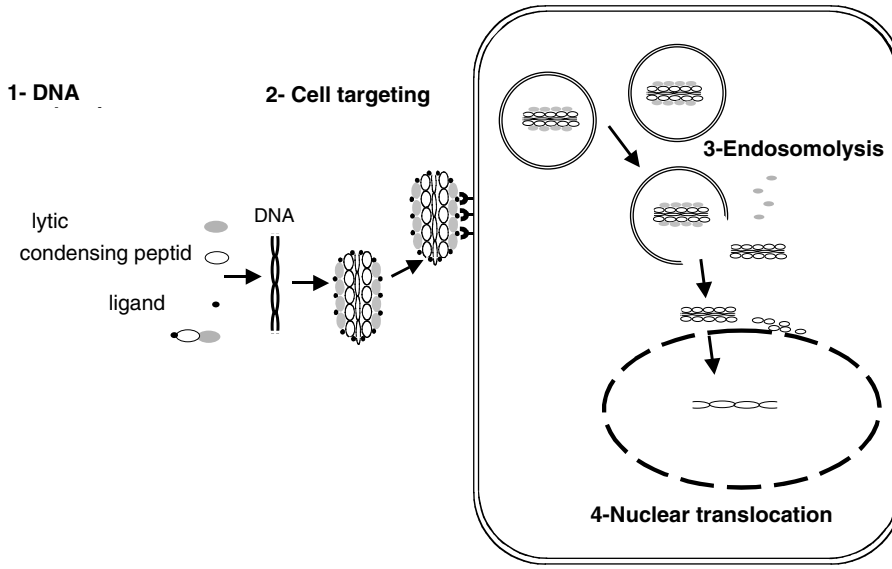

FIGURE 5.2 The four major steps in peptide-based gene delivery: (1) DNA binding and condensation, (2) cell targeting, (3) endosomal release of the plasmid or ODN, and (4) nuclear targeting.

cationic moiety, such as the polylysine DNA-binding domain. Noncovalent attachment of an NLS to DNA is preferable to enable complete release of DNA from the NLS-containing peptide following nucleocytoplasmic transport. However, a series of parameters need to be controlled and cannot be generalized, including the number of NLS molecules used and the ratio of NLS to DNA. Special attention is required when considering the mechanism of complex formation and the order of association of a multicomponent DNA carrier. The total amount of NLS is important because the import mechanism can be saturated by an excess of free NLS. Also, care has to be taken to avoid binding of the NLS within the DNA.

The NLS from the large T antigen of SV 40 (PKKKRKV) is one the most used in nonviral gene delivery systems.[4,5,9,81] Peptides containing NLS are able to condense DNA and to form a single transfection system without any further requirement. They have been shown to increase aggregation at the surface of the cell and to improve delivery. However, among the several examples described so far, the role of the NLS in nuclear accumulation of DNA appears to be controversial.[82,83] The association of an NLS to DNA was shown to increase transgene expression following cytoplasmic injection into zebrafish eggs.[84] Complexes of DNA with peptide scaffolds consisting of the M9 import sequence with a scrambled SV40 NLS peptide were used to improve binding via NLSs.[9,85] Peptides or proteins containing NLS, complexed or not to lipids, are used to improve nuclear transport through electrostatic binding of plasmids.[9] An NLS associated to a PNA sequence with a sequence-specific DNA-binding domain allows control of the number of attached molecules and of their binding sites in the DNA.[66,67]

5.4.2.1 Covalent Linkage of NLS to Condensing Agents

NLSs are also covalently linked to components of nonviral gene delivery systems.[86-88] For a single chimeric peptide, one of the most important criteria is sequence organization. In chimeric proteins containing a DNA-binding domain and an NLS, competition between these two moieties for DNA binding is prevented, and the accessibility of the NLS enhanced, by using neutral or anionic NLSs, or a longer NLS sequence with negatively charged residues upstream or downstream.

The presence of an SV40 NLS sequence linked to pLL increases transgene expression.[33,34] The association of fusion peptide with an NLS was shown to promote both rapid plasmid delivery into the nucleus and transgene expression.[50,51] A recent study has demonstrated that condensation of DNA with pLL-NLS can be used to enhance transfection of polyplex targeted to cells expressing the melanocyte stimulating hormone (MSH) receptor. A chimeric Gal4-α MSH fusion protein was associated with an optimized SV40 NLS. The NLS was used to compensate the antagonistic impact of GAL4 binding to DNA and nuclear targeting and to promote nuclear transfer of genes.[69-70]

5.4.2.2 NLS Linkage Directly to DNA

The influence of the number and localization of the NLS on the nuclear import of exogenous DNA are essential criteria participating in the controversy over the effect of the NLS. Several studies have developed strategies to attach an NLS directly to plasmid DNA by using either photoactivation[88] or cyclopropapyroloindole for conjugation.[86] Although the NLS–DNA conjugate was shown to associate with importin, such approaches offer no control as to the number of NLSs attached or their location within the DNA, two parameters essential for the success of this strategy. A critical number of NLSs (between 50 and 100, depending on the method used) attached to DNA are required for efficient transgene expression.[88,86] However, poor delivery of plasmids into the nucleus was observed when a large number of NLSs was linked to DNA.[86-89]

Another approach is to control the number and site of attachment of the NLS at specific points in the plasmid to avoid loss of transgene expression; the location of the NLS is an important parameter. A method described by Zanta et al. proposes to modify the ODN with NLS using maleimide chemistry followed by ligation of this site to a luciferase expression cassette to produce a vector containing a single-terminal NLS.[87] This approach was shown to improve gene expression following transfection, independently of the transfection system used, and also lead to peak expression after 12 h instead of 24 h in the absence of NLS.[87] Another method developed by Ludtke et al., involves the use of SV40 NLS conjugated to streptavidin bound to a biotinylated DNA fragment. The authors demonstrated that streptavidin–NLS promoted active nuclear uptake of linear DNA. However, this method seems to be limited to short DNA fragments.[89]

One NLS molecule seems to be sufficient to promote nuclear delivery of DNA. From a mechanistic point of view, the NLS docks the DNA onto the nuclear pore and the DNA is then translocated through the nuclear pore. As the DNA enters the

nucleus, it rapidly condenses into a chromatin-like structure. Multiple NLSs might therefore inhibit nuclear transport of two NLSs docked onto a nuclear pore.[87]

5.5 DESIGN AND EVALUATION OF NLS-CONTAINING CELL-PENETRATING PEPTIDES

The "ideal" NLS cargo complex is recognized by the nuclear import machinery through specific NLS sequences; this complex is driven into the nucleus where it enhances transgene expression. Efficient nuclear transport of cell-penetrating peptides requires essential steps that are controlled by several regulatory pathways. As such, these parameters need to be taken into account when designing a new peptide vector. Of particular relevance are accessibility of the NLS and availability of the import factors, regulation of affinity of the NLS for its import receptor, phosphorylation, existence of cytosolic or nucleoplasmic retention signals, and regulation of NPC permeability, as well as the possible regulation of the affinity of the cargo for the hydrophobic central channel. In this section, technical aspects will be described in order to evaluate and improve NLS-containing cell-penetrating peptides.[5,9,18,27]

5.5.1 Mechanism of Cell Delivery

The transfection or transport of cargo into cells involves a number of selective steps in addition to nuclear import. Understanding the behavior of cell-penetrating peptide and DNA or cargo complexes in cells is essential to improve their efficiency. Intracellular transport of drugs or cargo into the nucleus can occur through endocytosis or through an independent pathway. A large number of methods has been proposed to determine the mechanism of inhibition of specific stages of the endosomal pathway (Figure 5.3).[5-9]

Cytochalasin B, bafilomycin A, and chloroquine are drugs that interfere with the endosomal pathway and whose effects are observed at concentrations ranging from 5 to 25 μM.[90] Cytochalasin B depolymerizes microfilaments involved in phagocytosis without affecting other endocytotic processes such as receptor-mediated endocytosis.[91] The effects of cytochalasin B can be observed in a dose-dependent manner with a maximal effect at 50 μg/ml. Bafilomycin A and chloroquine interfere with the acidification of early and late endosomes, respectively. Bafilomycin A is a specific inhibitor of the vacuolar proton pump ATPase, and therefore prevents acidification of early endosomes and blocks formation of endosomal transport vesicles between early and late endosomes.[90,92] Chloroquine acts as a weak organic base and neutralizes the pH of late endosomes.[90,93] If the cell-penetrating internalization process occurs through the endosomal pathway, at least one of these inhibitors should dramatically affect expression of the transgene. Bafilomycin A inhibits and chloroquine increases expression of transgene delivered by cationic lipid or MPS vectors. (For review, see Brisson et al.[90])

In stark contrast with this internalization process, transfection mediated by the peptide carrier MPG (Figure 5.4) is absolutely not affected by either of these inhibitors, suggesting that MPG-dependent internalization is independent of the endosomal

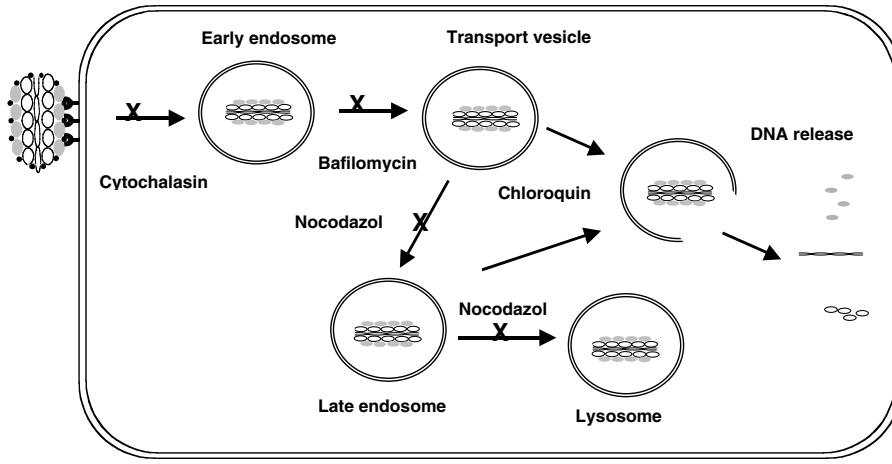

FIGURE 5.3 Mechanism of action of several cell-trafficking inhibitors. Penetration of a DNA formulation is blocked by cytochalasin B, an inhibitor of microfilament depolarization. The complexes then enter early endosomes, followed by formation of transport vesicles, which can be blocked by bafilomycin A, an inhibitor of vacuolar ATPase. Maturation of the transport vesicles into late endosomes can be inhibited by addition of chloroquin, a weak base. Finally, fusion of the late endosomes with lysosomal compartments can be blocked by nocodazole, which induces microtubule depolymerization.

pathway.[50,51] Cell-penetrating peptides can enter the nucleus through a mechanism independent of the importin pathway or by active transport dependent on energy. The question of energy is therefore an important parameter to be considered when characterizing the nuclear import mechanism. The endosomal pathway is energy-dependent, so incubation at 4°C constitutes one of the means of blocking that pathway; however, this may be limited to specific cell lines and may affect cell death or modify cellular composition.

5.5.2 Mechanism of Nuclear Transport

Several examples using NLS-containing peptides have been demonstrated to facilitate transfection of DNA.[6-10] However, only a fraction of these show a real effect of the NLS as a nuclear-facilitating agent. This effect should be investigated directly on nuclear import and nuclear accumulation of plasmid should be monitored to distinguish from secondary effects. In most cases, the NLS may contribute through nonspecific electrostatic interactions that enhance DNA complex formation or aggregation. It is therefore important to establish a correlation between transfection efficiency and interaction with the import machinery.

In all cases, control experiments should be performed with cell-penetrating peptides lacking an NLS or containing mutated or scrambled NLSs, to confirm the specific role of the NLS. SV40-derived NLS peptides were used and in control a reverse NLS showed no transfection[33] or nuclear import following microinjection into zebrafish eggs using luciferase reporter gene.[84] A specific M9-NLS sequence

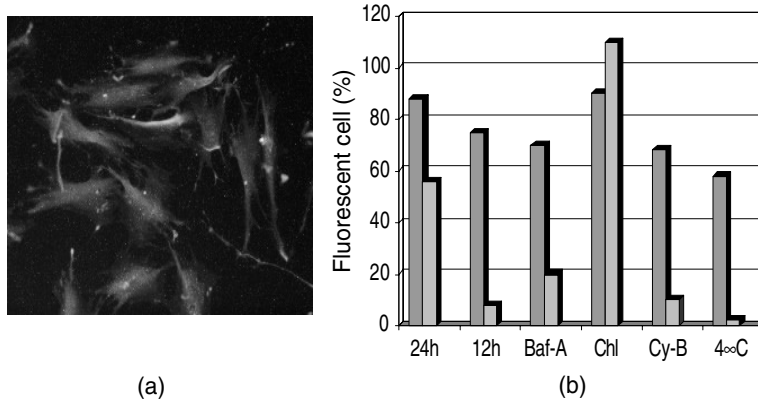

FIGURE 5.4 (Color Figure 5.4 follows p. 14.) MPG-mediated gene delivery mechanism. (a) MPG-mediated pcDNA3.1NT-GFP plasmid delivery in human fibroblast cell line HS-68. Cells were incubated in the presence of preformed MPG/DNA complexes for 1 h at 37°C, after which they were replaced in DMEM supplemented with 10% FCS. Expression of GFP is monitored 24 h later. (b) Mechanism of MPG-mediated gene delivery. Cells were incubated in the presence of preformed MPG/DNA (in red) complexes for 1 h at 4°C, or at 37°C in the absence or presence of several cell-trafficking inhibitors, bafilomycin A (Baf-A), chloroquin (Chl), and cytochalasin B (Cy-B). Following this treatment, cells were replaced in DMEM supplemented with 10% FCS and expression of GFP was monitored 12 or 24 h later. As a control, similar experiments were performed with a cationic lipid formulation (in blue).

noncovalently attached to plasmid DNA was shown to improve mammalian cell transfection significantly. Both NLS and electrostatic properties can be used to improve the effect of the NLS. M9 sequence, fused to a scrambled NLS for DNA binding and combined with Lipofectamine™ for transfection increases reporter gene expression ten-fold compared to scrambled M9 sequence.[85] Associating an NLS with a PNA is an excellent transfection tool, and NLS–PNA conjugates have been shown to be specific using scrambled NLS as a negative control.[66]

Several methods have been described to study the nuclear transfer of cell-penetrating peptide containing NLS.

1. *Interaction with importin factor.* Physical interaction with import factors can be monitored *in vitro* using recombinant proteins which yield information concerning specificity, affinity, and stoechiometry. Methods have been described using recombinant importin proteins and an ELISA-based binding assay.[33] *In vitro* binding assays reporting the binding of NLS to importin have revealed that the NLS is specific.
2. *Microinjection and cell permeabilization.* The direct effect of an NLS on nuclear transfer can be investigated by either microinjection into the cytoplasm or using methods for cell permeabilization. Digitonin permeabilization of the cell and direct injection of genetic material have been the methods of choice for study of NLS function.[71,94] However, these are limited by the quality and quantity of the preparation. DNA–NLS complexes

microinjected into the cytoplasm of living cells localized rapidly into the nucleus and were specifically inhibited by inhibitors of the NPC import pathway.[84]

3. *Utilization of inhibitors of nuclear import.* Nuclear import of cargo or DNA is an active process that is inhibited at 4°C or following energy depletion,[95] depending on cell culture methods. These methods are dependent on the cell lines and therefore special care should be taken. Nuclear import can be blocked by competitive NLS protein coinjection of BSA or of lectin-specific wheat germ agglutinin (WGA).[96] For example, WGA has been shown to compete with the α-importin pathway: WGA with NLS-streptavidine, suggesting that nuclear import of NLS covalently attached to a plasmid occurs through the α-importin pathway.[86] DNA M9 complex was shown to accumulate in nuclei and to translocate through NPCs by WGA blocking experiments.[85]
4. *Control of the cell cycle.* Gene expression following microinjection of DNA in the cytoplasm is generally quite inefficient, in fact, gene expression is much greater in dividing cells than in nondividing cells. Since the nuclear membrane is disintegrated during mitosis, the presence of an NLS is crucial for nuclear transfection of postmitotic cells. Experiments should also be performed on nondividing cells or in G1 arrested or synchronized cells and earlier expression (12 h after transfection) should be monitored.[87] Synchronization of cells is cell line-dependent and must be controlled. Different techniques such as serum deprivation, nocodazole, or thymidine blocks can be applied.[97]
5. *Monitoring nuclear accumulation.* Accumulation of plasmid in the nucleus can be determined by quantitative PCR with specific reporter vectors or by fluorescence microscopy following direct labeling of DNA or using traceable molecules.[98,99]

5.6 CONCLUSIONS

The nucleus constitutes both a major target for drugs and a major barrier for biologically active molecules. A large number of cell-penetrating peptides have been designed containing an NLS domain, which allows nuclear targeting. In the case of cell penetratin peptides or proteins containing an NLS, the role of the NLS is well established, but its function in nuclear transfer of DNA remains unclear. Several points need to be clarified to justify the requirement for an NLS and to improve the design and efficiency of novel NLS-containing cell-penetrating peptides. Standardization of experiments is essential because cell lines and problems in comparing different systems require some form of standardization. Also, progress needs to be made in order to limit toxicity of these novel molecular tools.

In conclusion, NLS-mediated transport is an essential technology or pathway to improve drug and gene therapies. The design of the next generation of peptide-based cell delivery systems is likely to combine properties of NLS with other cellular requirements, such as selectivity, signaling, and the knowledge of cell cycle regulations.

REFERENCES

1. Lindgren et al., Cell-penetrating peptides, *Trends Pharmacol. Sci.,* 21, 99, 2000.
2. Schwarze, S.R. and Dowdy, S.F., *In vivo* protein transduction: intracellular delivery of biologically active proteins, compounds and DNA, *Trends Pharmacol. Sci*., 21, 45, 2000.
3. Prochiantz, A., Messenger proteins: homeoproteins, TAT and others, *Curr. Opin. Cell Biol.,* 12, 400, 2000.
4. Gariepy, J. and Kawamura, K., Vectorial delivery of macromolecules into cells using peptide-based vehicles, *Trends Biotechnol*., 19, 21, 2001.
5. Morris, M.C. et al., Translocating peptides and proteins and their use for gene delivery, *Curr. Opin. Biotechnol.,* 11, 461, 2000.
6. Snyder, E.L. and Dowdy, S.F., Protein/peptide transduction domains: potential to deliver large DNA molecules into cells, *Curr. Opin. Mol. Ther.,* 2, 147, 2001.
7. Schwartz, J. and Zhang, S., Peptide-mediated cellular delivery, *Curr. Opin. Mol. Ther.,* 2, 162, 2000.
8. Bremner, K.H., Seymour, L.W., and Pouton, C.W., Harnessing nuclear localization pathways for transgene delivery, *Curr. Opin. Mol. Ther.,* 3, 170, 2001.
9. Mahato, R.I. et al., Peptide-based gene delivery, *Curr. Opin. Mol. Ther.,* 1, 226, 1999.
10. Hawiger, J., Cellular import of functional peptides to block intracellular signaling, *Curr. Opin. Immunol*., 9, 189, 1997.
11. Görlich, D. and Mattaj, I.W., Nucleocytoplasmic transport, *Science,* 271, 1513, 1996.
12. Mattaj, I.W. and Englmeier, L., Nucleocytoplasmic transport: the soluble phase, *Annu. Rev. Biochem*., 123, 265, 1998.
13. Goldfarb, D.S. et al., Synthetic peptides as nuclear localization signals, *Nature,* 322, 614, 1986.
14. Dingwall, C. and Laskey, R.A., Nuclear targeting sequences — a consensus? *Trends Biochem. Sci.,* 16, 477, 1991.
15. Robbins, J. et al., Two interdependent basic domains in nucleoplasmin nuclear targeting sequence: identification of a class of bipartite nuclear targeting sequence, *Cell*, 64, 615, 1991.
16. Landford, R.E., Kanda, P., and Kennedy, R.C., Introduction of nuclear transport with synthetic peptide homologous to the SV40 T-antigen transport signal, *Cell,* 46, 575, 1986.
17. Chan, C.K. and Jans, D.A., Enhancement of MSH receptor- and GAL4-mediated gene transfer by switching the nuclear import pathway, *Gene Ther.,* 8,166, 2001.
18. Kaffman, A. and O'Shea, E.K., Regulation of nuclear localization: a key door, *Annu. Rev. Cell Dev. Biol.,* 15, 291, 1999.
19. Nigg, E.A., Nucleocytoplasmic transport: signals, mechanisms and regulation, *Nature*, 386, 779, 1997.
20. Jans, D.A., Xiao, C.Y., and Lam, M.H., Nuclear targeting signal recognition: a key control point in nuclear transport? *Bioessays*, 22, 532, 2000.
21. Gorlich, D. and Kutay, V., Transport between the cell nucleus and the cytoplasm, *Annu. Rev. Cell Dev. Biol.,* 15, 607, 1999.
22. Allen, T.D. et al. The nuclear pore complex: mediator of translocation between nucleus and cytoplasm, *J. Cell Sci.,* 113, 1651, 2000.
23. Stoffler, D., Fahrenkrog, B., and Aebi, U., The nuclear pore complex: from molecular architecture to function dynamics, *Curr. Opin. Cell Biol*., 11, 391, 1999.
24. Sweitzer, T.D., Love, D.C., and Hanover, J.A., Regulation of nuclear import and export, *Curr. Top. Cell Regul.,* 36, 77, 2000.

25. Wente, S.R., Gatekeepers of the nucleus, *Science,* 288, 1374, 2000.
26. Ribbeck, K. and Gorlich, D., Kinetic analysis of translocation through nuclear pore complexes, *Embo. J.,* 20, 1320, 2001.
27. Catimel, B. et al., Biophysical characterization of interactions involving importin-alpha during nuclear import, *J. Biol. Chem.,* 276, 34189, 2001.
28. Kobe, B., Autoinhibition by an internal nuclear localization signal revealed by the crystal structure of mammalian importin alpha, *Nat. Struct. Biol.,* 4, 388, 1999.
29. Siomi, M.C. et al., Transportin-mediated nuclear import of heterogeneous nuclear RNP proteins, *J. Cell Biol.,* 138, 1181, 1997.
30. Bogerd, H.P. et al., Definition of a consensus transportin-specific nucleocytoplasmic transport signal, *J. Biol. Chem.,* 274, 9771, 1999.
31. Truant, R., Kang, Y., and Cullen, B., The human tap nuclear RNA export factor contains a novel transportin-dependent nuclear localization signal that lacks nuclear export signal function, *J. Biol. Chem.,* 274, 32167, 1999.
32. Hubner, S., Xiao, C.Y., and Jans, D.A., The protein kinase CK2 site (Ser111/112) enhances recognition of the simian virus 40 large T-antigen nuclear localization sequence by importin*, J. Biol. Chem.,* 272, 1719, 1997.
33. Chan, C.K., Senden, T., and Jans, D.A., Supramolecular structure and nuclear targeting efficiency determine the enhancement of transfection by modified polylysines, *Gene Ther.,* 19, 1690, 2000.
34. Chan, C.K. and Jans, D.A., Enhancement of polylysine-mediated transferrinfection by nuclear localization sequences: polylysine does not function as a nuclear localization sequence, *Hum. Gene Ther.,* 10, 1695, 1999.
35. Nakielny, S. et al., Transportin: nuclear transport receptor of a novel nuclear protein import pathway, *Exp. Cell Res.,* 229, 261, 1996.
36. Michael, W.M., Choi, M., and Dreyfuss, G., A nuclear export-signal in hnRNP A1: a signal mediated, temperature-dependent nuclear protein export pathway, *Cell*, 83, 415, 1995.
37. Cullen, B., Journey to the center of the cell, *Cell*, 105, 697, 2001.
38. Saphire, A.C.S. et al., Nuclear import of adenovirus DNA *in vitro* involves the nuclear protein import pathway and hsc70, *J. Biol. Chem.,* 275, 4298, 2000.
39. Kichler, A. et al., Efficient DNA transfection mediated by the C-terminal domain of human immunodeficiency virus type 1 viral protein R, *J. Virol.,* 74, 5424, 2000.
40. Jenkins, Y. et al., Characterization of HIV-1 vpr nuclear import: analysis of signals and pathways, *J. Cell Biol.,* 143, 875, 1998.
41. Vodicka, M.A. et al., HIV-1 Vpr interacts with the nuclear transport pathway to promote macrophage infection, *Gene Dev.*, 12, 175, 1998.
42. Truant, R. and Cullen, B.R., The arginine-rich domains present in human immunodeficiency virus type 1 Tat and Rev function as direct importin α-dependent nuclear localization signals, *Mol. Cell. Biol.,* 19, 1210, 1999.
43. Hong, J.S. and Engler, J.A., The amino terminus of the adenovirus fiber protein encodes the nuclear localization signal, *Virology*, 185, 758, 1999.
44. Zhang, L. et al., Preparation of functionally active cell-permeable peptides by single-step ligation of two peptide modules, *Proc. Natl. Acad. Sci. U.S.A.,* 95, 9184,1998.
45. Rojas, M. et al., Genetic engineering of proteins with cell membrane permeability, *Nat. Biotechnol.,* 16, 370, 1998.
46. Lui, K.Y. et al., Identification of functionally important sequence in the cytoplasmic tail of integrin beta 3 by using cell-permeable peptide-analogs, *Proc. Natl. Acad. Sci. U.S.A.,* 93, 11819, 1996.

47. Chaloin, L. et al., Conformations of primary amphipathic carrier peptides in membrane mimicking environments, *Biochemistry*, 36, 11179, 1997.
48. Chaloin, L. et al., Design of carrier peptide-oligonucleotide conjugates with rapid membrane translocation and nuclear localization properties, *Biochem. Biophys. Res. Commun.,* 243, 601, 1998.
49. Chaloin, L. et al., Improvement of porphyrin cellular delivery and activity by conjugation to a carrier peptide, *Bioconjug Chem.,* 12, 691, 2001.
50. Morris, M.C. et al., A new peptide vector for efficient delivery of oligonucleotide into nontransformed mammalian cells, *Nucleic Acids Res.*, 25, 2730, 1997.
51. Morris M.C. et al., A novel potent strategy for gene delivery using a single peptide vector as a carrier, *Nucleic Acids Res.*, 27, 3510, 1999.
52. Morris, M.C. et al., A new potent peptide carrier for the delivery of biologically active proteins into mammalian cells, *Nat. Biotechnol.,* 19, 1173*,* 2001.
53. Wagner, E., Effects of membrane-active agents in gene delivery, *J. Control. Rel.*, 53, 155, 1998.
54. Plank, C., Zauner, W., and Wagner, E., Application of membrane-active peptides for drug and gene delivery across cellular membrane, *Adv. Drug. Del. Rev.*, 34, 21, 1998.
55. Lear, J.D. and DeGrado, W.F., Membrane binding and conformational properties of peptides representing the NH2 terminus of influenza HA-2, *J. Biol. Chem.*, 262, 6500, 1987.
56. Parente, R.A. et al., Association of a pH-sensitive peptide with membrane vesicles: role of amino-acid sequence, *Biochemistry,* 29, 8713, 1990.
57. Wyman, T.B. et al., Design, synthesis and characterization of a cationic peptide that binds to nucleic acids and permeabilizes bilayers, *Biochemistry,* 27, 3008, 1997.
58. Gottschalk, S. et al., A novel DNA-peptide complex for efficient gene transfer and expression in mammalian cells, *Gene Ther.,* 3, 448, 1996.
59. Niidome, T. et al., Binding of cationic α-helical peptides to plasmid DNA and their gene transfer abilities into cells, *J. Biol. Chem*., 272, 15307, 1997.
60. Derossi, D., Chassaing, G., and Prochiantz, A., Trojan peptides: the penetratin system for intracellular delivery, *Trends Cell Biol.*, 8, 84, 1998.
61. Elliott, G. and O'Hare, P., Intercellular trafficking and protein delivery by a Herpesvirus structural protein, *Cell*, 88, 223, 1997.
62. Phelan, A., Elliott, G., and O'Hare, P., Intercellular delivery of functional p53 by the herpes virus protein VP22, *Nat. Biotechnol.,* 16, 440, 1998.
63. Pooga, M. et al., Cell penetration by transportan, *FASEB J.,* 12, 67, 1998.
64. Demidov, U.V. et al., Kinetics and mechanism of polyamide ("peptide") nucleic acid binding to duplex DNA, *Proc. Natl. Acad. Sci. U.S.A.,* 92, 2637, 1995.
65. Hyrup, B. and Nielsen, P.E., Peptide nucleic acids (PNA) synthesis, properties and potential applications, *Bioorg. Med. Chem.,* 4, 5, 1996.
66. Branden, L.J., Mohamed, A.J., and Smith, C.I.E., A peptide nucleic acid-nuclear localization signal fusion that mediates nuclear transport of DNA, *Nat. Biotechnol.,* 17, 784, 1999.
67. Branden, L.J., Christensson, B., and Smith, C.I.E., *In vivo* nuclear delivery of oligonucleotides via hybridizing bifunctional peptides, *Gene Ther.,* 8, 84, 2001.
68. Lin, Y.Z. et al., Inhibition of nuclear translocation of transcription factor NF-kappa B by a synthetic peptide containing a cell membrane-permeable motif and nuclear localization sequence, *J. Biol. Chem.*, 270, 14255, 1995.
69. Chan, C.K. et al., Mutual exclusivity of DNA binding and nuclear localization signal recognition by the yeast transcription factor GAL4: implications for nonviral DNA delivery, *Gene Ther.,* 9, 1204, 1998.

70. Chan, C.K. and Jans, D.A., Enhancement of MSH receptor- and GAL4-mediated gene transfer by switching the nuclear import pathway, *Gene Ther.,* 2, 166, 2001.
71. Ziemienowicz, A. et al., Import of DNA into mammalian nuclei by proteins originating from plant pathogenic bacterium, *Proc. Natl. Acad. Sci. U.S.A.,* 96, 3729, 1999.
72. Vidal, P. et al., Interaction of primary amphipatic vector peptides with membranes: conformational consequences and influence on cellular localisation, *J. Membr. Biol.*, 162, 159, 1998.
73. Sheldon, K. et al., Loligomers: design of *de novo* peptide-based intracellular vehicles, *Proc. Natl. Acad. Sci. U.S.A.,* 92, 2056, 1995.
74. Singh, D. et al., Penetration and intracellular routing of nucleus-directed peptide-based shuttles (loligomers) in eukaryotic cells, *Biochemistry*, 37, 5798, 1998.
75. Chaloin, L. et al., Synthetic primary amphipathic peptides as tools for the cellular import of drugs and nucleic acids, *Curr. Top. Pep. Prot. Res.,* 3, 153, 1999.
76. Anderson, W.F., Human gene therapy, *Nature*, 392, 25, 1998.
77. Ledley, F.D., Nonviral gene therapy: the promise of genes as pharmaceutical products, *Hum. Gene Ther.*, 6, 1124, 1995.
78. Luo, D. and Saltzman, M., Synthetic DNA delivery systems, *Nat. Biotechnol.*, 18, 33, 2000.
79. Vacik, M. et al., Cell-specific nuclear import of plasmid DNA, *Gene Ther.,* 6, 1006, 1999.
80. Fajac, I. et al., Sugar-mediated uptake of glycosylated polylysines and gene transfer into normal and cystic fibrosis airway epithelial cells, *Hum. Gene Ther.,* 10, 395, 1999.
81. Hawinger, J., Noninvasive intracellular delivery of functional peptide and proteins, *Curr. Opin. Chem. Biol.,* 3, 189, 1999.
82. Kaneda, Y., Iwai, K., and Uchida, T., Increased expression of DNA cointroduced with nuclear protein in adult rat liver, *Science*, 243, 375, 1989.
83. Fritz, J.D. et al., Gene transfer into mammalian cells using histone-condensed plasmid DNA, *Hum. Gene Ther.,* 7, 1395, 1996.
84. Collas, P. and Alestrom, P., Nuclear localization signals: a driving force for nuclear transport of plasmid DNA in zebrafish, *Biochem. Cell Biol.,* 75, 633, 1997.
85. Subramanian, A. et al., Nuclear targeting peptide scaffolds for lipofection of nondividing mammalian cells, *Nat. Biotechnol.,* 17, 873, 1999.
86. Sebestyen, M.G. et al., DNA vector chemistry: the covalent attachment of signal peptides to plasmid DNA, *Nat. Biotechnol.*, 16, 80, 1998.
87. Zanta, M.A., Belguise–Valladier, P., and Behr, J.P., Gene delivery: a single nuclear localization signal peptide is sufficient to carry DNA to the cell nucleus, *Proc. Natl. Acad. Sci. U.S.A.,* 96, 91, 1999.
88. Ciolina, C. et al., Coupling of nuclear localization signals to plasmid DNA and specific interaction of the conjugates with importin, *Bioconjug. Chem.*, 10, 49, 1999.
89. Ludtke, J.J. et al., A nuclear localization signal can enhance both the nuclear transport and expression of 1 kb DNA, *J. Cell Sci.*, 112, 2033, 1999.
90. Brisson, M. et al., Subcellular trafficking of the cytoplasmic expression system, *Hum. Gene Ther.,* 10, 2601, 1999.
91. Silverstein, S.C., Steinman, R.M., and Cohn, Z.A., Endocytosis, *Annu. Rev. Biochem.,* 46, 669, 1977.
92. Bowman, E.J., Siebers, A., and Altendorf, K., Bafilomycins: a class of inhibitors of membrane ATPases from microorganisms, animal cells and plant cells, *Proc. Natl. Acad. Sci. U.S.A.,* 85, 7972, 1988.
93. Maxfield, F.R., Weak bases and ionophores rapidly and reversibly raise the pH of endocytic vesicles in cultured mouse fibroblasts, *J. Cell Biol.,* 95, 676, 1982.

94. Görlich, D. et al., Distinct functions for the two importin subunits in nuclear protein import, *Nature*, 377, 246, 1995.
95. Melchior, F. et al., Inhibition of nuclear protein import by nonhydrolyzable analogues of GTP and identification of the small GTPase Ran/TC4 as an essential transport factor, *J. Cell Biol.,* 123, 1649, 1993.
96. Finlay, D.R. et al., Inhibition of *in vitro* nuclear transport by a lectin that binds to nuclear pores. *J. Cell Biol.,* 104, 189, 1987.
97. Davis, P.K., Ho, A., and Dowdy, S.F., Biological methods for cell-cycle synchronization of mammalian cells, *Biotechniques*, 30, 1322, 2001.
98. Vidal, P. et al., New strategy for RNA vectorization in mammalian cells. Use of a peptide vector, *C R Acad. Sci. III,* 320, 279, 1997.
99. Salman, H. et al., Kinetics and mechanism of DNA uptake into the cell nucleus, *Proc. Natl. Acad. Sci. U.S.A.,* 98, 7247, 2001.

6 Hydrophobic Membrane Translocating Sequence Peptides

Kristen Sadler, Yao-Zhong Lin, and James P. Tam

CONTENTS

6.1 INTRODUCTION

Advances in genomics and proteomics have led to the design of a significant number of therapeutic and diagnostic agents that target intracellular molecules. However, the delivery of such agents to the cytoplasm and nucleus is impeded by the cell membrane which is intrinsically impermeable to most peptides, proteins, and nucleic acids. To overcome this barrier, invasive techniques such as microinjection, electroporation, and application of pore-forming reagents have been used to introduce biologically active tools such as antibodies, synthetic peptides, and peptidomimetics into cells.[1-5] However, by their very nature, each of these techniques compromises the structural and functional integrity of the living cell. Furthermore, these techniques,

0-8493-1141-1/02/$0.00+$1.50

along with plasmid transfection used to introduce DNA fragments into cells,[6,7] also require complex sample manipulation, experienced technical staff, and purchase of single-purpose systems; the combination of these issues results in delivery techniques that are inaccessible to many research groups.

To allow simplified noninvasive delivery of peptides, proteins and oligonucleotides into intact cells a new method termed the "Trojan horse" approach has been developed. For this, the biologically active cargo is associated with a peptide intrinsically capable of penetrating the cell membrane lipid bilayer, resulting in delivery of the cargo to the intracellular space without lethal disruption of the membrane. Several peptides have been identified that can freely translocate across cell membranes and reside within the cytoplasm and nucleus without compromising normal cellular function. The majority of translocating peptides routinely used today have undergone sequence modifications such as amino acid substitution and formation of chimeras to produce variants with increased translocation activity compared to the original native sequences.

In the literature, there are two major classes of translocating peptides. The first category is highly cationic with arginine- or lysine-rich sequences. They include HIV-1 Tat peptide,[8] penetratin,[9] the chimeric transportan,[10] and heat shock protein Hsp70.[11] The second category is hydrophobic and based on protein signal sequences.[12] These peptides differ in size, composition, and, possibly, mechanism of entry; yet all exhibit translocation activity. The herpes simplex virus type 1 VP22 protein has also been reported to possess translocation activity that is not dependent on classical endocytosis or energy.[13] However, Lundberg and Johansson recently reported findings that suggest that the observed uptake is a product of artificial import and nuclear localization of VP22 during fixation.[14] O'Hare and Elliott agreed that some uptake during fixation does occur, but that this is a weak effect and insufficient to account for total transport activity.[15]

This chapter focuses on the identification and use of hydrophobic signal sequence-based peptides as translocation peptides; detailed descriptions of the remaining peptides may be found in other chapters of this handbook. Several aspects critical to the design of effective translocation peptides are also addressed, including the use of ligation strategies for coupling translocation peptides to cargoes and the identification of a potentially new class of translocation peptides.

6.2 SIGNAL HYPOTHESIS

Membrane translocating sequence (MTS) peptides are predominantly hydrophobic in character and therefore unlike the majority of translocating peptides also described in this book. These peptides are derived from secretory proteins that translocate through cellular membranes following synthesis and post-translational modifications. More than 20 years ago, Blobel and co-workers succinctly reported on the presence of a signal sequence and on the reliance of protein translocation on the interaction of this signal sequence with the membrane directly or the translocation machinery.[16-18]

Our understanding of the process by which a protein achieves its topological distribution within a cell or within a membrane has been shaped by Blobel's work.

The initial hypothesis proposed to answer questions such as whether there is a role for the N-terminal extension synthesized on secretory proteins and whether it is necessary for targeting was extended into a theory suggesting that signals exist to initiate and to terminate translocation.[17] This seminal work resulted in the establishment of the signal hypothesis and the 1999 Nobel Prize for Physiology or Medicine for Blobel. Currently understood mechanisms used by proteins to translocate across membranes are reviewed in Simon and Blobel.[18]

6.3 HYDROPHOBIC TRANSLOCATING PEPTIDES BASED ON THE SIGNAL SEQUENCE h-REGION

We now know that the signal sequence region consists of three distinct domains: a hydrophilic N terminus, a hydrophobic core, and a polar C terminus that usually defines a signal peptidase cleavage site.[19-22] The hydrophobic region (h-region) has been shown to play a central role in the ability of the protein to penetrate the membrane and, also, in the secondary conformation of the signal sequence.[23-28] Therefore, only the h-regions of certain signal sequences have been investigated as translocation peptides; the flanking residues that do not tend to influence translocation activity have been omitted. h-regions that generally range in length from 18 to 21 residues have been identified in over 100 proteins[29] and exhibit minimal primary structure homology. It appears that the average hydrophobic character of the h-region, and of the entire signal sequence, correlates more closely with observed translocation activity than the actual amino acid sequence.[30-32] Considering the translocating activity of the h-region peptides in the protein secretion process (protein export), these peptides have been recently tested for their ability to translocate and deliver cargo into living cells.[33] Lin et al. found that these h-region peptides are fully capable of importing other functional peptides and proteins into living cells.[33-36] Therefore, these h-region-based peptides have been termed membrane translocating sequence (MTS) peptides.

The following sections of this chapter describe the use of MTS peptides as translocation peptides in living cellular systems. The applications of MTS peptides in biological research and their potential in therapeutic development are also reviewed.

6.3.1 Development of SN50 Peptide: kFGF MTS Linked to NF-κB NLS

The hydrophobic MTS peptides are utilized most frequently for examination of intracellular signal transduction pathways and protein trafficking. The h-region of the signal sequence of Kaposi fibroblast growth factor (kFGF or FGF-4) was the first such peptide tested as an MTS.[33] In one of the earliest experiments designed to test the efficacy of the hydrophobic peptide, the 16-residue sequence AAVALLPAVLLALLAP from the h-region of kFGF was synthesized in tandem with a 25-residue peptide representing a nonhydrophobic region of the kFGF protein. The complete 41-residue peptide with the h-region located at the N terminus was radiolabeled through a tyrosine residue with ^{125}I and initially tested for uptake into cells *in vitro*. The peptide, termed ^{125}I-SKP, was found to be associated with NIH 3T3 cells

following a 30-min incubation; on average, 20 times more ^{125}I-SKP was associated with cells compared to a control peptide that lacked the MTS. The addition of the proteases Pronase and trypsin to the medium after incubation did not decrease the amount of radioactivity associated with the cells, indicating that the SKP peptide was at the very least buried in the membrane, if not present in the cytoplasm, and therefore inaccessible to the enzymes. Furthermore, cellular uptake was not inhibited by unlabeled SKP, thus excluding the possibility that the uptake was receptor mediated. It was also concluded that the peptide translocation was not reliant on large stores of ATP after it was shown that incubation with ATP-depleted cells did not prevent peptide uptake.

Once the translocation activity of the kFGF h-region had been confirmed, a peptide containing both the kFGF h-region and the nuclear localization sequence (NLS) of the nuclear factor-kappa B (NF-κB) p50 subunit was synthesized. The purpose was to produce a peptide that could translocate into intact cells and aid in the study of the role of the NF-κB NLS in the intracellular trafficking of this transcription factor.[33] The import of this chimeric peptide, termed SN50, into murine endothelial LE-II cells was monitored by confocal microscopy using an indirect immunofluorescence detection protocol. The import of SN50 was determined to be concentration-, time-, and temperature dependent, with maximum fluorescence observed after incubation at 37°C for 30 to 60 min at a concentration of 50 to 100 μg/ml.

Of equal importance was the biological activity of SN50; the peptide successfully competed with NF-κB complexes for the cellular machinery responsible for agonist-induced nuclear translocation of NF-κB. The inhibition of NF-κB nuclear translocation was concentration dependent, with the maximum inhibition occurring when the extracellular concentration of SN50 reached 50 μg/ml (18 μ*M*). This is the first example of the ability of an MTS to transport a functional domain into intact cells.

The SN50 peptide was used in a related study to delineate the mechanisms by which the nuclear import machinery recognizes the transcription factors NF-κB, AP-1, NFAT, and STAT1, each of which differs in NLS sequence.[37] Each of these transcription factors plays a critical role in the expression of genes important for cell growth, differentiation, and adhesion.[38,39] It was found that administration of SN50 to the medium containing human Jurkat T lymphocytes resulted in the uptake of the peptide by the activated cells. The imported SN50 was shown to inhibit nuclear import of NF-κB, AP-1, and NFAT at a high dose of 210 μg/ml in Jurkat cells. In other studies, however, lower doses of SN50 selectively and specifically inhibited NF-κB translocation in primary cells. For example, in primary human peripheral blood lymphocytes, lower doses of SN50 peptide (37.5 μg/ml) were shown to inhibit NF-κB only, without inhibiting AP-1 and NFAT.[40]

The ability of SN50 to inhibit the import and nuclear function of NF-κB without the use of disruptive methods led to the development of a new strategy to exert an immunosuppressive effect on activated T lymphocytes. Similar methods have been used to study factors critical to the growth and differentiation of many cell types as highlighted by the following examples.

6.3.2 Applications of SN50 Peptide

The peptide SN50 is now used as a general reagent in molecular biology due to its proven ability to prevent NF-κB-induced gene expression. Kilgore et al.[41] used SN50 in a study of the role of NF-κB in the up-regulation of certain proteins during formation of the membrane attack complex (MAC) of complement. Following activation of the complement cascade, the assembly of the MAC induces production of inflammatory mediators, e.g., IL-8, monocyte chemoattractant protein-1 (MCP-1); however, the mechanism by which this occurred was unknown. Through a detailed assessment of the nuclear activity of NF-κB in the presence and absence of SN50 following MAC formation, the authors concluded that MAC formation may serve to activate IL-8 and MCP-1 genes through activation and translocation of NF-κB.

In a second example of SN50 used as a general reagent, the peptide was employed to determine the role of NF-κB in the response of myocardial tissue to ischemia. Maulik et al.[42] speculated that NF-κB was involved in myocardial adaptation to ischemia. In this study rat hearts were rapidly excised and retrograde perfusion established before subjecting the hearts to ischemic stress and monitoring the adaptation. To define the role of NF-κB, the SN50 peptide was added to the perfusion buffer and hearts were exposed to 18 μ*M* of the peptide over a 15-min period. It was found that the beneficial effects of ischemic adaptation were blocked by pretreating the hearts with SN50. This shows that SN50 is capable of translocating not only into cell suspensions but also into tissue.

More examples of the recent uses of SN50 to delineate the role of NF-κB in signaling pathways are listed in Table 6.1. Results presented in these studies vary; in some cases NF-κB was found to be important in the pathway examined, but in other situations it has been determined that NF-κB is not involved.

6.3.3 kFGF MTS Aids in Translocation of Other Cargoes

Based on early success of the delivery of NF-κB NLS into intact cells when covalently linked to the kFGF MTS, Lin et al.[34] proceeded to link the same MTS to a different NLS, this time derived from the protein fibroblast growth factor-1 (FGF-1). The purpose of this assembly was to produce a reagent allowing examination of the functional role of the NLS in FGF-1-stimulated DNA synthesis and mitogenesis. A stepwise solid-phase peptide synthesis method was employed to produce this chimeric peptide (SA), with the MTS located at the N terminus separated from the NLS by a three-residue spacer (AAA). An indirect immunofluorescence assay was used to show that SA peptide migrated into NIH 3T3 cells with localization to the perinuclear areas and a thymidine incorporation assay showed that the peptide induced a mitogenic response in a manner similar to the entire FGF-1 protein. A peptide representing the NLS alone was not capable of inducing such a response and it was therefore concluded that the entire SA peptide was required for cell penetration and biological activity. This same peptide was also found to be effective in a range of other cell types, i.e., BALB/c3T3 murine fibroblasts, human vascular endothelial cells, and primary cultured hepatocytes.[74]

TABLE 6.1
Recent Applications of SN50 to Investigate Role of NF-κB in Various Signaling Pathways

Disease	Function under investigation	Ref.
Cancer	Leukemic cell proliferation via TNFα	43
	LHRH expression by ovarian cancers	44
	HeLa cell resistance to cisplatin	45
	Tumor cell adhesion via β1 integrin	46
	NGF as mitogen for breast cancer	47
	TRAIL as multiple myeloma therapeutic	48
Viral infection	Protein regulation by cytomegalovirus	49
	HIV-1 Tat modulaiton of ion channels	50
	HIV-1 Tat modulation of cAMP	51
	Flavivirus-induced apoptosis and replication	52
Lyme disease	Upregulation of MM-9 by *Borrelia burgdorferi*	53
Multiple sclerosis	Induction of iNOS in microglial cells	54
Huntington's disease	c-Myc and p53 induction of apoptosis	55
Parkinson's disease	Dopamine-induced apoptosis	56
Adult respiratory distress syndrome	Asbestos-induced TNFα gene expression	57
	Silica-induced TNFα–gene expression	58
	TNFα induction of chemokine IL-8	59
Asthma	Role of GATA3 in Th2 differentiation	60
Other	Induction of chemokines by spider venom	61
	Expression of LIF and IL-6 in endometrium	62
	Cyanide-induced apoptosis	63
	TNFα regulation of corneal fibroblast apoptosis	64
	TNFα regulation of uterine cell death	65
	Generation of GM-CSF by human monocytes	66
	TNFα-induced apoptosis	67–69
	Induction of IL-6 by TNFα	70
	Survival of cerebellar granule neurons	71
	Induction of cytokines by macrophages	72
	Insulin rescue of retinal neurons	73

The kFGF MTS has been covalently linked to several other peptides, including a cyclic, 10-residue inhibitor of enzyme oligosaccharyl transferase for translocation across the endoplasmic reticulum membrane *in vitro*;[75] a peptide representing an epidermal growth factor receptor (EGFR) autophosphorylation site;[35] a 12-residue peptide derived from the region surrounding phosphotyrosine 317 of the intracellular signaling protein Shc;[76] and a series of peptides representing binding sites of proteins involved in signaling pathways associated with activation of the G protein-coupled receptor 5-HT_{2C} in choroid plexus endothelial cells.[77] Moreover, the nuclear import of NF-κB has been inhibited by an SN50 analog, a peptide comprising two NLSs of NF-κB, one on either end of the kFGF MTS, to increase the efficacy of nuclear uptake.[78] This peptide was also synthesized using D-amino acids to increase resistance

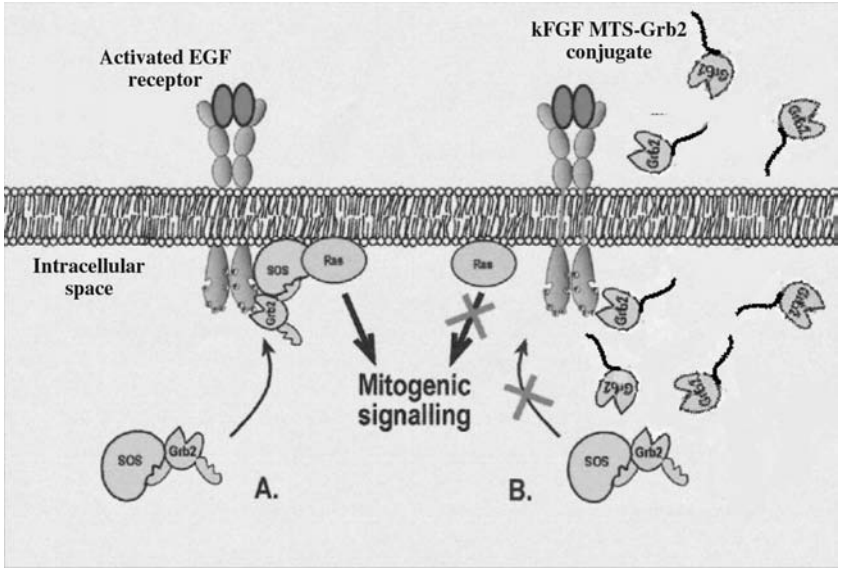

FIGURE 6.1 (Color Figure 6.1 follows p. 14.) The effect of kFGF MTS-Grb2 translocation on growth factor signaling. (A) The activated EGF receptor is phosphorylated and subsequently bound by the Grb2 SH2 domain, which in turn recruits Sos and Ras molecules. Activation of Ras leads to cellular responses including mitogenesis. (B) Introduction of the kFGF MTS-Grb2 conjugate results in the binding of this conjugate to the activated EGF receptor and inhibition of binding of native Grb2. Thus, Sos and Ras are not activated and cellular signaling is inhibited.

to proteolysis; the peptide blocked the nuclear import of NF-κB and it was determined that NF-κB plays an important role in acute inflammatory disease models.

The minimal peptide that inhibits Stat3 signaling has been identified by coupling phosphorylated peptides to the kFGF MTS.[79] Constitutive activation of Stat3 frequently accompanies various human malignancies; therefore, this peptide inhibitor is being investigated as a peptidomimetic for drug design. Croce and co-workers successfully synthesized a cell-permeant inhibitor of the Ca^{2+}-activated protease calpain by assembling a peptide containing the kFGF MTS and the minimal inhibitory sequence (24 residues) of the known calpain inhibitor, calpastatin.[80]

The ability of kFGF MTS to aid in translocation of large proteins has also been demonstrated.[36] A 12-residue MTS (AAVLLPVLLAAP) derived from the 16-residue h-region of the signal sequence of kFGF[81] was expressed adjacent to a fusion protein comprising *Schistosoma japonicum* glutathione *S*-transferase and the Grb2 SH2 domain,[82] resulting in a 41-kDa MTS-protein conjugate. The protein was found to be imported into every cell on a culture dish and the amount of protein taken up by each cell was up to several million copies, depending on extracellular concentration and incubation time. Exposure of cells to the MTS-protein conjugate resulted in inhibition of EGF-induced intracellular signaling and mitogenesis, as shown in Figure 6.1.

Based on the success of this protein import study, Zhao et al.[83] attached the same MTS covalently to antibodies, thus creating proteins capable of translocating into living fibroblast cells without affecting cell structure and viability. The internalized antibody appeared uniformly in the cytoplasm, whereas the nucleus showed significantly less antibody-positive material. Importantly, these imported antibodies can be detected by ELISA after extraction. More recently, by fusion to the 12-residue kFGF MTS, the DNA Cre recombinase has also been demonstrated to be cell-permeable and functional in cells *in vitro* and *in vivo*.[84]

In a significant step forward in the use of MTS peptides as therapeutic and diagnostic agents Li et al.[85] showed that the SA peptide containing the h-region of kFGF and the NLS of FGF-1[34] was capable of *in vivo* cargo delivery. The peptide was injected directly into the left lateral cerebroventricle of male Wistar rats to determine the effect of the presence of the FGF-1 NLS on food intake. Compared to previous studies in which other peptides encompassing the FGF-1 N terminus were investigated using a similar method,[86,87] the SA peptide exerted a far stronger inhibitory effect on food uptake. Because the MTS does not affect feeding behavior,[85] it may be concluded that the increased potency of SA peptide is most likely due to more effective intracellular delivery of the FGF-1 NLS. Another good example of the therapeutic application of MTS peptides is the role of an SN50 peptide analog in the inhibition of acute inflammatory disease models.[78]

6.3.4 Identification of Translocation Activity of Integrin β_3 h-Region

The favorable results achieved using the kFGF h-region and modified sequences as MTS peptides seem to have precluded the investigation of h-regions from other proteins as translocation peptides. Another sequence examined as a potential cell-permeant peptide vector is the h-region of human integrin β_3.[88] The hydrophobic peptide VTVLALGALAGVGVG[89] was synthesized in tandem with a set of four overlapping peptides representing segments of the cytoplasmic tail of human integrin β_3. This series of peptides was used to identify the region of the integrin β_3 cytoplasmic tail is involved in the regulation of fibrinogen binding to the extracellular domain. By incorporating the translocating peptide into the peptides tested, the authors successfully identified the major cell adhesion regulatory domain (CARD) of integrin β_3.

6.4 MECHANISM OF MTS MEMBRANE TRANSLOCATION

While the exact mechanism utilized by MTS peptides to translocate across the plasma membrane is still not known, several important clues have been uncovered. First, import is not sequence specific because synthetic peptides containing MTSs from distinct protein signal sequences or modified sequences can translocate into the intracellular space.[33,36,88] The translocation is also not limited to a particular cell type; efficient uptake has been observed with many cell types, e.g., human monocytes, endothelial cells, T lymphocytes, fibroblasts, murine endothelial cells, and mast cells.[90] This is in contrast to the cell-specific uptake associated with the 60-residue antennepedia homeobox domain (from which penetratin is derived), where the

expression of α-2,8-polysialic acid on cell surface neuronal cell adhesion molecules (NCAM) is required.[91] Uptake by T lymphocytes indicates that the mechanism involved does not depend on membrane caveolae because T lymphocytes do not express these structures.[37] The addition of inhibitors of the endosomal pathway to cell culture does not prevent the intracellular localization of MTS peptides; therefore, uptake does not rely on endocytosis.[33]

Furthermore, in a study using electron microscopy co-staining techniques, MTS-cargo peptides have been observed to translocate across the cell membrane by free penetration and without specific association with any membrane-bound vesicles, such as endosomes.[92] These observations, together with results suggesting that import of MTS peptides is ATP-independent and temperature-dependent, and that intact architecture of the plasma membrane is required,[33] lead to conclusions that translocation occurs directly through the lipid bilayer and that membrane fluidity and lateral mobility of membrane proteins influence this import process.

The secondary conformation adopted by MTS peptides is potentially responsible for membrane interaction. The residues located in the h-regions of signal sequences are often those with a propensity to form α-helices; data from circular dichroism (CD) studies show that various signal peptides can adopt an α-helical conformation in membrane-mimetic environments.[31,93-98] Similarly, the correlation of the stability of the helix–turn–helix conformation of h-regions with *in vivo* function is observed with the prokaryotic LamB protein.[99] Furthermore, it has been suggested that a helical hairpin structure makes hydrophobic peptides prone to interaction with membrane lipid[93-95,100] and that this interaction unloops the peptide, resulting in a transmembrane conformation.[101]

Du and co-workers performed a detailed study aimed at defining the conformational requirements of cell-permeant hydrophobic MTS peptides and the correlation between translocation activity and sequence topology.[102] For this, SA peptide with sequence AAVALLPAVLLALLAPAAANYKKPKL[34] and several variants were synthesized and analyzed for secondary conformation and translocating activity. The 16 N-terminal residues of SA represent the h-region of kFGF, which is separated from the NLS of FGF-1 by a trialanine spacer region. Results confirm that the MTS induces α-helix formation in membrane-mimetic environments and the authors concluded that a tendency to adopt α-helical conformation in a heterogeneous amphiphilic environment suggests a possible interaction with hydrophilic headgroups of plasma membrane lipids.

These findings suggest that signal sequence-based MTS peptides can be modified to retain or improve their import activity as long as the secondary conformation remains unchanged. In fact, Rojas et al. have designed a 12-residue MTS derived from the 16-residue h-region of kFGF mentioned above. They have shown that this shortened MTS peptide is also capable of efficiently delivering peptides and proteins into cells.[36] This 12-residue MTS may be the shortest hydrophobic translocating peptide reported thus far.

Du et al. also addressed the effect of the location of the MTS on peptide import function. It was found that the peptide still adopted an α-helical structure in the membrane-mimetic environment and was able to penetrate across the cell membrane when the MTS was attached at the C terminus of the NLS.[102] Thus, the site of

attachment did not significantly affect MTS peptide-translocating activity. However, when the SA peptide was synthesized partly as a retro peptide, i.e., with amino acid residues of the MTS in reverse order, the peptide failed to be imported into cells as determined by import and functional assays.[102] The side chain topology and the peptide amide bond direction of the MTS seem to be critical requirements for peptide import function; either of these factors may influence the ability of the peptide to form desirable secondary conformation for membrane interaction.

6.5 METHODS FOR ATTACHING CARGO AND TARGETING DOMAINS TO TRANSLOCATING PEPTIDES

Translocating peptides must be linked to at least one other module to be biologically valuable. First, they must be linked to a biologically active module, often referred to as cargo. Second, it may be necessary to target the biologically active module to a particular cell type or specific intracellular compartment, in which case inclusion of a third module that allows specific recognition through a receptor–ligand interaction is required.

In some cases it seems that the covalent linkage of cargo to translocating peptide is not essential for efficient delivery of the cargo. For example, the plasmids pGL2 luciferase and pCMV βgal were individually mixed with a multiple antigenic peptide (MAP) comprising eight branching units, with each unit containing the SV40 large T-antigen NLS (TPPKKKRKVEDP) and a lysine pentapeptide acting as a cytoplasmic translocation signal. The exposure of Chinese hamster ovary (CHO) cells to the admixture resulted in expression of both gene products and it was proposed that the cationic peptide associated with the negatively charged phosphate DNA backbone via electrostatic bonds.[103] A reliance on electrostatic interaction may be adequate for import of oligonucleotides that typically contain a negatively charged backbone; however, uptake of proteins and peptides that, by their very nature, differ in charge will likely always require covalent attachment to the peptide vector.

To date, one exception to this rule, in which the strength of the noncovalent interaction between biotin and avidin was exploited, has been reported. A biotinylated translocating peptide was synthesized and subsequently reacted with fluoresceinated streptavidin; this vector–cargo molecule was imported into cells, whereas fluoresceinated streptavidin alone was not.[104]

There are two general methods available for linking translocating peptides to peptide and protein cargo. First, the same method used to generate the cargo, whether chemically by stepwise solid-phase peptide synthesis or biologically by biosynthetic expression of recombinant protein, may be modified to include synthesis of the translocating peptide. This is a relatively straightforward task when solid-phase peptide synthesis is employed because the synthesis may be extended to include the extra peptide residues at either the C or N terminus (Figure 6.2A) or coupled using an orthogonal protection strategy to produce a peptide with a branched format.[33,34]

The inclusion of a translocation peptide in the expression of a recombinant protein requires that the plasmid encoding the protein be modified to contain the additional nucleotides that will encode the desired peptide sequence (Figure 6.2B).

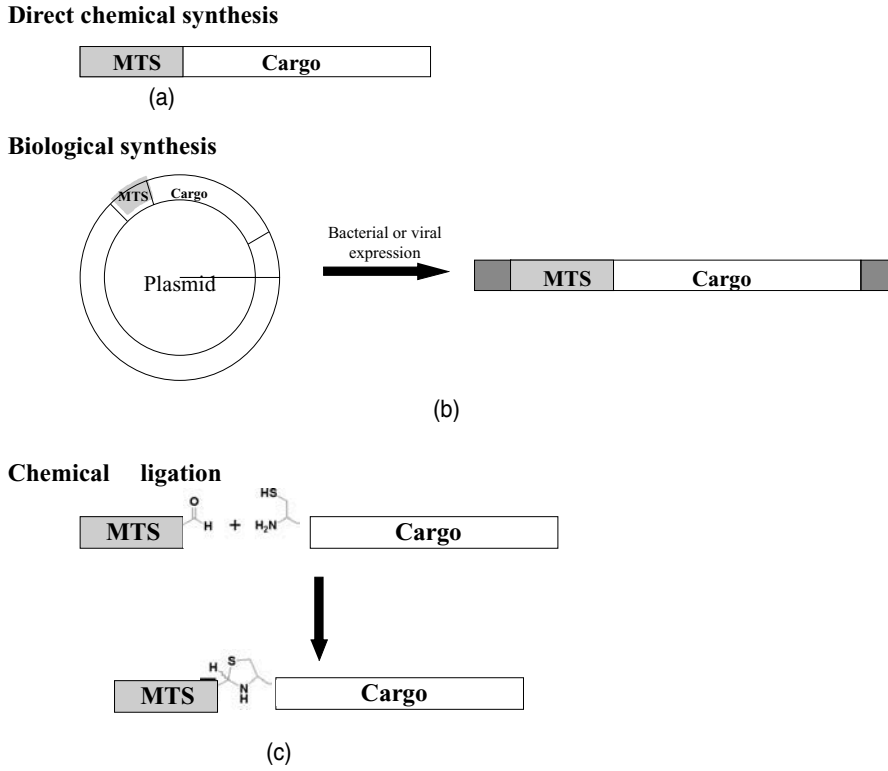

FIGURE 6.2 Schemes generally used to prepare MTS-cargo peptides and proteins. (a) Direct chemical synthesis where the MTS and cargo are synthesized in tandem. (b) Biological synthesis involves the incorporation of MTS and cargo DNA into a plasmid and expression in a bacterial or viral host system. Often remnant enzyme cleavage site residues flank the sequence of interest (hatched bars). (c) A general scheme for peptide ligation via thiazolidine ring formation is shown. An MTS bearing an aldehyde is ligated with a cargo peptide or protein containing an N-terminal cysteinyl moiety, resulting in the formation of a nonamide bond.

To date, translocating peptides have predominantly been attached to cargo proteins (and some peptides) using genetic recombination.[36,84,105-107] Using cell-permeable GST-GrbSH2-MTS protein as an example, the expression plasmid was constructed by ligating the double-stranded MTS into a BamH1 site of an expression plasmid for GST fusion protein.[36] The design of the plasmid further allowed the insertion of DNA fragments encoding GrbSH2 protein into the GST-MTS sequence. In this case the protein product was used to test the effect of the GrbSH2 domain on EGF-induced mitogenic signaling.[36] The main disadvantage associated with use of these types of continuous synthesis strategies is that a new synthesis must be performed for production of each vector–cargo molecule. The synthesis of peptides incorporating vector and cargo residues may also prove difficult as peptide length increases.

On the other hand, the vector and cargo may be synthesized separately and coupled together using a ligation strategy. One of the most commonly used ligation techniques in biological chemistry is the formation of a disulphide bond between peptides and proteins containing activated thiol groups. Disulphide bond formation has been used to link both peptide[108-110] and oligonucleotide[111,112] cargo to translocating peptide vectors. The nature of the disulphide bond requires that separation procedures used to isolate and characterize the desired product must not include any method that may reduce the disulphide bond, e.g., SDS-PAGE with reducing buffers. Another drawback associated with the formation of disulphide bonds is that a large quantity of byproducts usually results due to the nonspecific nature of the interaction, leading to low reaction efficiency. Formation of this type of bond has the advantage, however, of releasing the cargo as the disulphide bond breaks in the reducing environment of the cytoplasm, thereby minimizing interactions between the translocating peptide and the biologically active cargo *in vivo*.

The formation of other nonamide linkages between translocating peptide and cargo has also been investigated.[77,83,113] Independently prepared translocating peptide and cargo peptides have been linked by a single-step ligation through a nonamide thiazolidine linkage (Figure 6.2c) and the biological activity of the resulting peptides compared to counterparts synthesized by the conventional tandem synthesis method.[113] Combinations of two different MTSs and two different cargo peptides were used in this study: the h-region of kFGF and that of human integrin β_3[33,88] as MTSs, and peptides derived from the human integrin β_3 cytoplasmic tail and the NF-κB p50 NLS as cargo. A general and mild method for the chemoselective ligation of an aldehyde on one reactant with a 1,2-amino thiol moiety on a second reactant[114,115] was used to assemble the MTS-cargo peptides. An aldehyde functionality was generated at the C terminus of each MTS peptide by oxidation of an aminopropanediol moiety or a 1,2-amino alcohol moiety present at the C terminal following stepwise solid-phase peptide synthesis and cleavage from the solid support.

Preparation of the cargo peptides involved addition of a cysteine residue to the N terminus of the sequence. The ligations, performed under various conditions to optimize solubility of hydrophobic and functional peptide modules, were complete within 6 h and standard procedures used to purify the desired products. The results of the biological assays indicate that the hybrid peptides are functionally equipotent with those containing an amide linkage synthesized by the conventional method.

The thiazolidine ring formation protocol was employed by Chang et al.[77] to generate a series of peptides comprising the kFGF MTS and cargo peptides designed to examine the intracellular signaling mechanism of the 5-HT_{2C} receptor. In this case lysine and serine residues were added at the C terminus of the MTS peptide to serve as a linker and a masked aldehyde, respectively. The lysine was attached to the C terminus of the MTS by its primary amine, and then serine was attached at the side chain ε-amine. The serine residue was treated with an oxidizing agent to generate the reactive aldehyde moiety subsequently reacted with effector peptides containing N-terminal cysteines to form the vector–cargo product.

This method for the rapid preparation of functional cell-permeant peptides may be applied to virtually any peptide or protein containing an N-terminal cysteine and allows bulk preparation of translocating peptide that may be used in ligation to any

TABLE 6.2
Commonly Used Translocating Peptides

Name	Sequence
HIV Tat peptide	GRKKRRQRRRPPQC
Penetratin	RQIKIWFQNRRMKWKK
Penetratin analogue	RRWRRWWRRWWRRWRR
Transportan	GWTLNPPGYLLGKINLKALAALAKKIL
SV40 large T antigen NLS (monopartite)	PKKKRKV
Nucleoplasmin NLS (bipartite)	KRPAATKKAGQAKKKL
kFGF MTS	AAVALLPAVLLALLAP
kFGF MTS analogue	AAVLLPVLLAAP

such peptide. One advantage of this approach is the use of fully free peptides and proteins, which obviates the need for chemical modification that might affect biological activity. As well as being synthetically straightforward and compatible with existing solid-phase peptide synthesis methods, the thiazolidine formation reaction is site-specific and avoids potential interference with the biological activity of the cargo. Furthermore, shorter preparation time and high yields represent a definite advantage over conventional stepwise solid-phase synthesis of vector–cargo molecules. A plethora of chemoselective ligation methods is now available for the ligation of unprotected peptides and proteins through amide and nonamide linkages;[116] many of these may be applied to the production of translocating conjugates.

6.6 CATIONIC TRANSLOCATING PEPTIDES

Cationic translocating peptides are diverse and frequently used; the HIV Tat peptide was one of the earliest translocation peptides described after it was determined that the truncated peptide retained the translocation activity exhibited by the entire Tat protein.[117] The amino acid sequence of the highly charged Tat peptide is shown in Table 6.2. Able to localize rapidly to the nucleus once inside the cell, the Tat peptide has also been shown to transport covalently bound peptides and proteins into cells and tissues.[8] In one of the most notable studies, a Tat peptide/β-galactosidase fusion protein was shown to translocate into cells derived from various murine tissue types. The 120-kDa protein was also found to be enzymatically active within each different cell type.[118] Other proteins successfully delivered to intracellular space by the Tat peptide include p16INK, caspase3, RhoA, and p27kip1.[119-122]

The penetratin peptide, also referred to as pAntp, is frequently used to deliver peptides and small proteins into cells. This peptide is derived from a highly conserved region of homeoprotein transcription factors.[123] The 16-residue penetratin is routinely used as a vector (Table 6.2); however, internalization of a shorter 6-residue fragment has also been reported.[124] Even though there is a lack of sequence homology between penetratin and the Tat peptide, both consist predominantly of positively charged residues. It seems that the translocation activity of penetratin is dependent upon the distribution of the positively charged residues and two tryptophan residues that reside

TABLE 6.3
Cationic Peptides Tested by Futaki et al.[127] for Translocation Activity

Name	Sequence	# arginine residues
HIV-1 Rev	^{34}TRQARRNRRRRWRERQR^{50}	10
FHV coat	^{35}RRRRNRTRRNRRRVR^{49}	11
HTLV-II Rex	^{4}TRRQRTRRARRNR^{16}	8
BMV Gag	^{7}KMTRAQRRAAARRNRWTAR^{25}	7
P22 N	^{14}NAKTRRHERRRKLAIER^{30}	6
CCMV Gag	^{7}KLTRAQRRAAARKNKRNTR^{25}	6
λN	^{1}MDAQTRRRERRAEKQAQWKAAN^{22}	5
ϕ21 N	^{12}TAKTRYKARRAELIAERR^{29}	5
Yeast PRP6	^{129}TRRNKRNRIQEQLNRK^{144}	5

Source: Futaki, S. et al., *J. Biol. Chem.,* 276, 5836, 2001.

on the opposing side of a theoretical helical structure. Based on this observation, the naturally occurring penetratin peptide sequence has been subsequently modified to produce a more efficient translocating peptide (Table 6.2) consisting of only arginine and tryptophan residues.[9,125,126]

The translocation activity of several other positively charged peptides has been investigated by Futaki et al.[127] Peptides representing arginine-rich RNA-binding regions (Table 6.3) were shown to accumulate in the cytoplasm and nucleus of cells within 5 min of addition of 1 μ*M* of peptide, adding weight to the premise that those peptides rich in positively charged residues are efficient translocating peptides. Peptides containing more than seven arginines exhibited internalization activity similar to the HIV Tat peptide, whereas those with less arginine residue showed less extensive internalization. Again, there is a lack of sequence homology between all the peptides tested; however, all possess several arginine residues, thus implicating arginine as critical to translocation activity. The ability of arginine oligomers to act as translocating peptides and also to transport attached cargo such as cyclosporin A across biological membranes has been reported.[128,129]

Based on these observations, polypeptides and peptoids consisting of repeating units mimicking various characteristics of arginine have been tested as transportants.[130,131] The results generated led to conclusions that the guanidino headgroup is superior to other cationic subunits and that the length of the alkyl chain between the headgroup and backbone is also significant.

Possibly the longest translocation peptide, transportan is a 27-residue chimera (Table 6.2) composed of amino acid sequences derived from two different proteins. This peptide contains 13 residues from the highly conserved N-terminal region of galanin and the 14-amino acid-long wasp venom peptide toxin, mastoparan.[10] The most recent report of use of transportan describes the fusion of transportan to various proteins ranging in size from the 30-kDa green fluorescent protein to 150-kDa antibodies and the subsequent delivery of the large protein cargoes into different cell types.[104]

Naturally occurring nuclear localization signal (NLS) sequences responsible for the import of proteins into the nucleus have also been exploited as translocation peptides. These peptides are also cationic in nature and capable of traversing cell and nuclear membranes.[132-134] There are two types of NLS peptides: monopartite, which consist of a single cluster of basic residues, or bipartite, which contain two clusters of basic residues.[135-137] Examples of monopartite and bipartite NLS sequences are shown in Table 6.2.

According to the established model of nuclear translocation, the NLS sequence on the protein surface is bound by an import receptor complex located in the cytoplasmic side of the nuclear membrane. The protein is then directed to a nuclear pore[138-140] where a cascade of tightly regulated interactions results in delivery of the protein into the nucleus. The protein is subsequently released from the importin complex. Furthermore, because this is a unidirectional event, it is a highly efficient means for delivering biologically active molecules into the nucleus. The definition of an NLS sequence is vague because of the diversity of peptides that can apparently function in this manner.[136] However, a quantitative method developed by Hodel et al.[141] can distinguish between efficient and weak NLS peptides on the basis of their affinity for the importin complex.

6.7 ARGININE–PROLINE-RICH PEPTIDES AS TRANSLOCATING PEPTIDES

Peptides with a high content of arginine and proline are heavily represented in antimicrobial peptides, a particular class of peptides produced by a range of species; furthermore, these peptides translocate across the cell membrane.[142-144] Antimicrobial peptides are classified on the basis of their structure and peptide composition: linear peptides that form α-helices; cyclic peptides rich in disulphide bonds; and peptides with a high content of a particular amino acid, usually proline or glycine.[145] Examples of the arginine–proline-rich (RP-rich) peptides include PR-39,[146,147] abaecin,[148] apidaecin,[149] Bac5, and Bac7.[150,151] The bactericidal properties of amphipathic, α-helical peptides (cecropins, magainins) and the disulphide-containing peptides (defensins) are thought to relate to their ability to form a pore in the target membrane,[152,153] whereas the RP-rich peptides penetrate the membrane and subsequently kill cells by interfering with the protein synthesis machinery.[142,154,155]

The antimicrobial activity exhibited by RP-rich Bac7 is retained by the 24-residue peptide RRIRPRPPRLPRPRPRPLPFPRPG[156]that represents the N terminus.[157] To determine if this peptide and a series of truncated peptides could traverse the cell membrane each peptide was synthesized with a fluorophore attached to the N terminus and incubated with murine monocytes. It was found that peptides with both a high and low content of arginine could translocate into cells, dispelling the hypothesis that a high content of arginine was solely responsible for the translocation.[158] The maximum intracellular concentration of fluoresceinated peptides occurred within 5 min and then decreased at a steady rate, indicating that rapid translocation occurs. Preliminary cytotoxicity assays indicated that the fluoresceinated peptides are not cytotoxic at concentrations up to 100 μ*M* after exposure for 24 h.

61	RNTVNRLLPM	LRRKKNEKKN	EKIERNNKLK	**QPPPPPNPND**	**PPPPNPNDPP**	**PPNPNDPPPP**
121	**NPNDPPPPNA**	**NDPPPPNAND**	**PAPPNANDPA**	**PPNANDPAPP**	**NANDPAPPNA**	**NDPAPPNAND**
181	**PAPPNANDPP**	**PPNPNDPAPP**	**QGNNNPQPQP**	**RPQPQPQPQP**	**QPQPQPQPQP**	**RPQPQPQPGG**
241	NNNNKNNNND	DSYIPSAEKI	LEFVKQIRDS	ITEEWSQCNV	TCGSGIRVRK	RKGSNKKAED
301	LTLEDIDTEI	CKMDKCSSIF	NIVSNSLGFV	ILLVLVFFN		

FIGURE 6.3 Amino acid sequence of *P. berghei* CS protein.[165] The proline-rich repeat region is shown in bold.

6.8 PROLINE-RICH PEPTIDES AS TRANSLOCATING PEPTIDES

The translocation activity of a potentially new class of translocating peptides, proline-rich peptides, has been investigated. Even though each translocating peptide identified thus far has proven capable of traversing the cell membrane and delivering biologically active cargo into the cytoplasm and nucleus, several disadvantages are associated with use of these peptides. For example, even though the basic residues of cationic peptides seem to aid in interaction with the negatively charged lipid bilayer and increase translocation, such highly charged peptides are potentially cytotoxic. In a report published by Singh et al.,[159] a loligomer comprising eight copies of a polylysine sequence had a cytotoxic effect on various eukaryotic cells at concentrations above 5 μ*M*. Linear polymers of polylysine have also been shown to possess cytotoxic properties.[160]

In a preliminary study we have examined the translocation activity of a peptide derived from the proline-rich repeat region of the *Plasmodium berghei* circumsporozoite surface (CS) protein. The CS protein is the major surface protein of the *Plasmodium* sporozoite,[161] the causative agent of malaria. Both the CS protein and the entire sporozoite possess the ability to translocate from the extracellular environment to the cytoplasm of hepatocytes.[162-164] Sporozoites have even been shown to pass back through the membrane and exit cells without fatally disrupting the membrane.[164] This protein contains a large proline-rich repeat region, the sequence of the *P. berghei* CS protein[165] is shown in Figure 6.3. The sequence PPPPNPND-PPPPNPND was selected for examination of translocation activity; uptake of this peptide by murine monocytes was found to be greater than that of an RP-rich control peptide derived from Bac7.[158] The successful uptake of proline-rich peptides has led to ongoing studies in which the mechanism of uptake is elucidated. These proline-rich peptides have the desirable properties of being aqueous soluble and not highly charged and, therefore, more conducive to routine synthesis and delivery.

6.9 FUTURE PERSPECTIVES OF CELL-PERMEANT PEPTIDE TECHNOLOGY

Peptides should possess several critical properties to be considered translocating vectors:

- Sequence short to simplify synthesis
- Internalization not appreciably affected by coupling to cargo
- Cargo delivered to the desired compartment
- Biologically inactive vector

The kFGF MTS, penetratin, and HIV-1 Tat peptides all fulfill these criteria and are currently regarded as the leading translocating peptide vectors. Whether proline-rich peptides will also meet all of these requirements remains to be determined, although results obtained to date are promising. Until a definitive study is performed in which the ability of different translocating peptides to transport the same cargo into cells is directly compared, the choice of peptide will largely be influenced by the types of uses described in the literature.

The ultimate goal of our translocating peptide research is to design biologically active therapeutic compounds. For this, potentially three different segments must be included in a single compound: a targeting module, a penetrating module, and an effector module. The role of the targeting module would be to direct the attached penetrating and biologically active modules to specific cell types *in vivo*, e.g., cancer cells and virus-infected cells. One of the defining characterisitics of cancer cells is the overexpression of specific cell surface proteins[166-170] and this feature may be exploited in the design of anticancer agents.

Effective antiviral agents may also be assembled where a biologically active antiviral drug such as a reverse transcriptase inhibitor can be linked to a cell-permeant peptide vector and targeted to infected cells. Virus-infected cells often express virus-specific proteins on the cell surface during replication; therefore, identification of a suitable target may be simplified. For example, human cytomegalovirus chemokine receptor US28 is expressed at the cell surface[171] and a number of HIV surface proteins are expressed prior to virion formation and budding.[172] Furthermore, this approach could be applied to development of a compound aimed at decreasing the multidrug resistance (MDR) exhibited by cancer cells.

Many cancer types, including leukemia, multiple myeloma, lymphomas, and a variety of solid tumors, overexpress the cell surface protein P-glycoprotein (P-gp) that transports anticancer drugs out of cells before cytotoxic effects occur.[166] The administration of drugs capable of reversing this MDR is currently limited because of the toxic effect on normal tissues. The assembly of a molecule that can target and bind to the overexpressed P-gp protein, penetrate through the cell membrane, and deliver a chemotherapeutic agent to the cancer cell resulting in cell death is highly desirable.

A major concern raised by Derossi et al.[9] is that the high efficiency of internalization exhibited by translocating peptides *in vitro* could have a detrimental effect on *in vivo* delivery because the peptide may be captured by cells at the delivery point and not reach target cells. Attachment of a targeting module addresses this concern to a certain extent. Ideally, the penetrating module would be completely masked by the targeting module and unavailable for nonspecific membrane interaction. Upon binding to the target receptor the target module would undergo a conformational change and expose the penetrating module to the lipid bilayer, thus allowing translocation to commence.

In conclusion, the production of drugs and diagnostic tools involves not only the design of the empirical three-dimensional conformation of the biologically active component but also the rational design of an effective intracellular delivery system for subcellular activity. Hydrophobic MTS peptides have already proven their worth as peptide vectors through the delivery of peptides and proteins to the intracellular

environment. We can now look beyond routine laboratory use of translocating peptides to development of effective agents for *in vivo* clinical and diagnostic use.

REFERENCES

1. Wang. K., Feramisco, J.R., and Ash, J.F., Fluorescent localization of contractile proteins in tissue culture cells, *Methods Enzymol*., 85, 514, 1982.
2. Wang, Z. and Moran, M.F., Requirement for the adapter protein GRB2 in EGF receptor endocytosis, *Science*, 272, 1935, 1996.
3. Buday, L. and Downward, J., Epidermal growth factor regulates p21ras through the formation of a complex of receptor, Grb2 adapter protein, and Sos nucleotide exchange factor, *Cell*, 73, 611, 1993.
4. Giorgetti–Peraldi, S. et al., Cellular effects of phosphotyrosine-binding domain inhibitors on insulin receptor signaling and trafficking, *Mol. Cell Biol*., 17, 1180, 1997.
5. Fitzgerald, E.M. and Dolphin, A.C., Regulation of rat neuronal voltage-dependent calcium channels by endogenous p21-ras, *Eur. J. Neurosci*., 9, 1252, 1997.
6. Henkel, T. et al., Intramolecular masking of the nuclear location signal and dimerization domain in the precursor for the p50 NF-kappa B subunit, *Cell*, 68, 1121, 1992.
7. Perlmutter, R.M. and Alberola-Ila, J., The use of dominant-negative mutations to elucidate signal transduction pathways in lymphocytes, *Curr. Opin. Immunol*., 8, 285, 1996.
8. Schwarze, S.R. and Dowdy, S.F., *In vivo* protein transduction: intracellular delivery of biologically active proteins, compounds and DNA, *Trends Pharmacol. Sci*., 21, 45, 2000.
9. Derossi, D., Chassaing, G., and Prochiantz, A., Trojan peptides: the penetratin system for intracellular delivery, *Trends Cell Biol*., 8, 84, 1998.
10. Pooga, M. et al., Cell penetration by transportan, *FASEB J*., 12, 67, 1998.
11. Fujihara, S.M. and Nadler, S.G., Intranuclear targeted delivery of functional NF-kappaB by 70 kDa heat shock protein, *EMBO J.*, 18, 411, 1999.
12. Hawiger, J., Cellular import of functional peptides to block intracellular signaling, *Curr. Opin. Immunol*., 9, 189, 1997.
13. Elliott, G. and O'Hare, P., Intercellular trafficking and protein delivery by a herpesvirus structural protein, *Cell*, 88, 223, 1997.
14. Lundberg, M. and Johansson, M., Correspondence: is VP22 nuclear homing an artifact? *Nat. Biotechnol*., 19, 713, 2001.
15. O'Hare, P. and Elliott, G., Correspondence: is VP22 nuclear homing an artifact? *Nat. Biotechnol*., 19, 713, 2001.
16. Blobel, G. and Dobberstein, B., Transfer to proteins across membranes. II. Reconstitution of functional rough microsomes from heterologous components, *J. Cell Biol*., 67, 852, 1975.
17. Blobel, G., Intracellular protein topogenesis, *Proc. Natl. Acad. Sci. U.S.A.,* 77, 1496, 1980.
18. Simon, S.M. and Blobel, G., Mechanisms of translocation of proteins across membranes, *Subcell. Biochem*., 21, 1, 1993.
19. von Heijne, G., Signal sequences. The limits of variation*, J. Mol. Biol*., 184, 99, 1985.
20. Briggs, M.S. and Gierasch, L.M., Molecular mechanisms of protein secretion: the role of the signal sequence, *Adv. Protein Chem*., 38, 109, 1986.
21. Gierasch, L.M., Signal sequences, *Biochemistry*, 28, 923, 1989.
22. von Heijne, G., The signal peptide, *J. Membr. Biol*., 115, 195, 1990.

23. Briggs, M.S. et al., *In vivo* function and membrane binding properties are correlated for *Escherichia coli* lamB signal peptides, *Science*, 228, 1096, 1985.
24. Kendall, D.A., Bock, S.C., and Kaiser, E.T., Idealization of the hydrophobic segment of the alkaline phosphatase signal peptide, *Nature*, 321, 706, 1986.
25. Yamamoto, Y. et al., Engineering of the hydrophobic segment of the signal sequence for efficient secretion of human lysozyme by Saccharomyces cerevisiae, *Biochem. Biophys. Res. Commun*., 149, 431, 1987.
26. Kendall, D.A. and Kaiser, E.T., A functional decaisoleucine-containing signal sequence. Construction by cassette mutagenesis, *J. Biol. Chem*., 263, 7261, 1988.
27. Bird, P., Gething, M.J., and Sambrook, J., The functional efficiency of a mammalian signal peptide is directly related to its hydrophobicity, *J. Biol. Chem*., 265, 8420, 1990.
28. Chou, M.M. and Kendall, D.A., Polymeric sequences reveal a functional interrelationship between hydrophobicity and length of signal peptides, *J. Biol. Chem*., 265, 2873, 1990.
29. Prabhakaran, M., The distribution of physical, chemical and conformational properties in signal and nascent peptides, *Biochem. J*., 269, 691, 1990.
30. Watson, M.E., Compilation of published signal sequences, *Nucleic Acids Res*., 12, 5145, 1984.
31. Hoyt, D.W. and Gierasch, L.M., Hydrophobic content and lipid interactions of wild-type and mutant OmpA signal peptides correlate with their *in vivo* function, *Biochemistry*, 30, 10155, 1991.
32. Ahn, K., Chen, D., and Kemper, B., Inverse relationship of cotranslational translocation with the hydrophobic moment of the bovine preproparathyroid hormone signal sequence, *Biochim. Biophys. Acta*, 1224, 459, 1994.
33. Lin, Y.Z. et al., Inhibition of nuclear translocation of transcription factor NF-kappa B by a synthetic peptide containing a cell membrane-permeable motif and nuclear localization sequence, *J. Biol. Chem*., 270, 14255, 1995.
34. Lin, Y.Z., Yao, S.Y., and Hawiger, J., Role of the nuclear localization sequence in fibroblast growth factor-1-stimulated mitogenic pathways, *J Biol Chem.,* 271, 5305, 1996.
35. Rojas, M., Yao, S., and Lin, Y.Z., Controlling epidermal growth factor (EGF)-stimulated Ras activation in intact cells by a cell-permeable peptide mimicking phosphorylated EGF receptor*, J. Biol. Chem*., 271, 27456, 1996.
36. Rojas, M. et al., Genetic engineering of proteins with cell membrane permeability, *Nat. Biotechnol*., 16, 370, 1998.
37. Torgerson, T.R. et al., Regulation of NF-kappa B, AP-1, NFAT, and STAT1 nuclear import in T lymphocytes by noninvasive delivery of peptide carrying the nuclear localization sequence of NF-kappa B p50, *J. Immunol*., 161, 6084, 1998.
38. Crabtree, G.R. and Clipstone, N.A., Signal transmission between the plasma membrane and nucleus of T lymphocytes, *Annu. Rev. Biochem*., 63, 1045, 1994.
39. Schindler, C. and Darnell, J.E. Jr., Transcriptional responses to polypeptide ligands: the JAK-STAT pathway, *Annu. Rev. Biochem*., 64, 621, 1995.
40. Kolenko, V. et al., Inhibition of NF-kappa B activity in human T lymphocytes induces caspase-dependent apoptosis without detectable activation of caspase-1 and -3, *J. Immunol*., 163, 590, 1999.
41. Kilgore, K.S. et al., Sublytic concentrations of the membrane attack complex of complement induce endothelial interleukin-8 and monocyte chemoattractant protein-1 through nuclear factor-kappa B activation, *Am. J. Pathol*., 150, 2019, 1997.
42. Maulik, N. et al., An essential role of NFkappaB in tyrosine kinase signaling of p38 MAP kinase regulation of myocardial adaptation to ischemia, *FEBS Lett*., 429, 365, 1998.

43. Liu, R.Y. et al., Tumor necrosis factor-alpha-induced proliferation of human Mo7e leukemic cells occurs via activation of nuclear factor kappaB transcription factor, *J. Biol. Chem*., 274, 13877, 1999.
44. Grundker, C. et al., Luteinizing hormone-releasing hormone induces nuclear factor kappaB-activation and inhibits apoptosis in ovarian cancer cells, *J. Clin. Endocrinol. Metab*., 85, 3815, 2000.
45. Eichholtz–Wirth, H. and Sagan, D., IkappaB/NF-kappaB mediated cisplatin resistance in HeLa cells after low-dose gamma-irradiation is associated with altered SODD expression, *Apoptosis*, 5, 255, 2000.
46. Andrews, E.J. et al., Tumor cell adhesion to endothelial cells is increased by endotoxin via an upregulation of beta-1 integrin expression, *J. Surg. Res*., 97, 14, 2001.
47. Descamps, S. et al., Nerve growth factor stimulates proliferation and survival of human breast cancer cells through two distinct signaling pathways, *J. Biol. Chem*., 276, 17864, 2001.
48. Mitsiades, C.S. et al., TRAIL/Apo2L ligand selectively induces apoptosis and overcomes drug resistance in multiple myeloma: therapeutic applications, *Blood*, 98, 795, 2001.
49. Cinatl, J., Jr. et al., Cytomegalovirus infection decreases expression of thrombospondin-1 and –2 in cultured human retinal glial cells: effects of antiviral agents, *J. Infect. Dis*., 182, 643, 2000.
50. Visentin, S., Renzi, M., and Levi, G., Altered outward-rectifying K(+) current reveals microglial activation induced by HIV-1 Tat protein, *Glia*, 33, 181, 2001.
51. Patrizio, M., Colucci, M., and Levi, G., Human immunodeficiency virus type 1 Tat protein decreases cyclic AMP synthesis in rat microglia cultures, *J. Neurochem*., 77, 399, 2001.
52. Liao, C.L. et al., Salicylates inhibit flavivirus replication independently of blocking nuclear factor kappa b activation, *J. Virol*., 75, 7828, 2001.
53. Kirchner, A. et al., Upregulation of matrix metalloproteinase-9 in the cerebrospinal fluid of patients with acute Lyme neuroborreliosis, *J. Neurol. Neurosurg. Psychiatry*, 68, 368, 2000.
54. Pahan, K. et al., Induction of nitric-oxide synthase and activation of NF-kappaB by interleukin-12 p40 in microglial cells, *J. Biol. Chem*., 276, 7899, 2001.
55. Nakai, M. et al., Kainic acid-induced apoptosis in rat striatum is associated with nuclear factor-kappaB activation, *J. Neurochem*., 74, 647, 2000.
56. Panet, H. et al., Activation of nuclear transcription factor kappa B (NF-kappaB) is essential for dopamine-induced apoptosis in PC12 cells, *J. Neurochem*., 77, 391, 2001.
57. Cheng, N. et al., Role of transcription factor NF-kappaB in asbestos-induced TNFalpha response from macrophages, *Exp. Mol. Pathol*., 66, 201, 1999.
58. Rojanasakul, Y. et al., Dependence of NF-kappaB activation and free radical generation on silica-induced TNF-alpha production in macrophages, *Mol. Cell Biochem*., 200, 119, 1999.
59. Dunican, A.L. et al., TNFalpha-induced suppression of PMN apoptosis is mediated through interleukin-8 production, *Shock*, 14, 284, 2000.
60. Das, J. et al., A critical role for NF-kappa B in GATA3 expression and TH2 differentiation in allergic airway inflammation, *Nat. Immunol.,* 2, 45, 2001.
61. Desai, A. et al., *Loxosceles deserta* spider venom induces NF-kappaB-dependent chemokine production by endothelial cells, *J. Toxicol. Clin. Toxicol*., 37, 447, 1999.
62. Laird, S.M. et al., Expression of nuclear factor kappa B in human endometrium; role in the control of interleukin 6 and leukaemia inhibitory factor production, *Mol. Hum. Reprod*., 6, 34, 2000.

63. Shou, Y. et al., Cyanide-induced apoptosis involves oxidative-stress-activated NF-kappaB in cortical neurons, *Toxicol. Appl. Pharmacol*., 164, 196, 2000.
64. Mohan, R.R. et al., Modulation of TNF-alpha-induced apoptosis in corneal fibroblasts by transcription factor NF-kappaB, *Invest. Ophthalmol. Vis. Sci*., 41, 1327, 2000.
65. Pampfer, S. et al., Activation of nuclear factor kappaB and induction of apoptosis by tumor necrosis factor-alpha in the mouse uterine epithelial WEG-1 cell line, *Biol. Reprod*., 63, 879, 2000.
66. Meja, K.K. et al., p38 MAP kinase and MKK-1 co-operate in the generation of GM-CSF from LPS-stimulated human monocytes by an NF-kappa B-independent mechanism, *Br. J. Pharmacol*., 131, 1143, 2000.
67. Niwa, M. et al., Nuclear factor-kappaB activates dual inhibition sites in the regulation of tumor necrosis factor-alpha-induced neutrophil apoptosis, *Eur. J. Pharmacol*., 407, 211, 2000.
68. Xiao, C., Ash, K., and Tsang, B., Nuclear factor-kappaB-mediated X-linked inhibitor of apoptosis protein expression prevents rat granulosa cells from tumor necrosis factor alpha-induced apoptosis, *Endocrinology*, 142, 557, 2001.
69. Han, Y.P. et al., TNF-alpha stimulates activation of pro-MMP2 in human skin through NF-(kappa)B mediated induction of MT1-MMP, *J. Cell Sci*., 114, 131, 2001.
70. Chae, H.J. et al., The p38 mitogen-activated protein kinase pathway regulates interleukin-6 synthesis in response to tumor necrosis factor in osteoblasts, *Bone*, 28, 45, 2001.
71. Koulich, E. et al., NF-kappaB is involved in the survival of cerebellar granule neurons: association of Ikappabeta phosphorylation with cell survival, *J. Neurochem*., 76, 1188, 2001.
72. Ropert, C. et al., Requirement of mitogen-activated protein kinases and I kappa B phosphorylation for induction of proinflammatory cytokines synthesis by macrophages indicates functional similarity of receptors triggered by glycosylphosphatidylinositol anchors from parasitic protozoa and bacterial lipopolysaccharide, *J. Immunol*., 166, 3423, 2001.
73. Barber, A.J. et al., Insulin rescues retinal neurons from apoptosis by a PI-3 kinase/Akt-mediated mechanism that reduces the activation of caspase-3, *J. Biol. Chem*., 276, 32814, 2001.
74. Komi, A., Suzuki, M., and Imamura, T., Permeable FGF-1 nuclear localization signal peptide stimulates DNA synthesis in various cell types but is cell-density sensitive and unable to support cell proliferation, *Exp. Cell Res.*, 243, 408, 1998.
75. Eason, P.D. and Imperiali, B., A potent oligosaccharyl transferase inhibitor that crosses the intracellular endoplasmic reticulum membrane, *Biochemistry*, 38, 5430, 1999.
76. Rojas, M. et al., An alternative to phosphotyrosine-containing motifs for binding to an SH2 domain, *Biochem. Biophys. Res. Commun*., 234, 675, 1997.
77. Chang, M. et al., Dissecting G protein-coupled receptor signaling pathways with membrane-permeable blocking peptides. Endogenous 5-HT(2C) receptors in choroid plexus epithelial cells, *J. Biol. Chem.,* 275, 7021, 2000.
78. Fujihara, S.M. et al., A D-amino acid peptide inhibitor of NF-kappa B nuclear localization is efficacious in models of inflammatory disease, *J. Immunol*., 165, 1004, 2000.
79. Turkson, J. et al., Phosphotyrosyl peptides block Stat3-mediated DNA-binding activity, gene regulation and cell transformation, *J. Biol. Chem*., Sep 28 [epub ahead of print], 2001.
80. Croce, K. et al., Inhibition of calpain blocks platelet secretion, aggregation, and spreading, *J. Biol. Chem.,* 274, 36321, 1999.

81. Delli Bovi, P. et al., An oncogene isolated by transfection of Kaposi's sarcoma DNA encodes a growth factor that is a member of the FGF family, *Cell,* 50, 729, 1987.
82. Lowenstein, E.J. et al., The SH2 and SH3 domain-containing protein GRB2 links receptor tyrosine kinases to ras signaling, *Cell*, 70, 431, 1992.
83. Zhao, Y. et al., Chemical engineering of cell penetrating antibodies, *J. Immunol. Methods*, 254, 137, 2001.
84. Jo, D. et al., Epigenetic regulation of gene structure and function with a cell-permeable Cre recombinase, *Nat. Biotechnol.,* 19, 929-33, 2001.
85. Li, A.J. et al., Strong suppression of feeding by a peptide containing both the nuclear localization sequence of fibroblast growth factor-1 and a cell membrane-permeable sequence, *Neurosci. Lett*., 255, 41, 1998.
86. Sasaki, K. et al., Effects of fibroblast growth factors and related peptides on food intake by rats, *Physiol. Behav*., 56, 211, 1994.
87. Li, A.J. et al., Fibroblast growth factor receptor-1 in the lateral hypothalamic area regulates food intake, *Exp. Neurol*., 137, 318, 1996.
88. Liu, X.Y. et al., Identification of a functionally important sequence in the cytoplasmic tail of integrin beta 3 by using cell-permeable peptide analogs, *Proc. Natl. Acad. Sci. U.S.A.,* 93, 11819, 1996.
89. Fitzgerald, L.A. et al., Protein sequence of endothelial glycoprotein IIIa derived from a cDNA clone. Identity with platelet glycoprotein IIIa and similarity to "integrin," *J. Biol. Chem*., 262, 3936, 1987.
90. Hawiger, J., Noninvasive intracellular delivery of functional peptides and proteins, *Curr. Opin. Chem. Biol*., 3, 89, 1999.
91. Joliot, A.H. et al., Alpha-2,8-Polysialic acid is the neuronal surface receptor of antennapedia homeobox peptide, *New Biol*., 3, 1121, 1991.
92. Lin, Y.Z. and Du, C., Unpublished results.
93. Briggs, M.S. and Gierasch, L.M., Exploring the conformational roles of signal sequences: synthesis and conformational analysis of lambda receptor protein wild-type and mutant signal peptides, *Biochemistry*, 23, 3111, 1984.
94. Batenburg, A.M. et al., Characterization of the interfacial behavior and structure of the signal sequence of *Escherichia coli* outer membrane pore protein PhoE, *J. Biol. Chem*., 263, 4202, 1998.
95. Batenburg, A.M. et al., Penetration of the signal sequence of *Escherichia coli* PhoE protein into phospholipid model membranes leads to lipid-specific changes in signal peptide structure and alterations of lipid organization, *Biochemistry*, 27, 5678, 1988.
96. Yamamoto, Y. et al., Conformational requirement of signal sequences functioning in yeast: circular dichroism and 1H nuclear magnetic resonance studies of synthetic peptides, *Biochemistry*, 29, 8998, 1990.
97. Rizo, J. et al., Conformational behavior of *Escherichia coli* OmpA signal peptides in membrane mimetic environments, *Biochemistry*, 32, 4881, 1993.
98. Chupin, V. et al., PhoE signal peptide inserts into micelles as a dynamic helix-break-helix structure, which is modulated by the environment. A two-dimensional 1H NMR study, *Biochemistry*, 34, 11617, 1995.
99. Bruch, M.D. and Gierasch, L.M., Comparison of helix stability in wild-type and mutant LamB signal sequences, *J. Biol. Chem*., 265, 3851, 1990.
100. McKnight, C.J., Briggs, M.S., and Gierasch, L.M., Functional and nonfunctional LamB signal sequences can be distinguished by their biophysical properties, *J. Biol. Chem*., 264, 17293, 1989.
101. de Vrije, G.J. et al., Lipid involvement in protein translocation in *Escherichia coli, Mol. Microbiol.*, 4, 143, 1990.

102. Du, C. et al., Conformational and topological requirements of cell-permeable peptide function, *J. Pept. Res*., 51, 235, 1998.
103. Singh, D. et al., Peptide-based intracellular shuttle able to facilitate gene transfer in mammalian cells, *Bioconjug. Chem*., 10, 745, 1999.
104. Pooga, M. et al., Cellular translocation of proteins by transportan, *FASEB J*., 15, 1451, 2001.
105. Perez, F. et al., Antennapedia homeobox as a signal for the cellular internalization and nuclear addressing of a small exogenous peptide, *J. Cell Sci*., 102, 717, 1992.
106. Perez, F. et al., Rab3A and Rab3B carboxy-terminal peptides are both potent and specific inhibitors of prolactin release by rat cultured anterior pituitary cells, *Mol. Endocrinol*., 8, 1278, 1994.
107. Schutze-Redelmeier, M.P. et al., Introduction of exogenous antigens into the MHC class I processing and presentation pathway by *Drosophila antennapedia* homeodomain primes cytotoxic T cells *in vivo*, *J. Immunol*., 157, 650, 1996.
108. Theodore, L. et al., Intraneuronal delivery of protein kinase C pseudosubstrate leads to growth cone collapse, *J. Neurosci*., 15, 7158, 1995.
109. Troy, C.M. et al., The contrasting roles of ICE family proteases and interleukin-1beta in apoptosis induced by trophic factor withdrawal and by copper/zinc superoxide dismutase down-regulation, *Proc. Natl. Acad. Sci. U.S.A.,* 93, 5635, 1996.
110. Fahraeus, R. et al., Inhibition of pRb phosphorylation and cell-cycle progression by a 20-residue peptide derived from p16CDKN2/INK4A, *Curr. Biol*., 6, 84, 1996.
111. Allinquant, B. et al., Downregulation of amyloid precursor protein inhibits neurite outgrowth *in vitro*, *J. Cell Biol*., 128, 919, 1995.
112. Troy, C.M. et al., Downregulation of Cu/Zn superoxide dismutase leads to cell death via the nitric oxide-peroxynitrite pathway, *J. Neurosci*., 16, 253, 1996.
113. Zhang, L. et al., Preparation of functionally active cell-permeable peptides by single-step ligation of two peptide modules, *Proc. Natl. Acad. Sci. U.S.A.,* 95, 9184, 1998.
114. Liu, C.F. and Tam, J.P., Chemical ligation approach to form a peptide bond between unprotected peptide segments, *J. Am. Chem. Soc*., 116, 4149, 1994.
115. Zhang, L. and Tam, J.P., Thiazolidine formation as a general and site-specific conjugation method for synthetic peptides and proteins, *Anal. Biochem*., 233, 87, 1996.
116. Tam, J.P., Yu, Q., and Miao, Z., Orthogonal ligation strategies for peptide and protein, *Biopolymers*, 51, 311, 1999.
117. Frankel, A.D. and Pabo, C.O., Cellular uptake of the tat protein from human immunodeficiency virus, *Cell*, 55, 1189, 1988.
118. Schwarze, S.R. et al., *In vivo* protein transduction: delivery of a biologically active protein into the mouse, *Science*, 285, 1569, 1999.
119. Ezhevsky, S.A. et al., Hypo-phosphorylation of the retinoblastoma protein (pRb) by cyclin D:Cdk4/6 complexes results in active pRb, *Proc. Natl. Acad. Sci. U.S.A.,* 94, 10699, 1997.
120. Nagahara, H. et al., Transduction of full-length TAT fusion proteins into mammalian cells: TAT-p27Kip1 induces cell migration, *Nat. Med*., 4, 1449, 1998.
121. Vocero–Akbani, A.M. et al., Killing HIV-infected cells by transduction with an HIV protease-activated caspase-3 protein, *Nat. Med.*, 5, 29, 1999.
122. Chellaiah, M.A. et al., Rho-A is critical for osteoclast podosome organization, motility, and bone resorption, *J. Biol. Chem.*, 275, 11993, 2000.
123. Derossi, D. et al., The third helix of the Antennapedia homeodomain translocates through biological membranes, *J. Biol. Chem*., 269, 10444, 1994.
124. Fischer, P.M. et al., Structure-activity relationship of truncated and substituted analogues of the intracellular delivery vector Penetratin, *J. Pept. Res*., 55, 163, 2000.

125. Williams, E.J. et al., Selective inhibition of growth factor-stimulated mitogenesis by a cell-permeable Grb2-binding peptide, *J. Biol. Chem*., 272, 22349, 1997.
126. Dunican, D.J. and Doherty, P., Designing cell-permeant phosphopeptides to modulate intracellular signaling pathways, *Biopolymers*, 60, 45, 2001.
127. Futaki, S. et al., Arginine-rich peptides. An abundant source of membrane-permeable peptides having potential as carriers for intracellular protein delivery, *J. Biol. Chem*., 276, 5836, 2001.
128. Rothbard, J.B. et al., Conjugation of arginine oligomers to cyclosporin A facilitates topical delivery and inhibition of inflammation, *Nat. Med*., 6, 1253, 2000.
129. Kown, M.H. et al., L-arginine polymer mediated inhibition of graft coronary artery disease after cardiac transplantation, *Transplantation*, 71, 1542, 2001.
130. Mitchell, D.J. et al., Polyarginine enters cells more efficiently than other polycationic homopolymers, *J. Pept. Res*., 56, 318, 2000.
131. Wender, P.A. et al., The design, synthesis, and evaluation of molecules that enable or enhance cellular uptake: peptoid molecular transporters, *Proc. Natl. Acad. Sci. U.S.A.,* 97, 13003, 2000.
132. Boulikas, T., Nuclear localization signals (NLS), *Crit. Rev. Eukaryot. Gene Expr*., 3, 193, 1993.
133. Collas, P. and Alestrom, P., Nuclear localization signals: a driving force for nuclear transport of plasmid DNA in zebrafish, *Biochem. Cell Biol*., 75, 633, 1997.
134. Moroianu, J., Nuclear import and export pathways, *J. Cell Biochem*., Suppl 32–33, 76, 1999.
135. Kalderon, D. et al., A short amino acid sequence able to specify nuclear location, *Cell*, 39, 499, 1984.
136. Dingwall, C. and Laskey, R.A., Nuclear targeting sequences — a consensus? *Trends Biochem. Sci.,* 16, 478, 1991.
137. Robbins, J. et al., Two interdependent basic domains in nucleoplasmin nuclear targeting sequence: identification of a class of bipartite nuclear targeting sequence, *Cell*, 64, 615, 1991.
138. Moroianu, J. et al., Mammalian karyopherin alpha 1 beta and alpha 2 beta heterodimers: alpha 1 or alpha 2 subunit binds nuclear localization signal and beta subunit interacts with peptide repeat-containing nucleoporins, *Proc. Natl. Acad. Sci. U.S.A.,* 92, 6532, 1995.
139. Radu, A., Moore, M.S., and Blobel G., The peptide repeat domain of nucleoporin Nup98 functions as a docking site in transport across the nuclear pore complex, *Cell*, 81, 215, 1995.
140. Gorlich, D. and Kutay, U., Transport between the cell nucleus and the cytoplasm, *Annu. Rev. Cell. Dev. Biol*., 15, 607, 1999.
141. Hodel, M.R., Corbett, A.H., and Hodel, A.E., Dissection of a nuclear localization signal, *J. Biol. Chem*., 276, 1317, 2001.
142. Casteels, P. and Tempst, P., Apidaecin-type peptide antibiotics function through a non-pore forming mechanism involving stereospecificity, *Biochem. Biophys. Res. Commun*., 199, 339, 1994.
143. Chan, Y.R. and Gallo, R.L., PR-39, a syndecan-inducing antimicrobial peptide, binds and affects p130(Cas), *J. Biol. Chem*., 273, 28978, 1998.
144. Castle, M. et al., Lethal effects of apidaecin on *Escherichia coli* involve sequential molecular interactions with diverse targets, *J. Biol. Chem*., 274, 32555, 1999.
145. Bulet, P. et al., Antimicrobial peptides in insects; structure and function, *Dev. Comp. Immunol*., 23, 329, 1999.

146. Agerberth, B. et al., Amino acid sequence of PR-39. Isolation from pig intestine of a new member of the family of proline-arginine-rich antibacterial peptides, *Eur. J. Biochem*., 202, 849, 1991.
147. Cabiaux, V. et al., Secondary structure and membrane interaction of PR-39, a Pro+Arg-rich antibacterial peptide, *Eur. J. Biochem*., 224, 1019, 1994.
148. Casteels, P. et al., Isolation and characterization of abaecin, a major antibacterial response peptide in the honeybee (Apis mellifera), *Eur. J. Biochem*., 187, 381, 1990.
149. Casteels, P. et al., Apidaecins: antibacterial peptides from honeybees, *EMBO. J*., 8, 2387, 1989.
150. Gennaro, R., Skerlavaj, B., and Romeo, D., Purification, composition, and activity of two bactenecins, antibacterial peptides of bovine neutrophils, *Infect. Immun*., 57, 3142, 1989.
151. Frank, R.W. et al., Amino acid sequences of two proline-rich bactenecins. Antimicrobial peptides of bovine neutrophils, *J. Biol. Chem*., 265, 18871, 1990.
152. Boman, H.G., Agerberth, B., and Boman, A., Mechanisms of action on *Escherichia coli* of cecropin P1 and PR-39, two antibacterial peptides from pig intestine, *Infect. Immun*., 61, 2978, 1993.
153. Gallo, R.L. and Huttner, K.M., Antimicrobial peptides: an emerging concept in cutaneous biology, *J. Invest. Dermatol*., 111, 739, 1998.
154. Bevins, C.L., Antimicrobial peptides as agents of mucosal immunity, *Ciba. Found. Symp*., 186, 250, 1994.
155. Shi, J. et al., Antibacterial activity of a synthetic peptide (PR-26) derived from PR-39, a proline-arginine-rich neutrophil antimicrobial peptide, *Antimicrob. Agents Chemother*., 40, 115, 1996.
156. Miao, Z. and Tam, J.P., Bidirectional tandem pseudoproline ligations of proline-rich helical peptides, *J. Am. Chem. Soc*., 122, 4253, 2000.
157. Scocchi, M., Romeo, D., and Zanetti, M., Molecular cloning of Bac7, a proline- and arginine-rich antimicrobial peptide from bovine neutrophils, *FEBS Lett*., 352, 197, 1994.
158. Sadler, K. and Tam, J.P., Unpublished results.
159. Singh, D. et al., Penetration and intracellular routing of nucleus-directed peptide-based shuttles (loligomers) in eukaryotic cells, *Biochemistry*, 37, 5798, 1998.
160. Arnold, L.J., Jr. et al., Antineoplastic activity of poly(L-lysine) with some ascites tumor cells, *Proc. Natl. Acad. Sci. U.S.A.,* 76, 3246, 1979.
161. Nussenzweig, V. and Nussenzweig, R.S., Circumsporozoite proteins of malaria parasites, *Cell*, 42, 401, 1985.
162. Hugel, F.U., Pradel, G., and Frevert, U., Release of malaria circumsporozoite protein into the host cell cytoplasm and interaction with ribosomes, *Mol. Biochem. Parasitol.,* 81, 151, 1996.
163. Frevert, U. et al., Malaria circumsporozoite protein inhibits protein synthesis in mammalian cells, *EMBO. J.,* 17, 3816, 1998.
164. Mota, M.M. et al., Migration of *Plasmodium* sporozoites through cells before infection, *Science*, 291, 141, 2001.
165. Eichinger, D.J. et al., Circumsporozoite protein of *Plasmodium berghei*: gene cloning and identification of the immunodominant epitopes, *Mol. Cell Biol*., 6, 3965, 1986.
166. Lum, B.L. et al., Molecular targets in oncology: implications of the multidrug resistance gene, *Pharmacotherapy*, 13, 88, 1993.
167. Boukerche, H. et al., A new Mr 55,000 surface protein implicated in melanoma progression: association with a metastatic phenotype, *Cancer Res*., 60, 5848, 2000.

168. Tendler, A., Kaufman, H.L., and Kadish, A.S., Increased carcinoembryonic antigen expression in cervical intraepithelial neoplasia grade 3 and in cervical squamous cell carcinoma, *Hum. Pathol*., 31, 1357, 2000.
169. Hewett, P.W., Identification of tumour-induced changes in endothelial cell surface protein expression: an *in vitro* model, *Int. J. Biochem. Cell. Biol*., 33, 325, 2001.
170. Lango, M.N., Shin, D.M., and Grandis, J.R., Targeting growth factor receptors: integration of novel therapeutics in the management of head and neck cancer, *Curr. Opin. Oncol*., 13, 168, 2001.
171. Fraile-Ramos, A. et al., The human cytomegalovirus US28 protein is located in endocytic vesicles and undergoes constitutive endocytosis and recycling, *Mol. Cell Biol.*, 12, 1737, 2001.
172. Doms, R.W. and Trono, D., The plasma membrane as a combat zone in the HIV battlefield, *Genes Dev.*, 14, 2677, 2000.

7 Arginine-Rich Molecular Transporters for Drugs: The Role of Backbone and Side Chain Variations on Cellular Uptake

Jonathan B. Rothbard, Erik Kreider, Kanaka Pattabiraman, Erin T. Pelkey, Christopher L. VanDeusen, Lee Wright, Bryan L. Wylie, and Paul A. Wender

CONTENTS

0-8493-1141-1/02/$0.00+$1.50

ABSTRACT

The goal of this review is to summarize previously published work on the design and biological activity of a family of guanidinium peptoid transporters that differ in the length of their side chains and to compare these results with a more recently designed family of transporters containing non-α-amino acids, i.e., variations along the backbone. The latter group of peptides differs by the spacing of the arginine subunits along the peptide backbone. When these analogs were assayed for cellular uptake, the most important feature was shown to be not the nature of the substituted amino acid, but rather the distance between each of the arginines.

When results of the two studies were compared a very similar pattern was observed. By increasing the conformational freedom of either the side chains of the peptoids or the backbone of peptides by the addition of methylene units, a significant enhancement in the rate of cellular uptake of the transporter was seen. Even though the conformational flexibility of peptoids and peptides is very different, addition of methylenes in either the backbone or the side chain results in enhanced cellular uptake, arguing that the flexibility of the guanidine headgroups can be accomplished in either of these ways. Typically, the biological activity of most biological ligands, particularly those functioning as inhibitors, increases with conformational restriction as preorganization in the form of the bound conformer favors tighter binding. The enhanced activity associated with increased conformational mobility observed for molecular transporters is in agreement with a dynamic transport system in which turnover rather than tightness of binding is critical for function.

7.1 INTRODUCTION

Biological barriers have evolved to prevent entry of xenobiotics into tissues and cells. However, these same barriers often limit or preclude uptake, and therefore the therapeutic benefit, of a variety of drugs. Consequently, most drugs must be restricted in physical properties to allow cellular and tissue uptake. This requirement greatly limits the universe of potential therapeutics to a very small number of compounds. The studies reviewed below were directed toward the goal of enhancing or enabling delivery of drugs through biological barriers by conjugation to transporter molecules.

Oligomers of arginine composed of six or more amino acids, either alone or when covalently attached to a variety of small molecules, cross biological membranes very effectively by an as yet undefined mechanism.[1] The chirality of the amino acid subunits in the arginine oligomers does not affect transport activity. In addition, a variety of other nonpeptide, guanidine-rich molecular transporters that do not share the composition or the spacing of a peptide have been shown to exhibit transport into cells.

The guanidine headgroup of arginine appears to be the key structural unit for cellular uptake.[1,2] The rate of uptake is dependent on both the concentration of the oligomers and their guanidine content, with a greater rate observed as the length of the peptide is increased up to approximately 15 residues. Oligomers beyond this length enter cells less effectively, precipitate serum proteins, and exhibit cellular cytotoxicity at high micromolar concentrations. Detailed kinetic analyses demonstrated that nonamers of arginine were significantly more effective at crossing biological membranes than

residues 49 to 57 of HIV tat and the 16 amino acid peptide from antennapedia, both widely used molecular transporters.[2] Interestingly, the activity of the HIV tat peptide closely mimicked that of a hexamer of arginine, which possesses the same arginine content.[2]

The goal of this review is to summarize previously published work on the design and biological activity of a family of guanidinium peptoid transporters that differ in the length of their side chains and to compare these results with a more recently designed family of transporters containing non-α-amino acids, i.e., variations along the backbone. The latter group of peptides differs by the spacing of the arginine subunits along the peptide backbone. Previous experiments have established clearly that the key structural unit necessary for transport was the guanidine headgroup and that only homopolymers containing more than five arginines exhibit significant biological activity. However, the importance of each headgroup and their spacing, both the distance they extend from the polymeric backbone and the distance between the headgroups along the backbone, has not been extensively investigated. Prior to these studies only individual alanine substitutions into a nine amino acid sequence in HIV tat were examined. These experiments demonstrated that the central glutamine is not required for activity, while replacement of any of the arginines results in a significant loss of uptake function.[2]

The experiments described in this review represent a portion of a broad effort to understand the fundamental structural requirements for transport across biological membranes and have led to the design of simple and cost effective transporters that could be used to deliver drugs and probe molecules into target tissues and cells as required for therapeutic applications. Peptoids have several advantages over peptides[3] and were selected for comparative study. Even though both are synthesized in a stepwise fashion using solid phase synthesis, peptoids are constructed from significantly cheaper starting materials and, due to absence of a chiral center, do not epimerize and are more amenable to side chain modification. This latter feature was utilized to construct a family of polyguanidine peptoids that differed in the length and flexibility of their side chains. Comparison of their ability to enter cells led to the realization that an increase in the length and, consequently, conformational mobility of the side chains resulted in a higher rate of cellular uptake.

A possible rationalization of the increase in biological activity of the peptoids with more flexible side chains is that this enabled a higher percentage of guanidines to contact a biological membrane. Molecular modeling was used to determine whether this hypothesis has merit by determining the theoretical number of guanidine headgroups in an oligomer of arginine that would contact a common surface. To investigate the results of this modeling experimentally, the residues believed to be unimportant in the complex formation were substituted in turn with each of the naturally occurring amino acids. Surprisingly, when these analogs were assayed for cellular uptake, the most important feature was shown to be not the nature of the substituted amino acid, but rather the distance between each of the arginines. This was established by inserting non-α-amino acids between the arginine subunits, which both supported the hypothesis and also allowed the spacing to be optimized.

When results of the two studies were compared, a very similar pattern was observed. By increasing the conformational freedom of either the side chains of

peptoids or the backbone of peptides by the addition of methylene units, a significant enhancement in the rate of cellular uptake of the transporter was seen. Even though the conformational flexibility of peptoids and peptides is very different, addition of methylenes in either the backbone or the side chain results in enhanced cellular uptake, arguing that the flexibility of the guanidine headgroups can be accomplished in either of these two ways. Typically, the biological activity of most biological ligands, particularly those functioning as inhibitors, increases with conformational restriction as preorganization in the form of the bound conformer favors tighter binding. The enhanced activity associated with increased conformational mobility observed for molecular transporters is in agreement with a dynamic transport system in which turnover rather than tightness of binding is critical for function.

7.2 MATERIALS AND METHODS

7.2.1 General

Rink amide resin and Boc anhydride were purchased from Novabiochem. Diisopropylcarbodiimide, bromoacetic acid, fluorescein isothiocyanate (FITC-NCS), ethylenediamine, 1,3-diaminopropane, 1,4-diaminobutane, 1,6-diaminohexane, 1,8-diaminooctane, *trans*-1,6-diaminocyclohexane, and pyrazole-1-carboxamidine were all purchased from Aldrich®. All solvents and other reagents were purchased from commercial sources and used without further purification. The mono-Boc amines were synthesized from commercially available diamines using a literature procedure (10 equiv. of diamine and 1 equiv. of Boc_2O in chloroform followed by an aqueous work-up to remove unreacted diamine).[4]

7.2.2 Peptide Synthesis

Peptides were synthesized using solid phase techniques and commercially available Fmoc amino acids, resins, and reagents (PE Biosystems, Foster City, CA, and Bachem Torrence, CA) on an Applied Biosystems 433A peptide synthesizer as previously described.[1] Fastmoc cycles were used with O-(7-azabenzotriazol-1-yl)-1,1,3,3-tetramethyluronium hexfluorophosphate (HATU) substituted for HBTU/HOBt as the coupling reagent. All Fmoc amino acids were commercially available (Bachem, San Diego, CA). The peptides were cleaved from the resin using 96% trifluoroacetic acid, 2% triisopropyl silane, and 2% phenol for between 1 and 12 h. The longer reaction times were necessary to completely remove the Pbf protecting groups from the polymers of arginine. The peptides subsequently were filtered from the resin, precipitated using diethyl ether, purified using HPLC reverse phase columns (Alltech Altima, Chicago, IL), and characterized using electrospray mass spectrometry (Applied Biosystems, Foster City, CA).

7.2.3 Robotic Peptide Synthesis

Parallel solid-phase synthesis of the peptides listed in Table 7.1 was accomplished using an ABI robotics system, the Solaris 450, capable of 48 concurrent syntheses. Identical protected amino acids, resins, and solvents were used in the robotic system

TABLE 7.1
All Possible Permutations of the Insertion of between One and Six Aminocaproic Acids (aca) into a Heptamer of Arginine

	code			code			code	
1	0	RRRRRRR	23	3.1	RacaRacaRacaRRRR	43	4.1	RacaRacaRacaRacaRRR
2	1.1	RacaRRRRRR	24	3.2	RacaRacaRRacaRRR	44	4.2	RacaRacaRacaRRacaRR
3	1.2	RRacaRRRRR	25	3.3	RacaRacaRRRacaRR	45	4.3	RacaRacaRacaRRRacaR
4	1.3	RRRacaRRRR	26	3.4	RacaRacaRRRRacaR	46	4.4	RacaRacaRRacaRacaRR
5	1.4	RRRRacaRRR	27	3.5	RacaRRacaRacaRRR	47	4.5	RacaRacaRRacaRRacaR
6	1.5	RRRRRacaRR	28	3.6	RacaRRacaRRacaRR	48	4.6	RacaRacaRRRacaRacaR
7	1.6	RRRRRRacaR	29	3.7	RacaRRacaRRRacaR	49	4.7	RacaRRacaRacaRacaRR
8	2.1	RacaRacaRRRRR	30	3.8	RacaRRRacaRacaRR	50	4.8	RacaRRacaRacaRRacaR
9	2.2	RacaRRacaRRRR	31	3.9	RacaRRRacaRRacaR	51	4.9	RacaRRacaRRacaRacaR
10	2.3	RacaRRRacaRRR	32	3.10	RacaRRRRacaRacaR	52	4.10	RacaRRRacaRacaRacaR
11	2.4	RacaRRRRacaRR	33	3.11	RRacaRacaRacaRRR	53	4.11	RRacaRacaRacaRacaRR
12	2.5	RacaRRRRRacaR	34	3.12	RRacaRacaRRacaRR	54	4.12	RRacaRacaRacaRRacaR
13	2.6	RRacaRacaRRRR	35	3.13	RRacaRacaRRRacaR	55	4.13	RRacaRacaRRacaRacaR
14	2.7	RRacaRRacaRRR	36	3.14	RRacaRRacaRacaRR	56	4.14	RRacaRRacaRacaRacaR
15	2.8	RRacaRRRacaRR	37	3.15	RRacaRRacaRRacaR	57	4.15	RRRacaRacaRacaRacaR
16	2.9	RRacaRRRRacaR	38	3.16	RRacaRRRacaRacaR	58	5.1	RacaRacaRacaRacaRacaRR
17	2.10	RRRacaRacaRRR	39	3.18	RRRacaRacaRacaRR	59	5.2	RacaRacaRacaRacaRRacaR
18	2.11	RRRacaRRacaRR	40	3.19	RRRacaRacaRRacaR	60	5.3	RacaRacaRacaRRacaRacaR
19	2.12	RRRacaRRRacaR	41	3.20	RRRacaRRacaRacaR	61	5.4	RacaRacaRRacaRacaRacaR
20	2.13	RRRRacaRacaRR	42	3.21	RRRRacaRacaRacaR	62	5.5	RacaRRacaRacaRacaRacaR
21	2.14	RRRRacaRRacaR				63	5.6	RRacaRacaRacaRacaRacaR
22	2.15	RRRRRacaRacaR				64	6.1	RacaRacaRacaRacaRacaRacaR

Note: The individual peptides are referred to using codes that also include the number of substitutions in their format.

as previously described. The peptides were cleaved from the resin using trifluoroacetic acid, purified by reverse phase HPLC, and their structure confirmed using electrospray mass spectrometry (Applied Biosystems, Foster City, CA).

7.2.4 Peptoid Polyamine Synthesis

Peptoids were synthesized manually using a fritted glass apparatus and positive nitrogen pressure for mixing the resin following the literature procedure developed by Zuckerman.[3,5,6] Treatment of Fmoc-substituted Rink amide resin (0.2 mmol) with 20% piperidine/DMF (5 ml) for 30 min (2×) gave the free resin-bound amine, which was washed with DMF (3 × 5 ml). The resin was treated with a solution of bromoacetic acid (2.0 mmol) in DMF (5 ml) for 30 min. This procedure was repeated. The resin was then washed (3 × 5 mL DMF) and treated with a solution of mono-Boc diamine (8.0 mmol) in DMF (5 ml) for 12 h. These two steps were repeated until an oligomer of the required length was obtained. (Note: the solution of mono-Boc diamine in DMF could be recycled without appreciable loss of yield.) The resin was then treated with *N*-Fmoc-aminohexanoic acid (2.0 mmol) and DIC (2.0 mmol)

in DMF for 1 h and this was repeated. The Fmoc moiety was then removed by treatment with 20% piperidine/DMF (5 ml) for 30 min. This step was repeated and the resin was washed with DMF (3 × 5 ml). The free amine resin was then treated with fluorescein isothiocyanate (0.2 mmol) and DIEA (2.0 mmol) in DMF (5 ml) for 12 h. The resin was then washed with DMF (3 × 5 ml) and dichloromethane (5 × 5 ml). Cleavage from the resin was achieved using 95:5 TFA/triisopropylsilane (8 ml).

Removal of the solvent *in vacuo* gave a crude oil that was triturated with cold ether (20 ml). The crude mixture thus obtained was centrifuged, the ether was removed by decantation, and the resulting orange solid was purified by reverse-phase HPLC (H_2O/CH_3CN in 0.1% TFA). The products were isolated by lyophilization and characterized by electrospray mass spectrometry and, in selected cases, by ^1H NMR spectroscopy.

7.2.5 Perguanidinylation of Peptoid Polyamines

A solution of peptoid amine (0.1 mmol) dissolved in deionized water (5 ml) was treated with sodium carbonate (5 equivalents per amine residue) and pyrazole-1-carboxamidine (5 equivalents per amine residue) and heated at 50°C for 24 to 48 h. The crude mixture was then acidified with TFA (0.5 ml) and directly purified by reverse-phase HPLC (H_2O/CH_3CN in 0.1% TFA). The products were characterized by electrospray mass spectrometry and isolated by lyophilization and further purified by reversed-phase HPLC. The yield for the perguanidinylated peptoids was 60 to 70%, while their purity was >95%, as determined by analytical reversed-phase HPLC (H_2O/CH_3CN in 0.1% TFA).

7.2.6 Molecular Modeling

NAMD2,[7] developed at the University of Illinois, was used to evaluate the structure of an acetylated decamer of arginine with a carboxamidine terminus. The psfgen program was used to create the necessary psf and pdb input files. CHARMM parameters[8] were used to minimize the heptamer for 2000 steps, using a dielectric constant of 80. At this point, molecular dynamics were performed for 100 psec over which the average kinetic energy of the system was increased from 300 to 1000 K in 25° increments by reassignment every psec, holding at 1000 K once reached. Following 20 psec of equilibration, the system was reequilibrated to 300 K over 100 psec in 10° increments every psec, holding at 300 K once reached. The annealed structures were then analyzed using VMD.[9]

7.2.7 Cellular Uptake Assays

The peptides and guanidine-substituted peptoids were each dissolved in PBS buffer (pH 7.2) and their concentration determined by absorption of fluorescein at 490 nm ($\varepsilon = 67{,}000$). The accuracy of this method for determining transporter concentration was established by weighing selected samples and dissolving them in a known amount of PBS buffer. The concentrations determined by UV spectroscopy correlated with the amounts weighed out manually. The human T cell line, Jurkat, grown in 10% fetal calf serum in DMEM, was used for all the cellular uptake experiments.

Varying amounts of the peptides were added to 3×10^5 cells in a total of 200 µl, in wells of microtiter plates, and incubated for 3 min at 23ºC. The cells were spun, washed three times with cold PBS and resuspended in PBS containing 0.1% propidium iodide. The cells were analyzed by fluorescent flow cytometry (FACScan, Becton Dickinson, Milpitas, CA). Cells staining with propidium iodide were excluded from the analysis.

Data presented are the mean fluorescent signal for the 5000 cells collected. To prevent cellular uptake of the peptides, the cells were treated with sodium azide (1.0%) for 25 min prior to exposure to the peptides. Intracellular fluorescence was calculated by subtracting the fluorescence from cells treated with sodium azide from that observed from untreated cells.

7.3 RESULTS

7.3.1 Guanidino Peptoid Design and Cellular Uptake

A series of novel polyguanidine peptoid derivatives were designed that preserved the 1,4-backbone spacing of side chains of arginine oligomers, but had an oligoglycine backbone devoid of stereogenic centers. These peptoids, incorporating side chains of arginine but attached to the amide nitrogen, were selected because of their expected resistance to proteolysis[10] and potential ease of synthesis.[3,6] Furthermore, epimerization, frequently encountered in peptide synthesis, is not a problem in peptoid synthesis and the submonomer[3] approach to peptoid synthesis allows for facile introduction of other side chains. Although the preparation of an oligourea[11] and peptoid–peptide hybrid[12] derivatives of $Tat_{49\text{-}57}$ have been previously reported, their cellular uptake was not explicitly studied.

The desired peptoids were prepared using the submonomer[3] approach to peptoids, followed by attachment of a fluorescein moiety through an aminohexanoic acid spacer onto the amine termini. After cleavage from the solid-phase resin, the fluorescently labeled polyamine peptoids thus obtained were converted in good yields (60 to 70%) into polyguanidine peptoids by treatment with excess pyrazole-1-carboxamidine[13] (Scheme 7.1). Previously reported syntheses of peptoids containing isolated *N*-Arg units have relied on the synthesis of *N*-Arg monomers (5 to 7 steps) prior to peptoid synthesis and the use of specialized and expensive guanidine protecting groups (Pmc, Pbf).[14,15]

The compounds reported here represent the first examples of polyguanidinylated peptoids prepared using a perguanidinylation step. This method provides easy access to polyguanidinylated compounds from the corresponding polyamines and is especially useful for the synthesis of perguanidinylated homooligomers. Furthermore, this procedure eliminates use of expensive protecting groups (Pbf, Pmc). An additional example of a perguanidinylation of a peptide substrate using a novel triflyl-substituted guanidinylating agent has been reported recently.[16]

The cellular uptake into the human T cell line, Jurkat, of the set of fluorescently labeled polyguanidine peptoids of varying length, *N*-arg 5, 7, and 9, was analyzed by flow cytometry and compared to the corresponding *d*-arginine peptides r5, 7, and 9. The amount of measured fluorescence inside the cells treated with *N*-arg 5, 7, and

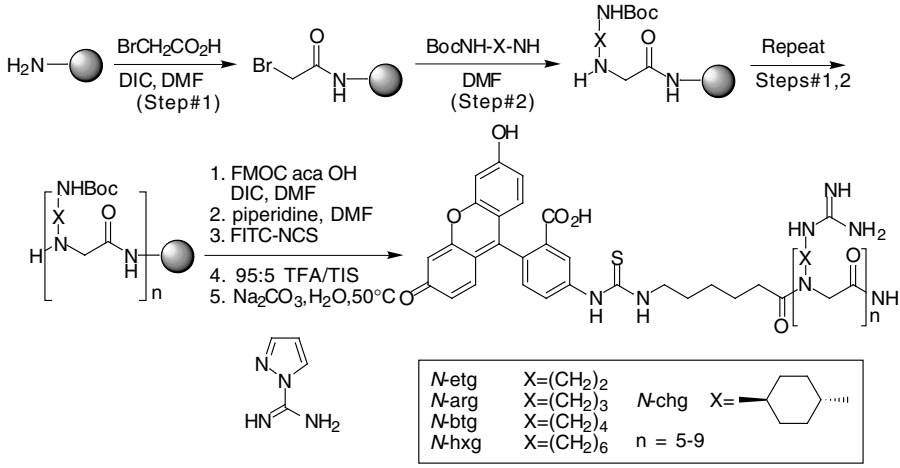

SCHEME 7.1 Preparation of guanidine-substituted peptoids.

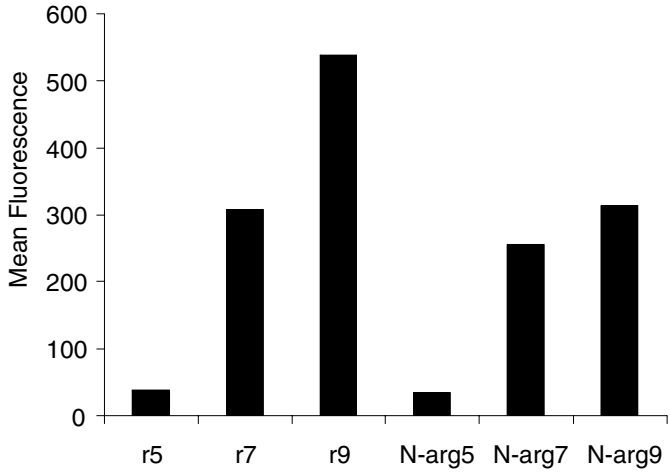

FIGURE 7.1 The length dependence of cellular uptake is observed for both polyguanidino peptoids and oligomers of *d*-arginine. The mean fluorescence from 5000 cells of a human T cell line, Jurkat, is shown after incubation with 12.5 μ*M* of each of the peptides for 5 min. Uptake was measured in triplicate at concentrations varying from 400 n*M* to 50 μ*M*. The data are shown at a single concentration for ease of presentation. Details of the assay are described in Section 7.2.

9 was found to be related to the number of guanidine residues in the peptoid, with the nonamer entering cells more effectively than the heptamer, which in turn was more effective than the pentamer (*N*-arg9 > *N*-arg7 > *N*-arg5) (Figure 7.1). These results are analogous to previously reported behavior for the different oligomers of

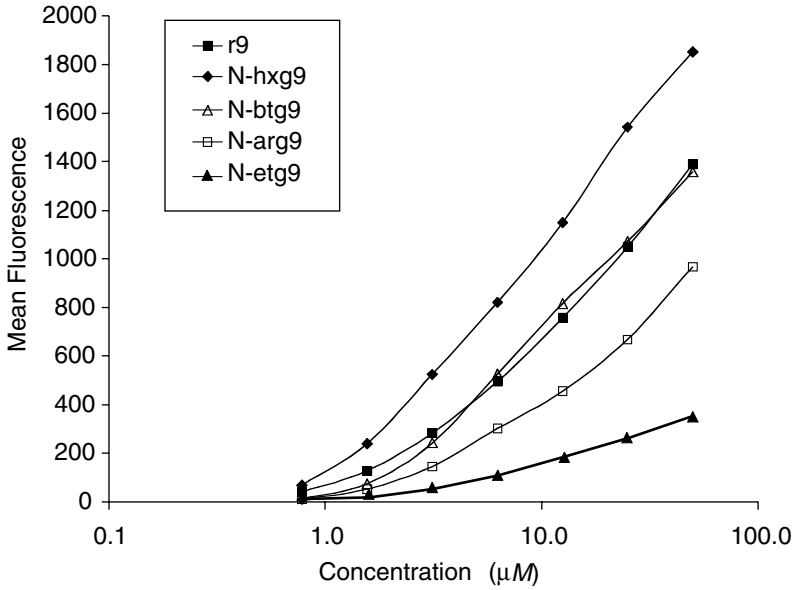

FIGURE 7.2 Relative cellular uptake of a set of guanidino peptoids with side chains of varying length. The mean fluorescence from 5000 cells of a human T cell line, Jurkat, is shown after incubation with each of the peptoids for 5 min. Uptake was measured in triplicate at concentrations varying from 80 n*M* to 50 μ*M*.

d-arginine (r9>r7>>r5). Importantly, the *N*-arg5, 7, and 9 peptoids showed only a slightly lower amount of cellular entry when compared to the corresponding homopolymers of arginine.

These results demonstrate that hydrogen bonding along the peptide backbone of arginine oligomers is not a required structural element for cellular uptake, oligomeric guanidine-substituted peptoids and other backbone systems (hydrocarbons, PEG, polyamines, etc.) can be utilized in place of arginine-rich peptides as molecular transporters. The addition of sodium azide inhibited internalization, suggesting that cellular uptake of peptoids was also energy dependent.

7.3.2 Role of the Side Chain Conformational Freedom of Guanidino Peptoids in Cellular Uptake

Following the demonstration that *N*-arg peptoids efficiently crossed cellular membranes, the effect of side chain length on cellular uptake was investigated by synthesizing guanidino peptoids with monomers of side chains containing two, three, four, or six methylenes between the backbone and the headgroup. Each of the monomers was used to prepare a set of peptoid pentamers, heptamers, and nonamers. The differential ability of each compound to enter T cells was assayed by flow cytometry as described in Section 7.2. Within each set of peptoids of the same length a similar pattern is observed (Figure 7.2 and data not shown): cellular uptake is enhanced as the number of methylenes in the side chain increases. In the case of

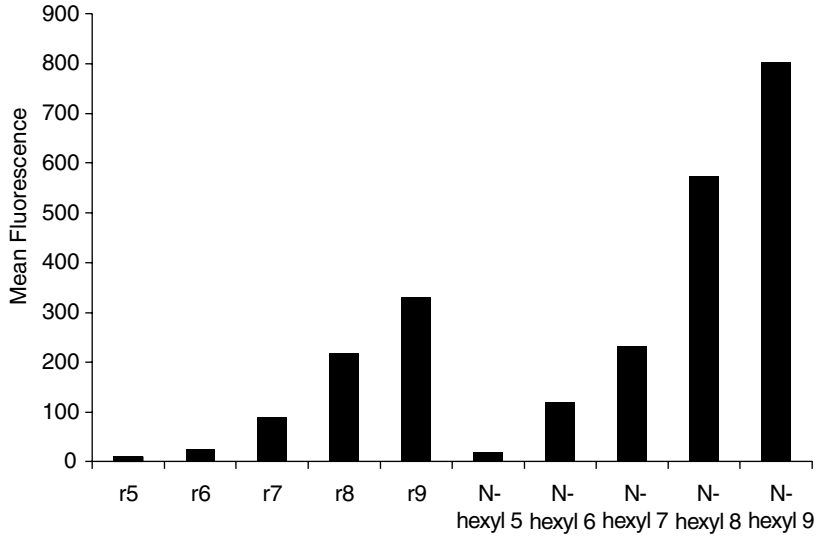

FIGURE 7.3 Guanidino peptoids with hexyl side chains enter cells more efficiently than oligomers of *d*-arginine of equal length. The mean fluorescence from 5000 cells of a human T cell line, Jurkat, is shown after incubation with 6.25 μ*M* of each of the peptides for 5 min. Uptake was measured in triplicate at concentrations varying from 400 n*M* to 50 μ*M*. Data are shown at a single concentration for ease of presentation.

the nonamers, the peptoid with four methylenes, *N*-butyl 9, is approximately equivalent to a nonamer of *d*-arginine, r9, with the peptoid with six methylenes in the side chain, *N*-hexyl 9, significantly more potent (Figure 7.2). The cellular uptake of the corresponding heptamers and pentamers also showed the same relative trend. In general, *N*-hexyl peptoids of n residues in length (where n = 5 to 9) enter cells as well as or better than peptide of n+1 residues (Figure 7.3).

To determine whether the enhanced cellular uptake was due to the increased hydrophobic nature or greater conformational freedom of the side chains, a set of peptoids was synthesized containing cyclohexyl side chains, *N*-cyclohex 5, 7, and 9 peptoids. These contained the same number of side chain carbons as the *N*-hexyl peptoids, but possessed significantly fewer degrees of conformational freedom. When assayed for cellular uptake, the *N*-cyclohex peptoid showed much lower cellular uptake activity than all of the previously assayed peptoids, including the *N*-ethyl peptoids (Figure 7.4). Therefore, the conformational flexibility and sterically unencumbered nature of the straight chain alkyl spacing groups — not the increased hydrophobic nature of the side chain — was the important factor in determining efficiency of cellular uptake.

7.3.3 Role of the Backbone Conformational Freedom of Guanidino Peptide Transporters in Cellular Uptake

For many secondary structures of the transporter, not all of the guanidino groups are capable of contacting a common surface involved in transport (either cell or

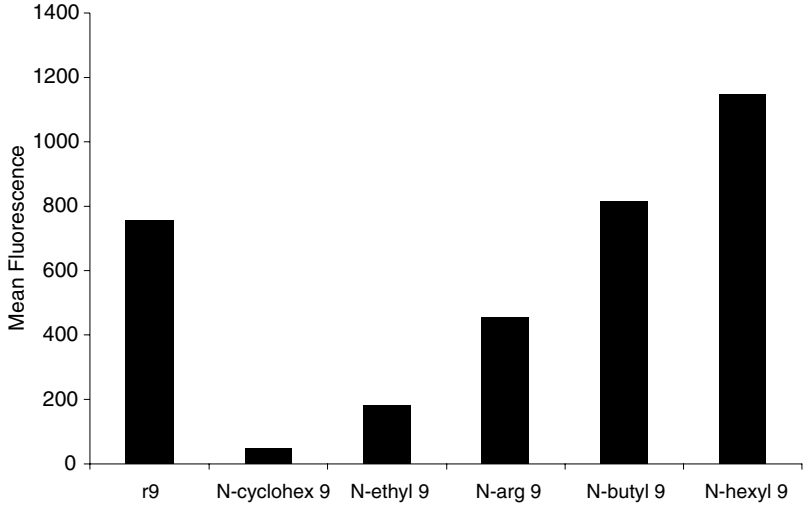

FIGURE 7.4 Enhanced cellular uptake correlates with increased conformational freedom and not hydrophobic content of the side chains of the transporter. Comparison of the cellular uptake of a set of guanidino peptoids containing nine subunits, but differing in their side chain composition. N-ethyl 9 contains two methylenes, N-arg, three, N-butyl, four, N-hexyl, six, and cyclohex, a cyclohexyl ring, approximately equivalent to N-hexyl in hydrophobic nature, but not conformational flexibility. The mean fluorescence from 5000 cells of a human T cell line, Jurkat, is shown after incubation with 12.5 μ*M* of each of the peptides for 5 min. Uptake was measured in triplicate at concentrations varying from 400 n*M* to 50 μ*M*. Data are shown at a single concentration for ease of presentation.

receptor). Consequently, arginines not in contact with the common surface could in principle be replaced with other residues without affecting transport.

Molecular modeling was used to generate secondary structures of the transporters and to determine the theoretical number of guanidine headgroups capable of contacting a common surface. Using NAMD2, a scalable molecular mechanics engine, the solution phase structures of a decamer of arginine were evaluated.[7] One of the low energy conformations found at 300 K positioned residues 2, 5, and 8 away from a surface plane making contact with the other residues (Figure 7.5). In this conformation, the maximum contacts with a common surface were made with the guanidine headgroups of residues 1, 3, 4, 6, 7, 9, and 10. The guanidine headgroups of the arginines at positions 2, 5, and 8 appeared unable to contact the surface for this family of conformers.

To test this hypothesis, a set of 17 peptides, substituting each of the naturally occurring amino acids, except arginine, cysteine, and tryptophan, into the three positions (2, 5, and 8) believed not in contact, were synthesized, conjugated with fluorescein, and assayed for cellular uptake (Figure 7.6).

All peptides were decamers containing seven equivalently spaced arginines. Not surprisingly, the peptides exhibited a wide range of abilities to enter the cells, depending on the substituted amino acid. Substitution with aspartic and glutamic acid resulted in analogues that entered cells relatively poorly. Previous experiments

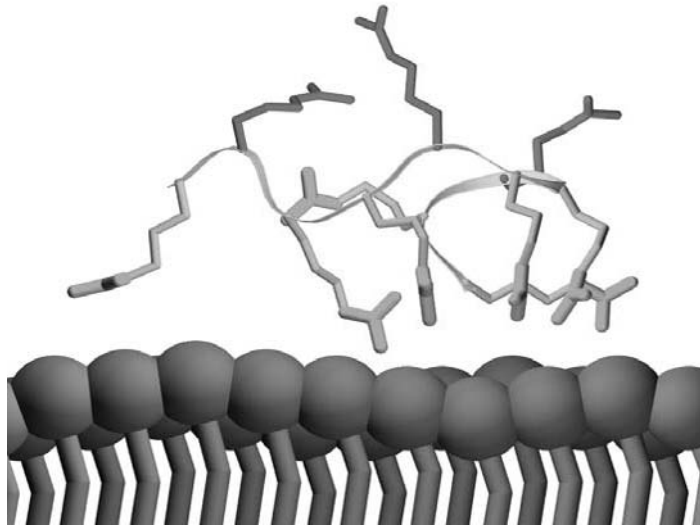

FIGURE 7.5 (Color Figure 7.5 follows p. 14.) A low energy conformation of Ac-R_{10}-$CONH_2$. Ribbon structure showing a representative decamer structure with the 2nd, 5th, and 8th side chains shown in red. The backbone of the decamer is represented by a green ribbon. Side chains able to access a common surface (purple) are shown in blue with yellow guanidinium groups.

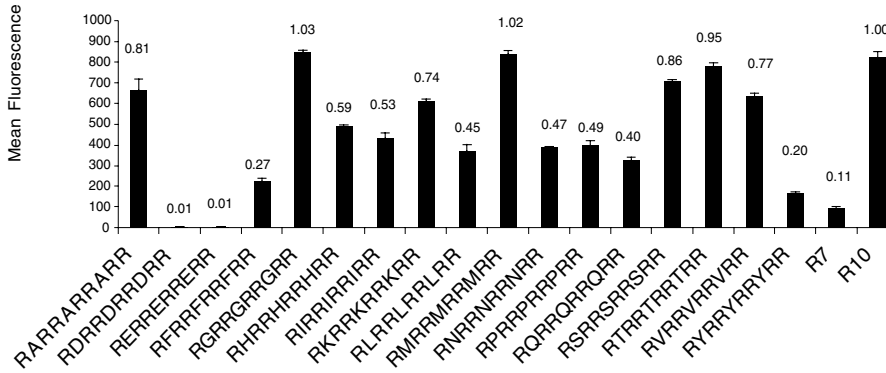

FIGURE 7.6 Differential cellular uptake of a set of decamers with each of the naturally occurring amino acids substituted in positions 2, 5, and 8 compared with R7 and R10. The mean fluorescence from 5000 cells of a human T cell line, Jurkat, is shown after incubation with 25 μ*M* of each of the peptides for 5 min. Uptake was measured in triplicate at concentrations varying from 400 n*M* to 50 μ*M*. Data are shown at a single concentration for ease of presentation; details of the assay are described in Section 7.2.

have established that the guanidine headgroup of arginine can form intramolecular salt bridges with either phosphate or carboxylate functionalities, and in so doing reduce the number of guanidines available for interaction with the cell surface (unpublished results). A similar effect could explain the relatively inefficient ability

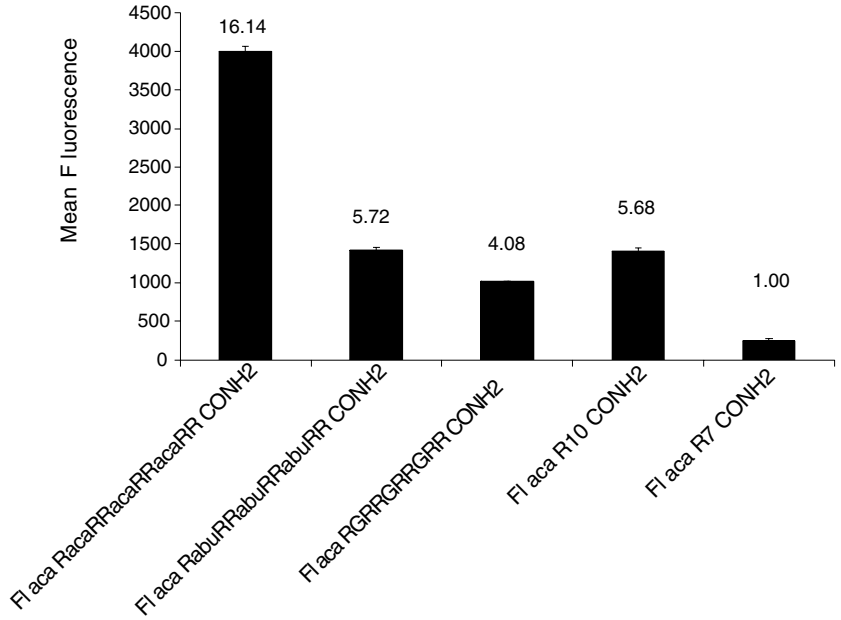

FIGURE 7.7 Relative ability of a set of decamer analogs with substitution at residues 2, 5, and 8 resulting in differential spacing between the arginines. The mean fluorescence from 5000 cells of a human T cell line, Jurkat, is shown after incubation with 12.5 μ*M* of each of the peptides for 5 min. Uptake was measured in triplicate at concentrations varying from 400 n*M* to 50 μ*M*. Data are shown at a single concentration for ease of presentation. The numbers above the histograms represent the relative uptake compared to hepta L-arginine, R7.

of the peptides substituted with the acidic amino acids to enter cells. Substitution with valine, alanine, glycine, methionine, and threonine resulted in analogues that entered cells as well as R10, even though they each contained only seven guanidino groups. This is in accordance with the hypothesis that not all of the guanidine headgroups are necessary for efficient cellular uptake.

Another factor contributing to cellular uptake is revealed when the peptides containing seven arginines and three variable residues are compared with R7 (Figure 7.6). With the exception of the acidic amino acid substitutions, all are superior to R7 — suggesting that an increase in the spacing between arginine residues also enhances cellular uptake.

To explore this hypothesis further, two decamers of arginine were synthesized: one with 4-aminobutyric acid (abu) and the other with 6-aminocaproic acid (aca) substituted for arginine at residues 2, 5, and 8. Their ability to enter lymphocytes was compared with the glycine-substituted analog and the two homopolymers, R7 and R10 (Figure 7.7).

The differential uptake of the peptides supported the hypothesis that increasing the spacing between the arginines results in greater cellular uptake. Glycine has a single methylene between the amino and carboxyl groups, 4-aminobutyric acid has three, and 6-aminocaproic acid has five. As the number of methylenes increased

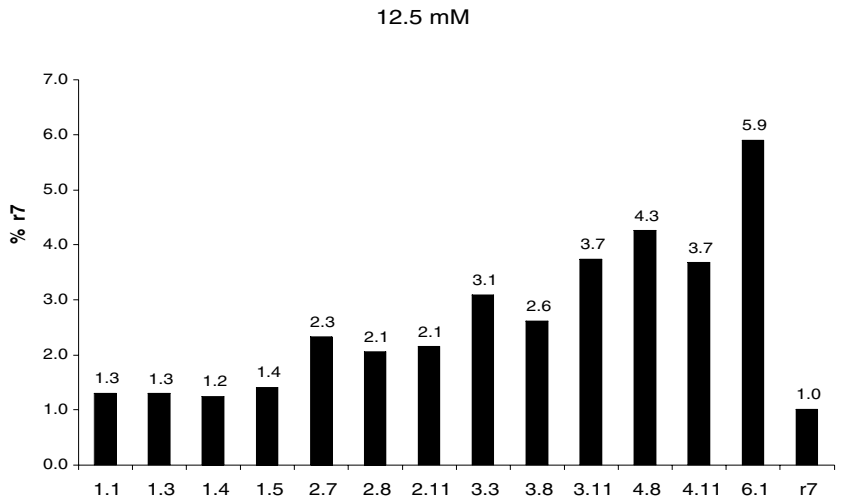

FIGURE 7.8 Differential uptake of heptamers of L-arginine with varying numbers of aminocaproic acid interspersed into the sequence. Codes refer to peptides listed in Table 7.1. Each peptide was assayed from 400 n*M* to 50 μ*M*, but only the differential uptake at 12.5 μ*M* is shown. Data above the bars are presented as relative uptake compared to hepta D-arginine, r7.

from one to three to five, the uptake relative to R7 increased by factors of four, five, and sixteen, respectively. The peptide with aminocaproic acid-spacing entered cells more effectively than R10.

The data in Figure 7.7 established that the spacing between arginine residues was a critical factor in the structure–activity relationship of cellular uptake. However, only a single substitution pattern was examined. A comprehensive analysis indicates that there are actually 63 unique sequences in which seven arginines are spaced by one to six nonconsecutive 1,6 aminocaproic acids (Table 7.1).

When the aca-spaced peptides were assayed for cellular uptake, a relatively simple pattern was observed. The rate of uptake is dependent on the aminocaproic acid content; the individual pattern of spacing was unimportant. Peptides with greater aminocaproic acid content exhibited faster rates of uptake than those containing fewer spacers. Peptides with an equal number of aminocaproic acids, but located differently within the sequence, entered cells comparably well (Figure 7.8 and data not shown). The most potent analog was the fully spaced compound, analog 6.1, which had six aminocaproic acids interspacing the seven arginines (Figure 7.8).

Such a simple pattern was consistent with the lack of a specific binding site in a putative receptor and supports the hypothesis that the peptides are contacting negatively charged species on the cell surface. An alternative explanation of the data is that, as more aminocaproic acids are introduced into the heptamer of arginine, the peptide becomes more protease resistant. Consequently, the peptides containing more aminocaproic acids have a higher effective concentration. Even though only a trace amount of serum was in the assay, this possibility should be considered.

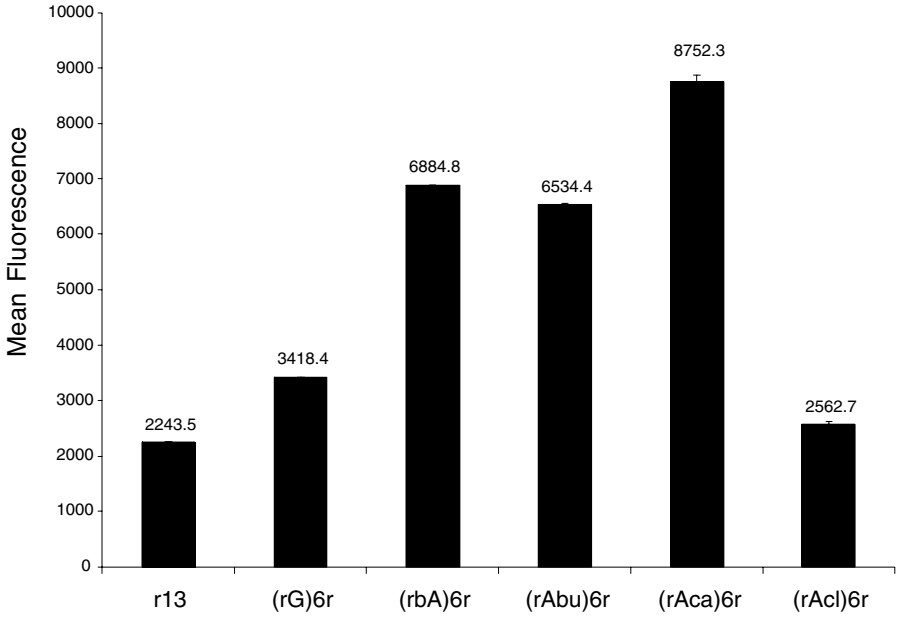

FIGURE 7.9 Cellular uptake increased as the spacing between the arginines increased until the residues were separated by 8-aminocaprylic acid. Comparison of the cellular uptake of a set of peptides containing seven arginine and either six alternating glycine ($CH_2 = 1$), β-alanine ($CH_2 = 2$), 4-aminobutyric acid ($CH_2 = 3$), 6-amino caproic acid ($CH_2 = 5$), or 8-aminocaprylic acid ($CH_2 = 7$) with both r13. The mean fluorescence from 5000 cells of a human T cell line, Jurkat, is shown after incubation with 12.5 μ*M* of each of the peptides for 5 min. Uptake was measured in triplicate at concentrations varying from 400 n*M* to 50 μ*M*. Data are shown at a single concentration for ease of presentation.

To attempt to distinguish between these possibilities and also to determine the optimal linear spacer, the set of peptides containing seven arginines with either six alternating glycine ($CH_2 = 1$), β-alanine ($CH_2 = 2$), 4-aminobutyric acid ($CH_2 = 3$), 6-amino caproic acid ($CH_2 = 5$), or 8-aminocaprilic acid ($CH_2 = 7$) residues were synthesized and assayed for cellular uptake (Figure 7.9). In this set of peptides *d*-arginine was used and any possibility of differential proteolysis was eliminated. With the exception of the peptide containing β-alanine being superior to that containing 4-amino butyric acid, a general trend of a faster rate of uptake into cells was observed when the spacing between the arginines increased, until a limit was reached with the 6-aminocaproic acid.

A possible explanation for the increased rate of uptake of substituted peptides is that they utilize a different mechanism for cell entry. A characteristic of arginine-rich transporters is that their ability to enter cells correlates with their arginine content. To test whether the spaced peptides share this characteristic, a set of spaced peptides with an arginine content ranging from five to seven were synthesized and assayed (Figure 7.10). Among a family of peptides with the arginine residues equally spaced, increasing the arginine content increased the rate of cellular uptake.

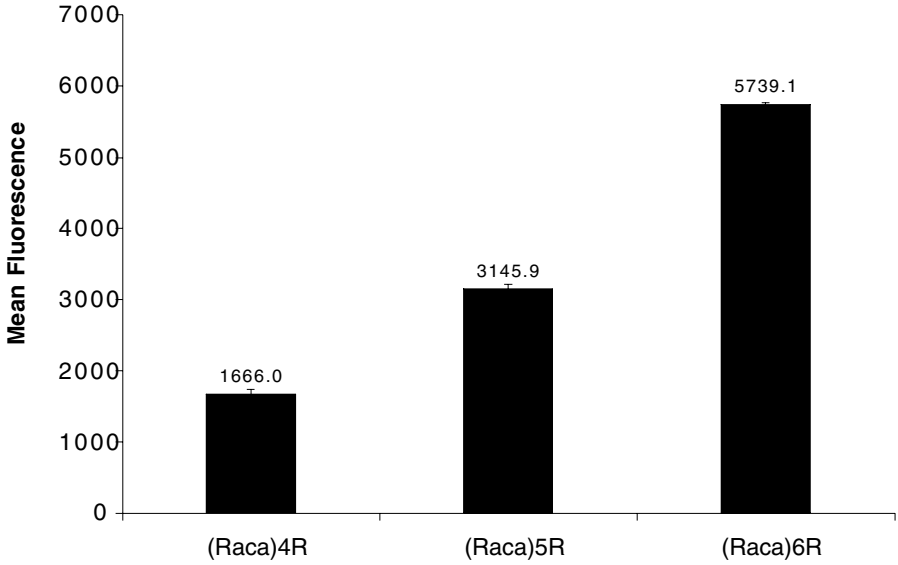

FIGURE 7.10 Peptides with greater arginine content exhibit faster rates of cellular uptake. Comparison of the cellular uptake of fluorescent peptides composed of either five, six, or seven arginines interspaced with 6-aminocaproic acid residues. Uptake was measured in triplicate at concentrations varying from 400 n*M* to 50 μ*M*, but only the differential uptake at 12.5 μ*M* is shown.

7.4 DISCUSSION

The fundamental goal of this research was to determine structural requirements for cellular uptake of guanidine-rich transporters and to use this information to develop simpler and more effective molecular transporters. Given the importance of the guanidino headgroup and the apparent insensitivity of the oligomer chirality revealed in our peptide studies, a novel series of polyguanidine peptoids was designed and synthesized. Incorporating the arginine side chain, the peptoids *N*-arg 5, 7, and 9 exhibited comparable cellular uptake to the corresponding *d*-arginine peptides r5, 7, and 9, indicating that the hydrogen bonding along the peptide backbone and backbone chirality are not essential for cellular uptake. This observation was consistent with molecular models of these peptoids, arginine oligomers, and $Tat_{49\text{-}57}$, all of which have a deeply embedded backbone and a guanidinium-dominated surface.

Molecular models further reveal that these structural characteristics are retained in varying degrees in oligomers with different alkyl spacers between the peptoid backbone and guanidino headgroups. Accordingly, a series of peptoids incorporating 2- (*N*-ethyl), 4- (*N*-butyl), and 6-atom (*N*-hexyl) spacers between the backbone and side chain were prepared and compared for cellular uptake with the *N*-arg peptoids (3-atom spacers) and *d*-arginine oligomers. The length of the side chains had a dramatic effect on cellular entry. The amount of cellular uptake was proportional to the length of the side chain, with *N*-hexyl > *N*-butyl > *N*-arg > *N*-ethyl. Cellular

uptake is improved progressively as the number of alkyl spacer units between the guanidine headgroup and the backbone is increased. Significantly, *N*-hexyl 9 was superior to r9, with the latter 100-fold better than Tat_{49-57}. This result led us to prepare peptoid derivatives containing longer octyl spacers (*N*-octyl) between the guanidino groups and the backbone. The limited solubility of this compound in aqueous buffers prevented evaluation of cellular uptake.

Because both perguanidinylated peptides and perguanidinylated peptoids efficiently enter cells, the guanidine headgroup (independent of backbone) is apparently a critical structural determinant of cellular uptake. However, the presence of several (over six) guanidine moieties on a molecular scaffold is not sufficient for active transport into cells, as the *N*-cyclohex peptoids did not efficiently translocate into cells. Thus, in addition to the guanidine headgroup, the conformational mobility of side chains plays a role in cellular uptake.

These studies identified a series of novel peptoids, of which 17 members were synthesized and assayed for cellular uptake. Significantly, the *N*-hexyl 9 transporter was found to be superior in cell uptake to r9 that was comparable to *N*-butyl 9. This research established that the peptide backbone and hydrogen bonding along that backbone are not required for cellular uptake and, most significantly, that an extension of the alkyl chain between the backbone and the headgroup provides superior transporters. In addition to better uptake performance, these novel peptoids offer several advantages over peptides, including lower cost of goods, ease of synthesis of analogs, and protease stability. Such features, along with their significant water solubility (>100 mg/ml), indicate that these novel peptoids could serve as effective transporters for molecular delivery of drugs, drug candidates, and other agents into cells.

The second goal of these studies was to determine whether all, or only a subset, of the headgroups in an oligomer were necessary for optimal activity, as modeling suggests that only a subset of side chains would contact most biological surfaces. The data shown in Figure 7.6 demonstrate that several decamers consisting of seven arginines interspersed at positions 2, 5, and 8 performed as well as the unsubstituted decamer of arginine. These data support the hypothesis that only a subset of the headgroups in the peptide transporter is necessary for uptake.

Significantly, with the exception of the analogs containing substitutions with aspartic and glutamic acid, all of the decamers containing seven arginines were more potent than heptaarginine homopolymers. These data indicate that, independent of the characteristics of the side chain, an increase in spacing between the arginine residues also leads to an increase in uptake. This second hypothesis is supported by the demonstration that, when non-α-amino acids were substituted into the second, fifth, and eighth positions, the rate of uptake increased as the number of methylenes in the non-α amino acids increased. However, this substitution pattern is only one of 63 different possible permutations of nonconsecutive spacer residues that can be placed into a heptamer of arginine. To determine the optimal spacing pattern for substituting up to six nonconsecutive 6-aminocaproic acid into a heptamer of arginine, substituted peptides were synthesized in parallel and then assayed for cellular uptake.

A simple pattern was observed. Greater cellular uptake was observed as the number of aca units in the analog increased. The exact location was unimportant, in that all analogs with a single aminocaproic acid are approximately equivalent and less effective than those with two spacing amino acids. Greater cellular uptake was seen as more aminocaproic acid residues were added until reaching the fully substituted analog containing six spacer amino acids alternating in the sequence with the seven arginines. As mentioned previously, these results are consistent with peptides containing greater aminocaproic acid content being more resistant to proteolysis and thereby increasing the effective concentration of the more highly substituted analogs.

Alternatively, the data supported the hypothesis that increasing the length between the arginines results in greater cellular uptake. Support for the latter hypothesis was generated by demonstrating a set of peptides containing seven *d*-arginines with either alternating glycine ($CH_2 = 1$), β-alanine ($CH_2 = 2$), 4-amino butyric acid ($CH_2 = 3$), 6-amino caproic acid ($CH_2 = 5$), or 8-aminocaprylic acid ($CH_2 = 7$) differentially entering cells. Uptake increased as the spacing between the arginines increased from $CH_2 = 1$ until $CH_2 = 5$, with the exception that the β-alanine-substituted peptide was slightly superior to the one containing 4-amino butyric acid. Uptake did not continually increase; the analog with 8-amino caprylic acid was less potent than the one containing aminocaproic acid.

The enhanced uptake when non α-amino acids were substituted into the peptide backbone was very similar to the effects seen when the side chains were extended in the peptoid series.[2] The fact that a similar pattern was seen when methylenes were substituted into the backbone or the side chain is noteworthy, not only due to the apparent symmetrical effect, but also because increasing flexibility into a ligand is counterintuitive for generating more potent ligands. These results, combined with earlier studies[1] demonstrating a lack of chiral recognition, emphasize that these compounds most likely are not interacting with a highly defined binding site characteristic of enzymes and protein receptors of most ligands. Typically, the biological activity of most biological ligands, particularly those functioning as inhibitors, increases with conformational restriction because preorganization in the form of the bound conformer favors tighter binding. In contrast, the enhanced activity associated with increased conformational mobility observed for molecular transporters is in agreement with a dynamic transport process in which turnover is critical for function.

The transporters are more likely forming ionic complexes with negatively charged entities on the surface of the biological membranes, most likely, the phosphates of phospholipids. The neutralization of the phosphate headgroups of lipids with polycations has been shown to have manifold effects due to neutralization of the charge, ranging from disruption of the order of the bilayer to release of associated membrane proteins into the media.[17]

The increased flexibility of the transporter might result in greater efficacy by allowing the molecule to adopt significantly different conformations necessary for the different steps in translocation. This possibility is consistent with a study demonstrating that a single, common secondary structure induced by model membrane systems was not observed for three transport peptides based on the antennapedia sequence.[18] Alternatively, the peptide might need to adopt single conformation for

biological activity, as is the case for amphipathic, antimicrobial peptides.[19,20] Increased flexibility in the backbone or the side chains could allow the guanidine headgroups to interact more effectively with negative charges on the cell surface. Using CPK models, increasing the number of methylenes between the arginines not only allows them to interact with negative charges further apart than homopolymers of arginine but, interestingly, also permits the guanidines to pack more closely and interact with putative negative charges that are closely spaced. Further experiments are needed to distinguish among these possible explanations.

REFERENCES

1. Mitchell, D.J. et al., Polyarginine enters cells more efficiently than other polycationic homopolymers, *J. Pept. Res.,* 56, 318, 2000.
2. Wender, P.A. et al., The design, synthesis, and evaluation of molecules that enable or enhance cellular uptake: peptoid molecular transporters, *Proc. Natl. Acad. Sci. U.S.A.,* 97, 13003, 2000.
3. Zuckermann, R. et al., Efficient method for the preparation of peptoids [oligo (N-substituted glycines)] by sub-nanomer solid phase synthesis, *JACS,* 114, 10646, 1992.
4. Pons, J. et al., A constrained diketopiperazine as a new scaffold for the synthesis of peptidomimetics, *Eur. J. Org. Chem.,* 1998, 853, 1998.
5. Murphy, J.E. et al., A combinatorial approach to the discovery of efficient cationic peptoid reagents for gene delivery, *Proc. Natl. Acad. Sci. U.S.A.,* 95, 1517, 1998.
6. Simon, R.J. et al., Peptoids: a modular approach to drug discovery, *Proc. Natl. Acad. Sci. U.S.A.,* 89, 9367, 1992.
7. Kale L. et al., NAMD2: greater scalability for parallel molecular dynamics, *J. Computational Physi.,* 151, 283, 1999.
8. MacKerell, B.D. et al., All atom empirical potential for molecular modeling and dynamics studies of proteins, *J. Phys. Chem.,* 102, 3586, 1998.
9. Humphrey, W., Dalke, A., and Schulten, K., VMD — visual molecular dynamics, *J. Mol. Graphics,* 14, 33, 1996.
10. Miller, S. et al., Proteolystic studies of homologous peptide and N-substituted glycine peptoid oligomers, *Bioorg. Phys. Lett.,* 4, 2657, 1994.
11. Tamilarasu, N., Huq, I., and Rana, T., High affinity and specific binding of HIV-1 TAR RNA by a Tat-derived oligourea, *JACS,* 121, 1597, 1999.
12. Hamy, F. et al., An inhibitor of the Tat/TAR RNA interaction that effectively suppresses HIV-1 replication, *Proc. Natl. Acad. Sci. U.S.A.,* 94, 3548, 1997.
13. Bernatowicz, M., 1H-pyrrole-1-carboxamidine hydrochloride: an attractive reagent for guanylation of amines and its application to peptide synthesis, *J. Org. Chem.* 57, 2497, 1992.
14. Kruijtzer, J. et al., Solid-phase syntheses of peptoids using Fmoc-protected N-substituted glycines: the synthesis of (retro) peptoids of Leu-enkephalin and substance P, *Chem. A Eur. J.,* 4, 1570, 1998.
15. Heizmann, G. and Felder, E.R., Synthesis of an N-3-guanidinopropylglycine (Narg) derivative as a versatile building block for solid-phase peptide and peptoid synthesis, *Pept. Res.,* 7, 328, 1994.
16. Feichtinger, K. et al., Triurethane-protected guanidines and triflyldiurethane-protected guanidines: new reagents for guanidinylation reactions, *J. Org. Chem.,* 63, 8432, 1998.

17. Bellet–Amalric, E. et al., Interaction of the third helix of *antennapedia* homeodomain and a phospholipid monolayer, studied by ellipsometry and PM-IR RAS at the air–water interface, *Biochim. Biophys. Acta,* 1467, 131, 2000.
18. Magzoub, M. et al., Interaction and structure induction of cell-penetrating peptides in the presence of phospholipid vesicles, *Biochim. Biophys. Acta,* 1512, 77, 2001.
19. Dathe, M. and Wieprecht, T., Structural features of helical antimicrobial peptides: their potential to modulate activity on model membranes and biological cells, *Biochim. Biophys. Acta,* 1462, 71, 1999.
20. Shai, Y., Mechanism of the binding, insertion and destabilization of phospholipid bilayer membranes by alpha-helical antimicrobial and cell non-selective membranelytic peptides, *Biochim. Biophys. Acta,* 1462, 55, 1999.

Section II

Mechanisms of Cell Penetration and Interactions of Cell-Penetrating Peptides with Plasma Membranes and Lipid Models

8 Interactions of Cell-Penetrating Peptides with Membranes

Laurent Chaloin, Nicole Van Mau, Gilles Divita, and Frédéric Heitz

CONTENTS

0-8493-1141-1/02/$0.00+$1.50

8.1 INTRODUCTION

Cellular uptake of therapeutic agents requires assistance of agents facilitating the crossing of the natural barrier, which is the plasma membrane. A large number of such agents have been developed in the recent past, mainly devoted to the transfer of nucleic acids and proteins. Among them, peptides appear to be very powerful tools for the transfer of DNAs; two main strategies are concerned: (1) covalent linkage between cargo and vector, thus forming a conjugate, and (2) formation of a complex between the two partners.

Within the peptides used in the first strategy, the first efficient vector developed is polylysine, which can act as vector for oligonucleotides.[1-5] Later, more sophisticated molecules such as the L-oligomers were proposed as vectors of cytotoxic agents with the aim to develop an anticancer strategy.[6,7] Simultaneously, fusion peptides[8] and peptides based on the KDEL sequence[9,10] were proposed as efficient vectors in the antisense strategy.

Although still based on peptide sequences, vectors issued from the homeodomain of Antennapedia were shown to translocate toward the nuclei of nervous cells in culture.[11-15] This α-helical peptide appears to be a very powerful agent, facilitating membrane crossing for both peptides[16,17] and oligonucleotides.[18] These properties led to a wider search for other translocating peptide sequences; among them, the so-called Tat-derived peptides from HIV1 were found.[19-21] Also, other peptides derived from natural sequences have been proposed. These are a peptide-based on neuropeptide Y,[22] shown to be an efficient vector for daunorubicin and doxorubicin although it requires the presence of a receptor, and a peptide issued from human calcitonin that acts through excised bovine nasal mucosa.[23]

As to the second strategy that involves the formation of complexes, besides the well documented approaches based on viruses,[24-27] liposomes,[28] cationic lipids,[29] or PEI,[30] peptidic vectors have also been investigated. All of them share the common presence of cationic residues, but differ mainly from each other by distribution of the basic residues along the peptide chain and thus by their ability to form an amphipathic structure.[31-42] According to the conformation involved in the formation of the amphipathic structure, these vectors are able to translocate charged molecules such as DNA or hydrophobic drugs.

All these peptides are short (below 40 residues) and constitute a series of vectors which validate the peptide approach. However, none of the peptidic vectors reported so far can be considered perfect. In order to attempt and define a new generation of nontoxic vector peptides with specific targeting, a prerequisite is to identify the mechanism leading to the cellular internalization process of vectors in the free form and when associated with the cargo. Two main processes with different mechanisms leading to cellular internalization must be examined: through the endosome pathway or by direct penetration into the cytoplasm.

In both cases, an obligatory step in such an approach is devoted to structural investigations for identification of structural requirements and their optimization for design of efficient vectors. The cellular internalization mechanism can be summarized as a three-step process; (1) uptake by the cellular membrane, (2) translocation through the membrane, and (3) release on the cytoplasmic side into the cell interior.

Most data available up to now are related to the two first steps, while those related to the third are more perspective-relevant.

8.2 STRUCTURAL DETERMINATIONS

Although much progress has been made recently in identification of peptide conformations in the presence of membranes or membrane mimicking media, determination of peptide structures in membranes remains a difficult task. This obligatory step for understanding the membrane crossing process requires conformational studies together with analysis of peptide–phospholipid interactions and their structural consequences.

We present here the most useful methods to be used for these two types of investigations and also point out their limits and the pertinence of their information. Two families of peptides will be used to illustrate the various information that can be obtained by the different techniques used in such situations. The first peptide family is composed of primary amphipathic peptides based on the association of a cationic nuclear localization sequence (NLS)[43] with either a signal peptide (SP)[44] or a sequence issued from a fusion peptide (FP).[45]

TABLE 8.1
Sequences of the Peptides of the SP–NLS Series

M-G-L-G-L-H-L-L-V-L-A-A-A-L-Q-G-A-W-S-Q-P-K-K-K-R-K-V	[1]
M-G-L-G-L-H-L-L-V-L-A-A-A-L-Q-G-A---------K-K-K-R-K-V	[2]

TABLE 8.2
Sequences of the Peptides of the FP–NLS Series and Related Peptides

G-A-L-F-L-G-W-L-G-A-A-G-S-T-M-G-A-W-S-Q-P-K-K-K-R-K-V	[3]
G-A-L-F-L-G-W-L-G-A-A-G-S-T-M-G-A----R----K-K-K-R-K-V	[4]
G-A-L-F-L-G-F-L-G-A-A-G-S-T-M-G-A-W-S-Q-P-K-S-K-R-K-V	[5]
G-A-L-F-L-A-F-L-A-A-A-L-S-L-M-G-L-W-S-Q-P-K-K-K-R-K-V	[6]

Both these series are composed of primary amphipathic peptides for which no folding is required for presenting the amphipathic character.

TABLE 8.3
Examples of Peptides Belonging to the Family of Secondary Amphipathic Peptides

K-L-A-L-K-L-A-L-K-A-L-K-A-A-L-K-L-A	from [31]
L-A-R-L-L-A-R-L-L-A-R-L-L-R-A-L-L-R-A-L-L-R-A-L	from [34]

For these two peptides folding into an α-helical form is required for presenting the amphipathic character.

8.2.1 Analytical Methods: Conformational Identifications

8.2.1.1 NMR

Besides crystal structure resolution, NMR is the most precise method for detailed identification of proteins and peptides structures. However, some limitations lie in the molecular weight of the particle under examination. While the structure of a protein of ~150 residues can be easily solved, an increase of its molecular weight by oligomerization or by incorporation into a lipidic medium (vesicles, for example) precludes obtaining resolved spectra. For peptides interacting with membranes, most investigations were carried out in the presence of micelles considered membrane-mimicking media and giving rise to resolved spectra. However, the question of membrane-relevance of the data obtained in such a medium must be raised. Indeed, nearly all studies show that peptides engaged in a micelle structure adopt a helical conformation. For example, this holds true for transportan[46] and for the primary amphipathic vectors based on the SP or FP sequences associated with the NLS motif.[47,48]

In the presence of phospholipids the situation differs strongly from that described earlier. While the SP-NLS peptides can adopt either an α-helical or a β-type structure, depending on the peptide/lipid ratio, no helical form could be detected for the FP–NLS peptide that remains in a β-sheet form, except[6] in Table 8.2, especially designed to adopt an α-helical conformation.

This remark does not imply that, when a helical form is found in SDS, the same form does not exist when the peptide is in the presence of phospholipids. Thus, the extrapolation of the findings in SDS to phospholipids must be taken very cautiously, especially when the peptides are nonordered in solution in water. On the contrary, when peptides show a tendency, even low, to adopt a helical conformation, measurements in SDS micelles are appropriate for structural identification.[49] This problem of conformational identification is overcome by using solid-state NMR, which has a great deal of potential for studies of membrane-embedded peptides.[50,51]

There are two fundamentally different types of structural constraints that can be obtained from solid-state NMR experiments. Distance constraints can be obtained from rotational resonance experiments. Unlike nuclear Overhauser effect constraints in solution NMR, distance constraints obtained in solid-state NMR are typically far more quantitative; the distances observed can be 1 nm or even greater, depending on the gyromagnetic ratios of the interacting nuclei. Such experiments do not require one-, two-, or three-dimensional order because the samples are spun in a magic angle spinner.

A second approach for structural constraints is to obtain orientational constraints by solid-state NMR. For this approach, samples need to be aligned with respect to the magnetic field direction, B_0, of the NMR spectrometer. Then the orientation-dependent magnitude of numerous nuclear spin interactions such as the anisotropic chemical shift and dipolar and quadrupolar interactions can be observed. Therefore, the quality of oriented samples should be high. Thus, the choice of lipid is also important from the standpoint of having a match between the lengths of the hydrophobic regions of the peptide or protein and lipid bilayer. Any peptide not in a lipid

environment with a bilayer normal aligned parallel with B_0 will result in less well-aligned peptide and protein preparations.

The choice of the orienting surface is dictated by a desire for relatively rigid surfaces that can be arranged and maintained in a sample container with the surface normally parallel to the magnetic field direction. Thin glass plates are appropriate for such preparations.

8.2.1.2 Circular Dichroism (CD)

CD is frequently used to identify the secondary structures of proteins or peptides; however, it has some drastic constraints with regard to the sample. For peptides or proteins in solution it is strongly recommended to record spectra in the far UV region, down to 180 nm, to obtain dependable information related to the conformation. Such a low wavelength precludes the use of most common buffers (hepes, acetate, etc.) and of salts based on chloride or bromide, for example. A membrane-mimicking situation requires the presence of phospholipids which will be organized forming vesicles. Except for a few synthetic phospholipids such as DOPG, which leads to transparent vesicles, most phospholipids form vesicles leading to milky solutions or suspensions with high scattering power. One issue to overcome these difficulties lies in the use of lysophospholipids or detergents such as SDS that form nonscattering micelles. However, a cautious interpretation of the data is required since a micelle has geometrical constrains that do not exist for membranes.[47]

However, CD can allow us to determine the orientation of helical sections of peptides or proteins in membrane. To do this, membranes are prepared in a multilayer array and CD spectra are measured at normal and oblique incident angles with respect to the planes of the layers. Taking into account the artifacts due to dielectric interfaces, linear dichroism, and birefringence, this method allows the detection of orientation modifications when the hydration state is varied.[52]

8.2.1.3 Fourier Transform InfraRed Spectroscopy (FTIR)

This spectroscopic approach appears to be one of the most powerful methods for the identification of peptide and protein secondary structures and thus for determination of conformational changes upon variations of the environment.[53-60] Under appropriate conditions this method also allows the determination of orientation of the peptide or protein with respect to an interface. In addition, infrared spectroscopy also provides information on all membrane components. Most data reported so far were obtained from solution and thus cannot account for the relative orientation of the bound peptide vs. the phospholipids.

To this end, several models have been constructed. Using polarized attenuated total reflection infrared spectroscopy, determination of the helical order parameter of a short α-helical peptide (melittin in that case) was revealed. It was also determined that the orientation of the helix depends on the hydration of the membrane preparation. Therefore, measurements of a fully hydrated state appear more appropriate, although they are carried out on monolayers. The first approach was carried out *in situ* using infrared refection (IRRAS) on phospholipid monolayers on a

Langmuir trough. A considerable improvement was provided by polarization modulation of the incident light (PMIRRAS), which has proved to be an efficient way to greatly increase surface absorption detectivity while getting rid of the intense isotropic absorption occurring in the sample environment.[61,62]

8.2.1.4 Diffraction

Since protein structure determination by classical x-ray crystallography is difficult to obtain for membrane protein, the alternative is to grow two-dimensional crystals by adsorbing proteins to ligand–lipid monolayers at the air–water interface. Using grazing incidence synchrotron x-ray diffraction and a setup of high angular resolution, narrow Bragg reflections are observed corresponding to a resolution of 10 A in plane and 14 A normal to the plane in the case of streptavidin. This approach is complementary to electron diffraction but avoids the process of transfer onto a grid and has the advantage of allowing *in situ* investigations.[63]

8.2.2 Interactions with Phospholipids and Their Consequences

8.2.2.1 The Monolayer Approach

Monolayers at the air–water interface are appropriate tools for investigating phospholipid–peptide interactions. Indeed, analysis of the adsorption or compression isotherms provides information on miscibility of the components forming the monolayer, together with information on interactions between these components. Analysis also provides crucial information concerning the state of the monolayer (below or above the collapse pressure or squeezing out of one monolayer component), when applying other methods that allow *in situ* observations such as infrared or grazing-incidence x-ray diffraction (see above). The management of this monolayer approach first requires a study in the absence of lipid; the influence of the presence of lipid is investigated in a second step.

8.2.2.2 Lipid-Free Air–Water Interface

Amphipathic peptides are surface-active molecules that, when in solution in water, adsorb spontaneously at the solution surface, thus lowering the surface tension γ. This parameter is measured by the Wilhelmy method and its variation as a function of the peptide concentration in the subphase provides the adsorption isotherm. Another method for studying proteins at the air–water interface consists in deposition as a drop of an aqueous solution of the peptide or as a drop of a solution in a volatile solvent on the water surface. The peptide molecules are organized at the surface in a monomolecular film that can be compressed using an hydrophobic barrier in order to increase the surface density. However, it is sometimes difficult to correlate the adsorption and compression isotherms because of conformational changes of the peptide during their adsorption process.

In order to identify conformational changes, transfer experiments can be carried out. These Langmuir–Blodgett transfers[64] are made at constant surface pressure onto solid supports such as germanium or CaF_2 for IR analyses.[65,66]

8.2.2.3 Lipid-Containing Air–Water Interface

Biological membranes are composed of lipid bilayers that constitute the major barrier for cell-penetrating peptides. These peptides are involved in exchange processes and lipid–peptide interactions may modify the lipid packing and thus the membrane properties.[67-72]

Monomolecular films are good investigative models since the thermodynamic relationship between monolayers and bilayer membranes is direct, and monomolecular films at the air–water interface overcome limitations such as regulation of lipid lateral-packing and lipid composition that occur in bilayers.[73] Measurements of peptide–lipid interactions can be achieved by forming a lipid monomolecular film at a given surface pressure close to the maximum obtained for the peptide at the air–water interface,[74] and by injecting aliquots of the peptide solution into the subphase.[74-77]

Mixed lipid–protein films can also be obtained by spreading on the water surface a mixture of the peptide and lipid dissolved in a volatile solvent[78-80] or by deposition of vesicles containing the desired mixture.[81] The conformational analysis of peptides interacting with lipids in an interfacial situation can be made by FTIR on Langmuir–Blodgett films transferred onto a germanium plate[82,83] or by CD when the transfer is made onto quartz plates.[84,85] Another advantage of monolayer lies in the fact that the lateral pressure can be varied and thus allows study of the influence of this pressure on the conformational state of the peptide.[86] However, such analyses have to be made with care since the transfer process can induce structural modifications. Thus, *in situ* methods have been developed accordingly.[87,88]

8.2.2.4 Bilayers

Contrary to monolayers, bilayer properties are more restricted but better models for plasmic membranes; therefore, most investigations have been carried out with liposomes. After uptake of the peptide by the liposomes, conformational analysis can be carried out by CD, x-ray or infrared spectroscopy.[89-93] For helix-rich peptides, insertion into the bilayers induces pore formation,[94] while other peptides interact only with receptors that are membrane-embedded. These receptor–peptide interactions can induce conformational changes and in some cases, can promote fusion processes.[95] Peptide-embedded analysis can also be carried out on bilayers obtained by the transfer protocol by Langmuir–Blodgett or Langmuir–Schaeffer methods.[96]

8.2.2.5 Fluorescence

Most proteins contain intrinsic fluorophores, which are the aromatic amino acids tryptophan (Trp), tyrosine (Tyr), and phenylalanine (Phe). Protein fluorescence is generally obtained by excitation at the absorption maximum near 280 nm or higher wavelengths. Under these conditions, Phe is not excited and hence cannot be considered an appropriate probe for fluorescence investigations on proteins. In fact, the most useful residue is Trp, since it can be selectively excited from 295 up to 305 nm and is sensitive to both specific and general environment effects. Briefly, two phenomena are currently used to describe the environment of a Trp residue: the wavelength of the

maximum emission and the quantum yield.[97] Others, such as polarization and lifetime measurements, are slightly more sophisticated and require specialized accessory equipment.[98]

The position of the emission spectrum's maximum provides information on the Trp environment. A low wavelength maximum (around 330 nm) is indicative of a Trp in a nonpolar environment, i.e., in contact with the phospholipid hydrocarbon chains; a high wavelength maximum (around 355 nm) reflects a polar environment close to the phospholipid headgroups.

Other types of measurements based on fluorescence properties, such as fluorescence transfer and quenching experiments, can be carried out. The latter deal with accessibility of quenchers such as I^-, Cs^+, trichloroethanol, or acrylamide to the probe,[99] while the former can be carried out using fluorescently labeled lipids.

8.2.2.6 Electron Paramagnetic Resonance (EPR) Spectroscopy

Similarly, to fluorescence, EPR spectroscopy also provides information about the interaction between peptides and membranes. This spectroscopic method is seldom used since it requires introducing the presence of side chain reactive residues such as cysteine in order to introduce an extrinsic spin label. The analysis of EPR spectra (width of the central line and peak-to-peak heights) provides the rotational correlation time, which is related to mobility of the particle (the vesicle containing the peptide) and that of the membrane-embedded peptide. For example, using this method, it was shown that spin-labeled Cys-pAntp binds DMPG or DOPG vesicles and not the neutral DMPC vesicles.[49]

8.2.2.7 Atomic Force Microscopy (AFM)

AFM allows observation of nanometer-sized particles and provides information on topographical organization of transferred monolayers[100-104] or bilayers.[105-108] AFM observation of monolayers requires transfer to a solid substrate and provides details on the domains existing in phase-separated thin films together with the localization of the protein. Generally, the observations deal with the hydrophobic side of the monolayer. Bilayers, which are more biologically relevant, are obtained by double transfer or by fusion of small unilamellar vesicles to a glass or mica surface; observations are made on the hydrophilic face of the bilayer. They allow identification of membrane domain and their constituents.

A final remark about the various methods reported here concerns their joined use. Indeed, it is highly recommended to describe the behavior of a lipid-interacting peptide using several approaches; otherwise, some dramatic misinterpretations can be made. This will be illustrated in an example in the next section.

8.2.2.8 An Example of Multidisciplinary Approach Based on Monolayers

A peptide based on the association of a signal peptide with a sequence issued from a positively charged nuclear localization motif (SP–NLS) (Table 8.1) was shown to act as a very efficient oligonucleotide carrier with a very rapid internalization process. In order to deepen understanding of the membrane-crossing process, a detailed study

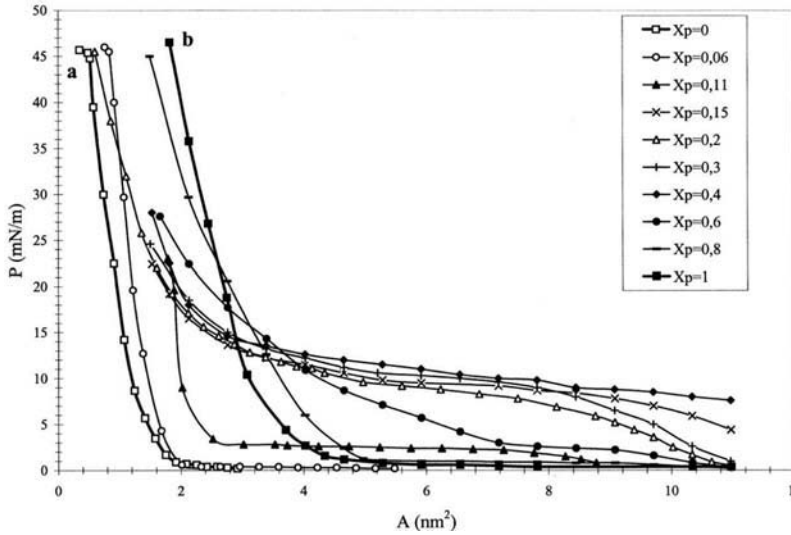

FIGURE 8.1 Variations of the surface pressure with the mean molecular area of mixed DOPC-[1] monolayers at various peptide molar fractions (x_P). (Adapted from Van Mau, N. et al., *J. Membr. Biol.,* 167, 241, 1999. With permission.)

of the membrane uptake of this peptide was undertaken using mainly monolayers AFM and FTIR.[57,58]

8.2.2.8.1 Monolayer Study

Because of its solubility properties, the peptide could be dissolved in the same volatile organic solvent mixture as the phospholipids (DOPC, DOPG, DPPC, and DPPG) and, hence, the peptide–lipid mixtures could be spread at the air–water interface. The various compression isotherms at various peptide molar fractions were recorded and are shown in Figures 8.1 and 8.2.

Analysis of the isotherm was made by plotting the variation of the mean molecular area as a function of the molar fraction at a given surface pressure. In all cases the variations of the mean molecular area showed positive deviations from additivity (Figure 8.3 and insets of Figure 8.2).[109,110] Such behavior can be considered indicative of strong peptide–lipid interactions with expansion of the mean molecular area. However, the deviation from linearity is larger in DOPC and DOPG than in DPPC and DPPG, suggesting that the nature of the peptide–lipid interactions could strongly depend on the nature of the fatty acid. Further investigations, based now on FTIR, showed clearly that the peptide underwent a conformational transition, going from an α-helical form at low peptide molar fraction to a β-type structure at higher molar fractions. This conformational transition was detected by examination of the position of the Amide I band, the major component of which moves from 1655 cm^{-1} (wavenumber characteristic of an α-helix) to 1625 cm^{-1} (wavenumber characteristic of a sheet structure)[111,112] upon increasing the peptide molar fraction (Figure 8.4). This holds true, at least, when the peptide interacts with DOPG, but probably also for DOPC. However, a transition occurs at very low peptide molar fractions, probably

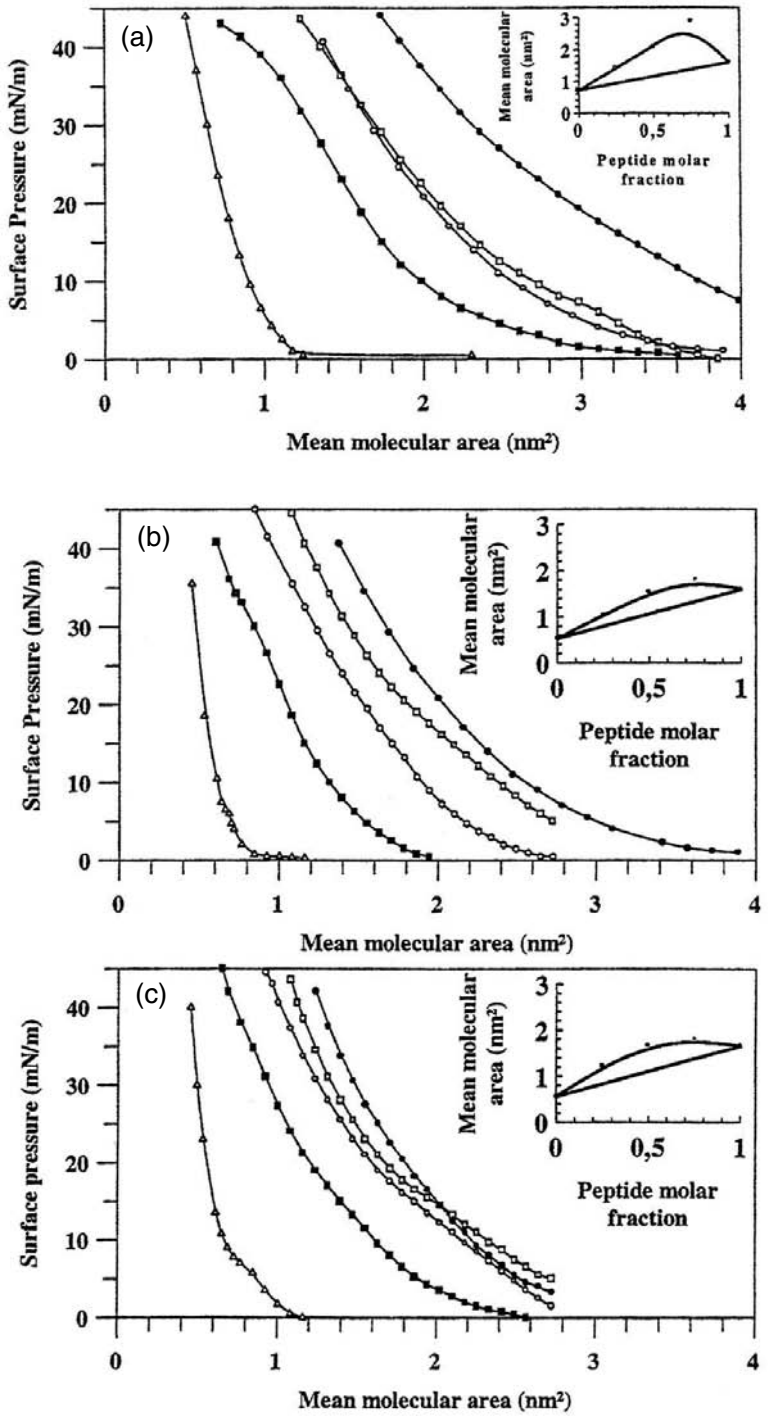
(a)
Surface Pressure (mN/m)
Mean molecular area (nm²)
Mean molecular area (nm²)
Peptide molar fraction
(b)
Surface Pressure (mN/m)
Mean molecular area (nm²)
Mean molecular area (nm²)
Peptide molar fraction
(c)
Surface pressure (mN/m)
Mean molecular area (nm²)
Mean molecular area (nm²)
Peptide molar fraction

FIGURE 8.2

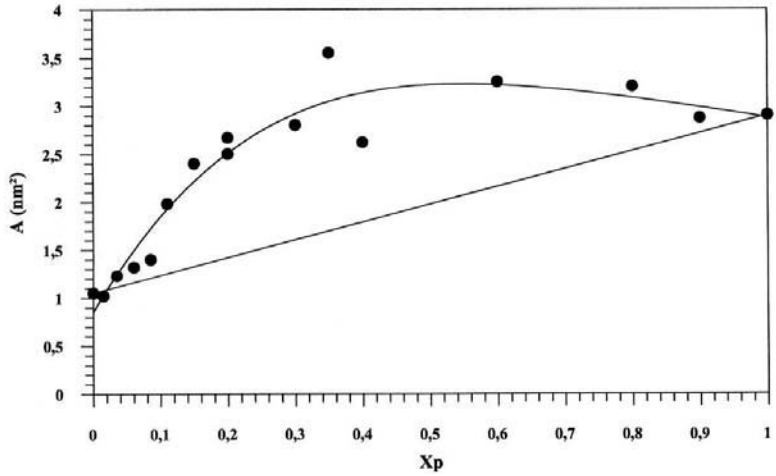

FIGURE 8.3 Variation at 15 mN/m of the mean molecular area of mixed DOPC-[1] monolayers as a function of the peptide molar fraction (x_P). The curve was calculated using a fourth order polynomial regression. (Adapted from Van Mau, N. et al., *J. Membr. Biol.,* 167, 241, 1999. With permission.)

because the two lipids are differently charged (one is negatively charged while the other is zwitterionic). For the two other lipids, no such structural changes could be detected, which is in agreement with the smaller deviation from linearity.

Turning back to the isotherms of peptide–DOPC mixtures, in a domain of peptide molar fractions $0.11 < x_p < 0.35$, a plateau of surface pressure is found at large molecular areas. These isotherms are characterized by constant surface pressures notably higher than those of the pure components in the same area domain. The high value of surface pressure suggests that strong hydrophobic interactions occur between the peptide and the lipid.[109,113] Such a behavior can be analyzed on the basis of the representation shown in Figure 8.5, which shows the variations of the surface pressure with the peptide molar fraction at a given mean molecular area. This figure reveals the existence of a transition pressure that remains almost constant in the molar fraction range $0.08 < x_p < 0.4$.

Applying the two-dimensional phase rule, the freedom degree F is given by the relationship $F = C - P_B - (q - 1)$, where C is the total number of components in the surface (lipid and peptide) and in the bulk, P_B is the number of bulky phases (the air and the water subphase), and q the number of surface phases. For the present conditions, F = 3 –q and, thus for x_p, below and above 0.08, $F = 1$; $q = 2$ and $F = 0$;

FIGURE 8.2 (opposite) Variations of the surface pressure with the mean molecular areas of mixed lipid-[1] monolayers at various peptide molar fractions (x_P). For A, B, and C the lipid is DOPG, DPPG, and DPPC, respectively. For clarity reasons, only a selected set of isotherms was shown. The insets show the variations, at 20 mN/m, of the mean molecular areas as a function of the peptide molar fractions. (Adapted from Vié, V. et al., *Biophys. J.,* 78, 846, 2000. With permission.)

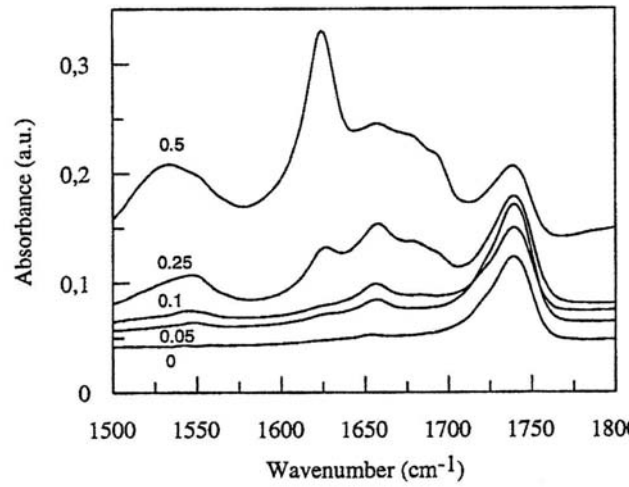

(a)

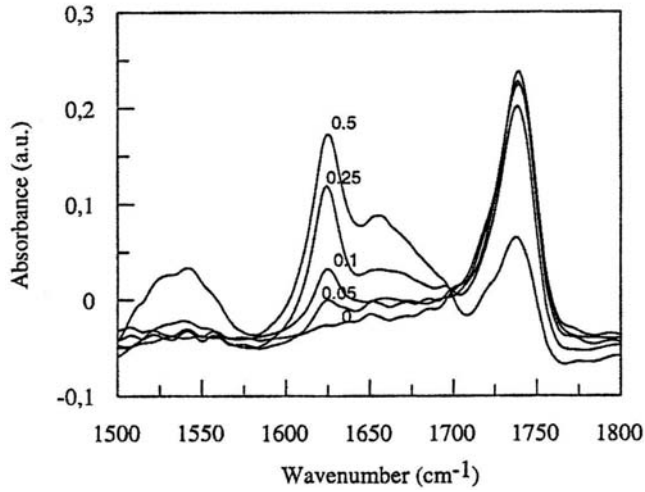

(b)

FIGURE 8.4 Variations of the FTIR spectra in the amide I and II bands region of mixed lipid-[1] multilayers as a function of the peptide molar fractions. The lipids are DOPG (A) and DPPG (B). The band centered around 1740 cm^{-1} corresponds to the lipidic carbonyls. (Adapted from Vié, V. et al., *Biophys. J.,* 78, 846, 2000. With permission.)

$q = 3$, respectively. This is a good indication that a phase separation occurs for $x_p = 0.08$. This behavior, together with the fact that an excess of peptide or of lipid generates low surface pressures, suggests that lipid–lipid and peptide–peptide interactions are lower than lipid–peptide interactions.

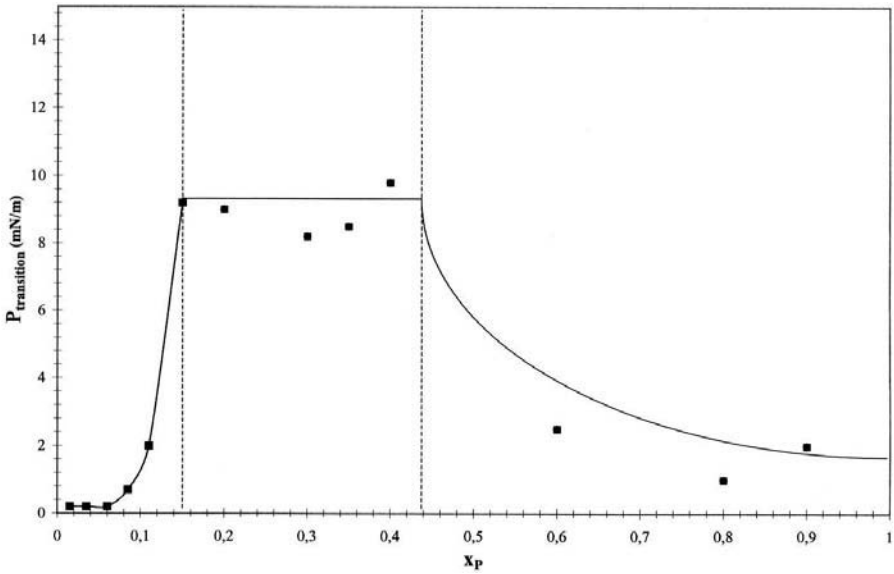

FIGURE 8.5 Variation of the transition surface pressure as a function of the lipid molar fraction (x_P). The data are provided from Figure 8.1. The dashed vertical bar shows the limits of the phase transitions. (Adapted from Van Mau, N. et al., *J. Membr. Biol.,* 167, 241, 1999. With permission.)

The phase separation deduced by analysis of the compression isotherms was confirmed by direct observations using AFM imaging on transferred monolayers. Figure 8.6 reveals strong changes on lipid-embedded particles when the peptide molar ratio is varied. The clear domains (Figure 8.6C) confirm the existence of peptide-induced phase separation; evolution of the shape of the particle is in accordance with a conformational change of the peptide with formation of mixed particles compatible with the FTIR observations.

8.2.2.8.2 Influence of the Sequence

Cell positioning: membrane associated or nuclear — Within the SP–NLS peptides (Table 8.1) and FP–NLS (Table 8.2), several variants have been synthesized. While single K to S mutations in the NLS sequences do not modify the final nuclear localization, removal of the W-S-Q-P linker can strongly modify the final cellular localization. For the SP–NLS peptides, the presence of this linker has no influence on final localization,[47] however, its absence in the FP-NLS series leads to a peptide that has a membrane-associated localization.[48] The origin of these different behaviors according to the nature of the hydrophobic sequence is still not clear and no rational explanation has been provided up till now, although some preliminary data suggest that the peptide–peptide interactions involving the N-terminal hydrophobic domain could play an important role.

Comparison between FP- and SP-NLS: a possible role of the conformation — A comparative study of peptides of the two series made on model membrane systems also provided some unexpected information. Using vesicles made of pure phospholipids

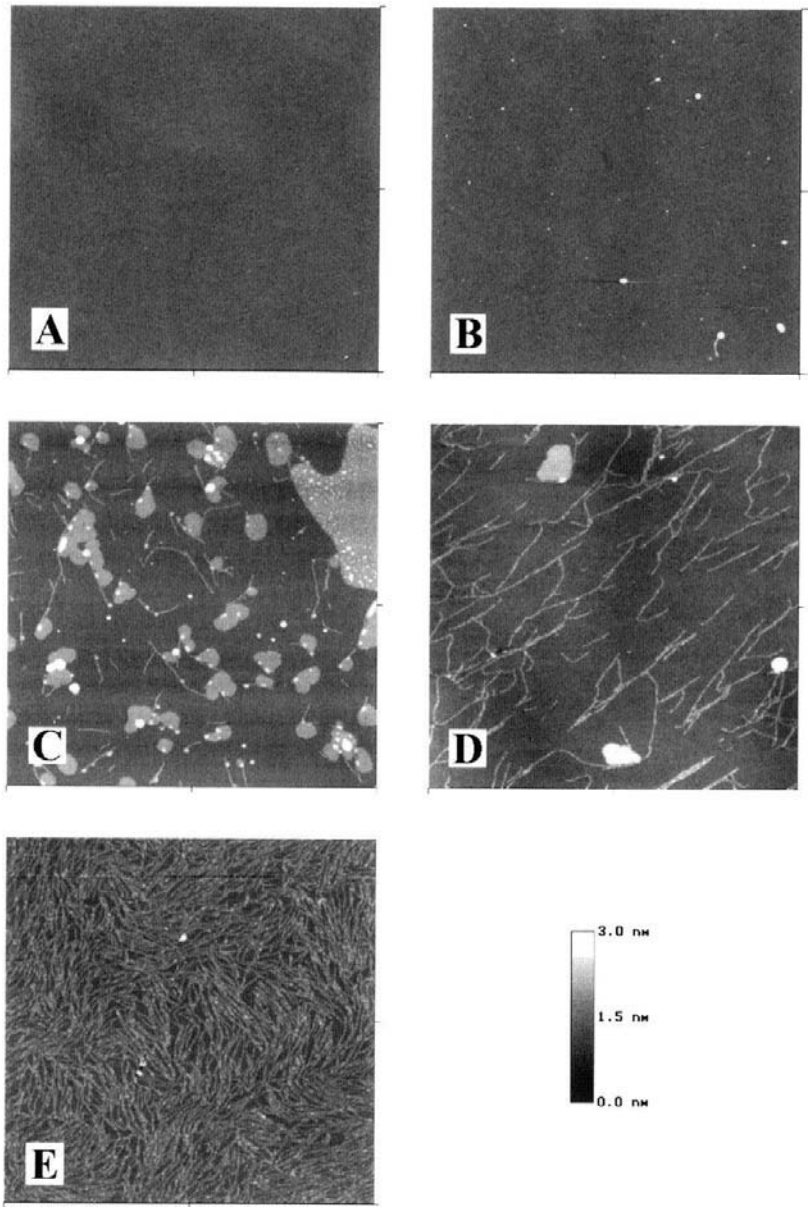

FIGURE 8.6 2×2 μm AFM scans of transferred peptide[1]-containing DOPC monolayers. $x_P = 0$, 0.01, 0.05, 0.1, and 0.25 for A, B, C, D, and E, respectively. (Adapted from Van Mau, N. et al., *J. Membr. Biol.,* 167, 241, 1999. With permission.)

(DOPC or DOPG), fluorescence measurements based on the Trp residues revealed that the SP–NLS peptide penetrates indifferently into neutral and negatively charged lipidic media,[47] while the FP–NLS peptide penetrates only in the negatively charged lipids. The same conclusion was obtained on the basis of monolayer experiments

that showed that the monolayer uptake of these two peptides was governed by the hydrophobic domains.[48] This observation raised the following question: since both peptides bear the same hydrophilic sequence, how can the lipid headgroup-dependent uptake be governed by the hydrophobic domain?

Some recent preliminary data suggest that the conformational state of this latter domain could be a determinant factor governing the membrane penetration of the shuttle peptides. Indeed, starting from the FP–NLS sequence, which is nonordered in water, several minor changes in the hydrophobic sequence lead to an α-helical peptide (peptide[6] of Table 8.2) that can penetrate indifferently into neutral and negatively charged model membranes.

8.3 CELLULAR INTERNALIZATION OF ANTENNAPEDIA

This well-known shuttle peptide based on the third helix of Antennapedia, (R-Q-I-K-I-W-F-Q-N-R-R-M-K-W-K-K) can also reach the cytoplasm and is eventually conveyed to the nucleus of cells in culture through a pathway that does not involve classical receptor-mediated endocytosis. Several observations, such as that the peptide is not able to induce channel formation, together with the consequences of replacing the two tryptophan residues by phenylalanines that did not modify the helical structure but abolished translocation, led to proposal of a model implying inverted micelles (Figure 8.7). The main reasons for favoring this model are the limited size of the polypeptidic cargo and its conformation, the requirement of Trp residues, multimer formation, and formation of hexagonal phases or inverted micelles.[14,114]

8.4 INTERNALIZATION VIA A VESICULAR PROCESS

Vesicular internalization is suggested to be associated with self-assembly induced perturbation of the lipid bilayer. This can be illustrated by study of the mechanisms involved in translocation of human calcitonin (hCT) through excised bovine nasal mucosa.[23] Using two carboxyfluorescein-labeled hCT fragments, it was shown that, in presence of the endocytosis inhibitor cytochalasin D, mucosal-to-serosal and serosal-to-mucosal hCT permeabilities were equal. Pathway visualization by confocal laser scanning microscopy showed punctated fluorescence indicating vesicular internalization. In contrast, the N-terminal fragment lacking the beta-sheet forming C terminus was not internalized. Circular dichroism showed that, when interacting with neutral and negatively charged liposomes, hCT adopts beta-sheet conformation. In a concentrated aqueous solution, beta-sheet formation induces hCT self-assembly and fibrillation. It was proposed that the high lipid partitioning and beta-sheet formation result in C terminus-restricted supramolecular self-assembly in lipid membranes. Condensed hCT self-assemblies may explain the high capacity of net mucosal-to-serosal hCT permeation, which compares favorably with the low transport capacity of receptor-mediated endocytosis.

8.5 INTERNALIZATION VIA RECEPTOR

One of the major problems in cancer chemotherapy is severe side effects that limit the dose of anticancer drugs because of their unselectivity for tumor vs. normal

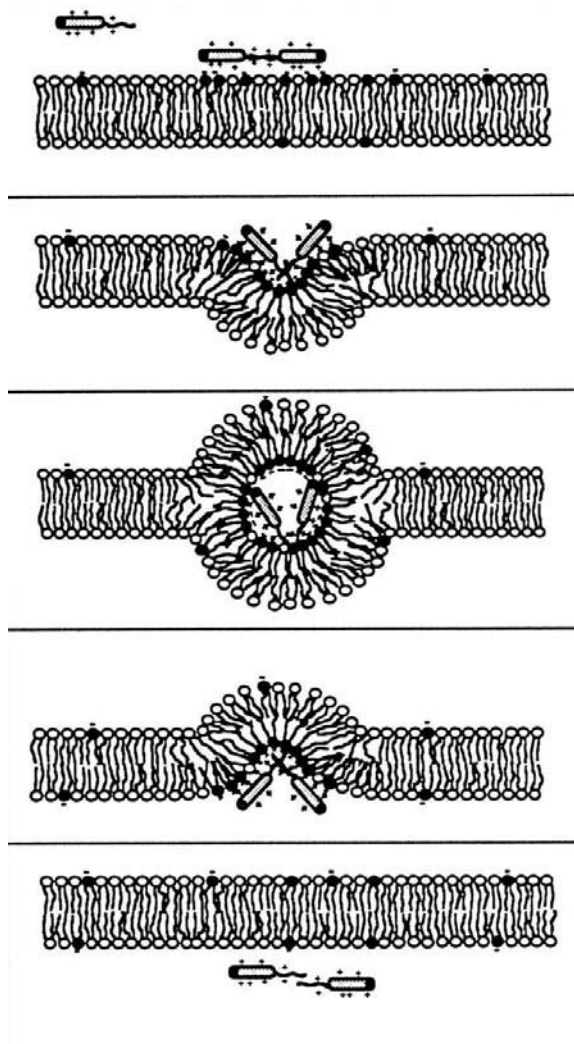

FIGURE 8.7 Model of internalization. In this model the peptide, arbitrarily represented as a dimer, recruits negatively charged phospholipids (filled circles) and induces the formation of an inverted micelle. The hydrophilic cavity of the micelle accommodates the peptide and, possibly, sequences attached to it can subsequently be released in the cytoplasmic compartment. (Adapted from Derossi, D. et al., *J. Biol. Chem.,* 271, 18188, 1996. With permission.)

cells. To this end, peptide–drug conjugates were designed to bind to specific receptors expressed on the tumor cells with subsequent internalization of the ligand–receptor complex.[22] Neuropeptide Y (NPY), a 36-amino acid peptide of the pancreatic polypeptide family, was chosen as model peptide because NPY receptors are overexpressed in a number of neuroblastoma tumors and their derived cell lines. Daunorubicin and doxorubicin, two widely used antineoplastic agents in tumor therapy, were covalently linked to NPY via two spacers that differ in stability.

Receptor binding of these conjugates was determined at the human neuroblastoma cell line SK-N-MC, which selectively expresses the NPY Y-1 receptor subtype; cytotoxic activity was evaluated using c cellular cytotoxicity assay. The different conjugates were able to bind to the receptor with affinities ranging from 25 to 51 n*M*, but only the compound containing the acid-sensitive bond showed cytotoxic activity comparable to the free daunorubicin and this cytotoxicity was Y-1 receptor-mediated. The intracellular distribution showed that the active conjugate releases daunorubicin, which is localized close to the nucleus, whereas the inactive conjugate is distributed distantly from the nucleus and does not seem to release the drug within the cell.

8.6 UNFOLDING FOR CONJUGATE CPP–PROTEIN

Some transduction domains of proteins such as Tat, Antennapedia, or VP22 appear to have the highest level of demonstrated protein-transduction efficiency. However, in some cases the transduction of full-length fusion proteins across the cell membrane results in an inactivation or denaturation of the protein. This suggested that transduction across the cellular membrane is a stringent process that partially or completely unfolds a protein.[20,21]

In fact, this is a common aspect for proteins that must penetrate into a membrane medium. Such a situation can be illustrated by the two following examples in which membrane-induced conformational changes were detected. The first concerns colicin A, which adopts the molten globule form to insert the membrane; the membrane-associated form differs from the hydrosoluble one only by the three-dimensional organization and not by the secondary structure.[115,116] In the second example, the toxin cry1Aa of *Bacillus thuringiensis,* the membrane uptake induces drastic conformational changes involving a loss of sheet structures.[96] Are these conformational changes reversible when the proteins are released into the aqueous medium? Almost nothing is known about this point, but it is likely that recovery of the native hydrosoluble form will be sequence- and medium-dependent.

8.7 ORIGIN OF THE TOXICITY

Some cell-penetrating peptides show strong toxic properties and, in order to understand the mechanism underlying these properties, several tests can be carried out. One consists in measurement of bacteriocidal activity for living organisms such as bacteria. Among them, mollicutes can be chosen because they represent the simplest, most cultivable, and most self-replicating organisms described thus far. Their cell envelope is composed only of the plasma membrane, which should facilitate analysis of the interactions between peptides and the bacterial cell surface.

The two series of peptides tested in a comparative manner revealed that the SP–NLS peptides (Table 8.1) were more active than those of the FP–NLS (Table 8.2) series. This was analyzed based on their effect on spiroplasma motility, cell morphology, membrane potential, and transmembrane ΔpH.[117]

All these experiments suggested that formation of transmembrane ion channel could be induced by carrier peptides, especially by those of the SP–NLS series.

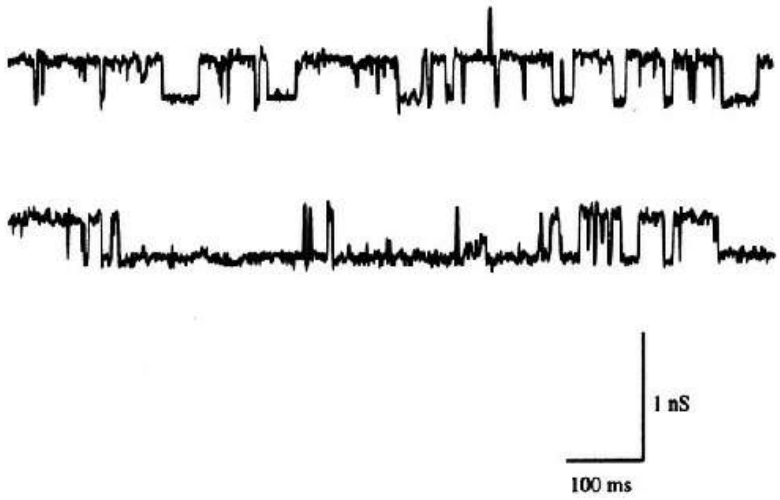

FIGURE 8.8 Single-channel trace obtained with peptide[1] when incorporated into planar lipid bilayers. (Adapted from Chaloin, L. et al., *Biochim. Biophys. Acta,* 1375, 52, 1998. With permission.)

Formation of ion channels was evidenced on membranes of *Xenopus* oocytes and on artificial planar lipid bilayers that allow an unambiguous assignment of the origin of ionophore activity. For both types of membranes, the peptide induces channel formation (Figure 8.8), thus providing an explanation for the toxic properties.[118]

8.8 CONCLUSIONS AND PERSPECTIVES

Although few investigations are related to the mechanism used by cell-penetrating peptides to penetrate into cells, the main general rule at least for shuttle peptides that do not use the endocytosis pathway, concerns the structure. Some points, such as the role of a linker sequence in the FP–NLS series, remain puzzling. The peptides must show amphipathic properties, which can appear either at the primary structural level or upon formation of an α-helix. However, for α-helical peptides, these amphipathic properties can generate toxicity through ion channel formation according to the peptide length. Up until now, no clear requirements have been established for the criteria that select the internalization pathway, through endocytosis or direct penetration into the cytoplasm.

Many aspects remain to be elucidated. They are mainly related to understanding the CPP–lipid relationship, including the influence of the peptide conformational state and the consequences on the lipid organization, as well as the influence of the cargo on the conformational state of the carriers. In addition, nothing is known about the mechanism of the release from the membrane into the cytoplasmic side of the cells. This point is crucial and should be investigated in the near future because the next generation of cell-penetrating peptides must bear labels that specifically recognize the target cells through a receptor, for example. All this information will allow

determination of permitted modifications of the peptide sequence without reduction of their properties for intracellular delivery of therapeutics.

REFERENCES

1. Westermann, P., Gross, B., and Hoinkis, G., Inhibition of expression of SV40 virus large T-antigen by antisense oligodeoxyribonucleotides, *Biomed. Biochim. Acta,* 48, 85, 1989.
2. Stevensen, M. and Iversen, P.L., Inhibition of human immunodeficiency virus type 1-mediated cytopathic effects by poly(L-lysine)-conjugated synthetic antisense oligodeoxyribonucleotides, *J. Gen. Virol.,* 70, 2673, 1989.
3. Leonetti, J.P. et al., Antiviral activity of conjugates between poly(L-lysine) and synthetic oligodeoxyribonucleotides, *Gene,* 72, 323, 1988.
4. Lemaitre, M., Bayard, B., and Lebleu, B., Specific antiviral activity of a poly(L-lysine)-conjugated oligodeoxyribonucleotide sequence complementary to vesicular stomatitis virus N protein mRNA initiation site, *Proc. Natl. Acad. Sci. U.S.A.,* 84, 648, 1987.
5. Degols, G. et al., Antiviral activity and possible mechanisms of action of oligonucleotides-poly(L-lysine) conjugates targeted to vesicular stomatitis virus mRNA and genomic RNA, *Nucleic Acids Res.,* 17, 9341, 1989.
6. Sheldon, K. et al., Loligomers: design of *de novo* peptide-based intracellular vehicles, *Proc. Natl. Acad. Sci. U.S.A.,* 92, 2056, 1995.
7. Gariepy, J. and Kawamura, K., Vectorial delivery of macromolecules into cells using peptide-based vehicles, *Trends Biotechnol.,* 19, 21, 2001.
8. Bongartz, J.P. et al., Improved biological activity of antisense oligonucleotides conjugated to a fusogenic peptide, *Nucleic Acids Res.,* 22, 4681, 1994.
9. Arar, K. et al., Synthesis and antiviral activity of peptide-oligonucleotide conjugates prepared by using N alpha-(bromoacetyl)-peptides, *Bioconjug. Chem.,* 6, 573, 1995.
10. Pichon, C. et al., Intracellular routing and inhibitory activity of oligonucleopeptides containing a KDEL motif, *Mol. Pharmacol.,* 51, 431, 1997.
11. Perez, F. et al., Antennapedia homeobox as a signal for the cellular internalization and nuclear addressing of a small exogenous peptide, *J. Cell Sci.,* 102, 717, 1992.
12. Derossi, D., Chassaing, G., and Prochiantz, A., Trojan peptides: the penetratin system for intracellular delivery, *Trends Cell Biol.,* 1998;8:84, 1998.
13. Derossi, D. et al., The third helix of the Antennapedia homeodomain translocates through biological membranes, *J. Biol. Chem.,* 269, 10444, 1994.
14. Derossi, D. et al., Cell internalization of the third helix of the Antennapedia homeodomain is receptor independent, *J. Biol. Chem.,* 271, 18188, 1996.
15. Brugidou, J. et al., The *retro-inverso* form of a homeobox-derived short peptide is rapidly internalised by cultured neurones: a new basis for an efficient intracellular delivery system, *Biochem. Biophys. Res. Commun.,* 214, 685, 1995.
16. Troy, C.M. et al., The contrasting roles of ICE family proteases and interleukin-1b in apoptosis induced by trophic factor withdrawal and by copper/zinc superoxyde dismutase downregulation, *Proc. Natl. Acad. Sci. U.S.A.,* 93, 5635, 1996.
17. Fahraeus, R. et al., Inhibition of pRB phosphorylation and cell-cycle progression by a 20-residue peptide derived from $p16^{CDKN2/INK4A}$, *Curr. Biol.,* 6, 84, 1996.
18. Prochiantz, A., Getting hydrophilic compounds into cells: lessons from homeopeptides, *Curr. Opin. Neurobiol.,* 6, 629, 1996.

19. Vivès, E., Brodin, P., and Lebleu, B., A truncated HIV-1 Tat protein basic domain rapidly translocates through the plasma membrane and accumulates in the cell nucleus, *J. Biol. Chem.,* 272, 16010, 1997.
20. Schwarze, S.R. et al., *In vivo* protein transduction: delivery of a biologically active protein into the mouse, *Science*, 285, 1569, 1999.
21. Schwarze, S.R., Hruska, K.A., and Dowdy, S.F., Protein transduction: unrestricted delivery into all cells? *Trends Cell Biol.,* 10, 290, 2000.
22. Langer, M. et al., Novel peptide conjugates for tumor-specific chemotherapy, *J. Med. Chem.,* 44, 1341, 2001.
23. Schmidt, M.C. et al., Translocation of human calcitonin in respiratory nasal epithelium is associated with self-assembly in lipid membrane, *Biochemistry,* 37, 16582, 1998.
24. Marin, M. et al., Targeted infection of human cells via major histocompatibility complex class I molecules by Moloney murine leukemia virus-derived viruses displaying single-chain antibody fragment-envelope fusion proteins, *J. Virol.,* 70, 2957, 1996.
25. Sharma, S. et al., Noninfectious virus-like particles produced by Moloney murine leukemia virus-based retrovirus packaging cells deficient in viral envelope become infectious in the presence of lipofection reagents, *Proc. Natl. Acad. Sci. U.S.A.,* 94, 10803, 1997.
26. Nguyen, D.M. et al., Gene delivery into malignant cells *in vivo* by a conjugated adenovirus/DNA complex, *Cancer Gene Ther.,* 4, 183, 1997.
27. Muzyczka, N., Use of adeno-associated virus as a general transduction vector for mammalian cells, *Curr. Top. Microbiol. Immunol.,* 158, 97, 1992.
28. Legendre, J.Y. and Szoka, F.C., *Liposomes for Gene Therapy,* Puisieux, F. et al., Eds., Editions de la Santé, Paris, 1995, 667.
29. Scherman, D. et al., Application of lipids and plasmid design for gene delivery to mammalian cell, *Curr. Opin. Biotechnol.,* 9, 480, 1998.
30. Boussif, O. et al., A versatile vector for gene and oligonucleotides transfer into cells in culture and *in vivo*: polyethylenimine, *Proc. Natl. Acad. Sci. U.S.A.,* 92, 7297, 1995.
31. Oehlke, J. et al., Cellular uptake of an alpha-helical amphipathic model peptide with the potential to deliver polar compounds into the cell interior non-endocytically, *Biochim. Biophys. Acta,* 1414, 127, 1998.
32. Chaloin, L. et al., Design of carrier peptide — oligonucleotide conjugate with rapid membrane translocation and nuclear localization properties, *Biochim. Biophys. Res. Commun.,* 243, 601, 1998.
33. Wyman, T.B. et al., Design, synthesis, and characterization of a cationic peptide that binds to nucleic acids and permeabilizes bilayers, *Biochemistry,* 36, 5616, 1997.
34. Niidome, T. et al., Binding of cationic alpha-helical peptides to plasmid DNA and their gene transfer abilities into cells, *J. Biol. Chem.,* 272, 15307, 1997.
35. Niidome, T. et al., Chain length of cationic α-helical peptide sufficient for gene delivery into cells, *Bioconjug. Chem.,* 10, 115, 1999.
36. Futaki, S. et al., Arginine-rich peptides. An abundant source of membrane-permeable peptides having potential as carriers for intracellular protein delivery, *J. Biol. Chem.,* 276, 5836, 2001.
37. Morris, M.C. et al., Translocating peptides and proteins and their use for gene delivery, *Curr. Opin. Biotech.,* 11, 461, 2000.
38. Morris, M.C. et al., A new peptide vector for efficient delivery of oligonucleotides into mammalian cells, *Nucleic Acids Res.,* 25, 2730, 1997.

39. Scheller, A. et al., Evidence for an amphipathicity independent cellular uptake of amphipathic cell-penetrating peptides, *Eur. J. Biochem.,* 267, 6043, 2000.
40. Pooga, M. et al., Cell penetration by transportan, *FASEB J.,* 12, 67, 1998.
41. Lindgren, M. et al., Cell-penetrating peptides, *TIPS,* 21, 99, 2000.
42. Pooga, M. et al., Cellular translocation of proteins by transportan, *FASEB J.,* 15, 1451, 2001.
43. Goldfarb, D.S. et al., Synthetic peptides as nuclear localization signals, *Nature,* 322, 641, 1986.
44. Briggs, M.S. and Gierasch, L.M., Molecular mechanisms of protein secretion: the role of the signal sequence, *Adv. Prot. Chem.,* 38, 109, 1986.
45. Slepushkin, V.A. et al., Investigation of human immunodeficiency virus fusion peptides. Analysis of interrelations between their structure and function, *AIDS Res. Hum. Retroviruses,* 8, 9, 1992.
46. Lindberg, M. et al., Secondary structure and position of the cell-penetrating peptide transportan in SDS micelles as determined by NMR, *Biochemistry,* 40, 3141, 2001.
47. Chaloin, L. et al., Conformations of primary amphipathic carrier peptides in membrane mimicking environments, *Biochemistry,* 36, 11179, 1997.
48. Vidal, P. et al., Conformational analysis of primary amphipathic carrier peptides and origin of the various cellular localizations, *J. Membrane Biol.,* 162, 259, 1998.
49. Magzoub, M. et al., Interaction and structure induction of cell-penetrating peptides in the presence of phospholipid vesicles, *Biochim. Biophys. Acta,* 1512, 77, 2001.
50. Cross, T., Solid-state nuclear magnetic resonance characterization of gramicidin channel structure, *Methods Enzymol.,* 289, 672, 1997.
51. Yang, J., Gabrys, C.M., and Weliky, D.P., Solid-state nuclera magnetic resonance evidence for an extended β strand conformation of the membrane-bound HIV-1 fusion peptide, *Biochemistry,* 40, 8126, 2001.
52. Wu, Y., Huang, H.W., and Olah, G.A., Method of oriented circular dichroism, *Biophys. J.,* 57, 797, 1990.
53. Tamm, L.K. and Tatulian, S.A., Infrared spectroscopy of proteins and peptides in lipid bilayers, *Q. Rev. Biophys.,* 30, 365, 1997.
54. Goormaghtigh, E., Cabiaux, V., and Ruysschaert, J.M., Determination of soluble and membrane protein structure by Fourier transform infrared spectroscopy. I. Assignments and model compounds. II. Experimental aspects, side chain structure, and H/D exchange. III. Secondary structure, in *Subcellular Biochemistry,* Vol. 23, *Physicochemical Methods in the Study of Biomembranes* (ed. H.J. Hilderson and G.B. Ralston), New York, Plenum Press, 329–450.
55. Goormaghtigh, E., Raussens, V., and Ruysschaert, J.M., Attenuated total reflection infrared spectroscopy of proteins and lipids in biological membranes, *Biochim. Biophys. Acta,* 1422, 105, 1999.
56. Haris, P.I. and Chapman, D., The conformational analysis of peptides using Fourier transform IR spectroscopy, *Biopolymers,* 37, 251, 1995.
57. Vié, V. et al., Detection of peptide–lipid interactions in mixed monolayers, using isotherms, atomic force micoscopy, and Fourier transform infrared analyses, *Biophys. J.,* 78, 846, 2000.
58. Van Mau, N. et al., Lipid-induced organization of a primary amphipathic peptide: a coupled AFM-monolayer study, *J. Membr. Biol.,* 167, 241, 1999.
59. Tatulian, S. and Tamm, L., Secondary structure, orientation, oligomerization, and lipid interactions of the transmembrane domain of influenza hemagglutinin, *Biochemistry,* 39 496, 2000.

60. Frey, S. and Tamm, L.K., Orientation of melittin in phospholipid bilayers. A polarized attenuated total reflection infrared study, *Biophys. J.,* 60, 922, 1991.
61. Blaudez, D. et al., Polarization-modulated FT-IR spectroscopy of spread monolayer at the air–water interface, *Appl. Spectrosc.,* 47, 869, 1993.
62. Cornut, I. et al., *In situ* study by polarization modulated Fourier transform infrared spectroscopy of the structure and orientation of lipids and amphipathic peptides at the air–water interface, *Biophys. J.,* 70, 305, 1996.
63. Lenne, P.F. et al., Synchrotron radiation diffraction from two-dimensional protein crystals at the air/water interface, *Biophys.,* J. 79, 496, 2000.
64. Schwartz, D., Langmuir–Blodgett film structure, *Surf. Sci. Rep.,* 27, 241, 1997.
65. Loeb, G.I., Infrared spectra of protein monolayers: paramyosin and β-lactoglobulin, *J. Colloid Interface Sci.,* 31, 572, 1969.
66. Loeb, G.I., Spectroscopy of protein monolayers: a transition in β-lactoglobulin films, *J. Polymer Sci.*, 34, 63, 1971.
67. Cserhäti, T. and Szögyi, M., Interaction of phospholipid with proteins and peptides. New advances 1990, *Int. J. Biochem.,* 24, 525, 1992.
68. Netz, R.R., Andelman, D., and Orland, H., Protein adsorption on lipid monolayers at their coexistence region, *J. Phys. II France,* 6, 1023, 1996.
69. Cornell, D.G. and Carroll, R.J., Electron microscopy of lipid-protein monolayers, *Colloids Surf.,* 6, 385, 1983.
70.. Zhao, J. et al., Effect of protein penetration into phospholipid monolayers: morphology and structure, *Colloids Surf. A: Physicochem. Eng. Aspects,* 171, 175, 2000.
71. Makievski, A.V. et al., Adsorption of proteins at the liquid–air interface, *J. Phys. Chem. B*, 102, 417, 1998.
72. Cho, D., Narsimhan, G., and Franses, E.I., Adsorption dynamics of native and pentylated bovine serum albumin at air–water interfaces: surface concentration/surface pressure measurements, *J. Colloid Interface Sci.,* 191, 312, 1997.
73. Brockman, H., Lipid monolayers: why use half a membrane to characterize protein–lipid interactions? *Curr. Opin. Struct. Biol.,* 9, 438, 1999.
74. Rafalski, M., Lear, J.D., and DeGrado, W.F., Phospholipid interactions of synthetic peptides representing the N-terminus of HIV gp41, *Biochemistry,* 29, 7917, 1990.
75. Chiang, C-M. et al., Conformational change and inactivation of membrane phospholipid-related activity of cardiotoxin V from Taiwan cobra venom at acidic pH, *Biochemistry,* 35, 9167, 1996.
76. Van Mau, N. et al., The SU glycoprotein 120 from HIV-1 penetrates into lipid monolayers mimicking plasma membranes, *J. Membr. Biol.,* 177, 251, 2000.
77. Nordera, P., Dalla Serra, M., and Menestrina, G., The adsorption of *Pseudomonas aeuginosa* exotoxin A to phospholipid monolayers is controlled by pH and surface potential, *Biophys. J.,* 73, 1468, 1997.
78. Vilallonga, F., Altschul, R., and Fernandez, M.S., Lipid–protein interactions at the air–water interface, *Biochim. Biophys. Acta,* 135, 406, 1967.
79. Colacicco, G., Applications of monolayer techniques to biological systems: symptoms of specific lipid-protein interactions, *J. Colloid Interface Sci.,* 29, 345, 1969.
80. Mita, T., Lipid–protein interaction in mixed monolayers from phospholipids and proteins, *Bull. Chem. Soc. Jpn.,* 62, 3114, 1989.
81. Verger, R. and Pattus, F., Lipid–protein interactions in monolayers, *Chem. Phys. Lipids,* 30, 189, 1982.
82. Silvestro, L. and Axelsen, P.H., Infrared spectroscopy of supported lipid monolayer, bilayer, and multilayer membranes, *Chem. Phys. Lipids,* 96, 69, 1998.

83. Silvestro, L. and Axelsen, P.H., Fourier transform infrared linked analysis of conformational changes in annexinV upon membrane binding, *Biochemistry,* 38, 113, 1999.
84. Burger, K.N.J. et al., The interaction of synthetic analogs of the N-terminal fusion sequence of influenza virus with a lipid monolayer. Comparison of fusion-active and fusion-defective analogs, *Biochim. Biophys. Acta,* 1065, 121, 1991.
85. Briggs, M.S. et al., Conformations of signal peptides induced by lipids suggest initial steps in protein export, *Science,* 233, 206, 1986.
86. Lindblom, G. and Quist, P.-O., Protein and peptide interactions with lipids: structure, membrane function and new methods, *Curr. Opin. Colloid Interface Sci.,* 3, 499, 1998.
87. Taylor, S.E. et al., Structure of a fusion peptide analogue at the air–water interface, determined from surface activity, infrared spectroscopy and scanning force microscopy, *Biophys. Chem.,* 87, 63, 2000.
88. Elmore, D.L. and Dluhy, R.A., Application of 2D IR correlation analysis to phase transitions in Langmuir monolayer films, *Colloids Surf. A: Physicochem. Eng. Aspects,* 171, 225, 2000.
89. Cortijo, M. et al., Intrinsic protein–lipid interactions. Infrared spectroscopic studies of gramicidin A, bacteriorhodopsin and Ca^{2+}-ATPase in biomembranes and reconstituted systems, *J. Mol. Biol.,* 157, 597, 1982.
90. Dempsey, C.E., The actions of melittin on membranes, *Biochim. Biophys. Acta,* 1031, 143, 1990.
91. Latal, A. et al., Structural aspects of the interaction of peptidyl-glycylleucine-carboxyamide, a highly potent antimicrobial peptide from frog skin, with lipids, *Eur. J. Biochem.,* 248, 938, 1997.
92. Cummings, C.E. et al., Structural and functional studies of a synthetic peptide mimicking a proposed membrane inserting region of a *Bacillus thuringiensis* δ-endotoxin, *Mol. Membr. Biol.,* 11, 87, 1994.
93. Tamm, L.K. and Tatulian, S.A., Infrared spectroscopy of proteins and peptides in lipid bilayers, *Q. Rev. Biophys.,* 30, 365, 1997.
94. Baty, D. et al., A 136-amino-acid-residue COOH-terminal fragment of colicin A is endowed with ionophoric activity, *Eur. J. Biochem.,* 30, 409, 1990.
95. Pécheur, I. et al., Protein-induced fusion can be modulated by target membrane lipids through a structural switch at the level of the fusion peptide, *J. Biol. Chem.,* 275, 3936, 2000.
96. Vié, V. et al., Lipid-induced pore formation of the *Bacillus thuringiensis* Cry1Aa insecticidal toxin, *J. Membr. Biol.,* 180, 195, 2001.
97. Lakowicz, J.R., in *Principles of Florescence Spectroscopy,* Plenum Press, New York, 1986.
98. Kenworthy, A.K., Petranova, N., and Edidin, M., High-resolution FRET microscopy of cholera toxin B-subunit and GPI-anchored proteins in cell plasma membranes, *Mol. Biol. Cell,* 11, 1645, 2000.
99. Lakey, J.H. et al., Membrane insertion of the pore-forming domain of colicin A. A spectroscopic study, *Eur. J. Biochem.,* 196, 599, 1991.
100. Edidin, M., Lipid microdomains in cell surface membranes, *Curr. Opin. Struct. Biol.,* 7, 528, 1997.
101. Zazadzinski, J.A. et al., Langmuir–Blodgett films, *Science,* 263, 1726, 1994.
102. Mou, J.D., Czalkowsky, M., and Shao, Z., Gramicidin A aggregation in supported gel state phosphatidylcholine bilayers, *Biochemistry,* 35, 3222, 1996.
103. ten Grotenhuis, E.R. et al., Phase behavior of stratum corneum lipids in mixed Langmuir–Blodgett monolayers, *Biophys. J.,* 71, 1389, 1996.

104. Vié, V. et al., Distribution of ganglioside G_{M1} between two-components, two phase phosphatidylcholine monolayers, *Langmuir,* 14, 4574, 1998.
105. Czajkowsky, D.M. et al., Direct visualization of surface charge in aqueous solution, *Ultramicroscopy,* 74, 1, 1998.
106. Gliss, C. et al., Direct detection of domains in phospholipid bilayers by grazing incidence diffraction of neutrons and atomic force microscopy, *Biophys. J.,* 74, 2443, 1998.
107. Hollars, C.W. and Dunn, R.C., Submicron structure of L-α-dipalmitoylphosphatidylcholine monolayers and bilayers probed with confocal, atomic force, and near field microscopy, *Biophys. J.,* 75, 342, 1998.
108. Hui, S.W. et al., The structure and stability of phospholipid bilayers by atomic force microscopy, *Biophys. J.,* 68, 171, 1995.
109. Gaines, G.L., Mixed monolayers, in *Insoluble Monolayers at Liquid–Gas Interfaces,* Prigogine, I., Ed., Interscience, New York, 281, 1966.
110. Crisp, D.J., A two dimensional phase rule. I. Derivation of a two-dimensional phase rule for planar interface. II. Some applications of a two dimensional phase rule for a single surface, in *Surface Chemistry,* Butterworths, London, 17, 1949.
111. Arrondo, J.L.R. et al., Quantitative studies of the structure of proteins in solution by Fourier-transform infrared spectroscopy, *Prog. Biophys. Mol. Biol.,* 59, 23, 1993.
112. Dong, A., Huang, P., and Caughey, W.S., Protein secondary structures in water from second-derivative amide I infrared spectra, *Biochemistry,* 29, 3303, 1990.
113. Taneva, S. and Keough, K.M.W., Pulmonary surfactant proteins SP-B and SP-C in spread monolayers at the air–water interface. I. Monolayers of pulmonary surfactant protein SP-B and phospholipids, *Biophys. J.,* 66, 1137, 1994.
114. Berlose, J.P. et al., Conformational and associative behaviours of the third helix of antennapedia homeodomain in membrane-mimetic environments, *Eur. J. Biochem.,* 242, 372, 1996.
115. van der Goot, F.G. et al., A "molten-globule" membrane insertion intermediate of the pore-forming domain of colicin A, *Nature,* 354, 408, 1991.
116. Bychkova, V.E., Pain, R.H., and Ptitsyn, O.B., The "molten globule" state is involved in the translocation of proteins across membranes? *FEBS Lett.,* 238, 231, 1988.
117. Beven, L. et al., Effect on mollicutes of peptides comprising a signal peptide or a fusion peptide and a nuclear localization sequence (NLS): a comparison with melittin, *Biochim. Biophys. Acta,* 1329, 357, 1997.
118. Chaloin, L. et al., Ionic channels formed by primary amphipathic peptides, *Biochim. Biophys. Acta,* 1375, 52, 1998.

9 Structure Prediction of CPPs and Iterative Development of Novel CPPs

Olivier Bouffioux, Frédéric Basyn, René Rezsohazy, and Robert Brasseur

CONTENTS

0-8493-1141-1/02/$0.00+$1.50

9.1 INTRODUCTION

Homeoproteins define a huge group of transcription factors sharing the evolutionary conserved homeodomain.[1] Representatives of this group of proteins are found in all the eukaryotic phyla, including yeasts, where they fulfill a wide range of biological functions. Among these functions, homeoproteins are involved in developmental processes such as the mating type switch in yeast, the main body axis patterning of animal embryos, limb development, regionalization of developing organs, and control of cell proliferation and differentiation.[2,3]

With a few exceptions, the homeodomain is 60 amino acids long; the structure determination of several representatives has shown a globular fold made of two antiparallel α-helices followed by a third, perpendicular one.[3-6] In some instances, the third α-helix may be followed by a kink and a short, fourth α-helix. The well-recognized function of the homeodomain is to bind DNA in a sequence-specific manner. Its third α-helix thus fits into the major groove of a cognate DNA site with amino acids contacting the base pairs. Furthermore, the extended N-terminal extremity of the homeodomain makes additional contacts within the DNA minor groove. The binding of the homeodomain to DNA also involves charge interactions, and basic residues in particular — namely, lysines and arginines — contribute by interacting with the phosphate groups of the DNA backbone.

Recently, it appeared that the homeodomain contributes to various other functions. It has been shown that, at least in some instances, homeodomains can act as an RNA binding domain,[6] define a transcriptional activation or repression domain,[6-9] modulate the activity of the protein,[10,11] and take part in protein-to-protein interactions.[12-15] Among these new roles, the most unforeseen was an involvement in the intracellular trafficking of homeoproteins as well as in cell-to-cell communication. Prochiantz and collaborators reported that the Antennapedia homeoprotein can indeed be taken up by live cells.[16] Internalization by cells was further shown to be conferred by a 16 amino acid-long peptide corresponding to the third α-helix of the homeodomain.[17] Furthermore, this α-helix also appeared to allow the protein to be conveyed to the cell nucleus.

Later on, the group of Prochiantz reported that the Engrailed homeoprotein can escape cells and that its commitment to the secretory pathway is provided by an 11-amino acid-long motif overlapping helices 2 and 3 of the homeodomain and corresponding to a functional nuclear export signal.[18,19] It was therefore proposed that the access of Engrailed to the secretory pathway may be conditioned by its transit to the nucleus.

All these data strongly suggest that the homeodomain transcription factors may act as signaling molecules and play a paracrine function. However, the biological phenomena relying on this possible paracrine function remain to be identified. The ability of Antennapedia to be taken up by cells has now been extended to other homeoproteins[20,21] (Rezsohazy, unpublished data).

Biophysical and cytological studies provided evidence that the cellular entry of homeoproteins, or of peptides corresponding to the third α-helix of their homeodomain now called penetratins, relies on a receptor- and energy-independent mechanism.[22] Indeed, penetratin can reach the intracellular milieu at either 37 or 4°C.

Furthermore, retro, enantio, and retro-inverso forms of penetratin can also efficiently enter live cells.[22] Therefore, the ability of penetratins to cross biological membranes should rely only on their physico-chemical properties. The only residue identified so far as critical for the translocation of penetratins through biological membranes is a Trp corresponding to the well-conserved position 48 in most of the homeodomains.[17,21,22] Indeed, substituting this residue by the otherwise hydrophobic phenylalanine appeared to be deleterious for crossing the peptide through lipid bilayers.

It has been suggested that penetratin might cross the cellular membrane by the transient formation of inverted micelles.[23,21] According to this model, the interaction between the peptide and membrane lipids should be critical for the internalization process. Several recent reports have addressed the question of physico-chemical parameters' conditioning the membrane crossing behavior of penetratins. They revealed that there is only a partial relationship between the lipid-binding affinity of penetratin variants and their capacity to cross biological membranes. Also, no correlation exists between the helical amphipathy of the variant peptides and their propensity to be internalized by cells.[24,25]

Although the mechanisms and determinants underlying translocation of penetratin through membranes remain to be characterized, it is obvious that, in its natural configuration — i.e., as an α-helix constitutive of a transcription factor — this short sequence promotes the cellular entry of large molecules. Furthermore, according to the different homeoproteins now shown to enter live cells, the penetratin sequence is functional even when located in the middle of the primary sequence of a long protein. However, since the only structural data available so far for homeoproteins are basically limited to the isolated homeodomain, it cannot be stated whether the penetratin α-helix must be solvent accessible to be functional. Nonetheless, in the different homeodomains or homeodomain–DNA complexes characterized so far, charges harbored by the polar amino acid residues of the third α-helix are exposed to the solvent or to the phosphate groups of the DNA. Strikingly, the tryptophan residue at position 48 in the homeodomain shown to be critical for crossing biological membranes takes part in the hydrophobic core of the homeodomain globular structure.

The recent discovery of cell-permeant peptides like penetratins, and others like the HIV Tat peptide or transportan[21,26] (see also other chapters in this book), has opened the perspective of using such peptides as carriers to allow intracellular delivery of different classes of molecules of pharmacological interest, in particular of hydrophilic compounds that hardly access the intracellular environment.[27-30] However, to evaluate the degree of freedom in designing new cell-permeant peptide derivatives or peptide–cargo combinations with the view of modulating cytological functions for therapeutic purposes, for example, it is important to elaborate predictive methods, taking into account constraints that condition the addressing of peptide vectors into live cells.

In order to get insight into molecular interactions between biological membranes and the numerous and unrelated classes of membrane proteins or membrane interacting proteins, modeling procedures have been developed and optimized.

To study peptide–bilayer interactions, we adopt a simulation approach using the Monte Carlo (MC) method, in which peptide–bilayer interactions are approached by the sum of different energy functions that mimic lipid perturbation, hydrophobicity, and electrostatic effects. All of these energies are named restraints because

the bilayer is simulated as a continuous domain. Indeed, this simple bilayer description is treated as a simple continuous hydrophobic domain, taking into account charge potential induced by the polar head groups of phospholipids. In this representation, proteins, peptides, or any amphiphilic molecules entering membrane are modeled at atomic resolution.

Such approaches have been used with success in the analysis of amphipathic peptides,[31-33] hydrophobic peptide,[31] tilted peptides,[34] and membrane protein.[35] Modeling results were similar to the experimental data when the latter were available. If the approximation of the bilayer as a hydrophobic–hydrophilic continuum is somewhat simplistic, the existence of such a continuum interface was shown by x-ray and neutron diffraction studies.[36,37] At 10 to 15 Å, head groups of phospholipids and water molecules are co-located. This picture is reinforced by several molecular dynamics (MD) simulations of pure lipid bilayers[32] or peptides in interaction with lipid bilayers,[38,39] but the later simulations are restricted to a few nanoseconds, which is insufficient to simulate the transfer of a molecule through the membrane.

This chapter about cell-permeant peptides will focus on modeling techniques recently developed to describe peptide behavior in context of their interaction with biological membranes and to provide a predictive method to further design peptide vectors aimed to address different classes of compounds into cells.

9.2 METHODS

9.2.1 Description of Water–Bilayer Interfaces

We postulate that the properties of membranes are constant in the plane of the bilayer (x/y plane). Thus, the lipid–water interfaces are described by a function, $C_{(Z)}$, which varies along the z axis only; z (in angstroms) is perpendicular to the plane of the membrane and its origin is at the center of the bilayer. $C_{(Z)}$ (Figure 9.1) is an empirical function varying from 1 (completely hydrophilic) to 0 (completely hydrophobic) derived from Milik and Skolnick.[40]

$$C_{(z)} = 1 - \frac{1}{1 + e^{\alpha(|z| - z_0)}} \tag{9.1}$$

where α and z_0 are mathematical parameters calculated so that $C_{(|Z = 18\ Å|)} = 1$ and $C_{(|Z = 13.5\ Å|)} = 0$ and so that the function is approximately constant from $-\infty$ to –18 Å (hydrophilic phase), from –13.5 to 13.5 Å (hydrocarbon core), and from 18 Å to ∞ (hydrophilic phase). Z = 13.5 Å is the distance at which the first polar heads appear,[41] and an interface of 4.5 Å gives the best results for simulations. The same interface width was used in the Monte Carlo technique developed by Milik and Skolnick.[40] This mathematical form of $C_{(Z)}$ was chosen because it is continuous and can be rapidly computed.

Because C does not vary into the plane x/y, a molecule is fully described by its internal geometry: two rotations (around x and y) and one translation (along z). The main simplification of this approach is that it totally neglects specific interactions between the molecule and lipids or other molecules buried in the membrane. However,

$$C_{(z)} = 1 - \frac{1}{1+e^{\alpha(|z|-z_0)}}$$

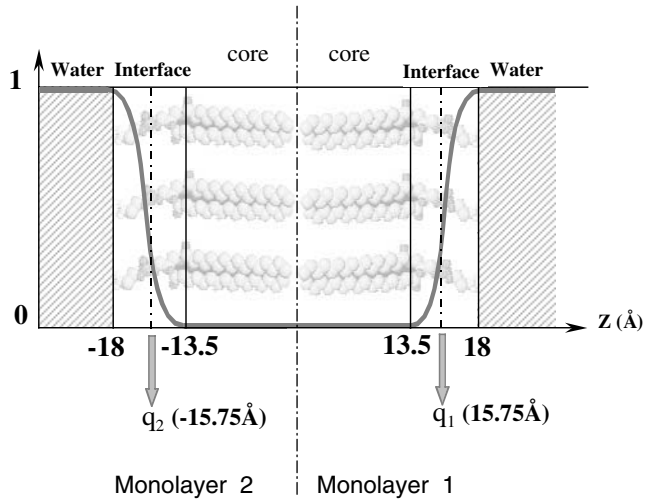

FIGURE 9.1 Model membrane of IMPALA.

generally these interactions do not seem crucial for folding membrane proteins, as the proteins may refold *in vitro* under nonbiological conditions.[42] This assumption is also made for the crystallization of integrated membrane proteins (IMPs) in which lipids are replaced by detergents. Moreover, the description is so simple that it could be easily adapted to other interfaces (e.g., monolayer, spherical, or discoidal).

9.2.2 Atomic Surface Hydrophobicity (First Restraint)

To calculate the hydrophobic and hydrophilic restraints, we use atomic surface transfer energies, a concept relying on the assumption that the overall transfer energy of a molecule, H, can be calculated as

$$H = \sum_{i=1}^{N} S_i E_{tr(i)} \tag{9.2}$$

where i is an index for the N atoms of the molecule, S (Å^2) the solvent-accessible surface calculated with Shrake and Rupley's algorithm with 192 points,[43,44] and E_{tr} (kJ/·mol·Å^2) is the transfer energy by surface of individual atoms (Table 9.1). A similar approach was successfully used on small molecules[45] by considering that

$$H = \sum_{i=1}^{N} E_{atr(i)} \tag{9.3}$$

TABLE 9.1
Atomic Surfaces Transfer Energies for the Seven Atomic Types[a]

Atomic types	Transfer energies per accessible surfaces (kJ/mol Å^2)
Csp3	–0.0150
Csp2	–0.0134
H (= 0)	–0.0397
H(/0)	0.0362
O	0.0403
N	0.1120
S	–0.1080

[a] Csp2, double-bonded and aromatic carbons; Csp3, single-bonded carbons; H (= 0), non-charged hydrogen (bound to C); H (/0), charged hydrogen; O, oxygen; N, nitrogen; S, sulfur.

where E_{atr} is the atomic transfer energy of one of the N atoms of the molecule considered. In addition we introduce a correcting factor that takes into account the fact that solvent interacts only with accessible atoms — known to be essential for a good description of the hydrophobic effect.[34,46] Our formulation is at least in line with two experimental facts: the hydrophobic effect is related to the nature and to the surface of solute in contact with solvent. To calculate the values of E_{tr}, we wrote an equation system by applying Equation 9.2 to 19 of the 20 natural amino acids (excluding proline for convenience). We used the experimental transfer energies measured by Fauchère and Pliska[47] as H values.

Following Brasseur,[45] seven atomic types were considered: double-bonded carbon (Csp2) (including aromatic cycles carbons), simple-bonded carbon (Csp3), oxygen (0), sulfur (S), nitrogen (N), uncharged hydrogen bonded to C (H = 0), and charged hydrogen (H/0). Thus, we can, for example, calculate the transfer energy of Phe and Asn (with the convention of Figure 9.2) as

$$H_{theo\ (ASN)} = E_{tr\ (Csp3)}(S2+S5) + E_{tr\ (Csp2)}(S3+S9) + E_{tr\ (H=0)}(S6+S7+S8+S13+S14) + E_{tr(H/0)}S10 + E_{tr\ (O)}(S4+S12) + E_{tr\ (N)}(S1+S11)$$

$$H_{theo\ (PHE)} = E_{tr\ (Csp3)}(S2+S5) + E_{tr\ (Csp2)}(S3+S9+S11+S13+S15+S17+S19) + E_{tr\ (H=0)}(S6+S7+S8+S12+S14+S16+S18+S20) + E_{tr(H/0)}S10 + E_{tr\ (O)}(S4) + E_{tr\ (N)}(S1)$$

where S1 to 20 are the accessible surfaces of atoms.

The system written that way consists of more equations than variables (19 vs. 7); hence, a unique solution does not exist and the system must be approximated. In their original publication, Fauchère and Pliska[47] deduced the measured transfer

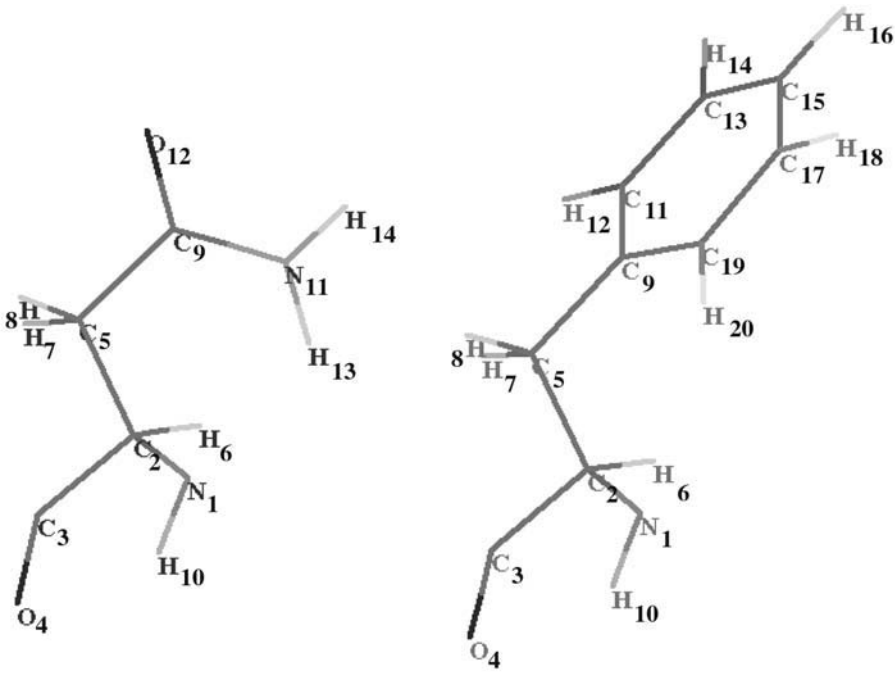

FIGURE 9.2 Structures of Phe and Asn used to optimize the atomic transfer energy scale.

energy of glycine from those of all other residues in order to obtain the transfer energies of the lateral side chains. Thus the error between experimental and calculated data for an amino acid x is

$$\delta_{(x)} = \left| \left(H_{theo(x)} - H_{theo(gly)} \right) - H_{exp(x)} \right|$$

The total error between the calculated and experimental H was minimized by a Monte Carlo procedure applied to the atomic transfer energy errors.

9.2.3 Lipid Perturbation (Second Restraint)

To build restraints of the lipid perturbation, one must define the general structural features of IMPs.[31] The observation of bacteriorhodopsin and photosynthetic reaction center[48] shows that IMPs are similar to soluble proteins with respect to surface area, interior hydrophobicity and packing, conservation of buried residues, and stability. The major difference between IMPs and soluble proteins is the nature of surface residues, which are more hydrophobic in IMPs than in globular proteins.[31] This feature has been used in many methods aimed at determining the transmembrane segments of IMPs. This striking segregation of hydrophobic and hydrophilic parts of the molecule imposed by the membrane properties is the hydrophobic effect. To simulate it, we calculate the hydrophobic restraint as

$$E_{int} = -\sum_{i=1}^{N} S_{(i)} E_{tr(i)} C_{(z_i)} \tag{9.4}$$

The general behavior of Equation 9.4 is that E_{int} increases when solvent-accessible hydrophilic atoms (i.e., $E_{tr} > 0$) penetrate the membrane and decreases when solvent-accessible hydrophobic atoms do. The more atoms are accessible, the larger is the effect.

E_{int} decreases when two hydrophobic or hydrophilic atoms come close together in the hydrophobic and hydrophilic phases, respectively. IMPs and water-soluble proteins tend to form compact structures. For water-soluble proteins this is explained by the fact that the protein minimizes its hydrophobic surface in contact with water. For IMPs, Rees and colleagues[48] suggested that interactions between adjacent lipids are disrupted and replaced by weaker interactions between the protein and lipids. E_{lip} accounts for perturbation of the lipid bilayer due to peptide insertion. It is defined as

$$E_{lip} = \alpha_{lip} \sum_{i=1}^{N} S_i C_{(Z_i)} \tag{9.5}$$

where α_{lip} is an empirical factor fixed to + 0.018. The concept of this equation is very simple: E_{lip} increases with the surface of the protein in contact with lipids. The assumption is made that lipids act as a pool of free-solvating CH_2 groups, although these groups are covalently linked in acyl chains.

9.2.4 Charge Simulation (Third Restraint)

More sophisticated methods exist to simulate electrostatic energy. Starting from an atomistic model of phosphatidyl choline phospholipid (PC) bilayers, La Rocca et al. calculated an average electrostatic potential along the bilayer.[32] This method exists for PC, a globally neutral lipid, but does not fit for charged monolayers. We have developed a method to mimic charge distribution of bilayers.

The electrostatic potential across the bilayer may be obtained by solving Poisson's equation:

$$\nabla \varepsilon(z) \nabla \Phi(z) = -\frac{\rho(z)}{\varepsilon_0} \tag{9.6}$$

where $\Phi(z)$, $\varepsilon(z)$, and $\rho(z)$ are the electrostatic potential, dielectric constant, and charge density, respectively, at position z. Water is treated as a z-dependent dielectric constant. Although this is a simplification, it captures the essentials of variation of the electrostatic potential along the bilayer normal at a similar level of approximation as the other elements of the empirical energy function used to represent the bilayer. At any point, the electrostatic potential resulting from Equation 9.6 will depend on

x, y, and z (where the xy plane is that of the membrane). However, on the time scale of peptide–bilayer interactions the peptide is assumed to be influenced by a potential averaged in the membrane plane:

$$\overline{\Phi}(z) = \frac{1}{S} \int \Phi(r)dxdy \tag{9.7}$$

where the integral in Equation 9.7 is extended on the surface of the xy plane over an area S. When the dielectric function is dependent upon z, the average potential $\Phi(z)$ is the solution of Equation 9.6 with an average charge distribution:

$$\varepsilon(z)\frac{d^2\overline{\Phi}(z)}{dz^2} + \frac{d\varepsilon}{dz}\frac{\overline{\Phi}(z)}{dz} = \frac{\overline{\rho}(z)}{\varepsilon_0} \tag{9.8}$$

where

$$\overline{\rho}(z) = \frac{1}{S}\int \rho(z)dxdy \tag{9.9}$$

and where the definition of the integral and of S are the same as in Equation 9.7. To make an average charge distribution, the mean and standard deviations of the z coordinate of each phospholipid atom type were calculated. The contribution from each atom type to the overall charge density of the bilayer was approximated as a Gaussian function with mean and standard deviations as calculated, and normalized to the partial charge per unit area of that atom type:

$$\overline{\rho}(z) = \frac{1}{A}\sum_i q_i G_i(z) \tag{9.10}$$

where A is the area per head group,[49] q_i is the partial charge of atom type i, G is a Gaussian function of the z coordinate for atom type i, and the sum is extended over all atom types of the phospholipid molecule. The resultant charge density of the bilayer is localized in a plane at –15.75 and +15.75 Å.

Imagine that a charge is distributed uniformly over the entire xy-plane (Figure 9.3), with a charge per unit area or surface density of charge, δ. We wish to calculate the electric intensity at the point P. Let the charge be subdivided into narrow strips parallel to the y-axis and of dx width. Each strip can be considered as a charged line. The area of a portion of a strip of length L is L dx, and the charge dq on the strip is

$$dq = \delta L dx$$

The charge per length unit, dλ, is therefore

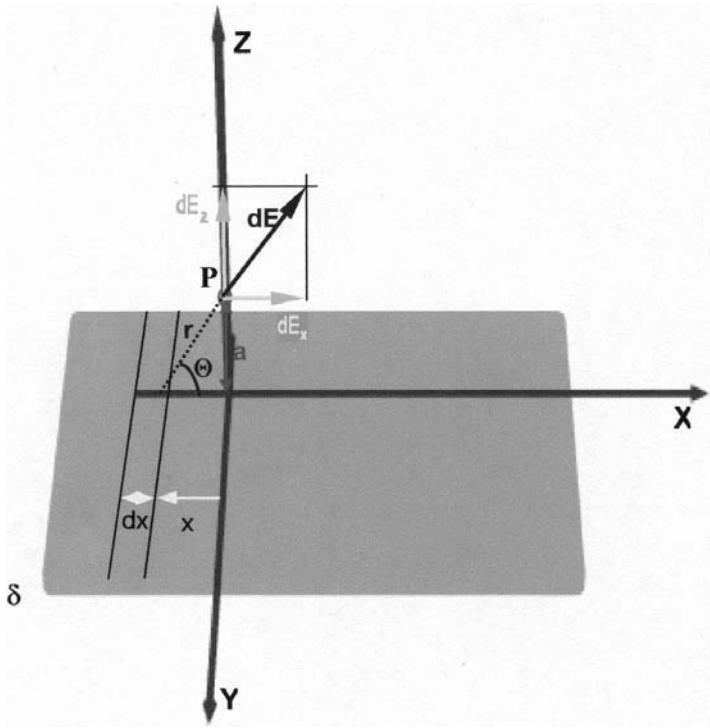

FIGURE 9.3 Schematic model for calculation of the electric intensity at P in the presence of a superficial density of charge δ.

$$d\lambda = \frac{dq}{L} = \delta\, dx$$

and at point P, a field dE, has a magnitude of

$$dE_q = 2k\delta \frac{dx}{r}$$

The field can be solved into two components dE_x and dE_z. By symmetry, the components dE_x will sum to zero for the entire sheet of charge. The resultant field at P is therefore in the z-direction, perpendicular to the sheet of charge. It is seen from the diagram that

$$dE_z = dE \sin \theta$$

and hence

$$E_q = \int dEz = 2k\delta \int_{-\infty}^{+\infty} \frac{\sin\theta.dx}{r}$$

But

$$\sin\theta = \frac{a}{r},\ r^2 = a^2 + x^2$$

Therefore

$$E_q = 2k\delta a \int_{-\infty}^{+\infty} \frac{dx}{a^2 + x^2} = 2k\delta a \left[\frac{1}{a}\tan^{-1}\frac{x}{a}\right]_{-\infty}^{+\infty}$$

$$\Rightarrow E_q = \frac{2\pi k\delta}{\varepsilon_{(z)}}$$

The model of the dielectric profile along the bilayer normal, $\varepsilon_{(z)}$, used by Flewelling and Hubbell[50] was adopted:

$$\varepsilon_{(z)} = \varepsilon_{pho} + \left(\varepsilon_{phi} - \varepsilon_{pho}\right)\left[1 + 10^{4(d+z)/h}\right]^{-1} \tag{9.11}$$

where $\varepsilon_{pho} = 2$ is the value of the dielectric constant in the hydrophobic core of the membrane, and $\varepsilon_{phi} = 78$ in bulk water. This function provides a smooth transition between the two constants in the interfacial region, defined by two parameters d and h that are the center and width of the transition region, respectively. The extent of the bilayer is $z = \pm (d + h/2)$. Equation 9.8 was solved using a finite difference algorithm.[51] A boundary condition of zero potential at $z = \pm 50$ Å (relative to the center of the bilayer at $z = 0$) was imposed.

Note that the distance a from the plane to the point P does not appear in the final result. This means that the intensity of the field set up by an infinite plane sheet of charge is independent of the distance from the charge. In other words, the field is uniform and normal to the plane of charge.

9.2.5 Procedure

In order to test the three restraints (hydrophobic, lipid perturbation, and charge simulation), we applied them to small peptides, the configurations of which have been experimentally determined. The structures of the peptides were helical and change of internal structure was not allowed. This drastically simplified the problem as follows:

1. Only three degrees of freedom were considered (two rotations and one translation) so that the Monte Carlo procedure used is efficient.
2. Since the structures were unchanged, Coulomb, Van Der Waals, hydrogen bonds, and torsion energies remained constants; thus the three variable parameters of the simulation are z_0, α, and α_{lip}.

This enabled us to rapidly determine a set of parameters leading to predictions in agreement with experimental data (see below).

The peptide structures were derived from the 9 ent.pdb. The molecules are fully described (H included, no heavy atoms) as this has an obvious effect on the accessible surface used in the calculations. A standard Monte Carlo procedure is then applied for $2 \cdot 10^5$ steps at 310 K by randomly translating (max. 1 Å) and rotating (max. 5°) the molecule at each step. Each Monte Carlo was run twice.

9.2.6 Monte Carlo Procedure

The total constraint E_i is calculated at the step i. The molecule undergoes a random translation and rotation at the step (i+1) where it is submitted to the constraint E_{i+1}.

- If $E_{i+1} < E_i$ the position at the step i+1 of the molecule is conserved and it undergoes another random movement where it will be submitted to the constraint E_{i+2} and compared to E_{i+1} …
- If $E_{i+1} > E_i$ the probability density function

$$f = e^{-\Delta E/kT} \ (0 \leq f \leq 1)$$

where $\Delta E = E_{i+1} - E_i$, k = Boltzman constant, T = temperature (in K), is compared to a random number Rnd ($0 \leq Rnd \leq 1$):

  - If Rnd < f, the position at point E_{i+1} is conserved and another random movement is applied from this position
  - If Rnd > f, the position at point E_{i+1} is rejected and a new random movement (translation and rotation) is applied to the molecule at the step i.

The probability for Rnd to be less than f is inversely correlated to ΔE, allowing the structure to converge towards a global minimum by jumping over the local minima.

9.2.7 Pex2Dstat Files

The results of the Monte Carlo simulations are saved in Pex2Dstat text files[52] (Figure 9.4A). These files consist of one array; each line corresponds to one step of the simulation. In this study, each Monte Carlo procedure was performed in 200,000 steps. Each column corresponds to a parameter analyzed during the simulation.

Current Pex2Dstat files are made of 27 columns among which the energetic restraints (col. 1, 2, 4, and 5), the molecule mass center penetration (col. 9), and the angle of the molecule vs. the bilayer model normal (col. 10) were considered for the present study.

Because of their size, Pex2Dstat files cannot be easily manipulated in their current form. Indeed, importing such files in a spreadsheet would give a worksheet

of 200,000 × 27 = 5,400,000 cells. In Figure 9.4B, we plotted all values of the total energetic restraint of a molecule as a function of the position of its mass center during the simulation.

In order to facilitate the analysis, a subsequent treatment of these huge files is applied. Since Monte Carlo is a minimization procedure, only the minimum values of the restraints need to be taken into consideration (gray points, Figure 9.4B); their extraction is carried out within a range of the mass center penetration (between +30 and –30 Å in this case). Between these two limits, a resolution step (0.5 Å in this case) is defined and we extract the lowest value of the energetic constraint within each 0.5 Å step (Figure 9.4C).

The results can also be plotted in three dimensions. In this case, each axis stands for a parameter of interest. As an example, Figure 9.4D shows evolution of the total energy restraint as a function of the mass center penetration of a molecule and as a function of its angle regarding the bilayer normal.

As an alternative we also looked for the envelope minima corresponding to the energy for the mass center penetration axis (between +30 and –30 Å with a step of 0.5 Å) and for the angle between the molecule and the bilayer normal axis (between 0 and 180° with a step of 3°), defining a two-dimensional mesh (Figure 9.4E).

9.2.8 Molecular Hydrophobicity Potential (MHP)

MHP is a three-dimensional plot of the potential of hydrophobicity of a molecule in order to visualize its amphipathy. Molecules and MHPs are drawn with WinMGM.[53] The hydrophobicity of a molecule is calculated using its partition coefficient between water and octanol. In order to visualize the amphipathy, a three-dimensional molecular plot of hydrophobicity was proposed by Fauchère et al.[47] for small molecules. The MHP approach was then extended to plot the surface of the isopotential contours of larger molecules.[35] We postulate that the hydrophobicity induced by an atom i and measured at a point M of space decreases exponentially with the distance between this point M and the surface of atom i. The molecular hydrophobicity potential at a point M in space is thus estimated according to the equation:

$$MHP_M = \sum_{i=1}^{N} E_{tri} \exp\left(r_i - d_i\right)$$

where N are all the atoms of the molecule, E_{tri} is the transfer energy of the atom i, r_i is the radius of the atom i, and d_i is the distance between the atom i and the point M. E_{tri} is the energy required to transfer an atom i from an hydrophobic to an hydrophilic medium. Atomic E_{tri} were calculated from the molecular E_{tr} compiled by Tanford,[54] assuming that molecular E_{tr} are the sum of the atomic E_{tr}. Atomic E_{tr} values were derived for seven different types of atoms.

The isopotential surfaces of protein hydrophobicity were then calculated by a cross-sectional computational method. A 1-Å-mesh-grid plane was set to sweep across the molecule by steps of 1 Å. At each step, the sum of the hydrophobicity

A

Hydrophobic restraint	Perturbation restraint	Charge gradient	Total restraint	Charge restraint	Rot X	Rot Y	Rot Z	Mass centre penetration	Angle1 vs. bilayer normal	Angle2 vs. bilayer normal	Z max	Z min	Surface Phi	Surface Phi	Surface inter	x coord atom 1	y coord atom 1	z coord atom 1	x coord atom 2	y coord atom 2	z coord atom 2	x coord atom 3	y coord atom 3	z coord atom 3	Surface (Å²)	Angle plan vs. bilayer normal
1.50	0.00	0.00	1.50	0.00	5.00	3.10	0.81	25.62	33.19	77.55	-18.37	-32.24	0.15	2403.43	0.00	12.59	-1.14	4.02	12.02	-1.67	2.80	11.14	-0.62	2.14	0.00	109.68
1.51	0.00	0.00	1.51	0.00	7.30	2.37	-1.00	27.00	34.76	80.29	-19.73	-33.62	0.01	2403.57	0.00	12.73	-0.78	3.67	12.12	-1.38	2.50	11.21	-0.37	1.82	0.00	108.67
1.51	0.00	0.00	1.51	0.00	9.56	4.51	2.36	25.67	33.16	80.23	-18.88	-32.37	0.06	2403.52	0.00	12.46	-1.15	4.43	11.30	-1.75	3.24	11.06	-0.73	2.48	0.00	105.37
1.51	0.00	0.00	1.51	0.00	9.24	7.91	-2.26	26.16	33.83	78.00	-19.73	-32.35	0.02	2403.56	0.00	12.68	-1.91	3.41	11.39	-2.41	2.21	11.16	-1.40	1.58	0.00	103.21
1.51	0.00	0.00	1.51	0.00	11.18	12.73	-4.24	27.38	35.58	76.42	-20.13	-34.82	0.01	2403.57	0.00	12.53	-2.87	3.04	11.82	-3.41	1.35	11.05	-2.29	1.25	0.00	98.20
1.51	0.00	0.00	1.51	0.00	14.09	12.43	0.19	26.55	36.56	78.87	-19.54	-33.88	0.02	2403.55	0.00	12.33	-2.63	4.15	11.64	-3.23	3.02	10.93	-2.16	2.21	0.00	96.65
1.51	0.00	0.00	1.51	0.00	15.98	12.11	4.67	28.13	37.43	80.60	-21.32	-35.31	0.00	2403.58	0.00	11.97	-2.42	5.19	11.38	-3.06	4.03	10.73	-2.02	3.13	0.00	95.85
1.51	0.00	0.00	1.51	0.00	20.95	10.24	8.37	28.28	37.00	85.81	-22.00	-35.01	0.00	2403.58	0.00	11.66	-1.57	6.14	11.16	-2.33	5.01	10.55	-1.39	3.98	0.00	94.34
1.51	0.00	0.00	1.51	0.00	24.87	11.74	9.33	23.18	31.32	88.62	-22.64	-35.82	0.00	2403.58	0.00	11.51	-1.45	6.44	11.01	-2.27	5.36	10.44	-1.39	4.25	0.00	91.82
1.51	0.00	0.00	1.51	0.00	29.08	13.79	6.60	27.45	31.35	91.49	-20.61	-33.96	0.00	2403.57	0.00	11.77	-1.33	5.96	11.19	-2.27	4.37	10.59	-1.45	3.83	0.00	88.13
1.51	0.00	0.00	1.51	0.00	26.05	14.36	9.75	27.62	83.62	88.57	-20.64	-34.51	0.00	2403.57	0.00	11.42	-1.82	6.52	10.88	-2.64	5.45	10.35	-1.76	4.33	0.00	89.10
1.51	0.00	0.00	1.51	0.00	29.39	14.98	11.67	27.45	90.82	91.84	-20.44	-34.08	0.00	2403.57	0.00	11.17	-1.49	7.01	10.66	-2.37	5.36	10.18	-1.57	4.78	0.00	86.82
1.50	0.00	0.00	1.50	0.00	28.27	16.83	12.47	26.21	88.38	89.52	-18.82	-33.42	0.09	2403.49	0.00	11.01	-2.06	7.11	10.49	-2.90	6.05	10.05	-2.04	4.87	0.00	85.84
1.53	0.01	0.00	1.54	0.00	31.43	11.57	8.04	24.23	34.53	84.82	-17.21	-31.01	1.57	2408.01	33.21	11.62	-0.63	6.37	11.11	-1.58	5.40	10.52	-0.84	4.21	0.00	83.04
1.49	0.00	0.00	1.49	0.00	27.56	16.56	6.34	25.31	86.37	83.10	-17.96	-32.52	0.47	2409.10	13.94	11.61	-2.07	6.09	11.00	-2.90	5.07	10.46	-2.03	3.94	0.00	86.36
1.47	0.00	0.00	1.48	0.00	28.40	18.51	6.15	25.40	86.34	88.32	-17.71	-32.35	0.77	2408.81	23.63	11.62	-2.37	5.36	10.97	-3.20	4.36	10.44	-2.33	3.83	0.00	84.25
1.47	0.00	0.00	1.47	0.00	28.33	18.02	2.26	25.27	87.36	89.09	-17.67	-32.72	0.84	2408.74	23.63	12.01	-2.28	5.15	11.30	-3.11	4.20	10.63	-2.24	3.11	0.00	84.71
0.65	0.08	0.00	0.72	0.00	27.35	18.46	-1.93	23.65	86.62	88.03	-15.97	-31.28	17.78	2391.79	130.66	12.34	-2.46	4.21	11.56	-3.27	3.30	10.87	-2.38	2.27	0.00	84.87
-0.36	0.29	0.00	-0.67	0.00	29.00	15.71	-6.70	22.18	83.71	91.01	-14.37	-29.08	67.20	2342.38	367.41	12.75	-1.74	3.24	11.33	-2.61	2.42	11.12	-1.79	1.43	0.00	86.07
0.24	0.11	0.00	0.36	0.00	29.00	15.71	-6.70	23.53	86.84	91.23	-15.62	-31.11	26.17	2383.41	173.01	12.72	-2.33	3.00	11.82	-3.20	2.25	11.04	-2.39	1.23	0.00	81.00
1.43	0.02	0.00	1.52	0.00	29.00	15.71	-6.70	23.74	93.08	96.04	-16.71	-30.43	5.57	2404.00	36.05	12.70	-0.91	3.72	11.35	-1.87	2.35	11.14	-1.16	1.87	0.00	85.09
0.37	0.11	0.00	0.48	0.00	29.00	15.71	-6.70	23.33	88.26	92.44	-15.65	-30.57	25.72	2383.85	211.17	12.73	-2.01	3.15	11.87	-2.90	2.40	11.08	-2.11	1.37	0.00	81.84
-0.26	0.15	0.00	-0.11	0.00	31.74	19.62	-9.44	23.31	86.37	90.44	-15.35	-31.00	35.77	2373.80	227.26	12.76	-2.45	2.72	11.84	-3.30	1.36	11.04	-2.47	0.39	0.00	81.33

FIGURE 9.4 Pex file example (top) and graphic representation (bottom). (See text for details.)

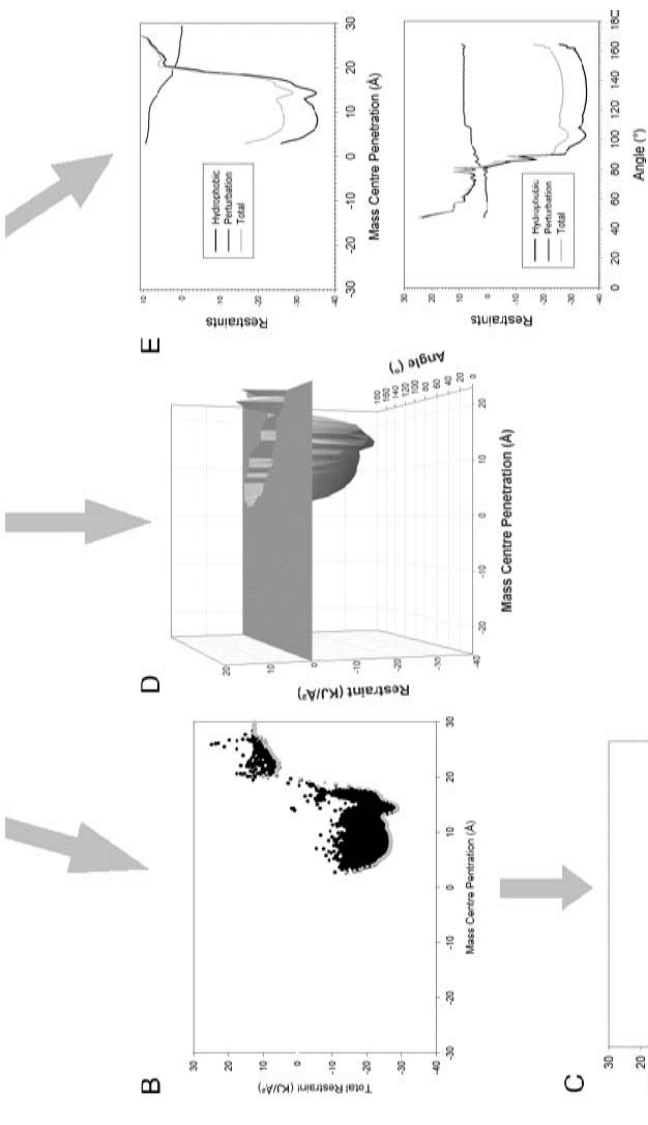

FIGURE 9.4 (continued)

and hydrophilicity values at all the grid nodes was calculated. The hydrophobic and hydrophilic MHP surfaces were then drawn by joining the isopotential values.

9.3 RESULTS

9.3.1 Efficiency of Monte Carlo Method Applied to Short Peptides and Membrane Proteins

9.3.1.1 Hydrophobic Peptides

Different peptides have already been studied in order to evaluate the Monte Carlo method by comparison with known experimental data. Different amphipathic, transmembrane[31] and tilted peptides[55] have been analyzed in this goal.

18A is a synthetic amphipathic peptide shown to be α-helical and adsorbed at the water–lipid interface.[56] In Figure 9.5, the restraint envelope is a function of the peptide mass center penetration and axis tilt with respect to the membrane surface. In its energy minimum position, the peptide is at the surface of the model bilayer. For the 18A peptide, the energy minimum is reached when the peptide is in membrane at about 16 Å of the bilayer center with a tilt of 10°, the position varies between 14-18 Å and 0-20° of angle of insertion, demonstrating that the peptide finds its local minimum in a position parallel to the interface, which corresponds to a perfectly amphipathic structure.

The M2δ peptide is a transmembrane α-helix present in the acetylcholine receptor that can induce the lysis of red blood cells.[57] The peptide is biamphipathic and, in the presence of a bilayer, it stands almost perpendicularly (around 70°) to the plane in a transmembrane configuration.[31]

The fusion peptide SIV (simian immunodeficiency virus) was among the first tilted peptides described by molecular modeling (Figure 9.5.C). Tilted peptides have 10 to 20 residues and a peculiar hydrophobicity profile. When analyzed in a helix

---

FIGURE 9.5 (opposite) The different plots correspond to the peptides 18A (A), M2δ (B), and SIV (C). IMPALA simulations are shown as 3D plots of the restraint energy vs. the penetration of the peptide mass center and vs. the angle of insertion of a reference vector. The reference vector is defined by 2 atoms of a helix or a strand, and the angle of this vector with the XY plane is the index of the peptide orientation in the bilayer. The protein mass center penetration in angstroms is plotted on the X axis (0 is the bilayer center); the Y axis is the angle in degrees of the reference vector. The restraint values are plotted along the Z axis. The energy minimum zones (light gray) locate the most favorable positions of the peptides. The 3D envelopes are calculated as follows: a 2D grid using as X axis the position of the molecule mass center between –15 and 15 Å, by steps of 0.5 Å, and along the Y axis, the angle of the helix with respect to the plane of the bilayer by steps of 3°. Next, for each grid knot, the minimal energy restraint is plotted. Data are extracted from the Pex2dstat files. The ribbon picture of the most stable conformation of each peptide is shown in the model membrane of IMPALA. The dotted line is the center of the bilayer (Z = 0 Å) and the black line defines where the polar heads of lipids start (z = ±13.5 Å). The gray line is the water–lipid interface (z = ±18 Å).

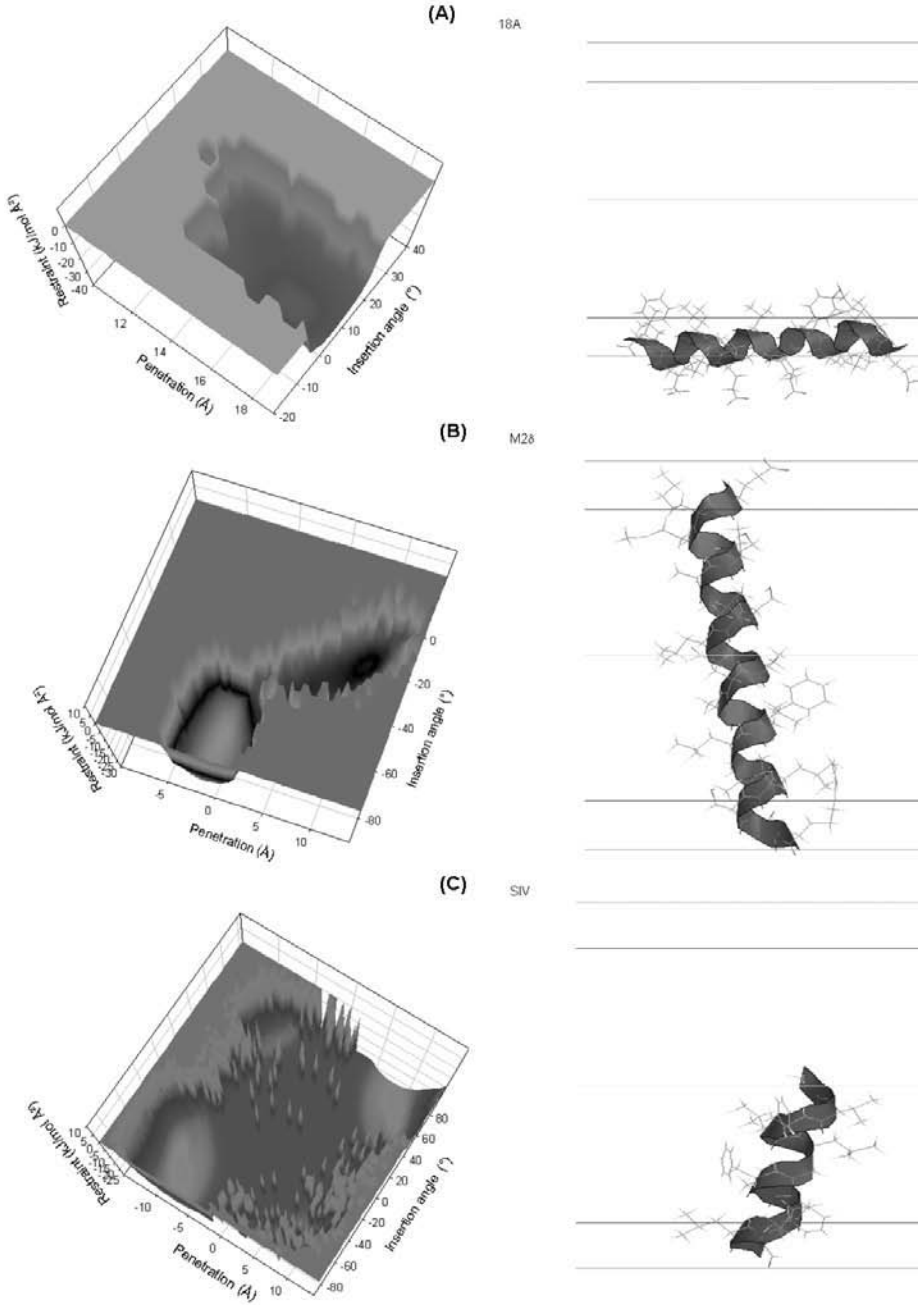
(A)
18A
Penetration (kJ/mol Å²)
Penetration (Å)
Insertion angle (°)
(B)
M2δ
Penetration (kJ/mol Å²)
Penetration (Å)
Insertion angle (°)
(C)
SIV
Penetration (kJ/mol Å²)
Penetration (Å)
Insertion angle (°)

FIGURE 9.5

conformation, the peptide hydrophobicity splits up in an asymmetric gradient: a more hydrophobic extremity at one side decreasing towards the other extremity of the helix.[45] These peptides insert in a tilted way with respect to the membrane interface and are able, *in vitro*, to destabilize the liposomal membranes and lead to their fusion.[58] The 3D envelope of the SIV fusion peptide shows that the surface of minimal energy is large, which means that the peptides may adopt an insertion angle which varies around 50°. In our calculations, the mass center penetration varies from (±) 8 to (±) 10 Å and the peptide inserts with an angle of about 50 to 60° with different local minima. Their tilted orientation, due to the hydrophobicity gradient, allows destabilizing the regular organization of the acyl chains of membrane lipids.

9.3.1.2 Membrane Proteins

Following validation of the method with peptides whose orientation is experimentally known, and since there was a good concordance between predictions and experimental observations, membrane proteins of known structure were processed. The formation of the dimer of Glycophorin A has been studied; the restraint terms increase the efficiency of the Monte Carlo algorithm to reach the dimer structure from monomers; this analysis was the first step to evaluate interactions between transmembrane parts of polytopic proteins.[59]

Bacteriorhodopsin was the first structurally described IMP.[60] It is found as a 2D crystal in the internal membrane of archaebacteria *Halobacterium salinarium*. Each monomer of the bacteriorhodopsin contains seven transmembrane α-helices and covalently binds a retinal chromophore by a lysine of the seventh transmembrane helix. In response to illumination, the geometry of the retinal is modified from a *trans* to a 13-*cis* configuration. This transconformation initiates a set of steps including a large conformational change of the protein and leads to translocation of a proton from the interior to exterior of the cell, which in turn puts the retinal and the protein back to their initial state. The transmembrane gradient of protons provides a way to capture and use light energy in order to allow ATP synthesis in the cell. Three of the helices are almost normal to the surface of the membrane, while four are tilted to 70°.[61,62] The reference vector for the insertion angle is localized into the first helix (Trp7-Phe22).

In Figure 9.6A, the 3D envelope shows a position of the protein mass center around –2 Å and an orientation of about –70°, which is in agreement with experimental observations. In the case of the β-Barrel proteins, the first IMP described was a porin of the external membrane of a gram-negative bacteria. Proteins with similar structures were further suspected in the external membranes of mitochondria and chloroplasts.[63]

Porins have a molecular weight between 28 and 48 kDa. They are made of 8 to 22 antiparallel strands organized in β-sheets making a barrel that delimits a channel. They are able to transfer small hydrophilic molecules, but no macromolecules, from outside to inside the cell and are associated with the peptidoglycan as well as the lipopolysacharides of the bacterial cell wall.[64]

Maltoporin, a homotrimer of β-barrel found in the external membrane of *Escherichia coli,* has been tested with our model of lipid bilayer. The function of this

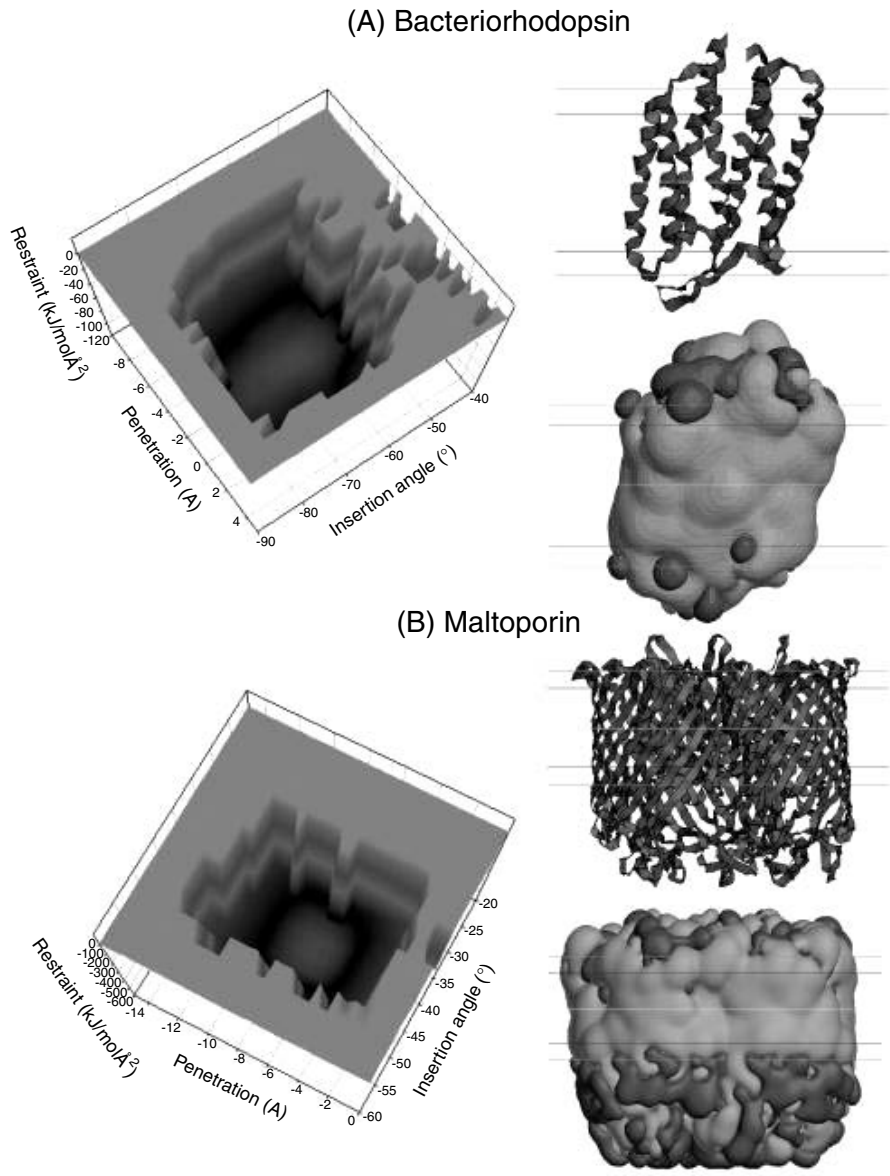

FIGURE 9.6 The different plots correspond to the bacteriorhodopsin (A) and to the maltoporin (B). 3D envelopes are shown as in Figure 9.5. An MHP plot is added. Dark gray surfaces of MHP are hydrophilic, light gray are hydrophobic.

protein is to facilitate diffusion of the maltodextrines across the *E. coli* cell wall. The protein structure was determined at a 2.4 Å resolution by Wang et al.[65] In the Monte Carlo minimization, the reference strand is the vector between the C_α of Thr40 and Gln48 of the monomer A. All strands are tilted to about 45° as compared

to the axis of the barrel. In Figure 9.6B, the 3D envelope of the restraints shows a local minimum at –40° for orientation of the β-sheet and a mass center penetration at about –7 Å. The mass center is shifted because of all the hydrophilic loops at the extremity of the pore of each monomer which move into an aqueous environment.

Validation of the method now allows testing *ab initio* or homology models of membrane proteins of unknown structures, to try to authenticate the insertion and structure of the model within a lipid environment.

9.3.2 Penetratin

Penetratins are cell-permeant peptides that can carry various sorts of cargoes into live cells and hence are now considered as vectors to develop new therapeutic tools. However, the mechanisms of penetratin cellular entry remain unknown. To get insight into the process of its membrane crossing and to provide a framework for further design of new derivatives, we have used the Monte Carlo method to model the penetratin membrane interactions.

For this aim, different analyses have been performed on:

Antennapedia homeodomain in complex with a double-stranded DNA cognate site (AntHD–DNA complex)
Antennapedia homeodomain alone (AntHD)
First helix of AntHD (RYQTLELEKEFHF)
Second helix of AntHD (RRRRIEIAHAL)
Third helix of AntHD corresponding to the penetratin sequence (pAntp; RQIKIWFQNRRMKWKK)

The AntHD–DNA complex structure, 9ent, has been determined by x-ray and NMR analysis.[66] The complex is represented in Figure 9.7A with each of the AntHD helices. For sake of clarity, hydrogen atoms are not represented but are accounted for in subsequent analysis. The 9ent structure and three homeodomain helices have been imported in the HyperChem V6 (Hypercube, Inc., Florida) software, and the AMBER force field has allowed us to attribute the atomic charges (Figure 9.7B).

The AntHD–DNA complex is highly negatively charged due to the phosphate groups of the double-strand DNA. The sum of the atomic charges, obtained from the AMBER force field, leads to a total charge of –18.23, whereas the AntHD peptide in the absence of the DNA sequence has a total charge of +11.76.

The first homeodomain helix (Figure 9.7B, top) contains three negatively charged (Glu), one positively charged (Arg), and two polar residues (Tyr, His). Nevertheless, according to the AMBER force field, its total charge is equal to zero. The second homeodomain helix (Figure 9.7B, middle) has five charged residues: four arginines at its N-terminal, a glutamic acid, and a polar amino acid (His). Its global charge is about +4.00. Among the 16 amino-acid residues of the penetratin sequence (Figure 9.7B, bottom), only four are hydrophobic. The others are charged or polar, conferring to this helix a global charge of +6.76.

If calculation of atomic charges gives information about the polarity of the Antennapedia homeodomain and its constitutive α-helices, calculation of molecular

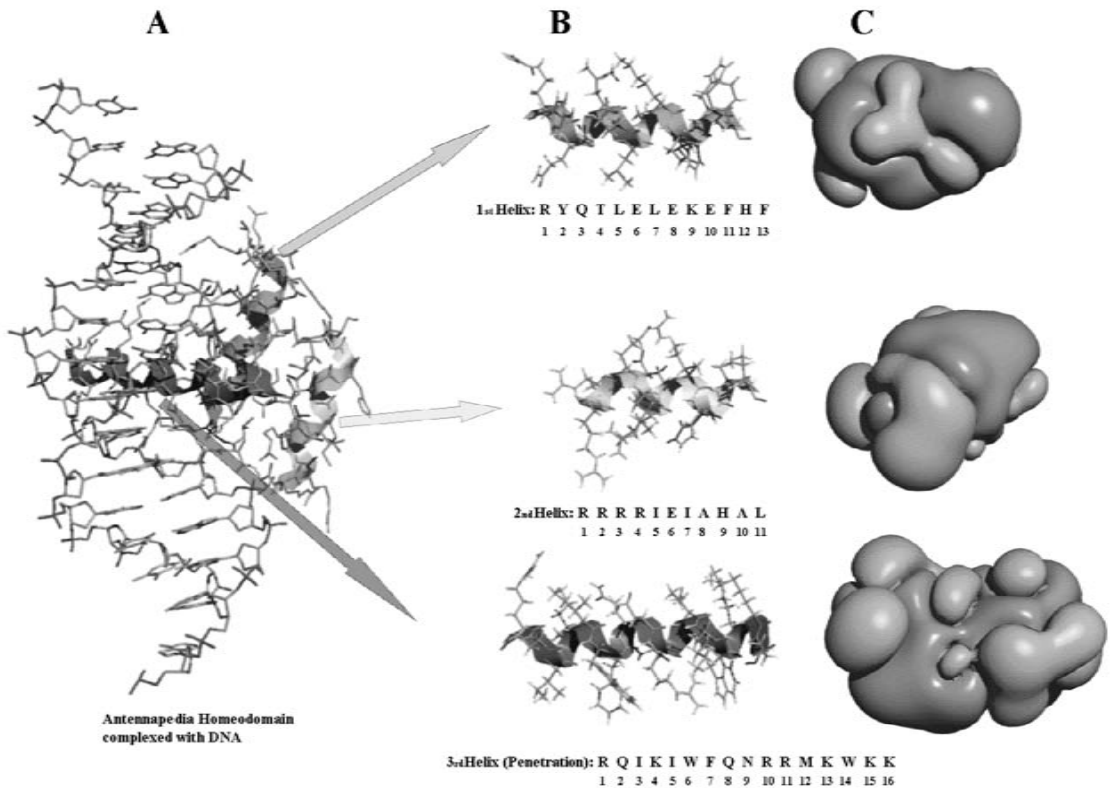

FIGURE 9.7 (Color Figure 9.7 follows p. 14.) AntHD–DNA complex from 9ent (A) and its constitutive helices (B). Column C represents molecular hydrophobicity potentials of each helix.

hydrophobicity potential (MHP) (Figure 9.7.C) provides an idea about the hydrophobicity distribution. Figure 9.7.C shows the partition of the hydrophilic (green) and the hydrophobic (orange) areas for each of the homeodomain helices. All helices are amphiphilic. The hydrophilic and hydrophobic partition is balanced for the first helix; a first hydrophilic domain is made of Arg1, Tyr2, and Cys3, followed by an important hydrophobic domain flanking a next hydrophilic domain defined by Glu6, Glu8, Lys9, and Glu10.

For the second helix, there is an evident segregation between a bulking hydrophilic domain (Arg1, Arg2, Arg3, and Arg4) and a C-terminal hydrophobic domain (Ile7, Ala8, Ala10, and Leu11). Finally, the penetratin helix (pAntp) has numerous hydrophilic domains spread all along the sequence. At the beginning of the sequence, one is due to Arg1 and Gln3. Then, a smaller hydrophilic domain is formed by the polar residues (Gln8, Asn9); charged residues are defining an important hydrophilic domain at the pAntp C-terminal extremity (Lys13, Lys15, and Lys16). An important hydrophobic domain is contributed by Trp6 and Phe7.

9.3.2.1 Uncharged Membrane Model

Figure 9.8 shows the Monte Carlo simulation results obtained for AntHD–DNA, AntHD, and the three homeodomain helices. The graph in the middle of the figure shows evolution of the global energetic restraint (hydrophobic and lipid perturbation restraints are summed) for each molecule or complex as a function of their mass center penetration Z ordinate. The two dotted lines mark the boundary of the phospholipid polar heads of the membrane external leaflets (between 18 and 13.5 Å) and the bilayer center corresponds to the 0 Å Z ordinate. The simulations were started with the molecule mass center located at 35 Å. At the end of the calculation, the lowest value of global energy restraint indicates the most probable position of the molecules in the bilayer.

Therefore, it is revealed from simulations that the AntHD–DNA complex stabilizes when its mass center is located at 34.5 Å from the bilayer center. When it approaches the bilayer, the energy restraint slowly, then severely, increases as the complex reaches 28.5 Å. Closer to the membrane, the restraint values are tremendous; the Monte Carlo procedure predicts that the complex cannot enter the bilayer. A similar profile is obtained for the homeodomain alone, even if the energy restraint is higher. The AntHD stabilizes at almost the same position as it does when in the AntHD–DNA complex (i.e., 27.5 Å).

If the energy restraint evolution curves for AntHD–DNA and AntHD penetrations are similar, the position of each subdomain (Figure 9.8A and 9.8B) are different at the restraint minimum value: for the AntHD–DNA complex, the third helix is in interaction with the double-strand DNA, and the other two helices, especially the first one (Figure 9.8C) are near the external sheet phospholipid polar heads. Conversely, when the DNA is removed, the third helix is close to the phospholipid heads; the other helices lie more distantly. This preferential interaction between the third helix and the phospholipids may be attributed to its amphiphilicity.

In order to go further in our analysis and to evaluate the contribution of each helix to interaction with the bilayer and, even more, to provide a model for penetratin

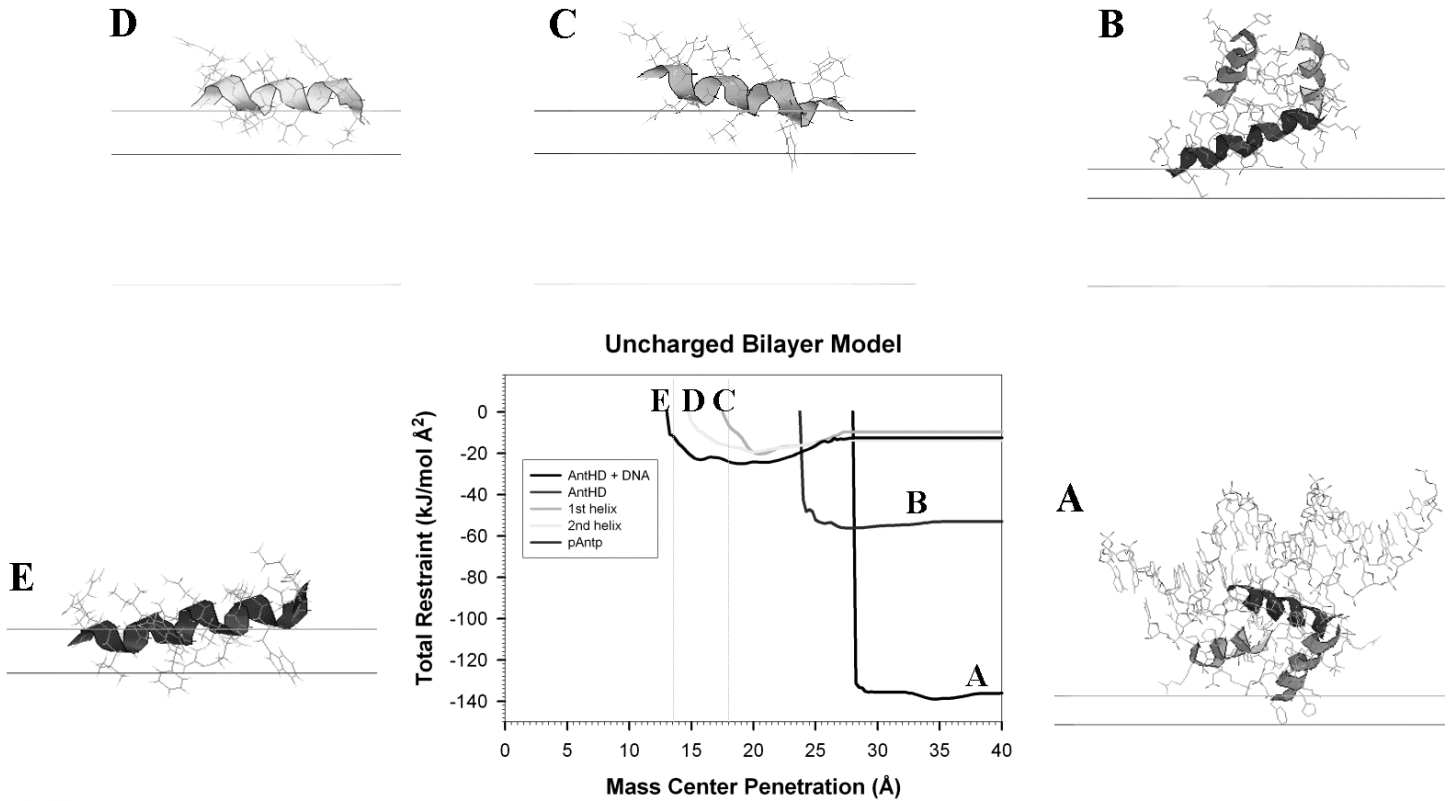

FIGURE 9.8 The center of the figure represents evolution of the total restraint vs. the mass center penetration of all simulated compounds in an uncharged bilayer model. Figures 9.8A, B, C, D, and E represent the position and the orientation of AntHD–DNA complex, AntHD, 1st helix, 2nd helix, pAntp, respectively, at the energy minimum value.

translocation across the bilayer, we applied the Monte Carlo procedure to each helix separately. The energy restraint evolution as a function of the mass center penetration shows that no helix can cross the uncharged bilayer model. However, the pAntp interacts more closely with the phospholipid polar heads (Figure 9.8E) than the second helix (Figure 9.8D), which adsorbs to the membrane, and than the first one (Figure 9.8C), which almost does not interact with the polar heads.

In conclusion, these Monte Carlo simulations performed with an uncharged bilayer model clearly show that no Antennapedia-derived peptide is predicted to cross the membrane. These results are in agreement with the MHP analysis: the charged and polar residues within the three homeodomain helices make them particularly hydrophilic so that they cannot enter the hydrophobic core of a biological membrane.

9.3.2.2 Charged Bilayer Model

Biological membranes are rarely symmetrical in lipid and protein composition. The uncharged model of lipid bilayer used in the first round of simulations described earlier mimics a membrane made of only neutral phospholipids (PL°). However, if the major membrane components of the eukaryotic organisms are PL°, it has been shown[67] that negatively charged phospholipids (PL^-) also enter in the composition of membranes. These PL^- are asymmetrically distributed between both leaflets of membranes. Moreover, the asymmetric distribution of PL° and PL^- is different according to the cell type and is actively controlled by specific protein machineries.

The asymmetric presence of PL^- causes an electrostatic gradient in biological membranes. To take this into account, we introduced charges in both leaflets. The question then was to determine to which extent the force field produced by the charge asymmetry might influence passage of peptides through the model membrane. In order to start such simulations, we chose to set up a model of the human erythrocyte membrane. Cullis et al.[67] have calculated a superficial charge density of 8 μC/cm^2 (0.005 e^-/Å^2) for the erythrocyte membrane. This charge density is due to the presence of PL^- in the internal leaflet of the erythrocyte membrane. We performed new simulations, considering that the internal sheet of the bilayer had a charge density ranging from 0.005 e^-/Å^2 to 0.04 e^-/Å^2.

The results of the different simulations are presented in Table 9.2. According to these simulations, penetratin should cross a membrane when the superficial charge density is 0.01 e^-/Å^2. When the superficial charge density reaches 0.04 e^-/Å^2, the Antennapedia homeodomain, as well as the first helix, partially penetrates the membrane, while the second helix and the penetratin cross this membrane. We detailed two simulations in order to further explain the mechanism.

Figure 9.9A shows evolution of the hydrophobic, lipid perturbation (E_{lip}), and charge sum restraints as a function of mass center penetration of the AntHD–DNA, when considering a superficial charge density of 0.02 e^-/Å^2 in the inner leaflet. The two dotted lines delimit the phospholipid polar heads of the external leaflet. The bilayer center is defined by the 0 Å ordinate. Because the complex does not cross the membrane, only the outer leaflet bearing the charge was plotted.

TABLE 9.2
Internalization of Simulated Peptides as a Function of the Inner Sheet Superficial Charge Density

Inner sheet charge ($e^-/Å^2$)	AntHD + DNA	AntHD	1st helix	2nd helix	pAntp
No charge	–	–	–	–	–
0.005	–	–	–	–	–
0.01	–	–	–	–	+
0.02	–	–	–	–	+
0.04	–	±	±	+	++

The AntHD–DNA complex stabilizes when its mass center is located at a distance of 28 Å, where the minimum value of the total restraint is reached. This is closer to the bilayer than when this one is uncharged, due to the charge restraint, which tends to bring the complex close to the membrane. Nevertheless, there is no membrane insertion because the hydrophobic restraint increases, thus impairing any insertion. From 28 to 25 Å, the total restraint increases, suggesting that a localization of the complex close to the membrane is unlikely.

The lipid perturbation restraint is low (maximum value: 8 kJ/mol.$Å^2$) compared with the other restraints. This is consistent since the complex only partially penetrates within the polar head domain; therefore, it does not disturb the acyl chains of the phospholipids. When the homeodomain is not associated with the DNA (Figure 9.9B), its mass center comes near the external bilayer leaflet because of the charge distribution in the internal leaflet. Here again, the hydrophilic and hydrophobic balance of the homeodomain prevents the crossing: the hydrophobic restraint is unfavorable from 28 Å and increases when the homeodomain mass center approaches the bilayer.

The same graphics have been made for simulations of the isolated helices (Figure 9.9C, D, E, bottom). Moreover, in every helix we chose two reference atoms to draw a segment parallel to the helix axis. This allowed us to follow the evolution of the total restraint as a function of the positions of the mass center and of the angles of the helix axis vs. the bilayer plane center (Figure 9.9C, D, E, top).

Now, considering each helix separately, it appears that, for the first helix, which is the less charged, the most probable position is reached when its mass center is located at 20 Å. When the mass center gets closer to the membrane both hydrophobic and charge restraints increase. At the energy minimum, the helix makes an angle of –5° (from the N-term to the C-term) with respect to the bilayer plane; several residues (Gln3, Leu7, Phe11) therefore enter within the polar heads domain (results not shown).

For the second helix observations are similar, but the charge restraint is more favorable (this helix has a charge of +4.00). The mass center is then located at the external limit of the polar heads of the external leaflet (18 Å). Here again, hydrophobic restraint prevents the penetration of the second helix into the hydrophobic

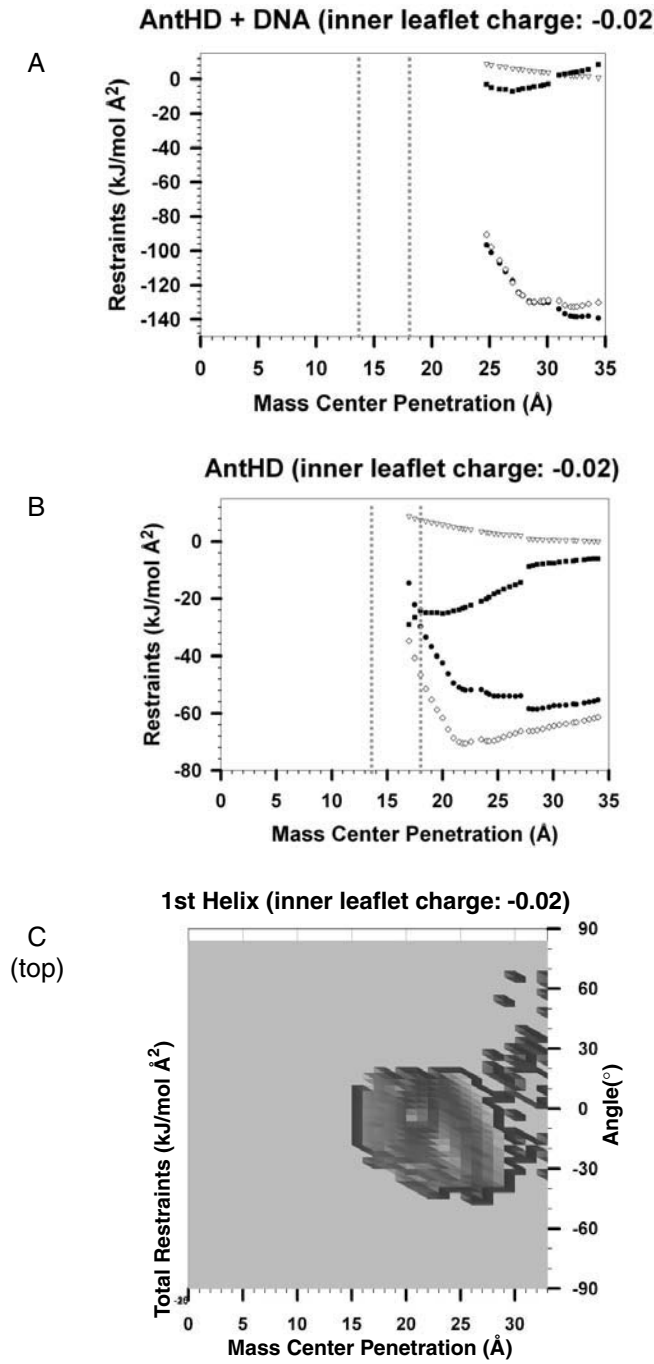

FIGURE 9.9 Evolution of the total restraint vs. mass center penetration of all simulated compounds in a charged bilayer model (inner leaflet charge: 0.02 $e^{-}/Å^{-2}$). (See text for details.)

(bottom)

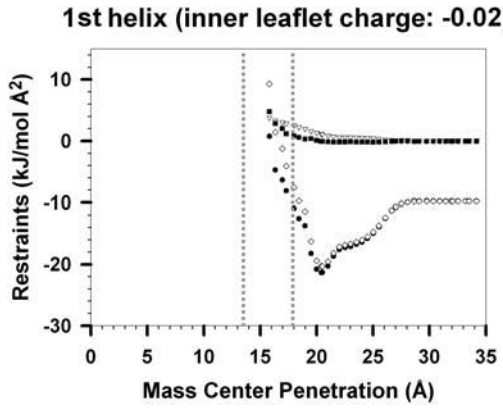

D
(top)

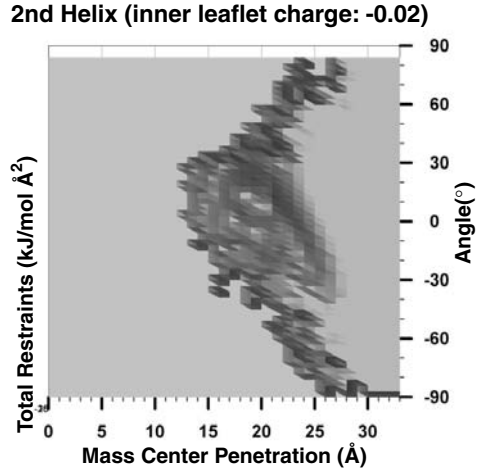

(bottom)

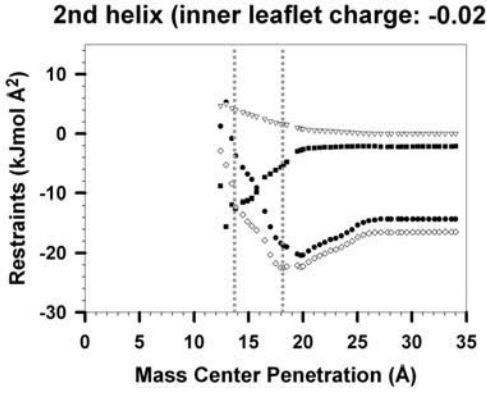

FIGURE 9.9 (continued)

E
(top)

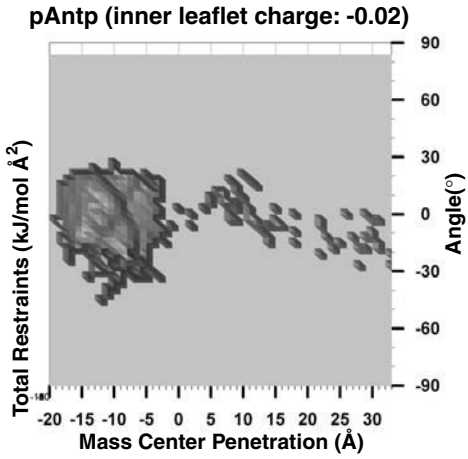

(bottom)

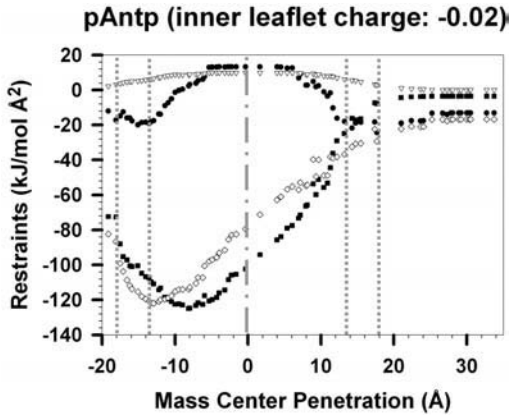

FIGURE 9.9 (continued)

core of the bilayer. The lipid perturbation restraint is similar to that calculated for the first helix and for the full-length homeodomain.

Finally, our simulations predict that, with such a charge distribution, the penetratin peptide may cross the bilayer due to the influence of membrane charges. This restraint is indeed greatly favorable during the bilayer crossing simulation. Furthermore, the evolution of the hydrophobic restraint suggests that the helix hydrophobic properties would not allow crossing the bilayer hydrophobic core in the absence of the superficial charge density located at the internal leaflet. However, although the charge restraint becomes unfavorable from –10 Å, the hydrophobic restraint, in turn, becomes favorable, and allows the mass center of the third helix to stabilize at –13 Å, forming a 3° angle with the bilayer plan. The discontinuous course during crossing (indicated by dots, Figure 9.9E, top) suggests that the crossing is very rapid. Lipid perturbation restraint stays at the same level as for the previous simulations (8 kJ/mol.Å^2), indicating that the crossing has no major destabilizing effects on the

phospholipid organization. Importantly, when pAntp has reached the energy minimum, its Trp6 residue interacts with the polar heads, whereas Trp14 is embedded within the hydrophobic core of the bilayer model.

Simulations were then performed with a superficial charge density at the inner leaflet of the bilayer model equal to 0.04 $e^{-}/Å^2$. As shown in Figure 9.10A, the AntHD–DNA complex is predicted to reach the same position as with the previous membrane model. The increase in charge density induces an increase of the charge restraint when the complex mass center reaches positions below 28 Å, but not before.

For the AntHD without DNA (Figure 9.10B), a partial crossing of the bilayer is observed, basically due to the charge restraint, since the hydrophobic restraint is largely unfavorable and the lipid perturbation restraint is important too (20kJ/mol.$Å^2$). In its final configuration, the AntHD mass center is located near the bilayer center (–4 Å), but this implies that part of the third helix interacts with the polar heads domain of the inner leaflet (Arg1, Arg10, Arg16 residues).

Taken separately, the first helix (Figure 9.10C) is predicted to enter the polar heads domain of the outer leaflet, with its mass center stabilizing at 15 Å. Then, the Monte Carlo procedure opens the way to a jump over the restraint barrier; indeed, using this method we switch between two local energy minima. The penetration of the first helix in the membrane is driven by the favorable charge restraint because the hydrophobic restraint is still unfavorable during the partial crossing.

The second helix entirely crosses the bilayer hydrophobic core (Figure 9.10D bottom) as an effect of the charge restraint, with the hydrophobic restraint, as for the previous simulations, unfavorable during the crossing. Here again, the absence of a continuous path to reach the most favorable position (Figure 9.10D top) is indicative of a rapid crossing.

The third helix, pAntp, crosses the membrane, too, but the energy minimum is less favorable than that reached in the case of helix 2 (Figure 9.10E bottom). Moreover, pAntp orientation at its energy minimum indicates that the helix forms an angle of –53° with the bilayer plane (Figure 9.10E top), with the pAntp N-terminal part buried within the hydrophobic core of the membrane and the C-terminal part interacting with the phospholipid polar heads of the inner leaflet.

9.4 CONCLUSIONS

We have developed a new computational method to simulate interactions between chemical compounds and a modeled membrane. This method has been tested and validated with peptides and proteins for which experimental data regarding their interactions with membranes were available. We applied this to the Antennapedia homeodomain and its derivatives, such as the penetratin cell-permeant peptides, in order to account for their behavior when facing membrane models. According to our analysis, in the case of an uncharged membrane model, neither the complete Antennapedia homeodomain nor its constitutive helices are able to cross the bilayer.

By refining our simulation methods in order to approach more reliably true biological membranes, we elaborated a charged bilayer model. In this context, we observe that, with the increase of the superficial charge density of the bilayer inner

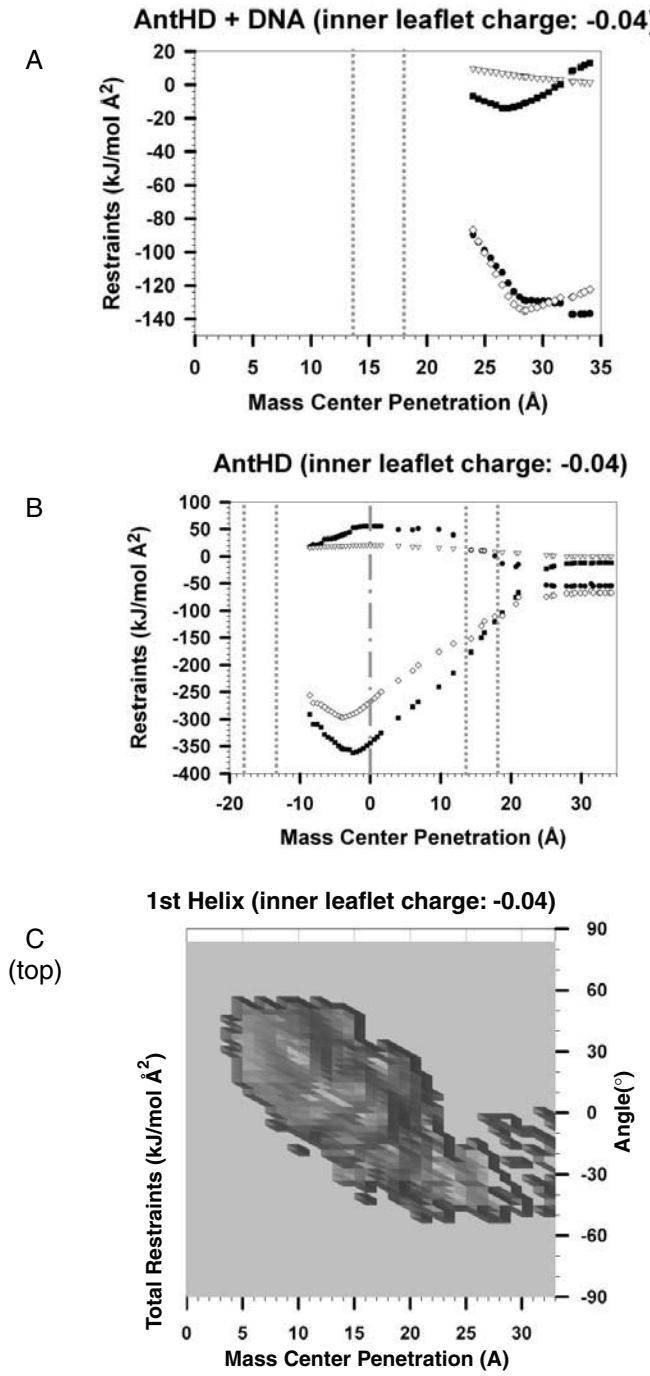

FIGURE 9.10 Evolution of total restraint vs. mass center penetration of all simulated compounds in a charged bilayer model (inner leaflet charge: 0.04 $e^{-}/Å^{-2}$). (See text for details.)

(bottom)

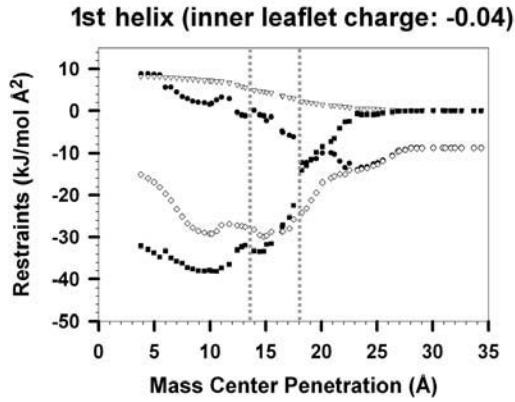

D
(top)

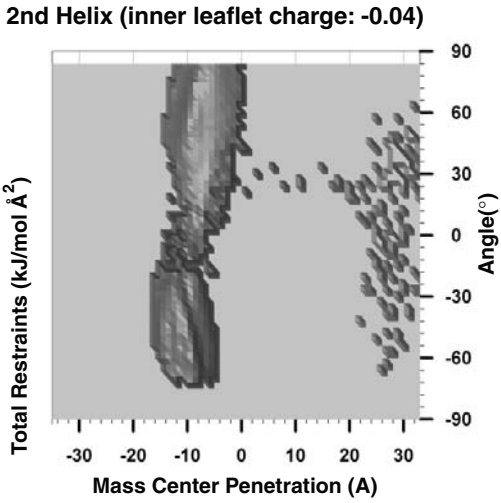

(bottom)

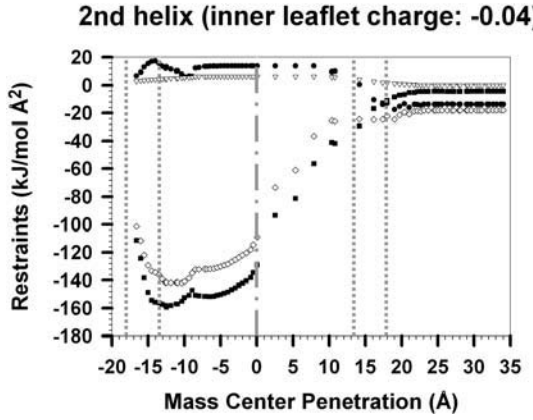

FIGURE 9.10 (continued)

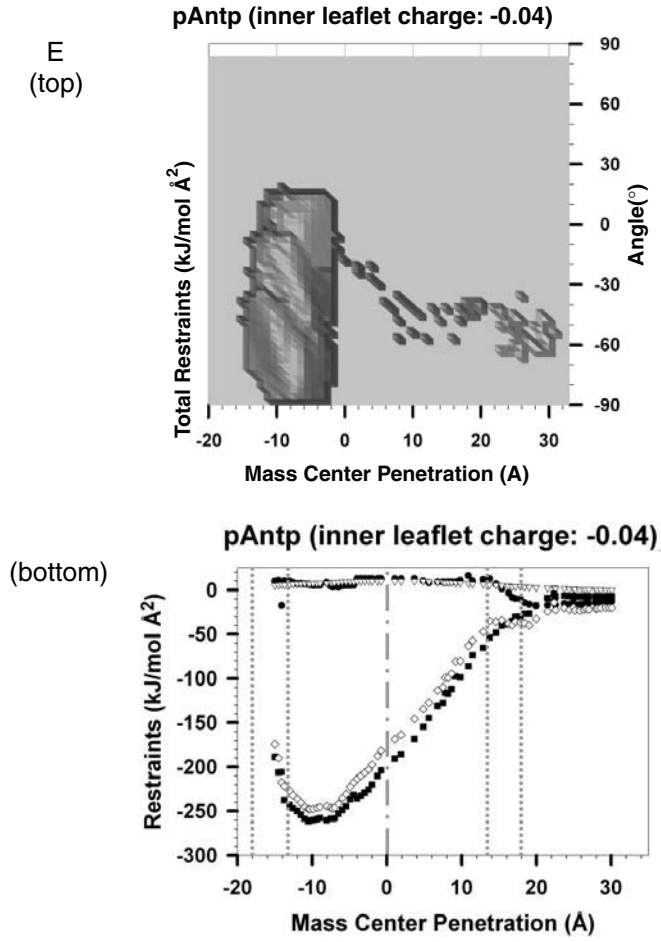

FIGURE 9.10 (continued)

leaflet, penetratin, the second helix, of the Antennapedia homeodomain, its first helix, and the entire homeodomain are predicted to penetrate, at least partially, in the membrane. Therefore, we suggest that the charge gradient within biological membranes would constitute an important factor for driving translocation of penetratins and homeodomains through biological membranes.

These results are not contradictory with, but rather complete, models built up according to previously published experimental data.[17,68,69] These models suggested formation of inverted micelle with negatively charged phospholipids during the crossing of biological membranes. Indeed the presence of PL^-, may constitute the first step enabling penetratin to interact with the membrane, to be followed by formation of inverted micelles. This new computer-based method should be very useful for screening and designing new peptide derivatives with cell-permeant potential.

ACKNOWLEDGMENTS

Olivier Bouffioux has been supported by the Ministère de la Région Wallonne, contract # 97/13649. Frédéric Basyn thanks the National Funds for Scientific Research of Belgium (FNRS) (Télévie) for financial support. René Rezsohazy is postdoctoral researcher at the National Funds for Scientific Research of Belgium. Robert Brasseur is research director at the National Funds for Scientific Research of Belgium. This work was supported by the European Community biotech contract BIO4-98-0227 and by the Interuniversity Poles of Attraction Program — Belgian State, Prime Minister's Office — Federal Office for Scientific, Technical, and Cultural Affairs PAI contract # P4/03.

REFERENCES

1. Banerjee–Basu, S., Ryan, J.F., and Baxevanis, A.D., The homeodomain resource: a prototype database for a large protein family, *Nucleic Acids Res.*, 28, 329, 2000.
2. Krumlauf, R., Hox genes in vertebrate development, *Cell*, 78, 191, 1994.
3. Wolberger, C., Homeodomain interactions, *Curr. Opin. Struct. Biol.*, 6, 62, 1996.
4. Passner, J.M. et al., Structure of a DNA-bound ultrabithorax-extradenticle homeodomain complex, *Nature*, 397, 714, 1999.
5. Piper, D.E. et al., Structure of a HoxB1-Pbx1 heterodimer bound to DNA: role of the hexapeptide and a fourth homeodomain helix in complex formation, *Cell*, 96, 587, 1999.
6. Niessing, D. et al., Homeodomain position 54 specifies transcriptional vs. translational control by Bicoid, *Mol. Cell*, 5, 395, 2000.
7. Schnabel, C.A. and Abate–Shen, C., Repression by HoxA7 is mediated by the homeodomain and the modulatory action of its N-terminal-arm residues, *Mol. Cell Biol.*, 16, 2678, 1996.
8. Zhang, H., Catron, K.M., and Abate–Shen, C., A role for the Msx-1 homeodomain in transcriptional regulation: residues in the N-terminal arm mediate TATA binding protein interaction and transcriptional repression, *Proc. Natl. Acad. Sci. U.S.A.*, 93, 1764, 1996.
9. Zhang, N. et al., Three distinct domains in the HOX-11 homeobox oncoprotein are required for optimal transactivation, *Oncogene*, 13, 1781, 1996.
10. Kim, Y.H. et al., Homeodomain-interacting protein kinases, a novel family of co-repressors for homeodomain transcription factors, *J. Biol. Chem*, 273, 25875, 1998.
11. Li, X., Murre, C., and McGinnis, W., Activity regulation of a Hox protein and a role for the homeodomain in inhibiting transcriptional activation, *EMBO J.*, 18, 198, 1999.
12. Zappavigna, V. et al., HMG1 interacts with HOX proteins and enhances their DNA binding and transcriptional activation, *EMBO J.*, 15, 4981, 1996.
13. Zappavigna, V., Sartori, D., and Mavilio, F., Specificity of HOX protein function depends on DNA–protein and protein–protein interactions, both mediated by the homeodomain, *Genes Dev.*, 8, 732, 1994.
14. Ohneda, K. et al., The homeodomain of PDX-1 mediates multiple protein–protein interactions in the formation of a transcriptional activation complex on the insulin promoter, *Mol. Cell Biol.*, 20, 900, 2000.
15. Zhang, H. et al., Heterodimerization of Msx and Dlx homeoproteins results in functional antagonism, *Mol. Cell Biol.*, 17, 2920, 1997.

16. Le Roux, I. et al., Neurotrophic activity of the Antennapedia homeodomain depends on its specific DNA-binding properties, *Proc. Natl. Acad. Sci. U.S.A.*, 90, 9120, 1993.
17. Derossi, D. et al., The third helix of the Antennapedia homeodomain translocates through biological membranes, *J. Biol. Chem*, 269, 10444, 1994.
18. Joliot, A. et al., Identification of a signal sequence necessary for the unconventional secretion of Engrailed homeoprotein, *Curr. Biol.*, 8, 856, 1998.
19. Maizel, A. et al., A short region of its homeodomain is necessary for Engrailed nuclear export and secretion, *Development*, 126, 3183, 1999.
20. Chatelin, L. et al., Transcription factor hoxa-5 is taken up by cells in culture and conveyed to their nuclei, *Mech. Dev.*, 55, 111, 1996.
21. Prochiantz, A., Messenger proteins: homeoproteins, TAT and others, *Curr. Opin. Cell Biol.*, 12, 400, 2000.
22. Derossi, D. et al., Cell internalization of the third helix of the Antennapedia homeodomain is receptor-independent, *J. Biol. Chem*, 271, 18188, 1996.
23. Berlose, J.P. et al., Conformational and associative behaviours of the third helix of antennapedia homeodomain in membrane-mimetic environments, *Eur. J. Biochem.*, 242, 372, 1996.
24. Drin, G. et al., Physico-chemical requirements for cellular uptake of pAntp peptide. Role of lipid-binding affinity, *Eur. J. Biochem.*, 268, 1304, 2001.
25. Scheller, A. et al., Evidence for an amphipathicity independent cellular uptake of amphipathic cell-penetrating peptides, *Eur. J. Biochem.*, 267, 6043, 2000.
26. Pooga, M. et al., Cell penetration by transportan, *FASEB J.*, 12, 67, 1998.
27. Pooga, M. et al., Cell penetrating PNA constructs regulate galanin receptor levels and modify pain transmission *in vivo*, *Nat. Biotechnol.*, 16, 857, 1998.
28. Prochiantz, A., Getting hydrophilic compounds into cells: lessons from homeopeptides, *Curr. Opin. Neurobiol.*, 6, 629, 1996.
29. Schwarze, S.R., Hruska, K.A., and Dowdy, S.F., Protein transduction: unrestricted delivery into all cells? *Trends Cell Biol.*, 10, 290, 2000.
30. Williams, E.J. et al., Selective inhibition of growth factor-stimulated mitogenesis by a cell-permeable Grb2-binding peptide, *J. Biol. Chem*, 272, 22349, 1997.
31. Ducarme, P., Rahman, M., and Brasseur, R., IMPALA: a simple restraint field to simulate the biological membrane in molecular structure studies, *Proteins*, 30, 357, 1998.
32. La Rocca, P., Shai, Y., and Sansom, M.S., Peptide-bilayer interactions: simulations of dermaseptin B, an antimicrobial peptide, *Biophys. Chem.*, 76, 145, 1999.
33. Vogt, B. et al., The topology of lysine-containing amphipathic peptides in bilayers by circular dichroism, solid-state NMR, and molecular modeling, *Biophys. J.*, 79, 2644, 2000.
34. Lins, L. and Brasseur, R., The hydrophobic effect in protein folding, *FASEB J.*, 9, 535, 1995.
35. Basyn, F. et al., Prediction of membrane protein orientation in lipid bilayer: a theoretical approach, *J. Mol. Graph. Model.*, 20, 235, 2001.
36. Wiener, M.C. and White, S.H., Structure of a fluid dioleoylphosphatidylcholine bilayer determined by joint refinement of x-ray and neutron diffraction data. III. Complete structure, *Biophys. J.*, 61, 437, 1992.
37. Bradshaw, J.P. et al., Oblique membrane insertion of viral fusion peptide probed by neutron diffraction, *Biochemistry*, 39, 6581, 2000.
38. Saiz, L. and Klein, M.L., Structural properties of a highly polyunsaturated lipid bilayer from molecular dynamics simulations, *Biophys. J.*, 81, 204, 2001.

39. Sankararamakrishnan, R. and Weinstein, H., Molecular dynamics simulations predict a tilted orientation for the helical region of dynorphin A(1-17) in dimyristoylphosphatidylcholine bilayers, *Biophys. J.*, 79, 2331, 2000.
40. Milik, M. and Skolnick, J., Insertion of peptide chains into lipid membranes: an off-lattice Monte Carlo dynamics model, *Proteins*, 15, 10, 1993.
41. White, S.H., Hydropathy plots and the prediction of membrane topology, in *Membrane Protein Structure: Experimental Approaches*, White, S.H., Eds., Oxford University Press, New York, 1994.
42. Popot, J.L., De Vitry, C., and Atteia, A., Folding and assembly of integral membrane proteins: an introduction, in *Membrane Protein Structure: Experimental Approaches*, White, S.H., Eds., Oxford University Press, New York, 2001.
43. Shrake, A. and Rupley J.A., Environment and exposure to solvent of proteins atoms. Lysozyme and insulin, *J. Mol. Biol.*, 79, 351, 1973.
44. Flower, D.R., SERF: a program for accessible surface area calculations, *J. Mol. Graph. Model.*, 15, 238, 1997.
45. Brasseur, R., Differentiation of lipid-associating helices by use of three- dimensional molecular hydrophobicity potential calculations, *J. Biol. Chem.*, 266, 16120, 1991.
46. Eisenberg, D. and McLachlan, A.D., Solvation energy in protein folding and binding, *Nature*, 319, 199, 1986.
47. Fauchère, J.L. and Pliska, V., Hydrophobicity parameter π of amino acid side chains from the partitioning of *N*-acetyl-amino-acid-amides, *Eur. J. Med. Chem*, 18, 369, 1983.
48. Rees, D.C. et al., Membrane protein structure and stability: implications of the first crystallographic analysis, in *Membrane Protein Structure: Experimental Approaches*, White, S.H., Ed., Oxford University Press, New York, 1994.
49. Heller, H., Shaefer, M., and Shulten, K., Molecular dynamics simulation of a bilayer of 200 lipids in the gel and in the liquid crystal phase, *J. Phys. Chem.*, 97, 8343, 1993.
50. Flewelling, R.F. and Hubbell, W.L., The membrane dipole potential in a total membrane potential model. Applications to hydrophobic ion interactions with membranes, *Biophys. J.*, 49, 541, 1986.
51. Press, W.H. et al., Numerical recipes in FORTRAN, in *The Art of Scientific Computing*, Cambridge University Press, 1992.
52. Thomas, A. et al., Pex, analytical tools for PDB files. I. GF-Pex: basic file to describe a protein, *Proteins*, 43, 28, 2001.
53. Rahman, M. and Brasseur, R., WinMGM: a fast CPK molecular graphics program for analyzing molecular structure, *J. Mol. Graph.*, 12, 212, 1994.
54. Tanford, C., *The Hydrophobic Effect: Formation of Micelles and Biological Membranes,* 1st ed., John Wiley & Sons, New York, 1973.
55. Lins, L. et al., Computational study of lipid-destabilizing protein fragments: towards a comprehensive view of tilted peptides, *Proteins*, 44, 435, 2001.
56. Lund-Katz, S. et al., Nuclear magnetic resonance investigation of the interactions with phospholipid of an amphipathic alpha-helix-forming peptide of the apolipoprotein class, *J. Biol. Chem.*, 265, 12217, 1990.
57. Kersh, G.J., Tomich, J.M., and Montal, M., The M2 delta transmembrane domain of the nicotinic cholinergic receptor forms ion channels in human erythrocyte membranes, *Biochem. Biophys. Res. Commun.*, 162, 352, 1989.
58. Martin, I. et al., Fusogenic activity of SIV (simian immunodeficiency virus) peptides located in the GP32 NH2 terminal domain, *Biochem. Biophys. Res. Commun.*, 175, 872, 1991.

59. Ducarme, P., Thomas, A., and Brasseur, R., The optimisation of the helix/helix interaction of a transmembrane dimer is improved by the IMPALA restraint field, *Biochim. Biophys. Acta*, 1509, 148, 2000.
60. Henderson, R. and Unwin, P.N., Three-dimensional model of purple membrane obtained by electron microscopy, *Nature*, 257, 28, 1975.
61. Luecke, H., Richter, H.T., and Lanyi, J.K., Proton transfer pathways in bacteriorhodopsin at 2.3 angstrom resolution, *Science*, 280, 1934, 1998.
62. Popot, J.-L., De Vitry, C., and Atteia, A., Folding and assembly of integral membrane proteins: an introduction, in *Membrane Protein Structure: Experimental Approaches*, Oxford University Press, White, S.H., Ed., New York, 1994, chap. 3.
63. Kuhlbrandt, W. and Gouaux, E., Membrane proteins, *Curr. Opin. Struct. Biol.*, 9, 445, 1999.
64. Buchanan, S.K., Beta-barrel proteins from bacterial outer membranes: structure, function and refolding [see comments], *Curr. Opin. Struct. Biol.*, 9, 455, 1999.
65. Wang, Y.F. et al., Channel specificity: structural basis for sugar discrimination and differential flux rates in maltoporin, *J. Mol. Biol.*, 272, 56, 1997.
66. Fraenkel, E. and Pabo, C.O., Comparison of x-ray and NMR structures for the Antennapedia homeodomain-DNA complex, *Nat. Struct. Biol.*, 5, 692, 1998.
67. Cullis, P.R., Fenske, D.B., and Hope, M.J., Physical properties and functional roles of lipids in membranes, in *Biochemistry of Lipids Lipoproteins and Membranes*, Vance, D.E. and Vance, J., Eds., Elsevier, Amsterdam, 1996, chap. 1.
68. Lindberg, M. and Graslund, A., The position of the cell penetrating peptide penetratin in SDS micelles determined by NMR, *FEBS Lett.*, 497, 39, 2001.
69. Magzoub, M. et al., Interaction and structure induction of cell-penetrating peptides in the presence of phospholipid vesicles, *Biochim. Biophys. Acta*, 1512, 77, 2001.

10 Biophysical Studies of Cell-Penetrating Peptides

Astrid Gräslund and L.E. Göran Eriksson

CONTENTS

0-8493-1141-1/02/$0.00+$1.50

10.1 INTRODUCTION

Cell-penetrating peptides, CPPs, are water-soluble but have the ability to translocate through various cell membranes with high efficiency and low lytic activity. The transport is nonendocytoic, does not require a chiral receptor, and is non-cell-type specific.[1-3] When covalently linked to "cargos" (polypeptides, oligonucleotides, particles, etc.) many times their own molecular mass, CPPs still retain their translocating ability.

Examples of CPPs are so-called Tat-derived peptides, as well as peptides based on sequences from certain transcription factors, signal sequences, chimeras between biological sequences, or completely synthetic (artificial) peptides. The most studied are those with sequences derived from homeodomains, where "penetratin" peptide is an archetype among the CPPs. Homeodomain (homeobox) proteins belong to a class of transcription factors involved in multiple morphological processes.[3] The sequences of penetratin, transportan, and a few other CPPs are shown in Table 10.1.

The mechanisms behind translocation of the CPPs are still mostly unknown, although it is clear that the molecular details of peptide–membrane interaction are fundamentally important for the translocation process. The role of any particular secondary structure in the process, though, remains disputed.

Background for the present review is the overall question of translocation mechanism of CPPs; however, with the lack of unambiguous experimental evidence regarding this question, we will mainly focus on membrane interaction properties of certain CPPs and analogues. Membrane model systems will be presented and the various biophysical methods used will be briefly described. We will also make a short comparison with studies on other classes of bioactive, membrane-interacting peptides in which more is known about the mechanisms of action.

10.2 SEQUENCES AND GENERAL PROPERTIES OF SELECTED CPPS

The sequences of selected CPPs discussed in this review are shown in Table 10.1, together with some variant sequences reported to have lost their translocating property. Penetratin, denoted pAntp, has a sequence corresponding to the 16 residues of the third α-helix (residues 43–58) from the Antennapedia homeodomain protein of *Drosophila*.[1,4-6] This third helix was found to be responsible not only for interaction with DNA by binding specifically to cognate sites in the genome, but also for translocation of the entire protein across cell membranes.[4,5] The pAntp peptide alone retains the membrane translocation properties and has therefore been proposed as a universal intercellular delivery vector.[1] A homologous peptide, pIsl, derived from the Islet-1 homeodomain, also behaves as an efficient CPP.[7]

Transportan is a chimeric 27-amino acid peptide with a sequence derived from the 1–12 residues of galanin and linked with a Lys to the sequence of the wasp

TABLE 10.1
Sequences of Selected Cell-Penetrating Peptides and Nonpenetrating Analogs

Name	Sequence	Translocation
Protein-derived		
Penetratin, pAntp	RQIKIWFQNRRMKWKK	yes[4]
Nonpenetratin	RQIKIFFQNRRMKFKK	no[14]
pIsl1	RVIRVWFQNKRCKDKK	yes[7]
Tat-derived	YGRKKRRQKKK	yes[3]
Peptide-derived chimera		
Transportan	GWTLNSAGYLLGKINLKALAALAKKIL	yes[8]
Nontransportan	LLGKINLKALAALAKKIL	no[15]
Signal-NLS	MGLGLHLLVLAAALQGAKKKRKVC	yes[12]
	GALFLGWLGAAGSTMGAWSQPKKKRKVC	yes[13]
	AAVALLPAVLLALLAPAAANYKKPKL	yes[11]

Note: Terminal groups may be substituted. Positively charged residues are underlined.

venom mastoparan.[8] The Tat sequence in Table 10.1 is derived from the HIV-1 Tat protein.[3] This protein was in fact the first example of a protein discovered to be translocated into cells.[9,10] The NLS-chimera peptides included in Table 10.1 are derived from hydrophobic parts of different signal peptide sequences fused with some nuclear localization sequence (NLS).[11-13]

Both the pAntp and transportan sequences have variants that have lost their translocating property, and selected nontransporting variants are also included in Table 10.1. With penetratin, critical substitutions of two residues — changing Trp into Phe — is enough to yield a nontransporting peptide.[14] With transportan, successive deletions from the N terminus showed that a peptide where residues 1–9 had been deleted had essentially lost its translocating property.[15]

There is no clear-cut biophysical difference between CCP and non-CPP variants of the peptides. The common denominator for all the peptides presented in Table 10.1 is that they are, more or less, positively charged at pH 7. In the case of chimeric CPPs, the charges are localized at the C-terminal part and originate from either an NLS-moiety or mastoparan (with transportan). The chimera have long stretches of hydrophobic residues (with no charges) at their N-terminal parts.

10.3 BIOMEMBRANE MIMETIC SOLVENTS AND MODEL SYSTEMS

CPPs are incorporated into any cell type and, today, the only common denominator is the ability to translocate through the plasma membrane. Transport studies are preferentially carried out with intact cells, using various microscopic techniques. However, the complexity of a biological cell and its handling make it difficult, or impossible, to apply other biophysical methods in a meaningful way. Hence, a more detailed biophysical molecular understanding requires studies with simplified model

systems. In this section a number of biomembrane models will be briefly presented. For more comprehensive knowledge, the vast literature in the membrane field, including *Handbook of Nonmedical Applications of Liposomes* (in four volumes)[16] is recommended. A brief summary relevant for CPP studies is given here.

Although the chemical composition of real biomembranes varies, their physical properties are mainly governed by the amphiphilic nature of the phospholipids forming a bilayer in water. In the model studies, well-characterized synthetic phospholipids should be used, instead of a mixture of ill-defined lipids from some natural source. Phospholipids with saturated fatty acid chains, with at least 14 carbons, form membranes with a sharp thermal phase transition between the gel state and the liquid crystalline state. Since the latter state exists *in vivo*, the system studies should be carried out above room temperature.

By choosing phospholipids with a thermal phase transition below room temperature, the nonbiological gel state is easily avoided. This is usually accomplished by having unsaturated fatty acids, although this means a higher risk for lipid oxidation to occur. Phospholipids with one of the chains (number 2) containing a single double-bond will have good and relevant properties. Compounds with the structure 1-palmitoyl-2-oleoyl-phosphatidyl-X (POP-X) have been frequently used. Here "X" denotes the "head group," giving rise either to the neutral, zwitterionic lipids (POPC, POPE) or the negatively charged lipids (POPG, POPS, POPA, etc.).

Biological membranes are electrically charged, where the fraction of charged phospholipids normally is low (order of 10 mol%). In order to mimic a more real system, it is therefore common to study membranes produced from mixtures of the two types of phospholipids. Phospholipids with the head group consisting of ethanolamine (X = E) frequently occur in natural membranes. However, for model systems this type of neutral phospholipid should not be used with high mol%, since a diacyl-PE molecule (for sterical reasons) does not form lamellar bilayers, but instead a hexagonal phase. For simple model studies there is no primary reason to include cholesterol or any other natural lipid molecule in the membrane composition.

In a biomembrane with low curvature, a phospholipid molecule occupies about 0.7 nm^2 in each layer of the bilayer. Below the thermal phase transition, in the gel state, the surface area will become smaller and the packing higher. The molecular shape as well as the electrical charge may cause an asymmetrical distribution of lipid components between the outer and inner monolayers of the membrane. The thickness of the bilayer depends on properties of the lipids, but is of the order of 5 nm. The transverse diffusion ("flip-flop") of lipids between the two layers is slow compared to the much more effective lateral, two-dimensional diffusion within each monolayer.

10.3.1 Liposomes and Vesicles

A monolayer of lipids can be formed at the air–water interface by the Langmuir technique; this type of preparation can be used for surface studies. A multilamellar arrangement of oriented bilayers will occur when lipids are deposited on a support and then hydrated. Such a specimen may be useful when studying the orientational dependence of a physical observable. The concept of liposome is used to any

preparation where amphiphilic lipids are hydrated by an aqueous medium and form bilayers, which self-close as a particle. Agitation alone (vortexing) results in dispersion of large multilamellar vesicles (LMV) with an onion-like structure formed by many lipid bilayers separated by water in layers. By repeated freeze-thawing, the particle size can be made more uniform. LMV is usually not a suitable model system for biophysical studies, since there is no single inner compartment. LMVs can be useful, however, for broad-band nuclear magnetic resonance (NMR) studies (^{2}H, ^{31}P) of the molecular order within a membrane

For biophysical studies various unilamellar vesicle preparations are useful model systems. The vesicle concept should be restricted to those particles with a single, unilamellar, membrane bilayer enclosing an inner compartment. Depending on the size of the vesicles, it is common to classify them as small (SUV; diameter 20 to 50 nm), large (LUV; 100 to 200 nm), and giant (GUV; 10 to 100 μm) unilamellar vesicles. The small vesicles (SUV) have large curvature, causing nonuniform tension. A larger vesicle should, in principle, better mimic the plasma membrane of a true biological cell because, with a large inner volume, the interior compartment can be more easily monitored. However, for optical spectroscopic studies, light scattering from large particles can be a severe problem. In such studies, SUV samples are usually preferred.

10.3.1.1 Small Unilamellar Vesicles (SUVs)

Disruption of LMV dispersions by ultrasound (sonication) will produce an SUV sample. The treatment is rather harsh and should be carried out with cooling and a protective nitrogen atmosphere. When a probe tip sonicator is employed, metal particles must be removed by centrifugation. Since the size of the vesicles has some distribution, ultracentrifugation or chromatography will make a sample more monodisperse. An SUV is metastable and should be stored only for a few days (above the transition temperature). Hydrolysis of the lipids may occur during sonication and the storage. The number of phospholipids required to form a typical SUV is on the order of 3000, with approximately 60% of the molecules occupying the outer layer. The large curvature will create a tighter packing of the lipids in the inner leaflet.

10.3.1.2 Large Unilamellar Vesicles (LUVs)

This type of preparation can also be useful for biophysical studies.[17] The simplest preparation procedure is to freeze-thaw an LMV suspension by several cycles, followed by extrusion repeatedly through a polycarbonate microfilter with, e.g., 100-nm pores. LUV samples may be stored in a refrigerator.

10.3.1.3 Giant Unilamellar Vesicles (GUVs)

This type of vesicles is observable by a light microscope and may be manipulated by microinjection.[18] GUVs can produced from phospholipids dissolved in a chloroform and methanol mixture. Hydration can take place either after removal of the solvent, or at the same time as the pressure is reduced to allow rapid evaporation from a water–organic solvent mixture; however, it is not evident that all the organic

solvent will disappear in that way. An alternative procedure is the so-called electroformation method, where a low-frequency AC field stimulates GUV formation. The stability of GUVs has been reported to be good, probably comparable to that of LUVs. A disadvantage with GUVs is that the ionic strength of the medium must be restricted.

10.3.2 Micelles, Bicelles, and Solvent Mixtures

Although phospholipid vesicles have many properties in common with biological membranes, they are not convenient for certain biophysical studies. For instance, as will be discussed later, no true high-resolution NMR spectrum will be recorded from a peptide (CPP) when it is bound even to an SUV, due to the high molecular weight and slow mobility of the complex in solution. For that reason other amphiphilic biomembrane mimetic systems have also been applied.

10.3.2.1 Micelles

Micelles can be produced by various amphiphiles, dissolved in an aggregated form above the critical micellar concentration (CMC) in aqueous media. The most common micelles are formed from sodium dodecyl sulfate (SDS), which forms small spherical micelles with a mean aggregation number of about 60 and a total molecular weight of about 20 kD. The CMC is about 10 m*M*. Since SDS is negatively charged, micelle stability becomes dependent on ionic strength. The micelle is very dynamic and the lifetime of the SDS molecules in the aggregate is short (< msec) compared to that of phospholipids in vesicles (order of hours).

10.3.2.2 Bicelles

A binary mixture of two phospholipids in water may form micelles with different shapes and properties.[19-22] The major component is a molecule able to form bilayers. Usually dimyristoyl-phosphatidylcholine (DMPC) is used. This zwitterionic molecule is mixed with a variable amount of zwitterionic dihexanoyl-phosphatidylcholine (DHPC), with lipid chains too short to be bilayer competent. The DMPC molecules will form a bilayer where the rim is covered by the DHPC molecules. The bicelle may be doped with charged lipids, like DMPG.[23] Bicelles have no inner aqueous compartment; like micelles, they are dynamic structures. Depending on lipid composition, concentration, temperature, etc., the bicellar samples can have either isotropic or anisotropic properties. The isotropic particles are small enough to allow high-resolution NMR.[24]

10.3.2.3 Solvent Mixtures

Many peptides when free in water have a low degree of secondary structure (random-coil state). By using mixtures of water and fluoroalcohols as solvents, a certain structural stabilization can take place, usually in the form of an α-helix. The general explanation for secondary structure induction in such solvent mixtures is that a

number of H-bonding water molecules are removed, therefore promoting intramolecular H-bonds. The most common alcohols used in such studies are trifluoroethanol (TFE) and hexafluoroisopropanol (HFP), which are water mixible; however, it has also been suggested that some aggregated solvent clusters could exist in aqueous mixtures.[25] Whether this type of solvent mixture should be considered a good membrane mimetic can be debated.

10.4 INTERFACIAL PHENOMENA — ELECTROSTATICS

Outside the charged membrane surface is the so-called interphase region, a region of solvent more strongly associated with the membrane than the bulk region, which is far away (∞) from the surface. In the theoretical treatment of the diffuse double layer one assumes that the interphase is also composed of two regions. Close to the surface is the Stern layer, where ions are attracted or repelled. Outside this region is a diffuse layer of ions, within which all the ionic particles, including charged peptides like CPPs, are assumed to obey a Boltzmann distribution. With an electrical potential $\phi(r)$ at a position r, the mean-field electrical interaction energy becomes $z_i e\phi(r)$, where z_i is valency of the ion ($\pm$) and e is electronic charge (F/N_A). For each ion, concentration (mol/dm^3) is assumed to become

$$c_i(r) = c_i(\infty)\ \exp\ [-z_i e\phi(r)/kT]$$

The net charge density (charges/m^3) in the aqueous phase at a point r is then

$$\rho(r) = \left(10^3 N_A e\right)\sum_i^{all} z_i c_i(r) = \left(10^3 N_A e\right)\sum_i^{all} z_i c_i(\infty)\exp\left[-z_i e\phi(r)/kT\right]$$

The Poisson equation is a fundamental result (from Gauss laws) in electrostatics connecting the electrical potential $\phi(r)$ and charge density $\rho(r)$:

$$\Delta\phi(r) = -\rho(r)/\varepsilon_o\varepsilon_r$$

In the one-dimensional case, the Laplace operator becomes $\Delta = d^2/dx^2$, where x is the distance from the Stern layer. With $x = \infty$, the limit is out in the bulk phase. When the medium is not a perfect dielectricum, variation in the permittivity (ε_r) can exist.

Even in the one-dimensional case, the combined Poisson–Boltzmann equation has no simple analytical solution; we must assume certain boundary conditions. A useful relation between the surface charge density, σ_0, and the surface potential $\phi(0)$, at x = 0, was derived by Grahame:[26]

$$\sigma_0^2 = 2\cdot 10^3 \varepsilon_o\varepsilon_r RT\sum_i^{all} c_i(\infty)\left\{\exp\left(-z_i e\phi(0)/kT\right) - 1\right\}$$

In this expression the ionic concentrations $c_i(\infty)$ of all ions in the bulk phase should be accounted for. At a fixed surface density (charges/m^2), the surface potential (volt) will become dependent on the concentration and valency of all the ions present in the bulk phase. The equation above is more general than the early Gouy–Chapman equation where, e.g., the exponent is simplified as a serial expansion (linearization). In the simplest theories the surface charge density is smeared out, without considering any "discreteness-of-charge" effects.[27,28]

At the Stern layer (x = 0) the surface potential is defined as $\phi(0)$. At a distance $x = 1/\kappa$ from the surface, the potential has decayed to $\phi(0)/e$. This characteristic length is the so-called Debye length, which is a measure of the extension of the diffuse layer. The full expression for the parameter κ includes the ionic strength, defined by

$$I = \tfrac{1}{2}\sum_{i}^{all} z_i^2 c_i$$

Since $\kappa \propto I^{1/2}$ it is clear that a higher ionic strength will result in a shorter Debye length ($1/\kappa$). Moreover, the surface potential $\phi(0)$ will become reduced due to screening. In this respect a multivalent ion will be very potent.

Besides the nonspecific screening effect, specific interactions (bindings) may exist between charged particles and a charged membrane. For instance, weak intrinsic bindings exist among the alkali ions to acidic phospholipids. This situation will result in reduced value of the surface potential and is not accounted for in the double-layer theory. The experimental surface potential (measured by electrophoresis as a zeta-potential) of a fully charged phospholipid vesicle (100 mol% PS, or PG) in 0.1 *M* NaCl is about –60 *m*V. With only 20 mol% of negative phospholipids, a value more relevant for many biological membranes, the surface potential of a bilayer becomes reduced to about –30 *m*V at the same salt concentration. If the salt concentration is decreased to only 0.01 *M* NaCl the surface potential of the low charge density vesicle will now also become about –60 *m*V. Hence, it is extremely important to have good control of the ionic strength when doing studies on the charged CCPs in model systems.

The relevant concentration in a membrane process is the local surface concentration. This should be used in order to understand intrinsic properties of the CPPs. Applying bulk concentration of ions will lead to apparent parameters, which will be dependent on the experimental conditions. Without proper corrections for the electrical potential effects, an apparent value for the binding constant (K_{app}) is measured. This value is related to the intrinsic (true) value (K_{int}) by

$$K_{app} = K_{int} \exp[-z_i e\phi(0)/kT]$$

The apparent binding constant will be orders of magnitude larger than the intrinsic one for a polycationic molecule (like a CPP) when $\phi(0)$ is negative (–*m*V). The

intrinsic binding at the membrane is usually described by an adsorption (mass action) isotherm (e.g., Langmuir) reflecting how the bound molecule (peptide) will become positioned at a site, until the surface becomes fully occupied (saturated).

10.5 BIOPHYSICAL METHODS TO STUDY PEPTIDE–MEMBRANE INTERACTIONS

Biomembranes are amphiphilic molecular assemblies able to stabilize peptide conformations upon interaction. When free, short peptides, as distinguished from globular proteins, do not normally have a more hydrophilic "outside" and a more hydrophobic "inside." Depending on the nature of the residues involved, a peptide will expose both hydrophobic and hydrophilic side chains to the surrounding medium. Peptides with low solubility may self-aggregate and form oligomers. Various spectroscopic methods are used to study the interactions between a peptide and a mixed solvent.

Among problems studied are, e.g., distribution of the peptide between the aqueous and amphiphilic phase, location and mobility of the peptide relative to the surface of the membrane mimetic phase, and induction of secondary structure in the peptide by the solvent. These studies are relevant for various other classes of peptides, such as hormones and antibiotic peptides. Other studies concern changes of the membrane induced by the peptide. Such changes range from complete disassembly (lysis) to pore formation or more subtle effects, which may be relevant for the group of peptides under consideration here. The most used spectroscopic techniques are briefly summarized below.

10.5.1 Fluorescence

The intrinsic fluorescence of tryptophan (or possibly tyrosine) residue may be investigated in order to determine the polarity of its environment.[29] The tryptophan emission peak wavelength is sensitive to polarity and shifts from ca. 356 nm in an aqueous phase to about 320 nm in a hydrophobic phase. In parallel, the quantum yield becomes enhanced in the hydrophobic phase. Artificial fluorescence probes can be attached to the peptide, cargo, or membrane and may report on interactions or change of state of its host. As a cargo, the green fluorescence protein (GFP) may be used as a natural test molecule. The topology of the peptide and membrane system may be monitored by experiments using quenchers or detecting fluorescence resonance energy transfer (FRET) between two fluorophores (donor–acceptor).

Polarization of fluorescence can be used to observe order and dynamics ("fluidity") of the membrane and perturbations caused by the peptide. Relatively low concentrations and volumes are needed for spectroscopic fluorescence studies: typically a few hundred μl of 1 μ*M* fluorophore, i.e., about 1 nmol, is enough to give a good fluorescence signal from tryptophan, as well as from any suitable external fluorescence probe. With fluorescence microscopy, in principle, single fluorescent molecules may be monitored by advanced techniques.[31]

10.5.2 Circular Dichroism

Circular dichroism (CD) spectroscopy detects the chirality of molecules as the small difference in absorbtivity for right- and left-hand circularly polarized light. Due to the chiral nature of the peptide bond and the different dihedral angles associated with different types of secondary structure, CD spectra report on secondary structures present in the amino acid chain. The spectral range for this type of peptide or protein study is usually 190 to 300 nm. The use of the CD method is mainly empirical; for analysis of the CD spectra of a protein or a peptide, one compares with standard spectra from proteins with well-known three-dimensional structures.[32]

It is possible to estimate percentages of typically five-component spectra: α-helix, antiparallel and parallel β-sheets, β-turn, and random coil. For globular proteins of the same kind used to create the standard set of spectra, this is a reliable evaluation. For short peptides, the results of such an analysis of a new CD spectrum are less clear-cut. However, they may be used as a first estimation of structures present and, particularly, to show directions of change under different conditions. The presence of a clear isodichroic point indicates a two-state situation.

CD spectra have similar requirements as to amounts of sample as fluorescence spectroscopy. Light scattering is a severe problem in the region around or below 200 nm when working with concentrated membrane samples or large particles. Oriented CD spectra from a peptide can be measured by use of aligned multibilayers deposited on a quartz plate.[33]

10.5.3 Fourier Transform Infrared Spectroscopy

Fourier transform infrared (IR) spectroscopy (FTIR) is a vibrational spectroscopy employing an interference technique. Similar to CD, IR spectra carry information about the presence of secondary structures in a peptide under various conditions.[34] The peptide bond has typical amide bands I and II in the IR region from 1680 to 1430 cm^{-1}, which can be best observed in a D_2O solvent. From these bands it is possible to evaluate secondary structures, which usually requires spectral deconvolution. FTIR sample requirements are typically small amounts of a very concentrated solution (few μl with <10 m*M* concentration), i.e., 10 to 50 nmol. Oriented samples can be studied using polarized light. The attenuated total reflection (ATR) technique can give significantly enhanced sensitivity.

10.5.4 Nuclear Magnetic Resonance

Nuclear magnetic resonance (NMR) spectroscopy gives molecular structure information at the atomic level. For studies of proteins and peptides, ^{1}H is the most commonly studied nucleus, but with isotope-labeled molecules ^{13}C and ^{15}N are also common nuclei studied in biomolecules. Three-dimensional structures in solution, as well as dynamics and sites of interactions between molecules, can be determined.[35,36] The limitation in the present context is that the object under study must have a relatively high mobility in order to give high-resolution NMR spectra. This

limits the applicability to molecular weights less than about 50 kD with conventional methods.

New methodology developments may raise this limit to a few hundred kD,[37] and solid-state NMR is applicable with larger objects, but the information content is more limited. At the present time this means that biomembrane mimetic solvents that allow detailed determination of atomic structure of an interacting peptide are limited to mixed organic solvents, detergent micelles, and, possibly, phospholipid bicelles; small unilamellar phospholipid vesicles and larger objects are not useful as solvents. NMR spectroscopy requires rather large amounts of sample for detailed studies, typically 0.5 ml of a 1-m*M* peptide, i.e., 500 nmol.

Besides studies of the peptide itself, NMR can also be applied to study of the phospholipids of model membranes. ^{31}P NMR (and ^{2}H NMR) has been used extensively to determine properties of membrane phases such as size, disruption into extended bilayers, phase transitions, or polymorphism.

10.5.5 Electron Paramagnetic Resonance

Electron spin (or paramagnetic) resonance (EPR) spectroscopy can be used to study CPPs if a spin labeling procedure is used. Spin labels, stable nitroxyl free radicals, can be attached to the peptide or included among the membrane constituents.[38] The aim of such studies is to determine interactions and mobility of the spin-labeled peptide exposed to solvent-containing membranes. The degree of binding and dynamics of a labeled peptide to a membrane particle can be estimated from EPR spectra. Information about peptide–peptide interactions may also be obtained. As with fluorescence labels, it is in principle possible to put one label on the peptide and another on the membrane and then investigate details of peptide–membrane interactions. The amount of sample needed for EPR-spin label studies is typically 50 µl of a 10-µ*M* solution, i.e., 0.5 nmol, which is similar to requirements for fluorescence and much less than those for NMR.

10.6 EXAMPLES OF SECONDARY STRUCTURE INDUCTION IN CPPS BY MEMBRANE-MIMETIC SOLVENTS

Many studies have reported induction of secondary structure in CPPs by interaction with membrane-mimetic solvents. We will not review all, but will give a few typical examples involving detergent micelles and phospholipid vesicles and illustrating use of different experimental techniques in the different model systems.

Most short peptides have only weak tendencies for ordered secondary structures in water; evidence from CD as well as NMR is typically interpreted as originating from a dominating "random coil" secondary structure. This is also true for CPPs like penetratin and transportan. Based on CD and NMR studies with aqueous fluoroalcohol (HFP or TFE) mixtures, an α-helical structure has been reported for penetratin,[6] and for a chimera of signal peptide sequences with a nuclear localization sequence (NLS; Table 10.1).[12,13] This situation is typical for many peptides in fluoroalcohol–water solvents, not just CPPs.

10.6.1 Structure Induction in Micelles

Detergent micelles, like mixed organic solvents, often induce helices in short peptides; CPPs are no exception. For penetratin, the induction of α-helix has been shown by NMR and CD in low (20 m*M*) and high (300 m*M*) SDS concentrations.[6,39] The induction of secondary structure in peptides by these solvents is often explained in terms of loss of hydrogen bonds from water.

There does not seem to be a close relationship between induction of α-helix by these membrane-mimetic solvents and the membrane translocation property. In fact, there are penetratin variants for which these solvents induce α-helical secondary structures; yet they have lost the ability to translocate. Moreover, there are examples of penetratin variants with proline insertions, which typically interrupt helical structures, but these peptides are still able to translocate. Transportan in SDS micelles gives a mixed structure: the C-terminal mastoparan part forms a well-developed α-helix, whereas the galanin part has a less well-defined secondary structure. Both parts are similar to structures of the corresponding parts of the galanin and mastoparan peptides, respectively, in the same solvent.[24,40]

10.6.2 Positioning in Micelles

In an attempt to carry NMR studies on peptides interacting with detergent micelles one step further, recent studies have aimed at determining the positioning of different parts of the peptide molecule relative to the surface and interior of the micelle. In these studies paramagnetic probes are used, which affect the linewidths of the resonances of nuclei in their neighborhood; these spin probes can be selected according to where they reside in the micellar system. Spin-labeled fatty acids, such as 12-doxyl and 5-doxyl stearic acid, are known to act inside and at the surface of the micelle, respectively. Paramagnetic ions, such as Mn^{2+} or water-soluble spin labels, affect parts of the peptide located outside the micelle. The selective effects on the peptide resonances are investigated and information on peptide positioning is obtained.[41]

Studies on transportan and penetratin in SDS micelles, using fatty acid spin labels as internal and Mn^{2+} ions as external paramagnetic probes, have been reported.[39,42] The SDS was in large excess in these experiments, typically 300 m*M* with 1 m*M* peptide. This corresponds to one peptide per five micelles, assuming 60 SDS per micelle. Results showed that the peptides are partly "hidden" inside the micelle and partly exposed outside the micellar surface. The helical parts of transportan and penetratin were found to be mostly buried by the micelle. For transportan, the most C-terminal residues and the central segment connecting the galanin and the mastoparan part were found to be exposed to the aqueous solvent. For penetratin, the most N-terminal residues were found to be exposed to the aqueous solvent. Therefore, a common denominator for transportan and penetratin in complex with SDS micelles is that they both have a helix buried in the interior of the micelle and an "anchor" at one or both ends of the helix.

The anchoring part is exposed at the outside of the micellar surface. This may speculatively be regarded as a crude model of a CPP in contact with a membrane-like environment with negative charge at the surface. The analysis of the shielding from the

different paramagnetic probes was not clear-cut for all residues, however, indicating that the systems are highly dynamic. In experiments with tryptophan fluorescence, the quenching properties of the two residues in penetratin were indistinguishable.[7]

In transportan and penetratin bound to the SDS micelles, the helical parts of the peptides are composed of 10 to 12 residues making about three turns of a helix (spanning approximately 16 Å). This corresponds to only about half the width of a typical phospholipid double layer. The possible importance of these features of the micelle-bound CPP for the translocation mechanism will be speculated on at the end of this chapter.

10.6.3 Structure Induction in Bicelles

Another recent approach is to use bicelles, disk-shaped objects composed of a suitable mixture of phospholipids with longer and shorter fatty acid chains. The phospholipds with the longer chains (e.g., DMPC) assemble to a bilayer making up the flat part of the disk, and the phospholipids with the shorter chains make up the rim. Certain preparations with suitable ratios of the phospholipid components give bicelles with molecular weights down to about 200 kD. Neutral and charged phospholipds may be mixed to obtain a variable surface charge of the bicelle. When bicellar solvents are used, it appears that relatively well-resolved NMR signals can be obtained from the peptide, but few reports on studies in such solvent systems have been published until now,[24] and not one with a CPP.

10.6.4 Structure Induction in Vesicles

As already pointed out, the more realistic membrane-mimetic systems are larger objects that are not amenable to high-resolution NMR studies. The practical limit for molecular weights directly accessible by NMR is around 50 kD, extended by transverse relaxation optimized spectroscopy (TROSY) techniques to a few hundred kD under favorable circumstances.[37] Certain ways around this practical problem have been devised, one of which is to use transferred nuclear Overhauser enhancement (NOE) experiments for structural information on peptides, which must be only weakly bound to the vesicle and therefore in rapid exchange between the free and bound states. These experiments combine the sharp linewidth of the peptide free in solution with some structural information (in terms of NOEs between resonances from protons close in space) on the bound peptide.

CD spectroscopy has been a method of preference for studies of structure induction by phospholipid vesicle systems. The overall conclusion for penetratin is that the charge of the membrane surface determines not only the strength of the interaction but also the dominating nature of the induced secondary structure. With highly negatively charged vesicles or high peptide–lipid ratios, the induced secondary structure is mainly a β-structure, whereas more neutral vesicles or low peptide–lipid ratios favor an α-structure.[43-45] This chameleon-like behavior of penetratin seems not to be followed by transportan, however, which keeps its partial α-structure unchanged, in phospholipid vesicles of different charges as well as in SDS micelles or in a 30% HFP mixture.

TABLE 10.2
Sequences of Selected Membrane-Active Peptides

Name	Sequence	Translocation	Lytic/Pore
Melittin	GIGAVLKVLTTGLPALISWIKRKRQQ-NH_2	yes	yes[33]
Magainin 2	GIGKFLHSAKKFGKAFVGEIMNS	yes	yes[47,48]
Mastoparan X	INWKGIAAMAKKLL-NH_2	yes	yes[47]
Buforin 2	TRSSRAGLQWPVGRVHRLLRK	yes	no[54]

Note: Positively charged residues are underlined.

Among the other CPPs included in Table 10.1, the Tat peptide had been discussed in terms of an amphipathic α-helix,[46] whereas two NLS-chimera seem to adopt β-structures with phospholipid vesicles, irrespective of the surface charge.[12,13]

10.7 POSSIBLE EFFECTS OF PEPTIDES ON MEMBRANES: COMPARISON WITH OTHER TYPES OF MEMBRANE-INTERACTING PEPTIDES

There is a vast amount of literature on membrane interactions and membrane effects by bioactive peptides. Biological effects have been compared with studies of interactions and structures in membrane model systems. In contrast to the more hydrophobic peptides, sometimes of an integral type, the highly amphipathic and water-soluble small peptides are more unpredictable in their biophysical behavior. Here we will only mention a few examples of the latter type of peptide and discuss various biological and physico-chemical effects defined for some peptides that may be relevant for understanding CPPs. We have selected the antimicrobial peptides, a widespread and much studied class of peptides.[47-51]

Antimicrobial and toxic peptides from various sources, exemplified by magainin (frog skin), melittin (bee venom), and mastoparan X (wasp venom), are examples of pore-forming peptides which, under certain conditions, cause the cell membrane to disrupt and lead to lysis of the cell. The sequences and a summary of their characteristic effects on biological membranes are shown in Table 10.2.

The overall view is that these peptides exert their cytotoxicity by permeabilizing cell membranes. The positively charged peptides are particularly toxic to bacterial membranes, which are negatively charged overall. A transmembrane potential (negative inside) has been found to increase the ability of peptides to induce cell lysis. The exterior side of the plasma membrane of mammalian cells is more neutral in charge (zwitterionic) and hence should have a lower affinity for the peptide. This is generally given as an explanation for the lower biological activity with mammalian cells as compared to bacterial cells, and thus the selective toxicity and the rescue of the host cells.

Amphiphaticity and aggregational states have been much discussed for the antimicrobial peptides, mostly in terms of (helical) secondary structures and membrane topology. The mechanisms of action have been suggested to include dynamic

pores in the form of peptide complexes. The peptide activities result in membrane leakage (permeation) and consecutive translocation of the peptide as well as the lipids in a transient manner.[47,48] This picture seems to be valid for peptides like melittin, magainin, and mastoparan X.

It has been suggested that each peptide has two physical states of binding to a phospholipid bilayer.[33,52,53] At low peptide-to-lipid molar ratios, the peptide becomes adsorbed in the membrane head-group region. In this state the peptide is still functionally inactive, but then causes thinning of the membrane bilayer. Above a threshold value for the molar ratio, the peptide forms a multiple-pore state. This lethal state depends on the composition and biophysical nature of the membrane, which could explain the susceptibility and specificity of the biological activity.

With buforin 2 peptide (from toad stomach) no membrane pores were detected, in agreement with the low lytic effect.[54] Interestingly, buforin efficiently translocates across lipid bilayers, but in this case without membrane permeabilization and lipid flip-flop induction. Its antimicrobial activity is even higher then for the pore-forming peptides. The toxic effect of buforin is suggested to be an interaction with intracellular nucleic acids.

The uptake of labeled buforin into *Escherichia coli* cells could be detected by fluorescence microscopy. However, the bacteria cells were not permeabilized to allow an influx of a DNA-staining probe. The cell-penetrating efficiency and antimicrobial activity of buforin and its analogs correlated with their α-helical contents.[55] It seems as if buforin in its behavior may have some properties in common with CPPs. Hence, it would be interesting to test whether buforin, or any of its analogs, can in fact pull a cargo into a cell as efficiently as some (arche)typical CPPs.

Molecular details of the membrane permeabilization process are not clear, but it is possible experimentally to observe changes in the macroscopic electric conductance in membrane model systems due to channel formation. The pores give rise to leakage of small molecules, such as dithionite or the fluorescent dye calcein, through the membrane. Models for the pore formation and structure have been much discussed.[33,47-53] In principle, two models are proposed: the "barrel-stave" and the "torus." The pore structures can be considered as formed by a bundle of membrane-interacting peptides with their polar surfaces turned towards the interior of the pore.

With the "carpet" model, the peptide lands on the bilayer leaflet, resulting in a membrane destabilization, without a defined oligomerization. As mentioned earlier, the structural modifications of the membrane are considered dynamic on variable timescales. However, in the case of magainin, a pore structure has even been crystallized and characterized by neutron diffraction.[53] For most pore-forming peptides there appears to be a good correlation among pore formation measured as leakage of the calcein dye, translocation of the peptide through the membrane, and the flip-flop process of membrane lipids.

The peptide translocation in vesicles was measured by observing the fluorescence resonance energy transfer between a tryptophan residue of the peptide and a fluorophore (acceptor) attached to the head group of a phospholipid. With a proper artificial fluorophore bound to the peptide, its translocation in a vesicle can also be followed by determination of accessibility of the peptide on the outside.

There should be a difference in the biological activities between the antimicrobial (pore-forming) peptides and CPPs, in that the latter must be much less cell toxic by their nature or design. At the molecular level, a superficial look at the peptide sequences shown in Tables 10.1 and 10.2 reveals very few obvious differences: positive charges and hydrophobic residues are well represented in both groups. An interesting reflection is that a peptide sequence such as mastoparan, which, like mastoparan X, belongs to the pore-forming group, may convert into the CPP group by acquiring an additional new N terminus from galanin. It seems as if the addition of a somewhat less hydrophobic sequence part makes the molecule less toxic and at the same time confers ability to carry conjugated cargoes across the membrane.

10.8 CPP TRANSLOCATION IN MODEL MEMBRANE SYSTEMS: THE CASE OF PENETRATIN

Some basic understanding of the mechanisms behind the CPP translocation phenomenon is urgent and challenging. For that reason, studies on membrane model systems are usually required. Will any of the CPPs, even without a cargo, be able to come across a bilayer of a unilamellar phospholipid vesicle? If the answer is yes, we need not speculate about any still unknown biological factor responsible for the translocation. We then just need to acquire better understanding of the biophysics of membranes. The thermodynamic energy dependence of the transport will be described in either a classical or an irreversible sense.

The first direct observation of translocation of penetratin across a vesicle membrane was reported by Thorén et al.,[56] who used fluorescence microscopy to observe labeled penetratin in the presence of giant vesicles (GUVs) prepared from soybean lipids. The authors reported that translocation took place with GUVs and with multilamellar liposomes (LMV). Even at the high peptide/lipid molar ratio (1:46) applied, penetratin did not cause any detectable membrane leakage.

In contrast, no evidence for any translocation was found by Drin et al.[57] when using fluorophore-labeled penetratin exposed to charged SUVs prepared from a POPC/POPG mixture (75/25) in saline. The peptide/lipid molar ratio was low (1:708) in this case. The penetratin remained on the outer leaflet of the SUVs, so the impermeable dithionite reagent could chemically extinguish the fluorescence. Similarly, no evidence of translocation was found when penetration was exposed to charged LUVs at a low peptide/lipid molar ratio.[43]

What may be the reasons for the conflicting results with the fluorescence methods? First, different vesicle types were used. GUVs seem to have relevant biomembrane mimetic properties, but a better defined lipid composition should be used. Whether the method of GUV preparation caused a transmembrane potential is not clear. The absence of translocation with SUVs might be a result of uneven bilayer packing, causing a strain too high for an effective transport. Perhaps more important, the studies were carried out with about one order difference in the peptide/lipid molar ratio. The surface potential may also have been different. Penetratin, with its chameleon-like properties, can adopt different secondary structures, depending on the experimental conditions (peptide/lipid ratio, surface charge, etc.).[45]

Interestingly, it has recently been reported[58] that penetratin could induce a transient aggregation of LUVs produced from a pure acidic phospholipid (DOPG). In this study a high peptide/lipid molar ratio was used, which should lower the surface potential. The aggregation was correlated with the occurrence of a concomitant, transient β-structure induction in the penetratin peptide. Upon the time-dependent disappearance of the vesicle (LUV) aggregation, the secondary structure of the peptide returned to an α-helical state. The authors suggested that peptide translocation could be responsible for this time-dependent phenomenon: if the penetratin escapes to the inside of the (aggregated) LUVs, the peptide surface concentration will become lower, which should favor the helical state and also electrostatically improve the colloidal stability of the vesicles. In summary, further critical studies with penetratin and other CPPs are required in order to establish and characterize any translocation in relevant membrane model systems.

10.9 CRITERIA FOR VARIOUS FORMS OF PEPTIDE ACTIVITIES ON MEMBRANES

In this context we would like to emphasize that it is important to define simple and robust criteria for the interpretation of the different terms: pore formation, translocation with cargo, etc. The meaning of these terms in a biological cell context is relatively clear; this is how the remarkable properties of the peptides were discovered. In the membrane model systems, however, there is a need to formulate operational definitions (protocols) of the different processes. For instance, one may define pore formation in a phospholipid vesicle by observing leakage above control level of a certain dye. It should also be emphasized that, although we discuss pore structures as if they were static, all these phenomena are dynamic and occur on various time scales. Further, one may define nonmediated translocation through a phospholipid vesicle membrane from the inside–outside distribution of the peptide. The distribution (topology) can be observed by fluorescence resonance energy transfer (FRET) properties between a fluorophore in the peptide and fluorescence-labeled lipids on either side of the bilayer, or simply by removing or destroying the exterior peptide fluorophore. Accompanying the peptide translocation, processes may exist like an induced lipid flip-flop process of the phospholipids across the bilayer.

For obvious reasons it is difficult to establish translocation (permeation) in a biological cell that undergoes lysis. Translocation in biological systems is therefore restricted as a phenomenon to such peptides, which do not cause drastic perturbances of the cell membrane. One could imagine a quantitative rather than qualitative difference between the pore-forming and translocating groups of peptides; CPPs may constitute a group with similar but milder effects on membrane integrity than the antimicrobial ones. In both cases, peptides should concentrate at the membrane surface. The interaction may cause weakening of the membrane barrier, which, in the pore forming case, will result finally in lethal permeability.

For good CPPs, on the other hand, disruption of the phospholipid assembly should be less serious and permanent, perhaps because the peptide does not so easily form aggregates at the membrane surface, or because it is only partially inserted

into the bilayer. A necessary, but not a satisfactory, criterion for any CPP is its own translocation. In order to be classified as a useful CPP, the peptide should also be able to carry cargo across a membrane. The size and nature of the cargo seems still to be an open question. However, a minimum requirement should be that the cargo is not just a part of the CPP peptide sequence itself, like an NLS-tag.

10.10 SPECULATIONS ON THE MECHANISMS OF CPP TRANSLOCATION

The only common obvious property among CPPs is their ability to permeate many types of living cells without damaging them. From cell culture studies it is believed that the spectacular transport of CPPs and a sizable cargo is not mediated by a chiral receptor, nor is it an energy-dependent process. Is there a common mechanism responsible for translocation of CPPs over plasma membranes? It is likely that CPPs of different types (Table 10.1) do not necessarily employ the same mechanism for their translocation.

We can distinguish two types of CPPs: one has many charged groups distributed along the molecule and another has relatively few charged residues terminating a long hydrophobic stretch. There is no consensus of primary sequence among CPPs; their origin and design are diverse (Table 10.1). The CPPs are more or less amphiphatic but they should be water-soluble with a low tendency to self-aggregate. Although some residues appear to be crucial, there is not always an all-or-none situation. A truncated analog can function, although with a reduced potency. The optimization of the properties is still based on empirical experiments. A number of basic amino acids (R, K) seem to be required. Arginine-rich peptides like pure Arg oligomers ($n < 9$) are even more potent than the parent CPPs.[59]

That the CPPs interact in some way with a membrane is a rather trivial finding from the model studies. However, the highly charged penetratin molecule interacts mainly by electrostatic attraction to an acidic phospholipid membrane, whereas other types of CPPs, like transportan and the other chimera, have a certain interaction even with a neutral membrane. In the case of negatively charged membranes, the interfacial concentration of a CPP will become very high. However, when the CPP is linked to a cargo, the total net charge of the assembly will be relevant. In the case of a polynucleotide cargo, the net charge might even hinder permeability if the surface potential is negative. Still, polynucleotides seem to come through.

In contrast to membrane-active antimicrobial peptides (melittin, magainin, etc.), so far no evidence exists for any pore formation leading to membrane leakage with CPPs. Moreover, a transient pore would be based on an oligomeric structure, which could hardly incorporate the many different types of cargos, including nanometer beads. Based on some membrane model experiments with penetratin, an inverted micelle model has been put forward.[6] However, the ^{31}P NMR spectra did not provide convincing evidence of a spectral (isotropic) component from lipidic particles, induced by penetratin. Nevertheless, it was suggested that penetratin, with its cargo, could be accommodated within an aqueous cavity of an inverted micelle, and then transiently internalized. Such a mechanism may not cause any leakage, but is as

complicated and unlikely as a pore model. Whether any of the CPPs are able to promote a transverse diffusion (flip-flop) of some phospholipids remains to be studied.

There is today no simple correlation between any degree of secondary structure induced in various model systems and the permeability efficiency of CPPs in cellular systems. Translocation of a charged CPP and a cargo across an *intact* membrane is energetically very unfavorable, even in the presence of proper transmembrane potential.

The CPP effect will depend on biophysical phenomena, not easily accounted for by structures, or molecular simulations in a short time window (~nsec). The function of the CPP tag could perhaps be as a magic agent to destabilize the membrane locally. Electrostatic perturbations within the membrane, primarily in the outer leaflet, may cause lateral rearrangement of acidic lipids. Besides membrane surface potential, interfacial dipole potential could be influenced. A discreteness-of-charge phenomenon may also be created, as suggested for studies on hepta-lysine.[28] A thinning of the membrane like the one reported with magainin,[60] combined with a reduction of local surface tension, may allow CPPs to intercalate the membrane. An intimate and flexible sealing between peptide side groups and lipid head groups will reduce leakage until the CPP slips snugly through and pulls the concomitant cargo inside. After this transient permeation the membrane must rapidly recover and heal. The detailed structural and thermodynamic description of such a hypothetic process remains to be worked out. From the biophysical point of view, to elucidate the mechanisms involved in CPP translocation and transport is still a challenge.

ACKNOWLEDGMENT

Work on this project in the authors' laboratory is supported by the Swedish Science Council.

REFERENCES

1. Derossi, D., Chassaing, G., and Prochiantz, A., Trojan peptides: the penetratin system for intracellular delivery, *Trends Cell Biol.*, 8, 84, 1998.
2. Lindgren, M. et al., Cell-penetrating peptides, *Trends Pharm. Sci.,* 21, 99, 2000.
3. Schwarze, S.R., Hruska, K.A., and Dowdy, S.F., Protein transduction: unrestricted delivery into all cells? *Trends Cell Biol.*, 10, 290, 2000.
4. Derossi, D. et al., The third helix of the Antennapedia homeodomain translocates through biological membranes, *J. Biol. Chem.*, 269, 10444, 1994.
5. Derossi, D. et al., Cell internalization of the third helix of the Antennapedia homeodomain is receptor-independent, *J. Biol. Chem.*, 271, 18188, 1996.
6. Berlose, J.-P. et al., Conformational and associative behaviours of the third helix of antennapedia homeodomain in membrane-mimetic environments, *Eur. J. Biochem.*, 242, 372, 1996.
7. Kilk, K. et al., Cellular internalization of a cargo complex with a novel peptide derived from the third helix of the Islet-1 homeodomain. Comparison with the penetratin peptide, *Bioconjugate Chem.*, 12, 911, 2001.
8. Pooga, M. et al., Cell penetration by transportan, *FASEB J.*, 12, 67, 1998.

9. Green, M. and Loewenstein, P.M., Autonomous functional domains of chemically synthesized human immunodeficiency virus tat trans-activator protein, *Cell*, 55, 1179, 1988.
10. Frankel, A.D. and Pabo, C.O., Cellular uptake of the tat protein from human immunodeficiency virus, *Cell*, 55, 1189, 1998.
11. Lin, Y.-Z., Yao, S., and Hawiger, J., Role of the nuclear localization sequence in fibroblast growth factor-1-stimulated mitogenic pathways, *J. Biol. Chem.*, 271, 5305, 1996.
12. Chaloin, L. et al., Conformations of primary amphipathic carrier peptides in membrane mimicking environments, *Biochemistry*, 36, 11179, 1997.
13. Vidal, P. et al., Interactions of primary amphipathic vector peptides with membranes. Conformational consequences and influence on cellular localization, *J. Membr. Biol.*, 162, 259, 1998.
14. Prochiantz, A., Getting hydrophilic compounds into cells: lessons from homeopeptides, *Curr. Opin. Neurobiol.*, 6, 629, 1996.
15. Soomets, U. et al., Deletion analogues of transportan, *Biochim. Biophys. Acta*, 1467, 165, 2000.
16. *Handbook of Nonmedical Applications of Liposomes, Volume IV: From Gene Delivery and Diagnostics to Ecology*, Lasic, D.D. and Yechezkel, B., Eds., CRC Press, Boca Raton, FL, 1996.
17. Jin, A.J. et al., Light scattering characterization of extruded lipid vesicles, *Eur. Biophys. J.*, 28, 187, 1999.
18. Fischer, A., Oberholzer, T., and Luisi, P.L., Giant vesicles as models to study the interactions between membranes and proteins, *Biochim. Biophys. Acta*, 1467, 177, 2000.
19. Sanders, C.R. and Schwonek, J.P., Characterization of magnetically orientable bilayers in mixtures of dihexanoylphosphatidylcholine and dimyristoyl-phosphatidylcholine by solid-state NMR, *Biochemistry*, 31, 8898, 1992.
20. Prosser, R.S., Hwang, J.S., and Vold, R.R., Magnetically aligned phospholipid bilayers with positive ordering: a new model membrane system, *Biophys. J.*, 74, 2405, 1998.
21. Sternin, E., Nizza, D., and Gawrisch, K., Temperature dependence of DMPC/DHPC mixing in a bicellar solution and its structural implications, *Langmuir,* 17, 2610, 2001.
22. Glover, K.J. et al., Structural evaluation of phospholipid bicelles for solution-state studies of membrane-associated biomolecules, *Biophys. J.*, 81, 2163-2001.
23. Struppe, J., Whiles, J.A., and Vold, R.R., Acidic phospholipid bicelles: a versatile model membrane system, *Biophys. J.*, 78, 281, 2000.
24. Vold, R.R., Prosser, R.S., and Deese, A.J., Isotropic solutions of phospholipid bicelles: a new membrane mimetic for high-resolution NMR studies of polypeptides, *J. Biomol. NMR*, 9, 329, 1997.
25. Kuprin, S. et al., Nonideality of water-hexafluoropropanol mixtures as studied by X-ray small angle scattering, *Biochem. Biophys. Res. Commun.*, 217, 1151, 1995.
26. Grahame, D.C., The electrical double layer and the theory of electrocapillarity, *Chem. Rev.,* 41, 441, 1947.
27. Peitzsch, R.M. et al., Calculations of the electrostatic potential adjacent to model phospholipid bilayers, *Biophys. J.,* 68, 729, 1995.
28. Murray, D. et al., Electrostatic properties of membranes containing acidic lipids and adsorbed basic peptides: theory and experiment, *Biophys. J.,* 77, 3176, 1999.
29. Lakowicz, J.R., *Principles of Fluorescence Spectroscopy,* 2nd ed., Kluwer Academic/Plenum Publishers, New York, 1999.

30. Santini, C.-L. et al., Translocation of jellyfish green fluorescent protein via the tat system of *Escherichia coli* and change of its periplasmic localization in response to osmotic up-shock, *J. Biol. Chem.*, 276, 8159, 2001.
31. Rigler, R., Fluorescence correlations, single molecule detection and large number screening. Applications in biotechnology, *J. Biotechnol.,* 41, 177, 1995.
32. *Circular Dichroism and the Conformational Analysis of Biomolecules*, Fasman, G.D., Ed., Plenum Press, New York, 1996.
33. Yang, L. et al., Barrel-stave model or toroidal model? A case study on melittin pores, *Biophys. J.*, 81, 1475, 2001.
34. Tamm, L.K. and Tatulian, S.A., Infrared spectroscopy of proteins and peptides in lipid bilayers, *Q. Rev. Biophys.*, 30, 365, 1997.
35. Wüthrich, K., The second decade — into the third millenium, *Nat. Struct. Biol. NMR,* Suppl. 5, 492, 1998.
36. Ferentz, A.E. and Wagner, G., NMR spectroscopy: a multifaceted approach to macromolecular structure, *Q. Rev. Biophys.,* 33, 29, 2000.
37. Pervushin, K., Impact of transverse relaxation optimized spectroscopy (TROSY) on NMR as a technique in structural biology, *Q. Rev. Biophys.,* 33, 161, 2000.
38. *Biological Magnetic Resonance, Vol. 14, Spin Labeling, The Next Mellennium*, Berliner, L.J., Ed., Plenum Press, New York, 1998.
39. Lindberg, M. and Gräslund, A., The position of the cell-penetrating peptide penetratin in SDS micelles determined by NMR, *FEBS Lett.*, 497, 39, 2001.
40. Öhman, A. et al., NMR study of the conformation and localization of porcine galanin in SDS micelles. Comparison with an inactive analog and a galanin receptor antagonist, *Biochemistry*, 37, 9169, 1998.
41. Damberg, P., Jarvet, J., and Gräslund, A., Micellar systems as solvents in peptide and protein structure determination, *Meth. Enzymol.,* 339, 271, 2001.
42. Lindberg, M. et al., Secondary structure and position of the cell-penetrating peptide transportan in SDS micelles as determined by NMR, *Biochemistry*, 40, 3141, 2001.
43. Drin, G. et al., Translocation of the pAntp peptide and its amphipathic analogue AP-2AL, *Biochemistry,* 40, 1824, 2001.
44. Magzoub, M. et al., Interaction and structure induction of cell-penetrating peptides in the presence of phosholipid vesicles, *Biochim. Biophys. Acta*, 1572, 77, 2001.
45. Magzoub, M., Eriksson, L.E.G., and Gräslund, A., Conformational states of the cell-penetrating peptide penetratin when interacting with phospholipid vesicles. Effects of surface charge and peptide concentration, *Biochim. Biophys. Acta*, in press.
46. Vivès, E., Brodin, P., and Lebleu, B., A truncated HIV-1 tat protein basic domain rapidly translocates through the plasma membrane and accumulates in the cell nucleus, *J. Biol. Chem.*, 272, 16010, 1997.
47. Matsuzaki, K., Magainins as paradigm for the mode of action of pore forming polypeptides, *Biochim. Biophys. Acta*, 1376, 391, 1998.
48. Matzuzaki, K., Why and how are peptide-lipid interactions utilized for self-defense? Magainins and tachyplesins as archetypes, *Biochim. Biophys. Acta,* 1462, 1, 1999.
49. Shai, Y., Mechanism of the binding, insertion and destabilization of phospholipid bilayer membranes by α-helical antimicrobial and cell nonselective membrane-lytic peptides, *Biochim. Biophys. Acta*, 1462, 44, 1999.
50. Shai, Y. and Oren, Z., From "carpet" mechanism to *de novo* designed diastereomeric cell-selective antimicrobial peptides, *Peptides*, 22, 1629, 2001.
51. Tossi, A., Sandri, L., and Giangaspero, A., Amphipathic, α-helical antimicrobial peptides, *Biopolymers*, 55, 4, 2000.

52. Huang, H.W., Action of antimicrobial peptides: two-state model, *Biochemistry*, 39, 8347, 2000.
53. Yang, L. et al., Crystallization of antimicrobial pores in membranes: magainin and protegrin, *Biophys. J.*, 79, 2002, 2000.
54. Kobayashi, S. et al., Interactions of the novel antimicrobial peptide buforin 2 with lipid bilayers: proline as a translocation promoting factor, *Biochemistry*, 39, 8648, 2000.
55. Park, C.B., Kim, H.S., and Kim, S.C., Mechanism of action of the antimicrobial peptide buforin II: Buforin II kills microorganisms by penetrating the cell membrane and inhibiting cellular functions, *Biochem. Biophys. Res. Commun.,* 244, 253, 1998.
56. Thorén, P.E.G. et al., The Antennapedia peptide penetratin translocates across lipid bilayers — the first direct observation, *FEBS Lett.*, 482, 265, 2000.
57. Drin, G. et al., Physico-chemical requirements for cellular uptake of pAntp peptide. Role of lipid-binding affinity, *Eur. J. Biochem.*, 268, 1304, 2001.
58. Persson, D., Thorén, P.E.G., and Nordén, B., Penetratin-induced aggregation and subsequent dissociation of negatively charged phospholipid vesicles, *FEBS Lett.*, 505, 307, 2001.
59. Futaki, S. et al., Arginine-rich peptides, *J. Biol. Chem.*, 276, 5836, 2001.
60. Ludtke, S., He, K., and Huang, H., Membrane thinning caused by magainin 2, *Biochemistry*, 34, 16764, 1995.

11 Toxicity and Side Effects of Cell-Penetrating Peptides

Margus Pooga, Anna Elmquist, and Ülo Langel

CONTENTS

11.1 INTRODUCTION

The main application of CPPs is to use them for cargo delivery of bioactive polar compounds lacking cellular uptake ability. These peptides may be used as carriers

0-8493-1141-1/02/$0.00+$1.50

in vitro, such as in studies of cellular events, as well as *in vivo* for drug delivery.[1,2] The mechanism exploited by cell-penetrating peptides to traverse the plasma membrane surrounding a cell is still unknown; however uncertainties regarding the mechanism have not hindered application of CPPs as carriers of many polar compounds lacking cellular uptake.

An ideal vector for transmembrane delivery would need to guarantee efficient transport of cargo into the cell interior. It should enter the cells without interfering with cellular processes or impairing the barrier function of plasma membrane surrounding cells (i.e., the ideal CPP should be nontoxic and side effect-free). First, the CPP (alone or conjugated with a cargo) must cross the plasma membrane — a lipid bilayer. Direct interaction of the peptide with lipids in the membrane is thought to be obligatory for cell penetration.[3] This interaction is accompanied by rearrangements of the membrane that, depending on properties and concentration of a particular CPP, could range from temporary to permanent and from subtle to profound. Second, the most often used delivery peptides are derived from naturally occurring proteins that carry different functions and possess various activities in cells. Whether the respective CPP is completely devoid of parent protein activities has not been sufficiently studied yet, nor if they gain new unexpected functions.

Most CPPs are positively charged under physiological conditions[3] and the impact of nonspecific interaction with cellular anions cannot be underestimated at concentrations achieved in cell-penetration assays. Here we give a brief overview about published data concerning nondesired biological activities of CPPs.

11.2 TOXICITY STUDIES OF CPPs

The primary structure and especially the net charge of CPPs are important factors influencing interaction with cellular membranes and also toxicity. Most CPPs are positively charged and some obtain an α-helical conformation in the membrane-mimicking environment. Some similarity can therefore be found with well-characterized antimicrobial peptides, which constitute a defense system against invading microorganisms in many organisms (for reviews see Ganz and Lehrer,[4] Boman,[6] and Simmaco et al.[5]). Both these types of peptides interact with the plasma membrane and enter the cells, though antimicrobial peptides assemble and multimerize at the membrane-forming pores. Pore formation is the main toxic mechanism of antimicrobial peptides. Upon interaction with the target membrane they fold from an unordered state into an amphipathic α-helix conformation. The target cell is lysed by a two-step mechanism: binding the peptide to the cell surface followed by membrane permeabilization (for a review see Dathe and Wieprecht[7]). Some CPPs, like the model amphipathic peptide (MAP), have features rather similar to antimicrobial peptides and the cellular uptake of the two peptide classes could proceed by a common mechanism.[8]

Most cell-penetrating peptides comprise an Arg- and Lys-rich region called the basic domain. Positively charged amino acids have been suggested to be pivotal in the electrostatic interaction with negatively charged head groups of phospholipids constituting cell plasma membranes.[9] Cell lytic peptides also contain a basic domain

as a typical amino acid motif which is presumably of similar function as that for CPPs. In addition, CPPs usually have a hydrophobic part that is suggested to induce integration of peptides into the cell membrane.[10] Some CPPs are amphipathic; like antimicrobial peptides, they adopt an α-helical structure under membrane-mimicking conditions.[11]

The toxicity and cell-lytic activity of antimicrobial peptides necessitate studies of CPPs' toxicity on plasma membranes and on general cellular level since similarities exist between these two classes of peptides. CPPs may act like toxic agents or peptides on proteins and lipids of cellular membranes, on cell proliferation, and also *in vivo,* causing cell death and inflammatory response. Further, some CPPs are derived from biologically active proteins, so the activities of these peptides must be evaluated before using them as carriers. Next we describe the most commonly used methods for assaying *in vitro* toxicity of different CPPs.

11.2.1 *In Vitro* Toxicity

The term *cytotoxicity* denotes a complex process spanning from the death of a single cell (general cytotoxicity) to the altering and gradual malfunction of the target cell/tissue (organ/cell-specific cytotoxicity). For evaluating short-term effects of bioactive compounds, a diversity of *in vitro* cell viability and cytotoxicity assays has been developed. These *in vitro* treatments are cheaper, easier to quantify, and ethically more acceptable than *in vivo* experiments.[12]

On the other hand, *in vitro* toxicity assays suffer from inherent limitations. In cell cultures it is usually difficult to recapitulate the respective *in vivo* situation with its complex pharmacokinetics. In general, significant differences often exist in drug exposure and concentration, metabolism, and excretion between *in vitro* and *in vivo* situations. Furthermore, only metabolism in the liver turns some substances toxic, which can be difficult to model in cell cultures. Analogously, the detoxification process that converts substances toxic to cells in culture into nontoxic ones for a living animal can be difficult to recreate *in vitro*. However, for initial testing of cytotoxicity, *in vitro* methods are very useful and informative, especially when studying compounds with putative membrane activity. *In vitro* toxicity assays track changes in cellular homeostasis triggered by the compounds of interest by estimating their general cytotoxicity or effect on cell viability and assessing integrity of the plasma membrane or metabolic activity, respectively.

11.2.1.1 Cell Membrane Permeability

The cell plasma membrane, a lipid bilayer, constitutes the first barrier against toxic agents, preventing hydrophilic molecules from entering the cell. The cellular homeostasis of ions and organic molecules is regulated at the plasma membrane with help from specific integral and peripheral proteins embedded in the lipid bilayer, i.e., transporters, receptors, channels, and pumps. Small and lipophilic substances are not hindered by the barrier and diffuse passively through the membrane.

There are several ways in which toxic agents may change the cellular membrane permeability. They may interfere with the functioning of membrane proteins, for

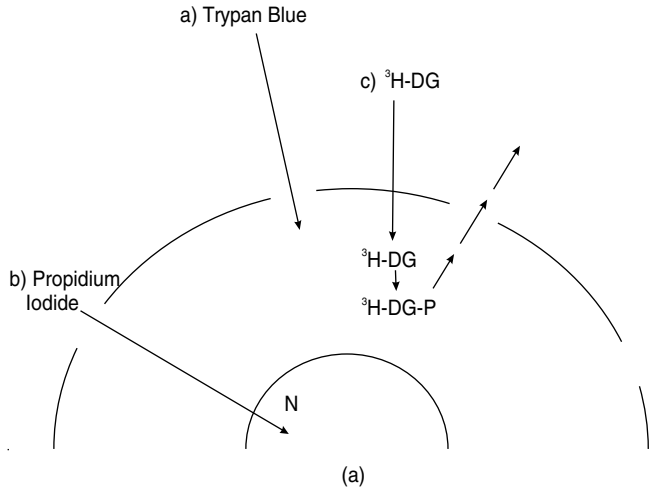

FIGURE 11.1a Methods used for estimating CPP-induced membrane toxicity. (a) Membrane-impermeable dyes (trypan blue, nigrosin, etc.) are excluded by living cells and can only enter into dead cells with damaged membranes. (b) Fluorescent DNA intercalating dyes are impermeable to cells and stain nuclei of damaged cells only. (c) Tritiated 2-deoxyglucose (DG) is taken up into the cells by glucose carriers and phosphorylated. The resulting ^{3}H-2-deoxyglucose-6-phosphate (DGP) efflux is only from cells with perforated membranes. (N = nucleus.)

instance by binding or cross-linking surface receptors. They may affect lipids by disturbing lipid organization or by lipid peroxidation as a consequence of free radical formation (e.g., ROS). Other agents act as detergents, dissolving membranes and forming permeable pores. Through these pores protons, metal ions and even proteins can leak out of the affected cell, causing collapse of the membrane potential and eventually cell death.

Good correlation between increased plasma membrane permeability and cell pathology enables rapid identification of dying or dead cells *in vitro.*[13] Exclusion of impermeable dyes by viable cells and leakage of cytosolic proteins or introduced markers from damaged cells are two ways to measure toxicity *in vitro.*[8,14]

11.2.1.1.1 Exclusion of Dyes

Most cells are impermeable to colloidal dyes such as nigrosin, trypan blue, and erythrosine B.[13,15,16] However, if the cell plasma membranes have been damaged or if the cells have died, dye exclusion ability will be lost yielding colored cells (Figure 11.1.a). The ability of cells to exclude the dye is so profound that it can be applied for measuring cell viability.[15] Usually the cells are stained in suspension, plated out, and viable cells counted using a hemocytometer. Several modifications, such as spectrophotometric analysis for quantification by Saijo[17] and a perfusion system for continuous reading of trypan blue uptake in cell monolayer cultures by Walum and co-workers,[16] have been suggested in order to decrease the subjectivity involved in this method. Similar to colloidal stains, impermeable fluorescent dyes such as dansyl lysine are often used to identify damaged or dead cells. DNA

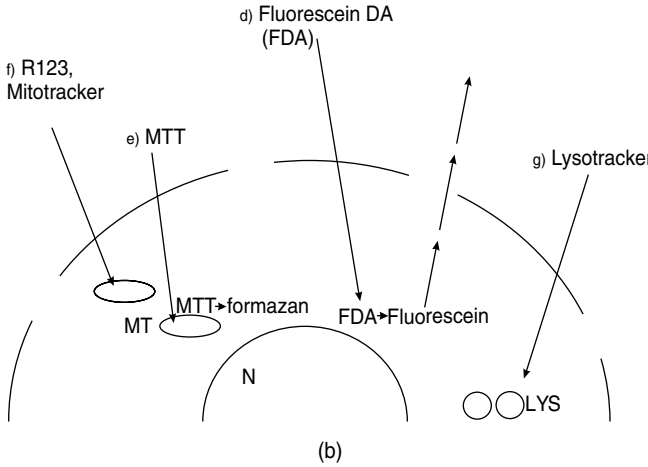

FIGURE 11.1b Methods used for estimating effects on cell viability. (d) Nonfluorescent, nonpolar fluorescein diacetate (FDA) diffuses into cells across the plasma membrane. The cellular esterases convert FDA into the fluorescent and polar fluorescein retained inside living cells. (e) Soluble MTT is converted into water-insoluble formazan crystals by mitochondrial enzymes of living cells. (f) R123 and Mitotracker® concentrate into mitochondria and (g) Lysotracker® into lysosomes of viable cells only. (N = nucleus; MT = mitochondria; LYS = lysosomes.)

intercalating dyes like ethidium bromide and, especially, propidium iodide (Figure 11.1.b), which is better suited to fluorescence microscopy, flow cytometry, and cell-sorting techniques, have gained more popularity.[18,19] New derivatives of propidium iodide (PI) are less cell-permeable and practically nonfluorescent when unbound to DNA, thus enabling a more sensitive detection system.

Dye exclusion assays are cheap, easy to perform, and well established over decades. However, these methods tend to overestimate viability, since cells unable to attach and proliferate (i.e., nonviable) may exclude the dye. Exclusion of trypan blue[20] (see Table 11.1) and propidium iodide[21] have been used for evaluation of CPP-induced toxicity.

11.2.1.1.2 Cytoplasmic Leakage

Another strategy for detection of cell plasma membrane damages is to estimate the outflow of cytosolic enzymes or cell-introduced probes.[22] The release of lactate dehydrogenase (LDH) into cell culture media[23] is one of the most traditional and frequently used leakage assays. LDH activity is measured by the conversion of NAD to NADH in the presence of excess lactate substrate. Release of LDH has been used in different toxicity assays and enables assessment of accumulated leakage over a remarkable time period. The major drawback with this method is the latency of LDH, since leakage of a high molecular weight enzyme is relatively slow as compared to dansyl lysine or PI nuclear staining.[19]

Another straightforward assay for determining the amount of viable cells is to measure radioactivity leakage from metabolically prelabeled cells after doping the

TABLE 11.1
Estimated Minimal Toxic Concentrations of CPPs *In Vitro*

Cell penetrating peptide	Minimal toxic concentration, μM			
	TPE[a]	DGP[b]	Others	Cell lines
KLALKLALKALKAALKLA-NH_2 (MAP)	4[8]	1[14]	4 (FDA[c])[8]	AEC, BMC
KLALKALKAALKLA-NH_2	Not toxic at 50[20]	N/A	N/A	AEC
KLGLKLGLKGLKGGLKLG-NH_2	Not toxic at 50[20]	N/A	N/A	AEC
GRKKRRQRRRPPQ-NH_2 (Tat (48–60))	N/A	Not toxic at 20[14]	N/A	BMC
RQIKIWFQNRRMKWKK (penetratin)	N/A	20[14]	50 (MC[d])[36]	U2OS, BMC
GWTLNSAGYLLGKINLKALAALAKK IL-NH_2 (transportan)	N/A	5[14]	N/A	BMC

[a] Trypane blue exclusion.
[b] 2-deoxyglucose-6-phosphate leakage.
[c] Fluorescein diacetate assay.
[d] Morphological changes.

cells with ^{14}C-thymidine, ^{35}S-methionine, ^{32}P, ^{3}H-uridine, ^{14}C-nicotineamide, etc.[24] However, these leakage assays do not allow proper detection of pores or temporal disturbances in the plasma membrane, since marker molecules of remarkable size like proteins and DNA cannot leak out through the small or short-living openings.

Detection of pores and temporal changes in the plasma membrane can be achieved by a more sensitive leakage assay in which the radioactive chromium (^{51}Cr) isotope is used. Living cells easily take up the reduced form of the isotope $^{51}Cr^{3+}$ in the form of $Na^{251}CrO_4$ salt.[25] Viable cells oxidize $^{51}Cr^{3+}$ to the membrane-impermeable $^{51}Cr^{2+}$ and its liberation enables quantitative estimation of membrane damage or cell death. The retention of $^{51}Cr^{2+}$ also shows that cells are viable since no radioactivity has been released from the cells.

A similar assay to estimate membrane intactness and cell viability by using tritiated 2-deoxyglucose was developed by Walum and Peterson.[22] The glucose analogue 2-deoxyglucose is taken up into cells via glucose carriers and then phosphorylated by hexokinase (Figure 11.1.c). The product, 2-deoxyglucose-6-phosphate (DGP), has been shown not to leave the cell via the plasma membrane when it is intact.[26] The efflux of radioactivity from cells preloaded with tritiated 2-deoxyglucose can be measured according to the method described previously,[22] which is quick, objective, easy to quantify, and does not use as detrimental ion $^{51}Cr^{3+}$. However, uptake of glucose (and $^{51}Cr^{3+}$ as well) varies between different cell lines and could in some cases be too low for detecting subtle changes in plasma membrane permeability. On the other hand, fast changes in membrane permeability induced by CPPs can be detected by the DGP assay.[14]

11.2.1.2 Viability Assays

Cell viability assays are based on counting living active cells instead of damaged or dead cells, which are counted in methods based on exclusion and leakage. These viability assays estimate the functioning of whole cells, usually assuming the intactness of the plasma membranes. Mainly, the activity of enzymes, pumps, and transporters is used for measuring cellular function, even under unfavorable conditions.

11.2.1.2.1 Enzymatic Assays

Many enzymatic viability assays are based on the activity of cytosolic esterases that convert neutral nonpolar esters of dyes that diffuse into the cells to colored or fluorescent substances. The products, which are polar or poorly soluble, cannot leave a cell via intact plasma membrane. The diacetyl derivative of fluorescein[27] was the first and, for a long time, the most commonly used compound for measuring viability enzymatically (Figure 11.1.d). An alternative compound for wider application is now provided by acetoxymethyl ester of calcein. This substance has the advantages of longer cellular retention time and lower pH sensitivity as compared to fluoresceinyl derivatives.

The functionality of mitochondria is assessed in the MTT assay described in the early eighties by Mosmann as a rapid colorimetric method for measuring cellular growth and survival.[28] It is based on the cleavage of a yellow, water-soluble tetrazolium dye, MTT, by succinate dehydrogenase (Figure 11.1.e). The tetrazolium ring is cleaved only in active mitochondria, resulting in a purple, water-insoluble MTT formazan product whose absorbency can be measured after dissolving the formed crystals in an organic solvent. MTT cleavage occurs only in active cells; the reaction is quick and no washing steps are required, which makes the method convenient and popular for measuring cytotoxicity, proliferation, and activation. However, a number of factors can significantly influence the cleavage of MTT,[29] such as cellular uptake and metabolism of glucose, cellular concentration of the reduced pyridine nucleotides NADH and NADPH, pH of media, and type of cell line. These parameters must be considered when establishing MTT assay conditions.

Both methods — the retention of fluorescein and the MTT assay — have been used to study effects of CPPs on cell viability[8,21,30] (see Table 11.2).

11.2.1.2.2 Uptake Assays

Maintenance of organelles and their specific environment is essential for cell survival. Some dyes sensitive to minor pH changes can diffuse into cells and will concentrate in acidic organelles, thereby reporting maintenance of organelle intactness and functionality. Acridine orange and neutral red can be used to reveal and assess the functioning of lysosomes.[31]

The dye rhodamine 123 (R123), which is sensitive to changes in membrane potential, concentrates in active mitochondria resulting in an intense fluorescence signal (Figure 11.1.f). This enables detection of mitochondria membrane intactness by the membrane potential and also visualization of these organelles.[32] Loss of R123 fluorescence is a rapid indicator of decreased cell viability and precedes the onset of propidium iodide staining of the nuclei. New derivatives of Mitotracker® and

TABLE 11.2
CPP-Induced Effect on Cell Viability as Determined by the MTT[a] Method

Cell-penetrating peptide	Conc., μM	Time, h	Viability	Cell line
KLALKLALKALKAALKLA-NH_2 (MAP)	10	0.5	50%[9]	AEC
C(Acm[b])GRKKRRQRRRPPQC[c] (Tat (48–60))	100	24	80%[31]	HeLa
C(Acm[b])FITKALGISYGRKKRRQRRRPPQC[c] (Tat (37–60))	100	24	40%[31]	HeLa
GRRRRRRRRRPPQ-C[c] (R_9-Tat (48–60))	100	24	70%[42]	RAW264.7[d]
GRQIKIWFQNRRMKWKKG (Gly-penetratin)	30	72	100[35]	IB4[e]

[a] 3-(4,5-dimethylthiazole-2-yl)-2,5-diphenyl tetrazolium bromide.
[b] Cys-acetamidomethyl.
[c] Fluorescein labeled cysteine.
[d] Mouse macrophage cells.
[e] Lymphoblastoid cell line.

Lysotracker® series offer more sensitive and selective ways for measuring the maintenance and functionality of mitochondria and lysosomes (Figure 11.1.f,g) and thereby cell viability.

11.2.1.2.3 Ion Pump Assays

Intracellular calcium concentrations reflect the ability of cells to respond to receptor-mediated events. Chelators such as fura 2, indo-1, indo-2, and their acetoxymethyl derivatives that fluoresce upon binding calcium can be used to monitor changes in intracellular calcium concentration as a cellular response to different compounds. The concentration at which the compound of interest starts to reveal detrimental effects on particular cells can only be reliably estimated by combining different cytotoxicity and viability assays.

11.2.2 CPP Toxicity *In Vitro*

The effects of CPPs on cell viability and toxicity have mainly been assessed by using three different short-term *in vitro* assays: dye uptake and exclusion,[20] MTT assay,[30] and deoxyglucose leakage.[14]

11.2.2.1 Model Amphipathic Peptides (MAPs)

The 18 amino acids-long model amphipatic peptide (MAP; Table 11.1) contains only amino acids Lys, Ala, and Leu. This peptide was created to study cellular uptake mechanisms of a perfect amphipathic helix. MAP shares many characteristics (e.g., charge and amphipathicity) with antimicrobial peptides and its toxicity is therefore expected to be rather high. The toxicity of MAP and its analogues has been examined on cell cultures by using both trypan blue exclusion and leakage of fluorescein. Indeed, by using trypan blue exclusion, initial indications of membrane perforation of calf aortic endothelial cells (AEC) were detectable from 4 μ*M* peptide concentration (Table 11.1).[8] The decrease in cellular activity to hydrolyze fluorescein diacetate was

detected at slightly lower MAP concentrations with an approximate EC_{50} value of 4 μ*M*. The following study from the same group investigated cellular uptake and membrane toxicity of MAP analogues designed by varying the parameters amphipathicity, hydrophobicity and net charge.[33]

Membrane toxicity was examined for some of the analogues by using the fluorescein leakage assay. Shortening MAP by four amino acids from the C terminus or substituting all Ala for Gly in full length peptide reduced the fluorescein leakage about three times as compared to MAP at 4.5 μ*M* concentration. However, the cell penetration efficacy of these MAP analogues was dramatically impaired (decreasing about tenfold). Cellular uptake was abolished when the peptide was shorter than 16 amino acids or when a negative net charge was introduced.[33] A later study reported that a 50 μ*M* extracellular concentration of these analogues did not induce membrane perforation of LKB Ez7 (subculture of AEC cell), referring again to a very low cellular uptake of these peptides.[20]

The strong effect of MAP on cell membrane permeability was confirmed by the DGP leakage assay. A peptide concentration of 1 μ*M* initiated leakage of DGP from human Bowes melanoma cells (BMC; Table 11.1).[14] Increased MAP concentrations totally disrupted cell plasma membranes, raising the efflux of DGP to the same level as for the positive control, 1% Triton X-100.

Oehlke and colleagues assessed the effect of MAP on AEC viability by the MTT assay.[8] Like trypan blue exclusion and fluorescein leakage assays, MAP initiated a decrease in viability at 4 μ*M* concentration, with an EC_{50} value of approximately 10 μ*M* (Table 11.2). To date, the effects of other MAP analogues on cell viability have not been studied.

There is some difference in toxicity threshold concentration of MAP estimated by DGP leakage and MTT assay. It could be explained by different sensitivity of the used cell lines (AEC and BMC) to MAP. However, the DGP leakage is a more suitable assay for detection of subtle and temporal changes in the cell plasma membrane permeability.

11.2.2.2 Tat

The Tat (48–60) peptide, opposite to MAP, seems to cause no or very little harm to cells. Even at 20 μ*M* peptide concentration, no increase in BMC membrane permeability could be detected when studying the DGP leakage (Table 11.1).[14] The MTT assay confirms very low cytotoxicity of Tat and its more basic analogues. Tat (48–60) was shown to affect cell viability only at high concentrations.[30] HeLa cell viability decreased to 80% when treated with 100 μ*M* Tat (48–60) for 24 h (Table 11.2). However, extension of the peptide chain at the N terminus by 10 amino acids, resulting in Tat (37–60), decreased the HeLa cells' viability to 40% under identical experimental conditions.[30]

11.2.2.3 Penetratin

Penetratin peptide causes only minor disturbances to plasma membranes. Treatment of BMC with 20 μ*M* penetratin for 15 min increased the DGP leakage to 5% over

basal level (Table 11.1). At lower penetratin concentrations, membrane leakage decreased in a dose-dependent manner with no detectable leakage under 10 μ*M* concentration.[14]

The effect of penetratin on cellular viability has been studied by MTT assay.[34] No effect on lymphoblastoid cell line IB4 viability was detected after 72 h of treatment with up to 30 μ*M* of penetratin (Table 11.2). Mazel and colleagues used D-penetratin as a vector for doxorubicin to increase the uptake of this cytotoxic drug.[35] The vector peptide did not cause any drop of human erythroleukemia cell line K562 (multidrug sensitive) and K562/ADR (multidrug resistant) viability as judged by the MTT method. In contrast, Garcia–Echeverria and collegues detected rounding up of the U2OS osteosarcoma cells after treatment with 50 μ*M* penetratin, suggesting that high concentrations of the peptide can be cytotoxic, at least to some cells.[36]

11.2.2.4 Transportan

The membrane toxicity of transportan lies somewhere between that of penetratin and MAP as estimated by the DGP leakage assay.[14] Transportan induced efflux of radioactivity from BMC at 5 μ*M* concentration diluted in serum-free culture medium (Table 11.1). At lower concentrations, no effect on plasma membrane permeability could be detected.

11.2.2.5 Arginine-Rich Peptides

The structure–activity relationship studies of Tat (48–60) peptides, corresponding to the Arg-rich domain of several transcription factors, revealed that peptides consisting mainly of Arg could efficiently penetrate through the cell plasma membrane. Futaki and co-workers studied the effect of basic peptides on cellular viability by using the MTT assay.[37] The basic stretch (49–57) in Tat peptide was replaced with only Arg residues, resulting in even more basic analogues than the original peptide. This Arg_9–Tat (48–60) peptide decreased viability of mouse macrophage RAW264.7 cells to 70% after treatment with 100 μ*M* for 24 h, while the original Tat (48–60) sequence reduced the viability to 40% under identical conditions (Table 11.2).

These results indicate that Arg-rich peptides, which are highly basic, can be of rather low toxicity to cells in culture and might thereby be suitable as carrier vectors. The peptides that comprise only Arg residues are efficiently internalized by the cells. Unfortunately, data about *in vitro* toxicity of these vector peptides are not yet available. However, cellular cytotoxicity increases with peptide length and Arg polymers of 12 kDa are cytotoxic at concentrations as low as 800 n*M*.[38]

11.2.2.6 Conclusions

The longer and more amphipathic peptides seem to affect cell plasma membranes more and thereby increase membrane permeability. As expected, MAP showed highest cell toxicity as judged by MTT, dye exclusion, and leakage assays, followed by transportan, penetratin, and Tat (48–60). On the first look, more membrane

disturbance is caused by CPPs with higher yield of accumulation into the cells (ratio between the intra- and extracellular concentration of CPP at the equilibrium), for instance, MAP and transportan. This suggests that the membrane-disturbing effects of CPPs, exerted at plasma membrane, depend primarily on their intracellular or membrane concentration and not so much on the applied concentration.

It is difficult to estimate the exact intracellular concentration of CPPs. The intramembrane concentration is even more difficult to assess, making correlation to membrane toxicity practically impossible. Usually, intracellular CPP concentration is determined by using fluorescein-labeled peptides. However, fluorescein is sensitive to its surrounding environment, which can cause not only errors when estimating the concentration, but also assumed change in intracellular localization pattern.[20]

Usually the CPP efficiency to translocate into cells as well as the toxicity is estimated on cells growing in culture where cells are at different stages in the cell cycle. The amphipathic synthetic peptide NAc-GALFLGWLGAAGSTMGAWSQP-KKKRKV-cysteamide has been shown to exert cell cycle-dependent toxicity.[39] This peptide is more toxic to proliferating cells than confluent H9C2 cells, but minimally or quiescent to differentiated cells. This fact must be considered when *in vitro* results are the only basis for explaining *in vivo* results.

11.2.3 Side Effects of CPPs *In Vitro*

Most described side effects of CPPs are based on *in vitro* toxicity data. This is mainly due to the high importance of a nontoxic delivery vector and the relative ease of finding a relevant assay. However, all the plausible side effects of CPPs cannot be comprehended by studying cell toxicity.

The remarkable high positive net charge of most CPPs causes their tight binding to polyanions. Indeed, penetratin binds heparin[40] and interacts strongly with polysialic acid of the cell-surface glycosides.[41] Probably most CPPs can interact strongly with DNA or RNA and the interaction with negatively charged polysialic acid has been suggested to mediate the efficient uptake of pAntp by neurons.[40]

The ability of CPPs to translocate into cells and their *in vitro* toxicity is relatively well characterized, but still other biological activities are only known for Tat peptide and transportan. The absence of data for other CPPs does not necessarily mean that they are devoid of side effects.

11.2.3.1 Transportan

The chimeric molecule of transportan comprises the fragment of neuropeptide galanin and a peptide from wasp venom — mastoparan. Indeed, transportan has some characteristic features of galanin: it interferes with galanin (^{125}I-galanin) binding to type 1 galanin receptors in BMC membranes, at rather low concentration (K_D 17.4 n*M*).[42] Transportan, like mastoparan, modulates the activity of membranous G-proteins. Surprisingly, in contrast to mastoparan, which activates G-proteins, transportan possesses an inhibitory effect (EC_{50} of 21.1 μ*M*) on them. It is not clear whether these effects of transportan are caused by direct binding of the peptide to the receptor and G-proteins or by changing membrane properties and thereby modulating

activity of the respective proteins. Modulation of G-protein activity by transportan can be considered a drawback for a peptide-type delivery vector. However, the concentration of transportan used in cell delivery experiments is an order of magnitude lower than what is necessary to influence G-protein activity.[42]

The predecessor of transportan, galparan (^{13}Pro-transportan) possesses activity in different experimental systems. Galparan activates Na^+,K^+-ATPase,[43] and induces acetylcholine release in the frontal cortex[44] and release of insulin from rat pancreatic β-cells.[45] Transportan can probably also have some analogous activity in these assays because of very similar structure to that of galparan. The above-mentioned activities of transportan can hardly have adverse effects when using it *in vitro*, since most of its side effects are exerted at higher concentrations than those used in cell delivery experiments. Furthermore, very few cell lines express galanin receptors and receptor-mediated effects of transportan can be avoided *in vitro* by choosing a cell line without galanin receptors.

11.2.3.2 Tat

Transcription transactivating factor of HIV, Tat, exerts a multitude of activities in addition to activation of viral gene expression and replication. The secreted factor Tat is implicated in angiogenesis,[46] and monocyte chemotaxis,[47] induces apoptosis in endothelial,[48] and neuronal cells,[49] potentiates glutamate excitotoxicity,[50] and decreases cAMP synthesis, to mention a few.

So far, it has not been established whether the respective activities of full-length Tat can be confined to certain regions in the protein or if the effects can be mimicked by short peptide sequences. However, a recent study by Jia and collaborators demonstrates that some effects of Tat whole protein can be exerted by the 12 amino acids-long peptide corresponding to basic region (known to penetrate into cells), or a peptide of 20 amino acids corresponding to the cysteine-rich domain.[51] The Tat (46–57) peptide inhibits binding of vascular endothelial growth factor (^{125}I-$VEGF_{165}$) to KDR and neuropilin receptors in human umbilical vein endothelial cells (HUVEC IC_{50} of 42 μ*M*). This peptide was able to inhibit VEGF induced ERK activation and mitogenesis in endothelial cells and inhibited angiogenesis *in vitro*. Tat (46–57) also inhibited ERK activation, mitogenesis, and angiogenesis induced by basic fibroblast growth factor.[51]

11.3 CPP TOXICITY *IN VIVO*

The limited number of reports describing *in vivo* application of cell-penetrating peptides does not afford generalizations about the toxicity of CPPs. Supposedly, no formal study about the general and acute toxicity of CPPs *in vivo* has been performed. However, in experiments that applied CPP-mediated delivery *in vivo*, toxic effects of cell-penetrating constructs and, sometimes, also the transport peptide have been estimated. In most cases, no toxicity or unwanted side effects have been detected. The *in vivo* studies with application of CPP-mediated transport will here be briefly summarized, concentrating mainly on observations that can be related to possible toxic effects.

Transportan and penetratin were used for delivery of a 21-mer antisense PNA to down-regulate the rat galanin receptor subtype 1 expression.[52] No signs of toxicity were observed when 4.5 μg of the cell-penetrating peptide–PNA constructs were repeatedly (three times in 12-h periods) administered intrathecally into lumbar spinal cords of female Sprague–Dawley rats.[52]

Bolton and colleagues have investigated the uptake and spread of fluorescently tagged penetratin in adult rat brain.[53] Intrastriatal injection of 10 μg of penetratin caused neurotoxic cell death and recruitment of inflammatory cells as judged by immunocytochemistry. Lowering the dose to 1 μg or less reduced toxicity and also recruitment of inflammatory cells.[53]

A recent study investigated delivery of β-galactosidase (β-gal) by an 11-amino acid-long peptide called the protein transduction domain (PTD) of Tat (amino acids 47–57), into mice tissue.[54] Following 4 to 8 h intraperitoneal administration (i.p.) of 100 to 500 μg of Tat PTD-β-gal, the enzyme activity was detectable in most tissues: liver, kidney, heart, muscle, lung, spleen, blood, etc. Even the brain showed strong β-galactosidase activity 4 h after i.p. injection of Tat-β-gal. Transduction of β-galactosidase into brain did not disrupt the blood–brain barrier of mice since Evans blue-albumin coinjected with Tat-β-gal could not penetrate into brain. Importantly, no signs of gross neurological problems or systemic distress were observed after 14 consecutive days of injection of a mouse with 1 mg of Tat PTD fusion protein per kilogram of body weight.[54]

Rothbard and co-workers conjugated the systemic and poorly cell-permeable drug cyclosporin A to a hepta-arginine oligomer (cyclosporin–Arg_7) to increase its cellular uptake.[55] One ear of dermatitis-induced mice was painted with a solution of cyclosporin–R_7 construct or with only the arginine–oligomer. The constructs entered the dermal cells where cyclosporin was released from the transporter peptide and reduced the inflammation dose dependently. The effect was local, cyclosporin was not detected in serum, and no reduction of inflammation of untreated ear was observed. Arginine–oligomer had no effect on the inflammation and no evidence of adverse consequences was seen during the studies.[55]

In summary, it is of great importance to evaluate CPPs' toxicity before applying them as drug transporters. Different strategies have been utilized for evaluating the modulation of cellular functions by CPPs. The initial cellular interaction of these peptides takes place at the cell plasma membrane and effects on the plasma membrane may alter homeostasis of the entire cell. Assays based on dye exclusion or uptake and leakage of cytoplasmic components have mainly been used for evaluating CPP-induced membrane toxicity. In general, amphipathic and positively charged peptides, like MAP, seem to be more toxic than other CPPs according to plasma membrane permeability assays (see Table 11.1). These CPPs show higher effect on the cellular viability that might be the outcome of damaged cell plasma membranes (see Table 11.2). After initial membrane interaction, some CPPs may interact with DNA. Every compound that binds to genetic material must be considered a potential genotoxic agent; however, so far, no data are published concerning CPPs and genotoxicity.

In conclusion, more *in vivo* investigations are needed to clarify the CPP concentrations tolerated without toxicity problems. Unexpected side effects that are not

revealed as toxicity or an inflammatory response cannot be excluded, even though no signs of toxicity or inflammation are detected. One of the most serious aspects could be immune response against the transport peptide.[54] The primary structure (e.g., multiple positive charges and bulky aromatic side chains in penetratin and transportan) of several CPPs suggests these to be rather immunogenic.[56,57] On the other hand, short peptides are not usually inducing an immune response. The development and availability of several CPPs with different primary structures will hopefully help to avoid toxicity problems in the future.

ACKNOWLEDGMENTS

This work was supported by grants from the EC Biotechnology Project BIO4-98-0227, Swedish Institute Visby Program, Swedish Royal Academy of Sciences, Swedish Research Councils TFR and NFR and Estonian Science Foundation (ESF4007), and the James McDonnel Foundation.

ABBREVIATIONS

AEC	Aortic endothelial cells
BMC	Bowes melanoma cells
CPP	Cell penetrating peptide
DGP	Deoxyglucose-6-phosphate
FDA	Fluorescein diacetate
HUVEC	Human umbilical vein endothelial cells
LDH	Lactate dehydrogenase
MAP	Model amphipathic peptide
MTT	(3-(4,5-dimethylthiazol-2-yl)-2,5-diphenyl tetrazolium bromide
PI	Propidium iodide
PNA	Peptide nucleic acid
PTD	Protein transduction domain
TPE	Trypan blue exclusion
VEGF	Vascular endothelial growth factor

REFERENCES

1. Schwarze, S.R., Hruska, K.A., and Dowdy, S.F., Protein transduction: unrestricted delivery into all cells? *Trends Cell Biol.,* 10, 290, 2000.
2. Schwarze, S.R. and Dowdy, S.F., *In vivo* protein transduction: intracellular delivery of biologically active proteins, compounds and DNA, *Trends Pharmacol. Sci.,* 21, 45, 2000.
3. Lindgren, M. et al., Cell-penetrating peptides, *Trends Pharmacol. Sci.,* 21, 99, 2000.
4. Ganz, T. and Lehrer, R.I., Antimicrobial peptides of vertebrates, *Curr. Opin. Immunol.,* 10, 41, 1998.
5. Simmaco, M., Mignogna, G., and Barra, D., Antimicrobial peptides from amphibian skin: what do they tell us? *Biopolymers,* 47, 435, 1998.

6. Boman, H.G., Gene-encoded peptide antibiotics and the concept of innate immunity: an update review, *Scand. J. Immunol.,* 48, 15, 1998.
7. Dathe, M. and Wieprecht, T., Structural features of helical antimicrobial peptides: their potential to modulate activity on model membranes and biological cells, *Biochim. Biophys. Acta,* 1462, 71, 1999.
8. Oehlke, J. et al., Cellular uptake of an alpha-helical amphipathic model peptide with the potential to deliver polar compounds into the cell interior nonendocytically, *Biochim. Biophys. Acta,* 1414, 127, 1998.
9. Derossi, D. et al., Cell internalization of the third helix of the Antennapedia homeodomain is receptor-independent. *J. Biol. Chem.,* 271, 18188, 1996.
10. Du, C. et al., Conformational and topological requirements of cell-permeable peptide function, *J. Pept. Res.,* 51, 235, 1998.
11. Oehlke, J. et al., Extensive cellular uptake into endothelial cells of an amphipathic beta-sheet forming peptide, *FEBS Lett.,* 415, 196, 1997.
12. Acosta, D. et al., An *in vitro* approach to the study of target organ toxicity of drugs and chemicals, *In Vitro Cell Dev. Biol.,* 21, 495, 1985.
13. Kaltenback, J.P., Kaltenback, M.H., and Lyons, W.B., Nigrosin as a dye for differentiating live and dead ascites cells, *Exp. Cell Res.,* 15, 112, 1958.
14. Hällbrink, M. et al., Quantification of cellular uptake and comparison of some cell penetrating peptides, *Biochim. Biophys. Acta,* 1515, 101, 2001.
15. Melamed, M.R., Kamentsky, L.A., and Boyse, E.A., Cytotoxic test automation: a live-dead cell differential counter, *Science,* 163, 285, 1969.
16. Walum, E., Peterson, A., and Erkell, L.J., Photometric recording of cell viability using trypan blue in perfused cell cultures, *Xenobiotica,* 15, 701, 1985.
17. Saijo, N., A spectrophotometric quantitation of cytotoxic action of antiserum and complement by trypan blue, *Immunology,* 24, 683, 1973.
18. Jones, K.H. and Senft, J.A., An improved method to determine cell viability by simultaneous staining with fluorescein diacetate-propidium iodide, *J. Histochem. Cytochem.,* 33, 77, 1985.
19. Juurlink, B.H. and Hertz, L., Ischemia-induced death of astrocytes and neurons in primary culture: pitfalls in quantifying neuronal cell death, *Brain Res. Dev. Brain Res.,* 71, 239, 1993.
20. Scheller, A. et al., Evidence for an amphipathicity independent cellular uptake of amphipathic cell-penetrating peptides, *Eur. J. Biochem.,* 267, 6043, 2000.
21. Wender, P.A. et al., The design, synthesis, and evaluation of molecules that enable or enhance cellular uptake: peptoid molecular transporters, *Proc. Natl. Acad. Sci. U.S.A.,* 97, 13003, 2000.
22. Walum, E. and Peterson, A., Tritiated 2-deoxy-D-glucose as a probe for cell membrane permeability studies, *Anal. Biochem.,* 120, 8, 1982.
23. Mitchell, D.B. and Acosta, D., Evaluation of the cytotoxicity of tricyclic antidepressants in primary cultures of rat hepatocytes, *J. Toxicol. Environ. Health,* 7, 83, 1981.
24. Thelestam, M. and Mollby, R., Cytotoxic effects on the plasma membrane of human diploid fibroblasts — a comparative study of leakage tests, *Med. Biol.,* 54, 39, 1976.
25. Zawydiwski, R. and Duncan, R., Spontaneous 51Cr release by isolated rat hepatocytes: an indicator of membrane damage, *In Vitro,* 14, 707, 1978.
26. Smith, D.E. and Gorski, J., Extrogen control of uterine glucose metabolism. An analysis based on the transport and phosphorylation of 2-deoxyglucose, *J. Biol. Chem.,* 243, 4169, 1968.

27. Rotman, B. and Papermaster, B.W., Membrane properties of living mammalian cells as studied by enzymatic hydrolysis of fluorogenic esters, *Proc. Natl. Acad. Sci. U.S.A.,* 55, 134, 1966.
28. Mosmann, T., Rapid colorimetric assay for cellular growth and survival: application to proliferation and cytotoxicity assays, *J. Immunol. Methods,* 65, 55, 1983.
29. Vistica, D.T. et al., Tetrazolium-based assays for cellular viability: a critical examination of selected parameters affecting formazan production, *Cancer Res.,* 51, 2515, 1991.
30. Vivés, E., Brodin, P., and Lebleu, B., A truncated HIV-1 Tat protein basic domain rapidly translocates through the plasma membrane and accumulates in the cell nucleus, *J. Biol. Chem.,* 272, 16010, 1997.
31. Borenfreund, E. and Puerner, J.A.,, Toxicity determined *in vitro* by morphological alterations and neutral red absorption, *Toxicol. Lett.,* 24, 119, 1985.
32. Mitchell, P., Keilin's respiratory chain concept and its chemiosmotic consequences, *Science,* 206, 1148, 1979.
33. Scheller, A. et al., Structural requirements for cellular uptake of alpha-helical amphipathic peptides, *J. Pept. Sci.,* 5, 185, 1999.
34. Fenton, M., Bone, N., and Sinclair, A.J., The efficient and rapid import of a peptide into primary B and T lymphocytes and a lymphoblastoid cell line, *J. Immunol. Methods,* 212, 41, 1998.
35. Mazel, M. et al., Doxorubicin-peptide conjugates overcome multidrug resistance, *Anticancer Drugs,* 12, 107, 2001.
36. Garcia–Echeverria, C. et al., A new Antennapedia-derived vector for intracellular delivery of exogenous compounds, *Bioorg. Med. Chem. Lett.,* 11, 1363, 2001.
37. Futaki, S. et al., Arginine-rich peptides. An abundant source of membrane-permeable peptides having potential as carriers for intracellular protein delivery, *J. Biol. Chem.,* 276, 5836, 2001.
38. Mitchell, D.J. et al., Polyarginine enters cells more efficiently than other polycationic homopolymers, *J. Pept. Res.,* 56, 318, 2000.
39. Pellegrin, P. et al., Cell cycle dependent toxicity of an amphiphilic synthetic peptide, *FEBS Lett.,* 418, 101, 1997.
40. Joliot, A.H. et al., alpha-2,8-Polysialic acid is the neuronal surface receptor of antennapedia homeobox peptide, *New Biol.,* 3, 1121, 1991.
41. Prochiantz, A., Messenger proteins: homeoproteins, TAT and others, *Curr. Opin. Cell. Biol.,* 12, 400, 2000.
42. Pooga, M. et al., Cell penetration by transportan, *FASEB J.,* 12, 67, 1998.
43. Langel, Ü. et al., A galanin-mastoparan chimeric peptide activates the Na+,K(+)-ATPase and reverses its inhibition by ouabain, *Regul. Pept.,* 62, 47, 1996.
44. Consolo, S. et al., Galparan induces *in vivo* acetylcholine release in the frontal cortex, *Brain Res.,* 756, 174, 1997.
45. Östenson, C.G. et al., Galparan: a powerful insulin-releasing chimeric peptide acting at a novel site. *Endocrinology,* 138, 3308, 1997.
46. Ensoli, B. et al., Tat protein of HIV-1 stimulates growth of cells derived from Kaposi's sarcoma lesions of AIDS patients, *Nature,* 345, 84, 1990.
47. Albini, A. et al., Identification of a novel domain of HIV tat involved in monocyte chemotaxis, *J. Biol. Chem.,* 273, 15895, 1998.
48. Park, I.W. et al., HIV-1 tat induces microvascular endothelial apoptosis through caspase activation, *J. Immunol.,* 167, 2766, 2001.

49. Ramirez, S.H. et al., Neurotrophins prevent HIV Tat-induced neuronal apoptosis via a nuclear factor-kappaB (NF-kappaB)-dependent mechanism, *J. Neurochem.,* 78, 874, 2001.
50. Haughey, N.J. et al., HIV-1 Tat through phosphorylation of NMDA receptors potentiates glutamate excitotoxicity, *J. Neurochem.,* 78, 457, 2001.
51. Jia, H. et al., Cysteine-rich and basic domain HIV-1 Tat peptides inhibit angiogenesis and induce endothelial cell apoptosis, *Biochem. Biophys. Res. Commun.,* 283, 469, 2001.
52. Pooga, M. et al., Cell penetrating PNA constructs regulate galanin receptor levels and modify pain transmission *in vivo*, *Nat. Biotechnol.,* 16, 857, 1998.
53. Bolton, S.J. et al., Cellular uptake and spread of the cell-permeable peptide penetratin in adult rat brain, *Eur. J. Neurosci.,* 12, 2847, 2000.
54. Schwarze, S.R. et al., *In vivo* protein transduction: delivery of a biologically active protein into the mouse, *Science,* 285, 1569, 1999.
55. Rothbard, J.B. et al., Conjugation of arginine oligomers to cyclosporin A facilitates topical delivery and inhibition of inflammation, *Nat. Med.,* 6, 1253, 2000.
56. Hopp, T.P. and Woods, K.R., Prediction of protein antigenic determinants from amino acid sequences, *Proc. Natl. Acad. Sci. U.S.A.,* 78, 3824, 1981.
57. Kyte, J. and Doolittle, R.F., A simple method for displaying the hydropathic character of a protein, *J. Mol. Biol.,* 157, 105, 1982.

12 Quantification of Cell-Penetrating Peptides and Their Cargoes

Maria Lindgren, Mattias Hällbrink, and Ülo Langel

CONTENTS

12.1 INTRODUCTION

The detection of intracellular cell-penetrating peptides (CPPs) poses several obstacles — for example, the difficulty of distinguishing membrane-bound CPP from intracellularly localized CPP. In this chapter we focus on methods used in quantifying the efficiency of CPP internalization, as well as the quantification of cargoes delivered by CPPs.

For efficient detection of a translocated CPP, a reporter group is generally attached to the active amino acid sequence; this group could also be called cargo

0-8493-1141-1/02/$0.00+$1.50

because it is indeed translocated by the aid of the transport peptide. The most frequently applied reporter group in *in vitro* studies so far is biotin, which is detected with fluorescently labeled streptavidin–avidin visualized in a fluorescence microscope or quantified by, for example, fluorescence-activated cell-sorting (FACS) analysis or fluorescence spectrophotometry.

Various cargo molecules, oligonucleotides (ONs), peptide nucleic acid (PNA), drugs, peptides, and proteins have been successfully transported by CPPs into a great selection of cell types (for review, see Lindgren et al.[1]). More recently, CPPs have also been applied in *in vivo* studies. Chemical conjugation by disulfide bonds or in-chain synthesis (for peptides and PNA) are the two main methods for conjugation of cargo to the CPP. In addition, recombinantly expressed fusion proteins have been used for the Tat protein and Tat peptides. The importance of detachment of the cargo from the transport peptide in case of intracellularly cleavable disulfide bonds is a debated matter. It could be argued that if the CPP is not disturbing the cargo's intracellular activity a detachment is not necessary. The CPP could, in fact, provide a useful protection against degradation.

Despite all of the quantification methods available today, with exception of direct antibody detection, it is the amount of a cargo–reporter group that is measured and not the amount of the CPP, as would be desired. In experiments where only a qualitative indication of intracellular delivery is sufficient, biotin is a useful label, but when quantification of the uptake is essential, fluorescence labeling of the CPP or cargo is more convenient.

In this chapter, various methods to quantify the efficiency of CPP uptake are compared. Emphasis is on methods in which the main interest has been to characterize the CPP itself. There are also a great number of publications where the focus has been on activity of the cargo delivered by the CPP; these are only briefly reviewed in this chapter.

12.2 QUANTIFICATION METHODS

The concentration range of CPP used during uptake experiments is crucial for exact quantification. A cell-penetrating peptide is defined as a peptide primarily entering the cell — not via endocytosis or by pore formation. Several CPPs cause pore formation or have lythic activity, e.g., transportan and model amphipatic peptide (MAP), but it is negligible[2] at low concentrations (lower than 5 μ*M*). In contrast, endocytosis contributes to the uptake of Tat fragments.[3] As described in Chapter 11, dye leakage assays or tritiated-glucose leakage can be used to detect and quantify membrane disturbing effects of CPPs.

Another important challenge when quantifying CPP uptake is to distinguish between membrane- or cell-associated peptide and intracellular CPP. For example, Oehlke et al. (see Chapter 4) have used a method in which the membrane-bound peptide is modified in order to discriminate it from intracellular MAP.[4] In the studies of 2-amino benzoic acid (Abz)-labeled transportan (Figure 12.1), a trypsin treatment has been applied.[5] Furthermore, acid wash and oil centrifugation,[6] and reduction-sensitive 7-nitrobenz-2-oxo-1,3-diazol (NBD) fluorophore[7] have been utilized for the distinction between membrane-associated and internalized CPP. However, inactivation

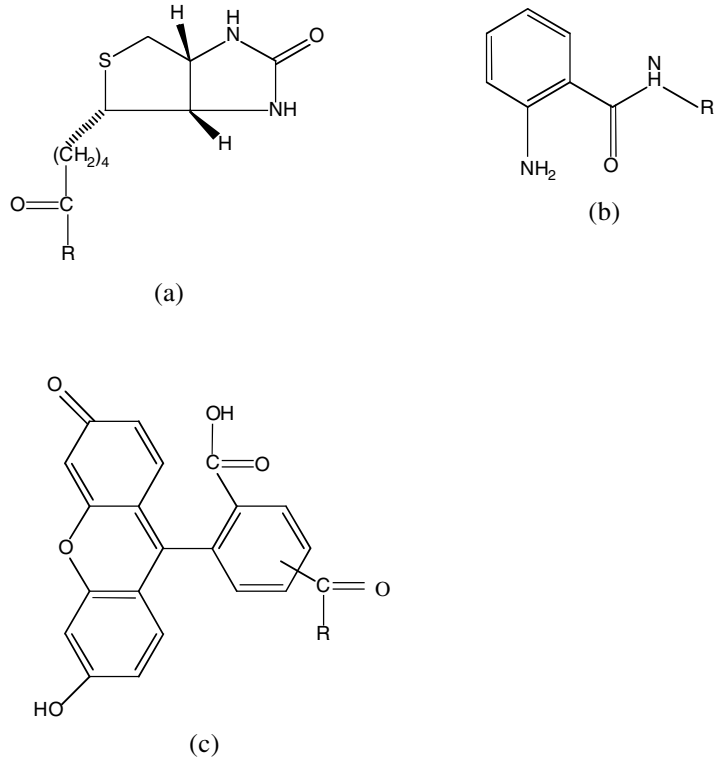

FIGURE 12.1 Structures of three reporter groups used in studies of transportan. (a) Biotinyl-, (b) 2-amino benzoyl (or Abz, λ_{ex}: 320 nm, λ_{em}: 420 nm), and (c) the fluorescein group (λ_{ex}: 494 nm, λ_{em}: 520 nm). The R denotes the attachment of the label to the primary amino group on the CPP.

of the label (NBD-group, for example) on CPPs that readily flow out from cells, e.g., MAP and transportan, could yield results biased toward lower uptake.

Scheller et al. discovered a wash-out effect connected to amphipaticity of the MAPs.[8] Analogues with lower hydrophobic moment had a lower resistance to wash-out. The higher ability of amphipathic peptides to associate with intracellular structures is suggested to be the main contributor to this phenomenon. Methods reviewed in this chapter on quantification of cell-penetrating peptides and their cargoes are as follows:

- Radiolabeling*
- Biotinylation*/Cell-ELISA
- Fluorescence microscopy/Spectrophotometer/FACS
- HPLC detection
- Immunodetection
- Detection of enzyme activity
- Fluorogenic construct assay*

* Practical examples of the method follow the text.

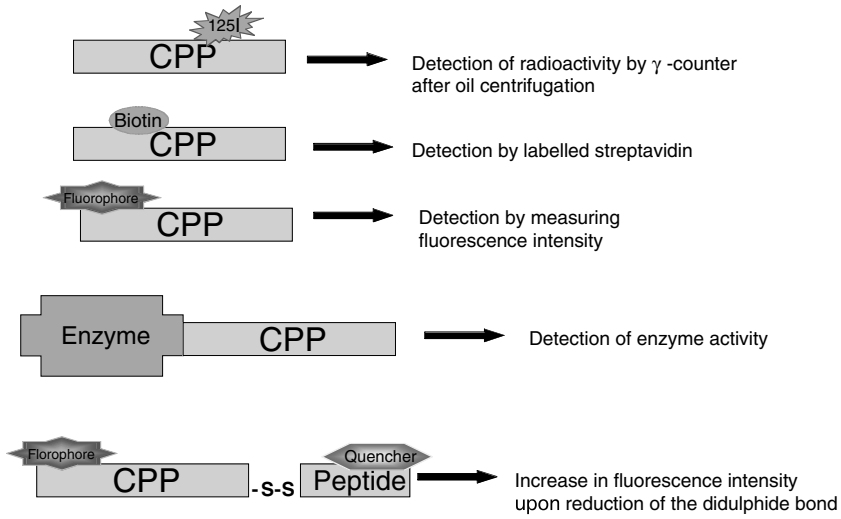

FIGURE 12.2 (Color Figure 12.2 follows p. 14.) Summary of the various detection methods used to quantify the internalization of CPPs by application of different labeling strategies. In general, the CPP is labeled with a reporter group, added to adherent cells or cells in solution, and the quantification of the CPP is carried out according to the method indicated in the figure.

- Detection of bioactivity of peptide cargo
- Detection of DNA/PNA antisense effects
- Quantification of drug activity

12.2.1 Studies of Cell-Penetrating Peptides Using Reporter Groups

This chapter is divided into two parts: one dealing with studies of CPPs and the other, very briefly, with quantification of cargoes delivered by CPPs. The reporter group, or label, is here defined as an addition to the CPP that will make it detectable. The exception is the immunodetection of the Tat peptide in which no reporter group is used. Detection methods used for these studies are summarized in Figure 12.2.

12.2.1.1 Radiolabeling

Two radioisotopes, ^{3}H and ^{125}I, have been used for radioactive labeling of peptides. Iodination is preferred because it is easier to perform and reproducible, even though the half-life of ^{125}I is only 60 days compared to tritium's 12 years. The most common methods used for peptide iodination are Chloramine-T and the [^{125}I]-Bolton–Hunter reaction.[9] For the Chloramine-T method, a Tyr residue is required in the sequence, as the aromatic side chain is the acceptor of the iodine isotope. Here, a major drawback is the possible oxidation of Trp and Cys/Met residues.

The Bolton–Hunter iodination is an acetylation of a primary N-terminal α-amino group or an ε-amino group of Lys by N-succinimidyl-3-(4-hydroxy, 5-^{125}I-iodophenyl) propionate. In the case of a sequence containing several Lys residues, the

reaction yields heterogeneously labeled products, which makes it difficult to estimate specific activity. For the studies of transportan, peptide iodination was carried out by the Chloramine T method.[6]

Example 12.1
Preparation and Internalization of ^{125}I-Labeled Transportan Peptides

Peptide iodination was carried out by the Chloramine T method.[10] $Na^{125}I$ (specific activity 16.1 mCi/mg, concentration 0.1 mCi/mL) was mixed with 5 eq. of the peptide, and phosphate buffer was added in tenfold excess.[5] The Chloramine T solution was prepared at a concentration of 2 mg/ml in phosphate buffer, pH 7.4. After 2 min of incubation, adding sodium metabisulfit (2.4 mg/ml in phosphate buffer, pH 7.4) stopped the reaction. The peptides were purified on a reversed-phase, column SEP-PAK 51910 (Millipore) using stepwise gradient of acetonitrile in water. The iodination was performed using 1 mCi $Na^{125}I$ and 4.9 nmol of biotinylated peptide for transportan and transportan 2, while transportan 3 was iodinated using 5 mCi of $Na^{125}I$ and 12.6 mmol, respectively. The fractions with the highest specific activity of radiolabeled peptides were used in the uptake experiments. The radiolabeled peptides, in HEPES-buffered Krebbs Ringer solution, were added to Bowes melanoma cells in suspension. The incubation was made on a mildly shaking waterbath at 37ºC. To separate the extracellular peptide, the cell suspensions were centrifuged through a mixture of 40% dioctyl phalate and 60% dibutyl phalate and washed in an acidic solution (0.2 *M* acetic acid in 0.5 *M* NaCl, pH 2.5). The fractions were counted in a γ-counter (Packard, Meriden, CT). As a control of the intactness of the cells during the incubation time, only $Na^{125}I$, instead of labeled peptide, was added.

12.2.1.2 Biotinylation and Cell-ELISA

Biotin (Figure 12.1) has been widely used as a reporter group on CPPs, as it is considered a less disturbing modification compared to the widely used fluorophores, which can interact with plasma membranes by themselves. Indirect immunofluorescence detection of biotin is more time consuming than direct visualization of a chromophore, but enables greater flexibility of methods (see Example 12.2).

Fisher and colleagues used a cell-ELISA for quantification of biotinyl–penetratin.[11] In short, 50,000 cells per well were seeded and, after overnight incubation, biotinylated penetratin (40 μ*M*) was added. Cells were rinsed, fixed, and permebilized with 3% Tween 20. Endogenous alkaline phosphatase activity was blocked by 1% bovine serum albumin (BSA) in phospahate-buffered saline (PBS) at 65°C for 60 min. Alkaline phosphatase labeled-streptavidin was added for 30 min at room temperature and developed by substrate addition; absorbance was measured at 405 nm.

12.2.1.3 Fluorescence Microscopy, Spectrophotometer, and FACS

Today, a wide variety of fluorophores is in use, with fluorescein perhaps the most common (Figure 12.1). However, fluorescein is sensitive to photobleaching and,

additionally, its hydrophobicity and size can alter the properties of the peptide. The 2-aminobenzoic acid fluorophore (Abz, Figure 12.1) is small, stable, and photoresistent,[12] and does not alter the hydrophobicity of the peptide to the same extent as fluorescein and rhodamine do. However, Abz is not easily visualized in fluorescence microscopy due to its deep blue color (λ_{em} 420 nm), but it is useful for spectrometry detection.

The coupling of the fluorophore to the CPP is usually carried out by covalent linkage to the N-terminal α-amino group or ε-amino group of Lys of the peptide. For fluoresceinyl-modification, the succinimidyl ester (Molecular Probes, Holland) can be used in a five-fold excess to the peptidyl-resin in *t*-Boc peptide chemistry. In solid phase peptide synthesis with Fmoc chemistry, the fluorescein isothiocyanate was applied in the presence of diisopropylethyl amine (DIEA). The Abz group can be introduced by a routine amino acid-coupling step. The labeling is preferably carried out before cleavage of the peptide from the solid support to ensure specific linkage of the fluorophore. Labeling during solid phase synthesis has the further advantage of avoiding the time and low yield of labeling the peptide in solution, because it is critical to remove any unreacted dye, which can greatly complicate subsequent experiments.[13]

Flow cytometry or fluorescence-activated cell sorting (FACS) is a convenient way of quantifying the content of fluorescently labeled peptide. This method has been used by Garcia–Echeverria et al. for detecting FITC labeled-penetratin.[14] FACS is a sensitive method; less than 100 fluorophores per particle or cell have been detected by this method.[14] After CPP treatment of the attached cells, they are treated with trypsin and fixed in a 10% paraformaldehyde solution prior to cell sorting analysis.

Confocal fluorescence microscopy quantification of fluorophore-labeled CPP was described by Scheller et al.[15] and also in Chapter 4. An on-line protocol was employed that would avoid biasing the internalization results by outflow of the peptides. Briefly, cells are seeded on coverslips and treated with peptide. Three regions of interest are scanned in the cytosol and one in the nucleus of three selected cells. The fluorescence resulting from the incubation media is removed as background fluorescence. After a 30-min assessment, cell viability is checked by addition of tryphan blue.[15]

The NBD (7-nitrobenz-2-oxo-1, 3-diazol; NBD) fluorophore group, stable in Fmoc cleavage conditions,[16] has been used to label CPPs.[7] The main advantage with this label is the sensitivity toward reduction agents, such as dithionite, that can be used to inactivate extracellular and membrane-bound label. Moreover, the NBD group changes fluorescence characteristics in a hydrophobic environment toward an emission blue shift (from 537 to 530 nm) as well as an increase in intensity. This property makes it possible to measure membrane partition coefficients of the labeled peptide.

Example 12.2
Quantification of Biotin/Abz/FITC-Labeled CPP

Either the N terminus or the ε-amino group of a Lys residue could be used for labeling with biotin, Abz, or FITC. In the case of labeling *p*VEC, a novel CPP,[17] the

N-terminal α-amino group was used for attachment. The peptide was synthesized by standard *t*-Boc solid phase peptide synthesis. For FITC labeling of the same peptide, the α-amino group of the peptide was deprotected and 100 mg of peptidyl-resin was incubated with five-fold excess of 4(5)-carboxyfluorescein succinimidyl ester (Molecular Probes, Holland) for 24 h at room temperature in a 1:1 mixture of dimethyl formamide (DMF)/dimethyl sulfoxide (DMSO), with five-fold excess of DIEA. For biotin or Abz, three-fold excess of HOBt and TBTU activated biotin or *t*-Boc-Abz in DMF was incubated with the peptidyl-resin for 30 min at RT. The peptides were cleaved from the resins (with liquid HF at 0°C for 30 min) in the presence of scavenger (*p*-cresol). The purity of the peptides was checked by HPLC analysis on Nucleosil 120-3 C_{18} column (0.4×10 cm). Molecular mass of each synthetic peptide was determined on a Voyager MALDI-TOF.[5,17]

Cellular internalization assay: The cells used for internalization experiments were seeded at the density of 10,000 cells/glass coverslip (10 mm diameter) in 24-well plates. One day post seeding, the cells were semiconfluent and media were changed to serum-free media containing 10 μ*M* of labeled peptide. After 60 min of incubation at either 37 or 4°C, the cells were washed three times with phosphate-buffered saline (PBS) and fixed with 3% (v/v) paraformaldehyde solution in PBS for 15 min. For indirect detection of biotinylated peptide, the fixed cells were permeabilised with 0.5% Triton X-100 in PBS and sites for nonspecific binding were blocked with 5% bovine serum albumin (BSA) in PBS. The biotin moieties were visualized by incubation with Texas red-labeled streptavidin (1:200 in blocking solution, Molecular Probes, Holland) for 1 h at room temperature. The cell nuclei were stained with Hoechst 33258 (0.5 μg/ml, Molecular Probes, Holland). After washing with PBS, the preparates were mounted in Fluoromount G water base (Electron Microscopy Science, PA, USA).

Quantitative uptake of fluorescence-labeled peptide: Cells were seeded in 12-well plates at the density of 100,000 cells/well and incubated overnight to adhere. Twelve hours after seeding, the cells were washed once with serum-free media and treated with 10 μ*M* peptide, dissolved in serum-free media, for 60 min at 37°C. The cells were washed twice with HEPES-buffered Krebs–Ringer solution (HKR) and detached by trypsin treatment for 3 min. The cells were centrifuged at $4000 \times g$ for 10 min at 4°C and resuspended in 200 μl of HKR. The fluorescence was measured in a fluorescence spectrophotometer (F-2000, Hitachi, Japan). The concentration of fluorescence-labeled peptide was calculated from a standard curve of the peptide in HKR. Alternatively, the cells were detached before peptide treatment and the peptide was added to the cells in suspension and incubated on a shaking 37°C water bath. Then the outer membrane-bound peptide was degraded by a 4-min trypsin treatment, after which the cells were spun down, washed, and resuspended in HKR and the fluorescence intensity measured. For the wavelength applied, see Figure 12.1.

12.2.1.4 HPLC Detection

Oehlke et al. have used high-performance liquid chromatography to quantify uptake of fluorescein-labeled cell-penetrating peptides[4] (for further details, see Chapter 4). In order to separate cell surface-bound and internalized peptide, treated cells were

exposed to diazotized 2-nitroaniline, which selectively modifies Lys side chains. As the reagent does not cross the plasma membrane, only peptides exposed to the extracellular medium are modified, resulting in increased hydrophobicity and subsequent increased HPLC retention time. This allows separation of intracellular and surface-bound peptide.

This procedure has the advantage that the reagent is highly reactive even at 0°C, so that the results are not biased by efflux processes because they are suppressed at this temperature. An additional advantage is that the various metabolites of the peptide can be isolated and characterized by mass spectroscopy. Furthermore, the use of a fluorescence detector in the HPLC equipment increases the sensitivity of this analysis.

12.2.1.5 Immunodetection

In order to quantify the uptake of Tat (37–72), Vivés and colleagues used both fluorescein labeling and direct immunodetection, using a monoclonal antibody against the Tat basic cluster.[18] Quantification was done by FACS analysis. This detection by the monoclonal antibody is a direct quantification of the CPP, and not via a reporter group.

12.2.1.6 Detection of Enzyme Activity

Internalization of RNAse A, β-Galactosidase, horseradish peroxidase, and *Pseudomonas* exotoxin A by Tat fragment (residues 37–72) was studied by Fawell et al.[3] The uptake was monitored colorimetrically and by cytotoxicity measurements. Quantification was carried out by measuring absorbance of the respective substrate produced by the CPP internalized enzymes.

12.2.1.7 Fluorogenic Construct Assay

Resonance energy transfer (RET) quenching is a process in which a molecule with an absorbance spectra overlapping the emission spectra of a flourophore quenches the fluorescence when the molecules are in close proximity. Several such fluorophore-quencher pairs have been found, e.g., DABCYL/EDANS[19] and Abz/3-nitro-Tyr.[12] The amount of quenching is dependent on the distance between the molecules as well as the spectral overlap.

The Abz flourophore is compatible with Fmoc and *t*-Boc chemistries. It is resistant to photobleaching and has a well characterized amino acid-like quencher, 3-nitro-Tyr, which is stable under both main types of peptide chemistries.

We have used a short fluorescently labeled peptide, with the sequence: Abz-Cys-LKANL as cargo in delivery quantification.[2] The CPPs contained a Cys-residue used for covalent attachment of the cargo–peptide via a disulfide bond, and a 3-nitro-Tyr extension acting as a quencher to the Abz group, which resulted in a reduction-sensitive fluorogenic construct (Figure 12.2). The cellular uptake of the construct is registered as an increase in the fluorescence intensity when the disulfide bond of the CPP–S-S cargo construct is reduced in the intracellular milieu.

With this method, it is possible to monitor in real time the intracellular degradation of the disulfidebond, and hence the cellular uptake of the constructs by increase in apparent fluorescence. Moreover, it eliminates the need to separate membrane-bound and internalized peptide. However, in order to isolate the uptake kinetic constant, it is necessary to find the intracellular reduction rate constant. In this case, it was done by first measuring intracellular glutathione concentration and then measuring reduction of the constructs in the presence of lipid vesicles.

Additionally, it is necessary to confirm that the cargo peptide cannot be internalized after extracellular reduction of the construct and to confirm that the increase in fluorescence is not caused by glutathione outflow due to peptide-induced membrane leakage.

We used this technique to compare uptake and cargo delivery efficiency of four different CPPs: penetratin, Tat (48–60), transportan, and model amphipathic peptide (MAP). Our data show that MAP has the fastest uptake, followed by transportan, Tat (48–60) and penetratin. Similarly, MAP has the highest cargo delivery efficiency, followed by transportan, Tat (48–60) and, last, penetratin.[2]

Example 12.3
Quantification of Model Peptide S-S CPP Construct[2]

One equivalent of CPP-(3-nitro-Tyr)-Cys(NPys) and 2 eq. of free thiol containing Abz-Cys-cargo–peptide were dissolved in a deoxygenated mixture of 3:2:1 dimethyl sulfoxide/N-methyl pyrrolidon/0.1 *M* sodium acetate, pH 4.5. The mixture was stirred for 4 h under nitrogen flow, and subsequently purified on reverse phase HPLC and characterized on a Voyager MALDI-TOF (Applied Biosystems). The yield of the desired heterodimers was approximately 30%.

Cells were washed and harvested by scraping into HEPES-buffered Krebbs–Ringer solution (HKR) containing 0.5 g/l glucose and subsequently counted in a Neubauer chamber. In 96-well plates, approximately 250,000 cells in 50 µl were added to wells containing 150 µl of peptide construct dissolved in HKR to reach concentrations of 0.1, 0.5, 1, 5, or 10 µ*M*. The cells were kept suspended by shaking between readings and the temperature was held constant at 37°C throughout the experiment. After 70 min, 5 µl 100 m*M* dithiothreitol (DTT) was added to reduce all remaining constructs. The fluorescence intensity value obtained after DTT reduction was used to define 100% of reduction. The fluorescence intensity was found to be dependent linearly on construct concentration. Fluorescence was measured (λ_{ex}: 320 nm, λ_{em}: 420 nm) in a Spectramax Gemini XS (Molecular Devices, USA) 96-well fluoroscence spectrophotometer. After the experiment, the cells were harvested by centrifugation and counted again in order to ascertain that no substantial lysis of the cells had occurred. Intracellular glutathione concentration was determined using a glutathione assay kit (Calbiochem, USA) according to the manufacturer's instruction.

Determination of reduction rate constants in the presence of lipid vesicles: Ten mg of phosphatidyl choline and 5 mg of phosphatidyl serine (Sigma, Sweden) were dispersed into 1 ml of HKR by vigorous vortex mixing. The mixture was sonicated with a probe tip sonicator in 25°C for 30 min. The resulting vesicles were purified

by gel filtration on sephadex G50; they were diluted to a final concentration of 2 mg/ml in HKR. Construct was added to yield a lipid-to-peptide ratio of 1000:1 and the mixture incubated for 10 min, after which glutathione (100 and 500 μ*M*; 1 and 2 m*M*) was added. Fluorescence increase was measured in a Hitachi F-2000 spectroflourimeter and the data analyzed fitting a numerical procedure in accordance to the following reaction scheme:

$$[\text{Glutathione}] + [\text{CPP-S-S-Cargo}] \xrightarrow{k} [\text{Free cargo-SH}] + [\text{HS-CPP}]$$

using Dynafit software[20] (Biokin Ltd., USA). To confirm that the cargo peptide could not be internalized after extracellular reduction of the construct, independent uptake experiments were performed with the unconjugated cargo peptide. After 60 min of incubation, no significant uptake could be measured.

To confirm that the increase in fluorescence is not caused by glutathione outflow due to peptide induced membrane leakage, cells were incubated in 5 μ*M* of the inactive [Pro[19]]–transportan construct together with 10 μ*M* of biotinyl–MAP, the peptide showing most membrane disturbance. Only modest (<1% of total) fluorescence increase above baseline was detected. This experiment also excludes the possibility that unspecific interaction with extracellular proteins would enhance the reduction significantly.

As an additional control, the cells and constructs were mixed and immediately reduced with DTT. The resulting fluorescence intensity was similar to that obtained at the end of the uptake experiments, showing that the observed saturation is not due to quenching of the flourophore intracellularly.

12.2.2 Quantification of Biological Activity of Cargo Delivered by CPPs

In addition to the studies characterizing CPPs, a great number of publications have as their main interest the delivery of an intracellularly active cargo. Large proteins, peptides, and oligonucleotides, as well as peptide nucleic acids, have been reported to be intracellularly introduced by different CPPs (Table 12.1). Here we present a few examples of CPP-delivered cargo in which the uptake has been indirectly quantified by measurements of the activity of the cargo.

The cargoes are divided into three classes of compounds; peptides, ON and PNA, and small molecules or drugs. The distinction from reporter group studies is that the efficiency of internalization is done by quantifying the cargo and not the CPP.

12.2.2.1 Detection of Bioactivity of Peptide Cargo

A 12-residue peptide containing the autophosphorylation site of the epidermal growth factor receptor (EGFR) was internalized by coupling it to a signal sequence-derived CPP. The peptide inhibited intracellular protein–protein interaction and thereby inhibited Ras- and mitogen-activated protein kinase activation, which was measured by Ras nucleotide exchange in SAA cells.[21] A recent review describes the design of cell-permeable phosphopeptides for modulation of intracellular signaling

TABLE 12.1
Examples of Quantification Methods of Cargos Delivered by CPPs by Their Intracellular Activity

Active Cargo	Cargo Details	CPP	Quantification Method
Peptide	Autophosphorylation site of EGFR, 12 residue peptide	Signal sequence derived CPP	Inhibition of Ras/MAP kinase activation measured by Ras nucleotide exchange in SAA cells[21]
	εIF4E-binding motifs analogues, 12 residue peptides	Penetratin	Dose-dependent measurements of cell survival by the MTT assay[23]
Antisense	βAPP antisense, 25-mer oligonucleotide	Penetratin	Down-regulation of amyloid precursor protein to study effects on neurite outgrowth; quantified by immunoprecipitation and pulse-chase experiments[28]
	GalR1 antisense, 21-mer PNA	Transportan, Penetratin	Estimation of pain transmission by the flexor–reflex assay and western blot detection[25]
Drug	Doxorubicin	Penetratin	Quantification of radio-labeled doxorubicin in brain tissue [26,29] and cytotoxcicity measurements by the MTT assay[27]

pathways.[22] Furthermore, penetratin has been used for delivery of εIF4E-binding motifs analogues.[23] The effect of the peptides was dose-dependent measurements of cell survival by the MTT (3-[4,5-dimethylthiazol-2-yl]-2,5-diphenyltetrazolium bromide) assay.

12.2.2.2 Detection of DNA/PNA Antisense Effects

The antisense effect in general is quantified either by analysis of protein content or quantification of mRNA levels. This detection of the extent of the effect is usually accompanied by a functional or biological assay (Table 12.1).

The membrane translocation signal (MTS) from Ig(v) light chain has been coupled via peptidase-sensitive linker to the nuclear localization signal (NLS), residues 127–132, or SV40T-ag.[24] The MTS–NLS chimera coupled to antisense (AS) β-COM oligodeoxynucleotide (ODN), directed against L-type Ca^{2+} channel, was shown to block mRNA translation.

Furthermore, transportan has previously been used for the intracellular delivery of 21-mer antisense PNA complementary to the galanin receptor type 1 mRNA.[25] For further details, see Chapter 16 on antisense application of CPPs.

12.2.2.3 Quantification of Drug Activity

Rousselle et al.[26] describe the delivery of the antineoplastic agent doxorubicin across the blood–brain barrier using the peptides penetratin and SynB1. The peptides deliver

doxorubicin, *in vivo,* both when tested in brain perfusion and when i.v. injected. Doxorubicin passage into the brain was quantified in *in situ* hybridization by radiolabeling. In a further study of peptide-vectorized doxorubicin, a dose-dependent inhibition of cell growth was detected with IC_{50} concentrations of vectorized doxorubicin at 3 μM and the drug alone at 65 μM.[27]

12.3 SUMMARY

Methods to quantify the internalization of cell-penetrating peptides are still in development. Those reviewed here have several drawbacks and are not ideal for all applications. A variety of new fluorophores may solve problems of sensitivity, photobleaching, and pH dependence, but will also be applicable for FRET or RET-Q studies. Measuring the change in fluorescence usually has a sensitivity higher than for direct measurement.

Today the development of mass spectrometry enables quantification of peptides and proteins by, for example, MALDI-TOF and may yield a future tool for studying CPPs. The main advantage would be that identification of the species present in the experiments could be carried out simultaneously with the actual quantification.

For a higher sample throughput a cell-ELISA with a sensitive luciferase or RET-Q system of detection would be highly convenient. Therefore, further development of assays for CPP quantification is needed. An ideal would be an assay in which all the methodological considerations in this chapter and the rest of this book are taken into assessment.

REFERENCES

1. Lindgren, M. et al., Cell-penetrating peptides, *Trends Pharmacol. Sci.*, 21, 99–103, 2000.
2. Hällbrink, M. et al., Cargo delivery kinetics of cell-penetrating peptides, *Biochim. Biophys. Acta,* 1515, 101–109, 2001.
3. Fawell, S. et al., Tat-mediated delivery of heterologous proteins into cells, *Proc. Natl. Acad. Sci. U.S.A.*, 91, 664–668, 1994.
4. Oehlke, J. et al., Cellular uptake of an alpha-helical amphipathic model peptide with the potential to deliver polar compounds into the cell interior nonendocytically, *Biochim. Biophys. Acta*, 1414, 127–139, 1998.
5. Lindgren, M. et al., Translocation properties of novel cell-penetrating transportan and penetratin analogues, *Bioconjug. Chem.*, 11, 619–626, 2000.
6. Pooga, M. et al., Cell penetration by transportan, *FASEB J.*, 12, 67–77, 1998.
7. Drin, G. et al., Physico-chemical requirements for cellular uptake of pAntp peptide. Role of lipid-binding affinity, *Eur. J. Biochem.*, 268, 1304–1314, 2001.
8. Scheller, A. et al., Evidence for an amphipathicity independent cellular uptake of amphipathic cell-penetrating peptides, *Eur. J. Biochem.*, 267, 6043–6050, 2000.
9. Bolton, A.E. and Hunter, W.M., The labelling of proteins to high specific radioactivities by ionization to a ^{125}I-containing acylating agent, *Biochem. J.,* 133, 529–538, 1973.
10. Kask, K. et al., Binding and agonist/antagonist actions of M35, galanin(1-13)-bradykinin(2-9)amide chimeric peptide, in Rin m 5F insulinoma cells, *Regul. Pept.*, 59, 341–348, 1995.

11. Fischer, P.M. et al., Structure-activity relationship of truncated and substituted analogues of the intracellular delivery vector penetratin, *J. Pept. Res.*, 55, 163–172, 2000.
12. Meldal, M. and Breddam, K., Anthranilamide and nitrotyrosine as a donor-acceptor pair in internally quenched fluorescent substrates for endopeptidases: multicolumn peptide synthesis of enzyme substrates for subtilisin Carlsberg and pepsin, *Anal. Biochem.*, 195, 141–147, 1991.
13. Wang, Y.L., Fluorescent analog cytochemistry: tracing functional protein components in living cells, *Methods Cell Biol.*, 29, 1–12, 1989.
14. Garcia–Echeverria, C. et al., A new Antennapedia-derived vector for intracellular delivery of exogenous compounds, *Bioorg. Med. Chem. Lett.*, 11, 1363–1366, 2001.
15. Scheller, A. et al., Structural requirements for cellular uptake of alpha-helical amphipathic peptides, *J. Pept. Sci.,* 5, 185–194, 1999.
16. Gazit, E. and Shai, Y., The assembly and organization of the alpha 5 and alpha 7 helices from the pore-forming domain of *Bacillus thuringiensis* delta-endotoxin. Relevance to a functional model, *J. Biol. Chem.*, 270, 2571–2578, 1995.
17. Elmquist, A. et al., VE-Cadherin-Derived Cell-Penetrating Peptide, pVEC, with carrier functions, *Exp. Cell Res.*, 269, 237–244, 2001.
18. Vives, E., Brodin, P., and Lebleu, B., A truncated HIV-1 Tat protein basic domain rapidly translocates through the plasma membrane and accumulates in the cell nucleus, *J. Biol. Chem.*, 272, 16010–16017, 1997.
19. Matayoshi, E.D. et al., Novel fluorogenic substrates for assaying retroviral proteases by resonance energy transfer, *Science*, 247, 954–958, 1990.
20. Kuzmic, P., Program DYNAFIT for the analysis of enzyme kinetic data: application to HIV proteinase, *Anal. Biochem.*, 237, 260–273, 1996.
21. Rojas, M. et al., An alternative to phosphotyrosine-containing motifs for binding to an SH2 domain, *Biochem. Biophys. Res. Commun.*, 234, 675–680, 1997.
22. Dunican, D.J. and Doherty, P., Designing cell-permeant phosphopeptides to modulate intracellular signaling pathways, *Biopolymers*, 60, 45–60, 2001.
23. Herbert, T.P. et al., Rapid induction of apoptosis mediated by peptides that bind initiation factor eIF4E, *Curr. Biol.*, 10, 793–796, 2000.
24. Chaloin, L. et al., Design of carrier peptide-oligonucleotide conjugates with rapid membrane translocation and nuclear localization properties, *Biochem. Biophys. Res. Commun.*, 243, 601–608, 1998.
25. Pooga, M. et al., Cell penetrating PNA constructs regulate galanin receptor levels and modify pain transmission *in vivo, Nat. Biotechnol.*, 16, 857–8561, 1998.
26. Rousselle, C. et al., New advances in the transport of doxorubicin through the blood–brain barrier by a peptide vector-mediated strategy, *Mol. Pharmacol.*, 57, 679–686, 2000.
27. Mazel, M. et al., Doxorubicin–peptide conjugates overcome multidrug resistance, *Anticancer Drugs*, 12, 107–116, 2001.
28. Allinquant, B. et al., Downregulation of amyloid precursor protein inhibits neurite outgrowth *in vitro, J. Cell Biol.*, 128, 919–927, 1995.
29. Rousselle, C. et al., Enhanced delivery of doxorubicin into the brain via a peptide-vector-mediated strategy: saturation kinetics and specificity, *J Pharmacol. Exp. Ther.*, 296, 124–131, 2001.

13 Kinetics of Uptake of Cell-Penetrating Peptides

Matjaž Zorko, Mattias Hällbrink, and Ülo Langel

CONTENTS

13.1 INTRODUCTION

The study of internalization kinetics of cell-penetrating peptides (CPPs) is an important tool for understanding the uptake process. Not only does it reveal the rate by which CPPs are taken up by cells, but it can also give additional insights, particularly in combination with other methods. For instance, the quantity of a CPP maximally

0-8493-1141-1/02/$0.00+$1.50

accepted by the cell can be predicted. Studies of uptake kinetics are essential in order to achieve a better understanding of the structure–activity relationship of CPPs. Furthermore, data on the efficiency and limitations of CPPs for the transfer of different cargoes in different cells could be amassed. Finally, studies of kinetics could provide a very important contribution for elucidation of the mechanisms by which CPPs pass membranes and enter cells.

It might, therefore, look quite surprising that few detailed kinetic studies of CPP internalization into cells, cell compartments, or model lipid vesicles have been undertaken. In a way, this is understandable since this field is relatively young. Additionally, kinetic studies of CPP internalization are demanding in terms of finding a reliable methodology. Despite the problems listed, some kinetic data have been collected and analyzed for transportans (TP), penetratin, peptides derived from nuclear transcription activator protein (Tat), and model amphipathic peptide (MAP or KLAL); the internalization kinetics of TP has been most thoroughly studied. This chapter reviews the kinetic studies of CPP internalization.

In the first part of the chapter, we summarize methods used for collecting the kinetic data together with procedures for their analysis. Special attention is given to the significance and reliability of kinetic parameters obtained by different methods. In the second part, we discuss the results and conclusions derived from studies of the most frequently used CPPs: TP, penetratin, Tat, and MAP and their analogs. Within scope of the limited data available, we try to compare the rate and the yield of internalization of different CPPs. In addition, we analyze the structure of the cargo transported by CPP and its effect on the translocation rate.

It should be stressed that, at relatively high concentration (1 μM and higher), CPPs can induce membrane leakage by membrane permeabilization.[1] CPP-induced membrane leakage could lead to cell damage and, eventually, to cell death. In this sense, some CPPs resemble the antimicrobial or lytic toxic peptides, for instance the well-known components of bee and wasp venom, melittin and mastoparan.[2] However, CPPs can efficiently penetrate cell membrane at much lower concentrations without inducing any damage to the biological membranes. In this chapter we focus on "pure" pore-free internalization of CPPs into cells under physiologically and, potentially, pharmacologically relevant conditions. Therefore, we mainly consider kinetic data obtained at CPP concentrations that are presumably lower than those required for membrane permeabilization.

13.2 METHODOLOGICAL CONSIDERATIONS

Any kinetic study of CPP internalization, with a goal to determine the rate of CPP internalization, comprises the following steps: incubation of cells with a CPP at suitable concentration, detection of the amount of CPP internalized into the cells as a function of time, and subsequent analysis of the collected data. A hypothetical scheme summarizing the steps of CPP uptake by cells is presented on Figure 13.1. This scheme is an attempt to explain the available kinetic data on CPP uptake; however, as such, it has not been adequately proven yet. Thus, the evaluation of this scheme still remains an issue for further studies.

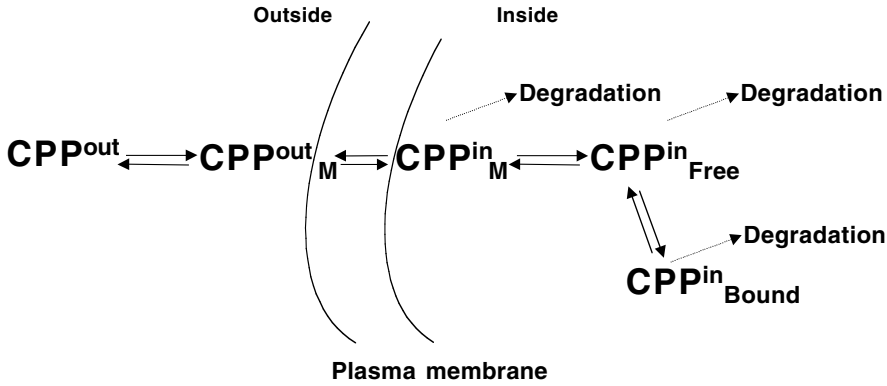

FIGURE 13.1 Schematic presentation of a CPP uptake by cells. CPP^{out} and CPP^{in} represent the peptide outside and inside the cells, respectively. M denotes the hypothetical membrane-bound state of the CPP; free denotes the possible nonbound or cytosolic fraction of the CPP; bound denotes the state of CPP in interaction with intracellular (cytosolic or nuclear) structures, e.g., proteins or phospholipid membranes; degradation indicates the possibility for CPP to be degraded by proteases yielding the shift in all-over equilibrum.

13.2.1 Cells

Transport of CPPs across membranes has most frequently been studied with cultured cells, but, in some cases, also with artificial lipid vesicles, tissues, and even organs *in vivo*.

A number of different mammalian cells has been used for internalization studies of CPPs. Kinetic experiments have been performed with calf aortic,[3] porcine, and human umbilical vein endothelial cells, human neuroblastoma and hepatoma cells,[4] human leukemia cells,[5,6] human Bowes melanoma cells,[7,8] and human epidermoid carcinoma cells.[6] No special cell cultivating procedures are needed for internalization studies. Cells are usually grown to 70 to 80% confluence in flasks or dishes.

It is convenient to detach cells from the surface of flasks or dishes and prepare a suspension of cells to assure a uniformly accessible cell surface prior to incubation with CPP. Detachment of cells can be achieved by scraping cells of the surface (dishes or flasks with the removable upper wall are very convenient), or by short trypsin treatment. In the first case, some cells will be damaged; in the latter case, the cell surface proteins might be affected by trypsin. Cells can be collected by mild centrifugation (usually at 1500 rpm for 10 min) and resuspended in suitable buffer solution. Prior to incubation of the obtained cell suspension with a CPP, it is necessary to determine the "concentration" of the cell suspension (number of cells per volume by means of cell counter or flow cytometer) as well as to estimate the average cell volume.

13.2.2 Incubation of Cells with CPP

During the incubation of cells with a CPP, a fraction of the peptide will be taken up by the cells, while another fraction of CPP molecules will be bound to the cell

surface with electrostatic and hydrophobic interactions (Figure 13.1). Most CPPs are positively charged at physiological pH and thus could interact with negatively charged groups on the cell surface. In order to determine the rate of internalization, the internalized fraction of CPP must be separated from noninternalized, and its amount estimated as a function of the incubation time. The loosely bound CPP can be removed from the cell surface, e.g., by a short-time incubation of the cells in ice-cold acidic solution (e.g., 5 min in the mixture of 0.2 *M* acetic acid and 0.5 *M* NaCl, pH 2.5; see Pooga et al.[8]).

Surface-bound CPP can be removed also by short treatment of cells with trypsin,[7] or the amount of this fraction can be separately quantified by modification of the adsorbed CPP[4] and subtracted from the amount of total cell-associated CPP in order to calculate the amount of internalized CPP. If the surface-bound CPP comprises only a very small part of the total amount of cell-associated CPP (5% or less), the kinetics of the uptake of labeled CPP is not substantially affected by this small fraction of the loosely membrane-attached CPP. In this case, any treatment of cells to remove loosely membrane-bound CPP can be omitted.[9]

Detached cells can be collected by centrifugation and washed; subsequently, the amount of the internalized CPP inside the cells is determined. An alternative technique is by centrifugation of cells for 15 sec at $6000 \times g$ through a mixture of 40% dinonylphthalate and 60% dibutylphthalate[8] or 75:25 mixture of silicon and mineral oil.[6] The bottoms of the centrifugation tubes containing the precipitated cells are then cut off and the amount of CPP in the cells and in the remaining incubation solution can be determined separately. This technique is preferable if the outflow of the CPP from the cells is fast. Sometimes a separation of the cells from the incubation solution is not necessary. This largely depends on the method by which the CPP is detected. Some approaches exploiting detection of CPP by fluorescence make it possible to bypass the separation procedure. They are briefly described below.

13.2.3 Detection of CPP

Different methods can be used to detect CPPs and to assess their concentrations (see Chapter 12). In general, CPPs cannot be directly observed in their intact form with methods suitable for kinetic measurements. Therefore, the peptide must be specially modified to allow reliable detection of rather small amounts that are usually internalized. In most internalization kinetic studies, the CPP itself or the cargo molecules (in CPP–cargo constructs) have been labeled by radioactive isotopes or fluorophore molecules.

Radioactive labeling of a CPP can be performed with ^{125}I-iodination,[8] e.g., using the chloramine-T method,[10] which can be exploited only when Tyr is present in the sequence. Labeling of cargo molecule has the advantage that the delivery of a cargo molecule into the cells can directly be traced and that there is a possibility to choose from a large variety of commercially available labeled compounds that could be used as cargo. One example is the synthesis of a construct where a commercially available radiolabeled antineoplastic agent, ^{14}C-doxorubicin, was used as cargo coupled to penetratin.[11]

In principle, the CPP or cargo molecules could be labeled with a variety of different radionuclids, e.g., ^{35}S, ^{32}P, or ^{3}H. Some tritiated short peptides have been used in internalization studies,[12] but these peptides do not classify as CPPs and are not reviewed here. Radioactive chelated technetium (^{99m}Tc) coupled to Tat peptide was transported into the cells.[6] To our knowledge, labeling of CPPs with other radionuclides has not been performed.

The use of a radioactively labeled CPP or CPP–cargo construct has an advantage over other methods due to high sensitivity. The main disadvantage of this detection method is the necessity for separation of the cell-internalized fraction of the labeled compound from the bulk remaining in the incubation solution. This prevents the design of kinetic experiments enabling continuous monitoring of the amount of cell-internalized CPP or CPP–cargo construct. Additionally, by this method, the fraction of CPP or CPP–cargo construct firmly inserted into the cell membranes cannot easily be differentiated from the fraction in cytoplasm and inner organelles.

Different fluorophores have been used to label CPPs and to trace their translocation into cells. Fluorescein and fluorescein derivatives,[4,6,11] NBD (7-nitrobenz-2-oxo-1,3-diazol),[5] and Abz (2-amino benzoic acid)[1,7] have been most frequently used. After the incubation of a cell with the labeled CPP, the solution is removed and the concentration of the labeled CPP inside the cells determined either directly[7] or by fluorescent flow cytometry.[5] Protocols have been developed to determine the amount of internalized CPP from cell lysate using HPLC.[4]

With fluorescently labeled CPPs, it is possible to quench fluorescence in the incubation solution after selected incubation time by addition of suitable quencher while the fluorescence of the labeled CPP inside the cells remains unchanged due to inability of quencher to penetrate into the cells. In this way, the fluorescence of NBD–penetratin in the incubation solution was irreversibly quenched by addition of sodium dithionite and the concentration of NBD–penetratin internalized into the cells was determined without any additional separation procedure of cells and incubation solution.[5]

Lorenz et al. have devised a method of confocal laser scanning microscopy (CLSM) to quantify the cytosolic portion of CPP uptake[13] (see Chapter 4). In short, attached cells are incubated with fluorescently labeled peptide and the time course of the fluorescence inside and outside the cells is monitored. The signal is corrected for the superimposition of the background fluorescence resulting from nonideal confocal properties of the microscope. With this method, it is possible to monitor the uptake of a CPP in real time.

Not only CPPs, but also cargo molecules in a CPP–cargo construct can be labeled with fluorophore. The amount of a labeled cargo transported into the cells by a CPP could be determined by one of the methods described above.

Recently, a new convenient strategy has been developed for characterization of uptake kinetics of CPPs. CPP–cargo constructs were synthesised where small pentapeptide cargo molecules, carrying a fluorophore, Abz, were coupled to different CPPs (TP, penetratin, Tat, and MAP) labeled with the fluorescence quencher 2-nitrotyrosine via disulphide bond, a bond readily reduced in the intracellular milieu.[1] The intensity of the resulting fluorescence inside the cells is proportional to the amount

of the internalized and liberated cargo, while the fluorescence of CPP–cargo construct in the incubation solution remains quenched. In this way, a continuous real-time quantitative monitoring of the cargo internalization into cells via CPP was achieved.

The method has a number of advantages. Convenient and reliable kinetic data are obtained in each single experiment where all experimental points obtained for the internalization process are measured in virtually identical conditions (same set of cells, same incubation solution, etc.), thus decreasing the scattering of data. It is assumed that the disulphide bond keeping the quencher in close proximity to fluorophore is reduced by gluthatione in the cytoplasm. If so, the portion of CPP–cargo construct that remains firmly associated with cell membranes has less chance to be reduced and made visible. Consequently, mainly the concentration of free cargo in the cytosol is determined. This approach is a method of choice for studying kinetics of internalization of CPP–cargo constructs in micromolar and submicromolar concentration ranges.

Lower sensitivity of methods based on measuring fluorescence is a main drawback in comparison with methods based on radioactivity measurements. The detection limit for fluorescence methods is close to the concentrations where some CPPs (MAP and TP, see Hällbrink et al.[1]) could disturb membranes. For these CPPs, following the internalization at lower concentrations (below 0.1 μM) seems much safer. This can be reliably achieved by use of radioactively labeled CPP.

13.2.4 Quantification of CPPs in Membranes

The quantification of the fraction of CPP or CPP–cargo construct inserted into the membrane and the amount actually free in the cytosol (Figure 13.1) is an important issue in kinetic studies. In constructing kinetic models to describe the dynamics of internalization of a CPP into cells, the insertion of the CPP and CPP–cargo construct into the membrane should be considered an important intermediate step of the uptake that must be directly or indirectly taken into the account during model prediction. Interaction of the CPP and CPP–cargo constructs with membranes is also an important physiological issue. CPPs are potentially aimed to be used for the internalization of drugs and it is important to know (or predict) the quantity of the drug transported and available in the cytosol, and the amount temporarily deposited in membranes. Different techniques exist for assessing the fraction of peptide adsorbed to membranes, e.g., treating the membrane with acids, treatment of cells with trypsin, or modification of the absorbed CPP, as mentioned above.

The determination of a membrane-associated fraction of a CPP is sometimes a difficult issue. Attempts have been made to evaluate this fraction by determination of the partition coefficients of CPPs between water and lipid environment. *n*-Octanol is often used as a rough approximation modeling the lipid part,[8] with known drawbacks.[14] Transportan peptide provides a clear example for this. As determined by Soomets et al., water–octanol partition coefficient for TP was determined to be 15,[9] but the confocal micrography revealed the presence of TP mainly in the cellular membrane structures.[8] This can be explained by the amphiphilic character of TP, enabling insertion of the hydrophobic side into the membrane, while the hydrophilic

part remains in the water phase. Besides, molecular modeling studies have shown that TP and TP analogues that possess the properties of CPP can be stable and deeply inserted into lipid bilayer.[9]

As opposed to TP, penetratin interacts mainly with membrane surface to which it is adsorbed by electrostatic interactions, as revealed from spectroscopic studies.[5] This clearly demonstrates that no single common mechanism governs interaction between different CPPs and membranes, and calls for detailed studies of this process, for instance, similar to those undertaken with the family of Trp-pentapeptides.[14]

13.2.5 Additional Consideration

The mechanisms of internalization have not yet been clarified for CPPs. In order to characterize kinetics of CPP uptake, it is necessary to determine that the internalization data are obtained under conditions in which the CPP is not internalized by endocytosis, mediated transport, pore formation, or a combination of these.

Exclusion of pore formation can be verified by leakage experiments in which cells are first loaded with a suitable labeled-molecule and then leakage of the labeled molecule from the cells is followed after the addition of CPP.[1] All types of protein-mediated transport can be ruled out if the internalization is not saturable, i.e., if the rate of internalization is linearly dependent on the increasing initial concentration CPP and does not show tendency to reach plateau. This is additionally checked by introducing a competitor peptide in excess, which should not substantially influence the rate of internalization of the studied CPP. When the uptake is measured with a labeled CPP, a nonlabeled CPP can be used as a competitor.[8] Active transport, which is energy dependent, is suppressed by substances that deplete cell energy,[8,12] experiments carried out at 4°C could yield additional information. Finally, endocytosis can be inhibited by hyperosmolar solution of glucose, which blocks the formation of clathrin-coated pits,[15] or by phenylarsine oxide treatment, which cross-links the thiol groups of membrane surface proteins.[16]

13.3 TYPES OF KINETIC EXPERIMENTS AND DATA ANALYSIS

The CPP uptake kinetics often follows the rules of simple first-order process

$$CPP^{out} \xrightarrow{k^I} CPP^{in} \qquad \text{Scheme 13.1}$$

where k^I is the first-order rate constant. This is seemingly controversial in light of a complex uptake scheme described in Figure 13.1. However, knowing that CPPs often accumulate in the cells, the simplification of the kinetic scheme seems reasonable. In several cases such simplification has yielded valuable information in studies of CPP uptake.

13.3.1 Single Time Point Measurements

The simplest way to measure kinetics of CPP internalization is a so-called single point experiment in which the amount of internalized CPP is determined at only

one time point. The benefit of simplicity, speed, and small amount of used material is lost in the fact that a single point experiment will not give kinetic constants and, consequently, information obtained might be useful only for rough evaluation. Similar, to some enzyme kinetics studies in which the time interval of quasi-linear dependence of the amount of transformed substrate per time is independently determined and then only one point inside this interval is routinely used,[17] this approach has been sometimes used for comparison of the initial rates of internalization of various analogues of CPPs. However, if the initial rate of internalization is substantially different for different analogues, the linear interval of internalization rate must be separately determined for each analogue; otherwise the comparison is not justified. An alternative solution would be the choice of two time points in the expected linear interval at which the amount of internalized CPP is determined; if the rates of internalization calculated at each of two points do not differ substantially, the obtained result could be considered the proper initial rate.

13.3.2 Uptake Measurements as a Function of Time

A better approach is to monitor the concentration of the internalized CPP as a function of time. In order to obtain reliable results, kinetic data should be collected over a time interval long enough to approach concentration equilibrium between CPP internalized in the cells and that in the surrounding solution. This can be done at one fixed concentration of CPP or, better, at several concentrations of CPP. When a fixed concentration of CPP is used, the obtained data allow for calculation of the rate constant of internalization and also the yield of internalization at the chosen concentration of CPP. The quality of the calculated kinetic parameters depends greatly on the number and reliability of the measured experimental points. Since the mechanism of CPP internalization is not known, any analysis of kinetic data is either phenomenological or model based. As a first approximation, first-order kinetics of internalization can usually be assumed and kinetic parameters are obtained by fitting Equation 13.1 to the experimental points:

$$[A] = [A]_{\infty}\left(1 - e^{-kt}\right) \tag{13.1}$$

where [A] is the concentration of internalized CPP at time point t, $[A]_{\infty}$ is the final concentration of CPP inside the cells, and k is the first-order rate constant. Parameters that are fitted are k and $[A]_{\infty}$. The latter is the maximal concentration of CPP internalized at given initial concentration of CPP outside the cells ($[A]_0$) and makes possible calculation of the internalization yield expressed by $([A]_{\infty}/[A]_0) \times 100$. Sometimes it is more illustrative to convert the first-order rate constant into half-time of internalization ($t_{0.5}$) using the equation $t_{0.5} = \ln 2/k$.

Goodness of fit should be tested for the whole time interval of the progress curve and analysis of residuals should be carried out (the algorithm for this is usually incorporated into the fitting program) in order to observe possible trends in discrepancy between the calculated curve and experimental points. If goodness of fit is not

satisfactory, the proposed first-order rate mechanism is probably not obeyed. In this case other equations might be applied, usually arising from more complex internalization mechanisms or internalization models. Even if the fitting is good, one must always be aware that the result applies only to the chosen concentration of CPP and that, in another concentration range, CPP could internalize in accordance with a different model.

13.3.3 Progress Curves at Different CPP Concentrations

The best approach is to follow the progress curves of internalization at several initial concentrations of CPP. This is demanding in terms of material and time consumption since a great number of experimental points is required, but the method yields important advantages. First, the kinetic parameters obtained are valid for the whole interval of used CPP concentrations and are therefore much more reliable. Even more important, the procedure allows checking the order of the reaction and verifying the complex kinetic models. If the first-order kinetics of internalization is proposed, the rate constant should not be dependent on the initial concentration of CPP, while the second-order kinetics requires linear relationship of the first-order rate constant on the initial concentration of the CPP.

This can be verified by treating each progress curve separately using a suitable computer program as described above for a fixed concentration experiment and checking the concentration dependency of the obtained rate constants. Some computer programs (see Dynafit, or a program of Stojan[18]) allow treatment of all obtained progress curves simultaneously, using either the explicitly derived equation for the predicted mechanism or a numerical treatment of the system. For more complex kinetic mechanisms, explicit equations are difficult or even impossible to obtain and a numerical treatment is the only solution.

13.4 RESULTS FROM CPP UPTAKE KINETICS MEASUREMENTS

In this section we shall present and discuss results of kinetic studies performed so far with four main classes of CPP: TP, penetratin, Tat, and MAP peptides.

13.4.1 Transportan

For internalization studies, [^{125}I]–transportan and biotinyl–transportan were applied[8] and the internalization of TP into a number of different cell lines was inspected. For kinetic studies, mainly Bowes cells were used. As revealed from visualization of the internalized biotinyl–transportan by indirect immunofluorescence using confocal microscopy, the process of internalization into different cells was rapid. The initial process was very fast: the cells were intensely stained after 1 min incubation at 37°C with 10 μ*M* biotinyl–transportan. After the first 5 min, the peptide was localized mostly in the plasma membrane and cytosolic membranous structures (endosomes, endoplasmatic reticulum, Golgi). Staining of the nuclear membrane and nuclei was slight, but clearly visible. After 15 to 30 min, biotinyl–transportan was preferentially concentrated in the nuclear membrane and the nuclei.

Measuring the radioactivity of [^{125}I]–transportan after internalization in Bowes cells showed that more than 50% of the maximal internalization of TP is achieved in the approximate interval of 3 min between adding TP to the suspension and centrifugation used to separate free and bound label, during which time all solutions were kept on ice. At all concentrations under study (5 to 500 n*M*), the time course of uptake is similar. Incubation of the cell suspension at 37°C with labeled transportan first induces fast increase of TP concentration in the cells. In 15 to 25 min, maximal intracellular concentration is achieved.

The maximal uptake of labeled transportan depends slightly on the peptide concentration in the solution. The relative uptake is higher at lower concentrations: 16.3 and 9.2% of the total amount of peptide at 5 and 500 n*M*, respectively. Taking into the account volumes of the cells and the surrounding solution, it was estimated that the concentration of [^{125}I]–transportan inside the cells is at least twofold higher than the concentration of free ligand outside them. The fraction of the label internalized into the cells did not persist on the maximal level, but rather slowly decreased over the period studied. In parallel to the decrease of radioactivity inside cells, the fraction of radioactivity outside started to increase. The decrease of radioactivity inside the cells could be interpreted as outflow of radioactively labeled fragments of the degraded TP from the cells. Interestingly, immunochemical staining showed no decrease in label in the cells after 4 h.

One explanation to this discrepancy is the possible cleavage of the peptide bond between Gly^{12} and Lys^{13} that would leave the [^{125}I] label on Tyr^{9} and the biotin label on Lys^{13} on different peptide fragments; it is possible that fragments retaining radioactivity behave differently from fragments with the biotin attached. The cleavage of the parent peptide galanin between amino acids Gly^{12} and Pro^{13} by membrane-bound proteases in spinal cord material has been demonstrated, supporting this interpretation.[19] Additionally, it has been shown that [^{125}I]–biotinyl–transportan is degraded when incubated with membranes.

The observed time course of the radioactivity in the cells was simulated by the following kinetic model:

$$A \underset{k_2}{\overset{k_1}{\rightleftharpoons}} B \xrightarrow{k_3} C \underset{k_5}{\overset{k_4}{\rightleftharpoons}} D \qquad \text{(Scheme 13.2)}$$

where A and B represent [^{125}I]–biotinyl–transportan outside and inside the cells, C and D are radioactive peptide fragment (or fragments) inside and outside the cells, and k denotes the first-order rate constants for corresponding processes. It is reasonable to speculate that the binding of the peptide to the membrane surface is fast enough for it to be ignored as an independent step, at least in this time resolution. Thus, this scheme is close to the scheme shown in Figure 13.1. The amount of radioactive peptides in the cells (B + C) and the corresponding rate constants were calculated by a numerical treatment of the experimental data using a modified regression computer program of Stojan.[18]

The advantage of this approach is the simultaneous fitting of the curves for all five initial concentrations (A_0) of [^{125}I]–biotinyl–transportan. Consequently, values obtained for the rate constants ($k_1 = 0.019\ min^{-1}$, $k_2 = 0.15\ min^{-1}$, $k_3 = 0.058\ min^{-1}$, $k_4 = 0.27\ min^{-1}$, and $k_5 = 0.0039\ min^{-1}$) are equally valid for all curves. The ratio between constants for uptake of TP (k_1) and its release (k_2) and the ratio of volumes outside and inside the cells are in accordance with a maximal accumulation of [^{125}I]–biotinyl–transportan detected in the cells (see above). On the other hand, the ratio of the constants for uptake (k_4) and release (k_5) of the degradation products corresponds to the ratio of intracellular (2 to 5 µl) and extracellular (100 µl) volumes. This suggests that degradation products do not accumulate in the membranes and that transportan could be degraded in the cells.

Not only the maximal fraction of TP that internalizes into the cells (9 to 16% of total amount of peptide; see above), but also the distribution of TP between membranes and inner cellular solutions is of particular interest, although difficult to determine. Additional experiments by the authors[8] revealed that the fraction released from the outer surface of the cells after treating cells with the acidic solution was less than 2%, pointing to a very small amount of TP that was loosely bound to the outer membrane surface.[8,9] Even less is known about the interaction of TP with the inner hydrophobic leaflet of the membrane. Molecular modeling revealed a possibility of a stable interaction between the lipid bilayer and TP,[9] and membrane-specific staining procedure disclosed the presence of TP in practically all membrane structures of the cell.[8]

Very little is known regarding differences in the specificity of TP for various types of the cell membranes. However, intracellular distribution of TP coincides with staining of high mannose-containing membrane proteins by FITC-conjugated concavalin A. It is interesting that, after longer incubations (more than 1 h), TP concentrates in the nuclear membrane and nuclei, where it localizes predominantly in the nucleoli.[8] More detailed studies of the localization of TP have not been carried out yet; neither has the kinetics of internalization of TP in particular cell structure been undertaken.

13.4.2 Transportan Analogues

A number of transportan analogs have been synthesized. These analogues can be divided into two classes: first, the analogues denoted TP2–TP6 where specific parts in the original TP sequence were replaced by other sequences,[7] and second, the TP analogues, denoted TP7–TP15, derived from TP by deletion of groups of amino acids from various parts of the original TP sequence.[9]

As described in detail in Chapter 3, TP is a chimeric peptide composed of two natural peptides: galanin (1–13) fragment of neuropeptide galanin in N terminus and mastoparan, a component of wasp toxin, in C terminus. In analogues TP2–TP6, each part of TP was selectively modified in order to reveal its role in the cell internalization.[7] The differences between TP and TP2 peptides are in the C-terminal where transportan 2 contains the inactive mastoparan analogue, Mas 17.[20] In TP3, the galanin part of the peptide was exchanged by the synthetic vasopressin antagonist

to elucidate the receptor dependency of the internalization. In TP4 mastoparan part was replaced by crabrolin, a peptide from hornet venom. TP5 and TP6 were obtained by introduction of Pro into TP sequence as a replacement of amino acids at positions 6 or 6 and 7, respectively.

The order of cellular uptake estimated by immunofluorescence was TP, TP2 > TP3, TP5, TP6 > TP4. This speaks for the great importance of mastoparan part and its amphipathic properties for the ability of these types of peptides to translocate cellular membranes, while modifications in galanin part have much less dramatic effect. In immunofluorescence experiments, longer incubation times were used; therefore, results might reflect the yield and not the rate of cellular uptake.

For this reason, it was important to compare data on immunofluorescence with time courses of cellular uptake of [^{125}I]-labeled peptides. Iodination on Tyr was successfully carried out with TP, TP2, and TP3 — peptides with highest demonstrated cellular localization (cf. above). All listed [^{125}I]–TPs were internalized into Bowes melanoma cells, even at 10 n*M* concentration, and time courses of cell penetration of the peptides were comparable. The efficiency and time course of uptake were in accordance with earlier results shown for TP,[8] but the biphasic kinetic behavior, characterized by slow decrease of cellular concentration of TP after reaching maximal value (see above), was not observed with TP2 and TP3. In the case of TP3, this might be because of lack of a cleavage point between Gly^{12} and Lys^{13}, while in the case of TP2 the reason is not clear (see degradation steps in Figure 13.1). Thus, analysis according to Scheme 13.2 (see above) could not be applied for comparison of internalization kinetics of TP, TP2, and TP3. Therefore, a simplified approach was used in which experimental data for the time courses of cellular uptake for all three peptides in question were approximated to the first-order scheme and Equation 13.1 was used for fitting time course curves to the experimental points.

Results confirmed that the immunofluorescence method mainly detects yield of uptake and does not necessarily reflect rate of penetration. The maximum uptake of labeled TP and TP2 were nearly identical, 9.8 and 10.7% of total peptide, respectively, while the same value for TP3 was significantly lower: 6% of total peptide added. On the other hand, the rate of cell penetration was nearly the same for all three peptides and was characterized by half-life ($t_{0.5}$) of uptake of 14 to 17 min.

The second class of TP analogues (TP7–TP15) was obtained by truncation of amino acids in the original TP sequence with the aim to minimize the undesired biological activities of TP (the affinity for galanin receptors and the interaction with G-proteins), but to retain the cell-penetration efficiency of the peptide.[9] In the first subgroup of the TP analogues, amino acids were deleted from the N terminus of TP, yielding three, six, or nine amino acid residues shorter peptides (TP7, TP10, and TP8), respectively. In the second subgroup, the peptides were truncated in the middle of the sequence (TP9 and TP11). The third subgroup represents peptides truncated at the N terminus and in the middle of the sequence (TP12–TP14). Finally, in TP15, the amino acids were deleted at the N and C termini as well as in the middle of the TP sequence.

Most of the short TP analogues have retained the ability to penetrate Bowes cells. As estimated from immunofluorescence experiments, the deletion of three or six residues from the N terminus of TP (TP7 and TP10, respectively) or two residues

from the middle (TP9), did not influence the penetration efficiency of peptides, since they internalized similarly to TP. However, the localization of these three peptides is not identical (see Chapter 3 for details). Further shortening of the N-terminal part by nine amino acid residues led to the loss of penetration ability. Deletions from the N terminus or from the middle of the TP molecule decreased (TP12, TP14, and TP11) or abolished (TP13) the internalization. Combination of deletions in the N and C termini and also in the middle of the sequence completely inactivated the peptide; TP15 did not internalize at all.

In order to compare rate and yield of internalization of the best penetrating short analogues of TP, characteristic half-lives of internalization were calculated from the first-order kinetics approximation (Equation 13.1). TP is the fastest penetrator, with a half-life of internalization of $t_{0.5} = 3.4$ min. Deletion analogues of TP show somewhat slower internalization with $t_{0.5}$ of 4.3, 8.6, 6.5, and 10.7 min for TP7, TP10, TP9, and TP12, respectively. These results are in accordance with results obtained with analogues in which substantial parts of the TP sequence were replaced by sequences of different other peptides or their fragments (cf. above). It was thus demonstrated that the modifications in C-terminal moiety of TP (mastoparan part) have more dramatic negative effect on cell penetration rate and efficacy than modifications in N-terminal part (galanin part). The most important result, however, is a discovery of TP10 that is an effective CPP and does not possess the ability to interplay with the activation process of G-proteins.[9]

13.4.3 Penetratin and Penetratin Analogues

Although penetratin was the first CPP described,[21] kinetic data on the internalization of penetratin into cells are scarce. Drin et al. presented the time course of internalization of NBD-labeled penetratin into K562 cells,[5] showing that uptake of penetratin (at 1.6 μ*M* initial concentration at 37°C) into the cells was rapid. The concentration of the internalized peptide reached plateau after 1 h of incubation. From the data (Drin et al.,[5] Figure 3) the value of $t_{0.5}$ of 17 min was recalculated assuming first-order kinetics.

Hällbrink et al. have followed the uptake of penetratin associated with a small peptide cargo into the Bowes cells.[1] The time course of the penetratin uptake was roughly consistent with the first-order kinetics (1 μ*M* initial concentration at 37°C) and with the $t_{0.5}$ of around 56 min. It is difficult to say whether the discrepancy between the results in Drin et al.[5] and those obtained in Hällbrink et al.[1] are due to different cells or to the impact of cargoes.

A number of different penetratin analogues has been synthesized.[5,7,21] They have been tested for the maximal amount internalized in different cells and vesicles, but none of them has been used in studies of kinetics of internalization.

13.4.4 Tat and Tat Analogues

To date, more than ten Tat-derived short peptides have been shown to translocate into the interior of different cells (see Chapter 1). Kinetic experiments were carried out with fluorescein-labeled Tat (49–57)[22] and Tat (48–60) coupled to small peptide

cargo and labeled with Abz.[1] Cellular uptake of Tat (49–57) was analyzed according to Michaelis kinetics in parallel with penetratin and two model poly-L-Arg peptides, allowing only approximate comparison of rate of internalization of these peptides and not giving proper kinetic parameters. As it was shown, Tat (49–57) was internalized almost twice as slowly as penetratin.[22] This is not in accordance with the results of Hällbrink et al. who found that a first-order rate constant for Tat was 1.7-fold higher than that for penetratin.[1]

A number of Tat analogues were synthesized and tested in T-Jurkat cells.[22] One family of analogues comprises a truncated Tat (49–57) (the shortest peptide was Tat 51–57); another family of peptides was obtained by L-Ala-scan technique. All analogues exhibited diminished cellular uptake. These results suggest that the cationic residues of the Tat peptide play a principal role in its uptake, although detailed kinetic parameters for these analogues were not obtained.

13.4.5 MAP and MAP Analogues

As shown by Oehlke et al., the internalization of the so-called model amphipathic peptide (MAP) proceeded roughly linearly throughout a period of 60 min.[4] With longer incubation periods, the amount of internalized peptides starts to decrease due to enzymatic cleavage of MAP within the incubation solution. The rate of internalization is dependent on the concentration of MAP and is approximately in accordance with first-order kinetics. A similar result was obtained by Hällbrink et al.,[1] who observed approximately first-order internalization kinetics of small peptide cargo attached to MAP.[1]

Scheller et al. have tested internalization of 15 MAP analogues with stepwise alterations of hydrophobicity, hydrophobic moment, and hydrophilic face, but with unchanged positive charge and helix forming propensity.[3] Here, the fastest internalization into the aortic endothelial cells was achieved with an analogue denoted IX that was taken up approximately 25-fold faster than the original MAP (for details see Chapter 4).

13.4.6 Comparison of CPPs and the Effect of Cargo on the Rate of Internalization

Hällbrink et al. have undertaken the only complete comparative study on the rate and yield of penetration of small cargo with TP, penetratin, Tat, and MAP, respectively.[1] The approximately first-order kinetics of internalization of cargo with all tested CPPs was observed. The fasted uptake was achieved with MAP ($t_{0.5}$ = 7 min), followed by TP ($t_{0.5}$ = 12 min), Tat ($t_{0.5}$ = 34 min), and penetratin ($t_{0.5}$ = 56 min). The efficiency of cargo delivery into the cells, expressed by the apparent cellular transport equilibrium constant (K_{io}), matches the rate of cellular uptake. The fastest penetrator, MAP, was also the most effective delivery vector (K_{io} = 417), followed by TP (K_{io} = 353), Tat (K_{io} = 107), and penetratin (K_{io} = 71). Unfortunately, the high efficiency and rate of cargo delivery into the cells is compensated by the potency of membrane leakage induction. In case of MAP peptide, intensive leakage of radioactive 2-[^{3}H]-deoxyglucose-6-phosphate from the cells was followed already at 1 μ*M* concentration. TP was not effective at this concentration, but at higher

concentrations the membrane leakage increased. Tat peptide did not induce any leakage at all, even at highest concentrations used (20 μ*M*), while a negligible effect was detected for penetratin.

The effect of a cargo on the translocation velocity is of great interest. Cargoes transported by CPPs are very different in structure and in size, ranging from organic molecules of low molecular mass (e.g., biotin, fluorescein), over peptides, DNA, and PNA fragments, to proteins of around 150 kDa. It is expected that a cargo could have an influence on the rate of internalization of CPP–cargo construct. However, as it was shown, small cargoes usually do not influence the rate of translocation substantially.[8]

The data on kinetics of translocation of CPP coupled to medium- and large-size cargos are not available. From immunofluorescence studies utilizing confocal microscopy, it could be deduced that TP attached to protein cargos of up to 150 kDa internalizes more slowly than TP itself, as estimated visually from the dynamics of fluorescence appearance in the cells.[8,23] Exact characterization of how much slower this process is has not been carried out.

Biotinyl–TP could be detected in cells after a few minutes and reached maximal intracellular concentration after 20 min of incubation.[8] Transportan attached to green fluorescence protein (GFP, molecular mass 28 kDa), avidin–TRITC (molecular mass 66 kDa), and polyclonal antibody (molecular mass 150 kDa) were detected in the cytoplasm substantially later, on average after 30 min of incubation. However, in some cases, e.g., with noncovalently attached monoclonal antibody against biotin to biotinyl–TP, the construct was detected in the cell after 2 h incubation.[23]

Proteins have also been translocated by the Tat (47–57) carrier.[24] Successful translocation of partially denatured β-galactosidase into different mouse cells was achieved, but the experiments do not allow comparison of rate of translocation between the Tat (47–57)–β-galactosidase construct and Tat (47–57). Interestingly, β-galactosidase was refolded inside the cells and regained its full physiological role.

13.5 CONCLUSIONS AND FUTURE PERSPECTIVE

Methods of kinetics have already proven their usefulness by providing valuable data on the rate of CPP internalization and by establishing the link between rate and yield of cellular uptake, as well as structure of CPP. Complete study of cellular penetration kinetics with all CPPs and various cargo molecules would give additional valuable information and allow constructing kinetic models for cell penetration of each individual CPP, leading to a better understanding of principles that govern the internalization of CPPs. Establishing methodological procedures for convenient and reliable real-time monitoring of internalization is an important first step.

ACKNOWLEDGMENTS

This work was supported by grants from the EC Biotechnology Project BIO4-98-0227, Swedish Research Councils TFR and NFR, and grants from the Ministry of Science, Education, and Sport of the Republic of Slovenia.

REFERENCES

1. Hällbrink, M. et al., Cargo delivery kinetics of cell-penetrating peptides, *Biochim. Biophys. Acta*, 1515, 101, 2001.
2. Tosteson, M.T. et al., Melittin lysis of red cells, *J. Membr. Biol.,* 87, 35, 1985.
3. Scheller, A. et al., Structural requirements for cellular uptake of α-helical amphipathic peptide, *J. Peptide Sci.*, 5, 185, 1999.
4. Oehlke, J. et al., Cellular uptake of an α-helical amphipathic model peptide with the potential to deliver polar compounds into cell interior non-endocytotically, *Biochim. Biophys. Acta*, 1414, 127, 1998.
5. Drin, G. et al., Physico-chemical requirements for cellular uptake of pAntp peptide, *Eur. J. Biochem.,* 268, 1304, 2001.
6. Polyakov, V. et al., Novel Tat-peptide chelates for direct transduction of Technetium-99m and Rhenium into human cells for imaging and radiotherapy, *Bioconjugate Chem.,* 11, 762, 2000.
7. Lindgren, M. et al., Translocation properties of novel cell penetrating transportan and penetratin analogues, *Bioconjugate Chem.,* 11, 619, 2000.
8. Pooga, M. et al., Cell penetration by transportan, *FASEB J.*, 12, 67, 1998.
9. Soomets, U. et al., Deletion analogues of transportan, *Biochim. Biophys. Acta*, 1467, 165, 2000.
10. Gavin, J.R. et al., Insulin receptors in human circulating cells and fibroblasts, *Proc. Natl. Acad. Sci. U.S.A.,* 69, 747, 1972.
11. Rousselle, C. et al., New advances in the transport of Doxorubicin through the blood-brain barrier by peptide vector-mediated strategy, *Mol. Pharmacol.,* 57, 679, 2000.
12. Oehlke, J. et al., Evidence for extensive and nonspecific translocation of oligopeptides across plasma membranes of mammalian cells, *Biochim. Biophys. Acta*, 1330, 50, 1997.
13. Lorenz, D. et al., Mechanism of peptide-induced mast cell degranulation. Translocation and patch-clamp studies, *J. Gen. Physiol.,* 112, 577, 1998.
14. White, S.H. and Wimley, W.C., Membrane protein folding and stability: physical principles, *Annu. Rev. Biophys. Biomol. Struct.,* 28, 319, 1999.
15. Heuser, J.E. and Anderson, R.G., Hypertonic media inhibit receptor-mediated endocytosis by blocking clathrin-coated pit formation, *J. Cell Biol.,* 108, 389, 1989.
16. Frost, S.C. and Lane, M.D., Evidence for the involvement of vicinal sulfhydryl groups in insulin-activated hexose transport by 3T3-L1 adipocytes, *J. Biol. Chem.,* 260, 2646, 1985.
17. McKenzie, F.R., Basic techniques to study G-protein function, in *Signal Transduction. A Practical Approach,* Milligan, G., Ed., Oxford University Press, New York, 1992, chap. 2.
18. Stojan, J., Analysis of progress curves in an acetylcholinesterase reaction: a numerical integration treatment, *J. Chem. Inf. Comput. Sci.,* 37, 1025, 1997.
19. Bedecs, K., Langel, Ü., and Bartfai, T., Metabolism of galanin and galanin (1 to 16) in isolated cerebrospinal fluid and spinal cord from rat, *Neuropeptides,* 29, 137, 1995.
20. Soomets, U. et al., From galanin and mastoparan to galparan and transportan, *Curr. Top. Pept. Protein Res.,* 2, 83, 1997.
21. Derossi, D. et al., Cell internalization of the third helix of the Antennapedia homeodomain is receptor-independent, *J. Biol. Chem.,* 271, 18188, 1996.
22. Wender, P.A. et al., The design, synthesis, and evaluation of molecules that enable or enhance cellular uptake: peptoid molecular transporters, *Proc. Natl. Acad. Sci. U.S.A.,* 97, 13003, 2000.

23. Pooga, M. et al., Cellular translocation of proteins by transportan, *FASEB. J.,* 15, 1451, 2001.
24. Schwarze, S.R. et al., *In vivo* protein transduction: delivery of a biologically active protein into the mouse, *Science,* 285, 1569, 1999.

14 Signal Peptides

Kenta Nakai

CONTENTS

0-8493-1141-1/02/$0.00+$1.50

ABSTRACT

Signal peptides are amino-terminal (N-terminal) extensions of polypeptides that target them from the cytosol to the cytoplasmic (plasma) membrane of prokaryotes and to the membrane of the endoplasmic reticulum (ER) of eukaryotes. After the targeting, they direct the linked proteins to translocate the membrane and are usually cleaved after the translocation. Signal peptides are also called signal sequences or leader sequences; however, the term "signal sequence" can sometimes be confusing because of the broader meaning of "protein-sorting signal." Signals for the translocation of the mitochondrial inner membrane and the chloroplast thylakoid membrane are homologs of signal peptides. Although most signal peptides are likely to be recognized by specific molecules within the cell, some of them spontaneously interact with the membrane and are inserted into it, at least *in vitro*. Thus, they are closely related to so-called cell-penetrating peptides, the main theme of this book. In addition, understanding signal peptides should be useful for a wide range of application areas such as biotechnology and clinical investigation.

14.1 BRIEF RETROSPECTION

Günter Blobel was awarded the Nobel Prize in Physiology or Medicine "for the discovery that proteins have intrinsic signals that govern their transport and localization in the cell" (from the press release) in 1999, a memorable year for the study of signal peptides. Of course, there were great pioneers in the study of protein secretion before Blobel, including George Palade, who shared the Nobel Prize in Physiology or Medicine with two others in 1974. Palade discovered that secreted proteins in eukaryotic cells first translocate into the lumen of ER and are then transported through the Golgi apparatus and secretory vesicles before they are finally secreted into the outside of the cell. Indeed, Blobel started his major works at Palade's laboratory at the Rockefeller Institute. In 1971, Blobel and Sabatini proposed a first version of the signal hypothesis that the N-terminal extension of secreted proteins serves as a signal directing them to and across the ER membrane. In 1975, Blobel and Dobberstein formulated their signal hypothesis based on results of their *in vitro* assay system.[1,2]

The signal hypothesis states the steps of newly synthesized proteins that translocate across the ER membrane. In light of current knowledge, the modern version of the hypothesis can be described as follows:[3-5]

1. In the cytosol, the ribosome binds mRNA regardless of whether it codes a secretory protein.
2. The ribosome begins to synthesize the polypeptide according to the bound mRNA.
3. When about 80 amino acid residues protrude from the ribosome, the peptide can interact with the signal recognition particle (SRP). If the polypeptide includes an N-terminal signal peptide, the SRP recognizes it and transiently stops translation of the polypeptide.
4. The SRP–ribosome complex moves to the ER membrane and the SRP binds to the membrane-bound SRP receptor. Then, the translation restarts.
5. The ribosome binds to the translocon channel on the ER membrane.
6. The gate of the translocon opens and the ribosome pushes the elongated polypeptide into the pore of the channel.
7. During or after translation, a signal peptidase cleaves the signal sequence.
8. When the completed protein is released, the complex is dissociated and the channel pore closes.

This hypothesis can also explain the assembly process of integral membrane proteins in which signal or signal-like hydrophobic segments start transfer across the membrane while other hydrophobic segments serve as the stop-transfer signal.[6-9] The validity of the signal hypothesis has been verified by many later experiments. Its basic idea also holds for translocation in prokaryotes; furthermore, proteins destined to other compartments such as mitochondria and chloroplasts also have specific sorting signals.

Because the signal hypothesis was so beautiful, people believed in a quite simple dogma based on it: although there is no simple consensus sequence pattern between amino acid sequences of signal peptides, they are believed to code a common function. Namely, the signal peptide cotranslationally directs the protein to the SRP-dependent pathway in eukaryotes while it post-translationally directs the protein to the Sec system (the protein translocation system dependent on SecA/SecYEG) in prokaryotes.[10] However, recent studies have begun to clarify that the real situation is a little more complex. Thus, the main purpose of this review is to introduce recent developments in the study of protein translocation, including computational and genome-wide studies.

14.2 PROTEIN SECRETION PATHWAYS IN BACTERIA

Early studies of protein secretion in bacteria were focused on genetic studies because of the difficulty of construction of *in vitro* translocation assay. At first, the parallelism between prokaryotic and eukaryotic systems was recognized; namely, that SecB protein and SecYEG channel were analogous to SRP and translocon, respectively, although this translocation process occurs post-translationally in prokaryotes. However, it turned out that there are several other translocation pathways, including the cotranslational SRP-dependent pathway, in bacteria (Figure 14.1). The translocation pathways of archaea are recently described elsewhere.[11,12]

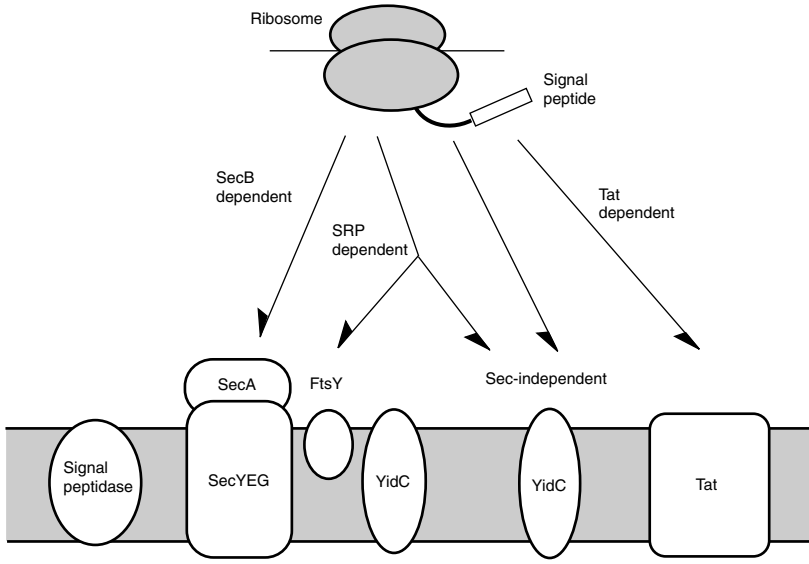

FIGURE 14.1 Protein targeting pathways to the cytoplasmic membrane in bacteria. Pathways are roughly classified based on the Sec (SecA/SecYEG) dependence. In *E. coli*, Sec-dependent pathways are either SecB-dependent or SRP-dependent but another Sec-dependent pathway may exist. For some SRP/SecYEG-dependent proteins, SecA may not be required. The role of YidC is under investigation but it is related to both Sec-dependent and Sec-independent pathways. Signal peptidases also affect the fate of signal peptides.

14.2.1 SecB-Dependent Pathway

SecB protein plays an important (but not essential) role in translocation of proteins across the cytoplasmic membrane of Gram-negative bacteria. The Sec-system was originally thought to be totally SecB-dependent and the pathway was called "general secretory pathway" (GSP).[13] The current view[14-20] of a SecB-dependent pathway is that a preprotein (i.e., a protein with a signal peptide) protruding from a ribosome is recognized by SecB, which keeps the preprotein in an unfolded state (the translocation-competent state); the SecB–preprotein complex somehow moves to the membrane-bound SecYEG–SecA complex. SecB tightly interacts with SecA and then the preprotein is passed to the SecYEG protein-conducting channel; the preprotein starts translocation and SecB is released. Recent findings related to molecular recognition are further described next.

14.2.1.1 SecB

As noted, SecB first recognizes a nascent protein. Thus, the central issue of signal recognition could be its substrate specificity, which has been, however, a controversial matter. For one thing, SecB binds to many unfolded proteins *in vitro*[21] while it shows highly selective binding *in vivo*.[22] For another thing, there is apparently contradicting evidence on whether SecB is a specific signal-recognition factor or not.[23-25] Most studies seem to support the notion that SecB is a general chaperone

that binds denatured mature portions of proteins.[17,26,27] If so, how does SecB discriminate preproteins from others?

To reconcile the paradox, a kinetic partitioning model, which indicates that retardation of protein folding by signal peptides is the major factor for SecB to discriminate its substrates, has been proposed by Hardy and Randall.[28,29] However, the binding rate of SecB is much faster than rates of protein synthesis and its folding[21] and the substrate specificity of SecB does not seem to explain its *in vivo* preference with preproteins.[27] Mutations on signal peptides or on early mature regions can change apparent SecB dependency; thus the ability to interact with the transport machinery of a protein may be the key factor to determining its apparent SecB dependency.[30] Recently, the crystal structure of SecB from *Haemophilus influenzae* was determined,[31] which shed some light on this paradox, although the structure binding its substrate would be desirable for detailed discussion.[18,19]

SecB is a highly acidic homotetramer. A mutational study implies that the tetramer is a dimer of dimers,[32] which was confirmed by the x-ray structure. In its quaternary structure, SecB seems to have two long grooves that are proposed to be the unfolded polypeptide binding sites.[31] The groove consists roughly of two subsites: one lined with conserved aromatic residues, the other a shallow floor rich in hydrophobic residues. Possibly, proteins in their translocation-competent state wrap around SecB. The SecB tetramer also has two potential SecA-binding sites, which are solvent-exposed flat surfaces rich in acidic residues. In addition, four exposed arms of SecB may embrace the SecA protein. Thus, subsequent binding among SecB, SecA, and preprotein could be the determinant of specific signal recognition.

14.2.1.2 SecA

In *Escherichia coli*, SecA is a large protein (901 residues) that works as a homodimer.[33,34] SecA is a part of the bacterial protein translocase complex; it binds to SecY through its N-terminal domain but also loosely binds to anionic phospholipids possibly through its C-terminal domain.[35-37] The exact role of SecA in preprotein translocation has not been fully understood; its RNA helicase activity is not required *in vivo* for efficient protein translocation.[38] SecA also has the ATPase activity: its binding to SecB[39] and to anionic phospholipids[40,41] induces its conformational change, thus stimulating its ATPase activity, especially in the presence of SecYEG.

Synthetic signal peptides were originally reported as inhibitors of ATPase activity without their mature portion,[40,42] although some recent experiments show that they stimulate ATPase activity in the presence of lipids.[43,44] However, a soluble N-terminal fragment of SecA was shown to bind signal peptides more tightly and this binding inhibits its ATPase activity.[45] It has been regarded that SecA is an ATP-driven motor protein and pushes preproteins into the membrane.[46] According to the membrane insertion hypothesis, SecA cycles insertion and deinsertion processes with the preprotein by utilizing the driving force of ATP hydrolysis,[47,48] but the detailed mechanism has yet to be elucidated.[19] As another driving force, the proton motive force (pmf) also seems to contribute significantly to the (late stage of) translocation process.[49]

14.2.1.3 SecYEG and Related Proteins

Three integral membrane proteins, SecY (PrlA), SecE, and SecG constitute the SecYEG complex, which is the central component of the translocase (or translocon).[19,34,50] This complex plays an active role in protein translocation because some mutations of SecY can affect the topology of substrate membrane proteins.[51] Other proteins, including YidC[52] and the SecDFyajC (SecD, SecF, and YajC) heterotrimer,[53] are also involved. There remain possibilities of yet uncharacterized factors. SecYEG is likely to exist in both monomeric and tetrameric forms.[54] Controversy still exists on whether the SecYEG monomer constitutes a functional channel or works as a tetramer.[55,56]

Homologous proteins of YidC exist in mitochondria (Oxa1p) and chloroplasts (Alb3) but not in ER.[52] Oxa1p and Alb3 play a key role in the assembly of mitochondrial inner membrane proteins and chloroplast thylakoid membrane proteins, respectively. YidC helps translocation of membrane proteins, possibly by clearing the channel of SecYEG translocase, thus preventing the jamming of its substrates;[57] however, it also seems to be able to translocate proteins independently from the translocase. The SecDFyajC complex controls SecA membrane cycling to regulate the movement of the translocating preprotein.[53]

14.2.2 SRP-Dependent Pathway in Bacteria

Since it had been widely believed that protein translocation directed by signal peptides occurs post-translationally in prokaryotes,[10] the discovery of *E. coli* genes homologous to the SRP components lead to a great interest on whether they really play significant roles in protein translocation or not. With subsequent extensive analyses, it turned out that the bacterial SRP system is essential, selectively translocating a group of proteins.[58-60] An important point is that this system also recognizes signal peptides or the first transmembrane segments; thus, there must be some discrimination mechanism between signal peptides (see Section 14.4.3.1).

14.2.2.1 Ffh and 4.5S RNA

Although potential involvement of additional proteins and RNAs cannot be ruled out, the bacterial SRP system (SRP and its receptor) basically consists of two proteins and one RNA. Like mammalian SRP, bacterial SRP is a ribonucleoprotein complex, but it simply consists of Ffh and 4.5S RNA.[61] Ffh is named as a homolog of the mammalian SRP54 subunit (i.e., Fifty-Four Homolog). It consists roughly of two major domains: the NG domain, which is related to GTPase activity and binding to FtsY, and the M domain, related to binding to 4.5S RNA and to signal peptides.

A crystal structure of Ffh from a thermophilic bacterium, *Thermus aquaticus*, was determined.[61] Subsequently, a crystal structure of the complex between domain IV of 4.5S RNA and the M domain of Ffh was solved.[62] From previous studies on the amino acid sequence of Ffh, the M domain was proposed to contain the methionine-bristle, where the unbranched thioester side chain of methionine enables flexible accommodation of a variety of signal sequences like bristles of a brush.[4,63] From crystallographic studies, the speculation was partly confirmed; however, a probably

more important structure, the finger-loop structure, was observed. Furthermore, it was found that the proposed signal peptide-binding groove lies alongside the RNA backbone. Thus, it is likely that RNA and protein constitute a signal peptide-binding site.[62]

This hypothesis is consistent with an observation that RNA increases the affinity of Ffh for signal peptides.[64] In fact, signal peptides bind the RNA component of SRP.[65] It seems that the 4.5S RNA stabilizes the hydrophobic finger loop,[66] thus catalyzing the assembly of Ffh and the FtsY receptor.[67] Then, SRP binds the ribosome-nascent chain complex (RNC) and targets it to the membrane-bound FtsY.

14.2.2.2 FtsY

FtsY, the receptor of bacterial SRP, is homologous to eukaryotic SRα. Its structure is roughly divided into two domains: the NG-domain, which has GTPase and Ffh binding activities, and the N-terminal domain (A-domain in *E. coli*), which is not well conserved across species but responsible for its membrane targeting. In the eukaryotic system, the signal receptor (SR) is bound by SRβ, an integral membrane protein. Since the homolog of SRβ has not been discovered in bacteria, how FtsY binds the membrane is not known.

A crystallographic structure of the *E. coli* NG domain was determined.[68] Interestingly, the structure of the NG domain of FtsY is similar to the NG domain of Ffh, although its meaning is not well understood. Anyway, in a GTP-dependent manner, RNC is released from the SRP/FtsY complex to the SecYEG complex,[69] although some inner membrane proteins containing long periplasmic loops do not require the Sec-translocase.[70,71] Then, the ribosome restarts the translation, leading to cotranslational translocation of the nascent polypeptide; however, the details of each step are not known. SRP may operate downstream of SR-mediated targeting of ribosomes to the inner membrane in *E. coli*.[72] SecA is necessary for this pathway, but its role is still under investigation.[73] It has been reported that SecA is not necessary for the targeting but is required for subsequent translocation of multispanning, hydrophobic membrane proteins.[74]

14.2.3 TAT-Dependent Pathway

In this chapter the word "Tat" means not the Tat protein of HIV (as in Chapter 1) but the twin arginine translocation pathway of proteins. Recent studies have clarified that bacteria have another protein translocation pathway independent of the general secretory pathway for a subset of periplasmic proteins.[75,76] The pathway was named Tat protein export pathway because the signal peptides that direct joined proteins to this pathway are similar to usual signal peptides but have a characteristic twin-arginine translocation motif (see Section 14.4.3.1); the system was also called Mtt for membrane targeting and transport.[77-80] Although not all bacteria use this translocation system, it is analogous to the ΔpH-dependent pathway across the thylakoid membrane of plant chloroplasts.[81-83] The most intriguing feature of the Tat-dependent pathway (and the ΔpH-dependent pathway) is that it can translocate folded proteins directly. Thus, it makes sense that many of the substrates of this pathway are

periplasmic cofactor-binding proteins. Although it seems possible that the pathway proofreads the folding state of its substrates, even malfolded proteins may pass through it.[84] The system also translocates oligomerized proteins; in fact, a protein without the Tat signal can safely translocate the membrane as a complex by a so-called hitchhiker mechanism.[85]

Although details of its transport mechanism have not been fully investigated, at least four integral membrane proteins are involved in the translocation system in *E. coli*: TatA, TatB, TatC, and TatE.[86] TatA, TatB, and TatC are coded in the same *tatABCD* operon and TatA, TatB, and TatE are similar in sequence. Whether these proteins comprise a channel is not known. The translocation is driven by the proton motive force. Which protein recognizes the signal is also an enigma, but recently DmsD (YnfI) has been proposed as a Tat leader-binding protein.[87] Another study based on two paralogous TatC proteins in *Bacillus subtilis*, indicated that TatC seems to be a specificity determinant of the pathway.[88]

14.2.4 Unknown or Factor-Independent Pathway

14.2.4.1 Insertion of Procoat Proteins

After the entire genome sequences of many bacteria were determined, some possibility still existed of yet-uncharacterized protein translocation pathways. Some excreted (i.e., secreted to the extracellular medium, which means an additional translocation across the outer membrane in Gram-negative bacteria) proteins translocate the inner membrane with a variety of their own transport machinery.[89,90] Although such pathways are out of the scope of this review, it seems noteworthy that SecB is likely to be involved in one of the branches, the ABC-mediated pathway.[91,92] Other proteins even appear to translocate the membrane without the aid of other protein factors. For example, procoat, i.e., precursor of coat, proteins of bacteriophages Pf3 and M13 have been well studied as model systems for Sec-independent protein transport.[93-95] Neither SRP nor SecB is required for these transports.[96]

Previously, it had been thought that insertion occurs spontaneously for these proteins, partly because they are rather small and partly because they can be inserted into the membrane of liposomes when electrochemical potential is between both sides of the membrane.[94] However, when the expression of YidC was depleted, the translocation of newly synthesized M13 procoat proteins was almost completely inhibited.[97] Thus, YidC not only facilitates Sec-dependent protein translocation but also helps Sec-independent proteins to be inserted into the membrane.[52] A recent study using various procoat mutants showed that substrate proteins can bind to SecA but cannot activate its ATPase activity, in some cases.[98] Another study suggests that YidC is involved in the lateral transfer of transmembrane domains of substrates from the translocase into the lipid bilayer.[99]

14.2.4.2 Energetic Aspects

Although the *in vivo* role of spontaneous insertion mechanisms becomes unclear, the interaction of signal peptides with lipids might be of special interest.[41,100] Signal

peptides are thought to be inserted into the membrane in a helix–beak–helix conformation consistent with the classical helical hairpin hypothesis.[101,102] At this process, the length of the hydrophobic region of signal peptides seems to play an important role.[103] The interaction between their positively charged N termini and the anionic phospholipids is also important for determining the orientation of insertion.[104] Namely, positively charged residues are not favored for transportation across the membrane; this seems to be the major determinant of the topology of membrane proteins (the positive-inside rule).[105,106]

In another study, the proton motive force (pmf), which renders the cytoplasm basic and the periplasm acidic, was shown to inhibit membrane translocation of positively charged residues within membrane proteins.[107,108] However, the determinants of the positive-inside rule seem still to be controversial.[109] Negatively charged residues are also likely to be involved in the translocation.[110] When there are no charged amino acids around the signal peptide, anionic lipids stimulate its translocation in a direction opposite to the positive-inside rule, possibly because of its helix dipole moment.[111] Factors that influence the efficiency and specificity of signal peptides will be discussed in Section 14.4.3.1.

14.3 PROTEIN SECRETION PATHWAYS IN EUKARYOTES

In eukaryotes, it is quite established that proteins transported through the secretory pathway have a signal peptide, including an uncleavable signal anchor, on their N terminus and are first transported to the ER, although there are some exceptions. Unlike the bacterial system, most of the signal peptides are cotranslationally recognized by SRP, although some proteins are transported through the post-translational pathway, especially in yeast. In addition, chloroplasts (and mitochondria) seem to have their own transport system directed by signal peptide-related signals. Here, eukaryote-specific topics are briefly summarized.[4,5,112-117] Translocation via signal peptide-like signals within mitochondria and chloroplasts is reviewed elsewhere.[52,118-120]

14.3.1 Cotranslational Pathway

14.3.1.1 Targeting to the ER

Mammalian SRP consists of 6 proteins and 1 RNA (7S RNA). All known SRP-related sequences are maintained in a public database (SRPDB).[121] SRP54, a homolog of bacterial Ffh, recognizes signal peptides and has GTPase activity. Although still controversial, the nascent polypeptide-associated complex (NAC), which is an abundant cytosolic heterodimer, has been proposed to first contact the nascent polypeptide chain emerging from the ribosome and to strengthen the specificity of SRP for binding signal peptides and for targeting to the ER.[122-124] Although ribosome–nascent chain (RNC) complexes can be targeted and bind to the ER membrane without the aid of SRP, the binding of RNC complexes with SRP gives it a competitive advantage.[125]

SRP binds to the SRP receptor (SR) on the ER. Unlike bacteria, SR is a heterodimer consisting of SRα and SRβ. SRα, a peripheral subunit, is homologous to bacterial FtsY while SRβ, an integral membrane, does not have its bacterial counterpart. Both subunits of SR have a GTPase domain. With the binding of SRP and SR, the GTPase activities of SRP54 and SRα increase. Then, the RNC complex is passed to the translocon and the SRP is dissociated.[126] SRβ coordinates signal peptide release from SRP.[127]

14.3.1.2 Translocon Complex

In mammals and yeasts, the translocon is thought to consist basically of three subunits, Sec61α (Sec61p), Sec61β (Sbh1p), and Sec61γ (Sss1p).[116] Sec61α and Sec61γ are similar to bacterial SecY and SecE, respectively, while Sec61β, a non-essential protein, is not similar to SecG. For translocation of at least some mammalian preproteins, the TRAM (translocating chain-associated membrane) protein plays an important role.[128] TRAM is an integral membrane protein and seems to recognize signal peptides.[129] However, the exact role of TRAM is still unclear and no homologs of TRAM exist in yeast.

The translocon is thought to form an aqueous gated pore.[130] Although there may be other receptors for the RNC, Sec61α directly binds to it.[131] Moreover, the Sec61-complex seems to recognize the signal sequence specifically, which is crucial in regulating translocation efficiency.[132-135] Thus, signal peptides are recognized at least twice by different proteins. The translocation of polytopic membrane proteins is thought to be basically the same as that of secreted proteins.[136] Due to the complete sequencing of the yeast genome, a homolog of Sec61p, Ssh1p, was discovered. Although *SSH1* is not an essential gene, recent studies show that Ssh1p acts with Sss1p and Sbh2p (a close homolog of Sbh1p) as a second, functionally distinct translocon.[137,138]

14.3.2 Post-Translational Pathway

In both yeast and mammalian cells, relatively few proteins translocate the ER membrane post-translationally.[139] In yeast, its molecular mechanism is rather known. Unlike the cotranslational pathway, SRP, SR, and TRAM are not involved in this pathway. Instead, several additional proteins are required.

14.3.2.1 Additional Membrane Proteins

As with the cotranslational pathway, translocation occurs through the Sec61 complex. In addition, several membrane proteins, including three integral (Sec62p, Sec63p, and Sec71p) and one peripheral (Sec72p), are required. These proteins form a stable heterotetrameric complex which also interacts with the Sec61 translocon. Homologs of Sec62p and Sec63p also exist in mammals.[140] According to a current model, a preprotein first binds to the Sec62p–Sec71p–Sec72p (and possibly Sec63p) complex, which is signal peptide-dependent but ATP-independent.[141] Then, the preprotein is possibly transferred to the Sec61 complex in an ATP-dependent manner (see below). Sec63p is partly similar to bacterial DnaJ protein, which stimulates the ATPase activity of DnaK, a bacterial hsc70 (heat shock cognate 70) molecular

chaperone.[142,143] Indeed, Sec63p stimulates the ATPase activity of Kar2p (BiP), which belongs to the DnaK family (see below).

14.3.2.2 Role of Chaperone Proteins

Although how preproteins are targeted to the translocation site on ER is not known, they are bound by cytosolic chaperones such as Ssa1p and Ydj1p at an early stage. Again, Ssa1p belongs to the DnaK/Hsp70 family, while Ydj1p belongs to the DnaJ family. Thus, they are believed to maintain the preproteins in a loosely folded, translocation-competent conformation. The interaction between Ssa1p and Ydj1p is required to promote protein translocation.[144]

In the lumen of yeast ER, two DnaK–Hsp70-family proteins exist: Kar2p (BiP) and Lhs1p. As noted above, Kar2p binds to Sec63p and stimulates initiation of translocation. Sec63p and Kar2p are also required for the SRP-dependent translocation process.[145] Another Hsp70 family lumenal protein, Lhs1p (Grp170–Orp150 in mammals), is also essential for translocation with the Sil1p protein, although the exact role remains to be determined.[146] Sec61p recognizes the signal peptides and its gate is opened;[147] then, the substrate preprotein is pushed into the translocon channel with the ATP-dependent functions of Sec63p and Kar2p.[148]

14.4 SEQUENCE FEATURES AND SPECIFICITY

In early signal peptide research, it was most surprising that there are a great variety of sequences for representing a sole function of signal peptides; indeed, the title of a review at that time was "Unity in function in the absence of consensus in sequence."[149] However, as described above, the situation turned out to be much more complex than expected.[150,151] Since different translocation pathways are dependent on signal peptides, the signal peptides must specify their own targeting routes. In addition, signal peptidases are also responsible for the fate of preproteins because uncleaved signal peptides can work as signal anchors. Here, our current understanding on this issue is reviewed.

14.4.1 General Features

14.4.1.1 Tripartite Structure

In a classical view, signal peptides exist at the N terminus of proteins and have the tripartite structure that is conserved across every species, instead of a concrete consensus sequence.[152] Namely, the main body of signal peptides is the central hydrophobic core (h-region), where hydrophobic residues are rich typically for about 7 to 15 amino acids (aa). The amino-terminal side of the h-region is called the n-region; this often contains positively charged residues while its carboxy-terminal region (c-region) contains more polar residues than the h-region. The c-region ends at the cleavage site. A weak consensus sequence pattern is found around the cleavage site, known as the (–3, –1) rule (see below).[153,154] Subtle differences exist between these features in different species; for example, signal peptides of *B. subtilis* tend to be longer than those of *E. coli*.[155-159]

14.4.1.2 Signal Anchors

Polytopic (multispanning) membrane proteins often do not have cleavable signal peptides, although their most N-terminal transmembrane segment is thought to act as an uncleavable signal peptide (see below).[8,9] However, some polytopic membrane proteins are exceptional in that their most N-terminal polar segment translocates across the membrane (the N-tail phenomenon).[160,161] Such an N-tail can be as long as 100 residues. The mechanism of N-tail translocation is not well understood but the effects of neighboring transmembrane segments have been observed.[162,163]

In an *in vitro* system, SecA, SecB, and electrochemical potential were necessary for a long N-tail translocation.[164] Although it is generally established that signal peptides have sufficient information for their targeting to the membrane and their translocation, there are some reports describing the contribution of other parts; for example, human UDP-glucuronosyltransferase 1A6 has an internal signal sequence that can direct the protein to the ER even when its N-terminal signal sequence is deleted.[165] Prion protein also has a second ER targeting signal at its C terminus.[166] Another recent surprise was that a signal peptide can target to ER and to mitochondria.[167] In this case, an endoprotease cleavage of its N terminus can activate a cryptic mitochondrial targeting signal. Interestingly, the topologies of proteins targeted to each site were different, suggesting the difference of their membrane assembly mechanisms.

14.4.2 Signal Peptidases

Signal peptidases are membrane-bound proteases that specifically remove signal peptides from preproteins after their translocation. In eubacteria, they are classified into two (or three) types: type I, type II, (and type III) signal peptidases.[168]

14.4.2.1 Distribution of Type I Signal Peptidases

Type I signal (or leader) peptidases cleave most signal peptides; their homologs exist in the ER, mitochondrial inner membrane, and chloroplast thylakoid membrane in eukaryotes, as well as the plasma membrane of archaea.[168,169] Of these, they are further divided into two types: the P (prokaryotic)-type for eubacterial, mitochondrial, and chloroplastic peptidases and the ER-type for eukaryotic and archaeal peptidases.[170] The P-type signal peptidases employ a serine–lysine catalytic dyad mechanism instead of the standard serine–histidine–aspartic acid catalytic triad mechanism of serine proteases.[168] In the ER-type, the lysine of the catalytic dyad is hisidine.[169]

Although most components for protein translocation are contained for only one copy in a genome, some bacteria contain multiple paralogous copies of type I signal peptidases. For example, seven copies were found in *B. subtilis*, two of which are encoded in plasmids. Surprisingly, one of the five genes encoded in the chromosome, SipW, seems to belong to the ER-type.[170] In addition, it was found that only two of the five genes are of major functional importance and that their difference cannot be explained from the structure of their catalytic site.[171]

14.4.2.2 Specificity of Type I Signal Peptidases

As noted above, signal peptides have a weak consensus pattern around their cleavage site known as the (–3, –1) rule.[153] Namely, the residues at positions –3 and –1 from the cleavage site are small (and neutral) such as alanine in most cases. In eukaryotes, this requirement is less stringent, allowing glycines and serines as well as alanines; it is more stringent in thylakoid membrane.[169,172,173] With experimental analyses, this rule was confirmed as the substrate specificity of type I signal peptidases. However, because the consensus pattern is so weak, many other potential consensus sites could be around the authentic site in a preprotein. More importantly, it seems difficult to discriminate signal-anchored proteins from proteins with cleavable signal peptides by mere existence of such a consensus pattern.[151]

Several experiments show that the degree of hydrophobicity in h-region affects the cleavage.[174] For example, signal peptides become uncleavable when their h-region is artificially extended.[175] The three-dimensional structure of a catalytic N-terminal fragment of *E. coli* type I signal peptidase gives some hints on this enigma.[176,177] The structure shows that the c-region must be in an extended conformation; since transmembrane segments in integral membrane proteins are generally longer and more hydrophobic than the h-region of signal peptides, these segments may not be able to be properly positioned at the catalytic site. However, this idea was challenged by a recent experiment in which both the lack of transmembrane region of signal peptidases and mutations in the h-region of signal peptides did not affect the correct cleavage site selection.[178]

Structures of the mature protein can also affect the cleavage. For example, removal of N-terminal cytoplasmic tail of a type II membrane anchor protein could lead to the cleavage of its transmembrane region;[179] in another example, the transmembrane region near the C terminus can affect the cleavage of signal peptides.[180] Thus, the prediction of signal-anchored proteins is still a difficult problem (see Section 14.5.1).

14.4.2.3 Other Types of Signal Peptidases

Type II signal peptidases (signal peptidases II) are found in eubacteria but not in archaea. These peptidases cleave the signal peptides of so-called lipoproteins (lipid-modified proteins) after the lipid modification. They show a clearer substrate specificity than type I peptidases: the lipobox, is typically represented as LA(G/A) | C, where | denotes the cleavage site.[181,182] The cysteine residue is linked by a fatty acid and the protein is anchored at the membrane with this lipid molecule. The leucine at the –3 position may be other large hydrophobic residues. In *B. subtilis*, signal peptidase II is required for efficient secretion of α-amylase, a nonlipoprotein.[183] Therefore, the substrate specificity of signal peptidase II may not be restricted to lipoproteins.

The third type of signal peptidase is PilD (XcpA), which specifically cleaves preproteins related to pilus biogenesis,[184-186] which is related to the so-called type II protein export pathway.[187] In this pathway, the leader sequences are exceptional in that they are basic and short. PilD not only cleaves these leader peptides but also subsequently monomethylates the newly exposed N-terminal phenylalanine.

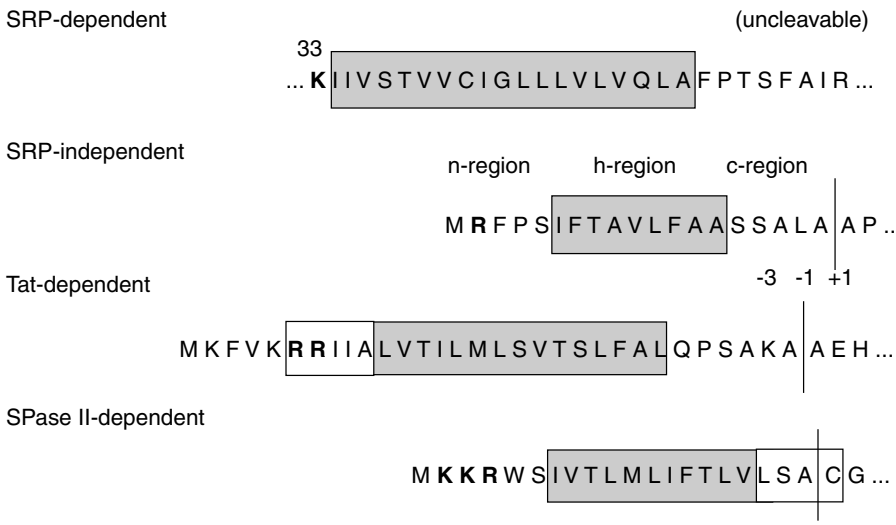

FIGURE 14.2 Various types of signal peptides. In bacteria, many of SRP-dependent signal peptides are signal anchors of multispanning membrane proteins while most mammalian signal peptides are SRP-dependent but cleavable. In an example of SRP-independent signal peptides, the labels of the tripartite structure are shown. In addition, basic residues (K and R) in the n-region are shown in bold face; hydrophobic h-regions are shown with gray boxes; cleavage sites are shown with vertical lines with the labels of important positions around them. In a Tat-dependent signal peptide, the most important region, including the twin-arginine motif, is boxed. In an SPase II-dependent signal peptide, the lipobox motif around the cleavage site is boxed, too.

14.4.3 Determinants of Specificity

As described earlier, prokaryotes and eukaryotes have multiple translocation pathways dependent on signal peptides. Therefore, there must be some specificity determinants within the amino acid sequence of preproteins (Figure 14.2). In addition, signal peptides must be distinguished from other sorting signals within eukaryotic cells.[188] Last, it might be possible that signal peptides could carry the information of the final localization site, i.e., the outer membrane of Gram-negative bacteria. Here, such sequence determinants of signal peptides are discussed.

14.4.3.1 Eubacterial Signal Peptides

If a signal peptide can specify one of the available translocation pathways, it might be also possible that it can specify the final localization site (e.g., the periplasm or the outer membrane of *E. coli*) of the protein where it resides. In fact, some statistical analyses showed that fine sequence features of signal peptides somehow correlate with the final localization sites.[189,190] Although it is widely believed that signal peptides do not determine final localization,[191] these results may reflect some correlation between localization sites and their targeting pathways.

The specificity determinants for various pathways are not well understood. An important question is how the distinction between the SecB-dependent pathway and the SRP-dependent pathway is made.[59] The SRP-dependent pathway is utilized by a subset of inner membrane proteins while the SecB-dependent pathway is utilized mainly by proteins at periplasm and outer membrane.[58,69] It is considered that SRP-dependent signal peptides are more hydrophobic in their h-region. Increasing the hydrophobicity of an SRP-independent signal peptide changed its SRP-dependence.[96] Only functional signal peptides were shown to bind and aggregate the RNA component of SRP.[65] In addition, another factor — trigger factor — seems to play an important role in the selection.[192]

The presence of flanking charged residues also affects specificity of signal peptides. The reason why the n-region often harbors positively charged residue seems to be understood in terms of the positive-inside rule and the loop model.[8,41] Similarly, in a Sec-independent translocation of membrane proteins, it was shown that the effect of the proton motive force on positively or negatively charged residues becomes more significant when hydrophobicity of the translocating segment is low.[108,193] The longer the hydrophobic region becomes, the more N-terminal translocation is favored.[194] The presence of flanking charged residues and the degree of hydrophobicity seem to contribute additively to determination of the topology of signal-anchor proteins.[195]

Signal peptides for the Tat-dependent pathway are somewhat similar to typical signal peptides, but their length is typically longer, due mainly to the extension of the n-region.[17] In addition, their degree of hydrophobicity is lower than that of usual Sec-type signal peptides.[196] However, the most conspicuous feature of the Tat-dependent signal is the unique twin-arginine motif that locates immediately upstream of the h-region. The motif is represented as (S/T)RRXFLK, where X represents an arbitrary residue. The arginine residues are invariant in chloroplasts[197,198] but only one substitution of them into lysine seems to be tolerated to some extent in bacteria.[199,200] The phenylalanine (F) is also important but can be changed to leucine (L). Surprisingly, the presence of the last lysine retards the transport.[199]

Basically, signals for the Tat-dependent pathway seem interchangeable between bacteria and chloroplasts.[201] However, in contrast to Sec-dependent signal peptides, the Tat-dependent signal peptides may not be universally recognized across species.[202] Not all Sec-dependent signal peptides can be converted into Tat-dependent by simply adding the motif, probably because of the nature of the bound proteins. In addition, one or two lysine residues in the c-region can work as a "Sec-avoidance" motif.[203] By increasing the hydrophobicity of a Tat-dependent signal peptide, the signal containing the Tat motif could be converted into Sec-dependent, thus proving the importance of low hydrophobicity of Tat-dependent signals.[196]

14.4.3.2 Eukaryotic Signal Peptides

In eukaryotic cells also, it is most likely that SRP dependence of signal peptides is determined by their own amino acid sequence;[150,204] their hydrophobicity seems to be the major determinant of this dependency. Other factors such as their 3D structure

can also affect the dependency. For example, based on the mutational study, it was proposed that kinked signal peptides may approach SRP more closely.[205] In another study, leucine-rich or chemically denatured signal peptides were shown to increase the tendency for interacting with SRP.[206] Thus, SRP may have a chaperone function by maintaining the favorable conformation of signal peptides during their targeting.

The recognition of signal peptides must compete with the recognition of other sorting signals in eukaryotic cells. However, apart from recognition of signal anchors and some exceptions, sequence features of signal peptides are rather unique and prediction of signal peptides from given amino acid sequences is relatively easier than prediction of mitochondrial targeting signals or chloroplast transit signals (see the following section). According to our extensive search of the optimized rule for signal sequence detection, only the sum of the hydropathy value[207] from the 6th residue to the 25th residue was a sufficiently powerful predictor.[208]

14.5 PREDICTIVE AND PROTEOME ANALYSES

In the post-genomic era, prediction of signal peptides and the systematic analyses of secreted proteins within a proteome are of special importance. Prediction of signal peptides enables us to annotate open reading frames with no known homologous proteins. It can be used for screening candidates for drug targets. This situation might explain a part of the reason why a prediction program, SignalP, was enthusiastically welcomed; its paper is cited in ISI's Red Hot Research list of 1997.[173] Not only theoretical works but also direct experimental studies on secreted proteins are now becoming major projects. Of course, both kinds of studies are desirable in order to stimulate each other.

14.5.1 Prediction Algorithms

Predictive recognition of signal peptides has been most successful among predictions of various protein-sorting signals. Most of these algorithms can also predict cleavage sites. Although attempts have been made to detect candidate proteins dependent on the Tat-dependent pathway, all currently available prediction methods seem to deal with Sec-dependent signal peptides only. In addition, the distinction between SRP-dependent and SRP-independent pathways has not been attempted, probably because of lack of sufficient data.

It should also be noted that the existence of signal peptide is not always clear in a biological sense; a fraction of proteins with "weak" signal peptides can remain in the cytosol.[134] Moreover, it seems difficult to describe the optimized features of signal peptides because they are recognized by different proteins, e.g., SRP and translocon. The prediction of signal peptides has recently been reviewed by several authors, including myself.[188,209-211] Essentially, there are two approaches for the prediction of signal peptides: window-based methods and global structure-based methods. The former is conveniently divided into weight matrix methods and artificial neural network-based methods.

14.5.1.1 Weight Matrix Methods

Various methods have been developed for the computational detection of molecular signals. When the signal to be detected is highly conserved, search of its consensus sequence, i.e., the pattern represented by regular expression such as NX(S/T), would be sufficient. However, because molecular signals usually allow functionally conservative mutations and because their degrees of allowance can vary for each position, the weight matrix (or the position-specific scoring matrix; PSSM) method is usually favored: namely, based on a compilation of known signals, the contribution according to their frequency for each residue at each position is stored as a matrix scanned over the target sequences to find places that give higher summation scores than a predefined threshold.[212]

Weight matrix method, then, is the simplest form of so-called window-based methods, in which a window of fixed length is examined at each position of the target sequence. This method was successfully applied to signal peptide prediction by von Heijne.[213] The matrix corresponds to positions from –13 to +2 in terms of the cleavage site. Thus, the sequence features of h-region and c-region, especially the (3, –1) rule, should contribute to the score calculation. Two kinds of matrices (for prokaryotes and eukaryotes) were constructed but these two were rather similar. Although von Heijne's method was originally developed for the detection of cleavage sites, it is sufficiently useful to detect the presence of (cleavable) signal peptides.

Recently, a prediction method very similar to the weight matrix method was proposed by Chou.[214] Then, the method was expanded to include the interresidue correlation around the –3, –1, and +1 positions (the subsite coupling model).[215] That is, conditional probabilities between these residues were introduced. This method showed 92% accuracy in detecting signal peptides in an objective test.

14.5.1.2 Artificial Neural Network-Based Methods

A direct way to improve the simple weight matrix method is to let pattern representation incorporate the effect of internal gaps or the correlation between different positions. Artificial neural networks (ANNs) have been used in various problems of bioinformatics to meet the latter need.[211,216] The ANN method is a sort of machine-learning method in which a number of numeric parameters are iteratively adjusted (or *learned*) to better distinguish positive and negative data. The weight matrix method of signal peptide prediction was elaborated using this method by several authors.[217,218] Among them, Neilsen et al.'s method has been most successful.[173]

In their algorithm, two kinds of networks were constructed for each of the three systems (Gram-positive bacteria, Gram-negative bacteria, and eukaryotes). One network outputs the S-score, which shows the likelihood of an input sequence segment with a fixed length (19 and 27 for bacteria and eukaryotes, respectively) being a part of a signal peptide, the other network outputs the C-score, which is an indicator on whether the input segment includes a cleavage site or not. Scanning the input sequence with the two networks, these two scores are calculated at each position. By combining these scores with a sort of averaging, the presence of signal peptide

and its cleavage site is predicted. The authors reported that their algorithm, SignalP, can predict the presence of signal peptides with high accuracy (72.4% for eukaryotes) and the program has been widely used. Later, SignalP was incorporated in TargetP, which can also predict the presence of mitochondrial targeting signals and chloroplast transit signals.[219] In version 2.0 of SignalP, the hidden Markov model method (see below) is also incorporated (http://www.cbs.dtu.dk/services/SignalP-2.0/).

One of the potential problems of the ANN-based approach is that the method often uses too many numeric parameters compared with the size of the training data used. In such a case, overfitting of the network to the training data is a danger; i.e., the network may memorize the examples without extracting general sequence features. To overcome this difficulty, Jagla and Schuchhardt used the adaptive encoding artificial neural network method in which they could reduce the number of parameters to one tenth without loss of prediction accuracy.[220] The approach of Bannai et al. grows from a motivation to overcome the difficulty that learned knowledge is very hard to interpret from the obtained parameter sets.[208] Thus, they extensively searched a much simpler parameter space directly interpretable as prediction rules.

14.5.1.3 Global Structure-Based Methods

The other category of signal peptide prediction methods is an approach trying to recognize the three-domain (tripartite) structure of signal peptides. A pioneering work on this approach was done by McGeoch.[221] In his algorithm, the start site of the h-region was first searched within the N-terminal 12 residues; then, the length of the h-region and the maximally hydrophobic eight-residue segment in it were used to judge the presence of signal peptide. Later, the method was refined using discriminant analysis in a general purpose prediction program of subcellular localization sites, PSORT/PSORT II.[222-224] At that time, the third variable, net charge of the n-region, was also considered.

Note that McGeoch's algorithm does not take the (–3, –1) rule into account. Therefore, it cannot predict the cleavage site. However, this feature was used in PSORT to detect signal anchors (uncleavable signal peptides) by combining von Heijne's and McGeoch's algorithms; namely, a protein is predicted to have a signal anchor when McGeoch's method predicts positively and von Heijne's algorithm negatively.[222] However, as mentioned earlier, it is difficult to exactly predict signal anchors exactly only from the absence of potential cleavage sites.

Hidden Markov model (HMM) has been widely used in various problems of speech recognition and bioinformatics, including representation of protein functional domains and gene finding.[216,225] It is a kind of probabilistic method where a predefined model is optimized from a set of training data and then the constructed model is used to scan target sequences. One of the strengths of HMM is that it can flexibly model various sequence features, including the tripartite structure of signal peptides. An application of HMM to signal peptide prediction was done by Nielsen and Krogh.[226] Their program, named SignalP-HMM, can predict cleavable signal peptides and also signal anchors by modeling the structure of type II signal anchor.

Recently, an objective assessment of signal peptide prediction methods was undertaken using newly obtained data.[227] In short, von Heijne's weight matrix method was inferior to modern HMM or ANN methods, especially in correctly locating cleavage sites, partly because it was handicapped with a very old dataset. The accuracy of SignalP ver.2 and that of SignalP-HMM ver.2 were comparable, but the latter was slightly superior in analysis of recently accumulated (and thus were not used for training) data.

14.5.2 From Proteome to Secretome

The last topic of this review is the comprehensive analysis of secreted proteins by theoretical or experimental study. Such an analysis is often called secretome analysis.[158,228]

Since the predictions of signal peptides and transmembrane regions are relatively reliable, potential secreted proteins are detectable as proteins having a cleavable signal peptide but not any other transmembrane segments. Several people have attempted to estimate how many proteins are secreted in a proteome.[229] For example, Schneider estimated ratios of secretory proteins coded in various genomes by using an ANN method based on the amino acid composition of full-length sequence.[230] For bacteria living in mild conditions, the ratios ranged between 15 and 30%. According to another analysis using TargetP, about 10% of *Arabidopsis thaliana* and human genes were estimated to code secretory proteins.[219]

Recently, prediction results of 180 secretory and 114 lipoprotein signal peptides in *B. subtilis* were tested by a set of proteome experiments.[158,231] Surprisingly, the authors concluded that the theoretical predictions reflect actual composition of the extracellular proteins for about 50%. Note that this figure does not always mean the direct prediction accuracy of current algorithms; one major reason was that many proteins lacked apparent signal peptides; some cytoplasmic proteins and cell-bound lipoproteins were also found in the extracellular medium. Perhaps "exceptional" secretion pathway for these proteins exists like various secretion pathways of Gram-negative bacteria.[186] In spite of difficulty of prediction, it is certain that these proteome studies will provide invaluable data sources for improving the prediction scheme.

At last, I would like to apologize to the many researchers whose important references were not cited. In addition, I omitted several interesting topics including various mutations on signal peptides and the fate of signal peptide fragments after cleavage.[151,232,233]

ACKNOWLEDGMENTS

I thank Koreaki Ito and his lab members for critically reading the manuscript. This work was supported by Grant-in-Aid for Scientific Research on Priority Areas (C) "Genome Information Science" from the Ministry of Education, Culture, Sports, Science, and Technology of Japan.

REFERENCES

1. Blobel, G. and Dobberstein, B., Transfer of proteins across membranes. 1. Presence of proteolytically processed and unprocessed nascent immunoglobin light chains on membrane-bound ribosomes of murine myeloma, *J. Cell Biol*., 67, 835, 1975.
2. Blobel, G. and Dobberstein, B., Transfer of proteins across membranes. 2. Reconstitution of functional rough microsomes from heterologous components, *J. Cell Biol.*, 67, 852, 1975.
3. Briggs, M.S. and Gierasch, L.M., Molecular mechanisms of protein secretion: the role of the signal sequence, *Adv. Protein Chem.*, 38, 109, 1986.
4. Walter, P. and Johnson, A.E., Signal sequence recognition and protein targeting to endoplasmic reticulum membrane, *Annu. Rev. Cell Biol*., 10, 87, 1994.
5. Keenan, R.J. et al., The signal recognition particle, *Annu. Rev. Biochem.*, 70, 755, 2001.
6. Blobel, G., Intracellular protein topogenesis, *Proc. Natl. Acad. Sci. U.S.A.,* 77, 1496, 1980.
7. Spiess, M., Head or tails — what determines the orientation of proteins in the membrane, *FEBS Lett*., 369, 76, 1995.
8. von Heijne, G., Getting greasy: how transmembrane polypeptide segments integrate into the lipid bilayer, *Mol. Microbiol.*, 24, 249, 1997.
9. van Geest, M. and Lolkema, J.S., Membrane topology and insertion of membrane proteins: search for topogenic signals, Microbiol. Mol. Biol. Rev., 64, 13, 2000.
10. Bassford, P. et al., The primary pathway of protein export in *E. coli*, *Cell*, 65, 367, 1991.
11. Pohlschröder, M. et al., Protein translocation in the three domains of life: variations on a theme, *Cell*, 91, 563, 1997.
12. Eichler, J., Archaeal protein translocation: crossing membranes in the third domain of life, *Eur. J. Biochem*., 267, 3402, 2000.
13. Pugsley, A., The complete general secretory pathway in Gram-negative bacteria, *Microbiol. Rev.,* 57, 50, 1993.
14. Ito, K., The major pathways of protein translocation across membranes, *Genes Cells*, 1, 337, 1996.
15. Danese, P. and Silhavy, T., Targeting and assembly of periplasmic and outer-membrane proteins in *Escherichia coli*, *Ann. Rev. Genet.*, 12, 59, 1998.
16. Driessen, A.J.M., Fekkes, P., and van der Wolk, J.P.W., The Sec system, *Curr. Opin. Microbiol*., 1, 216, 1998.
17. Fekkes, P. and Driessen, A.J.M., Protein targeting to the bacterial cytoplasmic membrane, *Microbiol. Mol. Biol. Rev.*, 63, 161, 1999.
18. Driessen, A.J.M., SecB, a molecular chaperone with two faces, *Trends Microbiol*., 9, 193, 2001.
19. Driessen, A.J.M., Manting, E.H., and van der Does, C., The structural basis of protein targeting and translocation in bacteria, *Nat. Struct. Biol.*, 8, 492, 2001.
20. Mori, H. and Ito, K., The Sec protein-translocation pathway, *Trends Microbiol.,* 9, 494, 2001.
21. Fekkes, P., den Blaauwen, T., and Driessen, A.J.M., Diffusion-limited interaction between unfolded polypeptides and the *Escherichia coli* chaperone SecB, *Biochemistry*, 34, 10078, 1995.
22. Kumamoto, C.A. and Francetic, O., Highly selective binding of nascent polypeptides by an *Escherichia coli* chaperone protein *in vivo*, *J. Bacteriol*., 175, 2184, 1993.

23. Park, S. et al., Modulation of folding pathways of exported proteins by the leader sequence, *Science*, 239, 1033, 1988.
24. Randall, L.L., No specific recognition of leader peptide by SecB, a chaperone involved in protein export, *Science*, 248, 860, 1990.
25. Watanabe, M. and Blobel, G., High-affinity binding of *Escherichia coli* SecB to the signal sequence region of a presecretory protein, *Proc. Natl. Acad. Sci. U.S.A.,* 92, 10133, 1995.
26. Topping, T.B. and Randall, L.L., Determination of the binding frame within a physiological ligand for the chaperone SecB, *Protein Sci*., 3, 730, 1994.
27. Knoblauch, N.T.M., Schneider–Mergener, J., and Bukau, B., Substrate specificity of the SecB chaperone, *J. Biol. Chem.*, 274, 34219, 1999.
28. Hardy, S.J. and Randall, L.L., A kinetic partitioning model of selective binding of nonnative proteins by the bacterial chaperone SecB, *Science*, 251, 439, 1991.
29. Randall, L.L. and Hardy, S.J.S., High selectivity with low specificity: how SecB has solved the paradox of chaperone binding, *Trends Biochem. Sci.*, 29, 65, 1995.
30. Kim, J., Luirink, J., and Kendall, D.A., SecB dependence of an exported protein is a continuum influenced by the characteristics of the signal peptide or early mature region, *J. Bacteriol*., 182, 4108, 2000.
31. Xu, Z., Knafels, J.D., and Yoshino, K., Crystal structure of the bacterial protein export chaperone SecB, *Nat. Struct. Biol.,* 7, 1172, 2000.
32. Murén, E.M. et al., Mutational alterations in the homotetrameric chaperone SecB that implicate the structure as dimer of dimers, *J. Biol. Chem*., 274, 19397, 1999.
33. Duong, F. et al., Biogenesis of the gram-negative bacterial envelope, *Cell*, 91, 567, 1997.
34. Manting, E.H. and Driessen, A.J.M., *Escherichia coli* translocase: the unravelling of a molecular machine, *Mol. Microbiol.*, 37, 226, 2000.
35. Oliver, D.B., SecA protein: autoregulated ATPase catalysing preprotein insertion and translocation across the *Escherichia coli* inner membrane, *Mol. Microbiol.*, 7, 159, 1993.
36. Snyders, S., Ramamurthy, V., and Oliver, D., Identification of a region of interaction between *Escherichia coli* SecA and SecY proteins, *J. Biol. Chem.*, 272, 11302, 1997.
37. Dapic, V. and Oliver, D., Distinct membrane binding properties of N- and C-terminal domains of *Escherichia coli* SecA ATPase, *J. Biol. Chem*., 275, 25000, 2000.
38. Schmidt, M.O., Brosh, R.M. Jr., and Oliver, D.B., *Escherichia coli* SecA helicase activity is not required *in vivo* for efficient protein translocation or autogenous regulation, *J. Biol. Chem*., 276, 37036, 2001.
39. Kim, J. et al., Evidence that SecB enhances the activity of SecA, *Biochemistry*, 40, 3674, 2001.
40. Lill, R., Dowhan, W., and Wickner, W., The ATPase activity of SecA is regulated by acidic phospholipids, SecY, and the leader and mature domains of precursor proteins, *Cell*, 60, 271, 1990.
41. van Voorst, F. and de Kruijff, B., Role of lipids in the translocation of proteins across membranes, *Biochem. J.*, 347, 601, 2000.
42. Cunningham, K. and Wickner, W., Specific recognition of the leader region of precursor proteins is required for the activation of translocation ATPase of *Escherichia coli*, *Prot. Natl. Acad. Sci. U.S.A.,* 86, 8630, 1989.
43. Miller, A., Wang, L., and Kendall, D.A., Synthetic signal peptides specifically recognize SecA and stimulate ATPase activity in the absence of preprotein, *J. Biol. Chem*., 273, 11409, 1998.

44. Wang, L., Miller, A., and Kendall, D.A., Signal peptide determinants of SecA binding and stimulation of ATPase activity, *J. Biol. Chem*., 275, 10154, 2000.
45. Triplett, T.L. et al., Functional signal peptides bind a soluble N-terminal fragment of SecA and inhibit its ATPase activity, *J. Biol. Chem.*, 276, 19648, 2001.
46. Schekman, R., Translocation gets a push, *Cell*, 78, 911, 1994.
47. Economou, A. and Wickner, W., SecA promotes preprotein translocation by undergoing ATP-driven cycles of membrane insertion and deinsertion, *Cell*, 78, 835, 1994.
48. Eichler, J. and Wickner, W., Both an N-terminal 65-kDa domain and a C-terminal 30-kDa domain of SecA cycle into the membrane at SecYEG during translocation, *Proc. Natl. Acad. Sci. U.S.A.,* 94, 5574, 1997.
49. Nishiyama, K. et al., Membrane deinsertion of SecA underlying proton motive force-dependent stimulation of protein translocation, *EMBO J*., 18, 1049, 1999.
50. Economou, A., Bacterial preprotein translocase: mechanism and conformational dynamics of a processive enzyme, *Mol. Microbiol*., 27, 511, 1998.
51. Prinz, W.A. et al., The protein translocation apparatus contributes to determining the topology of an integral membrane protein in *Eschericha coli*, *J. Biol. Chem*., 273, 8419, 1998.
52. Luirink, J., Samuelsson, T., and de Gier, J.-W., YidC/Oxa1p/Alb3: evolutionarily conserved mediators of membrane protein assembly, *FEBS Lett*., 501, 1, 2001.
53. Duong, F. and Wickner, W., The SecDFyajC domain of preprotein translocase controls preprotein movement by regulating SecA membrane cycling, *EMBO J.*, 16, 4871, 1997.
54. Collinson, I. et al., Projection structure and oligomeric properties of a bacterial core protein translocase, *EMBO J.*, 20, 2462, 2001.
55. Yahr, T.L. and Wickner, W.T., Evaluating the oligomeric state of SecYEG in preprotein translocase, *EMBO J*., 19, 4393, 2000.
56. Manting, E.H. et al., SecYEG assembles into a tetramer to form the active protein translocation channel, *EMBO J.*, 19, 852, 2000.
57. Samuelson, J.C. et al., Function of YidC for the insertion of M13 procoat protein in *Escherichia coli*: translocation of mutants that show differences in their membrane potential dependence and *Sec* requirement, *J. Biol. Chem*., 276, 34847, 2001.
58. Ulbrandt, N.D., Newitt, J.A., and Bernstein, H.D., The *E. coli* signal recognition particle is required for the insertion of a subset of inner membrane proteins, *Cell*, 88, 187, 1997.
59. de Gier, J.-W.L. et al., The *E. coli* SRP: preferences of a targeting factor, *FEBS Lett*., 408, 1, 1997.
60. Herskovits, A.A., Bochkareva, E.S., and Bibi, E., New prospects in studying the bacterial signal recognition particle pathway, *Mol. Microbiol.*, 38, 927, 2000.
61. Keenan, R.J. et al., Crystal structure of the signal sequence binding subunit of the signal recognition particle, *Cell*, 94, 181, 1998.
62. Batey, R.T. et al., Crystal structure of the ribonucleoprotein core of the signal recognition particle, *Science*, 287, 1232, 2000.
63. Bernstein, H.D. et al., Model for signal sequence recognition from amino-acid sequence of 54K subunit of signal recognition particle, *Nature*, 340, 482, 1989.
64. Zheng, N. and Gierasch, L.M., Domain interactions in *E. coli* SRP: stabilization of M domain by RNA is required for effective signal sequence modulation of NG domain, *Mol. Cell*, 1, 79, 1997.
65. Swain, J.F. and Gierasch, L.M., Signal peptides bind and aggregate RNA, *J. Biol. Chem*., 276, 12222, 2001.

66. Cleverley, R.M., Zheng, N., and Gierasch, L.M., The cost of exposing a hydrophobic loop and implications for the functional role of 4.5S RNA in the *Escherichia coli* signal recognition particle, *J. Biol. Chem.*, 276, 19327, 2001.
67. Peluso, P. et al., Role of 4.5S RNA in assembly of the bacterial signal recognition particle with its receptor, *Science*, 288, 1640, 2000.
68. Montoya, G. et al., Crystal structure of the NG domain from the signal-recognition particle receptor FtsY, *Nature*, 385, 365, 1997.
69. Valent, Q.A. et al., The *Escherichia coli* SRP and SecB targeting pathways converge at the translocon, *EMBO J.*, 17, 2504, 1998.
70. Whitley, P. et al., *Sec*-independent translocation of a 100-residue periplasmic N-terminal tail in the *E. coli* inner membrane protein proW, *EMBO J.*, 13, 4653, 1994.
71. Cristóbal, S. et al., The signal recognition particle-targeting pathway does not necessarily deliver proteins to the Sec-translocase in *Escherichia coli*, *J. Biol. Chem.*, 274, 20068, 1999.
72. Herskovits, A.A. and Bibi, E., Association of *Escherichia coli* ribosomes with the inner membrane requires the signal recognition particle receptor but is independent of the signal recognition particle, *Prot. Natl. Acad. Sci. U.S.A.,* 97, 4621, 2000.
73. Qi, H.-Y. and Bernstein, H.D., *SecA* is required for the insertion of inner membrane proteins targeted by the *Eschericha coli* signal recognition particle, *J. Biol. Chem.*, 274, 8993, 1999.
74. Neumann–Haefelin, C. et al., SRP-dependent co-translational targeting and SecA-dependent translocation analyzed as individual steps in the export of a bacterial protein, *EMBO J.*, 19, 6419, 2000.
75. Weiner, J.H. et al., A novel and ubiquitous system for membrane targeting and secretion of cofactor-containing proteins, *Cell*, 93, 93, 1998.
76. Santini, C.-L. et al., A novel Sec-independent periplasmic protein translocation pathway in *Escherichia coli*, *EMBO J.*, 17, 101, 1998.
77. Berks, B.C., Sargent, F., and Palmer, T., The Tat protein export pathway, *Mol. Microbiol.*, 35, 260, 2000.
78. Wu, L.F. et al., Bacterial twin-arginine signal peptide-dependent protein translocation pathway: evolution and mechanism, *J. Mol. Microbiol. Biotechnol.*, 2, 179, 2000.
79. Robinson, C. and Bolhuis, A., Protein targeting by the twin-arginine translocation pathway, *Nat. Rev. Mol. Cell Biol.*, 2, 350, 2001.
80. Sargent, F., A marriage of bacteriology with cell biology results in twin arginines, *Trends Microbiol.*, 9, 196, 2001.
81. Settles, A.M. and Martienssen, R., Old and new pathways of protein export in chloroplasts and bacteria, *Trends Cell Biol.*, 8, 494, 1998.
82. Dalbey, R.E. and Robinson, C., Protein translocation into and across the bacterial plasma membrane and the plant thylakoid membrane, *Trends Biochem. Sci.*, 24, 17-22, 1999.
83. Dalbey, R.E. and Kuhn, A., Evolutionarily related insertion pathways of bacterial, mitochondrial, and thylakoid membrane proteins, *Ann. Rev. Cell Dev. Biol.*, 16, 51-87, 2000.
84. Hynds, P.J., Robinson, D., and Robinson, C., The Sec-independent twin-arginine translocation system can transport both tightly folded and malfolded proteins across the thylakoid membrane, *J. Biol. Chem.*, 273, 34868, 1998.
85. Rodrigue, A. et al., Co-translocation of a periplasmic enzyme complex by a hitchhiker mechanism through the bacterial Tat pathway, *J. Biol. Chem.*, 274, 13223, 1999.
86. Sargent, F. et al., Overlapping functions of components of a bacterial Sec-independent protein export pathway, *EMBO J.*, 17, 3640, 1998.

87. Oresnik, I.J., Ladner, C.I., and Turner, R.J., Identification of a twin-arginine leader-binding protein, *Mol. Microbiol.*, 40, 323, 2001.
88. Jongbloed, J.D. et al., TatC is a specificity determinant for protein secretion via the twin-arginine translocation pathway, *J. Biol. Chem.*, 275, 41350, 2000.
89. Thanassi, D.G. and Hultgren, S.J., Multiple pathways allow protein secretion across the bacterial outer membrane, *Curr. Opin. Cell Biol.*, 12, 420, 2000.
90. Fernández, L.A. and Berenguer, J., Secretion and assembly of regular surface structures in Gram-negative bacteria, *FEMS Microbiol. Rev.,* 24, 21, 2000.
91. Binet, R. et al., Protein secretion by Gram-negative bacterial ABC exporters — a review, *Gene*, 192, 7, 1997.
92. Delepelaire, P. and Wandersman, C., The SecB chaperone is involved in the secretion of the *Serratia marcescens* HasA protein through an ABC transporter, *EMBO J.*, 17, 936, 1998.
93. Kuhn, A., Major coat proteins of bacteriophage Pf3 and M13 as model systems for Sec-independent protein transport, *FEMS Microbiol. Rev.*, 17, 185–190, 1995.
94. Soekarjo, M. et al., Thermodynamics of the membrane insertion process of the M13 procoat protein, a lipid bilayer traversing protein containing a leader sequence, *Biochemistry*, 35, 1232, 1996.
95. Kiefer, D. and Kuhn, A., Hydrophobic forces drive spontaneous membrane insertion of the bacteriophage Pf3 coat protein without topological control, *EMBO J.*, 18, 6299, 1999.
96. de Gier, J.-W.L. et al., Differential use of the signal recognition particle translocase targeting pathway for inner membrane protein assembly in *Escherichia coli*, *Proc. Natl. Acad. Sci. U.S.A.,* 95, 14646, 1998.
97. Samuelson, J.C. et al., YidC mediates membrane protein insertion in bacteria, *Nature*, 406, 637, 2000.
98. Roos, T. et al., Indecisive M13 procoat protein mutants bind to SecA but do not activate the translocation ATPase, *J. Biol. Chem.*, 276, 37909–37915, 2001.
99. Urbanus, M.L. et al., Sec-dependent membrane protein insertion: sequential interaction of nascent FtsQ with SecY and YidC, *EMBO Rep.*, 2, 524, 2001.
100. McIntosh, T.J., Vidal, A., and Simon, S.A., The energetics of binding of a signal peptide to lipid bilayers: the role of bilayer properties, *Biochem. Soc. Trans*., 29, 594, 2001.
101. Engelman, D.M. and Steitz, T.A., The spontaneous insertion of proteins into and across membranes: the helical hairpin hypothesis, *Cell*, 23, 411, 1981.
102. Chupin, V. et al., PhoE signal peptide inserts into micelles as a dynamic helix-breaα-helix structure, which is modulated by the environment. A two-dimensional ^{1}H NMR study, *Biochemistry*, 34, 11617, 1995.
103. Killian, J.A., Hydrophobic mismatch between proteins and lipids in membranes, *Biochim. Biophys. Acta,* 1376, 401, 1998.
104. van Klompenburg, W. and de Kruijff, B., The role of anionic lipids in protein insertion and translocation in bacterial membranes, *J. Membrane Biol.*, 162, 1, 1998.
105. von Heijne, G., The distribution of positively charged residues in bacterial inner membrane proteins correlates with the trans-membrane topology, *EMBO J.*, 5, 3021, 1986.
106. von Heijne, G., Transcending the impenetrable: how proteins come to terms with membranes, *Biochim. Biophys. Acta*, 947, 307, 1988.
107. Monné, M. et al., Positively and negatively charged residues have different effects on the position in the membrane of a model transmembrane helix, *J. Mol. Biol*., 284, 1177, 1998.

108. Schuenemann, T.A., Delgado–Nixon, V.M., and Dalbey, R.E., Direct evidence that the proton motive force inhibits membrane translocation of positively charged residues within membrane proteins, *J. Biol. Chem.*, 274, 6855, 1999.
109. van de Vossenberg, J.L.C.M. et al., The positive inside rule is not determined by the polarity of the $\Delta\psi$, *Mol. Microbiol.*, 29, 1125, 1998.
110. Kiefer, D. et al., Negatively charged amino acid residues play an active role in orienting the Sec-independent Pf3 coat protein in the *Escherichia coli* inner membrane, *EMBO J.*, 16, 2197, 1997.
111. Ridder, A.N.J.A. et al., Anionic lipids stimulate Sec-independent insertion of a membrane protein lacking charged amino acid side chains, *EMBO Rep.*, 2, 403, 2001.
112. Rapoport, T.A., Rolls, M.M., and Jungnickel, B., Approaching the mechanism of protein transport across the ER membrane, *Curr. Opin. Cell Biol.,* 8, 499, 1996.
113. Sakaguchi, M., Eukaryotic protein secretion, *Curr. Opin. Biotech.*, 8, 595, 1997.
114. Wilkinson, B.M., Regnacq, M., and Stirling, C.J., Protein translocation across the membrane of the endoplasmic reticulum, *J. Membr. Biol.*, 155, 189, 1997.
115. Stroud, R.M. and Walter, P., Signal sequence recognition and protein targeting, *Curr. Opin. Struct. Biol.*, 9, 754, 1999.
116. Johnson, A.E. and van Waes, M.A., The translocon: a dynamic gateway at the ER membrane, *Ann. Rev. Cell Dev. Biol.*, 15, 799, 1999.
117. Agarraberes, F.A. and Dice, J.F., Protein translocation across membranes, *Biochim. Biophys. Acta*, 1513, 1, 2001.
118. Koehler, C.M., Protein translocation pathways of the mitochondrion, *FEBS Lett.*, 476, 27, 2000.
119. Robinson, C., Thompson, S.J., and Woolhead, C., Multiple pathways used for the targeting of thylakoid proteins in chloroplasts, *Traffic*, 2, 245, 2001.
120. Truscott, K.N., Pfanner, N., and Voos, W., Transport of proteins into mitochondria, *Rev. Physiol. Biochem. Pharmacol.,* 143, 81, 2001.
121. Gorodkin, J. et al., SRPDB (signal recognition particle database), *Nucl. Acids Res.*, 29, 169, 2001.
122. Wiedmann, B. et al., A protein complex required for signal-sequence-specific sorting and translocation, *Nature*, 370, 434, 1994.
123. Wickner, W., The nascent-polypeptide-associated complex: having a "NAC" for fidelity in translocation, *Proc. Natl. Acad. Sci. U.S.A.,* 92, 9433, 1995.
124. Beatrix, B., Sakai, H., and Wiedmann, M., The α and β subunit of the nascent polypeptide-associated complex have distinct functions, *J. Biol. Chem.*, 275, 3783, 2000.
125. Neuhof, A. et al., Binding of signal recognition particle gives ribosome/nascent chain complexes a competitive advantage in endoplasmic reticulum membrane interaction, *Mol. Biol. Cell*, 9, 103, 1998.
126. Song, W. et al., Role of Sec61a in the regulated transfer of the ribosome-nascent chain complex from the signal recognition particle to the translocation channel, *Cell*, 100, 333, 2000.
127. Fulga, T.A. et al., SRβ coordinates signal sequence release from SRP with ribosome binding to the translocon, *EMBO J.*, 20, 2338, 2001.
128. Görlich, D. et al., A protein of the endoplasmic reticulum involved early in polypeptide translocation, *Nature*, 357, 47, 1992.
129. Voigt, S. et al., Signal sequence-dependent function of the TRAM protein during early phases of protein transport across the endoplasmic reticulum membrane, *J. Cell Biol.*, 134, 25, 1996.

130. Matlack, K.E.S., Mothes, W., and Rapoport, T.A., Protein translocation: tunnel vision, *Cell*, 92, 381, 1998.
131. Raden, D., Song, W., and Gilmore, R., Role of the cytoplasmic segments of Sec61α in the ribosome-binding and translocation-promoting activities of the Sec61 complex, *J. Cell Biol*., 150, 53, 2000.
132. Jungnickel, B. and Rapoport, T.A., A posttargeting signal sequence recognition event in the endoplasmic reticulum membrane, *Cell,* 82, 167, 1995.
133. Siegel, V., A second signal recognition event required for translocation into the endoplasmic reticulum, *Cell*, 82, 167, 1995.
134. Belin, D. et al., A two-step recognition of signal sequences determines the translocation efficiency of proteins, *EMBO J.*, 15, 468, 1996.
135. Mothes, W. et al., Signal sequence recognition in cotranslational translocation by protein components of the endoplasmic reticulum membrane, *J. Cell Biol.*, 142, 355, 1998.
136. Bibi, E., The role of the ribosome-translocon complex in translation and assembly of polytopic membrane proteins, *Trends Biochem. Sci*., 23, 51, 1998.
137. Wilkinson, B.M., Tyson, J.R., and Stirling, C.J., Ssh1p determines the translocation and dislocation capabilities of the yeast endoplasmic reticulum, *Dev. Cell*, 1, 401, 2001.
138. Robb, A. and Brown, J.D., Protein transport. Two translocons are better than one, *Mol. Cell*, 8, 484, 2001.
139. Rapoport, T.A. et al., Posttranslational protein translocation across the membrane of the endoplasmic reticulum, *Biol. Chem.*, 380, 1143, 1999.
140. Tyedmers, J. et al., Homologs of the yeast Sec complex subunits Sec62p and Sec63p are abundant proteins in dog pancreas microsomes, *Proc. Natl. Acad. Sci. U.S.A.,* 97, 7214, 2000.
141. Lyman, S.K. and Schekman, R., Binding of secretory precursor polypeptides to a translocon subcomplex is regulated by BiP, *Cell*, 88, 85, 1997.
142. Brodsky, J.L., Post-translational protein translocation: not all hsc70s are created equal, *Trends Biochem. Sci*., 21, 122, 1996.
143. Zimmermann, R., The role of molecular chaperones in protein transport into the mammalian endoplasmic reticulum, *Biol. Chem*., 379, 275, 1998.
144. McClellan, A.J. and Brodsky, J.L., Mutation of the ATP-binding pocket of *SSA1* indicates that a functional interaction between Ssa1p and Ydj1p is required for post-translational translocation into the yeast endoplasmic reticulum, *Genetics*, 156, 501, 2000.
145. Young, B.P. et al., Sec63p and Kar2p are required for the translocation of SRP-dependent precursors into the yeast endoplasmic reticulum *in vivo*, *EMBO J.*, 20, 262, 2001.
146. Tyson, J.R. and Stirling, C.J., *LHS1* and *SIL1* provide a lumenal function that is essential for protein translocation into the endoplasmic reticulum, *EMBO J.,* 19, 6440, 2000.
147. Plath, K. et al., Signal sequence recognition in posttranslational protein transport across the yeast ER membrane, *Cell*, 94, 795, 1998.
148. Pilon, M. and Schekman, R., Protein translocation: how Hsp70 pulls it off, *Cell*, 97, 679, 1999.
149. Randall, L.L. and Hardy, S.J.S., Unity in function in the absence of consensus in sequence: role of leader peptides in export, *Science*, 243, 1156, 1989.
150. Zheng, N. and Gierasch, L.M., Signal sequences: the same yet different, *Cell*, 86, 849, 1996.

151. Martoglio, B. and Dobberstein, B., Signal sequences: more than just greedy peptides, *Trends Cell Biol.*, 8, 410, 1998.
152. von Heijne, G., Signal sequences. The limits of variation, *J. Mol. Biol.*, 184, 99, 1985.
153. von Heijne, G., How signal sequences maintain cleavage specific, *J. Mol. Biol.*, 173, 243, 1984.
154. Jain, R.G., Rusch, S.L., and Kendall, D.A., Signal peptide cleavage regions. Functional limits on length and topological implications, *J. Biol. Chem.*, 269, 16305, 1994.
155. Simonen, M. and Palva, I., Protein secretion in *Bacillus* species, *Microbiol. Rev.*, 57, 109, 1993.
156. Nagarajan, V., Protein secretion, in *Bacillus subtilis* and Other Gram-Positive Bacteria: Biochemistry, Physiology, and Molecular Genetics, Sonenshein, A.L., Hoch, J.A., and Losick, R., Eds., *American Soc. Microbiol.,* 713, 1993.
157. Nakai, K., Refinement of the prediction methods of signal peptides for the genome analyses of *Saccharomyces cerevisiae* and *Bacillus subtilis*, in *Genome Informatics 1996*, Universal Academy Press, Inc., Tokyo, Japan, 1996, 72.
158. Tjalsma, H. et al., Signal peptide-dependent protein transport in *Bacillus subtilis*: a genome-based survey of the secretome, *Microbiol. Mol. Biol. Rev.*, 64, 515, 2000.
159. Karel, H.M. et al., Translocation of proteins across the cell envelope of Gram-positive bacteria, *FEMS Microbiol. Rev.,* 25, 437, 2001.
160. Cao, G. and Dalbey, R.E., Translocation of N-terminal tails across the plasma membrane, *EMBO J.*, 13, 4662, 1994.
161. Dalbey, R.E., Kuhn, A., and von Heijne, G, Directionality in protein translocation across membranes: the N-tail phenomenon, *Trends Cell Biol.*, 5, 380, 1995.
162. Monné, M. et al., N-tail translocation in a eukaryotic polytopic membrane protein. Synergy between neighboring transmembrane segments, *Eur. J. Biochem.*, 263, 264, 1999.
163. Nilsson, I. et al., Distant downstream sequence determinants can control N-tail translocation during protein insertion into the endoplasmic reticulum membrane, *J. Biol. Chem.*, 275, 6207, 2000.
164. McMurry, J.L. and Kendall, D.A., An artificial transmembrane segment directs SecA, SecB, and electrochemical potential-dependent translocation of a long amino-terminal tail, *J. Biol. Chem.*, 274, 6776, 1999.
165. Ouzzine, M. et al., An internal signal sequence mediates the targeting and retention of the human UDP-glucuronosyltransferase 1A6 to the endoplasmic reticulum, *J. Biol. Chem.*, 274, 31401, 1999.
166. Hölscher, C., Bach, U.C., and Dobberstein, B., Prion protein contains a second endoplasmic reticulum targeting sequence located at its C terminus, *J. Biol. Chem.*, 276, 13388, 2001.
167. Bhagwat, S.V. et al., Dual targeting property of the N-terminal signal sequence of P450A1. Targeting of heterologous proteins to endoplasmic reticulum and mitochondria, *J. Biol. Chem.*, 274, 24014, 1999.
168. Paetzel, M., Dalbey, R.E., and Strynadka, N.C., The structure and mechanism of bacterial type I signal peptidases. A novel antibiotic target, *Pharmacol. Ther.*, 87, 27, 2000.
169. Dalbey, R.E. et al., The chemistry and enzymology of the type I signal peptidases, *Protein Sci.*, 6, 1129, 1997.
170. Tjalsma, H. et al., Functional analysis of the secretory precursor processing machinery of *Bacillus subtilis*: identification of a eubacterial homolog of archaeal and eukaryotic signal peptidases, *Genes Dev.*, 12, 2318, 1998.

171. van Roosmalen, M.L. et al., Distinction between major and minor *Bacillus* signal peptidases based on phylogenetic and structural criteria, *J. Biol. Chem*., 276, 25230, 2001.
172. Howe, C.J. and Wallace, T.P., Prediction of leader peptide cleavage sites for polypeptides of the thylakoid lumen, *Nucl. Acids Res.*, 18, 3417. 1990.
173. Nielsen, H. et al., Identification of prokaryotic and eukaryotic signal peptides and prediction of their cleavage sites, *Protein Eng.*, 10, 1, 1997.
174. Sakaguchi, M. et al., Functions of signal and signal-anchor sequences are determined by the balance between the hydrophobic segment, *Prot. Natl Acad. Sci. U.S.A.,* 89, 16, 1992.
175. Nilsson, I., Whitley, P., and von Heijne, G., The COOH-terminal ends of internal signal and signal-anchor sequences are positioned differently in the ER translocase, *J. Cell Biol.*, 126, 1127, 1994.
176. Paetzel, M., Dalbey, R.E., and Strynadka, N.C., Crystal structure of a bacterial signal peptidase in complex with a β-lactam inhibitor, *Nature*, 396, 186, 1998.
177. von Heijne, G., Life and death of a signal peptide, *Nature*, 396, 111, 1998.
178. Carlos, J.L. et al., The role of the membrane-spanning domain of type I signal peptidases in substrate cleavage site selection, *J. Biol. Chem.*, 275, 38813, 2000.
179. Roy, P. et al., Transformation of the signal peptide/membrane anchor domain of a type II transmembrane protein into a cleavable signal peptide, *J. Biol. Chem.*, 268, 2699, 1993.
180. Rehm, A. et al., Signal peptide cleavage of a type I membrane protein, HCMV US11, is dependent on its membrane anchor, *EMBO J.*, 20, 1573, 2001.
181. Klein, P., Somorjai, R.L., and Lau, P.C.K., Distinctive properties of signal sequences from bacterial lipoproteins, *Protein Eng.*, 2, 15, 1988.
182. von Heijne, G., The structure of signal peptides from bacterial lipoproteins, *Protein Eng*., 2, 531, 1989.
183. Tjalsma, H. et al., The role of lipoprotein processing by signal peptidase II in the Gram-positive eubacterium *Bacillus subtilis*, *J. Biol. Chem*., 274, 1698, 1999.
184. Strom, M.S., Nunn, D.N., and Lory, S., Posttranslational processing of type IV prepilin and homologs by PilD of *Pseudomonas aeruginosa*, *Methods Enzymol.*, 235, 527, 1994.
185. Lory, S. and Strom, M.S., Structure-function relationship of type-IV prepilin peptidase of *Pseudomonas aeruginosa* — a review, *Gene*, 192, 117, 1997.
186. Fernandez, L.A. and Berenguer, J., Secretion and assembly of regular surface structures in Gram-negative bacteria, *FEMS Microbiol. Rev.*, 24, 21, 2000.
187. Nunn, D., Bacterial type II protein export and pilus biogenesis: more than just homologies? *Trends Cell Biol.*, 9, 402, 1999.
188. Nakai, K., Protein sorting signals and prediction of subcellular localization, *Adv. Protein Chem*., 54, 277, 2000.
189. Sjöström, M. et al., Signal peptide amino acid sequences in *Eschericha coli* contain information related to final protein localization. A multivariate data analysis, *EMBO J*., 6, 823, 1987.
190. Edman, M. et al., Different sequence patterns in signal peptides from Mycoplasmas, other Gram-positive bacteria, and *Escherichia coli*: a multivariate data analysis, *Proteins, Struct. Funct. Genet.*, 35, 195, 1999.
191. Tommassen, J., van Tol, H., and Lugtenberg, B., The ultimate localization of an outer membrane protein of *Escherichia coli* K-12 is not determined by the signal sequence, *EMBO J*., 2, 1275, 1983.

192. Beck, K. et al., Discrimination between SRP- and SecA/SecB-dependent substrates involves selective recognition of nascent chains by SRP and trigger factor, *EMBO J.*, 19, 134, 2000.
193. Delgado–Partin, V.M. and Dalbey, R.E., The protein motive force, acting on acidic residues, promotes translocation of amino-terminal domains of membrane proteins when the hydrophiobicity of the translocation signal is low, *J. Biol. Chem.*, 273, 9927, 1998.
194. Rösch, K. et al., The topogenic contribution of uncharged amino acids on signal sequence orientation in the endoplasmic reticulum, *J. Biol. Chem.*, 275, 14916, 2000.
195. Wahlberg, J.M. and Spiess, M., Multiple determinants direct the orientation of signal-anchor proteins: the topogenic role of the hydrophobic signal domain, *J. Cell Biol.*, 137, 555, 1997.
196. Cristóbal, S. et al., Competition between Sec- and TAT-dependent protein translocation in *Eschericha coli*, *EMBO J.*, 18, 2982, 1999.
197. Chaddock, A.M. et al., A new type of signal peptide: central role of a twin-arginine motif in transfer signals for the ΔpH-dependent thylakoidal protein translocase, *EMBO J.*, 14, 2715, 1995.
198. Brink, S. et al., Targeting of thylakoid proteins by the ΔpH-driven twin-arginine translocation pathway requires a specific signal in the hydrophobic domain in conjunction with the two-arginine motif, *FEBS Lett*., 434, 425, 1998.
199. Stanley, N.R., Palmer, T., and Berks, B.C., The twin arginine consensus motif of Tat signal peptides is involved in Sec-independent protein targeting in *Escherichia coli*, *J. Biol. Chem.,* 275, 11591, 2000.
200. Hinsley, A.P. et al., A naturally occurring bacterial Tat signal peptide lacking one of the "invariant" arginine residues of the consensus targeting motif, *FEBS Lett*., 497, 45, 2001.
201. Mori, H. and Cline, K., A signal peptide that directs non-Sec transport in bacteria also directs efficient and exclusive transport on the thylakoid ΔpH pathway, *J. Biol. Chem*., 273, 11405, 1998.
202. Blaudeck, N. et al., Specificity of signal peptide recognition in tat-dependent bacterial protein translocation, *J. Bacteriol*., 183, 604, 2001.
203. Bogsch, E., Brink, S., and Robinson, C., Pathway specificity for a ΔpH-dependent precursor thylakoid lumen protein is governed by a "Sec-avoidance" motif in the transfer peptide and a "Sec-incompatible" mature protein, *EMBO J.*, 16, 3851, 1997.
204. Ng, T.W., Brown, J.D., and Walter, P., Signal sequences specify the targeting route to the endoplasmic reticulum membrane, *J. Cell Biol.*, 134, 269, 1996.
205. Matoba, S. and Ogrydziak, D.M., Another factor besides hydrophobicity can affect signal peptide interaction with signal recognition particle, *J. Biol. Chem*., 273, 18841, 1998.
206. Zheng, T. and Nicchitta, C.V., Structural determinants for signal sequence function in the mammalian endoplasmic reticulum, *J. Biol. Chem*., 274, 36623, 1999.
207. Kyte, J. and Doolittle, R.F., A simple method for displaying the hydropathic character of a protein, *J. Mol. Biol.*, 157, 105, 1982.
208. Bannai, H. et al., Extensive feature detection of N-terminal protein sorting signals, *Bioinformatics*, 18, 298, 2002.
209. Claros, M.G., Brunak, S., and von Heijne, G., Prediction of N-terminal protein sorting signals, *Curr. Opin. Struct. Biol.*, 7, 394, 1997.
210. Nielsen, H., Brunak, S., and von Heijne, G., Machine learning approaches for the prediction of signal peptides and other protein sorting signals, *Protein Eng*., 12, 3, 1999.

211. Nakai, K., Prediction of *in vivo* fates of proteins in the era of genomics and proteomics, *J. Struct. Biol*., 134, 103, 2001.
212. Staden, R., Searching for patterns in protein and nucleic acid sequences, *Methods Enzymol*., 183, 193, 1990.
213. von Heijne, G., A new method for predicting signal sequence cleavage sites, *Nucl. Acids Res.,* 14, 4683, 1986.
214. Chou, K.C., Prediction of protein signal sequences and their cleavage sites, *Proteins Struct. Funct. Genet.,* 42, 136, 2001.
215. Chou, K.C., Using subsite coupling to predict signal peptides, *Protein Eng*., 14, 75, 2001.
216. Baldi, P. and Brunak, S., *Bioinformatics: Adaptive Computation and Machine Learning*, 2nd ed., MIT Press, Cambridge, MA, 2001.
217. Ladunga, I. et al., Improving signal peptide prediction accuracy by simulated neural network, *Comput. Appl. Biosci.*, 7, 485, 1991.
218. Schneider, G., Rohlk, S., and Wrede, P., Analysis of cleavage-site patterns in protein precursor sequences with a perceptron-type neural network, *Biochem. Biophys. Res. Commun.*, 194, 951, 1993.
219. Emanuelsson, O. et al., Predicting subcellular localization of proteins based on their N-terminal amino acid sequence, *J. Mol. Biol.*, 300, 1005, 2000.
220. Jagla, B. and Schuchhardt, J., Adaptive encoding neural networks for the recognition of human signal peptide cleavage sites, *Bioinformatics*, 16, 245, 2000.
221. McGeoch, D.J., On the predictive recognition of signal peptide sequences, *Virus Res*., 3, 271, 1985.
222. Nakai, K. and Kanehisa, M., Expert system for predicting protein localization sites in gram-negative bacteria, *Proteins: Struct. Funct. Genet.,* 11, 95, 1991.
223. Nakai, K. and Kanehisa, M., A knowledge base for predicting protein localization sites in eukaryotic cells, *Genomics*, 14, 897, 1992.
224. Nakai, K. and Horton, P., PSORT: a program for detecting sorting signals in proteins and predicting their subcellular localization, *Trends Biochem. Sci*., 24, 34, 1999.
225. Durbin, R. et al., *Biological Sequence Analysis: Probabilistic Models of Proteins and Nucleic Acids*, Cambridge University Press, London, 1998.
226. Nielsen, H. and Krogh, A., Prediction of signal peptides and signal anchors by a hidden Markov model, *Intell. Syst. Mol. Biol*., 6, 122, 1998.
227. Menne, K.M., Hermajakov, H., and Apweiler, R., A comparison of signal sequence prediction methods using a test set of signal peptides, *Bioinformatics*, 16, 741, 2000.
228. Greenbaum, D. et al., Interrelating different types of genomic data, from proteome to secretome: 'oming in on function, *Genome Res.*, 11, 1463, 2001.
229. Ladunga, I., Large-scale predictions of secretory proteins from mammalian genomic and EST sequences, *Curr. Opin. Biotechnol.*, 11, 13, 2000.
230. Schneider, G., How many potentially secreted proteins are contained in a bacterial genome? *Gene*, 237, 113, 1999.
231. Antelmann, H. et al., A proteomic view on genome-based signal peptide predictions, *Genome Res.*, 11, 1484, 2001.
232. Chan, D., Ho, M.S., and Cheah, K.S., Aberrant signal peptide cleavage of collagen X in Schmid metaphyseal chondrodysplasia. Implications for the molecular basis of the disease, *J. Biol. Chem.*, 276, 7992, 2001.
233. Weihofen, A. et al., Release of signal peptide fragments into the cytosol requires cleavage in the transmembrane region by a protease activity that is specifically blocked by a novel cysteine protease inhibitor, *J. Biol. Chem.,* 275, 30951, 2000.

Section III

Applications of Cell-Penetrating Peptides

15 Cell-Penetrating Peptide Conjugations and Magnetic Cell Labels

Ching-Hsuan Tung and Ralph Weissleder

CONTENTS

15.1 INTRODUCTION

Cellular plasma membrane and intracellular membranes represent natural barriers to a large number of exogeneous (and endogenous) molecules. To overcome this delivery barrier for therapeutic and diagnostic drugs, a variety of strategies has been proposed to ferry agents through cellular membranes. These strategies include receptor mediated uptake,[1,2] fluid phase endocytosis (pinocytosis),[3] direct fusion with the

0-8493-1141-1/02/$0.00+$1.50

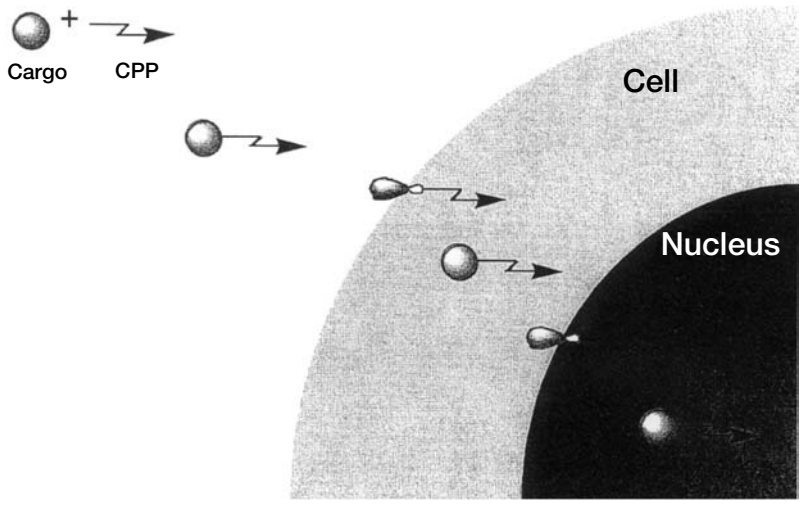

FIGURE 15.1 CPP delivery. CPP is able to deliver various types of biological active molecules through plasma membrane; some of them can even deliver cargo molecules into nucleus.

membrane lipid bilayer,[4] and use of peptide/protein-mediated translocation signals.[5,6] Recently reported cell-penetrating peptides (CPP), including the HIV–Tat,[7,8] the third helix of the homeodomain of Antennapedia,[9] transportant,[10,11] a peptide derived from antiDNA monoclonal antibody,[1,2] VP22 herpes virus protein,[13,14] and other synthetic peptides,[15,16] provide a new way of delivering cargo molecules through cellular barrier (Figure 15.1). The large number of CPPs have been used as efficient delivery vehicles for various biological active molecules, such as proteins,[7,17-23] peptides,[8,24,25] oligonucleotides,[26-28] peptide nucleic acid,[29] plasmid DNA,[30-32] and imaging compounds (Table 15.1).[33-36]

Magnetic materials such as superparamagnetic nanoparticles, ferromagnetic beads, and paramagnetic chelators already play important roles in biotechnology and clinical medicine. However, their applications could be even broader if they could be efficiently delivered into cells rather than attaching them to the cell surface. Internalization would allow an entirely new application spectrum of these materials, including (1) *in vivo* tracking of labeled immune cells in intact micro- and macroenvironments over time, (2) tracking of stem and progenitor cells by imaging, (3) magnetic isolation of *in vivo* homed cells, and (4) using magnetic materials as nanosensors for intracellular readouts of protein or DNA and imaging gene expression. In this chapter we first describe conjugation strategies for attaching CPPs to different materials, then summarize our studies on labeling cells with Tat-assisted magnetic probes.

15.2 CONJUGATION TACTICS

We and other groups have used a number of different strategies to bioconjugate CPPs to payloads; the following section reviews some of them. Most frequently

TABLE 15.1
Some Examples of CPP-Assisted Delivery Systems

CPP	Cargos	Ref.
HIV-Tat	Peptide	36, 49
	Protein	7, 18, 50–52
	Oligonucleotide	28
	DNA	53
	Fluorescence tag	8, 33, 54
	Chelator	33
	Liposome	55
	Particles	34, 35
Antennapedia	Peptides	38, 56, 57
	Protein	58
	Oligonucleotide	59, 60
	PNA	29
Transportan	Peptide	56
	Protein	23
	PNA	29
Loligomer	Fluorescence tag	15
	Plasmid DNA	32
	Drug	61
Hydrophobic signal	Peptide	16, 24, 62
	Protein	4
	Oligonucleotide	27
Oligoarginine	Fluorescence tag	39–41
	Peptide	63
VP-22	Protein	13

used conjugating agents ("cross-linking agents") can be divided into two subgroups: homobifunctional conjugating reagents, which contain at least two identical reactive groups, and heterobifunctional reagents, which have two different reactive groups. The reactive groups usually include amines, sulfhydryls, and carboxylic acids. Other conjugating agents, such as photoreactive and biotin–avidine agents, are less frequently used in CPP conjugation and thus will not be discussed in this chapter.

15.2.1 Direct Synthesis of CPP Conjugates

Typically, CPPs are synthesized on an automatic synthesizer using solid phase peptide chemistry. If CPP conjugates can be synthesized on the synthesizer directly, the preparation would be convenient and straightforward. At least three questions must be answered before making the conjugates. First, will the cargo molecules survive in peptide synthesis and cleavage conditions? Second, does the cargo molecule have the right functional group for coupling? Third, how is a synthetic scheme designed? Usually this approach is only used for conjugating small synthetic compounds to CPP.

Two methods, Fmoc (9-fluorenylmethyloxycarbonyl) and Boc (tert-butyloxycarbonyl) chemistry, are typically used in peptide synthesis. In Fmoc chemistry, the N terminus and side chains of the amino acids are protected by Fmoc and t-butyl groups, respectively. On each cycle, the Fmoc group is removed with 20% piperidine. After synthesis, the peptide is cleaved from the support and side-chain deprotected with 90% trifluoroacetic acid (TFA). Boc chemistry needs stronger acids, i.e., TFA and hydrogen fluoride. TFA was used to remove the N-terminal t-Boc protecting-group on each cycle; hydrogen fluoride was needed to remove the side chain benzyl-protecting group and to cleave peptide off solid support. Thus the stability of the cargo molecules in all these chemical conditions is critical for conjugate preparation.

The common functional groups on peptide for cargo molecule attachment are N-terminal amino, side-chain amino, sulfhydryls, and carboxylic groups. These groups can be conveniently introduced by adding additional amino acids, such as lysine, cysteine, glutamic acid, or aspartic acid. The reactive functional groups can also come from non-nature amino acids or other synthetic linkers. The cargo molecules then can be anchored to the peptide through these functional groups.

The biggest advantage of performing conjugation on the solid support is that the structure of the conjugates is well defined. Using orthogonal deprotecting strategies, the cargo molecules can be attached to a specific position; even the peptide contains several identical functional groups. CPPs are good examples because most of them have several lysine residues. Applying cargo molecule to a specific lysine side chain can be done by selecting various protected lysine residues during the synthesis. The example shown below is to prepare a Tat peptide and metal chelator conjugate used for cell imaging.[33]

Example 15.1
Synthesis of Tat-macrocyclic chelator conjugate

Gly-Arg-Lys-Lys-Arg-Arg-Gln-Arg-Arg-Arg-Gly-Tyr-Lys(DOTA)-NH_2 (Figure 15.2)

1. Reagents:
   Amino acids: Boc-Gly, Fmoc-Arg(Pbf), Fmoc-Lys(Boc), Fmoc-Gln(Trt), Fmoc-Gly, Fmoc-Tyr(Bu) and Fmoc-Lys(Dde) (NovaBiochem, San Diego, CA).
   Resin: Rink amide MBHA resin (NovaBiochem, San Diego, CA).
   Coupling agents: 2-(1H-benzotriazole-1-yl)-1,1,3,3-tetramethyluronium hexafluorophosphate (HBTU)/N-hydroxybenzotriazole (HOBt) (NovaBiochem, San Diego, CA).
   Chelator: 1,4,7,10-tetraazacyclododecane-1,4,7-tris(acetic acid t-butyl ester)-10-acetic acid (DOTA-3tBu) (Macrocyclics, Richardson, TX).
2. The peptide was synthesized on an automatic peptide synthesizer (PS3, Rainin, Woburn, MA) by Fmoc chemistry at 0.1 mmol scale. To each cycle, four-fold excess on amino acid and coupling agents was used. The amino acid sequence and protecting groups are shown in Figure 15.2. Since the subsequent hydrazine treatment is able to remove the Fmoc

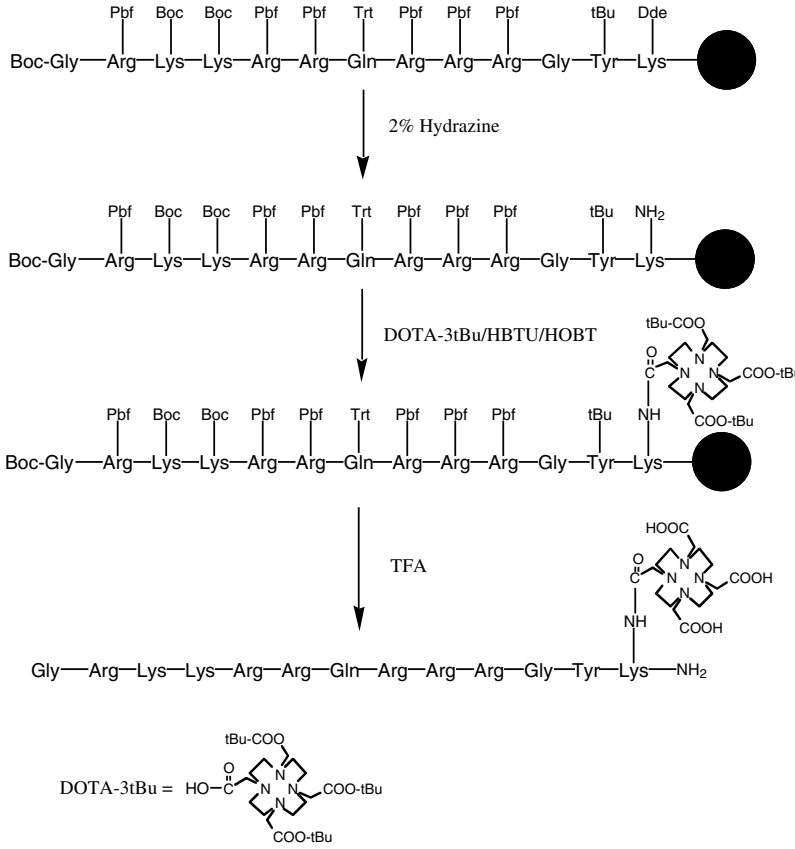

FIGURE 15.2 Synthetic scheme of Tat-DOTA. (From Bhorade, R. et al., *Bioconjug. Chem.,* 11, 301, 2000. With permission.)

group, Fmoc-Gly cannot be used for the last cycle. Instead, a t-Boc-Gly was used to cap the N-terminal amino group.

3. The Dde protecting group on the C- terminal lysine residue was selectively removed with 10 ml of 2% hydrazine in DMF (2×3 min). The other lysine residues were still protected by t-Boc groups.
4. The deprotected lysine residue was then reacted with four-fold excess of DOTA-3tBu with HOBT/HBTU in 5 mL of DMSO/diisopropylethylamine (20% v/v). The coupling efficiency was monitored by Ninhydrin reaction.
5. After synthesis the peptide was cleaved by 5 ml of TFA/thioanisole/ethandithiol/anisole (90/5/3/2) for 3 h, precipitated by methyl-t-butyl ether and purified by C18 reverse phase high pressure liquid chromatography.
6. Finally, the purified peptide was characterized by mass spectrum, MALDI-MS; $(M + H)^+$: 2131.4 (calc.), 2131.3 (found).

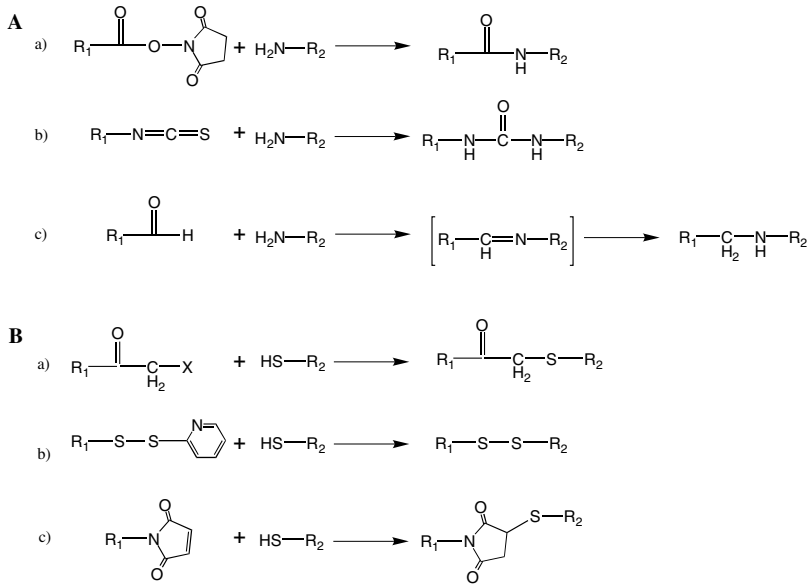

FIGURE 15.3 Common reactions of amino and sulfhydryl groups. (A) Reaction of amino groups with a) activated esters, b) isothiocyanates, and c) aldehydes. (B) Reaction of sulfydryl groups with a) haloacetyls, b) pyridyl disulfides, and c) maleimides.

15.2.2 Solution Phase Conjugation

A number of proteins, peptides, oligonucleotides, oligonucleotide analogs, and particles have been linked to CPPs using solution phase conjugation. Cargo molecules and CPPs were linked through two reactive ends, usually amino or sulfhydryl groups, by bifunctional linkers (Figure 15.3). To prevent dimer formation, hetero-bifunctional linkers are preferable. The most commonly used bridges between CPPs and cargo molecules are disulfide, maleimide, thioether, and amide linkage. The reactives for amino and sulfydryl are described in the following section.

15.2.2.1 Amine-Reactive Reagents

Aliphatic primary amine is commonly found at the N terminal of proteins or lysine side chain and has excellent reactivity, so it is widely applied in conjugation. Lysine ε-amine has good nucleophilic activity about pH 8.0, while the α-amino group is more basic than lysine and reactive at around pH 7.0. The optimal pH for amine reaction is between pH 8 and 9. At this pH range, other amine-containing groups, such as guanidinium group of arginine, amide group of glutamine and asparagine, imidazolium group of histidine, and aromatic amine of nucleic acids, are virtually unreactive. Buffers that contain free amine, e.g., Tris and glycine, should be avoided in the reaction.

Preactivated esters, isothiocynates and aldehyde are three often used reagents for amine conjugation (Figure 15.3A). Preactivated N-hydroxysuccinimide (NHS)

esters react with amine efficiently, and the amide linkages formed are stable in most conditions. Some linkers with NHS ester may have poor water solubility; in these cases, NHS can be replaced by sulfonate-NHS. Isothiocyanates like NHS esters are amine-reactive reagents: a stable thiourea bond was formed after the reaction. A number of isothiocyanates of fluorescence dye have been widely used in labeling biomolecules.

The third type of amine-reactive group is aldehyde, which will form an imine linkage. The aldehyde first reacts with amine to form an intermediate Schiff base, which can be selectively reduced by mild reducing agent sodium cyanoborohydride to give a stable alkylamine bond. This type of linkage is used often to react with sugar because the sugar molecule can be readily oxidized into aldehyde by sodium periodate. However, the reaction is not limited to aliphatic amines; it can also react with aromatic amines. CPPs such as Tat, antennpedia, transportan, and others have multiple lysine residues. Any modification on these lysine side chains may abolish their penetrating capability; therefore, instead of amino groups, a sulfhydryl group is usually introduced for CPP attachment.

15.2.2.2 Sulfhydryl-Reactive Reagents

Sulfhydryl-specific reactions include α-haloacetyls, pyridyl disulfides, and maleimides, (Figure 15.3B). Reacting with maleimide and haloacetyl groups will form thiol ether bonds, and with thiol–pyridyl will form a disulfide linkage that is cleavable. All these thiol-specific reactions happen rapidly in the physiological pH range, pH 6.5 to 8.0, at or below room temperature. Since thiol and amino groups have different optimum pH, the selectivity of the reactions can be controlled well.

Although the thiol–ether bond created from haloacetyl group is a stable bond, the ones from maleimide or pyridyle disulfide are not. The disulfide linkage can be readily cleaved under reducing conditions. If a reversible linkage on the CPP conjugate were preferred, the disulfide bond would be an ideal choice. The maleimide linkage is stable at neutral pH; once the pH is above 8, side reactions may occur.[37]

Compared to amino groups, thiol groups are less commonly found in most proteins; thus the sulfhydryl reactive group can provide means of selective modification at a defined site. For synthetic compounds, a sulfhydryl group can be conveniently generated during synthesis. Peptides can be functionalized by adding a cysteine residue at the N terminus, C terminus, or even at an internal position. If an oligonucleotide is involved in conjugation, many ready-to-use thiol linkers for oligonucleotide 3′ or 5′-terminal modification are also commercially available.

15.2.2.3 Heterobifunctional Conjugation

Checking the amino acid sequences of CPPs, it is found that the positively charged arginine and lysine residues are the two most dominant amino acids. Compared to the amino group of lysine, the guanidinium group of arginine is inert at the optimal pH range for amine reaction. Arginine residue would cause no trouble during conjugation, but the lysine residues might, especially multiple lysine residues. Heterobifunctional linkers usually have two distinct reactive groups that allow for sequential

conjugation with specific groups on cargo molecules and CPPs. Using heterobifunctional reagents, the most labile group should be reacted first to ensure effective cross-linking and avoid unwanted polymerization. The second reaction can then be initiated after cleaning the excess reagents and byproducts from the first. Linker selection is based on the reactive group on either molecule. The majority of commercially available heterobifunctional linkers contain an amine-reactive at one end and a thiol-reactive at the other.

If the CPP were modified to have a thiol group as previously described, the first step of the conjugation usually begins by reacting the activated ester with the amino group on the cargo molecules at basic pH. Then the CPP is attached to the activated first component through a thiol-specific reaction. The commonly used linkers include m-Maleimidobenzoyl-N-hydroxysuccinimide (MBS), N-succinimidyl 3-(2-pyridyldithio)propionate (SPDP), iodoacetic anhydride, and other similar analogs.

Here we use an example to illustrate the solution conjugation approach. A magnetic particle and the Tat peptide were linked using SPDP. The described protocol can also be applied in CPP and protein conjugation.

Example 15.2

Preparation of superparamagnetic iron oxide particle and Tat peptide conjugate (Figure 15.4).[34,35]

1. Reagents:
   Gly-Arg-Lys-Lys-Arg-Arg-Gln-Arg-Arg-Arg-Gly-Tyr-Lys(FITC)-Cys-NH_2
   (the italicized amino acids correspond to CPP signal of the Tat protein)
   N-succinimidyl 3-(2-pyridyldithio)propionate (SPDP) (Molecular Biosciences, Boulder, CO)
2. An amine terminated cross-linked monodispersed superparamagnetic iron oxide colloid (CLIO-NH_2) was prepared as described.[35] The particles consist of a small monocrystalline, superparamagnetic iron oxide core, stabilized by a cross-linked dextran coating to improve stability that was aminated. The particle core measures approximately 5 nm and the overall particle size is 45 nm as determined.
3. CLIO-NH_2 (31.2 mg Fe, 557 μmol) in 2.4 mL of 0.1 *M* phosphate buffer, pH 7.4 was added 2 mL of SPDP in DMSO (25 m*M*, 50 μmol). The reaction mixture was allowed to stand for 3 h at room temperature.
4. Low molecular impurities such as excess reagent and NHS were removed by a gel filtration Sephadex G-25 columns (20 cm, Sigma Chemical, St. Louis, MO) equilibrated with 0.01 *M* Tris, 0.02 *M* citrate, pH 7.4 buffer. The pooled void volume of 4.4 mL was recovered, containing 2-pyridyl disulfide derivatized CLIO at a concentration of 7 mg Fe/mL (0.125 *M*).
5. To measure the number of 2-pyridyl disulfide groups attached, 0.2 mL of the solution above was added to 0.2 mL of 50 m*M* DTT in 0.1 *M* phosphate, pH 7.4. The mixture was allowed to stand for 30 min at room temperature. A microconcentrator, 30 kDa cutoff (Amicon, Beverly, MA), was used to separate the product of the reduction, pyridine-2-thione, from iron. The concentration of pyridine-2-thione was quantitated using an

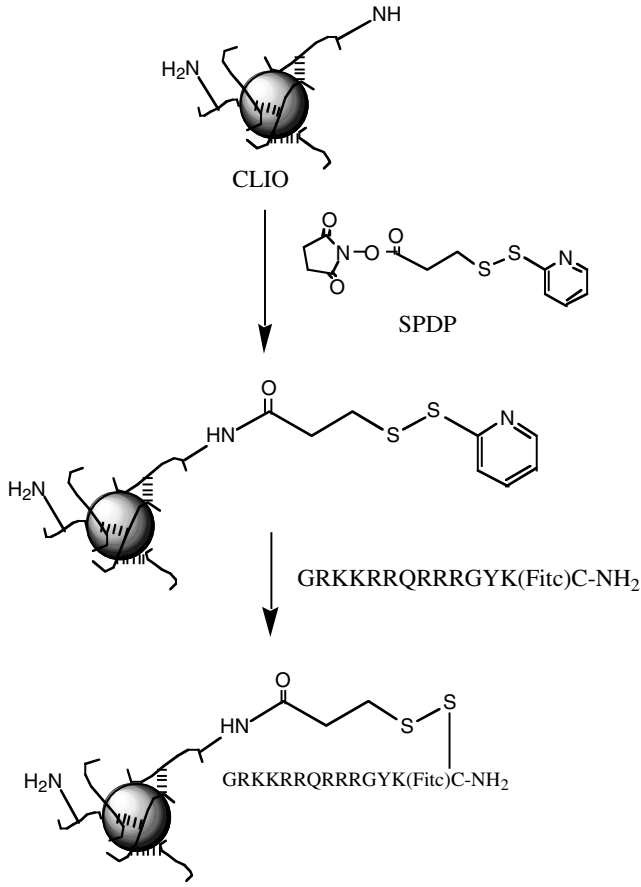

FIGURE 15.4 Synthetic scheme of CLIO–Tat. (From Josephson, L. et al., *Bioconjug. Chem.,* 10, 186, 1999. With permission.)

extinction coefficient at 343 nm of 8100 M^{-1} cm^{-1}. On average, each particle contains 14 2-pyridyl disulfide groups.

6. To 2.3 mL of 2-pyridyl disulfide derivatized CLIO (16.1 mg/Fe, 288 μmol) was added 1.9 mL of Tat peptide (803 μ*M*, 1.52 μmol, as determined by FITC absorbance, extinction coefficient of 73000 M^{-1} cm^{-1} at 494 nm in 0.1 *M* phosphate buffer). The mixture was allowed to react overnight at room temperature.
7. The solution was applied to a second 20-cm Sephadex G-25 column equilibrated as above and the excluded volume containing CLIO–Tat was saved.
8. To measure the number of Tat groups attached, the colloid was reacted with DTT and applied to a microconcentrator as above. Released peptide in the filtrate was quantitated using FITC fluorescence read against a standard of FITC. The average number of Tat peptides per CLIO particle was 4.1 per particle.

In some cases, bifunctional linkers are not needed for conjugation. The most often seen example is a disulfide-linked conjugate. If both cargo molecule and CPP have thiol groups, they may link directly without any tethers. However, there is a risk of having a mixture of homodimer of cargo molecules or CPPs. To prevent this, one of the thiol group can be derivatized with 2,2′-dithiobis(5-nitropyridine) to have a 2-thio-5-nitropyridyl protected/activated thiol group.[29,38] Thereafter, the reaction is the same as described in the Example 15.2. If the CPP has no reactive amino group in its sequence, the carboxyl end can be activated by carbodiimides and then react with the amino group on the cargo molecule. For example, the recently reported polyarginine and polyguanidine peptoids[39-41] would be ideal compounds for this type of coupling. Other approaches, such as peptide fragment condensation and protein expression, are described in various chapters of this book.

15.3 TAT PEPTIDE DELIVERS MAGNETIC COMPOUNDS INTO MAMMALIAN CELLS

15.3.1 Cellular Internalization of Superparamagnetic Nanoparticles

We originally developed different nanometer sized iron oxide particles[42] for cell labeling by phagocytosis,[43] receptor-mediated endocytosis,[44,45] and fluid phase endocytosis.[46] Although the latter mechanism can be used to label lymphocytes,[46] the amount of internalized marker is low, necessitating administration of large amounts of cells for their *in vivo* detection.[47] We therefore concluded that alternative ways of cell labeling should be developed in order to track smaller numbers of cells *in vivo*.

Residues 48–57 of HIV Tat protein, Gly-Arg-Lys-Lys-Arg-Arg-Gln-Arg-Arg-Arg, were designed to shuttle magnetic nanoparticles into cells.[34,35] We subsequently showed that this powerful new technique allows (1) tracking of relatively few cells *in vivo* (<10 cells per voxel), (2) magnetic recovery and isolation of *in vivo* homed lymphocytes, and (3) study of transgenic or progenitor cells that are usually only available in small amounts. The preparation of CLIO–Tat was described in the Example 15.2. The utilized CLIO particles consisted of a small monocrystalline, superparamagnetic iron oxide core (5 nm) stabilized by a cross-linked aminated dextran coating to improve stability, resulting in an overall size of approximately 45 nm. To each particle, an average of 4–7 Tat peptide chains were attached.[35]

15.3.1.1 CLIO–Tat Is Internalized into Different Subsets of Lymphocytes and CD34+ Cells

The uptake of the CLIO–Tat and CLIO was compared in human hematopoietic CD34+ cells, mouse neural progenitor cells (C17.2), human CD4+ lymphocytes, and mouse splenocytes (Figure 15.5). Using radiolabeled CLIO–Tat particles, the labeling efficiencies were similar for the different cells, ranging from 10 to 30 pg of superparamagnetic iron/cell equivalent to 0.5 to 2×10^7 nanoparticles/cell.[34] The uptake of CLIO–Tat and CLIO was significantly different in every tested cell line.

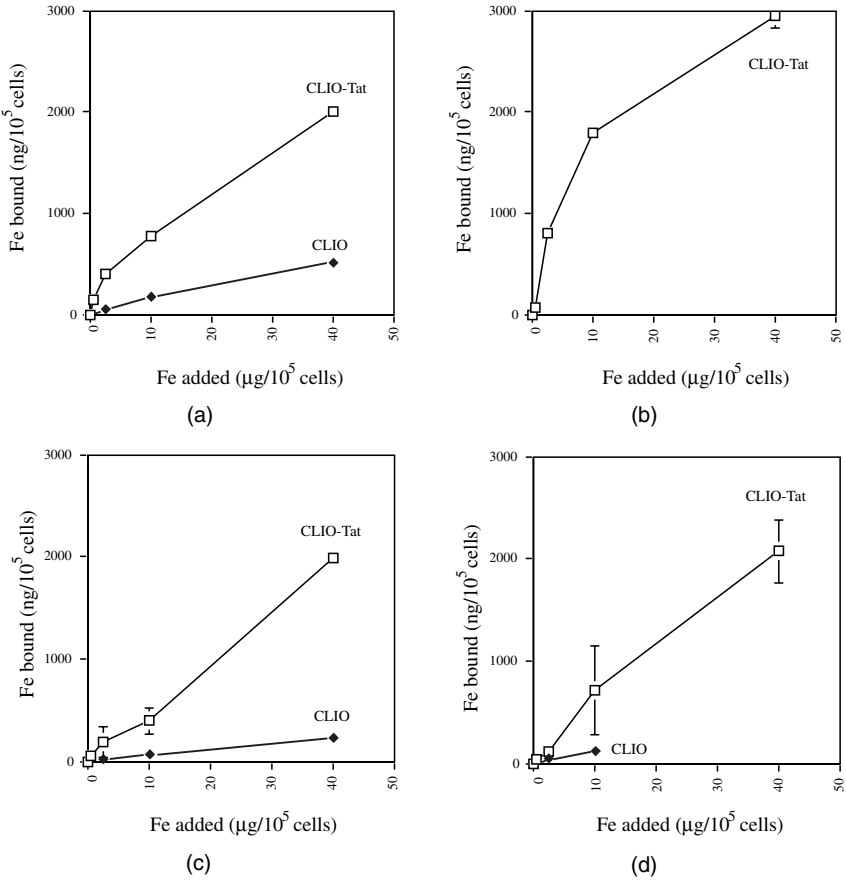

FIGURE 15.5 Quantitative uptake of CLIO–Tat into different cell types. Different cell types were incubated with increasing concentration of ^{111}In-CLIO–Tat or ^{111}In-CLIO for 1 h at 37°C. Mean ± SD of uptake is plotted for: (a) CD34+ cells, (b) mouse neural progenitor cells (C17.2), (c) human CD4+ lymphocytes, and (d) mouse splenocytes. (From Lewin, M. et al., *Nat. Biotechnol.,* 18, 410, 2000. With permission.)

Without the assistance of Tat peptide, the CLIO particle cannot pass through cell membrane efficiently.

15.3.1.2 Label Distribution in Dividing Cell Populations

The next two questions we addressed were (1) what is the intracellular magnetic half-life of CLIO–Tat in cells and (2) what is the fate of cellular CLIO–Tat in actively dividing cells? To answer the first question we performed time dependence studies using MR imaging of labeled lymphocytes. Results from these studies showed that the transverse relaxation time (T2, T2*) of magnetically labeled lymphocytes returned to normal approximately 7 to 14 days (depending on amount internalized) after labeling, indicating that the magnetic core of CLIO–Tat is biodegraded.

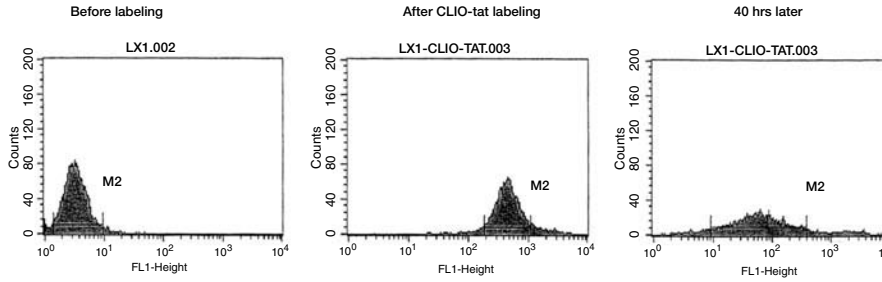

FIGURE 15.6 CLIO–Tat (containing an FITC label) appears to be distributed in roughly equal amounts to daughter cells after cell division.

To answer the second question we labeled actively dividing human LX1 tumor cells (doubling time of 20 h) with CLIO–Tat and performed FACS analysis before labeling, immediately after labeling, and 40 h (2 division cycles) after labeling (Figure 15.6). Data from these studies support the hypothesis that CLIO–Tat is equally distributed to progeny cells, similar to the case for many cellular fluorescent stains.

15.3.1.3 CLIO–Tat Is not Toxic to Cells at Concentrations Used for Magnetic Labeling

In order to determine the dose at which Tat labeled particles become toxic to cells, a trypan blue exclusion assay was initially performed. For these studies, mouse lymphocytes were incubated with Tat-labeled particles ranging from 7 to 700 nmol peptide per 10^6 cells for 3 h followed by trypan blue staining. Tat-labeled particles were nontoxic to cells at incubation concentrations <150 nmol peptide/10^6 cells, corresponding to approximately 4×10^6 internalized particles per cell. We also performed ^{51}Cr release assays. Our data show that for the different target-to-effect ratios and the different doses of CLIO–Tat there was little difference in the function of NK cells to lyse the target cells.

15.3.1.4 CLIO–Tat Labeling Allows Magnetic Sorting of Lymphocytes Labeled *In Vitro*

The following experiments were performed to determine feasibility of magnetically sorting CLIO–Tat-labeled lymphocytes. Mouse splenic lymphocytes were labeled CLIO–Tat (10 to 20 μg Fe/10^6 cells) for 1 h at 37°C. Cells were then washed and mixed with unlabeled lymphocytes (50/50%). The cell mixture was then subjected to a single magnetic sorting procedure using a commercially available separator (Milteny Biotec). The cells were passed through a column containing polyethylene-coated iron particles (0.5 mm diameter) and analyzed using FACS analysis (Figure 15.7). Fluorescence emission was sampled through a 560-nm dichroic long-pass filter and passed through a 530/30 nm bandpass filter.

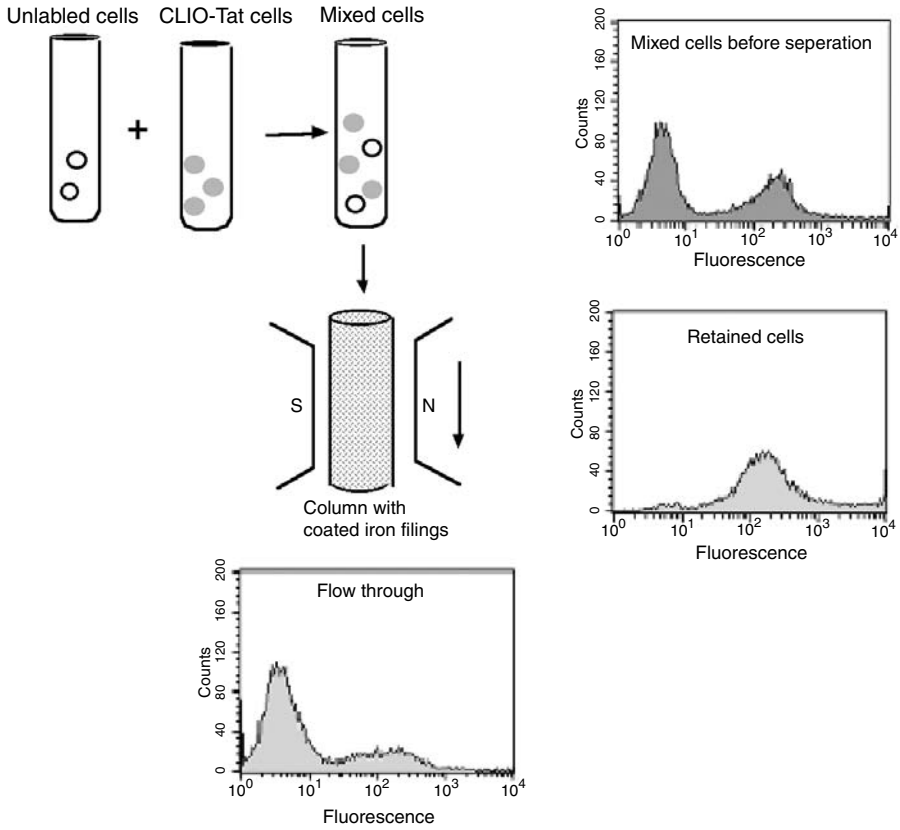

FIGURE 15.7 Left: experimental set up. The FACS graphs from the three different cell populations are shown on the right and bottom. Top right: mixed cells before separation; bottom right: labeled cells after separation; bottom left: supernatant after separation. Separated cells were 96% pure.

Our data show that CLIO–Tat-labeled lymphocytes were 96.8% pure after the first separation cycle (approximately 1 min). The parent cell solution (supernatant) was depleted from labeled lymphocytes from 43.4 to 17.5% during the first pass. The mean fluorescence of CLIO–Tat-labeled cells was similar before and after separation (221.8 ± 7.7 vs. 206.1 ± 8.6 AU respectively). Lymphocytes labeled with non-labeled CLIO by fluid phase pinocytosis (20 ng Fe/million cells), could *not* be extracted with the separator, presumably because the internalized amount was too low. Virtually identical results were obtained when CD34+ cells were labeled with CLIO–Tat; using a 50/50% mixture of CLIO–Tat to unlabeled CD34+, a single magnetic separation yielded 98.95% pure CLIO–Tat-labeled CD34+ cells.

15.3.1.5 Recovery of *In Vivo* Injected Cells

We subsequently hypothesized that CLIO–Tat-labeled cells could be recovered after i.v. injection and *in vivo* homing. We therefore labeled mouse lymphocytes with

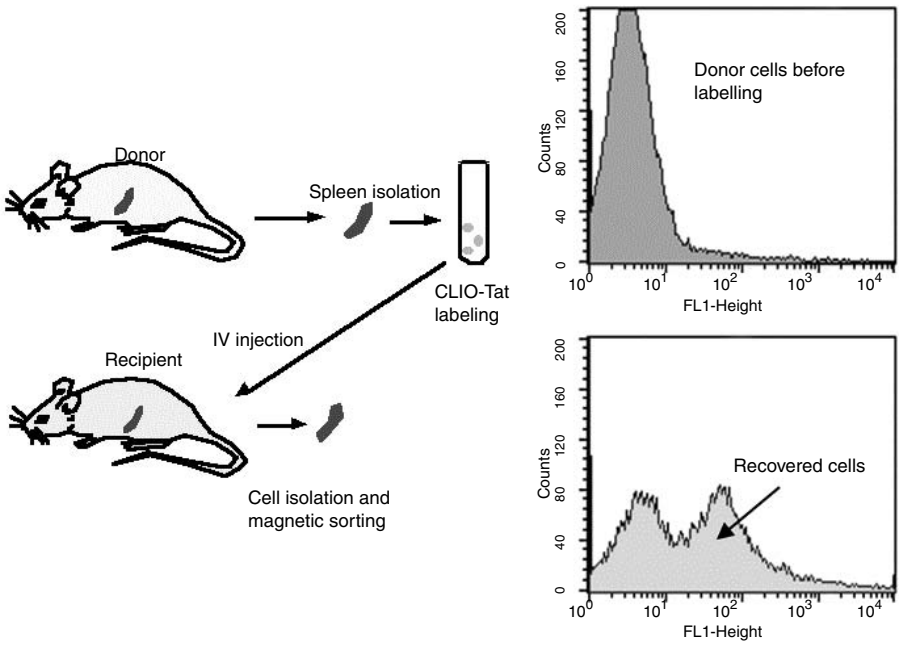

FIGURE 15.8 Cell recovery of CLIO–Tat-labeled cells. The FACS analysis of unseparated recipient splenocytes is shown on the right (top). *In vivo* recovered and magnetically separated cells are shown at the bottom right. The arrow points to the fluorescent CLIO–Tat cell population recovered from the spleen during the first round of magnetic separation.

CLIO–Tat as described above and injected them into recipient mice (Figure 15.8). Approximately 2×10^7 purified cells were injected into a recipient mouse through the tail vein and no adverse effects were observed. The recipient mouse was sacrificed after 24 h and the spleen excised. Splenic lymphocytes were isolated as described above and the obtained cell suspension subjected to FACS analysis before and after magnetic separation. Our data show that 44.9% of the lymphocytes adhering to the magnetic separator were fluorescently labeled and thus contained CLIO–Tat. Higher yields (>90% of cells) were observed after repeated runs through the magnetic separator. These results clearly attest to the feasibility of recovering i.v. injected CLIO–Tat-labeled cells.

15.3.1.6 High Resolution *In Vivo* MR Imaging of CLIO–Tat Labeled Cells

We then determined whether CLIO–Tat-labeled lymphocytes would be detectable in tumor environments. In earlier research we had quantitated the tumoral recruitment of different lymphocyte populations using isotope labeling techniques.[48] Briefly, a total of 3×10^7 labeled cells were administered i.v. into a nude mouse bearing a 9L glioblastoma implanted intracerebrally. At 0.3% of cells accumulating per g tumor (tumor weight 80 mg), one can expect approximately 7.5×10^3 cells within the tumor or 1.5×10^3 cells per image slice (Figure 15.9). MR imaging at high spatial resolution

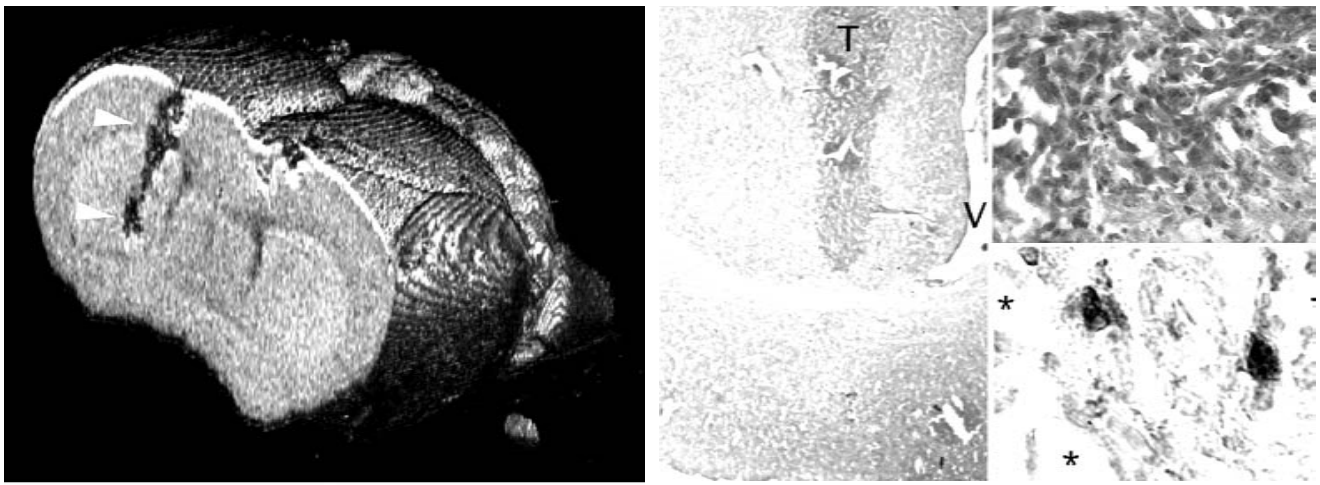

FIGURE 15.9 (Color Figure 15.9 follows p. 14.) Left: μNMR image of a mouse brain (isotropic voxel size of 39 μm; TR 150 msec, TE 3.6 msec, FA 34°) with an implanted 9L tumor growing in elliptical shape (arrowheads). Note that i.v.-injected labeled lymphocytes have accumulated in the tumor and significantly reduce the signal intensity (tumor without cells would have similar signal as normal brain with this NMR sequence). Approximately 1500 labeled cells are present within the section shown. Right: HE stains of the most inferior aspect of the tumor extending into the brain (T = tumor; V = ventricle; 7 μm section). Top right: higher magnification HE stain in tumor. Bottom right: high magnification Fe stain. CLIO–Tat-labeled lymphocytes appear dark and are seen in and adjacent to vessels marked with an asterisk.

(TR 150 msec, TE 3.6 msec, FA 34°, voxel size: $39 \times 39 \times 78$ μm) clearly showed that the labeled cells are detectable in the tumor bed and that very low cell numbers for the first time can be visualized by MR imaging.

15.3.2 Internalization of Paramagnetic Chelates

The above described cellular internalization of nanoparticles is a viable option for labeling cells for MR imaging, particularly when T2 weighted sequences are obtained. An alternative strategy, however, is to internalize small paramagnetic molecules into cells that can chelate lanthanides serving as paraqmagnetic or fluorescent reporters. We hypothesized that it should be feasible to internalize macrocyclic lanthanide chelators into cells using the same HIV–Tat-derived peptide sequence used for the CLIO–Tat attachment (Figure 15.10). In order to deliver various lanthanide elements into cells, we have attached 1,4,7,10-tetraazacyclododecane-N,N',N'',N'''-tetraacetic acid (DOTA) to the Tat peptide as described in Example 15.1 (Figure 15.10–top).[33] The Tat–DOTA was then subsequently labeled with gadolinium (Gd), dysprosium (Dy), or Indium-111 (^{111}In).

Fresh lymphocytes (1×10^6 cells) obtained from mouse spleen were incubated with various amounts of Tat–DOTA–^{111}In (25, 50, 100, 150, or 200 nmol) in 1 ml of RPMI 1620 medium at 37°C for 60 min. After incubation, cells were washed three times with Hanks buffered saline solution and then resuspended in RPMI 1620 medium. In parallel, DOTA–In^{111} without Tat peptide was used as a control. As shown in Figure 15.10–center, uptake increased with increasing amounts of Tat–DOTA conjugate without reaching saturation at 200 mol of peptide per million cells. On the contrary, uptake of DOTA–In^{111} was negligible at all concentrations.

To determine whether quantitative differences in cellular uptake between labeled and unlabeled lymphocytes would translate into differences by MR signal intensity, we labeled mouse lymphocytes by incubation with 150 μg Gd per 10^6 cells. MR imaging phantoms were prepared by placing 20 μL cell pellets into agarose and then sealing them with additional agarose to avoid air-induced susceptibility artifacts. The phantoms were then subjected to MR imaging at 1.5 T (Signa 5.5; GE Medical Systems, Milwaukee, WI) using a 5-in. surface coil. The imaging protocol consisted of a coronal T1 weighted spin echo (SE) sequence with a TR/TE of 300/11, and a slice thickness of 3 mm. The imaging results (Figure 15.10–bottom) showed that cells can be labeled paramagnetically and that the labeled cells appear hyperintense. These T1 markers would potentially be beneficial to improve signal-to-noise ratios for tracking cells using T1 weighted MR imaging techniques. Conversely, if the Tat–DOTA was labeled with Dy, the signal of Tat–DOTA–Dy-labeled cells was lower because of the predominant T2/T2* effect of the latter, which may be desirable for certain imaging studies.

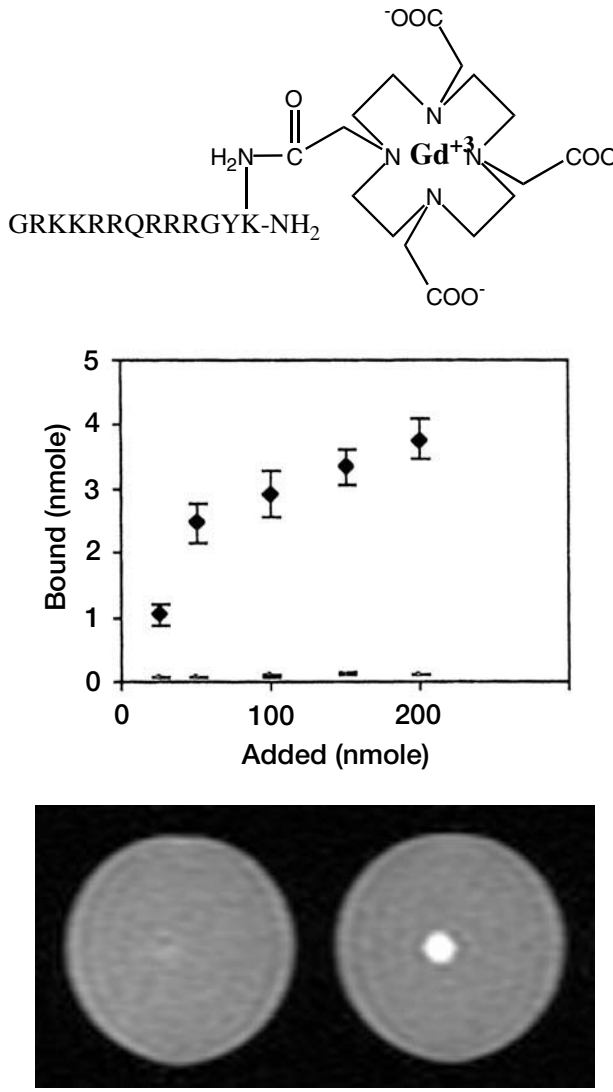

FIGURE 15.10 Top: Chemical structure of Tat-DOTA-Gd. The center ion can be replaced with Dy or In. Center: Uptake of Tat-DOTA-^{111}In and DOTA-^{111}In into mouse lymphocytes. Bottom: MR image of unlabeled (left) and Gd-Tat labeled cells (right) embedded in agar (T1 weighted spin-echo (TR/TE) 300/11). The labeled lymphocytes appear markedly hyperintense and are readily detectable. (From Bhorade, R. et al., *Bioconjug. Chem.,* 11, 301, 2000. With permission.)

REFERENCES

1. Dubowchik, G.M. and Walker, M.A., Receptor-mediated and enzyme-dependent targeting of cytotoxic anticancer drugs, *Pharmacol. Ther.*, 83, 67, 1999.
2. Reddy, J.A. and Low, P.S., Folate-mediated targeting of therapeutic and imaging agents to cancers, *Crit. Rev. Ther. Drug Carrier Syst.*, 15, 587, 1998.
3. Marecos, E. et al., Antibody-mediated vs. nontargeted delivery in a human small cell lung carcinoma model, *Bioconjug. Chem.*, 9, 184, 1998.
4. Rojas, M. et al., Genetic engineering of proteins with cell membrane permeability, *Nat. Biotechnol.*, 16, 370, 1998.
5. Prochiantz, A., Messenger proteins: homeoproteins, Tat and others, *Curr. Opin. Cell Biol.*, 12, 400, 2000.
6. Lindgren, M. et al., Cell-penetrating peptides, *Trends Pharmacol. Sci.*, 21, 99, 2000.
7. Fawell, S. et al., Tat-mediated delivery of heterologous proteins into cells, *Proc. Natl. Acad. Sci. U.S.A.,* 91, 664, 1994.
8. Vivés, E. et al., A truncated HIV-1 Tat protein basic domain rapidly translocates through the plasma membrane and accumulates in the cell nucleus, *J. Biol. Chem.*, 272, 16010, 1997.
9. Derossi, D. et al., Cell internalization of the third helix of the Antennapedia homeodomain is receptor-independent, *J. Biol. Chem.*, 271, 18188, 1996.
10. Pooga, M. et al., Cell penetration by transportan, *FASEB. J.*, 12, 67, 1998.
11. Soomets, U. et al., Deletion analogues of transportan, *Biochim. Biophys. Acta*, 1467, 165, 2000.
12. Avrameas, A. et al., Polyreactive anti-DNA monoclonal antibodies and a derived peptide as vectors for the intracytoplasmic and intranuclear translocation of macromolecules, *Proc. Natl. Acad. Sci. U.S.A.,* 95, 5601, 1998.
13. Phelan, A. et al., Intercellular delivery of functional p53 by the herpesvirus protein VP22, *Nat. Biotechnol.*, 16, 440, 1998.
14. Elliott, G. and O'Hare, P., Intercellular trafficking and protein delivery by a herpesvirus structural protein, *Cell*, 88, 223, 1997.
15. Sheldon, K. et al., Loligomers: design of *de novo* peptide-based intracellular vehicles, *Proc. Natl. Acad. Sci. U.S.A.,* 92, 2056, 1995.
16. Zhang, L. et al., Preparation of functionally active cell-permeable peptides by single-step ligation of two peptide modules, *Proc. Natl. Acad. Sci. U.S.A.,* 95, 9184, 1998.
17. Efthymiadis, A. et al., The HIV-1 Tat nuclear localization sequence confers novel nuclear import properties, *J. Biol. Chem.*, 273, 1623, 1998.
18. Pepinsky, R.B. et al., Specific inhibition of a human papillomavirus E2 trans-activator by intracellular delivery of its repressor, *DNA Cell Biol.*, 13, 1011, 1994.
19. Anderson, D.C. et al., Tumor cell retention of antibody Fab fragments is enhanced by an attached HIV TAT protein-derived peptide, *Biochem. Biophys. Res. Commun.*, 194, 876, 1993.
20. Bayley, H., Protein therapy-delivery guaranteed, *Nat. Biotechnol.*, 17, 1066, 1999.
21. Nagahara, H. et al., Transduction of full-length TAT fusion proteins into mammalian cells: TAT-p27Kip1 induces cell migration, *Nat. Med.*, 4, 1449, 1998.
22. Vocero–Akbani, A.M. et al., Killing HIV-infected cells by transduction with an HIV protease- activated caspase-3 protein, *Nat. Med.*, 5, 29, 1999.
23. Pooga, M. et al., Cellular translocation of proteins by transportan, *FASEB. J.*, 15, 1451, 2001.
24. Lin, Y.Z. et al., Inhibition of nuclear translocation of transcription factor NF-kappa B by a synthetic peptide containing a cell membrane-permeable motif and nuclear localization sequence, *J. Biol. Chem.*, 270, 14255, 1995.

25. Schluesener, H.J., Protection against experimental nervous system autoimmune diseases by a human immunodeficiency virus-1 Tat peptide-based polyvalent vaccine, *J. Neurosci. Res.*, 46, 258, 1996.
26. Morris, M.C. et al., A new peptide vector for efficient delivery of oligonucleotides into mammalian cells, *Nucleic. Acids Res.*, 25, 2730, 1997.
27. Antopolsky, M. et al., Peptide-oligonucleotide phosphorothioate conjugates with membrane translocation and nuclear localization properties, *Bioconjug. Chem.*, 10, 598, 1999.
28. Astriab–Fisher, A. et al., Antisense inhibition of P-glycoprotein expression using peptide-oligonucleotide conjugates, *Biochem. Pharmacol.*, 60, 83, 2000.
29. Pooga, M. et al., Cell penetrating PNA constructs regulate galanin receptor levels and modify pain transmission *in vivo*, *Nat. Biotechnol.*, 16, 857, 1998.
30. Elliott, G. and O'Hare, P., Intercellular trafficking of VP22-GFP fusion proteins, *Gene Ther.*, 6, 149, 1999.
31. Zhang, F. et al., A transfecting peptide derived from adenovirus fiber protein, *Gene Ther.*, 6, 171, 1999.
32. Singh, D. et al., Peptide-based intracellular shuttle able to facilitate gene transfer in mammalian cells, *Bioconjug. Chem.*, 10, 745, 1999.
33. Bhorade, R. et al., Macrocyclic chelators with paramagnetic cations are internalized into mammalian cells via a HIV-Tat derived membrane translocation peptide, *Bioconjug. Chem.*, 11, 301, 2000.
34. Lewin, M. et al., Tat peptide-derivatized magnetic nanoparticles allow *in vivo* tracking and recovery of progenitor cells, *Nat. Biotechnol.*, 18, 410, 2000.
35. Josephson, L. et al., High-efficiency intracellular magnetic labeling with novel superparamagnetic-Tat peptide conjugates, *Bioconjug. Chem.*, 10, 186, 1999.
36. Polyakov, V. et al., Novel Tat-peptide chelates for direct transduction of technetium-99m and rhenium into human cells for imaging and radiotherapy, *Bioconjug. Chem.*, 11, 762, 2000.
37. Ishii, Y. and Lehrer, S.S., Effects of the state of the succinimido-ring on the fluorescence and structural properties of pyrene maleimide-labeled alpha alpha-tropomyosin, *Biophys. J.*, 50, 75, 1986.
38. Theodore, L. et al., Intraneuronal delivery of protein kinase C pseudosubstrate leads to growth cone collapse, *J. Neurosci.*, 15, 7158, 1995.
39. Wender, P.A. et al., The design, synthesis, and evaluation of molecules that enable or enhance cellular uptake: peptoid molecular transporters, *Proc. Natl. Acad. Sci. U.S.A.,* 97, 13003, 2000.
40. Mitchell, D.J. et al., Polyarginine enters cells more efficiently than other polycationic homopolymers, *J. Pept. Res.*, 56, 318, 2000.
41. Futaki, S. et al., Arginine-rich peptides. An abundant source of membrane-permeable peptides having potential as carriers for intracellular protein delivery, *J. Biol. Chem.*, 276, 5836, 2001.
42. Shen, T. et al., Monocrystalline iron oxide nanocompounds (MION): physiocochemical propreties, *Magn. Reson. Med.*, 29, 599, 1993.
43. Schulze, E. et al., Cellular uptake and trafficking of a prototypical magnetic iron oxide label *in vitro*, *Invest. Radiol.*, 30, 604, 1995.
44. Shen, T.T. et al., Magnetically labeled secretin retains receptor affinity to pancreas acinar cells, *Bioconjug. Chem.*, 7, 311, 1996.
45. Moore, A. et al., Measuring transferrin receptor gene expression by NMR imaging, *Biochim. Biophys. Acta*, 1402, 239, 1998.
46. Schoepf, U. et al., Intracellular magnetic labeling of lymphocytes for *in vivo* trafficking studies, *BioTechniques*, 24, 642, 1998.

47. Weissleder, R. et al., Magnetically labeled cells can be detected by MR imaging, *J. Magn. Reson. Imaging*, 7, 258, 1997.
48. Schoept, U. et al., Intracellular magnetic labeling of lymphocytes for *in vivo* trafficking studies, *Biotechniques,* 24, 642, 1998.
49. Gius, D.R. et al., Transduced p16INK4a peptides inhibit hypophosphorylation of the retinoblastoma protein and cell cycle progression prior to activation of Cdk2 complexes in late G1, *Cancer Res.*, 59, 2577, 1999.
50. Schwarze, S.R. et al., *In vivo* protein transduction: delivery of a biologically active protein into the mouse, *Science*, 285, 1569, 1999.
51. Vocero–Akbani, A. et al., Transduction of full-length Tat fusion proteins directly into mammalian cells: analysis of T cell receptor activation-induced cell death, *Methods Enzymol.*, 322, 508, 2000.
52. Xia, H. et al., The HIV Tat protein transduction domain improves the biodistribution of beta-glucuronidase expressed from recombinant viral vectors, *Nat. Biotechnol.*, 19, 640, 2001.
53. Eguchi, A. et al., Protein transduction domain of HIV-1 Tat protein promotes efficient delivery of DNA into mammalian cells, *J. Biol. Chem.*, 276, 26204, 2001.
54. Vivés, E. et al., Structure-activity relationship study of the plasma membrane translocating protential of a short peptide from HIV-1 Tat protein, *Lett. Peptide Sci.*, 4, 429, 1997.
55. Torchilin, V.P. et al., TAT peptide on the surface of liposomes affords their efficient intracellular delivery even at low temperature and in the presence of metabolic inhibitors, *Proc. Natl. Acad. Sci. U.S.A.,* 98, 8786, 2001.
56. Lindgren, M. et al., Translocation properties of novel cell penetrating transportan and penetratin analogues, *Bioconjug. Chem.*, 11, 619, 2000.
57. Fenton, M. et al., The efficient and rapid import of a peptide into primary B and T lymphocytes and a lymphoblastoid cell line, *J. Immunol. Methods*, 212, 41, 1998.
58. Han, K. et al., Efficient intracellular delivery of GFP by homeodomains of *Drosophila* Fushi-tarazu and Engrailed proteins, *Mol. Cells*, 10, 728, 2000.
59. Troy, C.M. et al., Downregulation of Cu/Zn superoxide dismutase leads to cell death via the nitric oxide-peroxynitrite pathway, *J. Neurosci.*, 16, 253, 1996.
60. Allinquant, B. et al., Downregulation of amyloid precursor protein inhibits neurite outgrowth *in vitro*, *J. Cell Biol.*, 128, 919, 1995.
61. Bisland, S.K. et al., Potentiation of chlorin e6 photodynamic activity *in vitro* with peptide-based intracellular vehicles, *Bioconjug. Chem.*, 10, 982, 1999.
62. Rojas, M. et al., Controlling epidermal growth factor (EGF)-stimulated Ras activation in intact cells by a cell-permeable peptide mimicking phosphorylated EGF receptor, *J. Biol. Chem.*, 271, 27456, 1996.
63. Rothbard, J.B. et al., Conjugation of arginine oligomers to cyclosporin A facilitates topical delivery and inhibition of inflammation, *Nat. Med.*, 6, 1253, 2000.

16 Cell-Penetrating Peptides as Vectors for Delivery of Nucleic Acids

Andres Valkna, Ursel Soomets, and Ülo Langel

CONTENTS

16.1 INTRODUCTION

Gene expression underlies important biological processes, including development, immune defense, and tumorigenesis. Many pathological processes are known to result from mutations that alter the way that genes are switched on and off. A current goal in molecular medicine is the development of new strategies to interfere with gene expression in living cells in the hope that novel therapies for human disease will result from these efforts.

During recent years, oligonucleotides (ONs) and their stable analogs have received remarkable attention as a rational way to design sequence-specific ligands of nucleic acids. Antisense and ribozyme strategies are based on the formation of Watson–Crick bonds between ribozyme or oligodeoxynucleotide (ODN) and complementary RNA sequence.[1] An ODN can be used as a "decoy" to trap DNA-binding

0-8493-1141-1/02/$0.00+$1.50

proteins, thus preventing them from associating to their normal target. Oligonucleotides can also recognize double-helical DNA at specific sequences by forming Hoogsteen or reverse-Hoogsteen hydrogen bonds with purine bases on one of the duplex strands; this forms a local triple helix, a strategy known as "antigene" approach.

Transfection of *cis*-element ODNs (decoy ODNs) has been recently accepted as a powerful tool that could be useful in a new class of antigene strategies for gene therapy and in the study of transcriptional regulation. These ODN decoys will disturb the authentic *cis–trans* interaction leading to the removal of *trans*-factors from endogenous *cis*-elements with subsequent modulation of gene expression. Morishita et al. first demonstrated the use of decoy ODNs for the therapeutic manipulation of gene expression in 1995.[2] They demonstrated treatment of rat arteries with ODNs bearing the consensus of binding site for the E2F family of transcription factors. Recently several groups have reported on decoy ODN as an *in vivo* gene therapy reagent further highlighting therapeutic potential of these oligonucleotides.[3-7]

Targeting oligonucleotides to the DNA or DNA-binding molecule (the antigene or decoy) has advantages compared to targeting antisense ODNs:

1. There are only two alleles of the targeted gene, whereas there may be thousands of copies of an mRNA. Blocking mRNA translation by inducing sequence-targeted cleavage of the RNA chain does not stop the respective gene from transcription.
2. Gene transcription regulation is thought to bring the mRNA concentration down more efficiently and the effect is believed to last longer.

However, the therapeutic potential of ONs will not be fulfilled until their uptake by cells has been considerably improved. Recently, CPPs have been applied to improve the ON uptake.

16.2 TRANSPORT OF NAKED OLIGONUCLEOTIDES

Cellular delivery of naked ONs has been thought to be too slow for use in therapeutic applications. ONs are known to be transported through the lipid bilayer where the major mechanism behind an uptake of negatively charged ONs is receptor-mediated endocytosis.[8,9] Unfortunately, this process is energy-dependent and saturable. Adsorptive endocytosis and pinocytosis also contribute to ON uptake in a process involving a membrane protein. It has been demonstrated that a 30-kDa DNA-binding membrane protein[10,11] enhances the uptake of DNA molecules longer than 7 kb; this effect could be inhibited by other negatively charged molecules.[12]

Finally, reports exist that demonstrate different mechanisms for ON uptake not related to receptors. Some of these show internalization of ONs by the protein-independent mechanism of endocytosis or internalization by a caveolar, potocytotic mechanism rather than by receptor-mediated uptake.[13] Others have demonstrated the involvement of different transporter proteins[14-16] or pore-forming proteins.[17,18] Such contradiction in published results could be a consequence of cell-specific involvement of different ON transport pathways or different experimental conditions.

After internalization, naked ONs are localized in the lysosomal compartment and either degraded or released by exocytosis. The phosphodiester and phosphorothioate oligonucleotides have been shown to be localized in nucleus,[19,20] while methylphosphonates are found only in endosomes and lysosomes.[21] The addition of phosphodiester moieties to methylphosphonates alters the distribution of ONs from endosomes to nuclear and cytoplasmic compartments.[22]

16.3 DELIVERY STRATEGIES

Present gene therapy is accomplished using various vectors (carriers) to transfer the specific gene of interest into the cell. Here we briefly summarize traditional methods of nucleic acid delivery.

Vectors can be divided into two groups: viral or nonviral. Although viruses are the most efficient carriers available at present, they have certain disadvantages. These include attack by the immune system of the host resulting in damage to the introduced gene, limited size of the gene that can be delivered, targeting of certain cells only (e.g., dividing cells in case of retroviral vectors), integration with potential oncogenesis, and other unexpected responses of the viral gene *in vitro* and *in vivo* (for review see References 23 and 24).

Nonviral strategies involve inclusion of ONs into liposomes and cationic lipids (lipofectin, cytofectin, etc.), or attaching ONs covalently or electrostatically to specific or nonspecific carriers. Application of liposomes, often composed of cationic closed phospholipid bilayer membranes, is the most widely used method to aid ON uptake because they form stable electrostatic interactions with negatively charged ONs. The mechanism of liposome uptake is endocytosis followed by eventual fusion with lysosomes (for review, see References 25 and 26).

Several reports confirm the potential of lipofilization of nucleic acids e.g., with alkyl moieties,[27] cholesterol,[28,29] cholic acids,[30,31] or phospholipids to improve uptake. It has been proposed that cholesterol-conjugated ONs may be especially valuable in cancer treatment, since specific receptor-mediated uptake of LDL by tumor cells is elevated.

Several invasive strategies for ON uptake have been described. Microinjection technique allows delivery of nucleic acids without limitations in size. The disadvantage is that it is a monocellular technique that cannot be used *in vivo* (for review, see Kalkbrenner et al.[32]). Electroporation is another widely used invasive technique that uses electric field to form pores in cellular membrane (for review, see Swartz et al.[33]). As this is a physical process based on diffusion, it can be applied to any cell type to transport nucleic acids and analogs without length restrictions. The disadvantage here is that the cells must be in solution, thus preventing use of this technique *in vivo*; also, the rate of cell death is high.

Receptor-mediated endocytosis of biologically active peptides and proteins conjugated to ONs have the same drawback as liposome delivery: transported molecule appears in lysosomal vehicle. Increase in antisense effect was observed when ONs were conjugated with asialoglycoprotein,[34,35] epidermal growth factor,[8] and mannose receptor.[36]

16.4 PEPTIDE VECTORS FOR OLIGONUCLEOTIDE DELIVERY

In accordance with the definition, cell membrane penetration of CPPs takes place at 4°C and under conditions that prevent normal endocytosis.[37] Cellular penetration is not receptor-mediated; thus it is cell type-unspecific. This virtue allows using these delivery vehicles as universal transporters of conjugated hydrophilic macromolecules, including nucleic acids. Recent reports suggest that CPPs are able to transport these macromolecules across the blood–brain barrier,[38] enabling use of these delivery vectors in gene therapy applications. Here we summarize recent applications of CPPs in ON delivery (cf. Figure 16.1). In addition, peptides that do not strictly fulfill the definition of CPPs but have been used in nucleic acid delivery are briefly described (Sections 16.4.6 and 16.4.7).

16.4.1 Penetratin

The use of penetration in transmembrane delivery of nucleic acids was first demonstrated by Allinquant et al. in 1995.[39] Their study demonstrated that amyloid precursor protein (APP) antisense ODN was capable of transiently inhibiting neurite outgrowth and decreasing APP levels in embryonic cortical neurons *in vitro*. Oligonucleotide internalization was achieved by linking ODN to a polypeptide derived from *Drosophila melanogaster* Antennapedia gene homeobox. The encoded protein is a 60 amino acid-long highly conserved sequence responsible for membrane translocation. The whole Antennapedia homeodomain is not necessary for translocation through membrane; earlier site-directed mutagenesis studies demonstrated that the third helix of Antennapedia (amino acids 43–58) is the shortest fragment of the homeodomain capable of membrane penetration.[40]

Troy et al. demonstrated down-regulation of Cu^{2+}/Zn^{2+} superoxide dismutase (SOD1) activity and following apoptotic death in PC12 cells using penetratin-modified antisense ON (Table 16.1). This showed efficient cellular uptake in the presence of serum and also 100-fold increased effect compared to that with naked ONs.[41]

Simmons et al.[42] demonstrated that peptides derived from the third helix of the homeodomain of Antennapedia mediate the uptake of a novel type of DNA analog with backbone modification, a peptide nucleic acid (PNA; for review, see Reference 43) to human prostate tumor-derived cells DU145 (Table 16.1). These results were obtained by using fluorescence microscopy and FACS analysis; the latter showed that about 99% of DU145 cells were transfected by fluorescein- or rhodamine-labeled PNA oligomers at concentrations as low as 500 n*M* — efficiency rarely observed by other transfection techniques. Naked PNA did not internalize at that concentration. The authors did not observe any toxicity at conjugate concentrations up to 500 n*M* and showed that PNA–peptide conjugates *in vitro*, as well as unmodified PNAs, inhibit human telomerase, thus demonstrating that the peptide moiety does not interfere with hybridization.

Pooga et al. (Table 16.1) further proved the potential of this delivery vector in transmembrane delivery of PNA.[44] A 21-mer antisense PNA complementary to the human neuropeptide galanin receptor type 1 mRNA was used after coupling to the

penetratin by disulphide bridge. This construct blocked the expression of galanin receptors in Bowes cells. The intrathecal administration of the peptide–PNA construct resulted in a decrease in galanin binding in the dorsal horn and inability of galanin to inhibit the C fibers stimulation-induced facilitation of flexor reflex in rat.

Oligonucleotides are efficiently taken up by *retro-inverso* penetratin as demonstrated by Aldrian–Herrada (Table 16.1).[45] PNA antisense sequence for the AUG translation initiation region of prepro-oxytocin mRNA was covalently coupled to *retro-inverso* penetratin. This conjugate was internalized by cultured cerebral cortex neurons within minutes, while the uptake of naked PNA was slow. The internalization and functional activity also occurred after maintaining cells at 4°C for 5 min and then incubating them at the same temperature for 10 min with the penetratin–PNA; PNA alone was internalized too slowly to be studied by this method without causing cell damage. The result is consistent with the hypothesis of direct penetration across the cell membrane. They also showed that PNA and vector peptide–PNA decreased the prepro-oxitocin mRNA level in a dose- and time-dependent manner in cultured magnocellular neurons from the hypothalamic supraoptic nucleus as shown by RT- PCR.

Penetratin has been used to deliver other modified oligonucleotide analogs, most commonly, phosphorothioates used in antisense experiments. Astriab–Fisher et al.[46] demonstrated by fluorescence microscopy that application of penetratin and penetratin–ON conjugate resulted in accumulation in the cell nucleus. Cells treated with naked ON showed no intracellular localization. They also attained significant inhibition of P-glycoprotein, a multidrug-resistance gene1 (MDR1) expression product, with submicromolar amounts of phosphorothioate oligonucleotide in NIH 3T3 cells. The presence of 10% serum enhanced the antisense effects, a surprising finding anomalous to other similar studies. Unfortunately, this study does not describe the degree of CPP–ON conjugates needed to affect drug resistance and is restricted to estimating the potential of these constructs *in vivo*. This study uses, in parallel, another type of CPP, a Tat protein-derived peptide.

Villa et al.[47] have used penetratin to target PNA and phosphorothioate ODNs to human melanoma cell line JR8 (Table 16.1). Biotinylated PNA was utilized to detect internalization, which occurred only when penetratin was coupled to PNA, whereas naked oligomers did not enter the cells. Moreover, these constructs were able to inhibit telomerase activity in these cells, suggesting such constructs have high potential in cancer treatment.

Very recently, Kokunai et al.[48] demonstrated use of Antennapedia homeodomain in antisense ODN delivery to malignant glioma cell lines. They showed that these ODNs are capable of enhancing γ irradiation-induced apoptosis, probably by p21 antisense.

16.4.2 Tat

Astriab–Fisher et al.[46] demonstrated similar results with Tat (see Chapter 1) coupled to phosphorothioates as previously described with penetratin (Table 16.1). These results further strengthen the assumptions that the uptake mechanism for Tat and penetratin peptides, could be similar and they could form a subclass of nonamphiphilic CPPs.

TABLE 16.1
Examples of Transport of Nucleic Acids by CPP

Cargo type	Cargo function	Target cell/tissue	Applied CPP	Conjugation method	Ref.
deoxyoligonucleotides	antisense 21-mer	PC-12 cells	pAntp(43 to 58) RQIKIWFQNRRMKWKK	S–S	41
peptide nucleic acids	antisense 11-mer	DU145 cells	pAntp analog, GGRQIKIWFQNRRMKWKK	peptide bond	42
	antisense 21-mer	Bowes cells; rat spinal cord	Penetratin RQIKIWFQNRRMKWKK transportan GWTLNSAGYLLGKINLKALAALAKKIL	S–S	44
	antisense 16-mer	Cultured cerebral cortex neurons	retro-inverso-penetratin KKWKMRRNQFWVKVQR	attachment via βAla-Lys-βAla linker	45
	antisense 13-mer	JR8 cells	pAntp(44 to 58) QIKIWFQNRRMKWKK[a]	S–S	47
	19 25-mers X-chromosome silencing, interference mapping	C57BL/6 dermal fibroplasts	transportan GWTLNSAGYLLGKINLKALAALAKKIL	S–S	53
	6 mer	bEnd cells	pVEC LLIILRRRIRKQAHAHSK	peptide bond	63
phosphorothioates	antisense 20-mer	NIH 3T3 cells	pAntp analog, Ant-20 RQIKIWFQNRRMKWKKGGC Tat analog, Tat-20 RKKRRQRRRPPQC	S–S	46

	ss and ds 18- and 36-mers	fibroplasts HS68 and NIH-3T3 cells	MPG fusion sequence of HIV gp41 + nuclear localization sequence of SV40 T-antigen Ac-GALFLGFLGAAGSTMGA-WSQ-PKSKRKV-cysteamide	Noncovalent conjugation	57
	antisense 26-mer	cardiac H9C2 cells	MTS-NLS N-terminal part — signal peptide sequence of cayman crocodylus Ig(v) light chain- C-terminal part- simian virus SV40 large tumor antigen (T-ag) NLS MGLGLHLLVLAAALQGAKKKRKV	S–S	55
plasmids	Plasmid pRL-SV40 Plasmid pcDNA3.1NT-GFP	HS-68, NIH-3T3, C2C12 myoblasts, COS-7, CEM-SS	MPG fusion sequence of HIV gp41 + nuclear localization sequence of SV40 T-antigen Ac-GALFLGFLGAAGSTMGA-WSQ-PKSKRKV-cysteamide	Noncovalent conjugation	59
λ phage	Recombinant λ phage particle	COS-1; VA13/2RA; 293; NIH 3T3; HeLa; A431; mouse liver *in vivo*	Tat (43–60) MLGISYGRKKRRQRRRPPQT	Application of recombinant λ phage displaying Tat peptide on its surface	49

[a] Sequence according to the original report.

Recently, Eguchi et al.[49] demonstrated utilization of Tat peptide for gene transfer to various mammalian cell lines (Table 16.1). They constructed recombinant lambda phage particles displaying Tat peptide on their surfaces and carrying mammalian marker genes (GFP and firefly luciferase) as part of their genomes. In animal cells briefly exposed to Tat–phage, the expression of phage marker genes was induced. In contrast, recombinant phage displaying other functional peptides, like the peptide from integrin-binding domain (RGD) or a nuclear localization signal (NLS) similar to controls (wild type phage and naked DNA), could not induce detectable marker gene expression. The expression of marker genes induced by Tat–phage is not affected by temperature or by endosomotropic agents such as monensin and chloroquine (for further reading, see Galloway et al.[50]). However, expression is partially impaired by inhibitors of caveolae formation such as nystatin[51] and fillipin.[52]

The ability of Tat–phage to transport dsDNA was also shown *in vivo*. Constructs carrying GFP gene were injected intraparenchymally into the mouse liver. Livers were dissected in 2 days and the GFP expression observed by fluorescence microscopy. These data suggest that Tat peptide could be used in gene transfer *in vivo*. Also, the existence of classical endocytic pathway-independent mechanism for Tat-mediated uptake was obviously proved again.

16.4.3 Transportan

Transportan is a 27-amino acid artificial chimeric peptide developed by the authors.[37] This peptide has been demonstrated to locate through biological membranes and finally localize in the nucleus. The ability to transport antisense PNA molecules *in vitro* and *in vivo* was demonstrated in the article published shortly after introducing the peptide.[44] This report compares penetratin and transportan as transmembrane delivery vectors for PNA molecules, demonstrating similar effects with both vectors (see above).

A recent publication by Beletskii et al.[53] reported use of transportan to target several PNA oligomers to diploid female ES cells (Table 16.1). The study demonstrates the effect of PNA oligomers on inactivation of X chromosome (Xi) and formation of macrochromatin body (MCB). This complex is formed to silence the X chromosome in female mammals. Transportan coupled with 19-mer PNA complementary to noncoding Xist RNA, a noncoding RNA responsible for Xi silencing, inhibits Xist complexing with Xi. Such inhibition leads to disruption of association between Xi and H2A macrohistone. These results prove the potential of transportan as a cell-penetrating delivery vehicle.

16.4.4 MTS–NLS

Certain peptides from protein signal sequences have been shown to penetrate membranes. Membrane translocating sequences (MTS) are used by protein sorting machinery to target proteins into different intracellular compartments. Nuclear proteins are usually tagged with nuclear localization signals (NLSs). MTS–NLS conjugates have shown the ability to enter cells and localize in the nucleus.[54]

Peptides containing a hydrophobic N-terminal part (signal peptide sequence of C*ayman crocodylus* Ig(v) light chain) associated with an NLS (the C-terminal

hydrophilic part of Simian virus SV40 large tumor antigen) have been shown to act as carriers of nucleic acids at physiological and decreased temperatures (Table 16.1).[55] The ability of this peptide to act as carrier for nucleic acids was further investigated using antisense technology. Antisense phosphorothioate ODN covalently attached to the formerly described peptide was able to inhibit L-type Ca^{2+}channel β subunit synthesis in cardiac cell line H9C2.

Another report showed the use of MTS (MPM) derived from the hydrophobic region of signal peptide sequence of the Kaposi fibroblast growth factor, or of the above-mentioned MTS in complex with NLS of transcription nuclear factor NFκB.[56] The phosphorothioate ODNs were cross-linked to the carrier peptides by disulphide bond. These constructs translocated membranes and localized in the nucleus. Unfortunately, the constructs did not show any antisense effect *in vitro*. Experiments with a cell-free luciferase reporter assay were successful as all antisense sequences decreased luciferase expression by 60 to 80% of basal level at 2 μ*M*. The inhibition of luciferase expression by control sequences was observed by 10 to 20%. We explain it by the fact that the authors of this study used high concentrations of construct.

Morris et al.[57] developed a 27-amino acid-long peptide called MPG that contains a hydrophobic domain derived from the fusion sequence of HIV gp41 and a hydrophilic domain derived from the nuclear localization sequence of SV40 T-antigen (Table 16.1). Binding of both single- and double-stranded phosphorothioate ODNs to MPG occurs through electrostatic interactions, which involve basic residues of the peptide vector. MPG peptide translocates fluorescein-labeled phosphorothioate ODN conjugates into cultured mammalian cells in less than 1 h with high efficiency (90%, as measured by confocal microscopy). The speed of the uptake indicates that the mechanism does not follow the endosomal pathway. Experiments with MPG-mediated ON uptake on HS68 fibroblasts at low temperature to block the endosomal pathway confirm the assumption. At 4°C the oligonucleotides were also rapidly internalized into cells in the previously described time frame and localized to the nucleus.

Vidal et al.[58] used MPG peptide for transmembrane delivery of fluorescent-labeled single-stranded mRNA encoding the p66 subunit of the HIV-1 reverse transcriptase. In the presence of the peptide vector, the mRNA was delivered into the cytoplasm of HS68 human fibroblasts. The same authors used a similar strategy for gene delivery into cultured cells.[59] MPG promoted delivery and expression of the pRL-SV40 plasmid encoding the reporter *R. reniformis* luciferase in HS-68 and NIH 3T3 fibroblasts, C2C12 myoblasts and COS-7 cells, as well as human CEM-SS lymphoblasts (Table 16.1). The degree of transfection using MPG was at least two- and sevenfold higher than that obtained with Lipofectamine® for fibroblasts or COS-7 and C2C12 myoblasts, respectively. They also demonstrated that MPG-mediated delivery of a plasmid carrying full-length antisense cdc25C cDNA into mammalian fibroblasts promotes cell cycle arrest at the G2/M transition.

Zanta et al.[60] demonstrated that NLS peptide (PKKKRKVEDPYC) alone was sufficient to deliver 3.3 kbp CMV luciferase gene. The efficiency of transfection was enhanced 10- to 1000-fold as a result of addition of NLS. Whether the enhancement of transfection is caused by improved membrane penetration or just by

increased nuclear localization remains unclear as transfections were performed by standard transfection protocol by Transfectam® or branched polyethylenimine (PEI).

The same NLS has been demonstrated to be involved in antigene PNA delivery to intact cells in culture.[61] The cell lines derived from Burkitt's lymphomas presenting translocated and hyperexpressed c-myc oncogene. An NLS coupled to 17-mer anti-myc PNA, complementary to myc sequence of the second exon of the oncogene, caused rapid down-regulation of c-myc expression. PNA-myc-NLS construct was shown to be localized predominantly in the cell nuclei. The data shown in this paper do not explain the type of uptake; similarities to previously used constructs cause one to think about penetration.

The putative roles of NLS in membrane penetration is further confirmed by a recent study that utilizes a similar transfection strategy.[62] Brandén et al. coupled SV40 NLS directly to PNA/Cy-3 oligonucleotide complex. These complexes were injected into various mouse tissues. The complex transfected cells in subcutaneous, muscular, or hepatic tissue, as measured by fluorescense microscopy. Comparative transfections with PEI/Cy-3 complexes uncover differences in transfection; PEI-condensed ODNs are detected in the cell as large complexes with nonhomologous distribution, while NLS-PNA/ODN complexes show less aggregated intracellular dispersion. When using a PNA/Cy-3 complex without NLSs, no detectable transfection took place, indicating the crucial role of NLSs in this experimental system.

16.4.5 pVEC

A recent article by Elmquist et al.[63] reported on novel CPP, an 18-amino acid-long peptide derived from the murine sequence of the cell adhesion molecule vascular endothelial cadherin, amino acids 615–632. They show that human aortic endothelial cells, brain capillary endothelial cells, Bowes melanoma cells, and murine brain endothelial cells efficiently take up this peptide. pVEC is also shown to transport hexameric PNA molecule at physiological and decreased (4°C) temperatures.

16.4.6 Other Peptide Vectors

There are several examples of peptide-mediated transmembrane delivery of ON or dsDNA when utilized peptides are not strictly CPPs by definition. Whether this is a general virtue of these peptides or whether the delivery is dependent on cell type or experimental conditions remains to be discovered.

Recently, novel gene transfer technique, in which an amphiphilic α-helical peptide containing cationic amino acids is used as a gene carrier into cells, has been reported. Wyman et al.[64] studied a peptide, KALA (WEAK-LAKA-LAKA-LAKH-LAKA-LAKA-LKAC-EA), derived from the sequence of the amino-terminal segment of the HA-2 subunit of the influenza virus hemagglutinin involved in fusion of the viral envelope with the endosomal membrane. The peptide displays functions necessary in transfection process, e.g., condensing DNA and causing an endosome–membrane perturbation and transfection of cells.

At physiological pH, the KALA peptide exists in the α-helical conformation in spite of the number of positive charges from the protonated Lys side chains. The peptide undergoes an α-helical structure to mixed random coil if pH is decreased

from physiological to 5 pH, shown by CD spectra analysis. The ability of penetration through membranes was shown at neutral and negatively charged liposomes at pH range of 4 to 8.5, in which the KALA peptide induced 100% leakage of liposome-entrapped dyes. A similar mechanism is suggested by the authors to account for KALA peptide's ability to exit from endosomes and transfer ONs or DNA. The KALA peptide was also shown to be efficient in mediating transfection of various cells with plasmid DNA. Transferrin addition did not influence transfection efficiency, thus eliminating this type of uptake.

Fominaya et al.[65] demonstrated the use of the KALA peptide analog in gene delivery. This peptide delivered noncovalent complexes of peptide–psVLUC plasmid to various cell lines as detected by expressed luciferase activity measurements.

A peptide with similar amphiphilic α-helical properties was designed by Niidome et al.[66] They demonstrated that COS-7 cells efficiently take up noncovalently conjugated peptide–plasmid complexes and that these plasmids retain functionality and express luciferase. The treatment of cells with chloroquine, an inhibitor of lysosomal hydrolases, increased the expression of luciferase, pointing to endosomal type of uptake. Later works by this group show the importance of hydrophobic moieties in cellular uptake of these peptides.[67]

Very recently Good et al.[68] used a peptide KFFKFFKFFK to target antisense peptide nucleic acids to bacterial cells. This peptide, developed by Vaara and Porro,[69] does not exhibit antibacterial activity and is capable of penetrating bacterial cells. PNA–peptide conjugates specifically inhibit *Escherichia coli* gene expression and growth. PNA conjugates targeted to rRNA and mRNA encoding the essential fatty acid biosynthesis protein Acp inhibited cell growth. The anti-acpP PNA at 2 μ*M* concentration cured HeLa cells from K12 *E. coli* infection.

16.4.7 Polylysine and Loligomers

Polylysine (PLL) has been used successfully as a DNA carrier in receptor–mediated gene transfer; in such cases, PLL is conjugated to the ligand for cell surface receptors like glycoproteins,[70] insulin,[71] transferrin,[72] lectins,[73] etc. These conjugates are directed to specific cell surface receptors and their uptake is of a lysosomal type. Some reports suggest possible involvement of PLL in nonendocytotic mechanism.

Polylysine alone usually possesses low uptake rates of ONs.[74] A recent report demonstrates the uptake of plasmid DNA, conjugated to poly-(L)-Lys (PLL), poly-(D)-Lys, or poly-Orn, into alveolar adenocarcinoma cells, A549.[75] Several other reports assert that PLL uptake is nonspecific adsorptive endocytosis.[76,77]

A recent article by Sazani et al.[78] demonstates the uptake of antisense PNA molecules with 4-mer Lys moieties in C terminus. These constructs are efficiently taken up by HeLa S3 cells; they blocked aberrant and restored correct splicing of modified EGFP precursor mRNA, thus generating properly translated EGFP. The authors suggest that the PNA–$(Lys)_4$ construct is taken up by a mechanism similar to that of cell-penetrating homeodomain proteins, as incubation at decreased temperatures retained the same number of fluorescent cells.

Another group of vector peptides, called loligomers, consists of branched "squid-like" polylysine sequences. Design of loligomers is based on a concept that multi-

valent display of functional domains leads to enhanced binding avidity and functional capacity, as compared to linear PPL analogs. These synthetic peptides penetrate cells and locate in the nucleus. At 4°C, loligomers do not enter the cells, but rather associate with plasma membranes.[79] Interestingly, inhibitors of ATP synthesis, like 2-deoxyglucose and Na-azide, did not inhibit uptake of loligomers, leaving the type of uptake uncovered.

Conjugation of NLS sequences directs loligomers to the nucleus. Such constructs have been successfully used in gene transfer *in vitro*. Singh et al.[80] have demonstrated the use of loligomer 4 in transmembrane delivery of various plasmids. Loligomer 4 contains 8 NLS derived from SV40 large T antigene and eight pentalysine stretches.

16.5 CONCLUSIONS

Current developments in genomic research will rapidly lead to expansion in identification of defective genes causing a variety of diseases and disclose numerous novel therapeutic targets. Treatment of such diseases may include strategies ranging from gene delivery and replacement to antisense approaches. For the foreseeable future, the development of a nontoxic, easy-to-make, high-efficient vector should remain a major focus of ongoing research. Several reports reviewed here demonstrate successful applications of CPPs as nucleic acid delivery vehicles in various test systems. It seems that these vectors are powerful ON and gene delivery tools, often transcending the efficiency, in terms of gene transfer and integration (up to >99%), of other common transfection vectors.

ABBREVIATIONS

Ac	acetyl
APP	amyloid precursor protein
CD	circular dichroism
CPP	cell-penetrating peptide
ds	double stranded
EGFP	enhanced green fluorescent protein
FACS	fluorescence activated cell sorting
FISH	fluorescent *in situ* hybridization
LDL	low density lipoprotein
MPM	membrane-permeable motif
MTS	membrane translocating sequence
NLS	nuclear localization signal
ODN	oligodeoxynucleotide
ON	oligonucleotide
pAntp	antennapedia peptide
PLL	poly-lysine
PNA	peptide nucleic acid
pVEC	peptide from vascular endothelial cadherin
RT-PCR	reverse transcriptase polymerase chain reaction
S–S	disulphide bond

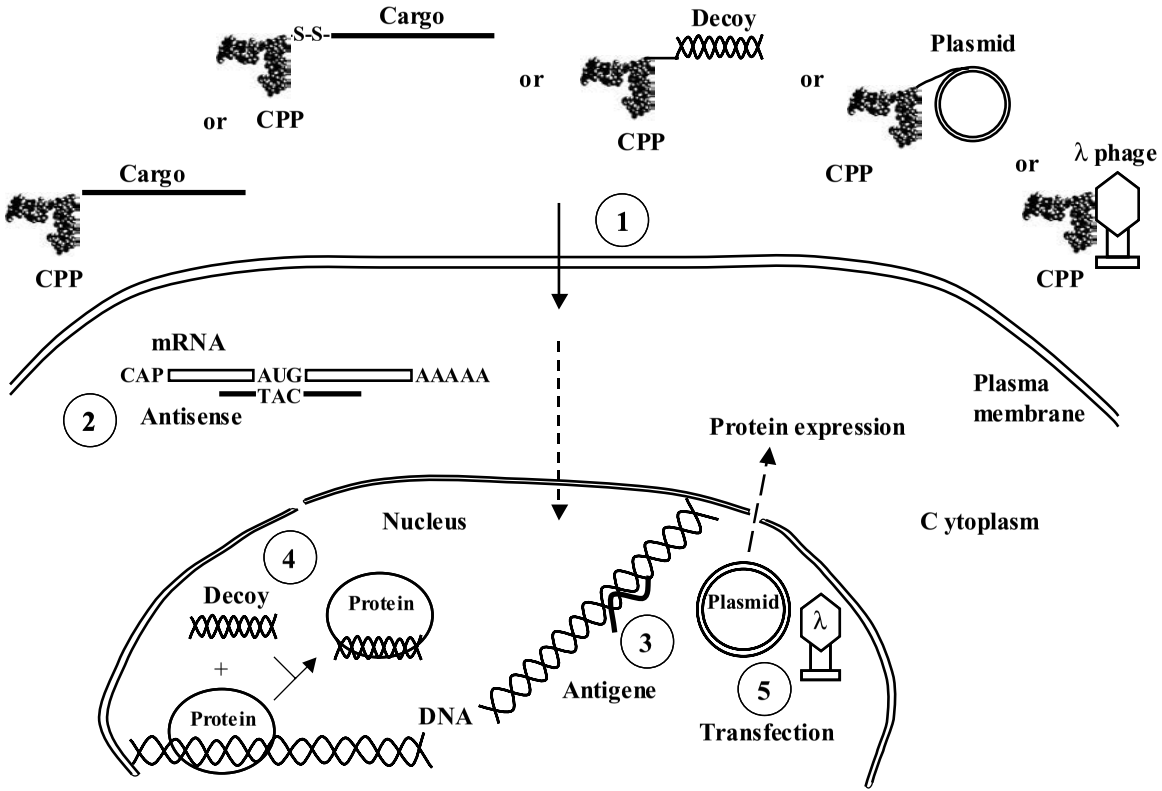

FIGURE 16.1 Schematic illustration of different CPP–cargo conjugates and their intracellular targets. Cargoes reported and reviewed in this chapter are ssDNA, dsDNA, ssPNA, ssPS, dsPS, plasmid. A model of transportan structure (From Lindberg, M. et al., *Biochemistry,* 40, 3141, 2001. With permission.) is shown as an example of CPP. 1 = denotes the process of internalization of conjugates, 2 = antisense effect of cargo, 3 = antigene effect of cargo, 4 = competitive binding of the ds decoy oligomer to the DNA-binding proteins (transcription factors, etc.), 5 = transfection with plasmid or phage.

REFERENCES

1. Delihas, N., Rokita, S.E., and Zheng, P., Natural antisense RNA/target RNA interactions: possible models for antisense oligonucleotide drug design, *Nat. Biotechnol.,* 15, 751, 1997.
2. Morishita, R. et al., A gene therapy strategy using a transcription factor decoy of the E2F binding site inhibits smooth muscle proliferation *in vivo*, *Proc. Natl. Acad. Sci. U.S.A.,* 92, 5855, 1995.
3. Feeley, B.T. et al., Nuclear factor-kappaB transcription factor decoy treatment inhibits graft coronary artery disease after cardiac transplantation in rodents, *Transplantation,* 70, 1560, 2000.
4. Ishibashi, H. et al., Sp1 decoy transfected to carcinoma cells suppresses the expression of vascular endothelial growth factor, transforming growth factor beta1, and tissue factor and also cell growth and invasion activities, *Cancer Res.,* 60, 6531, 2000.
5. Kawamura, I. et al., Intravenous injection of oligodeoxynucleotides to the NF-kappaB binding site inhibits hepatic metastasis of M5076 reticulosarcoma in mice, *Gene Ther.,* 8, 905, 2001.
6. Tomita, N. et al., Inhibition of TNF-alpha, induced cytokine and adhesion molecule. Expression in glomerular cells *in vitro* and *in vivo* by transcription factor decoy for NFkappaB, *Exp. Nephrol.,* 9, 181, 2001.
7. Park, Y.G. et al., Reduction in cyclin D1/Cdk4/retinoblastoma protein signaling by CRE-decoy oligonucleotide, *Biochem. Biophys. Res. Commun.,* 281, 1213, 2001.
8. Deshpande, D. et al., Enhanced cellular uptake of oligonucleotides by EGF receptor-mediated endocytosis in A549 cells, *Pharm. Res.,* 13, 57, 1996.
9. Nakai, D. et al., Cellular uptake mechanism for oligonucleotides: involvement of endocytosis in the uptake of phosphodiester oligonucleotides by a human colorectal adenocarcinoma cell line, HCT-15, *J. Pharmacol. Exp. Ther.,* 278, 1362, 1996.
10. Bennet, R.M. et al., The production and characterization of murine monoclonal antibodies to a DNA receptor on human leukocytes, *J. Immunol.,* 140, 2937, 1988.
11. Hefeneider, S.H. et al., Identification of a cell-surface DNA receptor and its association with systemic lupus erythematosus, *J. Invest. Dermatol.,* 94, 79S, 1990.
12. Francolini, M. et al., Evidence for nuclear internalization of exogenous DNA into mammalian sperm cells, *Mol. Reprod. Dev.,* 34, 133, 1993.
13. Zamecnik, P. et al., Electron micrographic studies of transport of oligodeoxynucleotides across eukaryotic cell membranes, *Proc. Natl. Acad. Sci. U.S.A.,* 91, 3156, 1994.
14. Goodarzi, G., Watabe, M., and Watabe, K., Binding of oligonucleotides to cell membranes at acidic pH, *Biochem. Biophys. Res. Commun.,* 181, 1343, 1991.
15. Akhtar, S. et al., The influence of polarized epithelial (Caco-2) cell differentiation on the cellular binding of phosphodiester and phosphorothioate oligonucleotides, *Antisense Nucleic Acid Drug Dev.,* 6, 197, 1996.
16. Yakubov, L.A. et al., Mechanism of oligonucleotide uptake by cells: involvement of specific receptors? *Proc. Natl. Acad. Sci. U.S.A.,* 86, 6454, 1989.
17. Wu-Pong, S., Weiss, T.L., and Hunt, C.A., Antisense c-myc oligonucleotide cellular uptake and activity, *Antisense Res. Dev.,* 4, 155, 1994.
18. Wu-Pong, S., Weiss, T.L., and Hunt, C.A., Antisense c-myc oligodeoxyribonucleotide cellular uptake, *Pharm. Res.,* 9, 1010, 1992.
19. Nestle, F.O. et al., Cationic lipid is not required for uptake and selective inhibitory activity of ICAM-1 phosphorothioate antisense oligonucleotides in keratinocytes, *J. Invest. Dermatol.,* 103, 569, 1994.

20. Noonberg, S.B., Garovoy, M.R., and Hunt, C.A., Characteristics of oligonucleotide uptake in human keratinocyte cultures, *J. Invest. Dermatol.,* 101, 727, 1993.
21. Shoji, Y. et al., Mechanism of cellular uptake of modified oligodeoxynucleotides containing methylphosphonate linkages, *Nucleic Acids Res.,* 19, 5543, 1991.
22. Giles, R.V., Spiller, D.G., and Tidd, D.M., Chimeric oligodeoxynucleotide analogues: enhanced cell uptake of structures which direct ribonuclease H with high specificity, *Anticancer Drug Des.,* 8, 33, 1993.
23. Smith–Arica, J.R. and Bartlett, J.S., Gene therapy: recombinant adeno-associated virus vectors, *Curr. Cardiol. Rep.,* 3, 43, 2001.
24. Riviere, I. et al., Retroviral-mediated gene transfer in primary murine and human T-lymphocytes, *Mol. Biotechnol.,* 15, 133, 2000.
25. Kompella, U.B. and Koushik, K., Preparation of drug delivery systems using supercritical fluid technology, *Crit. Rev. Ther. Drug Carrier Syst.,* 18, 173, 2001.
26. Chandran, S., Roy, A., and Mishra, B., Recent trends in drug delivery systems: liposomal drug delivery system — preparation and characterisation, *Indian J. Exp. Biol.,* 35, 801, 1997.
27. Uwai, Y. et al., Functional characterization of the rat multispecific organic anion transporter OAT1 mediating basolateral uptake of anionic drugs in the kidney, *FEBS Lett.,* 438, 321, 1998.
28. Krieg, A.M. et al., Modification of antisense phosphodiester oligodeoxynucleotides by a 5′ cholesteryl moiety increases cellular association and improves efficacy, *Proc. Natl. Acad. Sci. U.S.A.,* 90, 1048, 1993.
29. Letsinger, R.L. et al., Cholesteryl-conjugated oligonucleotides: synthesis, properties, and activity as inhibitors of replication of human immunodeficiency virus in cell culture, *Proc. Natl. Acad. Sci. U.S.A.,* 86, 6553, 1989.
30. Chow, T.Y., Juby, C., and Brousseau, R., Specific targeting of antisense oligonucleotides to neutrophils, *Antisense Res. Dev.,* 4, 81, 1994.
31. Janout, V. et al., Evidence for highly cooperative binding between molecular umbrella-spermine conjugates and DNA, *Bioconjug. Chem.,* 8, 891, 1997.
32. Kalkbrenner, F. et al., Nuclear application of antisense oligonucleotides by microinjection and ballistomagnetic transfer to identify G protein heterotrimers activating phospholipase C, *Methods Mol. Biol.,* 83, 203, 1997.
33. Swartz, M. et al., Sparking new frontiers: using *in vivo* electroporation for genetic manipulations, *Dev. Biol.,* 233, 13, 2001.
34. Wu, C.H. and Wu, G.Y., Targeted inhibition of hepatitis C virus-directed gene expression in human hepatoma cell lines, *Gastroenterology,* 114, 1304, 1998.
35. Wu, G.Y. and Wu, C.H., Specific inhibition of hepatitis B viral gene expression *in vitro* by targeted antisense oligonucleotides, *J. Biol. Chem.,* 267, 12436, 1992.
36. Gottschalk, S. et al., Folate receptor mediated DNA delivery into tumor cells: photosomal disruption results in enhanced gene expression, *Gene Ther.,* 1, 185, 1994.
37. Pooga, M. et al., Cell penetration by transportan, *FASEB J.,* 12, 67, 1998.
38. Schwarze, S.R. et al., *In vivo* protein transduction: delivery of a biologically active protein into the mouse, *Science,* 285, 1569, 1999.
39. Allinquant, B. et al., Down regulation of amyloid precursor protein inhibits neurite outgrowth *in vitro*, *J. Cell. Biol.,* 128, 919, 1995.
40. Derossi, D. et al., The third helix of the Antennapedia homeodomain translocates through biological membranes, *J. Biol. Chem.,* 269, 10444, 1994.
41. Troy, C.M. et al., Down regulation of Cu/Zn superoxide dismutase leads to cell death via the nitric oxide-peroxynitrite pathway, *J. Neurosci.,* 16, 253, 1996.

42. Simmons, C.G. et al., Synthesis and membrane permeability of PNA-peptide conjugates, *Bioorg. Med. Chem. Lett.,* 7, 3001, 1997.
43. Nielsen, P.E. et al., Sequence-selective recognition of DNA by strand displacement with a thymine-substituted polyamide, *Science,* 254, 1497, 1991.
44. Pooga, M. et al., Cell penetrating PNA constructs regulate galanin receptor levels and modify pain transmission *in vivo*, *Nat. Biotechnol.,* 16, 857, 1998.
45. Aldrian–Herrada, G. et al., A peptide nucleic acid (PNA) is more rapidly internalized in cultured neurons when coupled to a retro-inverso delivery peptide. The antisense activity depresses the target mRNA and protein in magnocellular oxytocin neurons, *Nucleic Acids Res.,* 26, 4910, 1998.
46. Astriab-Fisher, A. et al., Antisense inhibition of P-glycoprotein expression using peptide-oligonucleotide conjugates, *Biochem. Pharmacol.,* 60, 83, 2000.
47. Villa, R. et al., Inhibition of telomerase activity by a cell-penetrating peptide nucleic acid construct in human melanoma cells, *FEBS Lett.,* 473, 241, 2000.
48. Kokunai, T. et al., Overcoming of radioresistance in human gliomas by p21WAF1/CIP1 antisense oligonucleotide, *J. Neurooncol.,* 51, 111, 2001.
49. Eguchi, A. et al., Protein transduction domain of HIV-1 Tat protein promotes efficient delivery of DNA into mammalian cells, *J. Biol. Chem.,* 276, 26204, 2001.
50. Galloway, C.J. et al., Analysis of endosome and lysosome acidification *in vitro*, *Methods Enzymol.,* 157, 601, 1988.
51. Anderson, H.A., Chen, Y., and Norkin, L.C., Bound simian virus 40 translocates to caveolin-enriched membrane domains, and its entry is inhibited by drugs that selectively disrupt caveolae, *Mol. Biol. Cell,* 7, 1825, 1996.
52. Orlandi, P.A. and Fishman, P.H., Filipin-dependent inhibition of cholera toxin: evidence for toxin internalization and activation through caveolae-like domains, *J. Cell Biol.,* 141, 905, 1998.
53. Beletskii, A. et al., PNA interference mapping demonstrates functional domains in the noncoding RNA Xist, *Proc. Natl. Acad. Sci. U.S.A.,* 98, 9215, 2001.
54. Lin, Y.Z. et al., Inhibition of nuclear translocation of transcription factor NF-kappa B by a synthetic peptide containing a cell membrane-permeable motif and nuclear localization sequence, *J. Biol. Chem.,* 270, 14255, 1995.
55. Chaloin, L. et al., Design of carrier peptide-oligonucleotide conjugates with rapid membrane translocation and nuclear localization properties, *Biochem. Biophys. Res. Commun.,* 243, 601, 1998.
56. Antopolsky, M. et al., Peptide-oligonucleotide phosphorothioate conjugates with membrane translocation and nuclear localization properties, *Bioconjug. Chem.,* 10, 598, 1999.
57. Morris, M.C. et al., A new peptide vector for efficient delivery of oligonucleotides into mammalian cells, *Nucleic Acids Res.,* 25, 2730, 1997.
58. Vidal, P. et al., New strategy for RNA vectorization in mammalian cells. Use of a peptide vector, *C.R. Acad. Sci. III,* 320, 279, 1997.
59. Morris, M.C. et al., A novel potent strategy for gene delivery using a single peptide vector as a carrier, *Nucleic Acids Res.,* 27, 3510, 1999.
60. Zanta, M.A., Belguise–Valladier, P., and Behr, J.P., Gene delivery: a single nuclear localization signal peptide is sufficient to carry DNA to the cell nucleus, *Proc. Natl. Acad. Sci. U.S.A.,* 96, 91, 1999.
61. Cutrona, G. et al., Effects in live cells of a c-myc anti-gene PNA linked to a nuclear localization signal, *Nat. Biotechnol.,* 18, 300, 2000.
62. Brandén, L.J., Christensson, B., and Smith, C.I., *In vivo* nuclear delivery of oligonucleotides via hybridizing bifunctional peptides, *Gene Ther.,* 8, 84, 2001.

63. Elmquist, A. et al., VE-Cadherin-derived cell-penetrating peptide, pVEC, with carrier functions, *Exp. Cell Res.,* 269, 237, 2001.
64. Wyman, T.B. et al., Design, synthesis, and characterization of a cationic peptide that binds to nucleic acids and permeabilizes bilayers, *Biochemistry,* 36, 3008, 1997.
65. Fominaya, J. et al., An optimized amphiphilic cationic peptide as an efficient nonviral gene delivery vector, *J. Gene Med.,* 2, 455, 2000.
66. Niidome, T. et al., Chain length of cationic alpha-helical peptide sufficient for gene delivery into cells, *Bioconjug. Chem.,* 10, 773, 1999.
67. Niidome, T. et al., Required structure of cationic peptide for oligonucleotide-binding and -delivering into cells, *J. Pept. Sci.,* 6, 271, 2000.
68. Good, L. et al., Bactericidal antisense effects of peptide-PNA conjugates, *Nat. Biotechnol.,* 19, 360, 2001.
69. Vaara, M. and Porro, M., Group of peptides that act synergistically with hydrophobic antibiotics against gram-negative enteric bacteria, *Antimicrob. Agents Chemother.,* 40, 1801, 1996.
70. Fisher, K.J. and Wilson, J.M., Biochemical and functional analysis of an adenovirus-based ligand complex for gene transfer, *Biochem. J.,* 299, 49, 1994.
71. Siller–Lopez, F. et al., Truncated active matrix metalloproteinase-8 gene expression in HepG2 cells is active against native type I collagen, *J. Hepatol.,* 33, 758, 2000.
72. Zenke, M. et al., Receptor-mediated endocytosis of transferrin-polycation conjugates: an efficient way to introduce DNA into hematopoietic cells, *Proc. Natl. Acad. Sci. U.S.A.,* 87, 3655, 1990.
73. Midoux, P. et al., Specific gene transfer mediated by lactosylated poly-L-lysine into hepatoma cells, *Nucleic Acids Res.,* 21, 871, 1993.
74. Zhou, X.H., Klibanov, A.L., and Huang, L., Lipophilic polylysines mediate efficient DNA transfection in mammalian cells, *Biochim. Biophys. Acta,* 1065, 8, 1991.
75. Ramsay, E. et al., Examination of the biophysical interaction between plasmid DNA and the polycations, polylysine and polyornithine, as a basis for their differential gene transfection *in vitro*, *Int. J. Pharm.,* 210, 97, 2000.
76. Shen, W.C. and Ryser, H.J., Conjugation of poly-L-lysine to albumin and horseradish peroxidase: a novel method of enhancing the cellular uptake of proteins, *Proc. Natl. Acad. Sci. U.S.A.,* 75, 1872, 1978.
77. Leonetti, J.P., Degols, G., and Lebleu, B., Biological activity of oligonucleotide-poly(L-lysine) conjugates: mechanism of cell uptake, *Bioconjug. Chem.,* 1, 149, 1990.
78. Sazani, P. et al., Nuclear antisense effects of neutral, anionic and cationic oligonucleotide analogs, *Nucleic Acids Res.,* 29, 3965, 2001.
79. Sheldon, K. et al., Loligomers: design of *de novo* peptide-based intracellular vehicles, *Proc. Natl. Acad. Sci. U.S.A.,* 92, 2056, 1995.
80. Singh, D. et al., Penetration and intracellular routing of nucleus-directed peptide-based shuttles (loligomers) in eukaryotic cells, *Biochemistry,* 37, 5798, 1998.
81. Lindberg, M. et al., Secondary structure and position of the cell-penetrating peptide transportan in SDS micelles as determined by NMR, *Biochemistry,* 40, 3141, 2001.

17 Protein Transport

Jehangir S. Wadia, Michelle Becker–Hapak, and Steven F. Dowdy

CONTENTS

17.1 PROTEIN TRANSDUCTION

The average eukaryotic cell contains more than 10,000 different proteins that participate in normal cellular functions such as signal transduction, gene transcription, cell-to-cell communication, and protein trafficking. When deregulated, these are often involved in the onset and progression of disease. Importantly, proteins have been evolutionarily selected to perform very specific functions. Thus, the ability to manipulate the cellular level of these proteins or the ectopic expression of novel proteins has shown tremendous potential as a biological tool for studying cellular processes and may become a cornerstone in the effective treatment of human disease. For instance, the reconstitution of tumor-suppressor function by the introduction of tumor-suppressor proteins in cancer therapy or the replacement of defective proteins in genetic disease such as cystic fibrosis or Duchenne's muscular dystrophy are often considered the goal of effective treatment.[1]

In practice, however, the ideal pharmacological agents to achieve these goals and their associated delivery must overcome several key obstacles, including poor specificity, bioavailability, tissue distribution, and toxicity. These obstacles currently limit the usefulness of techniques such as drug therapy or genetic approaches and largely account for failure of the early promise afforded by introduction of recombinant protein technology. For instance, over the past century, the serendipitous discovery of certain drugs and small molecules which could be delivered easily and

0-8493-1141-1/02/$0.00+$1.50

act to manipulate protein function or levels has driven much of our early understanding of metabolic and signaling pathways within the cell. However, the usefulness of small molecules is often compromised by their narrow bioavailability profiles — either too polar for transport across the lipid membrane or too nonpolar for effective delivery. Furthermore, unlike "information-rich" proteins, small molecule therapy often suffers from lack of target specificity and is complicated by side effects and toxicity.[2]

Likewise, in recent years development of molecular techniques for gene delivery with the concomitant expression of specific gene products that can alter cellular phenotype, or with therapeutic biological activity, has been responsible for major advances in our understanding of cellular processes, although they have offered surprisingly little benefit in the management of genetic disorders.[3,4] Delivery of genetic material into eukaryotic cells through use of viral vectors such as adenoviruses or by nonviral mechanisms such as microinjection, electroporation, or chemically through use of cationic lipids or calcium phosphate, for instance, are problematic. The low efficiency of different nonviral vector systems and their immunogenicity, toxicity, and inability to target many cell types, coupled with subsequent transient and varied gene expression, have limited their efficacy *in vivo*. In fact, the often massive transgene overexpression induced through these systems has been considered a contributing factor in spurious experimental results.

17.2 PROTEIN TRANSDUCTION TECHNOLOGY

The ability to deliver full-length functional proteins into cells is problematic due to the bioavailability restriction imposed by the cell membrane. That is, the plasma membrane of the cell forms an effective barrier that limits the diffusion and intercellular uptake of molecules to those sufficiently nonpolar and smaller than approximately 500 Da in size. Efforts to increase the effectiveness of protein uptake by utilizing receptor-mediated endocytosis or through packaging of macromolecules into caged liposomal carriers suffers due to poor cellular uptake. Intracellular sequestration of these molecules into the endocytic pathway, preventing their release into the cellular environment, makes them incapable of interacting with their cellular targets.

The recent observation that certain intracellular proteins added exogenously into media are able to pass efficiently through the plasma membrane of cells has led to identification of a novel class of proteins from which peptide sequences termed "protein transduction domains" (PTDs) have been derived.[5,6] To date, several proteins have been demonstrated to possess transducing capabilities; the three most widely studied are the *Drosophila* antennapedia transcription protein (AntHD),[7-9] the herpes simplex virus structural protein VP22,[10] and the HIV-1 transcriptional activator Tat protein.[5,6] Furthermore, identification of short basic peptide sequences from these proteins (Antp: RQIKIWFQNRRMKWKK, Tat-(47–57): YGRKKRRQRRR), which confers cellular uptake has led to identification and synthesis of numerous new PTDs.[11-13]

Significantly, when covalently cross-linked to full-length proteins such as β-galactosidase or horseradish peroxidase, these PTDs are able to stimulate their

cellular uptake. These chimeric proteins are found within the cytoplasm and the nucleus and, remarkably, retain their enzymatic activity, thus indicating that these proteins remain functionally active. Transduction of these proteins occurs in a rapid process independent of receptors, occurs at 37 and 4°C, targets 100% of cells, and results in a concentration-dependent, uniform intracellular loading. These peptide domains have since been found to induce transduction of a wide variety of molecules in addition to proteins, such as DNA, drugs, and even inorganic 40-nm iron particles.

The advantages and versatility of protein transduction over viral transgene delivery were recently illustrated in a pair of papers from van der Noen's group. In a continuation of their previous studies that investigated transduction of β-galactosidase into rat salivary gland cells *in vivo* using retroviral vectors,[14,15] they more recently compared this to cellular uptake and activity of recombinant Tat-β-galactosidase protein into the same tissue by retrograde injection.[16]

In contrast to viral delivery, which has limited capacity to infect nondividing cells, all cell types were susceptible to Tat-mediated protein transduction. With Tat transduction it was possible to target 100% of the cells in a concentration-dependent manner, whereas viral delivery could achieve only 30 to 50% transduction efficiency with variable levels of expression within those cells. Furthermore, β-galactosidase activity could be detected intracellularly within ascinar cells from 10 min to 6 h following injection, while viral delivery was associated with a significantly delayed onset of enzyme activity, likely due to the added cellular requirement of transcription and translation of the β-galactosidase.

The direct delivery and efficient cellular uptake of transducing proteins offers several advantages over traditional DNA-based methods of manipulating the cellular phenotype. Consequently, a vast increase in use of PTD fusion to address biological questions and for the introduction of pharmacologically relevant proteins *in vitro* and *in vivo* has now begun.

17.3 DEVELOPMENT OF PTD FUSION PROTEINS

At present two methods are employed to generate chimeric proteins capable of cellular transduction: chemical conjugation of protein transduction domains to proteins or *in vivo* expression of in-frame recombinant fusions of transduction domains with full length proteins. In both cases the resulting chimeric proteins are able to be taken up by cells similar to the Tat protein or the antennapedia homeoprotein. Using this approach, it is possible to target virtually 100% of primary and transformed cells. Each cell contains nearly identical intracellular concentrations of biologically active protein readily manipulated by titrating the amount of exogenous protein. Furthermore, PTD fusion proteins are rapidly internalized and reach maximal intracellular loading in less than 5 min, suggesting that timing of treatment can be precisely controlled.

While the different protein transduction domains show similar characteristics for cellular uptake, it is clear that they vary in efficacy in transporting their cargo into the cell. Although no homology between the primary and secondary structure of these PTDs exists, the rate of cellular uptake has been found to correlate strongly to the number of basic residues present, specifically arginine. This indicates the

presence of a common, undefined internalization mechanism likely dependent on an interaction between the charged groups of the basic residues and lipid phosphates on the cell surface.[11,12]

To date, fusions created with PTDs consisting of Tat-(48–57) show markedly better cellular uptake than similar fusions using the 16-amino acid sequence from antennapedia or VP22. However, recently devised peptoid transducers such as the *retro-inverso* form of Tat-(57–48) or homopolymers of arginine appear to increase cellular uptake several-fold.[11,12] Moreover, although the antennapedia PTD can transduce into cells when associated with chemically synthesized peptides,[17,18] efficiency dramatically decreases with incorporation of larger proteins.

VP22 transduction is somewhat different from Tat or Antp. In this system, DNA encoding the entire VP22 protein is genetically fused to the gene of interest and first transfected into cells. The fusion transgene is transcribed and the translated protein transduces from the primary transfected cells into the surrounding cells to varying levels.[10,19] Exogenously added VP22 fusion proteins have been reported to be internalized, but little data about the efficiency of this protein delivery mode are available.

17.3.1 Cloning and Purification of Tat Fusion Proteins

In an effort to exploit Tat-mediated protein delivery as a powerful tool to study cellular biology and as a potential system for therapeutic delivery of full-length proteins, we have developed a bacterial expression system that permits rapid cloning and expression of in-frame fusion proteins using an N-terminal 11 amino acid sequence corresponding to the region 47–57 of Tat (YGRKKRRARRR). In addition, purification protocols were devised that appeared to increase the biological uptake and activity of these chimeric proteins.[20-22] In general, the cDNA encoding the open reading frame of the gene of interest is cloned in-frame downstream of the N-terminal 6xHis-Tat-HA (hemagglutinin-tagged) sequence in the pTat-HA expression vector.

Although, recombinant Tat fusion proteins may be expressed in soluble form within *Escherichia coli,* the majority of these proteins are insoluble and present in the bacterial inclusion bodies which, although more difficult to extract, are resistant to proteolytic degradation within the cell. Consequently, inclusion bodies generally contain full length, undegraded protein. Soluble proteins are purified from the bacterial pellet by sonication in a denaturant, such as in 8 *M* urea, which serves to solubilize proteins stored in inclusion bodies and also to denature those not folded correctly by bacteria. In this case, denaturation serves two purposes: (1) it aids in isolation of insoluble recombinant proteins and (2) unfolding complex tertiary protein structure has been observed to increase transduction efficiency over proteins purified under native conditions.[22]

Interestingly, this latter observation is in keeping with earlier findings that supported a role for protein unfolding in the increased cellular uptake of the Tat fusion protein Tat-DHFR.[23] It is possible that the higher energy (ΔG) of partial or fully denatured proteins increases efficiency of transduction compared to lower-energy correctly folded ones, in part, due to relief of steric hindrance surrounding the Tat domain. Once inside the cells, these denatured proteins are believed to be

refolded correctly by cellular chaperones such as HSP90 in order to regain biological activity.[24]

Following extraction from bacteria, the 6xHis-tagged recombinant proteins are purified by immobilized metal affinity chromatography, followed by ion exchange and, finally, gel filtration chromatography. Using this technique, full-length Tat fusion proteins of 15 to 121 kDa in size and spanning a wide variety of functional classes, including p16,[25] p27,[20] adenovirus E1A, HPV E7, Caspase-3,[26] HIV protease,[26] Cu,Zn-SOD,[27] eGFP,[28] Bcl-X_L,[29] Rho,[30] IκB,[31] p73 dominant-negative,[32] E2F-1 dominant-negative,[33] Cre recombinase (unpublished), CRAC[34] and pRB (unpublished), have been expressed, purified and shown to be competent for cellular uptake and biological activity. The purified Tat fusion proteins can be added directly into the media or used to inject and transduce whole animals.

In vitro, both primary and transformed cell types, including peripheral blood lymphocytes, diploid human fibroblasts, keratinocytes, bone marrow stem cells, osteoclasts, fibrosarcoma cells, leukemic T cells, osteosarcoma, glioma, hepatocellular carcinoma, renal carcinoma, and NIT 3T3 cells are transducible with recombinant proteins. The uptake of these proteins is rapid (<5 min) with uniform intracellular accumulation dependent primarily on the extracellular concentration. Moreover, these Tat fusion proteins are able to transduce rapidly and regain biological activity into all cells and tissues present in mice, including across the blood–brain barrier.

Although Tat-mediated transduction has recently been successful for a variety of protein sizes (15 to 120 kDa), biological functions, and even 40-nm spheres, it is impractical to expect Tat-mediated transduction approaches to work for every protein. Although the current approach utilizes bacterial expression, some proteins are poorly expressed in bacteria or require posttranslational modifications. Therefore, expression of these Tat fusion proteins systems such as yeast or baculovirus will obviously be exploited. Based on the rapid and unknown nature of the Tat PTD to transduce across the cell membrane, it is also unrealistic to expect transmembrane proteins to be presented as such with the current vectors for producing transducing proteins. However, as we observed when originally adapting the Tat-mediated transduction technology to specific biological problems in our laboratory, new and creative solutions using the technology will undoubtedly arise.

17.4 DELIVERY OF PTD-CONJUGATED MACROMOLECULES

17.4.1 Applications in Cell Culture

The transduction of PTD-linked peptides and proteins into cells is performed simply by adding the specified amounts to the tissue culture media. Normally, final media concentrations of 25 to 200 n*M* provide biological activity, although concentrations in excess of 1 μ*M* can be used. As an example of the utility of protein transduction, it is usually necessary to express a protein inside cells to study its effects on particular cellular events. Primary lymphocytes, however, are very difficult to transfect and require electroporation of DNA constructs. This process is very damaging, killing 90 to 99% of cells and yielding protein expression in less than 10% of those surviving.

An alternative method to electroporation was first described by Schutze–Redelmeier et al.[35] This group successfully transduced into T cells an antigenic peptide epitope subsequently presented at the cell surface in the MHC class I complex. Fenton et al. have also demonstrated the ability to transduce fluorescent-labeled Antp peptides into both quiescent and activated lymphocytes.[36] Our laboratory has expanded on this concept by transducing the Tat–E1A fusion protein (60 kDa) into ~100% of cells, both quiescent and cycling primary human lymphocytes in the population, in a concentration-dependent manner. The ability of Tat–E1A to bind endogenous p130 and pRB proteins (cellular targets of E1A) demonstrates that it retains its normal biological function. Moreover, this experiment was performed with a 2-year-old frozen preparation of Tat–E1A protein.

Transduction has also been effective in determining the regulatory role of the small GTPase Rho in mediating integrin signaling events in avian osteoclasts. Small GTPases, such as CDC42, Rac, and Rho, regulate the cytoskeletal architecture of the cell, depending on the type of extracellular signals received.[37-39] For instance, Rho plays a dual role in formation of actin stress fibers and assembly of focal adhesions in fibroblasts.[38] Osteoclasts are important for bone remodeling processes and therefore are highly mobile cells. They achieve this state by rapidly changing their actin cytoskeletal attachment structures (called podosomes).[40,41] *In vitro*, these processes are stimulated by the growth factor osteopontin (OP).[42] Dissecting the role of Rho in podosome formation has been hampered by the inability to manipulate osteoclasts since these cells are essentially resistant to introduction of expression constructs by transfection or retroviral infection.

However, the use of Tat-mediated transduction has allowed these barriers to be bypassed. Constitutively active and dominant-negative forms of Tat–Rho protein were generated and added to osteoclast cultures that contained the protein, based on anti-hemagglutinin (HA) immunostaining and confocal microscopy.[43] The constitutively active Tat–Rho^{V14} rapidly (15 to 30 min) stimulated actin stress fiber formation in a manner indistinguishable from OP during the early phases of treatment. Consistent with this finding, the dominant-negative Tat–Rho blocked the podosome-forming effects of OP. Thus, the utility of Tat-mediated transduction allows for experimentation of primary cells, such as osteoclasts, that are extremely difficult to manipulate.

Another powerful example of the utility of recombinant Tat fusion protein technology was the use of Tat–Cre recombinase to modify gene expression in culture and to induce gene deletion *in vivo* (Becker and Dowdy, manuscript in preparation). Cre recombinase is a 38 kDa protein from bacteriophage P1 that mediates the site-specific, intramolecular, or intermolecular recombination of DNA between a pair of 13 bp inverted repeat sequences called loxP sites; thus it permits precise deletion or activation of genes.[44-46] For example, NIH 3T3 cells containing the actin promoter separated from the β-galactosidase transgene by a loxP-'stop'-loxP motif and thereby preventing its expression were transduced with Tat–Cre protein. Unlike the poor efficiency afforded by DNA-based techniques to introduce Cre cDNA, transduction by Tat–Cre protein induced activation of β-galactosidase expression and activity in more than 95% of cells within 24 h (Figure 17.1).

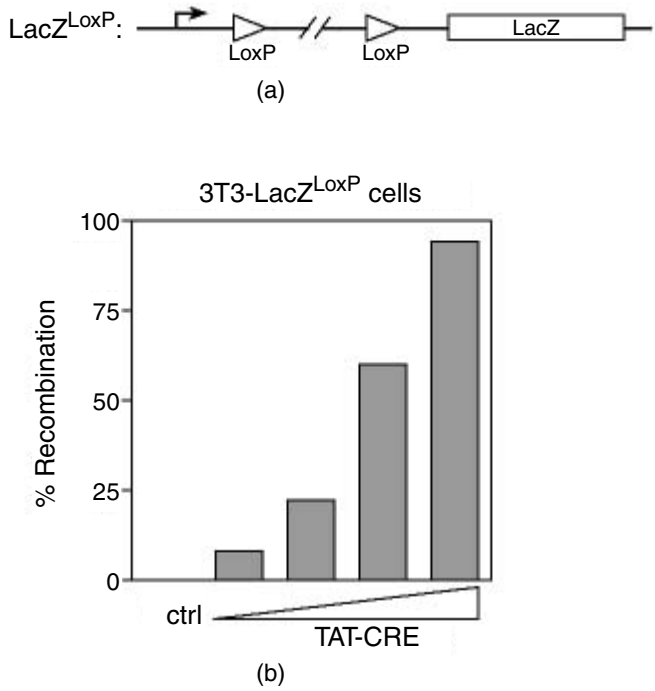

FIGURE 17.1 Recombination of LoxP sites by transducible Tat–Cre protein. NIH 3T3 harboring a transgene comprised of a promoter separated from the β-galactosidase gene by a LoxP-stop-LoxP motif was treated with Tat–Cre protein. Treated cells were assayed for β-galactosidase 24 h post-treatment by staining with X-gal.

Tat–Cre has also been used on primary splenocytes harvested from retinoblastoma loxP mice to cause recombination-specific excision of exon 19 from the retinoblastoma gene. After overnight incubation, PCR analysis and subsequent sequencing of the exon 19 region showed that, predominantly, all cells in culture contained the specific deletion of DNA sequence from exon 19 surrounding the loxP recombination sites, while cells treated with Cre were not recombined (Becker–Hapak et al., unpublished results). Moreover, these results could be reproduced *in vivo* following intraperitoneal administration of Tat–Cre and were only limited by proteolytic degradation in the serum. In both examples, exogenously applied Tat–Cre was able to pass through the plasma membrane, accumulate within the nucleus, and catalyze site-specific recombination between the loxP sites.

17.4.2 *In Vivo* Applications

As with any potential pharmacological approach, one must translate *in vitro* findings to animal models. Can PTDs deliver molecules into cells of entire organisms? Based on past and recent studies in model organisms, the answer is a resounding yes. In 1994, Fawell et al.[47] demonstrated a limited, but significant, capacity of Tat fusions to enter tissues *in vivo* in mice. Schutze–Redelmeier et al.[35] showed that intraperi-

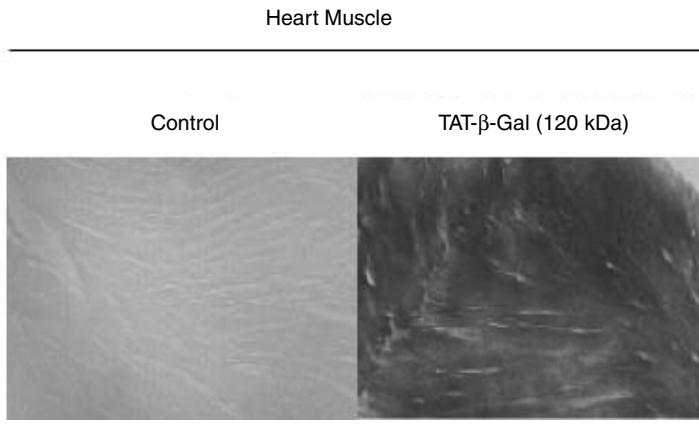

FIGURE 17.2 *In vivo* treated mice with Tat–β-galactosidase protein. Tissue sections of heart muscle from mice treated with intraperitoneally administered Tat–β-galactosidase protein or nontransducible control-β-galactosidase were assayed by X-gal overlay 4 h post-injection.

toneal (i.p.) injection of an Antp-antigenic peptide activated endogenous T cells in mice. Pooga et al.[48] have shown the ability of Antp-antisense PNA oligomers to penetrate the blood–brain barrier in rats. Additionally, Tat–GFP protein has been shown to transduce into *Drosophila* by painting the eyes with a solution containing Tat–GFP (C. Brachmann, carrie@pharmdec.wustl.edu; personal communication).

The therapeutic cache of recombinant Tat proteins, however, will be realized if the effectiveness of this delivery modality can be reproduced *in vivo* to introduce active proteins throughout all tissues. Recently, we have delivered a biologically active enzyme to all cells and tissues of mouse models.[21] Intraperitoneal delivery of 200 to 500 μg of Tat–β-galactosidase into mice, equivalent to 10 to 25 mg/kg body weight of protein, resulted in readily detectable β-galactosidase enzymatic activity in the majority of tissues assayed 4 h after injection, although maximal β-galactosidase loading of the tissues was found to occur within minutes. This difference is likely to represent the time required for refolding and subsequent enzymatic activity of the enzyme.

β-galactosidase activity was strongest in the liver, kidney, lung, heart, and spleen and, significantly, could cross through the blood–brain barrier and be found in the cell body layers of the brain (Figure 17.2). Importantly, Tat–β-galactosidase did not disrupt the blood–brain barrier as assayed by coinjection with Evan's blue dye. Thus, protein transduction technology has the demonstrated potential to introduce a 120-kDa enzyme into many, if not all, cells and tissues of a mammal. Importantly, this represents a molecule approximately 200 times larger than the current bioavailability size restriction.

Another study differentiated between normal and HIV-1-infected cells by inclusion of a viral-specific proteolytic cleavage site created in the Tat transducing protein. This so-called "Trojan horse" strategy selectively induced apoptosis in HIV-infected cells by exploiting the HIV protease.[26] A transducible Caspase-3 pro-apoptotic Tat PTD fusion zymogen was engineered that substituted HIV proteolytic cleavage sites

for endogenous Caspase cleavage sites. Tat–Caspase-3 was processed into an active form by the HIV protease in infected cells, resulting in initiation of the apoptotic cascade in infected cells, while uninfected cells were spared. These preclinical approaches to harness the therapeutic potential of protein transduction likely represent the tip of the iceberg as to what lies in store for the future, with significant improvements in transduction potential and creative approaches to target specific disease cells and tissues.

17.5 FUTURE DIRECTIONS AND CONSIDERATIONS

Although unrestricted access of proteins into cells is now possible, we have a poor grasp of how this technology works. Based on whole animal studies, all cells appear to be susceptible to protein transduction. At the molecular level, it is unclear how proteins behave when interacting with the cell membrane or if any particular molecule (such as a specific phospholipid) is necessary to mediate entry. Currently available limited data suggest that transduction across the cellular membrane results in a partial or complete unfolding of the protein that will likely differ from one protein to another. Therefore, once inside the cell, the transduced protein requires refolding to obtain biologically active proteins.

Another consideration is the intracellular half-life of the protein. As has already been observed with several genetically altered proteins, protein half-life can be dramatically extended. In our animal studies the Tat–β-gal protein served as an excellent "tester" enzyme to begin initially characterizing the ability to transduce large proteins in model mammalian organisms. However, administration of additional Tat fusion molecules to model organisms that generate phenotypic changes is necessary to determine how much promise *in vivo* protein transduction really holds. Basic pharmacological questions of tissue distribution, protein half-life, immunogenicity, and modes of delivery also need to be addressed in a quantitative fashion. Therefore, a complete understanding of protein transduction would not only facilitate rational drug design, but also improve the efficacy of *in vitro* experiments.

REFERENCES

1. Anderson, W., Human gene therapy, *Nature*, 392, 25–30, 1998.
2. Lebleu, B., Delivering information-rich drugs — prospects and challenges, *Trends Biotechnol.*, 14, 109–110, 1996.
3. Robbins, P.D. and Ghivizzani, S.C., Viral vectors for gene therapy, *Pharmacol Ther.*, 80, 35–47, 1998.
4. Robbins, P.D., Tahara, H., and Ghivizzani, S.C., Viral vectors for gene therapy, *Trends Biotechnol.*, 16, 35–40, 1998.
5. Frankel, A. and Pabo, C., Cellular uptake of the Tat protien from human immunodeficiency virus, *Cell*, 55, 1189–1193, 1988.
6. Green, M. and Loewenstein, P., Autonomous functional domains of chemically synthesized human immunodeficiency virus Tat trans-activator protein, *Cell*, 55, 1179–1188, 1988.

7. Joliot, A. et al., Antennapedia homeobox peptide regulates neural morphogenesis, *Proc. Natl. Acad. Sci. U.S.A.,* 88, 1864–1868, 1991.
8. Joliot, A.H. et al., alpha-2,8-Polysialic acid is the neuronal surface receptor of antennapedia homeobox peptide, *New Biol.*, 3, 1121–1134, 1991.
9. Le Roux, I. et al., Neurotrophic activity of the Antennapedia homeodomain depends on its specific DNA-binding properties, *Proc. Natl. Acad. Sci. U.S.A.,* 90, 9120–9124, 1993.
10. Elliott, G. and O'Hare, P., Intercellular trafficking and protein delivery by a herpesvirus structural protein, *Cell*, 88, 223–233, 1997.
11. Wender, P.A. et al., The design, synthesis, and evaluation of molecules that enable or enhance cellular uptake: peptoid molecular transporters, *Proc. Natl. Acad. Sci. U.S.A.*, 97, 13003–13008, 2000.
12. Futaki, S. et al., Arginine-rich peptides. An abundant source of membrane-permeable peptides having potential as carriers for intracellular protein delivery, *J. Biol. Chem.*, 276, 5836–5840, 2001.
13. Ho, A. et al., Synthetic protein transduction domains: enhanced transduction potential in vitro and in vivo, *Cancer Res.*, 61, 474–477, 2001.
14. Barka, T. and van der Noen, H., Retrovirus-mediated gene transfer into rat salivary glands in vivo, *Hum. Gene Ther.*, 7, 613–618, 1996.
15. Barka, T. and van der Noen, H., Retrovirus-mediated gene transfer into rat salivary gland cells *in vitro* and *in vivo, J. Histochem. Cytochem.*, 45, 1533–1545, 1997.
16. Barka, T., Gresik, E., and van der Noen, H., Transduction of TAT-HA-b-galactosidase fusion protein into salivary gland-derived cells and organ cultures of the developing gland, and into rat submandibular gland *in vivo, J. Histochem. Cytochem.*, 48, 1453–1460, 2000.
17. Kato, D. et al., Features of replicative senescence induced by direct addition of antennapedia-p16INK4A fusion protein to human diploid fibroblasts, *FEBS Lett.*, 427, 203–208, 1998.
18. Chen, Y.N. et al., Selective killing of transformed cells by cyclin/cyclin-dependent kinase 2 antagonists, *Proc. Natl. Acad. Sci. U.S.A.,* 96, 4325–4329, 1999.
19. Elliott, G. and O'Hare, P., Intercellular trafficking of VP22-GFP fusion proteins, *Gene Ther.*, 6, 149–151, 1999.
20. Nagahara, H. et al., Transduction of full-length TAT fusion proteins into mammalian cells: TAT-p27Kip1 induces cell migration, *Nat. Med.*, 4, 1449–1452, 1998.
21. Schwarze, S.R. et al., *In vivo* protein transduction: delivery of a biologically active protein into the mouse [see comments], *Science*, 285, 1569–1572, 1999.
22. Becker-Hapak, M., McAllister, S.S., and Dowdy, S.F., Tat-Mediated protein transduction into mammalian cells, *Methods*, 24, 247–256, 2001.
23. Bonifaci, N., Sitia, R., and Rubartelli, A., Nuclear translocation of an exogenous fusion protein containing HIV Tat requires unfolding, *AIDS*, 9, 995–1000, 1995.
24. Schneider, C. et al., Pharmacologic shifting of a balance between protein refolding and degradation mediated by Hsp90, *Proc. Natl. Acad. Sci. U.S.A.*, 93, 14536–14541, 1996.
25. Zezula, J. et al., p21cip1 is required for the differentiation of oligodendrocytes independently of cell cycle withdrawal, *EMBO Rep.*, 2, 27–34, 2001.
26. Vocero-Akbani, A.M. et al., Killing HIV-infected cells by transduction with an HIV protease- activated caspase-3 protein, *Nat. Med.*, 5, 29–33, 1999.
27. Kwon, H.Y. et al., Transduction of Cu,Zn-superoxide dismutase mediated by an HIV-1 Tat protein basic domain into mammalian cells, *FEBS Lett.*, 485, 163–167, 2000.
28. Caron, N.J. et al., Intracellular delivery of a Tat-eGFP fusion protein into muscle cells, *Mol. Ther.*, 3, 310–318, 2001.

29. Embury, J. et al., Proteins linked to a protein transduction domain efficiently transduce pancreatic islets, *Diabetes*, 50, 1706–1713, 2001.
30. Vocero-Akbani, A. et al., Protein transduction: delivery of Tat-GTPase fusion proteins into mammalian cells, *Methods Enzymol.*, 332, 36–49, 2001.
31. Abu-Amer, Y. et al., TAT fusion proteins containing tyrosine 42-deleted IkappaBalpha arrest osteoclastogenesis, *J. Biol. Chem.*, 276, 30499–30503, 2001.
32. Lissy, N.A. et al., TCR antigen-induced cell death occurs from a late G1 phase cell cycle check point, *Immunity*, 8, 57–65, 1998.
33. Lissy, N.A. et al., A common E2F-1 and p73 pathway mediates cell death induced by TCR activation, *Nature*, 407, 642–645, 2000.
34. Li, H. et al., Cholesterol binding at the cholesterol recognition/interaction amino acid consensus (CRAC) of the peripheral-type benzodiazepine receptor and inhibition of steroidogenesis by an HIV TAT-CRAC peptide, *Proc. Natl. Acad. Sci. U.S.A.,* 98, 1267–1272, 2001.
35. Schutze-Redelmeier, M.P. et al., Introduction of exogenous antigens into the MHC class I processing and presentation pathway by Drosophila antennapedia homeodomain primes cytotoxic T cells in vivo, *J. Immunol.*, 157, 650–655, 1996.
36. Fenton, M., Bone, N., and Sinclair, A.J., The efficient and rapid import of a peptide into primary B and T lymphocytes and a lymphoblastoid cell line, *J. Immunol. Methods*, 212, 41–48, 1998.
37. Ridley, A.J. and Hall, A., The small GTP-binding protein rho regulates the assembly of focal adhesions and actin stress fibers in response to growth factors, *Cell*, 70, 389–399, 1992.
38. Barry, S.T. et al., Requirement for Rho in integrin signaling, *Cell Adhes. Commun.*, 4, 387–398, 1997.
39. Zhong, C., Kinch, M.S., and Burridge, K., Rho-stimulated contractility contributes to the fibroblastic phenotype of Ras-transformed epithelial cells, *Mol. Biol. Cell*, 8, 2329–2344, 1997.
40. Kanehisa, J. and Heersche, J.N., Osteoclastic bone resorption: in vitro analysis of the rate of resorption and migration of individual osteoclasts, *Bone*, 9, 73–79, 1988.
41. Lakkakorpi, P.T. and Vaananen, H.K., Cytoskeletal changes in osteoclasts during the resorption cycle, *Microsc. Res. Tech.*, 33, 171–181, 1996.
42. Chellaiah, M. et al., c-Src is required for stimulation of gelsolin-associated phosphatidylinositol 3-kinase, *J. Biol. Chem.*, 273, 11908–11916, 1998.
43. Chellaiah, M.A. et al., Rho-A is critical for osteoclast podosome organization, motility, and bone resorption, *J. Biol. Chem.*, 275, 11993–2002, 2000.
44. Sauer, B., Inducible gene targeting in mice using the Cre/lox system, *Methods*, 14, 381–392, 1998.
45. Bethke, B.D. and Sauer, B., Rapid generation of isogenic mammalian cell lines expressing recombinant transgenes by use of Cre recombinase, *Methods Mol. Biol.*, 133, 75–84, 2000.
46. Le, Y. and Sauer, B., Conditional gene knockout using cre recombinase, *Methods Mol. Biol.*, 136, 477–485, 2000.
47. Fawell, S. et al., Tat-mediated delivery of heterologous proteins into cells, *PNAS*, 91, 664–668, 1994.
48. Pooga, M. et al., Cell penetration by transportan, *Faseb J.*, 12, 67–77, 1998.

18 Microbial Membrane-Permeating Peptides and Their Applications

K. R. Gunaratna, Mats Andersson, and Liam Good

CONTENTS

0-8493-1141-1/02/$0.00+$1.50

18.1 INTRODUCTION

This chapter reviews peptides that are able to permeate microbial cell membranes and enter cells. The existence of microbial-permeating peptides is surprising because peptides are generally considered too large to pass microbial cell barriers, which are typically more stringent than mammalian cells. Nevertheless, there are many clear examples of peptides able to permeate microbial cells without damage to host cells. Indeed, most of our knowledge of cell-permeating peptides and their potential practical applications stems from the discovery that the innate immune response in animals, plants, and insects involves the release of antimicrobial peptides.

Antimicrobial peptides have been shown to kill microbes with impressive potency and specificity and many research groups have sought to develop them as therapeutic agents for infectious disease treatment. In related applications, antimicrobial peptides could provide pathogen resistance to agricultural crops or be used in post harvest food preservation.[1] In all such cases, the objective is to develop peptides to augment the host's own defense mechanisms against pathogenic microorganisms.

The need is increasing for more prudent antibiotic usage and new strategies to fight antibiotic-resistant strains.[2] Despite early warnings during the 1940s, drug resistance has increased into a serious problem that can extend to "stand-by" antibiotics and even the newly introduced oxazolidinones.[3,4] To overcome this problem, antimicrobial peptides or their derivatives offer some exciting possibilities and "antibiotic peptides" may prove to be less susceptible to resistance mechanisms.[5] Effective antimicrobial peptides brought to market would lower our reliance on conventional antibiotics and help to overcome resistant strains.

A second possible application is to use permeating peptides as carriers for delivery of foreign substances into microorganisms.[6] The idea seems reasonable, given that many antimicrobial peptides appear to enter cells and act on intracellular targets.[1,7,8] Therefore, it should be possible to use permeating peptides to deliver foreign substances that otherwise would enter microbes only poorly. This application has the same objective as earlier efforts to use receptor-mediated oligopeptide transport mechanisms for antimicrobial delivery, but the cellular uptake mechanism is different.[9-11] The microbial-permeating peptides described here enter cells independent of classical receptor-mediated uptake, as is also the case for the eukaryotic cell-permeating peptides described in earlier chapters in this book (see Chapters 1 to 7, 16, and 17).

In this chapter, we first briefly describe microbial membranes and how they differ from mammalian cell membranes. Second, the chapter describes the origin and structures of antimicrobial peptides and their ability to permeate microbial cells. The chapter then focuses on practical applications for cell-permeating peptides in antimicrobial development and cellular delivery. Finally, we describe several research strategies to characterize the uptake of microbial cell-permeating peptides.

18.2 BACKGROUND

18.2.1 Microbial and Mammalian Cell Barriers

The cell membrane is formed by a phospholipid bilayer that is generally impermeable to fluids, ions, and most foreign substances. This would seem to isolate the cell from

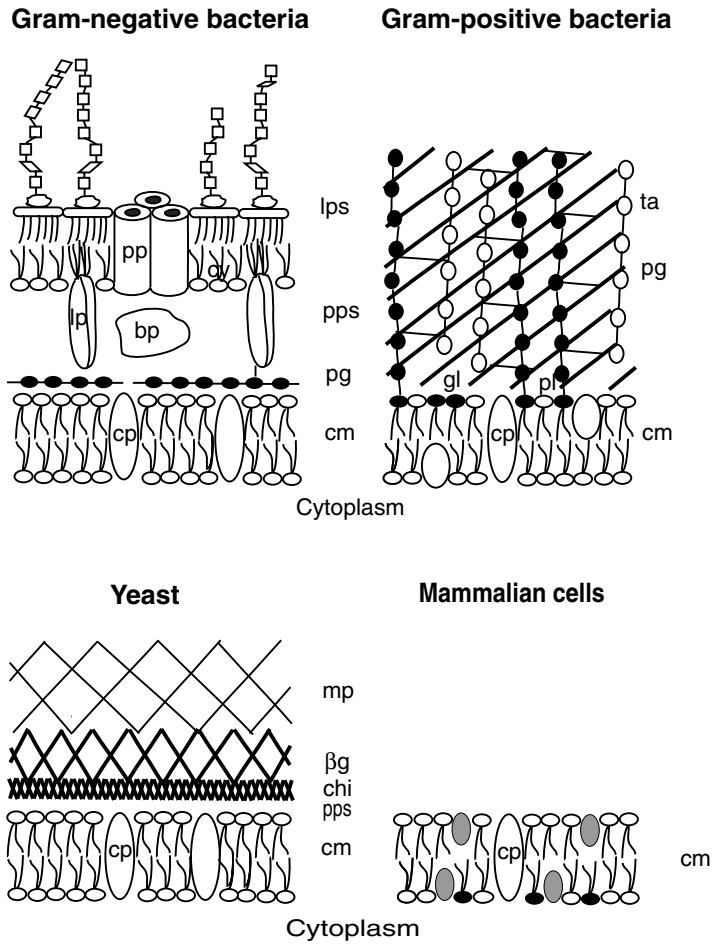

FIGURE 18.1 Microbial and mammalian cell barriers. The cell barriers of different types of cells are illustrated. LPS, lipopolysaccharide; PG, peptidoglycon; PL, phospholipid; GL, glycolipid; PPS, periplasmic space; CM, cytoplasmic membrane; BP, braun lipoprotein; LP, lipoprotein; CP, carrier protein; PP, pore protein; TA, teichoic acid; MP, mannoprotein; βG, beta-glucan; CHI, chitin. (See Figure 18.2 for details on lipid characteristics.)

its environment; however, cell membranes are in fact semipermeable to small molecules. In addition, microbial cell bilayers are coated with an extracellular matrix that provides a largely inert structural framework and protective barrier. The composition of the bilayer and the extracellular matrix varies with cell type, and these differences are important to the activities and cell type-specificity of cell-permeating peptides. Figure 18.1 illustrates cell barriers associated with different cell types.

The cell barriers of prokaryotic cells are multilayered structures that provide stringent protection against foreign substances in the cell's environment.[12] In the case of Gram-positive bacteria, the cell barrier consists of a phospholipid bilayer covered by a thick peptidoglycan layer and an outer capsule that varies in thickness

between species. In the case of Gram-negative bacteria, the cell barrier consists of two phospholipid bilayers, with the inner membrane surrounded by a peptidoglycan layer and the outer coated on the exterior by a lipopolysaccharide (LPS) layer (Figure 18.1).[13] The LPS layer provides Gram-negative bacteria with a particularly stringent sieve against foreign substances.

The cell barrier of eukaryotic cells typically presents less of an obstacle to permeating peptides because the main structure is the phospholipid bilayer. Most mammalian cells have little additional coating as protection. In contrast, fungal plasma membranes are enriched in inositol phosphoceramides and a thick outer protective cell wall composed of β-1,3 glucan and β-1,6 glucans and chitin.[14] In some cases the fungal cell wall can amount to as much as 40% of the dry cell mass. Therefore, fungi are similar to bacteria in having thick and complex barriers against cell-permeating peptides and other foreign substances.

18.2.2 Origins and Discovery of Microbial Cell-Permeating Peptides

Antimicrobial peptides were discovered as a group of small, cationic peptides, and it was soon found that these peptides possessed potent bactericidal and fungicidal properties.[15-17] Antimicrobial peptides have been isolated from most vertebrate and invertebrate material studied, such as the blood and epithelia of animals, plants, hemolymph of insects, and venom of scorpions. The multitude of peptides discovered, more than 500, are cataloged and updated in a database (www.bbcm.univ.trieste.it/~tossi/antimic.html). The diverse occurrence and similar activities of antimicrobial peptides indicate an ancient origin and conserved role in host immunity to pathogens.[18,19] Indeed, during the last two decades, antimicrobial peptides have become well recognized as important within the innate and the humoral immune responses.

18.2.3 Composition and Structure of Microbial Cell-Permeating Peptides

The naturally occurring antimicrobial peptides are normally 12–50 amino acids long (occasionally up to 80 amino acids) and share two main characteristics. First, they are polycationic with a positive net charge of more than +2 (due to an excess of primarily lysine and arginine residues). Second, they have the ability to form amphipathic structures with both positively charged and hydrophobic regions (see Figure 18.2b). The hydrophobic content is generally around 50% and this face promotes interaction with membrane lipids. The positively charged face promotes interaction with water and negatively charged lipids and cell wall structures. This organization is ideal for a molecule that needs to be soluble in water and also lipophylic.

Apart from their positive charge and amphipathic features, antimicrobial peptides can be categorized into different structural classes (Figure 18.2a), including peptides composed of α-helices, β-sheet, loops, and extended sequences. The most common classes are linear peptides that form amphipathic α-helices in contact with membranes and the cystein-containing peptides, which are usually β-sheet peptides constrained by two to four disulfide bonds. Less common are linear peptides with a

α-helical linear peptides

LL-37	LLGDFFRKSKEKIGKEFKRIVQRIKDFLRNLVPRTES
Cecropin P1	SWLSKTAKKLENSAKKRISEGIAIAIQGGPR

Peptides containing disulfide bonds

α-defensins	ACYCRIPACIAGERRYGTCIYQGRLWAFCC
β-defensin	DHYNCVSSGGQCLYSACPIFTKIQGTCYRGKAKCCK
bactenecin	RLCRIVVIRVCR

Peptides with one or two dominating amino acids

PR-39	RRRPRPPYLPRPRPPPFFPPRLPPRIPPGFPPRFPPRFPGKR-NH2
Indolicidin	ILPWKWPWWPWRR-NH2

(a)

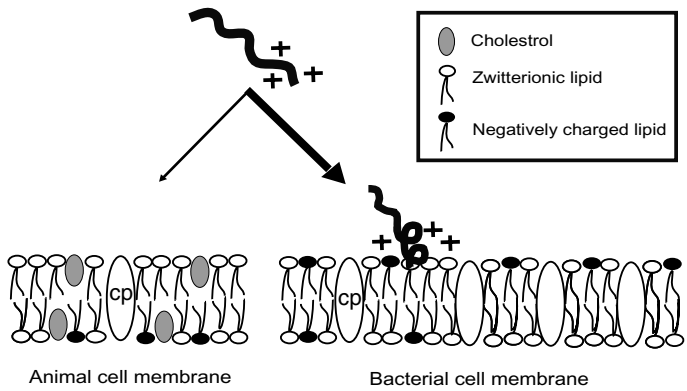

(b)

FIGURE 18.2 Structural classes of cell-permeating cationic antimicrobial peptides. (a) structural classes of natural antimicrobial peptides; (b) proposed basis for cell-type specific interaction based on cell surface charge differences between microbial and host cells.

predominance of one or two amino acids (usually R, P, W, G, or H) and loop peptides with just one disulfide bond. In all cases, however, it is clear that a minimum size is required to maintain antimicrobial activity, approximately that needed to span a lipid bilayer (around 12 amino acids). The membrane-disturbing activity of larger peptides and proteins (>40 amino acids) is usually confined to subdomains.

Linear peptides are susceptible to enzymatic degradation; microbial resistance to antimicrobial peptides can be provided by up-regulation of membrane-associated proteases.[20] Clearly, protease stability is an important feature that appears to be improved in natural antimicrobial peptides by the presence of disulfide bonds. For

example, the recently discovered theta-defensin from *Rhesus macaque* is a macrocyclic peptide with three disulfide bonds and a structure similar to protegrin from pig.[21] The same motif is also found in macrocyclic peptides from plants, although the cross-linking arrangement of disulfide bonds differs.[22] Interestingly, another macrocylic peptide AS-48, a plasmid-encoded peptide expressed by *Enterococcus faecalis*, shows remarkable structural similarities with porcine NK-lysin in terms of size and α-helical fold.[23] Therefore, among natural antimicrobial peptides, a range of structural arrangements can provide stable and active peptides.

When designing antimicrobial peptides, another strategy is to incorporate non-natural amino acids. For example, peptides containing D-amino acids can display improved antimicrobial activities because they retain their activity but are more resistant to proteases.[24-26] In our studies (Andersson et al., unpublished), we have noticed that *Mycobacterium smegmatis* is insensitive to certain α-helical peptides, while the corresponding D-forms have higher activities. Furthermore, it is possible to synthesize short cyclic amphiphilic peptides with both L- and D-amino acids, and these modified circular peptides display good protease resistance.[27]

18.3 MECHANISMS OF ACTION

18.3.1 Cell Uptake

18.3.1.1 Cell Permeation by Cationic Peptides

In broad terms, microbial cell permeation by peptides can be seen as a three-step process. The first event is an electrostatic attraction of the peptide to the membrane surface (Figure 18.2b). The second involves membrane disruption and penetration and, possibly, some reorganization of the peptide structure. As peptides accumulate at the surface and start to displace lipids, this would eventually lead to local disruptions of the membrane ("carpet model") or perhaps formation of transient peptide-lipid "wormhole" pores.[28-30] Such disorganization or pore formation could allow cellular components to leak out and weaken the bacterial wall, creating opportunities for peptides to translocate into the inner membrane and subsequently into the cytoplasm. It also seems possible for peptides to translocate without causing significant membrane disruption.[31,32] Finally, in the third step the peptide passes the membrane and gains access to intracellular processes.

In a more specific example, cationic peptide uptake into Gram-negative bacteria can be seen as a "self promoted" process, reflecting the fact that uptake is receptor independent.[5] According to this view, cationic peptides would contact the outer membrane through electrostatic attraction between positively charged antimicrobial peptides and negatively charged membrane lipids and the LPS layer. At this point peptides could compete for divalent cation binding sites within the outer cell membrane. In *Escherichia coli*, such competition would disrupt stabilizing cross-linking between LPS molecules and therefore reduce outer membrane integrity, which would provide opportunities for peptides to enter the membrane. The membrane charge gradient (inside negative) would then force cationic peptides into cells.

Although cationic peptide uptake into bacteria is viewed differently by many researchers, it is accepted that electrostatic attraction is often an important first step in uptake. Consistent with this, it is generally observed that increased salt concentrations shield the interaction and reduce peptide potency. Also, resistance can arise from cell barrier modifications that limit permeation. For example, resistant Salmonella cells contain modified LPS molecules with reduced membrane negative charge density.[33] Thus, an initial electrostatic attraction appears to be needed for cell-permeating peptides to enter cells. However, some variations and exceptions exist within this rule. For example, certain cationic peptides are more salt tolerant and some antimicrobial peptides are not cationic.[34]

Based on this general view of peptide permeation, numerous synthetic cationic peptides in the range of 10–20 amino acids have been made with variations in their amphipathic structure. The peptides have been subjected to a variety of biochemical analysis with artificial membranes in order to elucidate the mechanism of action, as reviewed.[28-30,35] However, given uncertainties surrounding the mechanism of action of cell-permeating peptides and the possibility for several different mechanisms, the design process remains uncertain.

18.3.1.2 Receptor-Mediated Transport of Peptides and Endocytosis

A variety of peptide sequences are known to enter microbial cells via receptor-mediated translocation or permeases; these mechanisms certainly offer opportunities to deliver foreign substances into microbial cells. Furthermore, receptor-mediated delivery is a very attractive approach for cellular delivery because of the potential for cell type specificity. The best known receptor-mediated transport mechanism in microorganisms involves the oligopeptide permeases, which import di- and trioligopeptides. There are multiple oligopeptide permeases in microbial cells, and overlapping substrate specificity between species. For more information on receptor-mediated uptake we direct readers to two excellent reviews.[36,37]

Endocytosis also offers a range of attractive possibilities for cell delivery; however, it is very complex and the intracellular fate of internalized vesicles is difficult to predict. Furthermore, most substances that undergo endocytosis are not released into the cytoplasm or able to reach the nucleus. Nevertheless, endocytosis is used by many bacterial toxins to reach the intracellular targets in eukaryotic hosts, so there are possibilities for practical applications.[38,39] We direct interested readers to an excellent recent review by Sandvig and van Deurs.[40]

18.3.2 Cell-Killing Mechanisms

18.3.22.1 Membrane Leakage

Membrane leakage is usually referred to as the main cytotoxic activity of antimicrobial peptides. However, it is not clear which events actually lead to microbial death by most antimicrobial peptides. There is no doubt that antimicrobial peptides interact with membranes, but several different hypotheses explain how this could lead to cell death. These include physical disturbance of membrane integrity, fatal

TABLE 18.1
Microbial Permeating Peptides with Intracellular Targets

Name	Putative intracellular target	Ref.
Nicin	Lipid II	72
PR-39	DNA and protein synthesis	8
Buforin 2	DNA/RNA	73
Histatins	Mitochondria	74
Bac5 and Bac7	Respiration	75
ENAP-2	Serine proteases	76

depolarization of energized bacteria, or leakage of essential intracellular components.[30,41,42]

18.3.2.2 Intracellular Target Inhibition

Early studies with antimicrobial peptides indicated that the mechanism of action could involve binding to intracellular targets and many more examples of this mode of action have recently been reported (Table 18.1). Several antimicrobial peptides, including defensins, interact with heat shock protein (HSP) 70 and DNA.[43,44] These peptides also can block general functions, including protein folding and protein synthesis. For example, PR-39 is known to rapidly (within minutes) stop DNA and protein synthesis in *E. coli*, apparently without causing cell lysis.[8] Indeed, several examples of antimicrobial peptides with intracellular targets involve processes such as transcription, translation, protease activity, and mitochondrial function[1,7,8,45- 47] (see also Table 18.1).

18.3.2.3 Dual Activities of Microbial Cell-Permeating Peptides

Many conventional antibiotics appear to kill cells via two or more mechanisms; permeating peptides also can act in multiple ways to kill cells. The two applications for cell-permeating peptides described below, cell permeabilization and cell delivery, potentially can be combined for greater overall activities. Indeed, cell wall permeabilization and toxic compound delivery could provide dual antimicrobial effects for improved overall activity.

Also, it is possible to recombine domains from different antimicrobial peptides to obtain new activity profiles, such as the cecropin–melittin hybrid and derivatives, which appear to have two distinct activity domains.[48,49] The recombined peptide shows greater overall activity and it appears that more than one cell-killing mechanism is involved. The design rules for such domain shuffling experiments remain uncertain, but there are opportunities to create more active hybrid peptides. For example, in our attempts to develop antimicrobial peptide–PNA conjugates, one can envision improved activity by invoking efficient cell wall permeabilization together with efficient antisense effects against an essential gene.[6]

18.3.3 Cell Type-Specific Activities

If microbial cell-permeating peptides are to prove useful in therapeutics, their cell-permeating properties must be largely specific for microbial cell membranes. Cell type-specificity is an important feature of conventional antibiotics that allows pathogen killing at concentrations that are not cytotoxic to host cells.[50] The activity of natural antimicrobial peptides and the safety of foods that contain such peptides indicates that antimicrobial peptides possess the needed specificity to be useful as therapeutics.[1] Many antimicrobial peptides and their derivatives display a therapeutic window in which they can kill microbial cells without damaging host cells.

Bacterial membranes have a more negatively charged outer leaf than mammalian cells, which provides some basis for selective activities. Tossi et al. studied 150 linear peptides and suggested that both position of the amphipathic structure and net charge can influence peptide specificity.[35] Also, the differing sterol content between mammalian and microbial membranes is often regarded as a reason for selectivity. Cholesterol inhibits antimicrobial peptide activity, possibly by providing improved membrane stability, but other differences could also affect activity. Furthermore, many antimicrobial peptides display selective activity against certain classes of microorganisms, such as Gram-positive bacteria or fungi.[51] Therefore, cell wall differences between species (Figure 18.1) provide a basis for cell type-specific killing by membrane active peptides, although the basis for this selectivity remains unclear.

18.4 METHODS

18.4.1 Antimicrobial Activity Assays

Several methods can be used to test antimicrobial activity. The three most common are the thin agar inhibition zone assay, microdilution assay, and colony forming units assay.[52,53] These methods are described in detail elsewhere, but a brief description is appropriate here.[54]

The inhibition zone assay is based on bacterial growth on agar plates. Small holes (usually 3 mm) are punched in the agar and small samples placed within. The plates are incubated and active peptides will diffuse and prevent microbial growth, seen as a zone of clearing. The diameter of the zone is proportional (exponential relationship) to peptide activity and can be given as zone diameter or as activity units relative to a standard peptide. The lethal concentration (LC) can be determined as the lowest amount of peptide needed to kill bacteria. The method is simple and the sensitivity is down to 30 ng for a peptide with an LC-value of approximately 1 μM; however, a disadvantage is that results are influenced by diffusion properties of the peptide and it is only suitable for rapid bacterial growth.

The microdilution assay involves bacterial growth in broth using microtitre plates with the addition of a serial dilution of peptides. The plates are incubated overnight and growth of bacteria is measured by monitoring turbidity. The peptide minimal inhibitory concentration (MIC) is taken as the lowest peptide concentration that prevents growth. This gives a value for bacteriostatic activity; for many antimicrobial

peptides this value is close to the LC values obtained. The minimal bactericidal concentration (MBC) is calculated by determining the number of colony-forming units during treatment. An aliquot from the microdilution assay is dispersed on agar plates and incubated. The MBC is usually defined as the lowest peptide concentration that prevents colony formation.

18.4.2 Cell Uptake Assays

Peptide uptake into cells can be assayed by direct and indirect methods. Early studies on microorganisms showed that the growth response of amino acid auxotrophic mutants to peptides can be used to indicate peptide entry; however, it is difficult to obtain quantitative data from the growth response. A more direct approach is to use radioactively labeled peptides and cell fractionation to assess localization and uptake kinetics. However, cell fractionation can be difficult and uncertain, especially with small microbial cells. Many researchers now prefer uptake assays based on colorimetric or fluorescent probes, which are easier to handle and better suited to measurements of uptake kinetics and cell localization.

18.4.2.1 Fluorescence Microscopy and FACS Analysis

There is a range of flexible fluorescent probes that can be attached covalently to peptides enables direct observation of peptide entry by using fluorescence microscopy and fluorescence-activated cell sorting (FACS). In broad terms, fluorescence microscopy can be used to indicate localization within a relatively small number of cells and FACS analysis can be used to profile uptake into a large number of cells. In our efforts to discover peptides that permeate into microbial cells, we have attached peptides to fluorescent probes and studied treated cells using fluorescence microscopy and FACS analysis. Figure 18.3 shows the microscopy image of GFP following peptide-mediated delivery into *Saccharomyces cerevisisae* and FACS analysis of the same cell population. In this example, the addition of the carrier peptide clearly improved cellular delivery.

18.4.2.2 Cell Permeabilization Assays

As mentioned earlier in the chapter, most antimicrobial peptides have potent cell wall activity, which often appears to be the major mechanism involved in cell killing. In other cases, killing also appears to involve binding to intracellular targets, but such peptides first must permeate the outer barriers to reach their internal targets (see Table 18.1). Therefore, whether cell wall activity involves permeabilization to cause cell leakage or permeation to gain access to the cell interior, some degree of membrane disturbance is involved. The most straightforward method to assess this disturbance is to use small fluorescent molecules or chromogenic probes that normally are excluded by cells but can gain access at points where the membrane is disturbed. By monitoring the cell entry and chemical conversion of such small molecule probes it is possible to gain insight into permeabilization kinetics and conditions that affect activity.

Several different fluorescent probes can be used to probe microbial membrane disturbance or permeabilization. For example, the hydrophobic fluorescent probe

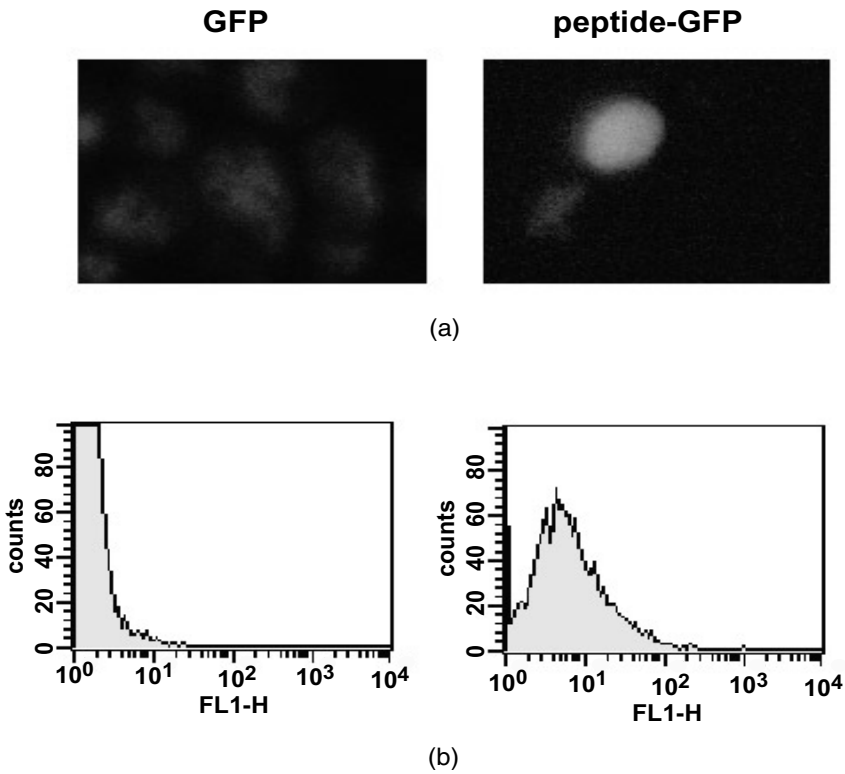

FIGURE 18.3 (Color Figure 18.3 follows p. 14.) Direct observation of peptide uptake by using fluorescent probes (a) fluorescence microscopy of a peptide–GFP (green fluorescent protein) fusion illustrating cellular localization within *S. cerevisiae*; (b) FACS analysis of a peptide–GFP fusion showing cellular delivery to a population of *S. cerevisiae* cells. The right shifted peak indicates increased GFP signal for the majority of cells.

N-phenol naphalene (NPN) can be used as an indicator of membrane integrity. In *E. coli* and other microbes, NPN normally is excluded by the outer membrane LPS layer, but can enter at points where membrane integrity is compromised. NPN has low fluorescence quantum yield in aqueous solution, but fluoresces strongly in the hydrophobic environment of a biological membrane. An alternative is to use propidium iodide, which fluoresces strongly if able to enter cells and bind nucleic acids.[55] These probes can be used with most types of microbial cells.

Gram-negative bacteria, which possess two cell membranes, are doubly challenging when attempting to assess membrane permeabilization. Nevertheless, in cells that express β-galactosidase and β-lactamase it is possible to monitor permeabilization of both membranes at the same time. For example, permeabilization of the outer membrane can be monitored using nitrocefin as a probe. Nitrocefin is normally excluded by the outer cell membrane but, if able to pass this barrier, can be cleaved by β-lactamase localized within the periplasmic space. Cleavage results in a color change from yellow

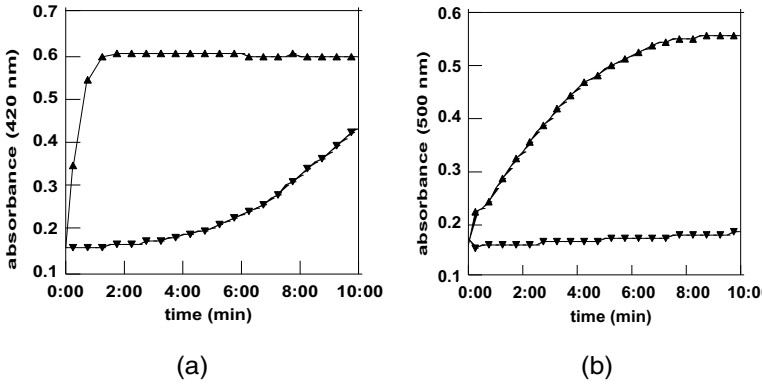

FIGURE 18.4 Indirect monitoring of peptide uptake into microorganisms. Concurrent measurements of *E. coli* outer and inner cell membrane permeabilization by polymyxin B. The symbols represent trials in the presence (▲) and absence (▼) of polymyxin B. For the left panel (a), increased absorbance indicates nitrocefin cleavage and permeabilization of the outer cell membrane. For the right panel (b), increased absorbance indicates ONPG cleavage and permeabilization of the inner cell membrane.

to red, which can be used to monitor outer membrane permeabilization. In a similar way, permeabilization of the inner membrane can be monitored by using the β-galactosidase substrate *o*-nitrophenyl-β-galactoside (ONPG) as a probe. In *E. coli* strain ML35p, which lacks *lac* permease, ONPG is blocked from cell entry by the inner membrane, but if able to pass this barrier, ONPG can be cleaved by β-galactosidase localized within the cytoplasm; this results in a color change from clear to yellow.[56] Figure 18.4 illustrates examples of *E. coli* cell permeabilization by the well known outer cell-permeabilizing peptide polymyxin B.

Permeabilization assays based on small molecule probes are relatively simple and provide useful information about peptide activities and permeabilization kinetics in a variety of environments. However, membrane disturbance is indicated only indirectly. Also, it is not possible to distinguish between permeabilization and permeation by peptides. This can be a disadvantage because certain peptides appear to cause very little membrane disturbance during membrane transport. Clearly there are shortcomings with the available direct and indirect methods to assess peptide permeation into microbial cells; however, in most studies the main objective is to compare a range of peptides in a variety of microorganisms.

18.5 APPLICATIONS

18.5.1 Antimicrobial Peptides as a New Source of Anti-Infective Agents for Medicine

There is an increasing need for new antimicrobial agents to combat resistant strains in the clinic, and antimicrobial peptides appear to offer attractive alternatives. Most importantly, antimicrobial peptides are active against strains that show antibiotic

resistance and resistance to antimicrobial peptides does not appear to arise rapidly.[57,58] This is probably because the antimicrobial peptide-killing mechanisms are largely distinct from those of small molecule antibiotics and antimicrobial peptides are typically cidal rather than static above their threshold concentration for activity. Another advantage with antimicrobial peptides is that their cell-permeating activities can potentiate conventional antibiotics when used in combination.[57]

As with all new drug ideas, several levels of difficulty exist with antimicrobial peptide development and the problems apply to most potential applications of cell-permeating peptides. Natural antimicrobial peptides are produced at site or delivered to the place of infection by white blood cells that produce the peptides, whereas peptides used as drugs must find their own way. Cell-permeating peptides are larger than most drugs and typically show poor stability and distribution properties in the body. Other problems are the uncertain design and development rules for antimicrobial peptides, *in vitro* studies provide only poor indications of *in vivo* efficacy, and peptides can be expensive to produce and purify. Because of these problems, screening efforts that show initial success can prove ultimately disappointing.

Given the uncertain mixture of positive and negative properties of antimicrobial peptides, the area is still regarded as rather risky and large pharmaceutical companies have shown relatively little interest (Table 18.2). Nevertheless, evidence from animal studies and clinical trials shows that antimicrobial peptides can provide effective antimicrobials.[59-63] Also, many problems that limit efficacy *in vivo* and efficient large scale production have been solved.[1] Finally, it has been very difficult to develop effective new small molecular weight antimicrobials that do not succumb to resistance.[64,65] Therefore, whereas the unconventional nature of antimicrobial peptides creates difficulties for clinical development, it is important to recognize that the unique properties of these peptides also provide very valuable alternative strategies. For the future, it seems likely that we will soon see drug approval for antimicrobial peptides for topical or oral therapy.

18.5.2 Microbial Cell-Permeating Peptides as Carriers for Foreign Substance Delivery

Microbial cells are typically very resistant to foreign substance uptake. As discussed above, this resistance is provided by the outer cell wall, which acts as a sieve blocking entry of many harmful compounds found in microbial environments.[12,66] Only small molecular weight substances are able to efficiently enter microorganisms by diffusion alone. Unfortunately, these barriers also limit the cell uptake of antimicrobial agents that otherwise would be useful in medicine. Most antibiotics and antimicrobials used in the clinic are small molecular weight substances, less than 500 g per mol. The observation that antimicrobial peptides can permeate cell barriers is surprising and opens possibilities to use these peptides to expand the range of substances that could be used as drugs against microorganisms.

The idea of using peptides to deliver foreign substances into microorganisms was introduced almost 30 years ago. The initial idea was to use two or three residue peptides that are substrates for oligopeptide permeases and link impermeant toxic compounds to the peptides for delivery (Figure 18.5). Impressive results were

TABLE 18.2
Antimicrobial Peptides or Derivatives in Clinical Development

Clinical application	Peptide	Type	Administration	Company	Stage of development
Diabetic foot ulcers	MSI-78 (magainin analog)	α-helical	Topical	Genaera (magainin)	Clinical trials completed
Catheter infection	MBI-226	α -helical	Topical	Micrologix Biothech	Clinical
Muscositis	IB-367 (protegrin analog)	β-sheet	Oral	Intrabiotics	Clinical
Gingivitis	P-113 (histatin analog)	unordered	Oral	Periodontix	Clinical
Antifungal			Systemic	Entomed	Preclinical
Meningococcal meningitis	Neuprex (BPI-fragment)	α-helical	Systemic	Xoma	Clinical

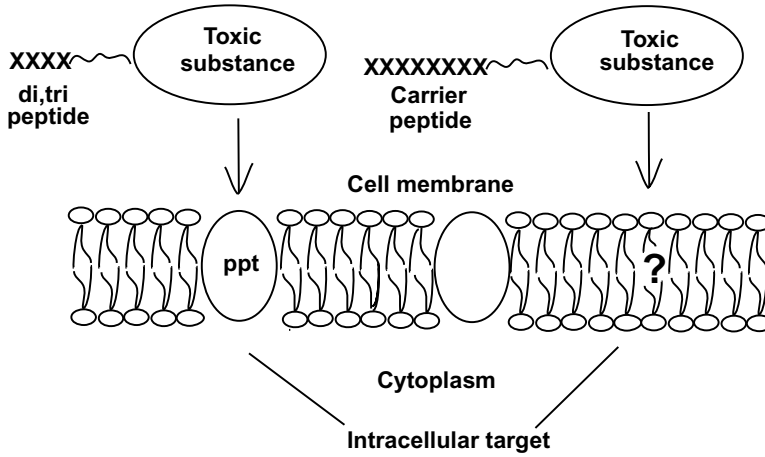

FIGURE 18.5 Generic strategies for peptide-mediated delivery of antimicrobials. The schematic illustrates a carrier peptide domain attached covalently by a flexible linker to a toxic domain. Di- and tripeptides could pass through core protein complex or peptide permease transporters. There are possibilities to use longer permeating peptide to deliver proteins and other substances into microbes, although the mechanisms involved remain uncertain.

reported for delivery into *E. coli* and *Salmonella typhimurium* and the idea was developed to produce the therapeutic alafosfalin, which showed modest clinical success.[9,10]

A limitation with the oligopeptide permease delivery approach, however, is that permeases are not able to efficiently transport substrates with cargoes attached, although certain permeases may be more promiscuous in this respect.[37] Another limitation is that oligopeptide permeases appear to mutate rapidly to change substrate specificity; therefore, it seems likely that microorganisms would become resistant to antimicrobials based on oligopeptide transport.

A related idea is to use cell wall-permeating peptides as vehicles to deliver toxic substances into microbes (Figure 18.5). At first glance it seems illogical to use peptides as delivery vehicles because they are relatively large in comparison to most drugs. Indeed, peptides are normally not considered cell permeable. However, natural antimicrobial peptides provide a clear precedent for this approach. Many natural antimicrobial peptides kill target cells not only by permeabilization, but also by inhibition of intracellular targets, as discussed earlier in this chapter. It seems clear that certain peptides can permeate cells to reach their main target; it should be possible to use such carrier domains to deliver attached foreign substances.

Cell-permeating peptides have been used to deliver a wide range of foreign proteins and oligonucleotides into mammalian cells (see Chapters 1 to 7, 16, and 17) and microbial cell-permeating peptides offer attractive possibilities for antimicrobial development. The challenge now is to identify peptides that can efficiently carry attached cargo molecules into cells with a high degree of microbial cell specificity. In our first attempt to use antimicrobial peptides as delivery vehicles, the objective was to improve cell uptake and activity of antisense peptide nucleic acids

(PNA) in *E. coli*. Antisense agents are designed to inhibit gene expression through sequence-specific nucleic acid binding, which normally requires formation of ten or more base pairs. Oligonucleotides of such lengths are typically too large for efficient passive cellular uptake by diffusion across lipid bilayers; cellular outer membrane structures can pose additional barriers.[67]

Recently, we introduced peptide nucleic acids (PNA) as antisense agents for bacterial applications.[68] Early experiments indicated very encouraging sequence specificity against reporter genes; however, uptake was limited by bacterial cell barriers.[69] This limitation is not surprising as *E. coli* and other Gram-negative bacteria have outer and inner bilayer membranes; the outer membrane contains a lipopolysacharide layer that stringently restricts the entry of foreign molecules.[12]

To provide carrier domains to improve cell uptake and potency, we first selected a range of short, cationic peptides that appeared to have cell-permeabilizing or cell-permeating activities against *E. coli*. These peptides were attached to PNA via flexible linkers.[6] Several of the peptides selected, in particular the KFFKFFKFFK peptide, provided efficient carriers for PNA. Indeed, an antisense peptide–PNA targeted to the essential *acpP* gene is bactericidal and shows encouraging bacterial cell specificity.[70,71] *E. coli* cells were grown in mixed culture with HeLa cells and the peptide–PNA efficiently cleared the human cell culture of inoculated bacteria without apparent harm to the HeLa cells, even when present at a concentration that was ten-fold higher than needed to kill the bacteria.[6] Therefore, microbial cell-permeating peptides can act as carriers for antisense agent delivery and can display toxic effects that appear largely specific against microbial cells.

ACKNOWLEDGMENTS

We thank the Swedish Science Council, Swedish Foundation for Strategic Research, and Pharmacia Corporation for support and our collegues for helpful comments on the manuscript.

REFERENCES

1. van 't Hof, W. et al., Antimicrobial peptides: properties and applicability, *Biol. Chem.,* 382, 597, 2001.
2. Davies, J., Inactivation of antibiotics and the dissemination of resistance genes, *Science,* 264, 375, 1994.
3. Tan, Y.T., Tillett, D.J., and McKay, I.A., Molecular strategies for overcoming antibiotic resistance in bacteria, *Mol. Med. Today,* 6, 309, 2000.
4. Murray, R.W. et al., Ribosomes from an oxazolidinone-resistant mutant confer resistance to eperezolid in a Staphylococcus aureus cell-free transcription-translation assay, *Antimicrob. Agents Chemother.,* 42, 947, 1998.
5. Hancock, R.E., Peptide antibiotics, *Lancet,* 349, 418, 1997.
6. Good, L. et al., Bactericidal antisense effects of peptide-PNA conjugates, *Nat. Biotechnol.,* 19, 360, 2001.

7. Carlsson, A. et al., Attacin, an antibacterial protein from Hyalophora cecropia, inhibits synthesis of outer membrane proteins in Escherichia coli by interfering with omp gene transcription, *Infect. Immun.,* 59, 3040, 1991.
8. Boman, H.G., Agerberth, B., and Boman, A., Mechanisms of action on Escherichia coli of cecropin P1 and PR-39, two antibacterial peptides from pig intestine, *Infect. Immun.,* 61, 2978, 1993.
9. Fickel, T.E. and Gilvarg, C., Transport of impermeant substances in E. coli by way of oligopeptide permease, *Nat. New Biol.,* 241, 161, 1973.
10. Ames, B.N. et al., Illicit transport: the oligopeptide permease, *Proc. Natl. Acad. Sci. U.S.A.,* 70, 456, 1973.
11. Payne, J.W., Drug delivery stystems: optimising the structure of peptide carriers for synthetic antimicrobial drugs, *Drugs Exp. Clin. Res.,* 12, 585, 1986.
12. Nikaido, H., Prevention of drug access to bacterial targets: permeability barriers and active efflux, *Science,* 264, 382, 1994.
13. Alberts, B. et al., *Molecular Biology of the Cell*, Garland Publishing Inc., New York, 1994.
14. Broach, J.R., Pringle, J.R., and Jones, E.W., *The Molecular and Cellular Biology of the Yeast Saccharomyces*, Cold Spring Harbor Laboratory Press, New York, 1997.
15. Steiner, H. et al., Sequence and specificity of two antibacterial proteins involved in insect immunity, *Nature,* 292, 246, 1981.
16. Selsted, M.E. et al., Primary structures of MCP-1 and MCP-2, natural peptide antibiotics of rabbit lung macrophages, *J. Biol. Chem.,* 258, 14485, 1983.
17. Zasloff, M., Magainins, a class of antimicrobial peptides from Xenopus skin: isolation, characterization of two active forms, and partial cDNA sequence of a precursor, *Proc. Natl. Acad. Sci. U.S.A.,* 84, 5449, 1987.
18. Fearon, D.T. and Locksley, R.M., The instructive role of innate immunity in the acquired immune response, *Science,* 272, 50, 1996.
19. Hoffmann, J.A. et al., Phylogenetic perspectives in innate immunity, *Science,* 284, 1313, 1999.
20. Guina, T. et al., A PhoP-regulated outer membrane protease of Salmonella enterica serovar typhimurium promotes resistance to alpha-helical antimicrobial peptides, *J. Bacteriol.,* 182, 4077, 2000.
21. Tang, Y.Q. et al., A cyclic antimicrobial peptide produced in primate leukocytes by the ligation of two truncated alpha-defensins, *Science,* 286, 498, 1999.
22. Derua, R., Gustafson, K.R. and Pannell, L.K., Analysis of the disulfide linkage pattern in circulin A and B, HIV-inhibitory macrocyclic peptides, *Biochem. Biophys. Res. Commun.,* 228, 632, 1996.
23. Gonzalez, C. et al., Bacteriocin AS-48, a microbial cyclic polypeptide structurally and functionally related to mammalian NK-lysin, *Proc. Natl. Acad. Sci. U.S.A.,* 97, 11221, 2000.
24. Maloy, W.L. and Kari, U.P., Structure-activity studies on magainins and other host defense peptides, *Biopolymers,* 37, 105, 1995.
25. Vunnam, S., Juvvadi, P., and Merrifield, R.B., Synthesis and antibacterial action of cecropin and proline-arginine-rich peptides from pig intestine, *J. Pept. Res.,* 49, 59, 1997.
26. Oren, Z. and Shai, Y., Cyclization of a cytolytic amphipathic alpha-helical peptide and its diastereomer: effect on structure, interaction with model membranes, and biological function, *Biochemistry,* 39, 6103, 2000.

27. Fernandez-Lopez, S. et al., Antibacterial agents based on the cyclic D,L-alpha-peptide architecture, *Nature,* 412, 452, 2001.
28. Shai, Y., Mechanism of the binding, insertion and destabilization of phospholipid bilayer membranes by alpha-helical antimicrobial and cell non-selective membrane-lytic peptides, *Biochim. Biophys. Acta,* 1462, 55, 1999.
29. Huang, H.W., Action of antimicrobial peptides: two-state model, *Biochemistry*, 39, 8347, 2000.
30. Matsuzaki, K., Why and how are peptide-lipid interactions utilized for self-defense? Magainins and tachyplesins as archetypes, *Biochim. Biophys. Acta,* 1462, 1, 1999.
31. Kobayashi, S. et al., Interactions of the novel antimicrobial peptide buforin 2 with lipid bilayers: proline as a translocation promoting factor, *Biochemistry,* 39, 8648, 2000.
32. Zhang, L., Rozek, A., and Hancock, R.E., Interaction of cationic antimicrobial peptides with model membranes, *J. Biol. Chem.,* 25, 25, 2001.
33. Guo, L. et al., Lipid A acylation and bacterial resistance against vertebrate antimicrobial peptides, *Cell,* 95, 189, 1998.
34. Friedrich, C. et al., Salt-resistant alpha-helical cationic antimicrobial peptides, *Antimicrob. Agents Chemother.,* 43, 1542, 1999.
35. Tossi, A., Sandri, L., and Giangaspero, A., Amphipathic, alpha-helical antimicrobial peptides, *Biopolymers,* 55, 4, 2000.
36. Naider, F. and Becker, J. M., Peptide transport in Candida albicans: implications for the development of antifungal agents, *Curr. Top. Med. Mycol.,* 2, 170, 1988.
37. Hancock, R.E.W., *Drug Transport in Antimicrobial and Anticancer Chemotherapy*, Marcel Dekker, New York, 1994.
38. Sandvig, K. and van Deurs, B., Endocytosis and intracellular transport of ricin: recent discoveries, *FEBS Lett.,* 452, 67, 1999.
39. Falnes, P.O. and Sandvig, K., Penetration of protein toxins into cells, *Curr. Opin. Cell Biol.,* 12, 407, 2000.
40. Sandvig, K. and van Deurs, B., Entry of ricin and Shiga toxin into cells: molecular mechanisms and medical perspectives, *Embo J.,* 19, 5943, 2000.
41. Westerhoff, H.V. et al., Magainins and the disruption of membrane-linked free-energy transduction, *Proc. Natl. Acad. Sci. U.S.A.,* 86, 6597, 1989.
42. Yang, L. et al., Crystallization of antimicrobial pores in membranes: magainin and protegrin, *Biophys. J.,* 79, 2002, 2000.
43. Kragol, G. et al., The antibacterial peptide pyrrhocoricin inhibits the ATPase actions of DnaK and prevents chaperone-assisted protein folding, *Biochemistry,* 40, 3016, 2001.
44. Sharma, S. and Khuller, G., DNA as the intracellular secondary target for antibacterial action of human neutrophil peptide-I against Mycobacterium tuberculosis H37Ra, *Curr. Microbiol.,* 43, 74, 2001.
45. Helmerhorst, E.J. et al., The cellular target of histatin 5 on Candida albicans is the energized mitochondrion, *J. Biol. Chem.,* 274, 7286, 1999.
46. Debono, M. and Gordee, R.S., Antibiotics that inhibit fungal cell wall development, *Annu. Rev. Microbiol.,* 48, 471, 1994.
47. Lupetti, A. et al., Candidacidal activities of human lactoferrin peptides derived from the N terminus, *Antimicrob. Agents Chemother.,* 44, 3257, 2000.
48. Boman, H.G. et al., Antibacterial and antimalarial properties of peptides that are cecropin-melittin hybrids, *FEBS Lett.,* 259, 103, 1989.
49. Andreu, D. et al., Shortened cecropin A-melittin hybrids. Significant size reduction retains potent antibiotic activity, *FEBS Lett.,* 296, 190, 1992.

50. Lehrer, R.I. and Ganz, T., Antimicrobial peptides in mammalian and insect host defence, *Curr. Opin. Immunol.,* 11, 23, 1999.
51. DeLucca, A.J. et al., Fungicidal activity of cecropin A, *Antimicrob. Agents Chemother.,* 41, 481, 1997.
52. Hultmark, D. et al., Insect immunity. Attacins, a family of antibacterial proteins from Hyalophora cecropia, *Embo J.,* 2, 571, 1983.
53. Wu, M. and Hancock, R.E., Interaction of the cyclic antimicrobial cationic peptide bactenecin with the outer and cytoplasmic membrane, *J. Biol. Chem.,* 274, 29, 1999.
54. Lorian, V., *Antibiotics in Laboratory Medicine*, 4th ed., Williams & Wilkins, Baltimore, 1996.
55. Mason, D.J. et al., Antimicrobial action of rabbit leukocyte CAP18(106-137), *Antimicrob. Agents Chemother.,* 41, 624, 1997.
56. Lehrer, R.I., Barton, A., and Ganz, T., Concurrent assessment of inner and outer membrane permeabilization and bacteriolysis in E. coli by multiple-wavelength spectrophotometry, *J. Immunol. Methods,* 108, 153, 1988.
57. Giacometti, A. et al., In-vitro activity and killing effect of polycationic peptides on methicillin-resistant Staphylococcus aureus and interactions with clinically used antibiotics, *Diagn. Microbiol. Infect. Dis.,* 38, 115, 2000.
58. Linde, C.M. et al., In vitro activity of PR-39, a proline-arginine-rich peptide, against susceptible and multi-drug-resistant Mycobacterium tuberculosis, *J. Antimicrob. Chemother.,* 47, 575, 2001.
59. Steinberg, D.A. et al., Protegrin-1: a broad-spectrum, rapidly microbicidal peptide with in vivo activity, *Antimicrob. Agents Chemother.,* 41, 1738, 1997.
60. Ahmad, I. et al., Liposomal entrapment of the neutrophil-derived peptide indolicidin endows it with in vivo antifungal activity, *Biochim. Biophys. Acta,* 1237, 109, 1995.
61. Welling, M.M. et al., Antibacterial activity of human neutrophil defensins in experimental infections in mice is accompanied by increased leukocyte accumulation, *J. Clin. Invest.,* 102, 1583, 1998.
62. Bals, R. et al., Augmentation of innate host defense by expression of a cathelicidin antimicrobial peptide, *Infect. Immun.,* 67, 6084, 1999.
63. Kisich, K.O. et al., Antimycobacterial agent based on mRNA encoding human beta-defensin 2 enables primary macrophages to restrict growth of Mycobacterium tuberculosis, *Infect. Immun.,* 69, 2692, 2001.
64. Tsiodras, S. et al., Linezolid resistance in a clinical isolate of Staphylococcus aureus, *Lancet,* 358, 207, 2001.
65. Gonzales, R.D. et al., Infections due to vancomycin-resistant Enterococcus faecium resistant to linezolid, *Lancet,* 357, 1179, 2001.
66. Hancock, R.E., The bacterial outer membrane as a drug barrier, *Trends Microbiol.,* 5, 37, 1997.
67. Wittung, P. et al., Phospholipid membrane permeability of peptide nucleic acid, *FEBS Lett.,* 365, 27, 1995.
68. Good, L. and Nielsen, P.E., Inhibition of translation and bacterial growth by peptide nucleic acid targeted to ribosomal RNA, *Proc. Natl. Acad. Sci. U.S.A.,* 95, 2073, 1998.
69. Good, L. et al., Antisense PNA effects in Escherichia coli are limited by the outer-membrane LPS layer, *Microbiology,* 146, 2665, 2000.
70. Vaara, M. and Porro, M., Group of peptides that act synergistically with hydrophobic antibiotics against gram-negative enteric bacteria, *Antimicrob. Agents Chemother.,* 40, 1801, 1996.
71. Cronan, J.E. and Rock, C.O., *Escherichia coli and Salmlonella: Cellular and Molecular Biology*, 2nd ed., American Society for Microbiology, Washington, D.C., 1996.

72. Breukink, E. et al., Use of the cell wall precursor lipid II by a pore-forming peptide antibiotic, *Science,* 286, 2361, 1999.
73. Park, C.B. et al., Mechanism of action of the antimicrobial peptide buforin II: buforin II kills microorganisms by penetrating the cell membrane and inhibiting cellular functions, *Biochem. Biophys. Res. Commun.,* 244, 253, 1998.
74. Tsai, H. and Bobek, L.A., Human salivary histatins: promising anti-fungal therapeutic agents, *Crit. Rev. Oral Biol. Med.,* 9, 480, 1998.
75. Skerlavaj, B., Romeo, D., and Gennaro, R., Rapid membrane permeabilization and inhibition of vital functions of gram-negative bacteria by bactenecins, *Infect. Immun.,* 58, 3724, 1990.
76. Couto, M.A., Harwig, S.S., and Lehrer, R.I., Selective inhibition of microbial serine proteases by eNAP-2, an antimicrobial peptide from equine neutrophils, *Infect. Immun.,* 61, 2991, 1993.

Index

C

D

E

F

G

H

I

K

L

M

N

O

P

Q

R

S

T